

https://dspace.org/

Effects of antiretroviral drugs on carcinogenesis in human breast and cervical cells

Adefolaju, Gbenga Anthony

2015-04-20
http://hdl.handle.net/10539/17452

Downloaded from a DSpace repository. https://dspace.org/

EFFECTS OF ANTIRETROVIRAL DRUGS ON CARCINOGENESIS IN HUMAN BREAST AND CERVICAL CELLS

By

GBENGA ANTHONY ADEFOLAJU



FACULTY OF HEALTH SCIENCES

A thesis submitted to the School of Anatomical Sciences,

Faculty of Health Sciences, University of the Witwatersrand,

in fulfilment of the requirements for the degree of

Doctor of Philosophy

Johannesburg, 2014

Supervisor: Professor Margot Jill Hosie

Co-Supervisor: Dr. Kathrine E. Theron

DECLARATION

I, Gbenga Anthony Adefolaju, declare that this thesis is my own work and where the work of others was consulted, it has been duly acknowledged. It is being submitted for the degree of Doctor of Philosophy in the University of the Witwatersrand, Johannesburg. It has not been submitted before for any degree or examination at this or any other University.

..... (Signature of Candidate)

……..day of……..2014

DEDICATION

This work is dedicated to

My supportive, beautiful, loving, caring and patient wife

Ololade Adesola ADEFOLAJU

My lovely sons

IreOluwa & IfeOluwa ADEFOLAJU

None of my accomplishments would have been possible without the kindness, love and support I obtained from

The entire family of

Pa Richard-Anike ADEFOLAJU

And

The entire family of

Pastor Frederick Ade-Agnes OMOLOLA

PUBLICATIONS AND PRESENTATIONS ARISING FROM THIS STUDY

Publications

- **Adefolaju GA**, Theron KE, Hosie MJ. (2013). Effects of HIV protease, nucleoside/non-nucleoside reverse transcriptase inhibitors on BAX, BCL-2 and apoptosis in two cervical cell lines. Biomed Pharmacother, http://dx.doi.org/10.1016/j.biopha.2013.08.007
- Thabethe KR, **Adefolaju GA**, Hosie MJ. (2013). An *In Vitro* Study of the Effects of Emtricitabine, Tenofovir Disoproxil Fumarate and Efavirenz on a Breast Cancer Cell Line, MCF-7. Journal of Basic and Applied Scientific Research (JBASR) 3(4)444-452

Conference Presentations

American Society for Cell Biology (ASCB), Annual Meeting in New Orleans, Louisiana, USA, December 14-18, 2013

EDITED ABSTRACT/CONFERENCE PROCEEDINGS:

Adefolaju GA, Theron KE, Hosie MJ. **(2013).** Effects of HIV protease, nucleoside/non-nucleoside reverse transcriptase inhibitors on Bax, Bcl-2 and apoptosis in two cervical cell lines, Abstract Number 1637.

ABSTRACT

Highly active antiretroviral therapy (HAART), a multidrug combination regimen, commonly consisting of Nucleoside Reverse Transcriptase Inhibitors, non- Nucleoside Reverse Transcriptase Inhibitors and Protease Inhibitors, has radically decreased mortality and morbidity rates among people living with HIV/AIDS and is currently the treatment of choice in South Africa and around the world. The emphasis of the original development of the antiretroviral drugs was on clinical effectiveness (reducing mortality), before all other considerations. Presently, emphasis has shifted from the initial short-term considerations to the long-term undesirable or harmful effects induced by this treatment regimen. Studies on the effects of HAART on the incidence and progression of HIV/AIDS associated cancers, non-Hodgkin's lymphoma, cervical cancer and Kaposi's sarcoma have provided contrasting data. While there has been a decrease in the incidence of Kaposi's sarcoma, HAART has reportedly not had a significant impact on the incidence of the other two AIDS defining malignancies, while some evidence even suggests an increase in these cancers. It has also been extensively reported that the widespread use of HAART has increased the risk of non-AIDS defining malignancies, including breast cancer.

Whether individual antiretroviral compounds or their combinations are oncogenic is therefore widely speculated. These speculations led to the investigation of the effects of some of the antiretroviral drugs used in the South African treatment guidelines on the expression of key apoptotic regulatory genes, *BAX* and *BCL-2* in two human breast, MCF-7 and MCF-10A and two human cervical cell lines, HCS-2 and NCE16IIA by Real Time qPCR gene expression and immunofluorescence. This is because cancer is initiated when there is an up-regulation of anti-apoptotic genes (e.g. BCL-2,) and down regulation of pro-apoptotic genes (e.g. BAX).

Because the formation of new blood vessels from pre-existing vasculature (angiogenesis) is required for cancer growth and development, this study also investigated the effects of the antiretroviral drugs on the expression levels of key angiogenic regulatory genes; hypothesising that the antiretroviral compounds might up-regulate pro-angiogenic $VEGF_{165a}$ and/or down-regulate anti-angiogenic $VEGF_{165b}$ gene expression. This study also evaluated the cytotoxicity of the antiretroviral drugs in normal and cancer cell lines of the breast and cervix at clinically relevant concentrations of the drugs and at different time points – 24, 48, 72 and 96 hours, employing the Neutral Red Toxicology/Viability Assay. In addition, the potential anti-apoptotic effects of the protease inhibitors - LPV/r were investigated by cell death detection ELISA and acridine orange staining.

This study shows that the antiretroviral drugs; tenofovir disoproxil fumarate, emtricitabine, efavirenz, lopinavir, ritonavir and the two triple combinations (all at clinically relevant concentrations which reflect their steady-state peak plasma concentrations in patients receiving these drugs) demonstrated varying degrees of cytotoxicity in the normal breast and cervical cells. The resulting DNA damage associated with cytotoxicity is strongly implicated in the processes of tumor initiation. The results of the qPCR data demonstrated differences in the response of the two tissue types used in this study, which, though is not statistically significant, showed trends and often opposite trends between the breast and cervical and between the normal and cancer cell lines. All the antiretroviral drugs and combinations tested did not significantly alter *BAX* and *BCL-2,* $VEGF_{165a}$ and $VEGF_{165b}$ gene expression in both cell lines. The protein localisation of BAX, BCL-2 and $VEGF_{165b}$ were also not altered.

The protease inhibitors - LPV/r exhibited significant ($p<0.05$) inhibition of Camptothecin induced apoptosis in the cervical cancer HCS-2 cell line but not in the normal immortalised NCE16IIA or the two breast cell lines. This anti-apoptotic property of HIV protease inhibitors, although shown here not to involve BAX or BCL-2 protein and RNA synthesis might promote the development of cervical cancer.

ACKNOWLEDGEMENTS

My heartfelt gratitude goes to my supervisors, Professor Margot Hosie and Dr Kate Theron, for their invaluable guidance, assistance and all round support throughout the course of this journey. You are the best mentors anyone can wish for. Through your warm and friendly but firm supervision, I have grown tremendously as a researcher.

My gratitude goes to the Head of School and all staff in the School of Anatomical Sciences, especially Mrs Hasiena Ali, Monica Gomes for their hard work and patience in assisting me with my techniques. My gratitude goes to Mrs Pamela Sharp for guidance in the use of the Confocal microscope. Many thanks to Alison and Glynis for promptly assisting me with "this or that" purchase.

I deeply appreciate the assistance of Karen Le Roux and Theresa Dix-Peek for giving me tips and hints that made my PCR experience much easier. I appreciate Dr Raquel Douarte-Lightfoot for making her PCR lab available.

I also acknowledge Dr Clem Penny for donating the breast cancer MCF-7 and normal immortalised breast MCF-10A cell lines. Thank you very much.

To all my friends who have given me love, support and encouragement throughout the years, thank you. Dr Moyo Ajao, thank you for touching my life.

My very deep gratitude goes to my family and in-laws. You are simply the best. Thank you for your prayers, encouragement and faith in me and my abilities throughout the years. I also say thank you; the giver of life, the one who began before the beginning began, the word made flesh; Jesus Christ.

Most importantly, I like to thank the love of my life – my wife, sister and friend – Ololade, we did this together! This trophy belongs to you. You gave me the most conducive home environment any man could wish for as I worked on this project. We went through the sleepless nights together. I love and appreciate you. To my beloved son and friend – IreOluwa, you contributed immensely to my sanity in difficult times. You were always welcoming me with your irresistible smiles and laughter. I love you!

TABLE OF CONTENTS **Page**

DECLARATION……..i

DEDICATION……..ii

PUBLICATIONS AND PRESENTATIONS…….iii

ABSTRACT……..iv

ACKNOWLEDGEMENTS ……....vii

TABLE OF CONTENTS…….viii

LIST OF FIGURES……..xiv

LIST OF TABLES……...xvii

LIST OF ABBREVIATIONS……xviii

CHAPTER 1: INTRODUCTION AND LITERATURE REVIEW……..……1

1.1 General Introduction…….....1

1.1.1 Antiretroviral Drug Classes…….5

1.1.2 HAART and its adverse effects…….....8

1.2 Drugs…….....11

1.2.1 Tenofovir Disoproxil Fumarate …….....11

1.2.2 Emtricitabine……...13

1.2.3 Efavirenz…….....14

1.2.4 Lopinavir/ritonavir……..15

1.2.5 Camptothecin…….……..17

1.3.1 Carcinogenesis…….....19

1.3.1.1 Carcinogenicity and Genotoxicity Reports on NRTIs…….19

1.3.1.2 Carcinogenicity and Genotoxicity Reports on NNRTIs……..20

1.3.1.3 Carcinogenicity and Genotoxicity Reports on Protease Inhibitors……..20

1.3.2 Breast Cancer……..21

1.3.3 Cervical Cancer……...23

1.4 Apoptosis and Regulatory Genes…….……..24

1.5 Angiogenesis and Regulatory genes……..27

1.6 Study Objectives……30

1.6.1 Broad Objectives…….30

1.6.2 Specific Objectives……..30

1.7 Anticipated Outcome……..31

CHAPTER 2: MATERIALS AND METHODS……..32

2.1 Kits, Antibodies and reagents…….32

2.2.1 Cells…….32

2.2.2 Cell Culture…….33

2.2.2.1 Pre-treatment culture conditions……..34

2.3.1 Drugs……...34

2.3.2 Stock Solutions of Antiretroviral Drugs……..34

2.3.3 Treatment…….35

2.4 Neutral Red Uptake Assay…….37

2.5 Reverse Transcription and Real time qPCR……..38

2.5.1 Total RNA Extraction…….39

2.5.1.1 RNA Gel Electrophoresis…….39

2.5.1.2 RNA Quantification…….40

2.5.2 Genomic DNA (gDNA) Removal……...40

2.5.3 Reverse Transcription for Complementary DNA (cDNA) Synthesis…….40

2.5.4 Primer Design…….41

2.5.5 Determination of qPCR Amplification Efficiencies……...43

2.5.6 qPCR Protocol…….43

2.5.7 Agarose Gel Electrophoresis of DNA…….44

2.5.8 qPCR Data Analysis……... 45

2.6 Immunofluorescence…….…….46

2.6.1 Bax and Bcl-2……..46

2.6.2 $VEGF_{165}$ …….46

2.6.3 Cell Staining……46

2.6.3.1 Optimization…….47

2.6.3.2 Immuno-staining……..47

2.7 Acridine Orange staining……....49

2.7.1 Induction of Apoptosis……49

2.7.2 Cell treatment and AO staining……...50

2.8 Cell Death Detection ELISA……..51

CHAPTER 3: RESULTS…….....53

3.1 Effects of Antiretroviral drugs on the viability of breast and cervical cells……..53

3.1.1 Effects of TDF on the viability of the cervical cells……...53

3.1.2 Effects of TDF on the viability of the breast cells……..53

3.1.3 Effects of FTC on the viability of the cervical cells……...55

3.1.4 Effects of FTC on the viability of the breast cells……..55

3.1.5 Effects of EFV on the viability of the cervical cells……...57

3.1.6 Effects of EFV on the viability of the breast cells……..57

3.1.7 Effects of ATP on the viability of the cervical cells……...59

3.1.8 Effects of ATP on the viability of the breast cells……..59

3.1.9 Effects of LPV on the viability of the cervical cells……...61

3.1.10 Effects of LPV on the viability of the breast cells……61

3.1.11 Effects of RTV on the viability of the cervical cells……63

3.1.12 Effects of RTV on the viability of the breast cells……...63

3.1.13 Effects of LPV/r on the viability of the cervical cells……..65

3.1.14 Effects of LPV/r on the viability of the breast cells…….65

3.1.15 Effects of TDF/FTC/LPV/r on the viability of the cervical cells…….67

3.1.16 Effects of TDF/FTC/LPV/r on the viability of the breast cells…….67

3.2 Effects of Antiretroviral drugs on apoptotic *BAX*; *BCL-2*, and angiogenic $VEGF_{165a}$ and $VEGF_{165b}$ gene expression in cervical and breast cell lines……...70

3.3 Immunofluorescence of BAX, BCL-2 and VEGF165b proteins in cancer (HCS-2) and normal cervical (NCE16IIA) and cancer (MCF-7) and normal breast (MCF-10A) cells exposed to antiretroviral drugs……..87

3.3.1 Immunofluorescence of BAX and BCL-2 proteins in HCS-2 and NCE16IIA cells exposed to antiretroviral drugs……...87

3.3.2 Immunofluorescence of BAX and BCL-2 proteins in MCF-7 and MCF-10A breast cells exposed to antiretroviral drugs……...110

3.3.3 Immunofluorescence of antiangiogenic VEGF $_{165b}$ protein in HCS-2 and NCE16IIA cells exposed to antiretroviral drugs……..……..…..133

3.3.4 Immunofluorescence of antiangiogenic VEGF $_{165b}$ protein in MCF-7 and MCF10-A cells exposed to antiretroviral drugs……..…...142

3.3.5 Effects of ARVs on the nuclear morphology of normal and cancer cervical and breast cell lines.....160

3.4 Protease Inhibitors and Apoptosis Inhibition……...164

3.4.1 Protease Inhibitors and apoptosis inhibition in cervical HCS-2 and NCE16IIA cells……165

3.4.2 Protease Inhibitors and apoptosis inhibition in breast MCF-7 and MCF10-A cells……171

CHAPTER 4: DISCUSSION……..177

4.1 Introduction……..177

4.2 Antiretroviral drugs and Cytotoxicity……..178

4.3 Do antiretroviral drugs alter the expression of apoptotic regulatory genes? ……...185

4.4 Antiretroviral drugs and the expression of angiogenic related genes……..189

4.5 Apoptosis Induction by Camptothecin…….192

4.6 Protease Inhibitors and Inhibition of Apoptosis……...193

4.7 HAART and Cervical Cancer……...199

4.8 HAART and Non-AIDS defining Malignancies……..200

4.9 Conclusion……204

REFERENCES…….206

APPENDICES……..221

Appendix A1: Solutions recipes…….221

Appendix A2: List of reagents and suppliers…….222

Appendix A3: Data sheets of all cell lines used…….223

Appendix B1: Procedure for total RNA extraction……227

Appendix B2: Procedure for RNA Gel Electrophoresis……228

Appendix B3: Procedure for Genomic DNA (gDNA) Removal……...229

Appendix B4: Optimization for Immunofluorescence……...229

Appendix B5: ABCAM immunofluorescence Staining protocol……...230

Appendix C1: Primer properties and products on target templates for all genes……...232

Appendix C2: Amplification Plots of primer pairs for all genes……...235

Appendix C3: Melt curves generated for PCR products for all primer pairs to confirm the absence of primer dimers and nonspecific amplification……..239

Appendix C4: Agarose gel electrophoresis of PCR products confirming the absence of nonspecific amplification……..246

Appendix D1-D16: Oneway analysis of effects of antiretroviral drugs on % viability of Cervical and Breast cells by time……....247-262

Appendix E: Oneway analysis of effects of ARVs on Fluorescence Intensity of protein staining on cervical and breast cell lines……...263-282

Appendix F: Oneway analysis of effects of ARVs on Nuclear Axes lengths (μm) by treatment groups in cervical and breast cells…….283-291

Appendix G: Oneway analysis of the anti-apoptotic effects of LPV/r on CPT induced apoptosis (Acridine Orange-G1) and DNA fragmentation (ELISA-G2) by groups……291-296

Appendix H: Ethics Clearance Certificate …….....297

LIST OF FIGURES **Page**

Fig. 1.1: Schematic diagram of the HIV-1 life cycle in a susceptible $CD4^+$ cell identifying distinct steps in HIV-1 life cycle as current target for antiretroviral drugs…...7

Fig. 1.2: Two Dimensional structure of tenofovir disoproxil fumarate……...12

Fig. 1.3: Two Dimensional structure of emtricitabine.....13

Fig. 1.4: Two Dimensional structure of efavirenz……14

Fig.1.5: Two Dimensional structure of lopinavir…….....16

Fig.1.6: Two Dimensional structure of ritonavir……..16

Fig.1.7: Two Dimensional structure of camptothecin……..16

Fig. 3.1A & B: Effects of TDF on the percentage viability of cervical (NCE16IIA/HCS2) and breast (MCF-10A /MCF-7) cells…….…….53-54

Fig. 3.2A & B: Effects of FTC on the percentage viability of cervical (NCE16IIA/HCS2) and breast (MCF-10A /MCF-7) cells…….…….55-56

Fig. 3.3A & B: Effects of EFV on the percentage viability of cervical (NCE16IIA/HCS2) and breast (MCF-10A /MCF-7) cells…….…….57-58

Fig. 3.4A & B: Effects of ATP on the percentage viability of cervical (NCE16IIA/HCS2) and breast (MCF-10A /MCF-7) cells…….…….59-60

Fig. 3.5A & B: Effects of LPV on the percentage viability of cervical (NCE16IIA/HCS2) and breast (MCF-10A /MCF-7) cells…….…….61-62

Fig. 3.6A & B: Effects of RTV on the percentage viability of cervical (NCE16IIA/HCS2) and breast (MCF-10A /MCF-7) cells…….…….63-64

Fig. 3.7A & B: Effects of LPV/r on the percentage viability of cervical (NCE16IIA/HCS2) and breast (MCF-10A /MCF-7) cells…….…….65-66

Fig. 3.8A & B: Effects of TDF/FTC/LPV/r on the percentage viability of cervical (NCE16IIA/HCS2) and breast (MCF-10A /MCF-7) cells…….…….67-68

Fig. 3.9A & B: Effects of TDF on *BAX*, *BCL-2, $VEGF_{165a}$ and $VEGF_{165b}$* mRNA expression in (NCE16IIA/HCS2) and breast (MCF-10A /MCF-7) cells….....71

Fig. 3.10A & B: Effects of FTC on *BAX*, *BCL-2, $VEGF_{165a}$ and $VEGF_{165b}$* mRNA expression in (NCE16IIA/HCS2) and breast (MCF-10A /MCF-7) cells…….73

Fig. 3.11A & B: Effects of EFV on *BAX*, *BCL-2, $VEGF_{165a}$ and $VEGF_{165b}$* mRNA expression in (NCE16IIA/HCS2) and breast (MCF-10A /MCF-7) cells…….75

Fig. 3.12A & B: Effects of ATP on *BAX*, *BCL-2, $VEGF_{165a}$ and $VEGF_{165b}$* mRNA expression in (NCE16IIA/HCS2) and breast (MCF-10A /MCF-7) cells…….....77

Fig. 3.13A & B: Effects of LPV on *BAX*, *BCL-2, $VEGF_{165a}$ and $VEGF_{165b}$* mRNA expression in (NCE16IIA/HCS2) and breast (MCF-10A /MCF-7) cells…….....79

Fig. 3.14A & B: Effects of RTV on *BAX*, *BCL-2, $VEGF_{165a}$ and $VEGF_{165b}$* mRNA expression in (NCE16IIA/HCS2) and breast (MCF-10A /MCF-7) cells…….....81

Fig. 3.15A & B: Effects of LPV/r on *BAX*, *BCL-2, $VEGF_{165a}$ and $VEGF_{165b}$* mRNA expression in (NCE16IIA/HCS2) and breast (MCF-10A /MCF-7) cells…….....83

Fig. 3.16A & B: Effects of TDF/FTC/LPV/r on *BAX*, *BCL-2, $VEGF_{165a}$ and $VEGF_{165b}$* mRNA expression in (NCE16IIA/HCS2) and breast (MCF-10A /MCF-7) cells……....85

Fig. 3.17A - K: Fluorescence micrographs of BAX and BCL-2 in cervical HCS-2 cells exposed to Growth Medium or Vehicle (A, B) and antiretroviral drugs (C-J)…..89-98

Fig. 3.18A - K: Fluorescence micrographs of BAX and BCL-2 in cervical NCE16IIA cells exposed to Growth Medium or Vehicle (A, B) and antiretroviral drugs (C-J)….99-109

Fig. 3.19A - K: Fluorescence micrographs of BAX and BCL-2 in breast MCF-7 cells exposed to Growth Medium or Vehicle (A, B) and antiretroviral drugs (C-J)...111-121

Fig. 3.20A - K: Fluorescence micrographs of BAX and BCL-2 in breast MCF-10A cells exposed to Growth Medium or Vehicle (A, B) and antiretroviral drugs (C-J)...122-132

Fig. 3.21A - K: Fluorescence micrographs of $VEGF_{165b}$ in cervical HCS-2 cells exposed to Growth Medium or Vehicle (A, B) and antiretroviral drugs (C-J)……...134-137

Fig. 3.22A - K: Fluorescence micrographs of $VEGF_{165b}$ in cervical NCE16IIA cells exposed to Growth Medium or Vehicle (A, B) and antiretroviral drugs (C-J)……...138-141

Fig. 3.23A - K: Fluorescence micrographs of $VEGF_{165b}$ in breast MCF-7 cells exposed to Growth Medium or Vehicle (A, B) and antiretroviral drugs (C-J)……...143-146

Fig. 3.24A - K: Fluorescence micrographs of $VEGF_{165b}$ in breast MCF-10A cells exposed to Growth Medium or Vehicle (A, B) and antiretroviral drugs (C-J)……...147-150

Figs. 3.25-3.32: Graphical representation of the effects of ARVs on BAX, BCL-2 and $VEGF_{165b}$ protein expression in (A) NCE16IIA (normal cervical); HCS-2 (cervical cancer) and (B) MCF-10A (normal breast); MCF-7 (breast cancer) cells…….151-158

Figure 3.33A - D: Effects of ARVs on the long (LA) and short (SA) axes lengths (μm) of the nuclei of normal cervical NCE16IIA (A), cancer cervical HCS-2 (B), normal breast MCF-10A (C) and cancer breast MCF-7 (D) cells……...162-163

Fig. 3.34: Effects of LPV/r on CPT mediated apoptosis in cervical HCS-2 cells evaluated by Acridine Orange Staining...……...166-167

Fig. 3.35: Effects of LPV/r on CPT mediated apoptosis in cervical NCE16IIA cells evaluated by Acridine Orange Staining……..168-169

Fig. 3.36: Effects of LPV/r on CPT mediated apoptosis in cervical HCS-2 and NCE16IIA cells evaluated by the Cell Death Detection ELISA...…….....170

Fig. 3.37: Effects of LPV/r on CPT mediated apoptosis in breast MCF-7 cells evaluated by Acridine Orange Staining...……...172

Fig. 3.38: Effects of LPV/r on CPT mediated apoptosis in breast MCF-10A cells evaluated by Acridine Orange Staining...……...174

Fig. 3.39: Effects of LPV/r on CPT mediated apoptosis in breast MCF-7 and MCF-10A cells evaluated by the Cell Death Detection ELISA...…….……..176

Fig. C1: Amplification Plots of BAX primer pairs……235

Fig. C2: Amplification Plots of BCL-2 primer pairs……..235

Fig. C3: Amplification Plots of $VEGF_{165a}$ primer pairs…….236

Fig. C4: Amplification Plots of $VEGF_{165b}$ primer pairs…….236

Fig. C5: Amplification Plots of TBP primer pairs…….237

Fig. C6: Amplification Plots of TFRC primer pairs……...237

Fig. C7: Amplification Plots of RPLP0 primer pairs…….238

Fig. C8: Melt curves generated for BAX PCR product to confirm the absence of primer dimers and nonspecific amplification……239

Fig. C9: Melt curves generated for BCL-2 PCR product to confirm the absence of primer dimers and nonspecific amplification……240

Fig. C10: Melt curves generated for $VEGF_{165a}$ PCR product to confirm the absence of primer dimers and nonspecific amplification……241

Fig. C11: Melt curves generated for $VEGF_{165b}$ PCR product to confirm the absence of primer dimers and nonspecific amplification……242

Fig. C12: Melt curves generated for TBP PCR product to confirm the absence of primer dimers and nonspecific amplification……243

Fig. C13: Melt curves generated for TFRC PCR product to confirm the absence of primer dimers and nonspecific amplification……244

Fig. C14: Melt curves generated for RPLP0 PCR product to confirm the absence of primer dimers and nonspecific amplification……245

Fig. C15: Agarose gel electrophoresis of PCR products confirming the absence of nonspecific amplification……...246

LIST OF TABLES **Page**

Table 1.1: Currently available ARVs drugs for the treatment of HIV infection…….4

Table 2.1: Preparation of stock and final concentrations of ARVs added to the cells…...35

Table 2.2: Treatment groups and drug concentrations administered for each cell line…..36

Table 2.3: Components of the Reverse Transcription reaction……...41

Table 2.4: Oligonucleotide sequences used for qPCR……42

Table 2.5: qPCR Reaction setup……. 43

Table 3.1: Summary of the effects of ARVs on normal and cancer cervical and normal and cancer breast cell lines with regard to cell survival using the Neutral Red assay……..……69

Table 3.2: Summary of the effects of ARVs on *BAX, BCL-2, VEGF165A* and *VEGF165B* mRNA expression in normal and cancer cervical and normal and cancer breast cell lines…….86

Table 3.3: Summary of the effects of ARVs on BAX, BCL-2 and VEGF165B protein expression (fluorescence intensity) and localisation in normal and cancer cervical and breast cell lines……...159

Table 3.4: Summary of the effects of ARVs on the nuclear morphology of normal and cancer cervical and breast cell lines...……161

Table A1: List of reagents and suppliers……222

Table C1: Bax primer properties and products on target templates……...232

Table C2: Bcl-2 primer properties and products on target templates……233

Table C3: VEGF165A primer properties and products on target templates……..233

Table C4: VEGF165B primer properties and products on target templates……..234

LIST OF ABBREVIATIONS

ΔCT	Change in threshold cycle
^{O}C	Degrees Celsius
ADM	AIDS defining malignancy
AIDS	Acquired Immunodeficiency Syndrome
AIF	Apoptosis inducing factor
ANOVA	Analysis of Variance
AO	Acridine Orange
ARV	Antiretroviral
ATCC	American Type Culture Collection
ATP	ATRIPLA
BAD	Bcl-2 antagonist of cell death
BAK	Bcl-2 Antagonistic Killer
BAX	Bc*l*-2 Associated Protein X
BCL-xL	B-cell lymphoma-extra large
BCL-2	B-cell Lymphoma bc*l*-2
BID	Bcl-2 interacting domain death agonist
BIM	Bcl-2 interacting mediator of cell death
BLAST	Basic sequence alignment search tool
BOX	Bcl-2 related ovarian killer
bp	base pair
BSA	Bovine serum albumin
CD4	Cluster of differentiation 4
cDNA	Complementary deoxyribonucleic acid
C_{max}	Steady-state plasma peak concentration
CO_2	Carbon dioxide
CPT	Camptothecin

CT	Threshold cycle
CYP3A	Cytochrome P450, family 3, subfamily A
DAPI	4',6-diamidino-2-phenylindole
dH_2O	Distilled water
DISC	Death Inducing Signalling Complex
DMSO	Dimethyl sulfoxide
DNA	Deoxyribonucleic Acid
DNase	Deoxyribonuclease
dNTP	Deoxynucleotide triphosphate
EDTA	Ethylene Diamine Tetraacetic Acid
EFV	Efavirenz
ELISA	Enzyme Linked Immunosorbent Assay
EMEM	Eagle's Minimal Essential Medium
FADD	Fas associated death domain
FAS	Fibroblast-associated
FAS-L	Fas ligand
FBS	Fetal Bovine Serum
FCS	Fetal Calf Serum
FDA	United States Food and Drug Administration
FITC	Fluorescein-isothiocyanate
FTC	Emtricitabine
gDNA	genomic DNA
HAART	Highly Active Anti-retroviral Therapy
HIV	Human Immunodeficiency Virus
HPV	Human papilloma virus
ICC	Immunocytochemistry
IDT	Integrated DNA Technologies

IgG	Immunoglobulin-G
JCRB	Japanese Collection of Research Bio-resources
KBM	Keratinocyte Basal Medium
kDA	Kilo Dalton
KS	Kaposi's Sarcoma
LPV	Lopinavir
mA	Milliamps
MEGM	Mammary Epithelium Growth Medium
MCL-1	Myeloid Leukaemia Cell differentiation protein
MIQE	Minimum Information for Publication of Quantitative Real-Time PCR Experiments
MOMP	Mitochondrial Outer Membrane Permeabilization
MOPS	4-Morpholine Propanesulphonic acid
mg	Milligram
ml	Millilitre
mm	Millimetre
mRNA	Messenger Ribonucleic acid
NADM	non-AIDS defining malignancy
NCBI	National Centre for Biotechnology Information
NHL	non-Hodgkin's Lymphoma
nM	Nanomolar
nm	Nanometre
nNRTI	non-Nucleoside/Nucleotide Reverse Transcriptase Inhibitor
NR	Neutral Red
NRTI	Nucleoside/Nucleotide Reverse Transcriptase Inhibitor
PBS	Phosphate Buffered Saline
PCR	Polymerase Chain Reaction

pH	Potential hydrogen
PI	Protease inhibitor
PlGF	Placental Growth Factor
PLWHA	People living with HIV/AIDS
PTPC	Permeability Transition Pore Complex
RNA	Ribonucleic Acid
RNase	Ribonuclease
RPLP0	*Homo sapiens* ribosomal protein, Large P0
RT	Reverse Transcription
RTV	Ritonavir
SA	South Africa
SIR	Standardized Incidence ratio
SMAC	Second mitochondria derived activator of caspases
TBP	*Homo sapiens* TATA Box Binding Protein
TDF	Tenofovir Disoproxil Fumarate
TFRC	Transferrin receptor
µl	Microlitre
µm	Micrometre
UNAIDS	United Nations Programme on AIDS
UTR	Un-translated Region
UV	Ultraviolet
VEGF	Vascular Endothelial Growth Factor
WHO	World Health Organisation

CHAPTER 1: INTRODUCTION AND LITERATURE REVIEW

1.1 General Introduction

The Human Immunodeficiency Virus/Acquired Immune Deficiency Syndrome HIV/AIDS pandemic have had a catastrophic effect on the world population. By 2012, HIV had infected a cumulative total of about 75 million, out of which about 36 million had died (UNAIDS Global AIDS Fact sheet, 2013).

UNAIDS GLOBAL FACT SHEET:

People living with HIV

- In 2012, there were 35.3 million [32.2 million–38.8 million] people living with HIV.

New HIV infections

- New HIV infections have fallen by 33% since 2001.
    - Worldwide, 2.3 million [1.9 million–2.7 million] people became newly infected with HIV in 2012, down from 3.4 million [3.1 million–3.7 million] in 2001.
    - New HIV infections among adults and adolescents decreased by 50% or more in 26 countries between 2001 and 2012.
- New HIV infections among children have declined by 52% since 2001.
    - Worldwide, 260 000 [230 000–320 000] children became newly infected with HIV in 2012, down from 550 000 [500 000–620 000] in 2001.

AIDS-related deaths

- AIDS-related deaths have fallen by 30% since the peak in 2005.
    - In 2012, 1.6 million [1.4 million–1.9 million] people died from AIDS-related causes worldwide compared to 2.3 million [2.1 million–2.6 million] in 2005.

Since the start of the epidemic, an estimated 36 million [30 million – 42 million] people have died of AIDS-related illnesses (UNAIDS Global AIDS Fact sheet, 2013).

Sub-Saharan Africa, which is home to just 10% of world's population, contains an overwhelming 70 percent of people living with HIV/AIDS (UNAIDS Global AIDS Fact sheet, 2013). South Africa (SA) has the highest number of people living with HIV in sub-Saharan Africa and in the world. It is for this reason that in November 2003, SA started the world's largest public sector rollout of Highly Active Antiretroviral Treatment (HAART) (Abdool Karim *et al.*, 2009; Kranzer *et al.*, 2010).

Prior to the advent of antiretroviral drugs, the management of the Human Immunodeficiency Virus-1 was essentially the management of AIDS-related illnesses and prevention against common opportunistic infections (Arts and Hazuda, 2012). Towards the close of the twentieth century, the development of inhibitors of two of the three most important enzymes (protease and reverse transcriptase) of the HIV-1 machinery dramatically changed the management of HIV patients (Arts and Hazuda, 2012). The introduction of regimens that combined the different drug classes further enhanced the overall effectiveness of the therapy (Arts and Hazuda, 2012).

Highly active antiretroviral therapy (HAART), a multidrug combination regimen, has dramatically reduced mortality and morbidity among Human Immunodeficiency Virus-1 (HIV-1) infected individuals (Nachega *et al.*, 2004; Sikora *et al.*, 2010) and is currently the treatment of choice in South Africa (Maqutu *et al.*, 2011). The multidrug combination therapy markedly stems HIV-1 replication and decreases the plasma viral load to levels almost undetectable by very sensitive clinical assays, which then leads to increased levels of circulating $CD4^+$ T-lymphocytes and a significantly reconstituted immune system (Autran *et al.*, 1997; Komanduri *et al.*, 1998; Lederman *et al.*, 1998). The development of combination therapy also became the foundation for preventing the evolution of drug resistance because the components of the combination act against two or more molecular

machinery of the virus (Arts and Hazuda, 2012).

If patients adhere appropriately to the HAART regimen, viral replication can be suppressed for many years, considerably increasing the life expectancy of HIV-infected individuals (Arts and Hazuda, 2012). Since HIV-1 is currently an incurable chronic infection, HAART on its own cannot resolve the HIV problem (Arts and Hazuda, 2012), so the option of continuing therapy for a lifetime, poses major problems, while the chances remain for continuous viral replication in reservoirs and compartments which may continually drive pathogenic disease processes (Finzi *et al.*, 1997; Finzi *et al.*, 1999).

Table 1.1 shows currently available antiretroviral (ARV) drugs used for the treatment of HIV infection (FDA: US Food and Drug Administration www.fda.gov).

Table 1.1: Currently available ARVs drugs for the treatment of HIV infection (FDA: United States Food and Drug Administration www.fda.gov). Highlighted drugs were used in this study.

ARV DRUG CLASS	ARV DRUG
Multi-class Combination Products	Atripla® efavirenz, emtricitabine & tenofovir disoproxil fumarate
	Complera® emtricitabine, rilpivirine, and tenofovir disoproxil fumarate
	Stribild® elvitegravir, cobicistat, emtricitabine, tenofovir disoproxil fumarate
Nucleoside Reverse Transcriptase Inhibitors (NRTIs)	Combivir® lamivudine and zidovudine; Emtriva® emtricitabine, FTC
	Epivir® lamivudine, 3TC, Epzicom® abacavir and lamivudine
	Hivid® zalcitabine, dideoxycytidine, ddC (no longer marketed)
	Retrovir® zidovudine, azidothymidine, AZT, ZDV
	Trizivir® abacavir, zidovudine, and lamivudine
	Truvada® tenofovir disoproxil fumarate and emtricitabine
	Videx EC® enteric coated didanosine, ddI EC; Videx® didanosine, dideoxyinosine, ddI
	Viread® tenofovir disoproxil fumarate, TDF; Zerit® stavudine, d4T; Ziagen® abacavir sulfate, ABC
non-Nucleoside Reverse Transcriptase Inhibitors (NNRTIs)	Intelence® etravirine; Rescriptor® delavirdine, DLV; Edurant® rilpivirine
	Sustiva® efavirenz, EFV; Viramune® nevirapine, NVP
Protease Inhibitors (PIs)	Agenerase® amprenavir, APV; Aptivus® tipranavir, TPV; Crixivan® indinavir, IDV
	Fortovase® saquinavir (no longer marketed); Invirase® saquinavir mesylate, SQV
	Kaletra® lopinavir and ritonavir, LPV/RTV
	Lexiva® Fosamprenavir Calcium, FOS-APV; Norvir® ritonavir, RTV
	Prezista® darunavir; Reyataz® atazanavir sulfate, ATV; Viracept® nelfinavir mesylate, NFV
Fusion Inhibitors	Fuzeon® enfuvirtide, T-20
Entry Inhibitors - CCR5 co-receptor antagonist	Selzentry® maraviroc
HIV integrase strand transfer inhibitors	Isentress® raltegravir; Tivicay® dolutegravir

1.1.1 Antiretroviral Drug Classes

Based on their mechanisms of action (De Clercq, 2005), antiretroviral constituent drugs can be divided into the following major classes:

Reverse transcriptase inhibitors (RTIs):

This class targets the construction of viral DNA and inhibits the activity of viral reverse transcriptase (De Clercq, 2005). There are two subcategories of RTIs based on different mechanisms of action: nucleoside analogue RTIs (NRTIs) and non-nucleoside-analogue RTIs (NNRTIs). NRTIs incorporate themselves into the viral DNA thus leading to chain termination, while NNRTIs alter the binding potential of the reverse transcriptase enzyme (De Clercq, 2005). RTIs can also be divided into three categories: Nucleoside analogue reverse transcriptase inhibitors (NARTIs or NRTIs), Nucleotide analogue reverse transcriptase inhibitors (NtARTIs or NtRTIs) and non-nucleoside reverse transcriptase inhibitors (NNRTIs).

The mechanism of action of NRTIs and NtRTIs are similar; these are equivalent to the naturally occurring deoxynucleotides used to synthesise the viral DNA. They compete with the naturally occurring deoxynucleotides to be incorporated into the elongating DNA chain of the Human Immunodeficiency Virus (Jochmans, 2008). Unlike the naturally occurring deoxynucleotides, however, NRTIs and NtRTIs lack a 3'-hydroxyl group on their deoxyribose moiety. Therefore, when an NRTI or an NtRTI is incorporated into the DNA, sequential formation of the next 5'-3' phosphodiester bond required to elongate the DNA chain is not present and therefore the DNA strand is terminated. This process is described as chain termination of viral DNA synthesis (Jochmans, 2008). While NRTIs and NtRTIs are described as competitive substrate inhibitors, NNRTIs, on the other hand, have a totally different mechanism of action. The NNRTIs are classified as non-competitive inhibitors of

the reverse transcriptase. They inhibit reverse transcriptase activity by binding at an alternate site on the enzyme different from the binding site of NRTIs and NtRTIs (De Clercq, 2005). Unlike NRTIs and NtRTIs, NNRTIs do not compete for incorporation into the viral DNA; rather they block the activity of protein domains of the reverse transcriptase required for the process of synthesising viral DNA (De Clercq, 2005).

Protease Inhibitors (PIs):

Protease inhibitors affect viral organisation by blocking the activity of HIV-1 protease, an enzyme utilised by HIV to split newly developing proteins required for assembling new virons (Richman, 2001). The HIV-1 protease is a complex enzyme comprising two similar halves with an active site positioned at the base of the cleft. In the final stages of the HIV life cycle, it is required for splitting of the larger viral precursor polypeptide chains into smaller, functional proteins, needed for maturing the HIV virion (Richman, 2001). HIV protease inhibitors particularly target the peptide bonds in the gag and gag-pol polyproteins which should be split by HIV-1 protease (Monini *et al.,* 2003). By inhibiting the HIV-1 protease, PIs structurally disorganise the virus, leading to the production of non-infectious viral particles (Monini *et al.,* 2003).

Fusion Inhibitors:

This class of drugs prevents the entrance of HIV into cells by blocking HIV from fusing with host cell membranes. HIV-1 needs the envelope glycoprotein complex (Env) to enter cells. The Env glycoprotein complex facilitates attachment to and eventually aids the fusion of HIV-1 to the membrane of host target cells (Eggink *et al.,* 2010). Env consist of three gp41 subunits necessary for membrane fusion. One of the currently approved fusion inhibitors, Enfuvirtide, is a peptide based on the gp41 sequence which competitively binds to gp41 and blocks the formation of the post-fusion structure (Eggink *et al.,* 2010).

Integrase Inhibitors:

This class of drugs inhibits the enzyme integrase, which is responsible for integrating viral DNA into the DNA of the infected cell. Integrating the reverse transcribed viral genome into host cell DNA represents an irreversible step during HIV infection (Messiaen *et al.*, 2013). This class of antiretroviral drugs targets the process of strand transfer while integration is taking place by binding in the catalytic core domain of the enzyme (Messiaen *et al.*, 2013).

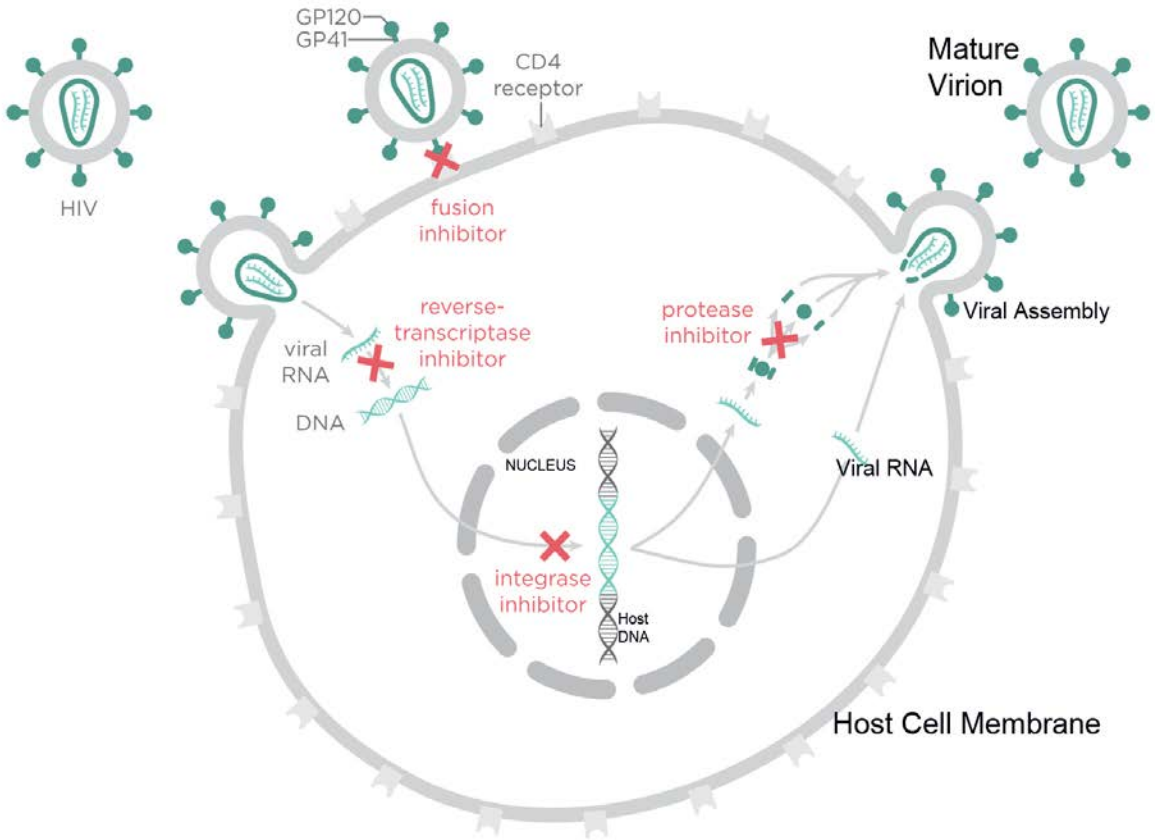

Figure 1.1: Schematic diagram of the HIV-1 life cycle in a susceptible $CD4^+$ cell identifying distinct steps in HIV-1 life cycle as current target for antiretroviral drugs (Adapted from Splettstoesser, 2013)

1.1.2 HAART and its Adverse Effects

The focus of the initial development of the antiretroviral drugs was on clinical effectiveness (lowering mortality) –all other considerations were secondary (Blas-Garcia *et al.,* 2010). However, as HIV infection and AIDS has been better managed, emphasis has shifted from the initial short-term considerations to the long-term undesirable or harmful effects induced by this treatment regimen (Blas-Garcia *et al.,* 2010). Continuous administration of the drugs in the cocktail has been associated with multiple adverse effects (Sikora *et al.,* 2010; Franzetti *et al*., 2013). For example, while NRTI drug combinations have provided improved anti-HIV therapy/prophylaxis, specific NRTIs are thought to be possible chemical carcinogens and mutagens (Olivero *et al.,* 1997; Blanche *et al.,* 1999; IARC 2000, Torres *et al.,* 2007) with their triphosphate derivatives inducing chain termination and cytotoxicity in healthy cells (Lewis *et al.,* 2001; Lewis *et al.,* 2003; Huber-Ruano and Pastor-Anglada, 2009).

Studies carried out on the effects of HAART with regards to the incidence and progression of HIV/AIDS associated cancers; non-Hodgkin's lymphoma, cervical cancer and Kaposi sarcoma, have provided contrasting data (Barbaro and Barbarini, 2007). While there has been a decrease in the incidence of Kaposi sarcoma, HAART has reportedly not had a significant impact on the incidence of the other two AIDS defining malignancies (Barbaro and Barbarini, 2007) - some evidence even suggests an increase in the incidence of these cancers (Engels *et al.,* 2008; Palefsky, 2009; Van der Burg and Palefsky, 2009).

On the other hand, it has been widely reported (Hessol *et al.,* 2007; Barbaro and Barbarini, 2007; Nguyen *et al.,* 2010) that the widespread use of HAART has increased the risk of non-AIDS defining malignancies (NADMs) including breast, kidney (Nguyen *et al.,* 2010), anal (Palefsky, 2009) and Hodgkin's lymphoma (Powles *et al.,* 2009).

In a review of the potential causes of the increased incidence of NADMs in the HAART era and also as a result of HAART use, Nguyen *et al.* (2010) lists as key factors, oncogenic viruses, (Epstein–Barr virus, Human papillomavirus, Hepatitis-B, Hepatitis-C), impaired immune surveillance, direct HIV-1 oncogenic effect, longer life expectancy associated with HAART (providing the longer latency period required for the development of certain malignancies) and other customary risk factors such as smoking, sun exposure, alcohol consumption, illicit drug use and genetic inheritance. Whether the antiretroviral compounds themselves are oncogenic is not clear (Powles *et al.,* 2009). Powles *et al.* (2009) reported that there may be an association between the use of NNRTIs and the development of non-AIDS defining malignancies, especially in Hodgkin's lymphoma.

Reports from *in vitro* studies confusingly suggest that the use of antiretroviral drugs could either lead to or potentially protect against the development of cancer (Olivero *et al.,* 2005; Gills *et al.,* 2007). This information, along with the evidence that the incidence of NADMs may be increasing (Powles *et al.,* 2009), has led to the opinion that HAART itself may have a negative effect on the risk of cancers (Franzetti *et al., 2013*). Assessing the correlation between the individual classes of ARV drugs and cancer risk becomes important because the oncogenic potential of different drug classes may be different (Olivero *et al.,* 2005; Gills *et al.,* 2007). Additionally, drugs within the cocktail may have effects on the DNA of host cells leading to genomic instability and carcinogenesis (Powles *et al.,* 2009). Studies by Torres *et al.* (2007) suggest that the improved chemoprotective effects of NRTI drug pairs used clinically may be associated with additive or synergistic phenomena that compound the long-term risk for cancer gene mutations and potential carcinogenesis.

A body of data (reviewed by Badley, 2005; Rizza and Badley, 2008) show that HIV PIs are anti-apoptotic, (which favours carcinogenesis) but the precise molecular mechanisms underlying these anti-apoptotic effects are still under active investigation *in vitro* and *in vivo*. Paradoxically, high-dose PIs have been shown to have pro-apoptotic effects, as demonstrated in implanted mouse models and transformed cell lines (Badley, 2005; Gills *et al.*, 2007).

The current work was designed to investigate the carcinogenic effects of some of the drugs in the South African HAART treatment guidelines individually and in combination on four human cell lines at clinically relevant concentrations. Recommended ARVs and combinations in South Africa include;

Emtriva® emtricitabine, FTC
Viread® tenofovir disoproxil fumarate, TDF
} (NRTIs)

Sustiva® efavirenz, EFV
} (NNRTI)

Kaletra® lopinavir and ritonavir, LPV/rtv
} (PIs)

1st Line: TDF + FTC/3TC + EFV ------- All new patients including pregnant women.

2nd Line: TDF + FTC/3TC + LPV/r –Protease Inhibitor based regimen. (2010 South African Antiretroviral Treatment Guidelines, Department of Health, RSA)

The normal and cancer cell lines of the breast and cervix used in this study were chosen as representations of AIDS-defining malignancies (Cervix) and non-AIDS-defining malignancies (Breast).

1.2 DRUGS

1.2.1 Tenofovir Disoproxil Fumarate (TDF)

VIREAD®, or generically, tenofovir disoproxil fumarate is a pro-drug of tenofovir which is a fumaric acid salt of bis-isopropoxycarbonyloxymethyl ester derivative of tenofovir. Tenofovir disoproxil fumarate (TDF) *in vivo* is converted to tenofovir, an acyclic nucleoside phosphonate (nucleotide) analog of adenosine 5'-monophosphate. Tenofovir acts against HIV-1 reverse transcriptase (Drug information, VIREAD® Gilead Sciences, 2010). The chemical name of tenofovir disoproxil fumarate is 9-[(*R*)-2[[bis[[(isopropoxycarbonyl)oxy]methoxy]phosphinyl]methoxy]propyl]adenine fumarate (1:1).

TDF has a molecular formula of $C_{19}H_{30}N_5O_{10}P \bullet C_4H_4O_4$ and a molecular weight of 635.52 (Drug information, VIREAD® Gilead Sciences, 2010). It is a nucleoside reverse transcriptase inhibitor widely used in the initial therapy for HIV-1 infection. It is orally administered to adults in a single daily dose of 300mg, which produces therapeutic plasma concentrations of up to $0.3 \pm 0.09\mu g/ml$ (Drug information, VIREAD® Gilead Sciences, 2010). Tenofovir is polar and ionized with poor oral bioavailability, so the disoproxil di-ester prodrug tenofovir disoproxil fumarate was produced to conceal the two ionic regions of the phosphonic acid, thereby enhancing transportation across gut membranes (Cihlar and Ray, 2010; Anderson *et al.*, 2011).

After the initial intestinal absorption, TDF is considered to be rapidly changed to a monoester by a carboxylesterase and then to tenofovir by a phosphodiesterase after passing through the liver and as such tenofovir becomes the predominant circulating compound (Naesens *et al.*, 1998; Kearney *et al.*, 2004).

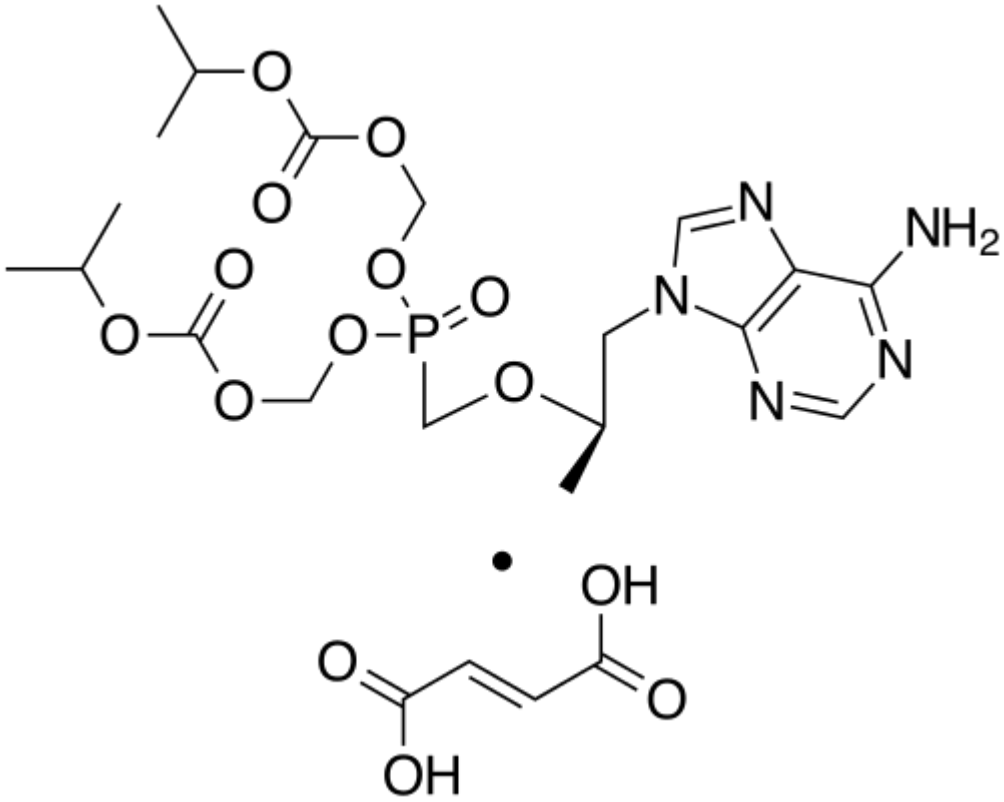

Figure 1.2: Two Dimensional structure of tenofovir disoproxil fumarate, a prodrug of tenofovir which is a nucleotide analog reverse transcriptase inhibitor (Drug information, VIREAD® Gilead Sciences, 2010)

The current South African practice guidelines recommend the use of TDF with one other NRTI and one NNRTI or one PI, thus potentially different combinations exist. Although regarded as a harmless drug, TDF-containing regimens have been linked to mutagenesis in the *in-vitro* mouse lymphoma assay (Drug information, VIREAD® Gilead Sciences, 2010), renal toxicity (Gitman *et al.*, 2007; Gilead sciences, 2010) glycosuria, proteinuria and calciuria (Drug information, VIREAD® Gilead Sciences, 2010).

1.2.2 Emtricitabine (FTC)

EMTRIVA® is the brand name for emtricitabine, a synthetic nucleoside analog with activity against human immunodeficiency virus type 1 (HIV-1) reverse transcriptase. The chemical name of emtricitabine is 5-fluoro-1-(2*R*,5*S*)-[2-(hydroxymethyl)-1,3-oxathiolan-5-yl]cytosine.

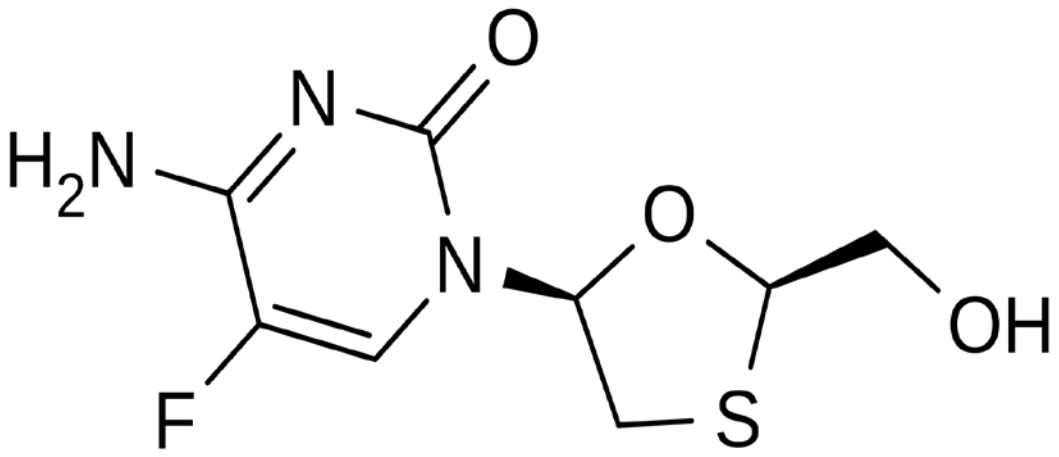

Figure 1.3: Two Dimensional structure of emtricitabine which is a nucleoside reverse transcriptase inhibitor (Drug information, EMTRIVA® Gilead Sciences, 2010).

Emtricitabine is the (-) enantiomer of a thio analog of cytidine, which differs from other cytidine analogues in that it has a fluorine in the 5-position of the benzene ring. It has a molecular formula of $C_8H_{10}F.N_3OS$ and a molecular weight of 247.24. Administering FTC to adults in a single daily dose of 200 mg produces therapeutic plasma concentrations of 1.8 ± 0.7μg/ml (Drug information, EMTRIVA® Gilead Sciences, 2010). FTC is associated with mitochondrial toxicity (Venhoff *et al.,* 2007), lactic acidosis and severe hepatomegaly with steatosis, even though the molecular pathways and cellular mechanisms remain largely unknown (Drug information, EMTRIVA® Gilead Sciences, 2010).

1.2.3 Efavirenz (EFV)

SUSTIVA® (efavirenz) is an HIV-1 specific, non-nucleoside reverse transcriptase inhibitor (NNRTI). The chemical name of Efavirenz is (S)-6-chloro-4 (cyclopropylethynyl)-1,4-dihydro-4-(trifluoromethyl)-2H-3,1-benzoxazin-2-one.

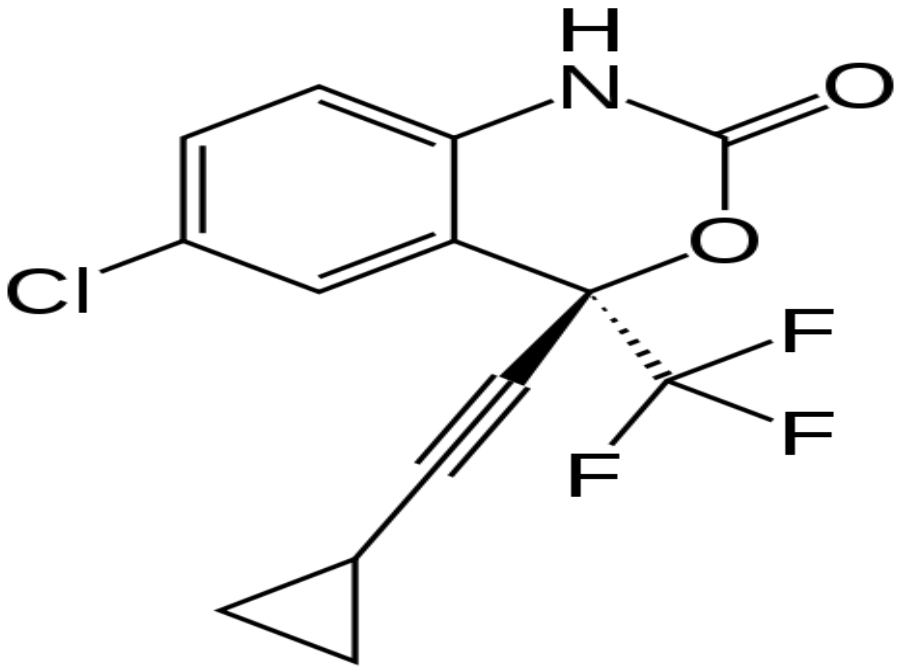

Figure 1.4: Two Dimensional structure of efavirenz; a non-nucleoside reverse transcriptase inhibitor (Fvasconcellos, 2008).

EFV has a molecular formula of $C_{14}H_9Cl.F_3NO_2$ and its molecular weight is 315.68 (Drug Information SUSTIVA® GILEAD SCIENCES 2010). It is utilised in the initial therapy for HIV-1. Administering EFV to adults in a single daily dose of 600 mg produces therapeutic plasma concentrations of up to 4.07±1.17μg/ml (Drug Information SUSTIVA® Gilead Sciences 2010). EFV containing regimens have been linked to lipid disturbances (Perez-Molina *et al.,* 2008) and hepatotoxicity (Blas-Garcia et al, 2010). Sikora *et al.* (2010) reported that EFV induces breast cancer cell growth by directly modulating oestrogen

receptors. Jover *et al.* (2004) suggest that an EFV based regimen is associated with breast enlargement.

1.2.4 LOPINAVIR/ritonavir (LPV/r)

LPV/r is a co-formulated boosted protease inhibitor marketed as KALETRA®. Lopinavir is an inhibitor of the HIV-1 protease while ritonavir inhibits the CYP3A-mediated metabolism of LPV, thereby providing increased plasma levels of LPV (Drug information, KALETRA® Abbott laboratories, 2010). LPV/r is considered to be a single antiretroviral agent because the levels of ritonavir achieved in plasma are subinhibitory and therefore the antiretroviral effect of the combination is based on the activity of lopinavir alone (Pierone *et al.*, 2006). Administering LPV/r to adults in a twice-daily dose of 400/100mg (or 800/200mg once daily) produces steady state plasma concentrations of 9.8$\pm$ 3.3 μg/ml (Drug information, KALETRA® Abbott laboratories, 2010).

The chemical name for Lopinavir is [1S-[1R*,(R*), 3R*, 4R*]]-N-[4-[[(2,6-dimethylphenoxy)acetyl]amino]3-hydroxy-5-phenyl-1-(phenylmethyl)pentyl]tetrahydro-alpha-(1-methylethyl)-2-oxo-1(2H)pyrimidineacetamide (Drug information, KALETRA® Abbott laboratories, 2010). Its molecular formula is $C_{37}H_{48}N_4O_5$, and its molecular weight is 628.80. Lopinavir is a white to light tan powder. It is freely soluble in methanol and ethanol, soluble in isopropanol and practically insoluble in water (Drug information, KALETRA® Abbott laboratories, 2010).

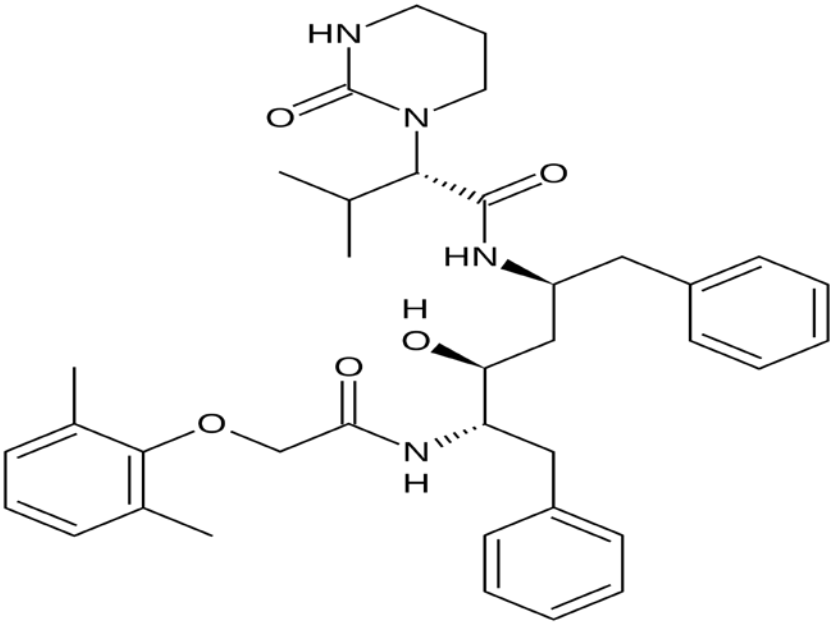

Figure 1.5: Two Dimensional structure of lopinavir; a protease inhibitor (Drug information, KALETRA® Abbott laboratories, 2010).

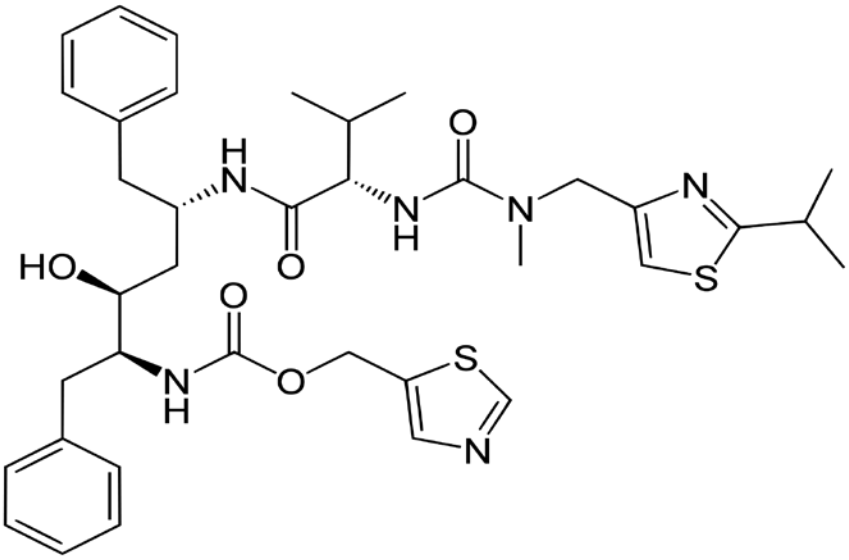

Figure 1.6: Two Dimensional structure of ritonavir; a protease inhibitor (Yikrazuul, 2008; Drug information, KALETRA® Abbott laboratories, 2010).

The chemical name for Ritonavir is 10-hydroxy-2-methyl-5-(1-methylethyl)-1- [2-(1-methylethyl)-4thiazolyl]-3,6-dioxo-8,11-bis(phenylmethyl)-2,4,7,12-tetraazatridecan-13-oic acid, 5-thiazolylmethyl ester, [5S-(5R*,8R*,10R*,11R*)]. Its molecular formula is $C_{37}H_{48}N_6O_5S_2$, and its molecular weight is 720.95. Ritonavir is a white to light tan powder and is insoluble in water.

Even though the absolute bioavailability of ritonavir had not been determined in humans at the beginning of this study and until now (Drug information, NORVIR® Abbott laboratories, 2013), across studies, administration of Kaletra® 400/100mg daily yields mean steady-state lopinavir plasma concentrations 15 to 20 times higher than those of ritonavir in HIV-1 patients (Drug information, KALETRA® Abbott laboratories, 2010). LPV/r at doses 0.5 times the human exposure in male rats results in the occurrence of hepatocellular adenoma and carcinoma (Drug information, KALETRA® Abbott laboratories, 2010). It has also been associated with the onset of diabetes or the aggravation of pre-existing diabetes (Drug information, KALETRA® Abbott laboratories, 2010).

1.2.5 Camptothecin

Camptothecin (CPT), a cytotoxic plant alkaloid compound (Fig. 1.7) obtained from the bark of the Chinese tree *Camptotheca acuminate*, was originally observed to impede leukaemia cell growth (Wall *et al.*, 1966). The chemical name of CPT is (*S*)-4-ethyl-4-hydroxy-1*H* pyrano[3',4':6,7]indolizino[1,2-b] quinoline-3,14-(4*H*,12*H*)-dione. CPT molecular Formula is C20H16N2O4 and its molecular weight is 348.4 (Product Information Camptothecin, Sigma, 2012).

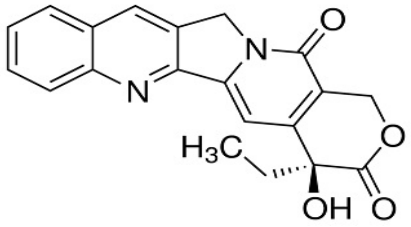

Figure 1.7: Two Dimensional structure of Camptothecin, a cytotoxic plant alkaloid compound (Product Information **(S)-(+)-**Camptothecin, Sigma, 2012).

CPT is a class I DNA topoisomerase inhibitor that reversibly induces single-strand DNA breaks, and as a result altering the replication capacity of the cell. Camptothecin binds to and stabilises the topoisomerase 1/DNA complex (Legarza and Yang, 2006). These topoisomerase-linked DNA strand breaks are rescindable pre-lethal lesions that inhibit DNA metabolism (Bertrand *et al.,* 1991; Pommier, 1997). But, when a DNA replication fork comes into contact with the cleavable complex, single-strand breaks are transformed to irreversible double-strand breaks (Hsiang *et al.,* 1985; 1989). Then, apoptosis is facilitated by the activation of caspases (Sanchez-Alcazar *et al.,* 2000).

In this study, CPT was used to induce apoptosis as has been widely reported (Nieves-Neira and Pommier, 1999; Rastogi *et al.,* 2006; Rudolf *et al.,* 2011). This was done so as to determine whether the protease inhibitors inhibit drug induced apoptosis in the cervical and breast cell lines since it had been reported (Phenix et al, 2001, Badley, 2005, Vlahakis *et al.,* 2007, Rizza and Badley, 2008) that protease inhibitors have potent anti-apoptotic effects in different cellular systems, the majority of which are immune cells. The anti-apoptotic effect of LPV/r was assessed to test whether these generalised effects are seen in the currently investigated cell lines.

1.3.1 Carcinogenesis

Carcinogenesis has been established as a multistep process with a large number of molecular events responsible for the initiation and progression of many human tumours (Grizzi and Chiriva-Internati, 2006). The detection of genomic modifications or changes that produce oncogenes with an assertive gain of function and tumour-suppressor genes with a suppressed loss of function has been important in this regard (Grizzi and Chiriva-Internati 2006). Results from numerous studies reveal that cancerous cells have a mutual collection of characteristics or "acquired capabilities" that function and are regulated at diverse multi-dimensional and progressive scales (Grizzi and Chiriva-Internati 2006; Wickstrom *et al.,* 2010).

These include the ability to create their own mitogenic signals, resist exogenous growth-restraining signals, elude programmed cell death and senescence, multiply endlessly, develop vasculature, and invade and metastasise in distant sites (Grizzi and Chiriva-Internati 2006). Carcinogenesis requires more than one mutation in a number of genes that control cell division, DNA repair and apoptosis (Wickstrom *et al.,* 2010). Non-mutagenic carcinogens are believed to encourage cancer initialisation by stimulating high rates of cell division, which often result in high error rates with regard to the inherent DNA repair mechanisms (Wickstrom *et al.,* 2010).

1.3.1.1 Carcinogenicity and Genotoxicity Reports on NRTIs

It has been shown that 7 out of 8 nucleoside reverse transcriptase inhibitors tested positive in one or more genotoxicity assays (except FTC). Abacavir, stavudine, tenofovir, zalcitabine, and zidovudine were shown to be rodent carcinogens (NTP, 1999) and tested positive in genotoxicity assays, including the *in vitro* human lymphocyte or mouse lymphoma assays. Zidovudine was positive in the Ames (bacterial reverse mutagenicity),

in vivo micronucleus, and *in vitro* hamster ovary cells assays (Wu *et al.,* 2012). All these corroborate the opinion that NRTIs, which are nucleoside analogues, are possibly genotoxic, while operating as chain terminators or through modification of the nucleotide pool (Wu *et al.,* 2012). Didanosine and lamivudine tested negative for carcinogenicity but tested positive for genotoxicity (NTP, 1999). This implies that genotoxicity data cannot be relied upon exclusively to predict tumorigenicity for this subclass of drugs (Wu *et al.,* 2012). Emtricitabine is the only NRTI that tested negative for both genotoxicity and carcinogenicity (NTP, 1999; Wu *et al.,* 2012). Zidovudine reportedly produced distinctive malignant vaginal tumors in both adult rats and mice (NTP, 1999) and also demonstrated transplacental carcinogenicity in pregnant mice; showing an increased tumor rate in the female reproductive tracts of the mice offspring (NTP, 1999).

1.3.1.2 Carcinogenicity and Genotoxicity Reports on NNRTIs.

NNRTIs have not been shown to be positive in genotoxicity assays, irrespective of their DNA synthesis chain termination properties. This has been attributed to the characteristics of NNRTIs non-competitive (versus NRTIs' competitive) inhibition of nucleoside phosphorylation (Wu *et al.,* 2012). In spite of the negative genotoxicity data, all NNRTIs are reportedly rodent carcinogens (delavirdine, etravirine, rilpivirine, efavirenz and nevirapine); all producing hepatocellular adenoma/carcinoma. Tumors of the lung and urinary bladder were also observed for efavirenz and delavirdine respectively (Wu *et al.,* 2012).

1.3.1.3 Carcinogenicity and Genotoxicity Reports on Protease Inhibitors.

With regards to PIs, nine out of ten have been shown to be carcinogenic in animals, including atazanavir, amprenavir, fosamprenavir, daurunavir, lopinavir, indinavir, tipranavir, nelfinavir and ritonavir (NTP, 1999; Wu *et al.,* 2012). Saquinavir was the only

PI that was not linked with carcinogenesis in rodents and among all PIs, atazanavir was the only agent that was genotoxic (tested positive by chromosomal aberration assay) (NTP, 1999; Wu *et al.,* 2012).

1.3.2 Breast Cancer

Breast cancer is the most common cancer seen in women worldwide (Oluwole *et al.,* 2005). Although HIV/AIDS is involved in carcinogenesis of some cancers, it has not been shown to cause breast cancer (Oluwole *et al.,* 2005). Some studies have reported the occurrence of breast cancer in young infected patients. Interestingly, the detected breast cancers demonstrate unusual characteristics when compared to breast cancer in uninfected patients. These unusual characteristics include poor differentiation, occurrence of metastasis at an earlier stage, poor prognosis and more ‘‘aggressiveness’’ (Voutsadakis and Silverman, 2002; Pantanowitz and Connolly, 2002; Oluwole, 2005). The acquired immunodeficiency syndrome that results from HIV infection weakens the immune system and therefore increases the chances of opportunistic infections and development of various cancers, including breast neoplasm (Pantanowitz and Connolly, 2002). It was suggested that malignancies, like breast cancer, will concurrently increase in HIV infected patients (Hajjar *et al*., 1992; Spina *et al*., 1994; Patil *et al*., 1995); however, this opinion is opposed by some authors who do not consider HIV to have a significant effect on the occurrence of breast cancer (Klassen *et al.,* 1997; Cooksley *et al.,* 1999; Silverberg and Abrams, 2007; Andrade *et al.,* 2011).

The occurrence of breast cancer in HIV infected patients was found to be increased in African and developing countries (Pantanowitz and Connolly, 2002). The vulnerability to malignant neoplasm is high in HIV infected people as a result of suppression of immunologic reaction to tumour cells and higher chances of oncogenic viral infections

(Pantanowitz and Connolly, 2002). HIV has been shown to have adverse effects on normal human mammary epithelial cells by inhibiting their growth (Pantanowitz and Connolly, 2002). However, HIV infected patients on antiretroviral treatment have a longer survival due to the treatment and therefore are at danger of developing breast cancer because its risk increases with age (Clay *et al.,* 2008; Phillips and Justman, 2009). Other studies suggest that the use of ARV drugs that prevent the wasting condition caused by AIDS might increase breast cancer risk by fat re-distribution from peripheral and gluteal tissues to the breast and abdomen as a result of increased production of oestrogen (Oluwole *et al.,* 2005; Sikora *et al.,* 2010). The total influence of HAART on the risk for NADM is far from concluded. In a recent meta-analysis (Shiels *et al.,* 2009), the standardized incidence ratio (SIR) of some NADMs including breast cancer, was substantially discrete prior to and in the HAART era. A Swiss HIV Cohort Study, a mega prospective cohort of people tracked for an average of 5 years after HAART, revealed no definite influence of HAART on SIRs of NADMs (Clifford *et al.,* 2005). However, another HIV/AIDS meta-analysis on a cohort conducted in England (Powles *et al.,* 2009), showed that a substantial total rise in the risk for NADMs accompanied HAART treatment. Non AIDS-defining cancers now generally account for more deaths in HIV infected individuals than AIDS defining cancers. Although traditional risk factors may account for part of this discrepancy, they certainly do not provide all the explanation for the explosion of these cancers in HIV affected people on HAART (Silverberg and Abrams, 2007). Engels *et al.* (2008) found that non-AIDS defining cancers comprise 58% of all cancer deaths post-HAART (1996-2002) in comparison to 31.4% in the pre-HAART era (1991-1995). This data strongly suggests that antiretroviral drugs influence cancer development and progression.

1.3.3 Cervical Cancer

Cervical cancer is aetiologically linked to the human papilloma virus and considered to be the second most malignant tumour globally (Stamataki *et al.,* 2010). South Africa is reported to have the highest incidence of cervical cancer in the world and is the most common cancer in coloured and black South African women (Denny, 2006; Gaym *et al.,* 2007). Cervical cancer, Kaposi sarcoma and non-Hodgkin's lymphoma are AIDS defining cancers (Barbaro and Barbarini, 2007, Engels *et al.,* 2008). The incidence of Kaposi sarcoma and non-Hodgkin's lymphoma have been reportedly reduced by HAART, the incidence of cervical cancer; however, is not declining and some evidence suggests that the incidence may even be increasing (Engels *et al.*, 2008; Palefsky, 2009; Van der Burg and Palefsky, 2009).

The institution of the combined antiretroviral therapy in 1996 (Dal Maso *et al.*, 2009) resulted in significant enhancement of clinical aftermaths and life prospect for individuals living with HIV/AIDS. It also provided the optimism that the enhanced immunological condition seen in the patients would lead to the elimination of human papilloma virus (HPV) infection in HIV-infected women, just as is the case for other opportunistic and AIDS-related infections, and lead to a significant decline in the occurrence and advancement of cervical neoplasia (Heard, 2009). However, a review (Bratcher and Sahasrabuddhe, 2010) of data from numerous studies has not shown a definite reduction in the problem and gravity of cervical disease since the beginning of HAART, as opposed to the other AIDS-associated cancers. Bratcher and Sahasrabuddhe (2010) reported that while the majority of published literature suggested that being on HAART has not caused a decline in the occurrence of cervical precancerous lesions and cervical intraepithelial

neoplasia in HIV-infected women, other studies found an increased chance in the post-HAART era.

1.4 Apoptosis and Regulatory genes

Apoptosis (programmed cell death) is a critical process that is dysregulated during tumourigenesis (Fiebig *et al.,* 2006). In many cancers, there is a consistent pattern of apoptosis inhibition and deregulation of cell and tissue homeostasis. There is a growing body of literature implicating apoptosis-related genes and their products in the development of cancer (Fiebig *et al.,* 2006; Eum and Lee, 2011).
The induction of apoptosis occurs via two major pathways: The extrinsic (death receptor) pathway and the intrinsic (mitochondria) pathway (Eum and Lee, 2011).

The extrinsic pathway is activated by the attachment of the FAS plasma-membrane death receptor (and related receptors like tumour necrosis receptor 1 and its family) to its extracellular ligand, FAS-L. When death stimuli take place, FAS-L binds to FAS and forms the death complex (Eum and Lee, 2011). The FAS/FAS-L complex enlists death domain-containing protein (FADD) and pro-caspase-8, which together forms the death-inducing signalling complex (DISC). Consequently, the protein complex activates its pro-caspase-8, which proceeds to trigger pro-caspase-3, the second to last enzyme for execution of the apoptotic process (Ouyang *et al.,* 2012).

The intrinsic pathway also leads to apoptosis but under the control of mitochondrial pro-enzymes. Most cell death in vertebrates occurs via the mitochondrial pathway of apoptosis (Llambi and Green, 2011). This pathway is controlled by the B-cell CLL/lymphoma 2 (BCL-2) family of proteins and they regulate the integrity of the mitochondrial outer membrane. When apoptosis arises as a result of cooperation among these proteins, the two

pro-death BCL-2 effector proteins: BCL-2-associated X protein (BAX) and BCL-2 antagonistic killer (BAK), disrupt the mitochondrial outer membrane in a process known as 'mitochondrial outer membrane permeabilisation' (MOMP) (Llambi and Green, 2011). If MOMP takes place, proteins located in the mitochondrial inter-membrane compartment enter the cytosol and activate caspases and cysteine proteases that coordinate the disassembling of the cell (Llambi and Green, 2011). If these caspase proteases are inhibited or their activation is hindered, apoptosis can still take place by disruption of mitochondrial performance (mitochondrial catastrophe). However, if a small number of mitochondria remain and divide to repopulate the cytoplasm, the cell can continue glycolysis and the cells may still survive (Llambi and Green, 2011). These phenomena may provide explanation as to why cancer cells usually exhibit malfunctions in the mitochondrial pathway downstream of MOMP (Llambi and Green, 2011). The process of MOMP is opposed by the pro-survival BCL-2 proteins, such as BCL-2, BCL-W, BCL-xL, A1/Bfl1 and MCL-1, which impede the capacity of BAX and BAK to permeabilise the outer mitochondrial membrane. The relevance of this process in cancer is highlighted by the remark that oncogenes, like *MYC*, which promotes proliferation, also promote cell death that is inhibited by the anti-apoptotic BCL-2 proteins (Llambi and Green, 2011).

The widely studied genes associated with apoptosis include *BCL-2*; the anti-apoptotic gene and *BAX*; a pro-apoptotic gene (Sjostrom and Bergh, 2001). Hypothetically, *BCL-2* over-expression renders a survival advantage for cancer cells; in contrast, an *in vivo* study has shown that expression of *BCL-2* was linked to a better prognosis in malignant diseases (Sjostrom and Bergh, 2001). For example in breast cancer, tumours expressing *BCL-2* were found to have oestrogen receptors and resulted in a better prognosis, therefore oestrogen has been suggested to be an up-regulator of *BCL-2* (Sjostrom and Bergh, 2001).

The BCL-2 protein is encoded by a gene which is triggered by the translocation of chromosomes in human follicular lymphomas (Gee *et al.,* 1994). This translocation is a cytogenetic defect of chromosomes and it overlaps the *BCL-2* gene with the immunoglobulin heavy chain locus, resulting in the over-expression of the BCL-2 protein (Gee *et al.,* 1994). BCL-2 occupies various locations within the cell including the inner mitochondrial membrane, the endoplasmic reticulum and the nuclear envelope (Gee *et al.,* 1994). The BCL-2 protein has two forms; an alpha 26KDa form or a beta 22KDa form. The process of programmed cell death is blocked by the BCL-2 alpha protein (Gee *et al.,* 1994). The alpha protein has also been reported to alter the cytotoxicity of some anticancer agents by preventing apoptosis from occurring (Gee *et al.,* 1994). The expression of BCL-2 can increase the life span of a cell, therefore increasing the likelihood of various genetic abnormalities (Gee *et al.,* 1994).

BAX is the most well studied member of the BCL-2 family with regards to its role in cancer and it serves as a key pro-apoptotic protein (Sjostrom and Bergh, 2001; Roucou *et al.,* 2005). BAX is located in the cytosol or found lightly affixed to the mitochondrial outer membrane (Roucou *et al.,* 2005). When the cell is exposed to a pro-apoptotic stimulus, BAX is translocated into the mitochondria from the cytosol. Once in place, it exposes its N-terminal domain by changing conformation and thereby forms an oligomer at the mitochondria (Roucou *et al.,* 2005). The translocation of BAX to the mitochondria results in the discharge of apoptogenic proteins exclusively found in the mitochondria; such as cytochrome c, endonuclease G, SMAC/DIABLO, Htr2/ Omi and AIF, initiating the caspase-dependent and independent pathways for apoptosis (Roucou *et al.,* 2005). BAX stimulation restores sensitivity to apoptosis induced by drugs or radiation. In contrast, its

over expression has the opposite effect in that it suppresses apoptosis (Sjostrom and Bergh, 2001).

1.5 Angiogenesis and Regulatory Genes

Angiogenesis, the formation of new blood vessels from pre-existing vasculature, is required for cancer growth and development. It is the growth and multiplication of a system of blood vessels that invades tumors, supplying nutrients and oxygen serving to remove wastes (Bates *et al.,* 2002). Tumor angiogenesis begins when cancer cells release factors that convey signals to neighbouring normal host cells and tissue. This process triggers specific genes in the host cells that consecutively synthesise proteins that promote the development of new blood vessels (Bates *et al.,* 2002).

The creation of new blood vessels is a complicated process that involves more than 50 co-dependent growth factors, cytokines, enzymes and receptors (Carmeliet, 2000), and several of them are from the vascular endothelial growth factor A (VEGFA), angiopoietin and ephrin families. The VEGF family performs important functions in vasculogenesis, angiogenesis and lymphangiogenesis. There are five members of the human VEGF family: VEGF (or VEGF-A), VEGF-B, VEGF-C, VEGF-D, and placental growth factor (PlGF) (Olofsson *et al.,* 1996; Joukov *et al.,* 1996; Achen *et al.,* 1998; Ferrara, 2004; Hoeben *et al.,* 2004). Alternative gene splicing of the respective human *VEGF* pre-mRNAs produces several isoforms of each gene. The VEGFA family of ligands have three receptor protein-tyrosine kinases (VEGFR1, VEGFR2, and VEGFR3) and two non-enzymatic receptors (neuropilin-1 and -2) (Roskoski, 2007). Many ligands of the VEGF family also attach to heparan sulphate proteoglycans that are located on the plasma membrane and the extracellular matrix (Roskoski, 2007). Binding sites for the *VEGF* gene were identified on vascular endothelial cells (Plouet and Moukadiri 1990; Vaisman *et al.,* 1990),

corresponding to VEGFR1 (Flt-1) (Shibuya *et al.,* 1990) and VEGFR2 (Flk-1/KDR) (Matthews *et al.,* 1991; Terman *et al.,* 1991; Terman *et al.,* 1992). Their presence on endothelial cells is responsible for *VEGF* specificity. VEGF-C and VEGF-D are bound by VEGFR3 (Flt-4) (Pajusola *et al.,* 1992), from the same receptor family.

VEGFA signalling denotes a complex but crucial rate-limiting phase in angiogenesis and as a result is the subject of concentrated research (Nowak *et al.,* 2008). The *VEGFA* gene consists of 8 exons set apart by 7 introns and spans 14 kilo bases (Houck *et al.,* 1991). *VEGF* pre-mRNA is differently spliced to generate mRNAs that encode about 12 isoforms that have been researched widely, some possessing pro-angiogenic and others possessing anti-angiogenic properties (Perrin *et al.,* 2005). One of the isoforms is $VEGF_{165}$, with 165 amino acids in its complete structure. However, recent evidence indicates that 2 families of VEGF proteins are formed by alternative splice-acceptor-site assortment in the 3′ untranslated region (UTR) within the terminal exon 8 to give 2 different C-terminal sequences that differ in only 6 amino acids (Bates *et al.,* 2002, Qiu *et al.,* 2009).

Proximal splice-acceptor-site selection in exon 8 results in classic proangiogenic $VEGF_{xxx}$ isoforms that contain the exon 8a sequence, whereas distal splice-acceptor-site selection produces anti-angiogenic $VEGF_{xxx}b$ isoforms that contain the exon 8b sequence (with xxx denoting the number of amino acids) (Qiu *et al.,* 2009). The proangiogenic isoforms encode a terminal 6–amino acid sequence of Cys-Asp-Lys-Pro-Arg-Arg, while the anti-angiogenic isoforms encode Ser-Leu-Thr-Arg-Lys-Asp. The most widely studied $VEGF_{xxx}b$ isoform is $VEGF_{165b}$, but other isoforms have also been identified at both the mRNA and protein levels (Qiu *et al.,* 2009). There is extensive expression of the $VEGF_{165b}$ transcript and protein in the majority of normal human tissues and in nonangiogenic

tissues. In contrast to the other VEGF isoforms, $VEGF_{165b}$ expression is reduced in angiogenic conditions, such as renal, prostate, colon, and skin cancers and proliferative diabetic retinopathy (Bates *et al.,* 2002; Perrin *et al.,* 2005). On the other hand, in nonangiogenic pathological conditions, like glaucoma, the anti-angiogenic $VEGF_{xxx}b$ isoforms are upregulated (Ergorul *et al.,* 2008). $VEGF_{165}b$ protein was reported to substantially and dose proportionally block $VEGF_{165}$-induced multiplication and movement of endothelial cells, vasodilation of mesenteric arteries, and angiogenesis in 2 separate prototypes of $VEGF_{165}$-induced vascular growth (Woolard *et al.,* 2004). $VEGF_{165b}$ has dimerisation and receptor-binding regions; therefore, it functions as a competitive inhibitor of $VEGF_{165}$; such that it binds to the receptor but fails to trigger the complete tyrosine phosphorylation of VEGF Receptor-2 and the subsequent signaling provoked by $VEGF_{165}$ (Woolard *et al.,* 2004). *$VEGF_{165b}$* therefore seems to be an intrinsic anti-angiogenic agent produced by alternate splicing. Reports indicate that the control of alternative splicing by growth and splicing factors represents an important step in influencing the comparative expression of proangiogenic versus anti-angiogenic VEGF isoforms (Nowak *et al.,* 2008; Qiu *et al.,* 2009; Rennel *et al.,* 2009).

Since the amino acid configuration of anti-angiogenic $VEGF_{165b}$ is 95% to 96% similar to that of $VEGF_{165a}$ (Woolard *et al.,* 2004; Qiu *et al.,* 2009), the majority of past studies that have investigated VEGF expression could not differentiate between these proangiogenic and anti-angiogenic VEGF isoforms. It is noted that the majority of these studies were conducted before the discovery of anti-angiogenic VEGF isoforms or used *in situ* hybridisation riboprobes, antibodies, and ELISAs that detect both $VEGF_{165a}$ and $VEGF_{165}b$ isoforms (Manetti *et al.,* 2011). One of the aims of the present study, therefore, was to investigate whether the expression of *VEGF* splice variants (*$VEGF_{165a}$* and

VEGF$_{165b}$) could be altered in breast and cervical cell lines exposed to different classes of antiretroviral drugs, individually and in combination.

1.6 STUDY OBJECTIVES

1.6.1 Broad Objectives

To determine the effects of some of the antiretroviral drugs (included in the 2010 South African Antiretroviral Treatment Guidelines), individually and in combination, on apoptosis and on the expression of apoptotic and angiogenic genes such as *BCL-2*-associated X protein (BAX), B-cell CLL/lymphoma 2 (*BCL-2*), vascular endothelial growth factor A (*VEGFA*), transcript variant 4 (*VEGF*$_{165a}$) and vascular endothelial growth factor A (*VEGFA*), transcript variant 7 (*VEGF*$_{165b}$) in normal and cancer human breast and cervical cell lines. This study looks at two cancers which are relevant in women living with HIV/AIDS. Cervical cancer; an AIDS associated cancer and breast cancer; a cancer commonly found in AIDS patients in the HAART era.

1.6.2 Specific Objectives

1. To assess the cytotoxicity of TDF, FTC, EFV and LPV/r (individually and at clinically relevant combinations) in normal and cancer cell lines of the breast and cervix at clinically relevant concentrations of the drugs and at different time points – 24, 48, 72 and 96 hours employing the Neutral Red Toxicology/Viability Assay.

2. To assess the effects of each of the drugs at clinically relevant concentrations on mRNA expression of *BAX*, *BCL-2*, *VEGF*$_{165a}$ and *VEGF*$_{165b}$ in each of the cell lines utilising Real Time Polymerase Chain Reaction (qPCR).

3. To assess the extent to which combinations of TDF/FTC/EFV; LPV/r and TDF/FTC/LPV/r alter the mRNA expression of *BAX*, *BCL-2*, $VEGF_{165a}$ and $VEGF_{165b}$ in each of the cell lines employing qPCR.

4. To investigate the extent to which each of the drugs (at clinically relevant concentrations) alter protein localisation of BAX, BCL-2 and $VEGF_{165b}$ in each of the cell lines, employing confocal microscopy on immunofluorescence. Fluorescence intensities reflecting protein quantities will be measured.

5. To investigate the extent to which combinations of TDF/FTC/EFV; LPV/r and TDF/FTC/LPV/r affect protein localisation of BAX, BCL-2 and $VEGF_{165b}$ in each of the cell lines employing confocal microscopy on immunofluorescence.

6. To determine whether the Protease Inhibitors LPV/r inhibit drug induced apoptosis in all four cell lines employing the Acridine Orange staining for the morphological evaluation of apoptotic cells and the Cell Death Detection Enzyme Linked Immunosorbent assay (ELISA) for the quantification of internucleosomal DNA fragmentation - an important hallmark of apoptosis.

1.7 Anticipated Outcome

It was projected that completion of the aforementioned specific aims would provide a comparative and comprehensive evaluation of the effects of tenofovir disoproxil fumarate, efavirenz, emtricitabine and lopinavir/ritonavir (individually and in combination) on apoptosis, apoptotic and angiogenic gene expression, which could indicate the potential for carcinogenesis. Insights gained from the experiments might lead to intervention strategies to attenuate oncogenicity without altering drug efficacy, thus improving the quality of life of HIV/AIDS patients that are mainly women in this instance.

CHAPTER 2: MATERIALS AND METHODS

2.1 Kits, Antibodies and reagents

The Neutral Red TOX-4 kit, Methanol, Acridine orange (AO), ethylenediamine-tetraacetic acid (EDTA) and Camptothecin (CPT) were purchased from Sigma Chemical Co. (St. Louis, MO, USA). Rabbit polyclonal anti-BAX antibody and mouse monoclonal anti-BCL-2 were purchased from DAKO (DK-2600 Glostrup, Denmark). Primary antibodies-polyclonal rabbit anti-human $VEGF_{165b}$ and secondary antibodies-goat anti rabbit Rhodamine conjugated and goat anti mouse FITC conjugated were purchased from ABCAM (Cambridge, UK). The GeneJET RNA Purification kit, DNase I, RNase-free kit and O'GeneRuler Low Range DNA Ladder were purchased from Thermo Scientific (Pittsburgh PA. USA). High Capacity cDNA Reverse Transcription Kit and Power SYBR® Green PCR Master Mix were purchased from Life Technologies (CA, USA). Oligos for qPCR were purchased from Integrated DNA Technologies, Inc. (Coralville, Iowa, USA). Agarose D-1 Low EEO-GQT was purchased from Conda Laboratories (Madrid, Spain).

2.2.1 Cells

Human squamous cell carcinoma cells (HCS-2) from the uterine cervix (Japanese Collection of Research Bio-resources, JCRB, Cell Bank) were cultured in Eagle's Minimal Essential Medium (EMEM) (Lonza, Verviers, Belgium) supplemented with 15% fetal calf serum (FCS) (Gibco, Germany) together with L-Glutamine (Gibco, Germany).

Transformed normal human cervical cells (NCE16IIA) (Japanese Collection of Research Bio-resources, JCRB, Cell Bank) were cultured in Keratinocyte Basal Medium KBM-GOLD (Lonza, Walkersville, MD USA) supplemented with human recombinant epidermal

growth factor, transferrin, hydrocortisone, epinephrine, insulin and bovine pituitary extract (Lonza, Walkersville, MD USA).

Human breast carcinoma MCF-7 cells (American Type Culture Collection Rockville, MD, USA) were cultured in DMEM medium (Gibco, MD, USA) containing 10% fetal bovine serum (Gibco, MD, USA).

Immortalized human breast epithelial cells, MCF-10A (American Type Culture Collection Rockville, MD, USA) were cultured in Mammary Epithelium Growth Medium (MEGM) (Lonza, Walkersville, MD USA) containing human recombinant epidermal growth factor, hydrocortisone, insulin and bovine pituitary extract (Lonza, MD, USA).

2.2.2 Cell Culture

Cells were propagated and sub-cultured according to supplier's instructions, available at;

http://cellbank.nibio.go.jp/~cellbank/en/search_res_det.cgi?ID=5979 (for HCS-2 cells)

http://cellbank.nibio.go.jp/~cellbank/en/search_res_det.cgi?ID=3303 (for NCE16IIA cells)

www.atcc.org/products/all/HTB-22.aspx (for MCF-7 cells)

www.atcc.org/en/Global/Products/1/6/3/A/CRL-10317.aspx (for MCF-10A cells). All cell data sheets are included in Appendix A3.

Briefly, cells were cultivated as a stationary monolayer in plastic tissue-culture dishes (Nunclon, Denmark) and were incubated at 37°C in a 5% CO_2 humidified environment. Cells were grown to 70-80% confluence and washed with 1X 0.1 M phosphate buffered saline (PBS) (Sigma, St. Louis, MO, USA) pH 7.4 and trypsinized with 2 ml of Trypsin-EDTA (Sigma, St. Louis, MO, USA). Following detachment, serum containing medium was added to deactivate the trypsin followed by centrifugation at the recommended rpm for each cell line in a Hermle Z400 centrifuge (HERMLE Labortechnik GmbH, Wehingen,

Germany), for 5 minutes. The supernatant was discarded and the cells were re-suspended in the appropriate culture media or freezing media for subculturing or storage respectively. Cells were stored at -80°C.

2.2.2.1 Pre-treatment culture conditions

The normal MCF-10A and NCE16IIA cells were cultured in serum-free media. MCF-7 and HCS-2 cells were synchronised by serum starvation for 24 hours (Razandi *et al.,* 2003; Pan *et al.,* 2006) prior to all experiments. After being cultured in complete medium for overnight attachment, MCF-7 and HCS-2 cells were incubated with serum-free media for 24 hours. The cells were then treated with the antiretroviral drugs (as described below; Table 2.2) in medium supplemented with serum for the indicated periods.

2.3.1 Drugs

Emtricitabine (FTC), tenofovir disoproxil fumarate (TDF), efavirenz (EFV), lopinavir (LPV) and ritonavir (RTV) were purchased from Toronto Research Chemicals (Toronto, Ontario. Canada). FTC and TDF were dissolved in distilled water, while EFV, LPV and RTV were dissolved in methanol (appropriate diluents obtained from the certificate of analysis for each drug; Toronto Research Chemicals, Toronto, Canada).

2.3.2 Stock Solutions of Antiretroviral Drugs

Stock solutions of the antiretroviral drugs used in this study were prepared as follows; 0.6mg TDF and 3.6mg FTC were weighed and dissolved in 1ml autoclaved distilled water. 40.7mg EFV, 98mg LPV and 6mg RTV were weighed and dissolved in 1ml methanol (appropriate diluents obtained from the certificate of analysis for each drug; Toronto Research Chemicals, Toronto, Canada). Table 2.1 shows the volume of stock concentrations added to the growth media to obtain the final concentrations and the final

diluent concentration. All drugs were kept frozen in stock solutions and were diluted to the required concentrations in the appropriate growth media (Section 2.2.1) before use.

Table 2.1: Preparation of stock and final concentrations of ARVs added to the cells

Drug	Original Stock Solution	Volume of stock added (µl)	Volume of Growth Medium added (µl)	2x concentration µg/ml	Final concentration added to cells µg/ml	% of diluent added to cells
TDF	0.6mg/ml dH_2O	10	9990	0.6 µg/ml	0.3 µg/ml	-
FTC	3.6mg/ml dH_2O	10	9990	3.6 µg/ml	1.8 µg/ml	-
EFV	40.7mg/ml meth	10	49990	8.14 µg/ml	4.07 µg/ml	0.01% meth
LPV	98mg/ml meth	10	49990	19.6 µg/ml	9.8 µg/ml	0.01% meth
RTV	6mg/ml meth	10	49990	1.2 µg/ml	0.6 µg/ml	0.01% meth

dH_2O= distilled water; meth=methanol

2.3.3 Treatment

The drugs were administered at clinically relevant concentrations which reflect their steady-state plasma peak concentration (C_{max}) (Apostolova *et al.*, 2010; Bumpus, 2011). The drug concentrations used in this study are the mean clinical C_{max} plasma concentrations achieved after daily oral administration of the drugs in HIV patients receiving HAART (Drug information, VIREAD®, EMTRIVA®, SUSTIVA®, Gilead Sciences, 2010; Drug information, NORVIR®, KALETRA®, Abbott laboratories, 2010; Apostolova et al. 2010; Bumpus, 2011). The cells were incubated with the drugs individually and in combination at the indicated concentrations (Table 2.2) for 24, 48, 72 and 96 hours. Untreated and vehicle control groups were exposed to growth medium and vehicle respectively (Groups 1 and 2).

Table 2.2: Treatment groups and drug concentrations administered for each cell line.

GROUP	TREATMENT
1	Growth Medium
2	0.01% Methanol
3	0.3µg/ml TDF
4	1.8µg/ml FTC
5	4.07µg/ml EFV
6	TDF+FTC+EFV (ATRIPLA)
7	9.8µg/ml LPV
8	0.6µg/ml RTV
9	LPV/r (KALETRA)
10	TDF+FTC+LPV/r

The cells were exposed to 0.3 µg/ml TDF; 1.8 µg/ml FTC; 4.07 µg/ml EFV, individually (Groups 3-5) and in combination (Group 6), as recommended by the 2010 South African antiretroviral treatment guideline and as in ATRIPLA®. Cells were also exposed to 9.8 µg/ml LPV (Group 7) and LPV/r (KALETRA®). Even though the absolute bioavailability of Ritonavir had not been determined in humans at the time of this study and until now (Drug information, NORVIR® Abbott laboratories, 2013), across studies, administration of Kaletra® 400/100 mg daily yields mean steady-state lopinavir plasma concentrations 15 to 20 times higher than those of ritonavir in HIV-1 patients (Drug information, KALETRA® Abbott laboratories, 2010). Therefore, a 9.8 µg/ml LPV: 0.6 µg/ml RTV ratio of lopinavir to ritonavir was used. In group 8, cells received 0.6 µg/ml RTV only. Another group of cells (Group 10) received a combination of TDF, FTC and LPV/r; recommended as a 2nd line regimen in the 2010 South African antiretroviral treatment guideline.

2.4 Neutral Red Uptake Assay

The Neutral Red Uptake cytotoxicity assay is a precise, easy and reproducible assay that allows for distinguishing between viable and non-viable cells (Borenfreund and Puerner, 1985). Neutral red is a weak cationic supravital dye that readily penetrates cell membranes by non-ionic diffusion and predominately accumulates intracellularly in lysosomes. Alterations to the lysosomal membrane integrity arising from the toxicity of substances reduces NR uptake thereby allowing the distinction between viable and damaged cells (Borenfreund and Puerner, 1985). After the viable cells have incorporated the dye, the dye is subsequently liberated from the cells and the degree of cytotoxicity, quantified by a spectrophotometer, is a measure of how many cells excluded the dye (Borenfreund and Puerner, 1985).

This assay was used to evaluate the cytotoxic effects of the NRTI/nNRTI and PIs used in this study. HCS-2, NCE16IIA, MCF-7 and MCF-10A cells were cultured as described (Section 2.2.2.1). For each cell line, 96-well Falcon tissue culture plates containing approximately 5000cells/well, in 125 µl of growth medium were treated with different media containing the test compounds and drug combinations (Table 2.1 and 2.2) for 24, 48, 72 and 96 hours. The negative control consisted of untreated cells, left in growth medium and diluent controls cells were exposed to 0.01% methanol. Each group consisted of four replicates. After treatment, the medium was removed and the protocol of Borenfreund and Puerner, (1985) was followed for the assay. Briefly, cells were rinsed in phosphate buffered saline (PBS). Neutral red medium was added to each well and plates were incubated for 2 hours at 37°C for the neutral red dye to be taken up by viable cells. Thereafter the NR solution was removed and cells were rinsed with PBS. The solubilising solution (1% acetic acid in 50% ethanol) was added to each well for 10 minutes in order to

extract the dye. The absorbance of the extracted dye was measured in a microplate reader (Anthos 2010 Model 17-550, Austria) at a wavelength of 540 nm. Background absorbance was read at 690 nm and subtracted from the 540 nm measurement. All experiments were repeated three times on three different days. The absorbance values were converted into percentage viability values as described in NICEATM, 2003. Statistical analysis was performed using JMP® (Version 10.0 SAS Institute Inc., Cary, NC). Data are reported as mean $\pm$ standard deviation. After verifying the normal distribution and the homogeneity of the variance using an F test ($p < 0.05$), a one way analysis of variance (where a significance level of $p < 0.05$ was set) was used to compare the results. All means were then compared using the Tukey-Kramer HSD. The effects of each treatment on percentage viability were compared between the breast cell lines and between the cervical cell lines using the Tukey-Kramer HSD. Comparisons were made at 24, 48, 72 and 96 hours.

2.5 Reverse Transcription and Real time qPCR

This section describes the use of reverse transcriptase and quantitative real-time polymerase chain reaction to study the expression of the apoptotic genes; *BAX* and *BCL*-2 and the angiogenic pathway-related genes; $VEGF_{165a}$ and $VEGF_{165b}$ mRNA in the cervical (cancer-HCS-2 and normal immortalized-NCE16IIA) and breast (cancer MCF-7 and normal immortalized-MCF10A) cells exposed to the antiretroviral drugs as described in Table 2.2. Total RNA was extracted (described below; Section 2.5.1) from the cells following treatment with the antiretroviral drugs or vehicle. The RNA extracts were reverse transcribed to cDNA using MultiScribe Reverse Transcriptase (described below; Section 2.5.3) and cDNA representing portions of each of the genes of interest were amplified with real-time qPCR. The relative expression of the specific genes of interest were normalised as a ratio to the amount of the two most stably expressed reference genes

according to the $2^{-\Delta\Delta C}$T method of Livak and Schmittgen (2001). Three reference genes were used for these experiments as follows; *Homo sapiens* TATA box binding protein (*TBP*), Transferrin receptor (*TFRC*) and *Homo sapiens* ribosomal protein, Large P0 (*RPLP0*).

2.5.1 Total RNA Extraction

Cells were cultured in 25 cm^3 plastic tissue-culture dishes (Nunclon, Denmark) as described (Section 2.2.2.1). For each cell line, total RNA was extracted from each group (Table 2.2), three different times on three different days from different experiments to generate the biological replicates required to validate the qPCR experiments (Bustin, 2002, Fleige and Pfaffl, 2006, Bustin *et al.,* 2009). After cells were exposed to the drugs for 96 hours, total RNA extraction was performed using the GeneJET RNA Purification kit (Van Phuc *et al.,* 2011) according to the manufacturer's instructions (Thermo Scientific, Pittsburgh PA. USA). The protocol was adapted from Chomczynski and Sacchi, (1987) and Boom *et al.,* (1990). The procedure for total RNA extraction is detailed in Appendix B1. RNA concentration and purity were determined using the Nanodrop®-1000 (NanoDrop® Technologies, USA) spectrophotometer (Derks *et al.,* 2008). RNA integrity was determined by gel electrophoresis (Derks *et al.,* 2008). The RNA was stored at -80°C in 10 µl aliquots for future use.

2.5.1.1 RNA Gel Electrophoresis

The formaldehyde agarose (FA) gel electrophoresis procedure described by the RNeasy Mini Handbook (QIAGEN®, USA) was followed. The procedure for RNA gel electrophoresis is detailed in Appendix B2. Illumination of the stained gels under UV light (254-366 nm) allowed bands of RNA to be visualised against a background of unbound

dye. Gel images were acquired with the BioRad Gel Doc® XR (Model 170-8170 Segrate, Milan. Italy). The integrity and size distribution of total RNA was checked by observing the stained RNA. The respective ribosomal bands appeared as sharp bands on the stained gel. The 28S ribosomal RNA band was present at approximately twice the intensity of the 18S ribosomal RNA band (RNeasy Mini Handbook, QIAGEN®, USA).

2.5.1.2 RNA Quantification

Quantification of RNA was done using a Nanodrop®-1000 spectrophotometer (NanoDrop® Technologies, USA). Readings were taken at 260 nm and 280 nm as described by the manufacturer. A 260/280 ratio of approximately 2 was regarded as pure quality (Derks *et al.*, 2008).

2.5.2 Genomic DNA (gDNA) Removal

Genomic DNA contamination was removed from total RNA using the DNase I, RNase-free kit (Thermo Scientific, Pittsburgh PA. USA) according to the protocol adapted from Kienzle *et al.*, (1996) and Sambrook and Russel, (2001). The procedure for gDNA removal is detailed in Appendix B3.

2.5.3 Reverse Transcription for Complementary DNA (cDNA) Synthesis

Using the High Capacity cDNA Reverse transcription kit (Life Technologies, California, USA) and as previously reported in Szwagierczak *et al.* (2010), cDNA was synthesised using MultiScribe™ Reverse Transcriptase from 700ng RNA. The reverse transcriptase reaction was carried out in a GeneAmp® PCR system 9600 Thermal Cycler for 10 mins at 25°C, 120 mins at 37°C and then the enzyme was deactivated for 5 mins at 85°C.

cDNA samples were either used immediately for real time PCR or stored at -20°C for later use. RNase-free and standard sterile protocols, according to the Minimum Information for Publication of Quantitative Real-Time PCR Experiments (MIQE) (Bustin, 2002; Fleige and Pfaffl, 2006; Bustin *et al.,* 2009) were exercised at all times and for all RNA, cDNA and qPCR procedures. Reagents were thawed on ice before use, and kept on ice while in use.

Table 2.3: Components of the Reverse Transcription reaction

Component	**Volume/Reaction (µL)**
10× RT Buffer	2
25× dNTP Mix (100 mM)	0.8
10× RT Random Primers	2
MultiScribe™ Reverse Transcriptase	1
RNase Inhibitor	1
RNA	Variable
Nuclease-free H_2O	added to increase total vol to 20
Total per Reaction	**20**

For all samples, the reverse transcription (RT) reaction was carried out without the reverse transcriptase enzyme to generate the minus RT controls. The minus RT samples were later amplified to confirm the absence of genomic DNA.

2.5.4 Primer Design

According to the MIQE guidelines (Bustin *et al.,* 2009), primers should be obtained from RTPrimerDB. RTPrimerDB is a public database for primer and probe sequences used in real-time PCR assays employing popular chemistries (SYBR Green I, Taqman, Hybridisation Probes, Molecular Beacon) to prevent time-consuming primer design and experimental optimisation, and to introduce a certain level of uniformity and standardisation among different laboratories.

The database is available online at http://medgen.ugent.be/rtprimerdb/. Primers for the human *BAX* gene was obtained from this database; Assay ID 1539. The RTPrimerDB website did not contain deposited primers for the other genes of interest required for this study, therefore, the appropriate forward and reverse primers were designed using the primer design tool of the National Centre for Biotechnology Information (NCBI) website at; http://www.ncbi.nlm.nih.gov/tools/primer-blast/

Designed primer pairs were then analysed with the Integrated DNA Technologies (IDT) SciTools Oligo Analyzer® 3.1 online tools. All primers were synthesised by IDT (Coralville, Iowa, USA) and all primer pairs were used at an annealing temperature of 60°C. Primer sequences are listed in Table 2.4. (See also Appendix C1).

Table 2.4: Oligonucleotide sequences used for qPCR

Gene	Sequences (5'-3' direction)	Product size (bp)
BAX Forward	CCT TTT CTA CTT TGC CAG CAA AC	148
BAX Reverse	GAG GCC GTC CCA ACC AC	
BCL-2 Forward	ATG TGT GTG GAG AGC GTC AAC C	122
BCL-2 Reverse	GCA TCC CAG CCT CCG TTA TC	
TBP Forward	TGA TGC CTT ATG GCA CTG GAC TGA	86
TBP Reverse	CTG CTG CCT TTG TTG CTC TTC CAA	
RPLP0 Forward	TGC AGC TGA TCA AGA CTG GAG ACA	178
RPLP0 Reverse	TCC AGG AAG CGA GAA TGC AGA GTT	
TFRC Forward	GGC ACC ATC AAG CTG CTG AAT GAA	133
TFRC Reverse	GTT GAT CAC GCC AGA CTT TGC TGA	
VEGF 165A Forward	CAA GAT CCG CAG ACG TGT AA	100
VEGF 165A Reverse	GCT TGT CAC ATC TGC AAG TA	
VEGF 165B Forward	CGC AGA CGT GTA AAT GTT CCT G	97
VEGF 165B Reverse	TTC CTG GTG AGA GAT CTG CAA G	

2.5.5 Determination of qPCR Amplification Efficiencies

For each primer pair, amplification efficiencies were determined by amplifying serial dilutions of cDNA. Data from these are used by the Applied Biosystem's ABI 7500 software to plot the slope and efficiency of the reaction for each primer pair. According to the MIQE guidelines (Bustin *et al.*, 2009), the ranges of accepted efficiencies are 90-110%. The amplification efficiencies for all primer pairs used were within this range. (Appendix C2).

2.5.6 qPCR Protocol

The Power SYBR® Green PCR Master mix was used for the qPCR procedure. This protocol contains adaptations from Mullis and Faloona (1987), Saiki *et al.* (1988) and Kwok and Higuchi (1989). The Power SYBR® Green PCR Master Mix is a premix of the components (except primers, template, and water) necessary to perform real-time PCR using SYBR® Green I dye with enhanced sensitivity and specificity (Life Technologies, California, USA, 2011). The SYBR Green dye binds to double-stranded (ds) DNA, thus providing a fluorescent signal that reflects the amount of ds-DNA product generated during PCR (Life Technologies, California, USA, 2011). The qPCR reaction was set up in MicroAmp® Optical 8-tube Strips (Life Technologies, CA, USA) as follows (Table 2.5)

Table 2.5: qPCR Reaction setup

Component	Volume per 20µl reaction	Final Concentration
Power SYBR® Green PCR Master Mix (2X)	10	1X
Forward Primer	0.4	200-400nM
Reverse Primer	0.4	200-400nM
Template	5	10ng
Water	4.2	
Total	**20**	

PCR reactions were amplified for 40 cycles prior to which the AmpliTaq Gold® DNA polymerase was activated for 10 mins at 95°C. Each cycle consisted of a denaturing step for 15 secs at 95°C, and annealing/extension step for 1 min at 60°C. PCR amplification was performed in a final volume of 20 µl using the Power SYBR® Green PCR Master Mix with the ABI 7500 and Step-One real-time PCR machines. To confirm the absence of nonspecific amplification, PCR products were separated on 3% agarose gels. Melt curves were generated for each PCR product using the Applied Biosystems ABI 7500 software (Appendix C3).

2.5.7 Agarose Gel Electrophoresis of DNA

A 3% (w/v) agarose gel was prepared per 50 ml gel as follows;

1.5 g agarose, 50 ml 1X TBE buffer (10X Tris Borate EDTA; 0.89 M Tris, 0.02 M EDTA, 0.89 M Boric Acid made up to 1000 ml with DEPC treated water pH $\pm$ 8.3). Agarose was boiled in a microwave until no crystals were visible and allowed to cool to hand warmth. Two (2) µl of ethidium bromide was added. Gel was poured into the casting unit and allowed to set for 30 minutes. Samples were prepared by mixing 1 volume of 6X DNA loading dye (Thermo Scientific, Pittsburgh PA, USA) and 5 volumes of DNA samples. After the gel was set, the aluminium gates and the combs were removed. The gel was placed into the tank containing 1X TBE. PCR products were loaded into the well and loading order recorded. An equal volume of O'GeneRuler Low Range DNA Ladder (Thermo Scientific, Pittsburgh PA, USA) was loaded into the first and last wells of each comb. Electrodes were then connected so that samples ran from negative to positive (from black to red leads). Gels were run at 100 V, 180 mA for 3 hours. Gel images were acquired with the BioRad Gel Doc® XR (Model 170-8170 Segrate, Milan. Italy) (Appendix C4).

2.5.8 qPCR Data Analysis

The relative mRNA expression levels of target genes in each sample were calculated using the qbase^{PLUS} software (Biogazelle, Zulte, Belgium). The stability of reference genes expression was evaluated using qbase^{PLUS} version 2.3. This software employs a pair-wise comparison model to calculate the stability of each reference gene, and selects the two or more most stable genes from a panel of reference genes for normalisation (Hellemans *et al.,* 2007). Genes were ranked based on a gene stability parameter *M*, where a low *M* value indicates high expression stability. In addition, the qbase^{PLUS} software also calculates the coefficient of variation (CV) to determine how stable a gene is expressed. PCR base line Cq values were exported from the ABI 7500 software as an Excel file (Microsoft, Redmond, WA, USA) and imported into the qbase^{PLUS} software. The data were then analysed using the default settings and the arithmetic mean of replicates was used. Data from standard curve experiments from the ABI 7500 software, imported into the qbase^{PLUS} software, was used to generate amplification efficiencies and standard errors that are used downstream by the qbase^{PLUS} software to determine normalised gene expression levels. The relative quantity of each target/sample combination was scaled to the average Cq of corresponding target (scale set to untreated control in the qbase^{PLUS} software). The relative expression of specific genes in the experiment were normalised as a ratio to the amount of the two most stably expressed reference genes according to the $2^{-\Delta\Delta C}$T method of Livak and Schmittgen (2001). To determine whether the expression of the genes of interest from the untreated differed significantly from those from the treated groups, the qbase^{PLUS} software was used to conduct the analysis of variance (ANOVA) with significance level set at $p<0.05$.

2.6 Immunofluorescence

2.6.1 BAX and BCL-2

The genes carrying the genetic information for BAX and BCL-2 proteins belong to the BCL-2 family, and they comprise the most biologically relevant classes of apoptosis regulators involved in the critical stages of apoptosis (Basu and Haldar, 1998). Generally, the relative ratio of pro-survival (BCL-2) and anti-survival (BAX) proteins is believed to determine cell sensitivity or resistance to the apoptotic stimuli (Ola *et al.*, 2011). BAX promotes apoptosis while BCL-2 inhibits it, therefore they were co-localised to determine whether the antiretroviral drugs used in this study affects apoptotic cell function through this pathway.

2.6.2 $VEGF_{165}$

$VEGF_{165b}$ behaves as a competitive inhibitor of $VEGF_{165a}$ by binding to its receptor but not stimulating the full tyrosine phosphorylation of the VEGFR-2 and the downstream signaling triggered by $VEGF_{165a}$ (Woolard *et al.*, 2004). $VEGF_{165b}$ is therefore considered to be an endogenous anti-angiogenic agent produced by alternative splicing (Woolard *et al.*, 2004). The effects of the antiretroviral drugs on $VEGF_{165b}$ localisation was determined by immuno-cytochemistry.

2.6.3 Cell Staining

The immunofluorescence staining procedure used in this study was adapted from the ABCAM® double labelling procedure, available at http://www.abcam.com/ps/pdf/protocols/Double%20immunofluorescence%20-simultaneous%20protocol.pdf (Appendix B5).

2.6.3.1 Optimization

A guide for cell staining was provided with the datasheet accompanying the primary and secondary antibodies used in this study, but to ensure specific antibody binding and optimal visualization of the target proteins, the following parameters required initial optimization; primary and secondary antibody dilutions, the blocking solution and duration and the duration of incubation with primary and secondary antibodies. The parameters optimized for immune-fluorescence are detailed in Appendix B4.

2.6.3.2 Immuno-staining

Cells ($1x10^4$) were plated on cover slips 1 day before the experiment. Cells were then cultured as described (Section 2.2.2.1). Cells were treated with the drugs at the indicated combinations and concentrations (Table 2.2) for 96 hours. Following treatment, cells were washed three times with 0.5% BSA in PBS, followed by fixation in 10% phosphate buffered formalin for 10 min. The fixed cells were rinsed in PBS and permeabilized with 0.05% Triton-X 100 in PBS, washed and blocked with 10% normal goat serum in PBS for 60 mins to eliminate non-specific binding of secondary antibody. Cells were then incubated with polyclonal rabbit anti-human BAX (1:1000 DAKO) and monoclonal mouse anti-human BCL-2 (1:100 DAKO) or polyclonal rabbit anti-human $VEGF_{165b}$ (5 μg/ml) (ABCAM). Following overnight incubation, the cells were washed and incubated for 2 hours with a FITC-conjugated goat anti-mouse antibody (1:500 ABCAM) and Rhodamine-conjugated goat anti-rabbit antibody (1:1000 ABCAM) in the dark. Slides were rinsed, nuclei counterstained in 4',6-diamidino-2-phenylindole (DAPI) 300 nm for 5mins, rinsed and mounted with Fluoromount (Sigma). Negative control groups were set up to ensure that the secondary antibodies were specific for their primary antibodies. The primary antibodies were substituted with 0.1% BSA/PBS and the normal protocol was carried out.

In a second negative control, the cells were treated in the same way as the experimental slides, but the secondary antibodies were substituted with PBS. The positive controls used in this study were HeLa cells, which had been shown to express BAX and $VEGF_{165b}$ (Tsuruta *et al.,* 2002, http://www.abcam.com/vegf-165b-antibody-mrvl561-ab14994.html, http://www.abcam.com/vegf-165b-antibody-ab90719.html, http://www.abcam.com/BAX-antibody-ab10813.html?productWallTab=Abreviews&applications=3688, http://www.ptglab.com/Products/BAX-Antibody-50599-2-Ig.htm) and HepG2 cells, shown to express BCL-2 (Tan *et al.,* 2009). These controls were set up to ensure that cross-reactivity was not taking place.

Cells were visualized using a Zeiss Laser Scanning Confocal Microscope 780 under a Zeiss 100X oil immersion objective. For digital image analysis, ZEN 2010 software was used. Slides were kept dark once fluorescent antibodies had been added to prevent bleaching. As fading of the fluorochromes will take place, images were analysed within the same time period. The image acquisition settings remained constant for all exposures. Images were taken and using the ZEN 2010 (Carl Zeiss, Germany) image analysis software, the intensity of the fluorescence of each micrograph was analysed. This was done by using the software to initially define the regions of interest (ROIs); namely, the nucleus and cytoplasm. The mean intensity of each ROI from the treatment groups (according to Table 2.2) was then analysed with the statistics software JMP® (Version 10.0 SAS Institute Inc., Cary, NC, USA). Data are reported as mean $\pm$ standard deviation. After verifying the normal distribution and the homogeneity of the variance using an F test ($p < 0.05$), a one way analysis of variance (where a significance level of $p < 0.05$ was set) was used to compare the results. Representative images are shown.

2.7 Acridine Orange Staining

Fluorescence light microscopy with differential uptake of fluorescent DNA binding dyes such as Acridine Orange (AO) provides a simple, rapid, and accurate method for measuring apoptosis and cell membrane integrity (Coligan *et al.,* 1995). Acridine Orange permeates all cells, making the nuclei appear green (Excitation; 488 nm laser line: Emitted fluorescence acquired at 500–560 nm (green region of spectrum, for AO). Live cells therefore have normal green nuclei; early apoptotic cells have bright green nuclei with condensed or fragmented chromatin; late apoptotic cells display condensed and fragmented chromatin and membrane blebbing (Ribble *et al.,* 2005; Yang *et al.,* 2013). This procedure was carried out to determine whether the protease inhibitors inhibit drug induced apoptosis in the cervical and breast cell lines since it had been reported (Phenix et al, 2001, Badley, 2005, Vlahakis *et al.,* 2007, Rizza and Badley, 2008) that protease inhibitors have potent anti-apoptotic effects in different cellular systems, the majority of which are immune cells. The anti-apoptotic effect of LPV/r was assessed to test whether these generalised effects are seen in the currently investigated cell lines.

2.7.1 Induction of Apoptosis

It was reported previously that 1 μM CPT significantly induced apoptosis in MCF-7 cells (Nieves-Neira and Pommier, 1999) and that 30 μM CPT significantly induced apoptosis in MCF10A cells (Rastogi *et al.,* 2006). For this study, these CPT concentrations were further optimised to determine the appropriate exposure time. In the breast cell lines, 1 μM CPT significantly increased the percentage of apoptotic MCF-7 cells from 3-4% (spontaneous apoptosis) to 15-18% following a 6 hour exposure, while the percentage of apoptotic MCF-10A cells increased from 1-2% to 8-9% following a 6 hour exposure to 30 μM CPT as determined by the AO staining. No literature was found describing the induction of

apoptosis with CPT in the cervical cell lines, so the CPT concentrations used to induce apoptosis in the cervical cell lines in this study were determined by optimisation experiments. HCS-2 and NCE16IIA cells were exposed to 1 μM CPT, 5 μM CPT, 10 μM CPT, 15 μM CPT, 20 μM CPT, 25 μM CPT, 30 μM CPT, 50 μM CPT for 6, 12, 18 and 24 hours. 25 μM CPT significantly increased the percentage of apoptotic HCS-2 cells from 1-2% (spontaneous apoptosis) to 10-12% following a 6 hour exposure, while the percentage of apoptotic NCE16IIA cells increased from 2% to 14-16% following a 6 hour exposure to 5 μM CPT.

2.7.2 Cell treatment and AO staining

HCS-2, NCE16IIA, MCF-7 and MCF-10A cells were cultured as described (Sections 2.2.1 and 2.2.2.1) on 22-mm square coverslips placed into 35-mm culture dishes (Costar, Cambridge MA, USA). Cells were treated with 0.01% methanol (vehicle) and the PI based combinations; LPV/r (in the appropriate medium; Section 2.2.1) for 96 hours before being stimulated (Phenix *et al.*, 2001) to undergo apoptosis with 25 μM CPT in EMEM (HCS-2), 5 μM CPT in KGM (NCE16IIA), 1 μM CPT in DMEM (MCF-7) and 30 μM CPT in MEGM (MCF-10A) for 6 hours. After induction of apoptosis, the CPT-containing medium was discarded, cells rinsed with PBS and 1ml AO dye mix (100 μg/ml AO in PBS) (Coligan *et al.*, 1995; Mironova *et al.*, 2007), was added into the culture dishes for 5 minutes. After AO staining, cells were rinsed with PBS and culture dishes were inverted and fixed with formaldehyde vapour for 1 minute to prevent the photo-damaging effects of continuous excitation on living cells due the photosensitizing effects of most fluorescent dyes (Canete *et al.*, 2001). Fluorescence images were captured using a Zeiss (Carl Zeiss MicroImaging GmbH, Germany) LSM 780 confocal microscope equipped with an argon ion laser of 25 mW (excitation wavelengths 458, 488 and 514 nm). A total of 600 cells per

cell line per group were counted from 3 independent experiments to determine the percentage of apoptotic cells. Data analysis was performed using JMP® (Version 10.0 SAS Institute Inc., Cary, NC). Data are reported as mean ± standard deviation. After verifying the normal distribution and the homogeneity of the variance using an F test ($p < 0.05$), a one way analysis of variance (significance level $p < 0.05$) was used to compare the results. If there was a significant difference between the means ($p<0.05$) then a Tukey-Kramer *post hoc* analysis was performed to determine which treatment groups were significantly different from each other.

2.8 Cell Death Detection ELISA

The Cell Death Detection ELISA plus kit (Roche Molecular Biochemicals, Mannheim, Germany) is used to measure changes in apoptosis (Liu *et al.,* 2003; Tu *et al.,* 2009). In this procedure, internucleosomal DNA fragmentation is quantitatively assayed by antibody mediated capture and detection of cytoplasmic mononucleosome and oligonucleosome associated histone-DNA complexes. Cells were cultured as described (Sections 2.2.1 and 2.2.2.1) in 96 well plates in duplicate. Cells were treated with 0.01% methanol (vehicle) and the PI based combination; LPV/r (in the appropriate medium; Section 2.2.1); for 96 hours before being stimulated (Phenix *et al.,* 2001) to undergo apoptosis with 25 μM CPT (HCS-2), 5 μM CPT (NCE16IIA), 1 μM CPT (MCF-7) (Nieves-Neira and Pommier, 1999) and 30 μM CPT (MCF10A) (Rastogi *et al.,* 2006) for 6 hours.

According to the protocol described by Liu *et al.,* (2003) and Tu *et al.,* (2009), cells were centrifuged (200 *g*), resuspended in 200 μl of the lysis buffer supplied in the kit and incubated for 30 min at room temperature. Nuclei were then pelleted at 200 g for 10 mins and 20 μl of the supernatant (cytoplasmic fraction) from treated group, untreated group, positive control and background control were transferred into the corresponding

streptavidin coated wells for the enzyme-linked immunosorbent assay (ELISA) according to the manufacturer's standard protocol (Tu *et al.,* 2009). Eighty (80) µl of the immunoreagent was added to each well containing the 20 µl supernatant or controls. The wells were covered with adhesive foil and incubated on a microplate shaker under gentle shaking (300 rpm) for 2 hours at room temperature. The solution was then removed by gentle pipetting; wells were rinsed three times with 250 µl incubation buffer and removed. One hundred (100) µl of the ABTS solution was pipetted into the wells and incubated on a plate shaker at 250 rpm until the colour development was sufficient for photometric analysis (approximately 10-20 minutes). One hundred (100) µl of the ABTS stop solution was added to each well. Absorbance was measured at 405 nm and 490 nm (reference wavelength) with a microplate reader (Anthos 2010 Model 17-550, Austria). Signals in wells containing the substrate only were subtracted as background. Data were analysed from three independent experiments. Data analysis was performed using JMP® (Version 10.0 SAS Institute Inc., Cary, NC). Data are reported as mean $\pm$ standard deviation. After verifying the normal distribution and the homogeneity of the variance using an F test ($p < 0.05$), a one way analysis of variance (significance level $p < 0.05$) was used to compare the results. If there was a significant difference between the means ($p<0.05$) then a Tukey-Kramer *post hoc* analysis was performed to determine which treatment groups were significantly different from each other.

CHAPTER 3: RESULTS

3.1 Effects of Antiretroviral drugs on the viability of breast and cervical cells

3.1.1 Effects of TDF on the viability of the cervical cells

After 24 and 48 hours of exposure, the NRTI, TDF, significantly ($p<0.05$) increased the viability of the normal cervical (NCE16IIA) cells; when compared to their control groups (Fig. 3.1A). With prolonged treatment (72 to 96 hours), these effects were not significantly different (Fig. 3.1A). The viability of the cancer cervical (HCS-2) cells was initially (24 to 48 hours) not altered by TDF, but at 72 hours, HCS-2 percentage viability became significantly ($p<0.05$) reduced when compared to the control group and the normal cervical cells (also at 72 hours) (Fig. 3.1A). After 96 hours of exposure to TDF, the cancer cervical cells exhibited reduced (but not significant $p<0.05$) viability when compared to its control and the normal cells at 96 hours (Fig. 3.1A).

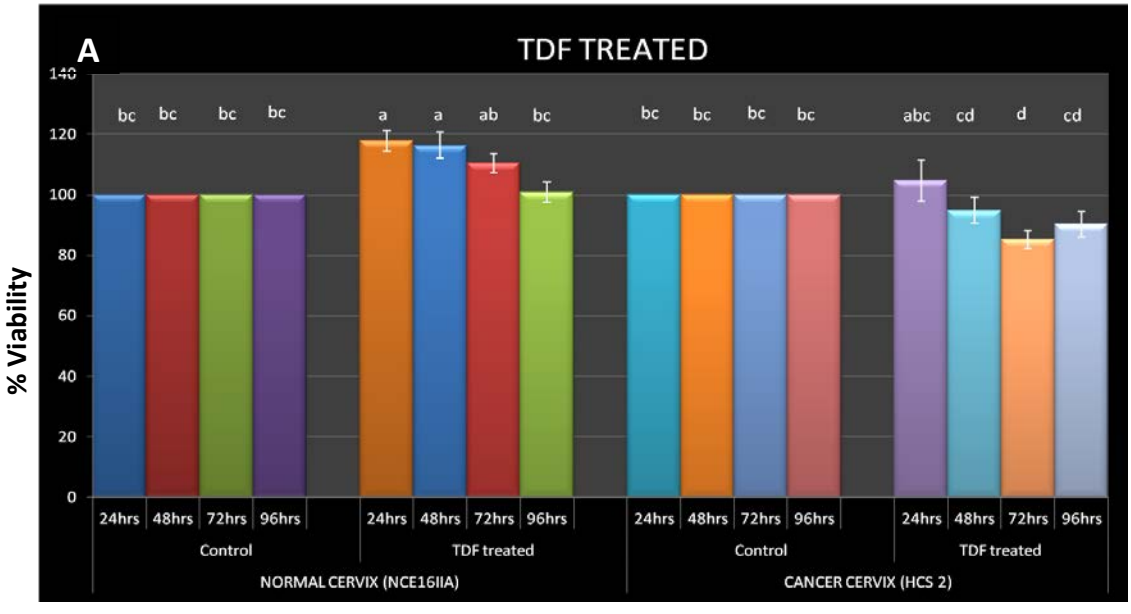

Fig. 3.1A: Effects of TDF on the percentage viability of normal cervical (NCE16IIA) and cervical cancer (HCS-2) cells. Cells were incubated with 0.3µg/ml TDF for 24 – 96 hrs. Graphs were plotted with mean ±SEM percentage viability from a mean of three independent experiments. Groups not connected by the same letter are significantly different ($p<0.05$).

3.1.2 Effects of TDF on the viability of the breast cells

The viability of the normal breast MCF-10A cells was significantly ($p<0.05$) reduced by TDF after 24 hours of exposure; when compared to its control (at 24 hours) and the cancer MCF-7 cells(also at 24 hours) (Fig. 3.1B). With prolonged treatment, the MCF-10A cells recovered from the initial cytotoxic effects of TDF such that after 48 hours and up to 96 hours, there were no significantly ($p<0.05$) different alterations to their viability when compared to their controls at the respective time points (Fig. 3.1B). At 48 hours, however, TDF significantly ($p<0.05$) reduced the viability of the cancer MCF-7 cells when compared to the normal MCF-10A cells (Fig. 3.1B). TDF produced no significant ($p<0.05$) alterations to the viability of the cancer MCF-7 cells at all time points when compared to their respective controls (Fig. 3.1B).

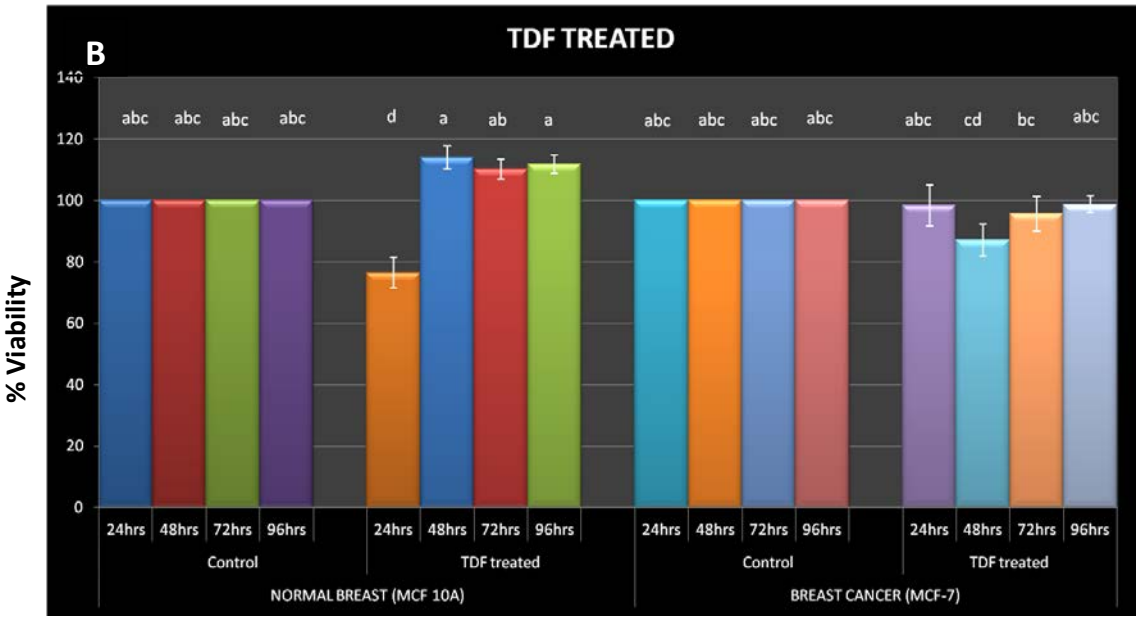

Fig. 3.1B: Effects of TDF on the percentage viability of normal breast (MCF-10A) and breast cancer (MCF-7) cells. Cells were incubated with 0.3µg/ml TDF for 24 – 96 hrs. Graphs were plotted with mean ±SEM percentage viability from a mean of three independent experiments. Groups not connected by the same letter are significantly different ($p<0.05$).

3.1.3 Effects of FTC on the viability of the cervical cells

The NRTI, FTC, exhibited no significant ($p<0.05$) alterations to the viability of the normal cervical (NCE16IIA) cells from 24 to 72 hours (Fig. 3.2A); however, at 96 hours, FTC significantly ($p<0.05$) reduced their viability (Fig. 3.2A); when compared to the control. FTC also significantly ($p<0.05$) reduced the viability of the normal cervical cells when compared to the cancer cervical HCS-2 cells at 96 hours (Fig. 3.2A). With respect to the cancer cervical cells, from 24 hours through 96 hours, FTC did not significantly ($p<0.05$) alter cell viability.

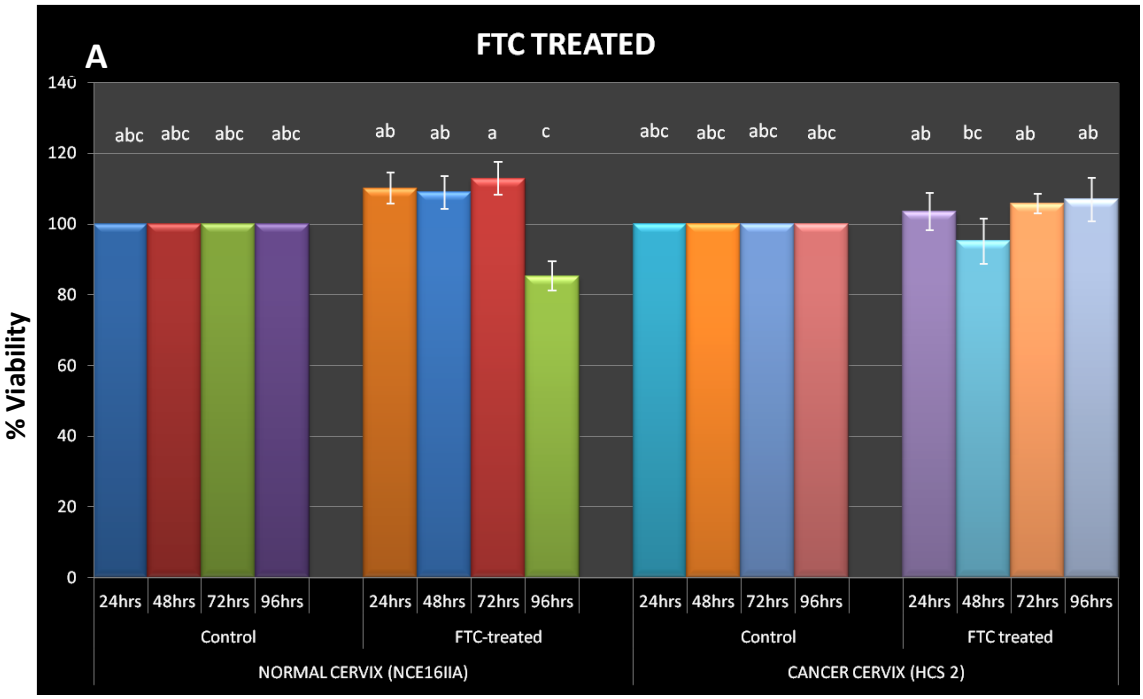

Fig. 3.2A: Effects of FTC on the percentage viability of normal cervical (NCE16IIA) and cervical cancer (HCS-2) cells. Cells were incubated with 1.8µg/ml FTC for 24 – 96 hrs. Graphs were plotted with mean ±SEM percentage viability from a mean of three independent experiments. Groups not connected by the same letter are significantly different ($p<0.05$).

3.1.4 Effects of FTC on the viability of the breast cells

FTC increased the viability of normal breast MCF10-A cells at 24 hours of exposure, however, the difference was not statistically significant ($p<0.05$) (Fig. 3.2B). From 48 through 96 hours, FTC did not significantly alter the viability of the normal breast MCF-10A cells (Fig. 3.2B). FTC significantly ($p<0.05$) reduced the viability of the cancer MCF-7 cells (when compared to the untreated control) after 48 hours of exposure (Fig. 3.2B). The effects of FTC on the cancer breast MCF-7 cells were not significantly different from the vehicle controls at 24, 72 and 96 hours (Fig. 3.2B).

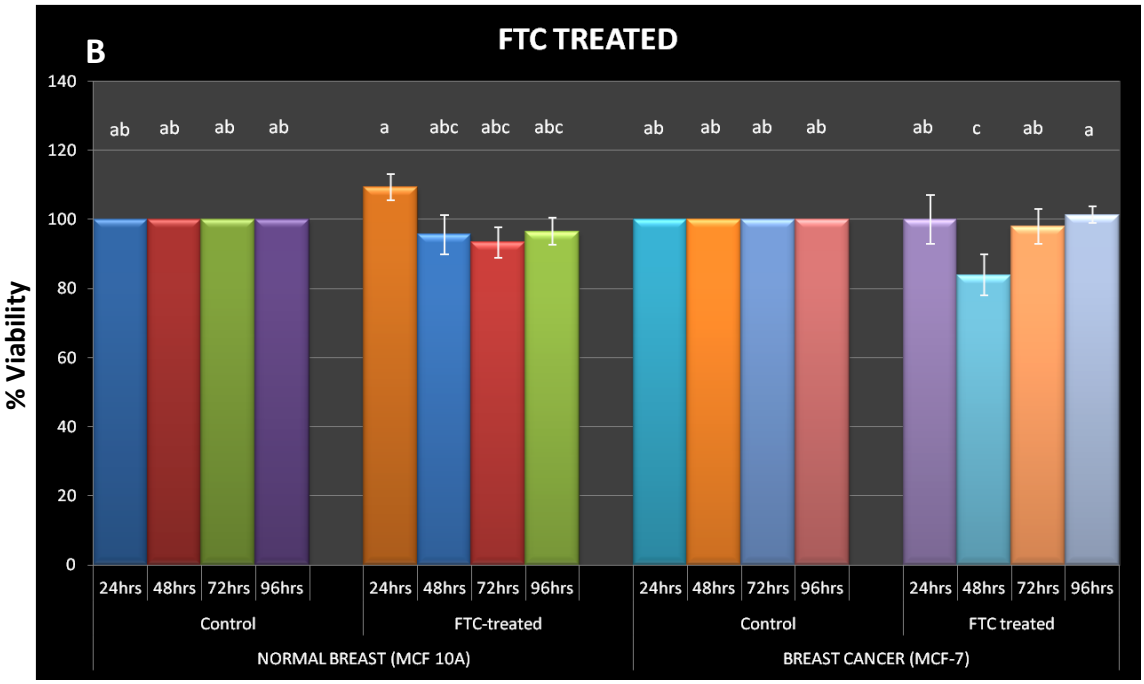

Fig. 3.2B: Effects of FTC on the percentage viability of normal breast (MCF-10A) and breast cancer (MCF-7) cells. Cells were incubated with 1.8µg/ml FTC for 24 – 96 hrs. Graphs were plotted with mean ±SEM percentage viability from a mean of three independent experiments. Groups not connected by the same letter are significantly different ($p<0.05$).

3.1.5 Effects of EFV on the viability of the cervical cells

The NNRTI, EFV, did not significantly ($p<0.05$) alter the viability of the normal (NCE16IIA) and cancer (HCS-2) cervical cells through all the time points tested when compared to their respective controls (Fig. 3.3A). However, at 48 hours, EFV showed opposing effects on the normal and cancer cervical cells. EFV significantly ($p<0.05$) reduced the viability of the normal NCE16IIA cells when compared to the cancer HCS-2 cells after 48 hours of exposure (Fig. 3.3A).

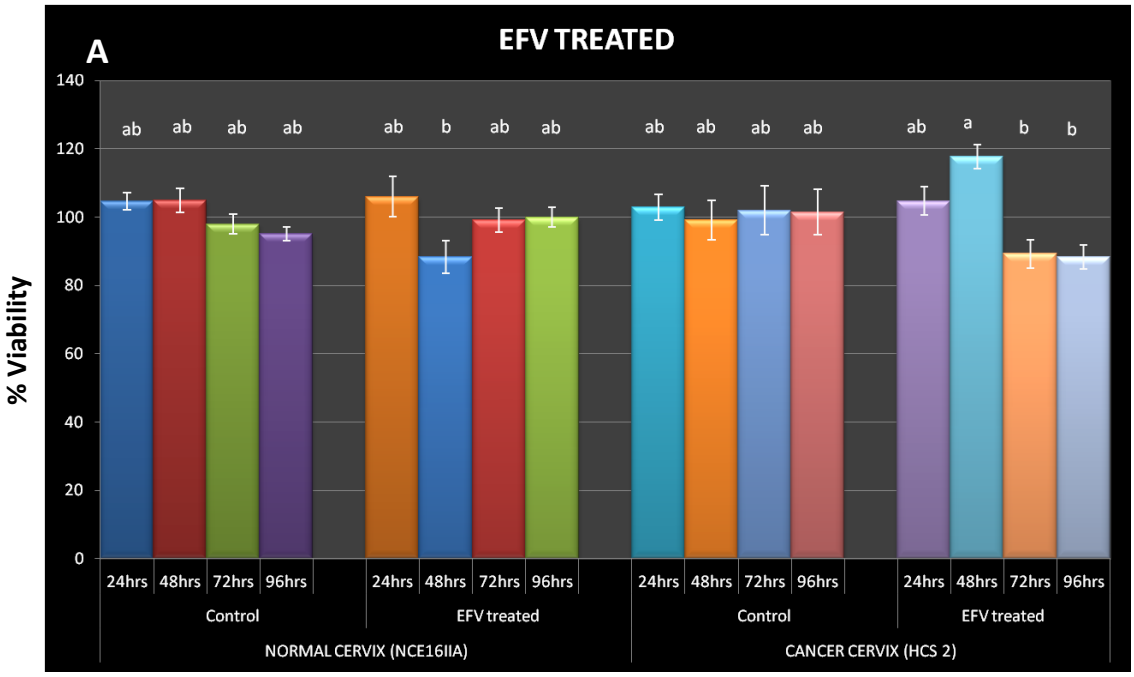

Fig. 3.3A: Effects of EFV on the percentage viability of normal cervical (NCE16IIA) and cervical cancer (HCS-2) cells. Cells were incubated with 4.07µg/ml EFV for 24 – 96 hrs. Graphs were plotted with mean ±SEM percentage viability from a mean of three independent experiments. Groups not connected by the same letter are significantly different ($p<0.05$).

3.1.6 Effects of EFV on the viability of the breast cells

EFV significantly ($p<0.05$) reduced the viability of the normal breast MCF-10A cells at all time points measured (24 to 96 hours); when compared to their control groups (Fig. 3.3B). EFV also significantly ($p<0.05$) reduced the percentage viability of the normal breast cells when compared to the percentage viability of the cancer breast MCF-7 cells at all time points (Fig. 3.3B). While EFV increased MCF-7 viability at 72 and 96 hours, this increase was not statistically significant (Fig. 3.3B).

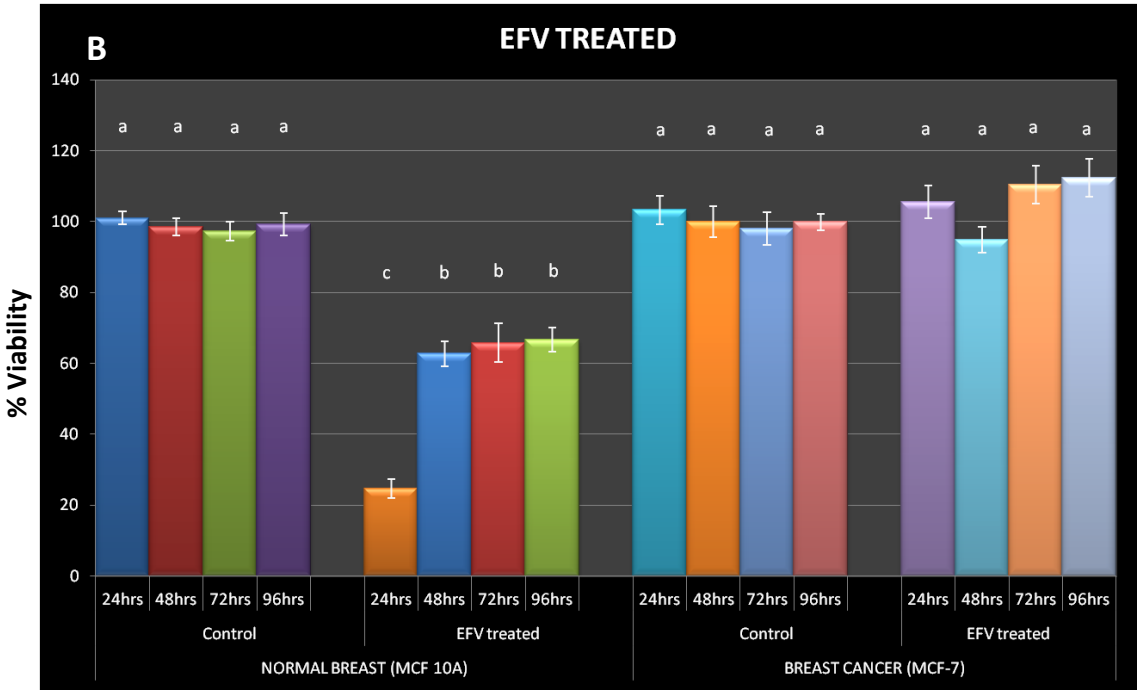

Fig. 3.3B: Effects of EFV on the percentage viability of normal breast (MCF-10A) and breast cancer (MCF-7) cells. Cells were incubated with 4.07µg/ml EFV for 24 – 96 hrs. Graphs were plotted with mean ±SEM percentage viability from a mean of three independent experiments. Groups not connected by the same letter are significantly different ($p<0.05$).

3.1.7 Effects of ATP on the viability of the cervical cells

The combination of TDF, FTC and EFV, as combined in ATRIPLA®, reduced the percentage viability of the normal cervical (NCE16IIA) cells from 24 to 96 hours, but the differences were not statistically significant ($p<0.05$) when compared to their vehicle controls (Fig. 3.4A). However, ATP significantly ($p<0.05$) reduced the viability of the NCE16IIA cells when compared to the cancer cervical HCS-2 cells at 48 and 72 hours (Fig. 3.4A). When compared to their controls, ATP did not significantly alter the viability of the cancer cervical HCS-2 cells from 24 through 96 hours (Fig. 3.4A).

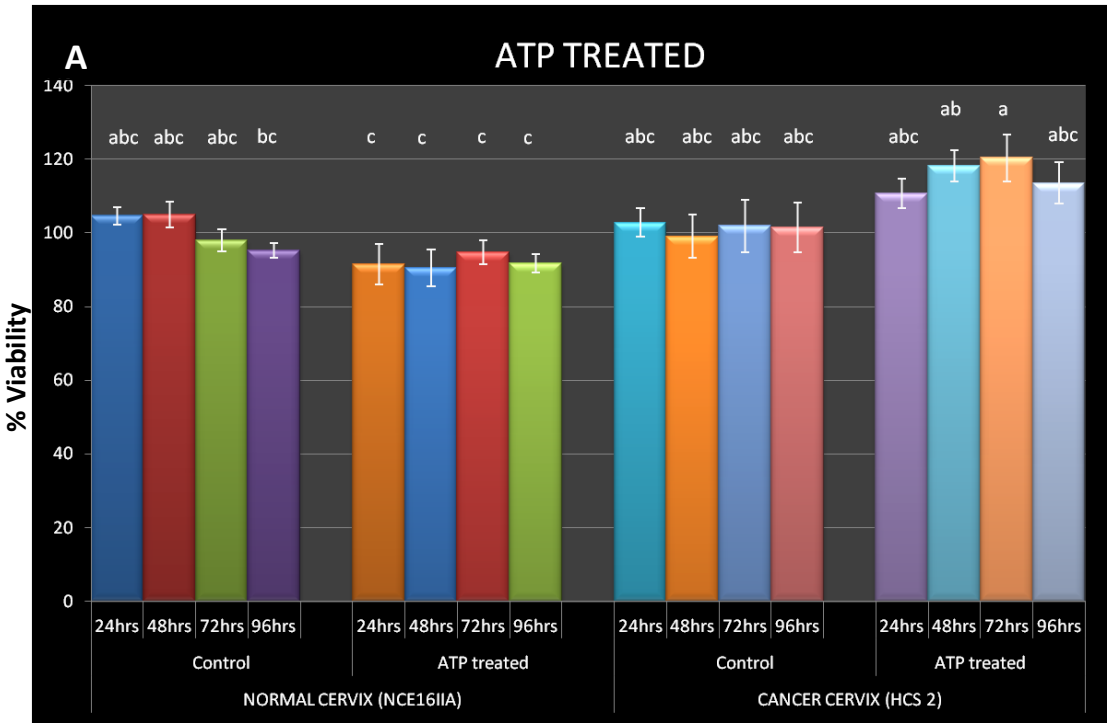

Fig. 3.4A: Effects of ATP on the percentage viability of normal cervical (NCE16IIA) and cervical cancer (HCS-2) cells. Cells were incubated with 1.8µg/ml FTC; 0.3µg/ml TDF; 4.07µg/ml EFV for 24 – 96 hrs. Graphs were plotted with mean ±SEM percentage viability from a mean of three independent experiments. Groups not connected by the same letter are significantly different ($p<0.05$).

3.1.8 Effects of ATP on the viability of the breast cells

ATP significantly ($p<0.05$) reduced the percentage viability of the normal breast MCF-10A cells after 24 hours when compared to the vehicle control (Fig. 3.4B). Also at 24 hours, there was a significant ($p<0.05$) difference between the percentage viability of the normal breast MCF-10A and the cancer breast MCF-7 cells (Fig. 3.4B). With continuous exposure (48 to 96 hours), ATP did not significantly alter the percentage viability of the normal and cancer breast cells (Fig. 3.4B).

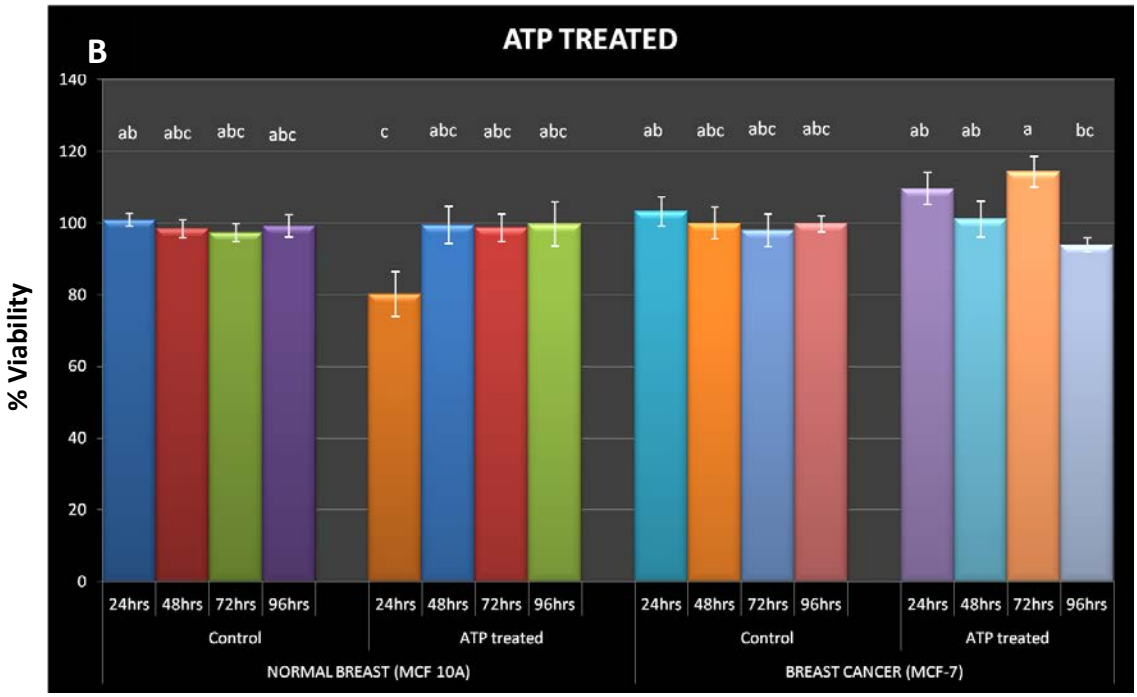

Fig. 3.4B: Effects of ATP on the percentage viability of normal breast (MCF-10A) and breast cancer (MCF-7) cells. Cells were incubated with 1.8µg/ml FTC; 0.3µg/ml TDF; 4.07µg/ml EFV for 24 – 96 hrs. Graphs were plotted with mean ±SEM percentage viability from a mean of three independent experiments. Groups not connected by the same letter are significantly different ($p<0.05$).

3.1.9 Effects of LPV on the viability of the cervical cells

The PI, LPV, did not significantly ($p<0.05$) alter the percentage viability of the normal and cancer cervical cells when compared to their vehicle controls from 24 to 96 hours (Fig. 3.5A). There were significant ($p<0.05$) differences, however, between the percentage viability of normal and cancer cells at 24 to 48 hours in response to LPV; with the viability of the normal cervical (NCE16IIA) cells significantly ($p<0.05$) reduced (Fig. 3.5A).

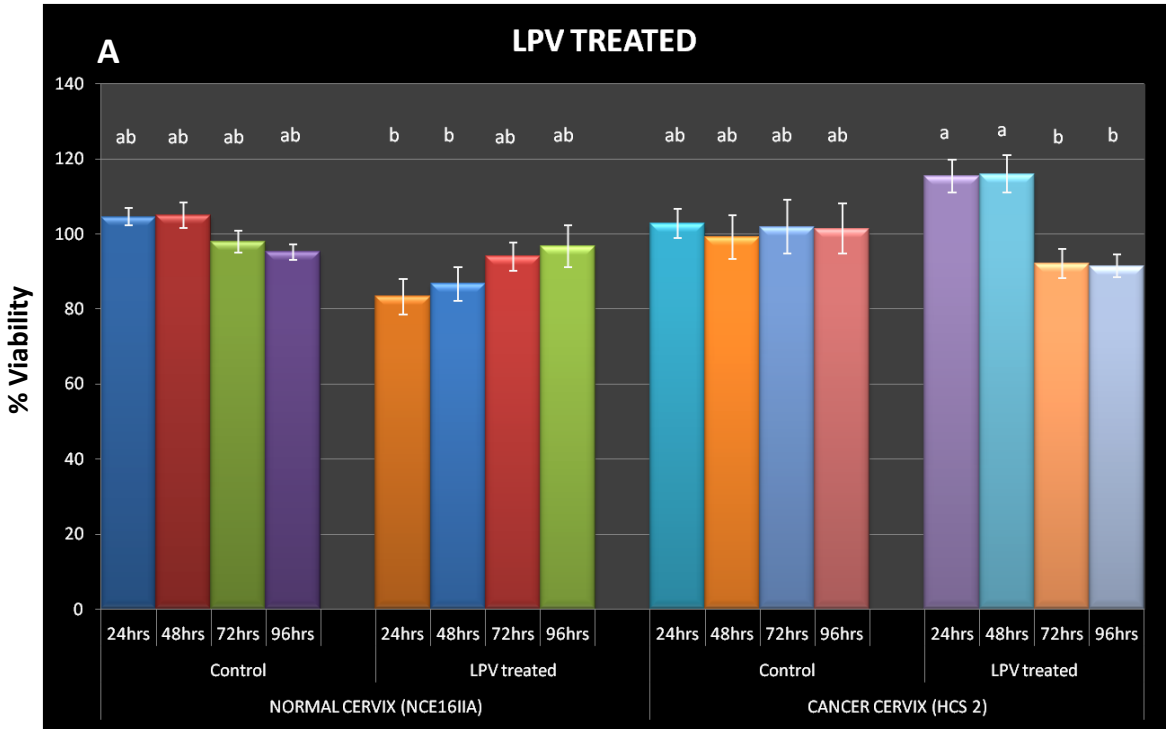

Fig. 3.5A: Effects of LPV on the percentage viability of normal cervical (NCE16IIA) and cervical cancer (HCS-2) cells. Cells were incubated with 9.8µg/ml LPV for 24 – 96 hrs. Graphs were plotted with mean ±SEM percentage viability from a mean of three independent experiments. Groups not connected by the same letter are significantly different ($p<0.05$).

3.1.10 Effects of LPV on the viability of the breast cells

LPV significantly ($p<0.05$) reduced the viability of the normal breast MCF-10A cells at 24 hours when compared to the vehicle control (Fig. 3.5B). Also at 24 hours, LPV significantly ($p<0.05$) reduced the percentage viability of the normal breast cells when compared to the cancer breast MCF-7 cells (Fig. 3.5B). With continuous exposure, the normal breast cells recovered from the initial cytotoxic effects of LPV, such that at 48 to 96 hours, there were no significant differences between the treated cells and their vehicle controls (Fig. 3.5B). LPV did not significantly ($p<0.05$) alter the percentage viability of the breast cancer MCF-7 cells from 24 to 96 hours when compared to their vehicle controls (Fig. 3.5B).

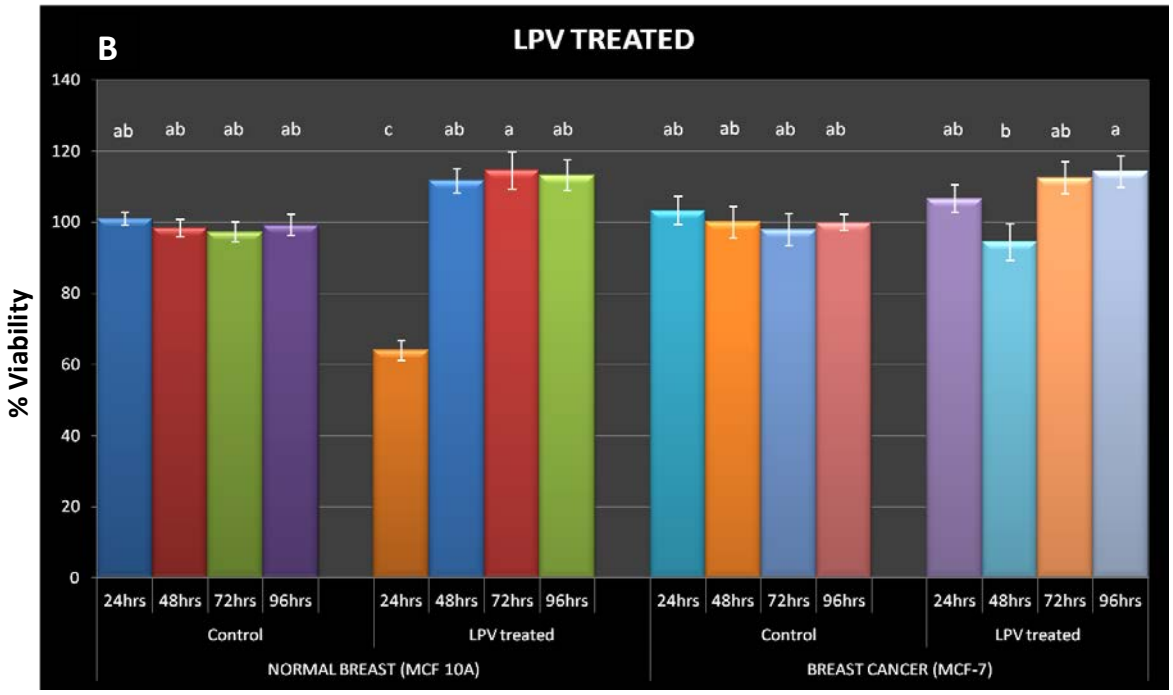

Fig. 3.5B: Effects of LPV on the percentage viability of normal breast (MCF-10A) and breast cancer (MCF-7) cells. Cells were incubated with 9.8µg/ml LPV for 24 – 96 hrs. Graphs were plotted with mean ±SEM percentage viability from a mean of three independent experiments. Groups not connected by the same letter are significantly different ($p<0.05$).

3.1.11 Effects of RTV on the viability of the cervical cells

The PI, RTV, did not significantly ($p<0.05$) alter the percentage viability of the normal (NCE16IIA) and cancer (HCS-2) cervical cells from 24 to 96 hours when compared to their respective vehicle controls and to each other at the respective time points (Fig. 3.6A).

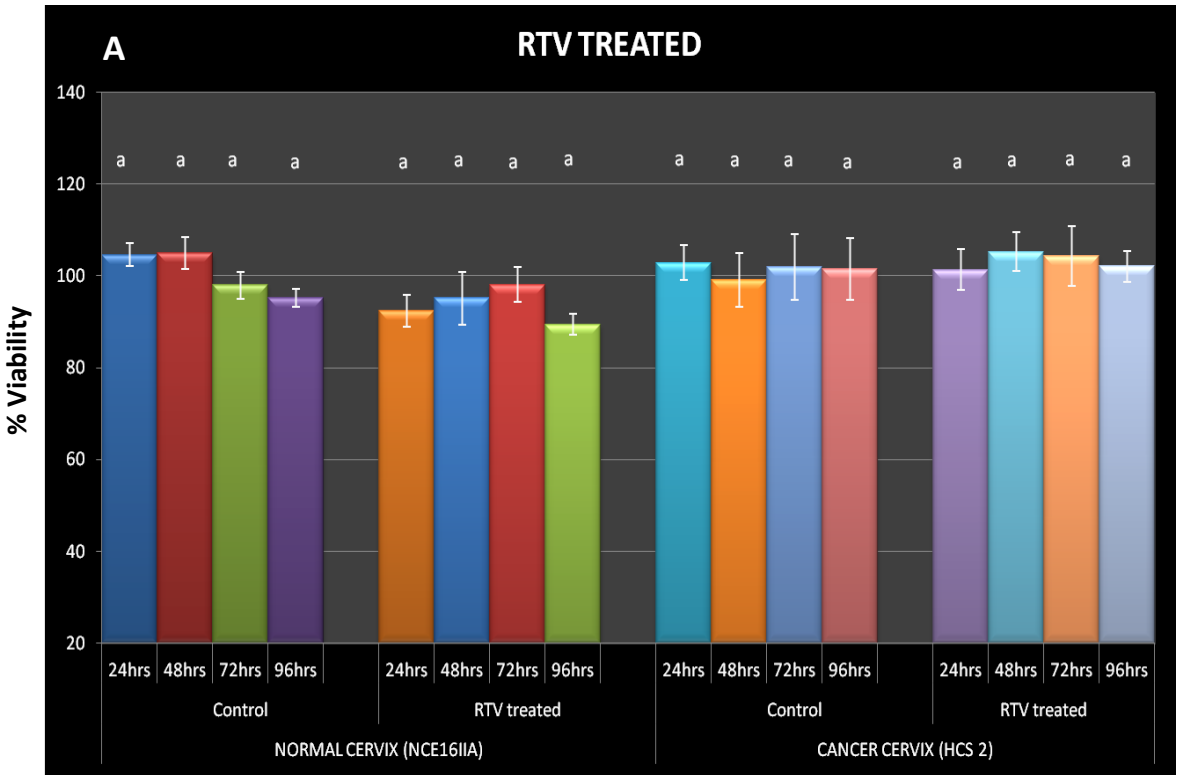

Fig. 3.6A: Effects of RTV on the percentage viability of normal cervical (NCE16IIA) and cervical cancer (HCS-2) cells. Cells were incubated with 0.6µg/ml RTV for 24 – 96 hrs. Graphs were plotted with mean ±SEM percentage viability from a mean of three independent experiments. Groups not connected by the same letter are significantly different ($p<0.05$).

3.1.12 Effects of RTV on the viability of the breast cells

RTV significantly ($p<0.05$) reduced the viability of the normal breast MCF-10A cells when compared to the vehicle control and the breast cancer MCF-7 cells at 24 hours (Fig. 3.6B). At 48 hours there was no significant ($p<0.05$) alteration in percentage viability between RTV treated and untreated in either cell line. At 72 hours, RTV treated MCF-10A cells demonstrated significantly ($p<0.05$) increased viability, while at 96 hours, there was no statistical significance in the difference between RTV treated and untreated MCF-10A cells (Fig. 3.6B). RTV did not alter the percentage viability of the breast cancer MCF-7 cells from 24 to 96 hours (Fig. 3.6B).

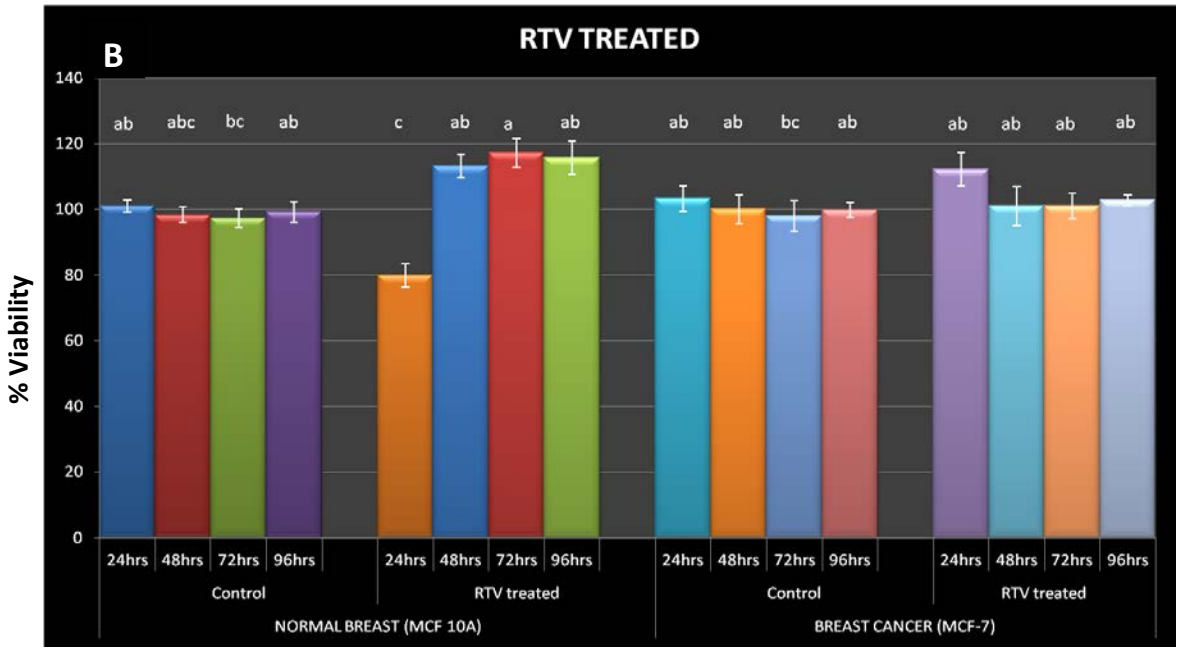

Fig. 3.6B: Effects of RTV on the percentage viability of normal breast (MCF-10A) and breast cancer (MCF-7) cells. Cells were incubated with 0.6µg/ml RTV for 24 – 96 hrs. Graphs were plotted with mean ±SEM percentage viability from a mean of three independent experiments. Groups not connected by the same letter are significantly different ($p<0.05$).

3.1.13 Effects of LPV/r on the viability of the cervical cells

The combination of LPV and RTV, as combined in KALETRA®, did not significantly ($p<0.05$) alter the percentage viability of the normal (NCE16IIA) and cancer (HCS-2) cervical cells from 24 to 96 hours when compared to their respective vehicle controls and to each other at the respective time points (Fig. 3.7A).

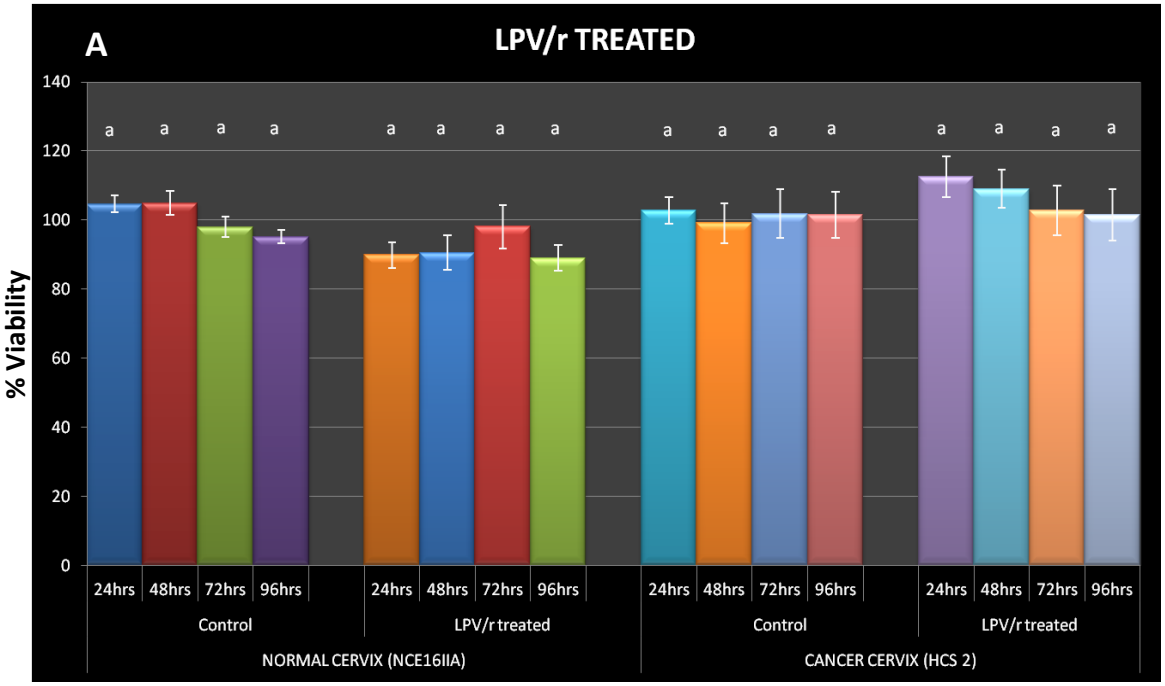

Fig. 3.7A: Effects of LPV/r on the percentage viability of normal cervical (NCE16IIA) and cervical cancer (HCS-2) cells. Cells were incubated with 9.8µg/ml LPV/0.6µg/ml RTV for 24 – 96 hrs. Graphs were plotted with mean ±SEM percentage viability from a mean of three independent experiments. Groups not connected by the same letter are significantly different ($p<0.05$).

3.1.14 Effects of LPV/r on the viability of the breast cells

The combination LPV/r did not significantly ($p<0.05$) alter the percentage viability of the normal (MCF-10A) and cancer (MCF-7) breast cells from 24 to 96 hours when compared to their respective vehicle controls and to each other at the respective time points (Fig. 3.7B).

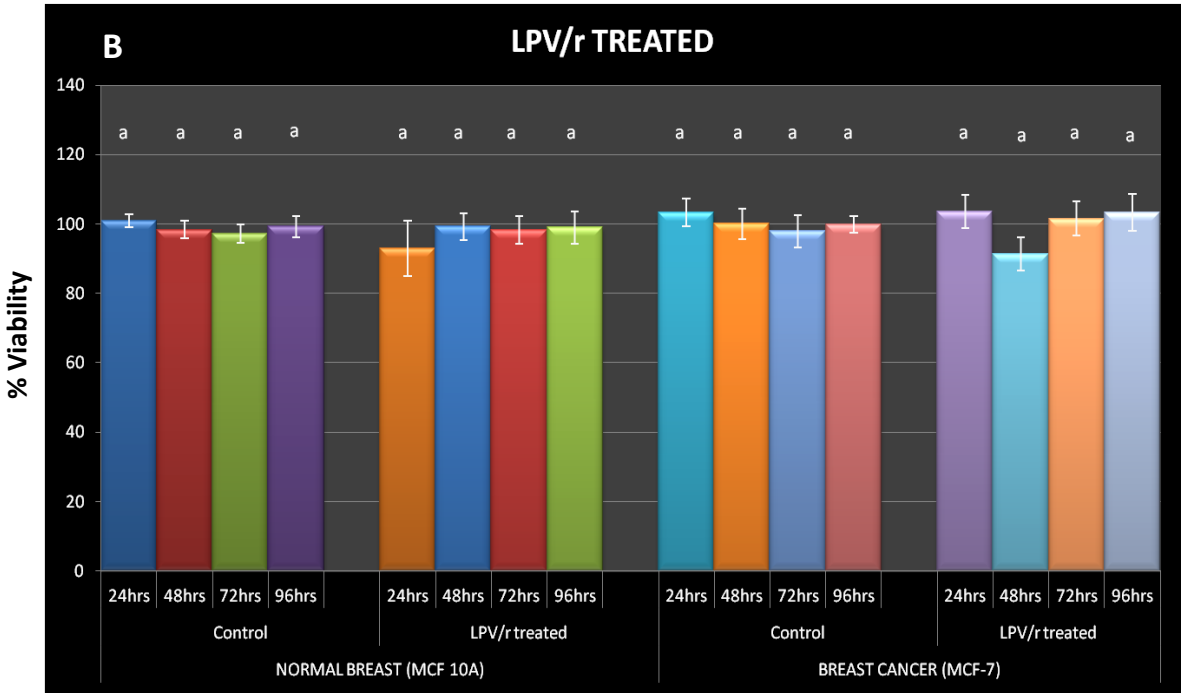

Fig. 3.7B: Effects of LPV/r on the percentage viability of normal breast (MCF-10A) and breast cancer (MCF-7) cells. Cells were incubated with 9.8µg/ml LPV/0.6µg/ml RTV for 24 – 96 hrs. Graphs were plotted with mean ±SEM percentage viability from a mean of three independent experiments. Groups not connected by the same letter are significantly different ($p<0.05$).

3.1.15 Effects of TDF/FTC/LPV/r on the viability of the cervical cells

TDF/FTC/LPV/r significantly ($p<0.05$) reduced the viability of the normal cervical (NCE16IIA) cells when compared to the vehicle control and the cervical cancer HCS-2 cells at 24 hours (Fig. 3.8A). At 48 hours, the viability of the NCE16IIA cells remained reduced when compared to the HCS-2 cells but the difference was not significant ($p<0.05$) when compared to the vehicle controls (Fig. 3.8A). With continuous exposure (72 to 96 hours), the combination had no significant effects on the percentage viability of the normal and cancer cervical cells (Fig. 3.8A).

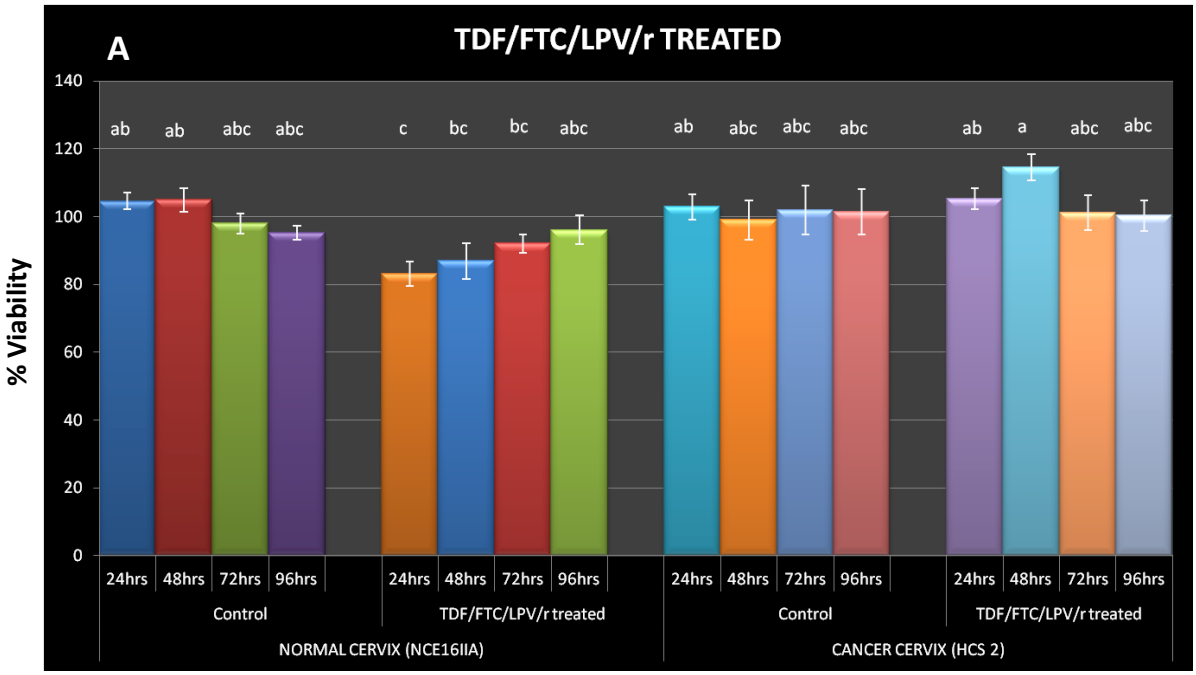

Fig. 3.8A: Effects of TDF/FTC/LPV/r on the percentage viability of normal cervical (NCE16IIA) and cervical cancer (HCS-2) cells. Cells were incubated with 1.8µg/ml FTC; 0.3µg/ml TDF; 9.8µg/ml; LPV/0.6µg/ml RTV for 24 – 96 hrs. Graphs were plotted with mean ±SEM percentage viability from a mean of three independent experiments. Groups not connected by the same letter are significantly different ($p<0.05$).

3.1.16 Effects of TDF/FTC/LPV/r on the viability of the breast cells

At 24 hours, the combination of TDF/FTC/LPV/r reduced the viability of the normal breast MCF-10A cells, but the reduction was not significantly ($p<0.05$) different from the vehicle control or from the breast cancer MCF-7 cells (at 24 hours) (Fig. 3.8B). At 48 hours, this combination significantly ($p<0.05$) reduced the viability of the cancer MCF-7 cells when compared to the normal MCF-10A cells. The effects of this combination on the breast cells at 48 hours were, however, not significantly different from their respective vehicle controls (Fig. 3.8B). At 72 hours, TDF/FTC/LPV/r significantly ($p<0.05$) increased the viability of the normal breast cells when compared to the vehicle control (Fig. 3.8B). At 72 and 96 hours, there were no significant differences between the viability of the normal and breast cancer cells (Fig. 3.8B).

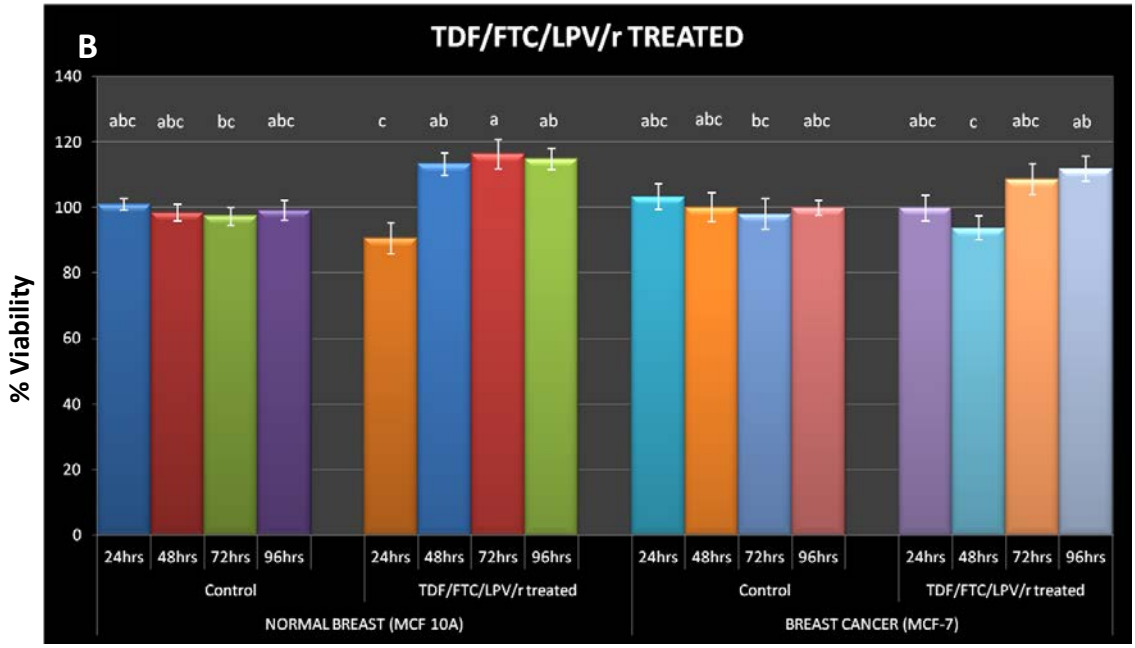

Fig. 3.8B: Effects of TDF/FTC/LPV/r on the percentage viability of normal breast (MCF-10A) and breast cancer (MCF-7) cells. Cells were incubated with 1.8µg/ml FTC; 0.3µg/ml TDF; 9.8µg/ml; LPV/0.6µg/ml RTV for 24 – 96 hrs. Graphs were plotted with mean ±SEM percentage viability from a mean of three independent experiments. Groups not connected by the same letter are significantly different ($p<0.05$).

Table 3.1: Summary of the effects of ARVs on normal and cancer cervical and normal and cancer breast cell lines with regard to cell survival using the Neutral red assay.

Drugs	Normal Cervical (NC)	Cancer Cervical (CC)	Normal Breast (NB)	Breast Cancer (BC)	Result	Remark
TDF	(+0)	(0-)	(-+)	(0-)	Promotes normal cell survival (NC initially and NB later) over cancer cells. Decreasing effect on both cancers.	Has an initial cytotoxic effect on cell survival in the normal breast. It has a slow ongoing effect in the cervix. Generally seems to promote normal cell survival over cancer cells
FTC	(+-)	0	(0-)	(-0)	Prolonged treatment show decreasing effects on normal cells. Favours CC with prolonged treatment	Has opposing effects on NC and CC after 96 hours of treatment.
EFV	(-0)	(+-)	(--)	(0+)	Promotes BC, decreases NB and CC.	Cytotoxic to normal breast cells, but favours breast cancer cells
ATP	(--)	(++)	(-0)	(+0)	Decreases NC promotes CC. Decreases NB at 24 hrs and has increasing effect on BC up to 72 hrs	Favours the survival of cancer cells compared to the normal
LPV	(-0)	(+0)	(-+)	(0+)	Promotes NB and BC. Decreasing effect on CC (72 to 96 hrs)	Generally appear to promote survival in the breast and CC in the short term
RTV	0	0	(-+)	0	Promotes NB.	Has opposing effects on NB and BC at 24 hours. Generally appears to promote survival in normal breast after an initial toxic effect
LPV/r	0	0	0	0	No effect	Interestingly, the combination of the two PIs has no effects on all cell lines
TDF/FTC /LPV/r	(-0)	(+0)	(-+)	(0+)	Has promoting effects on NB and BC. Has opposing effects on NC and CC at 24 and 48 hrs	Shows a trend towards breast cell survival

(0) = No effect on cell viability, (+) = increased cell viability, (-) = decreased cell viability.

3.2 Effects of Antiretroviral drugs on apoptotic *BAX*; *BCL-2,* and angiogenic $VEGF_{165a}$ and $VEGF_{165b}$ gene expression in cervical and breast cell lines

BAX is a pro-apoptotic gene that is involved in the release of cytochrome c from the inner mitochondrial membrane (Rosse *et al.,* 1998). *BCL-2* is a human proto-oncogene that modulates apoptotic pathways by regulating the release of pro-apoptotic molecules from the mitochondria. The effects of the antiretroviral drugs on *BAX* and *BCL-2* mRNA expression in all cell lines were investigated after a 96 hour exposure. The mRNA expression levels of the pro-angiogenic and anti-angiogenic VEGFA splice variants ($VEGF_{165a}$ and $VEGF_{165b}$) were also investigated.

3.2.1 The NRTI – TDF

TDF increased *BAX* and *BCL-2* gene expression in the two cervical cell lines, though to a lesser degree in the cancer cervical cells (Fig. 3.9A). TDF slightly up-regulated the pro-angiogenic $VEGF_{165a}$ in the normal cervical cells but slightly down-regulated both $VEGF_{165a}$ and the anti-angiogenic $VEGF_{165b}$ in the cervical cancer cells (Fig. 3.9A). With respect to the breast cell lines, TDF slightly down-regulated *BAX* in the normal and cancer cell lines (Fig. 3.9B). TDF increased and decreased *BCL-2* slightly in the normal and breast cancer cells respectively (Fig. 3.9B). In response to TDF, $VEGF_{165a}$ and $VEGF_{165b}$ were both slightly up-regulated in the normal breast cells and both down-regulated in the breast cancer MCF-7 cells, with $VEGF_{165a}$ more so than $VEGF_{165b}$ in both cases (Fig. 3.9B). In all breast and cervical cells treated with TDF, the differences in fold changes were not significantly ($p<0.05$) different from the untreated controls for *BAX, BCL-2,* $VEGF_{165a}$ and $VEGF_{165b}$ (Fig. 3.9). *BAX* was slightly up-regulated in the cervical cells, but down-regulated in the breast cell lines. In addition, the expression of *BCL*-2 followed

opposite patterns in the two cancer cell lines; increased in the cervical cancer and decreased in the breast cancer cells.

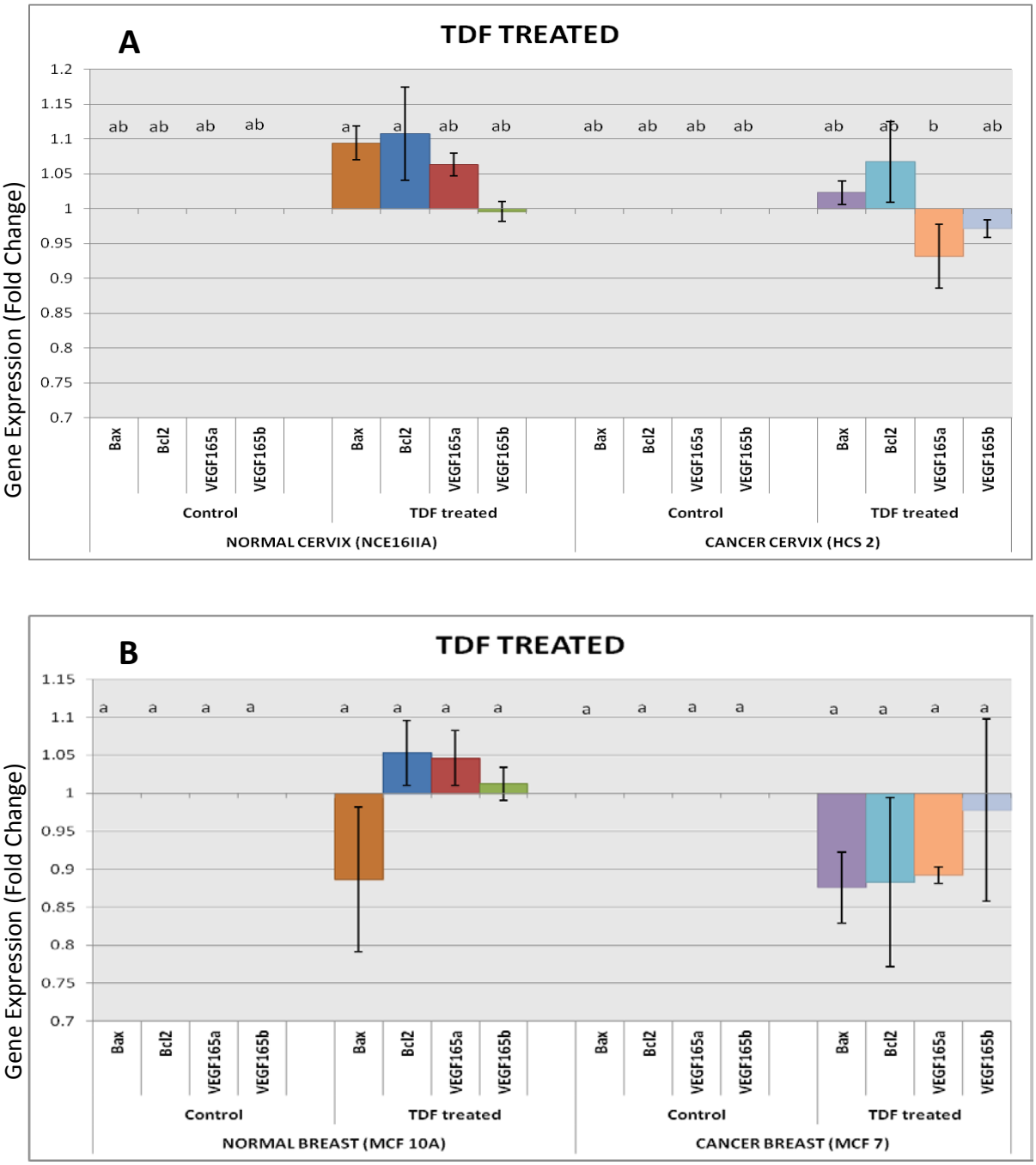

Figure 3.9: Effects of TDF on *BAX*, *BCL-2*, *VEGF*$_{165a}$ *and VEGF*$_{165b}$ mRNA expression in (**A**) NCE16IIA (normal cervical); HCS-2 (cervical cancer) and (**B**) MCF-10A (normal breast); MCF-7 (breast cancer) cells. Cells were incubated with 0.3µg/ml TDF for 96 hours. Data (mean ± SEM), are represented as fold changes of gene expression relative to values from the vehicle-treated cells (defined as 1) and representative of 3 independent experiments for RNA extraction. Groups not connected by the same letter are significantly ($p<0.05$) different.

3.2.2 FTC

After 96 hours of exposure, FTC slightly increased *BAX* expression in the normal cervical but not the cancer cervical cells (Fig. 3.10A). *BCL-2* expression was also slightly increased in both cervical cell lines. The expression of the pro-angiogenic $VEGF_{165a}$ was up-regulated by FTC in the normal but not the cancer cervical cells (Fig. 3.10A). FTC did not affect the levels of the anti-angiogenic $VEGF_{165b}$ (Fig. 3.10A) in the cervical cells.

FTC up-regulated *BAX* and *BCL-2* in the normal breast MCF-10A cells while *BAX* and *BCL-2* levels were down-regulated in the cancer breast MCF-7 cells (Fig. 3.10B). The levels of both the pro and anti-angiogenic $VEGF_{165}$ were down-regulated in the breast cancer MCF-7 cells (Fig. 3.10B). In all cell lines treated with FTC, the differences in fold changes were not significantly ($p<0.05$) different from the untreated controls for *BAX*, *BCL-2*, $VEGF_{165a}$ and $VEGF_{165b}$ (Fig. 3.10). FTC treatment produced opposite trends of *BAX* and *BCL*-2 mRNA expression in the two cancer cell lines; slightly up-regulated in the cervical cancer and down-regulated in the breast cancer cell line.

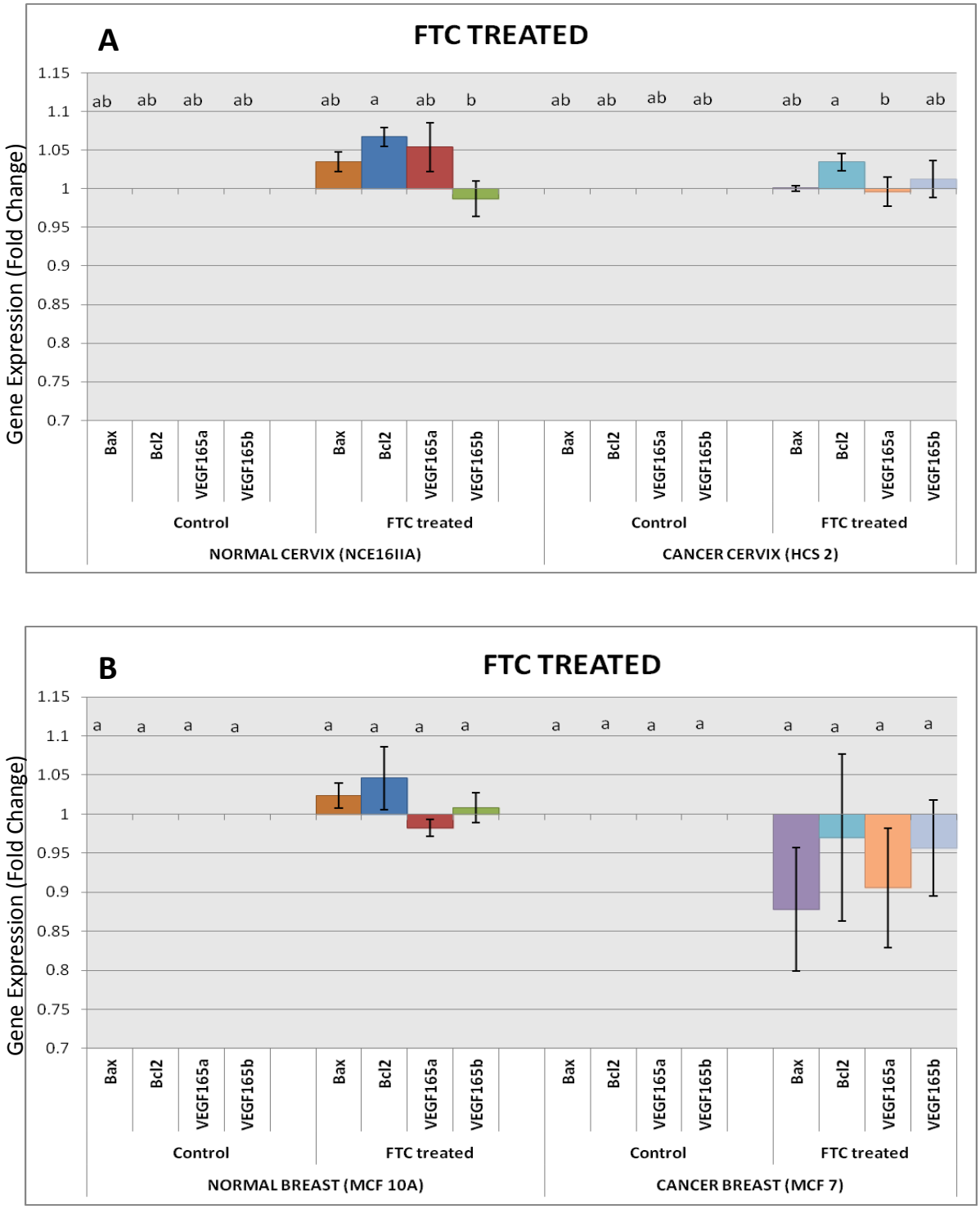

Figure 3.10: Effects of FTC on *BAX*, *BCL-2*, *VEGF*$_{165a}$ *and VEGF*$_{165b}$ mRNA expression in (**A**) NCE16IIA (normal cervical); HCS-2 (cervical cancer) and (**B**) MCF-10A (normal breast); MCF-7 (breast cancer) cells. Cells were incubated with 1.8µg/ml FTC for 96 hours. Data (mean ± SEM), are represented as fold changes of gene expression relative to values from the vehicle-treated cells (defined as 1) and representative of 3 independent experiments for RNA extraction. Groups not connected by the same letter are significantly ($p<0.05$) different.

3.2.3 EFV

In the normal cervical (NCE16IIA) cells, EFV slightly up-regulated *BAX* and down-regulated *BCL-2* expression, while in the cancer cervical HCS-2 cells, EFV down-regulated the levels of both *BAX* and *BCL-2* (Fig. 3.11A). EFV also slightly increased the levels of the pro-angiogenic $VEGF_{165a}$ in the normal cervical cells and slightly reduced the levels of both angiogenic $VEGF_{165}$ genes in the cervical cancer cells (Fig. 3.11A).

In the normal breast cells, EFV only slightly increased the levels of *BCL-2,* while in the breast cancer MCF-7 cells, the levels of *BAX, BCL-2 and* $VEGF_{165a}$ were slightly reduced (Fig. 3.11B). EFV also slightly increased the levels of the anti-angiogenic $VEGF_{165b}$ in the breast cancer cells (Fig. 3.11B). In all cell lines treated with EFV, the differences in fold changes were not significantly ($p<0.05$) different from the untreated controls for *BAX, BCL-2,* $VEGF_{165a}$ and $VEGF_{165b}$ (Fig. 3.11). However, EFV treatment produced opposing trends of *BCL*-2 mRNA expression in the two normal cell lines; slight down-regulation in the normal cervical and up-regulation in the normal breast cell line.

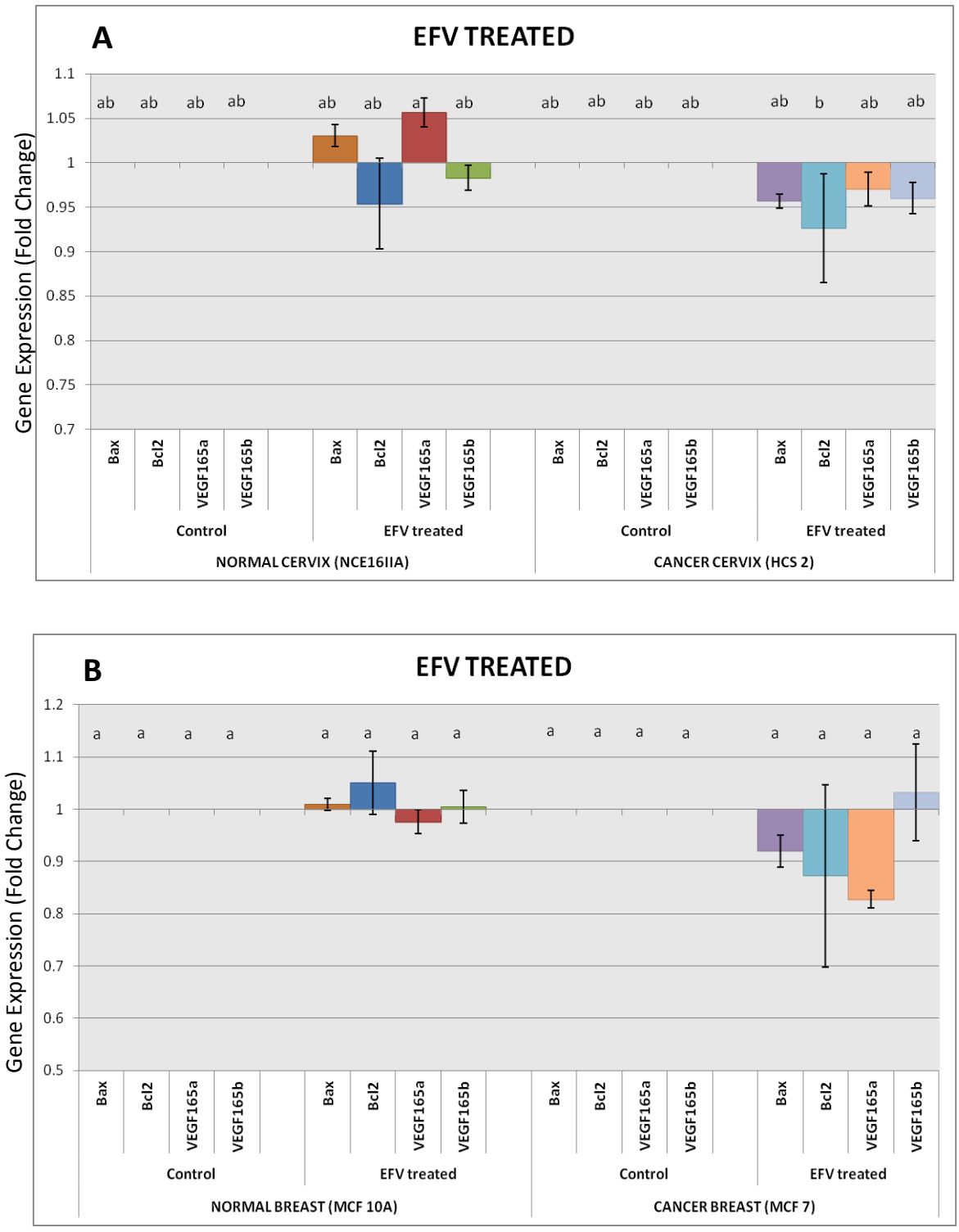

Figure 3.11: Effects of EFV on *BAX*, *BCL-2*, *VEGF*$_{165a}$ *and VEGF*$_{165b}$ mRNA expression in (**A**) NCE16IIA (normal cervical); HCS-2 (cervical cancer) and (**B**) MCF-10A (normal breast); MCF-7 (breast cancer) cells. Cells were incubated with 4.07µg/ml EFV for 96 hours. Data (mean ± SEM), are represented as fold changes of gene expression relative to values from the vehicle-treated cells (defined as 1) and representative of 3 independent experiments for RNA extraction. Groups not connected by the same letter are significantly ($p<0.05$) different.

3.2.4 ATP

ATP slightly increased the levels of *BAX* in the normal cervical cells but decreased the levels of *BAX* in the cervical cancer cells (Fig. 3.12A). The level of BCL-2 was also slightly increased in the normal cervical cells but not in the cervical cancer cells (Fig. 3.12A). The level of the pro-angiogenic $VEGF_{165a}$ was slightly increased in the normal cervical cells, but only slightly reduced in the cervical cancer cells (Fig. 3.12A).

In the normal breast MCF-10A cells, in response to ATP, *BAX* levels were slightly up-regulated while it was down-regulated in the breast cancer MCF-7 cells (Fig. 3.12B). *BCL-2* levels were decreased in the normal breast cells. $VEGF_{165a}$ levels were decreased in the breast cancer cells compared to the normal cells while the levels of $VEGF_{165b}$ were slightly increased in the normal breast but decreased in the breast cancer cells (Fig. 3.12B). In all cell lines treated with ATP, the differences in fold changes were not significantly ($p<0.05$) different from the untreated controls for *BAX*, *BCL-2*, $VEGF_{165a}$ and $VEGF_{165b}$ (Fig. 3.12). But opposite trends of *BCL*-2 mRNA expression were observed in the two normal cell lines in response to ATP treatment; slight up-regulation in the normal cervical and down-regulation in the normal breast cell line.

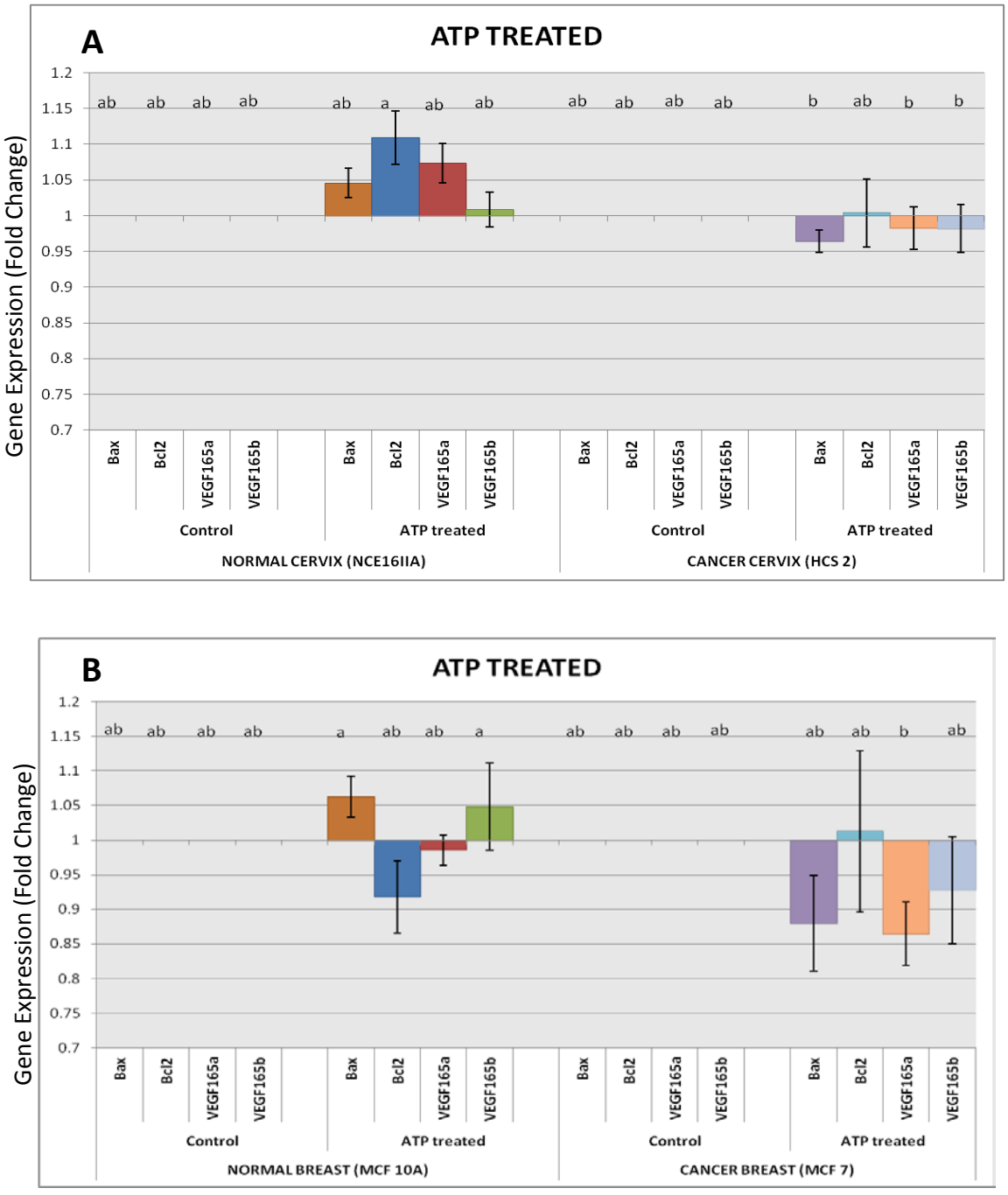

Figure 3.12: Effects of ATP on *BAX*, *BCL-2*, $VEGF_{165a}$ *and* $VEGF_{165b}$ mRNA expression in (**A**) NCE16IIA (normal cervical); HCS-2 (cervical cancer) and (**B**) MCF-10A (normal breast); MCF-7 (breast cancer) cells. Cells were incubated with 0.3µg/ml TDF; 1.8µg/ml FTC; 4.07µg/ml EFV for 96 hours. Data (mean ± SEM), are represented as fold changes of gene expression relative to values from the vehicle-treated cells (defined as 1) and representative of 3 independent experiments for RNA extraction. Groups not connected by the same letter are significantly ($p<0.05$) different.

3.2.5 LPV

After 96 hours of treatment, LPV slightly increased the *BAX* and *BCL-2* levels in the normal cervical (NCE16IIA) cells but decreased *BAX* and *BCL-2* levels in the cervical cancer HCS-2 cells (Fig. 3.13A). $VEGF_{165a}$ levels were slightly increased in the normal cervical cells while $VEGF_{165b}$ levels were slightly decreased in the cervical cancer cells (Fig. 3.13A).

In response to LPV, *BAX* levels were decreased in both normal and breast cancer cells (Fig. 3.13B). *BCL-2* levels were decreased in the normal breast cells while it was slightly increased in the breast cancer MCF-7 cells (Fig. 3.13B). The pro-angiogenic $VEGF_{165a}$ levels were decreased in both breast cell lines while $VEGF_{165b}$ levels were decreased in the normal breast cells only (Fig. 3.13B). LPV treatment produced opposing trends of *BAX* and *BCL*-2 mRNA expression in the two normal cell lines; slightly up-regulated in the normal cervical and down-regulated in the normal breast cell line. In all cell lines treated with LPV, the differences in fold changes were not significantly ($p<0.05$) different from the untreated controls for *BAX*, *BCL-2*, $VEGF_{165a}$ and $VEGF_{165b}$ (Fig. 3.13).

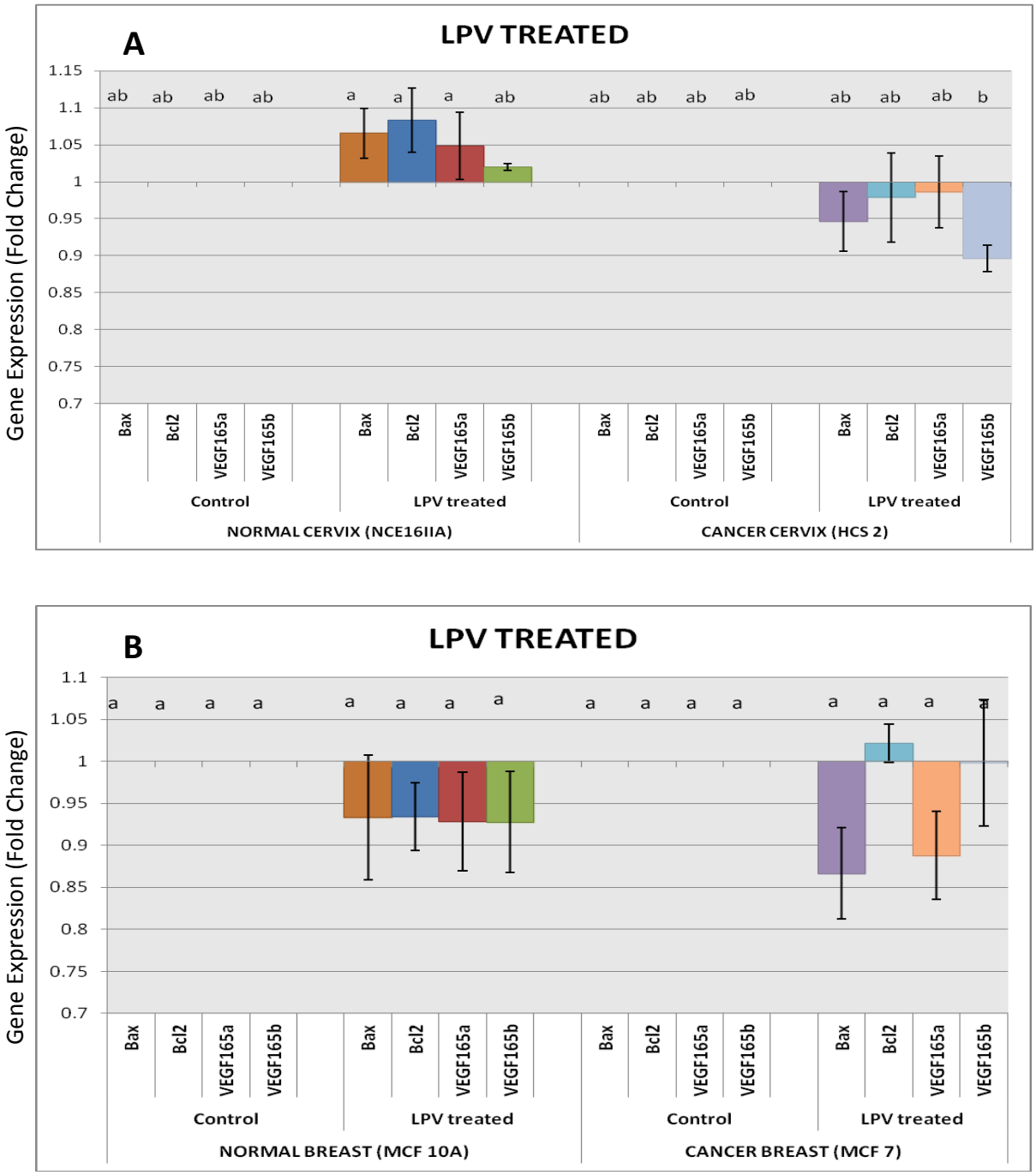

Figure 3.13: Effects of LPV on *BAX*, *BCL-2*, *VEGF*$_{165a}$ *and VEGF*$_{165b}$ mRNA expression in (**A**) NCE16IIA (normal cervical); HCS-2 (cervical cancer) and (**B**) MCF-10A (normal breast); MCF-7 (breast cancer) cells. Cells were incubated with 9.8µg/ml LPV for 96 hours. Data (mean ± SEM), are represented as fold changes of gene expression relative to values from the vehicle-treated cells (defined as 1) and representative of 3 independent experiments for RNA extraction. Groups not connected by the same letter are significantly ($p<0.05$) different.

3.2.6 RTV

In the normal cervical cells, RTV slightly increased the levels of *BAX* and *BCL-2* genes (Fig. 3.14A). In response to RTV, in the cancer cervical cells, *BAX* levels were slightly decreased, while *BCL-2* levels were slightly increased (Fig. 3.14A). The levels of the angiogenic genes $VEGF_{165a}$ and $VEGF_{165b}$ were also slightly increased in the normal cervical cells, while their levels were slightly decreased in the cervical cancer HCS-2 cells (Fig. 3.14A).

In response to RTV, *BAX* levels were slightly increased in the normal breast MCF-10A cells, but decreased in the breast cancer MCF-7 cells (Fig. 3.14B). *BCL-2* levels in both breast cells were decreased; but to a greater degree in the normal breast cells (Fig. 3.14B). The levels of the pro-angiogenic $VEGF_{165a}$ were also slightly decreased in the breast cancer MCF-7 cells but not in the normal breast cells (Fig. 3.14B). In all cell lines treated with LPV, the differences in fold changes were not significantly ($p<0.05$) different from the untreated controls for *BAX*, *BCL-2*, $VEGF_{165a}$ and $VEGF_{165b}$ (Fig. 3.14).

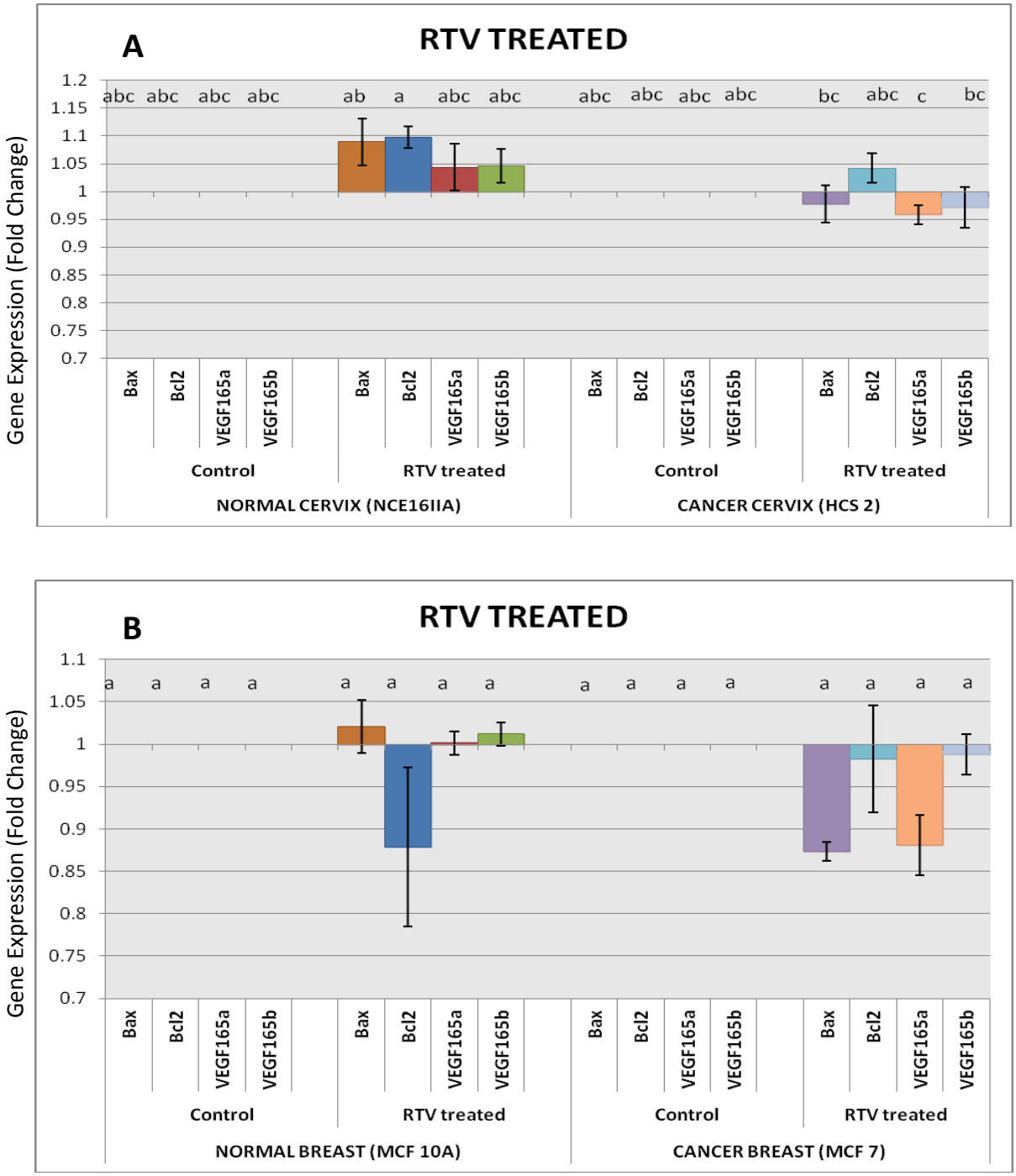

Figure 3.14: Effects of RTV on *BAX*, *BCL-2*, *VEGF*$_{165a}$ *and VEGF*$_{165b}$ mRNA expression in (**A**) NCE16IIA (normal cervical); HCS-2 (cervical cancer) and (**B**) MCF-10A (normal breast); MCF-7 (breast cancer) cells. Cells were incubated with 0.6µg/ml RTV for 96 hours. Data (mean ± SEM), are represented as fold changes of gene expression relative to values from the vehicle-treated cells (defined as 1) and representative of 3 independent experiments for RNA extraction. Groups not connected by the same letter are significantly ($p<0.05$) different.

3.2.7 LPV/r

LPV/r slightly increased *BCL-2* levels in the normal cervical (NCE16IIA) cells but decreased *BCL-2* levels in the cervical cancer HCS-2 cells (Fig. 3.15A). $VEGF_{165a}$ levels were slightly increased in the normal cervical cells while $VEGF_{165a}$ levels were slightly decreased in the cervical cancer cells (Fig. 3.15A). $VEGF_{165b}$ levels were slightly decreased in both cervical cell lines (Fig. 3.15A).

In response to LPV/r, *BAX* levels were slightly decreased in both normal and breast cancer cells (Fig. 3.15B). *BCL-2* and $VEGF_{165a}$ levels were slightly increased in the normal breast cells but their levels were slightly decreased in the breast cancer cells (Fig. 3.15B). $VEGF_{165b}$ levels were slightly increased in the breast cancer cell line (Fig. 3.15B). LPV/r produced similar trends of *BAX* and *BCL*-2 mRNA expression in the two cancer cell lines. In all cell lines treated with LPV/r, the differences in fold changes were not significantly ($p<0.05$) different from the untreated controls for *BAX*, *BCL-2*, $VEGF_{165a}$ and $VEGF_{165b}$ (Fig. 3.15).

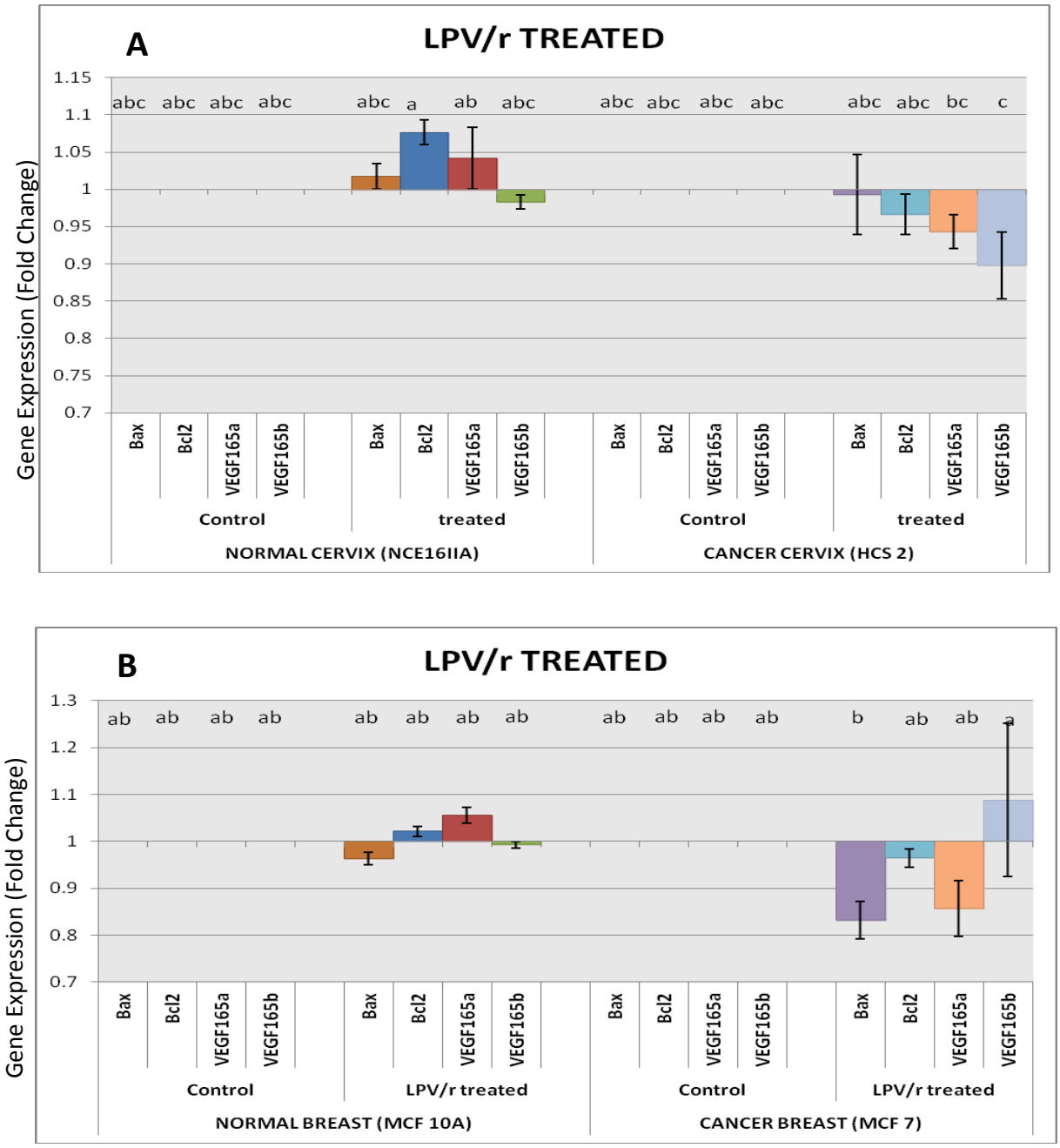

Figure 3.15: Effects of LPV/r on *BAX*, *BCL-2*, *VEGF*$_{165a}$ *and VEGF*$_{165b}$ mRNA expression in (**A**) NCE16IIA (normal cervical); HCS-2 (cervical cancer) and (**B**) MCF-10A (normal breast); MCF-7 (breast cancer) cells. Cells were incubated with 9.8µg/ml LPV; 0.6µg/ml RTV for 96 hours. Data (mean ± SEM), are represented as fold changes of gene expression relative to values from the vehicle-treated cells (defined as 1) and representative of 3 independent experiments for RNA extraction. Groups not connected by the same letter are significantly ($p<0.05$) different.

3.2.8 TDF/FTC/LPV/r

TDF/FTC/LPV/r slightly increased the *BAX* and *BCL-2* levels in the normal cervical (NCE16IIA) cells but slightly decreased *BAX* levels in the cervical cancer HCS-2 cells (Fig. 3.16A). $VEGF_{165a}$ levels were slightly increased in the normal cervical cells but slightly decreased in the cervical cancer cells (Fig. 3.16A). $VEGF_{165b}$ levels were slightly decreased in both cervical cell lines (Fig. 3.16A) but more so in the cancer cell line.

In the breast cell lines, this combination slightly increased *BAX* levels in the normal breast and slightly decreased *BAX* levels in the cancer MCF-7 cells. *BCL-2* levels were slightly increased in both breast cell lines (Fig. 3.16B). $VEGF_{165a}$ levels were slightly increased in the normal breast cells but were slightly decreased in the breast cancer cells (Fig. 3.16B). $VEGF_{165b}$ levels were slightly decreased in the normal breast cells but were not altered in the breast cancer cells (Fig. 3.16B). In all cell lines treated with LPV/r, the differences in fold changes were not significantly ($p<0.05$) different from the untreated controls for *BAX*, *BCL-2*, $VEGF_{165a}$ and $VEGF_{165b}$ (Fig. 3.16).

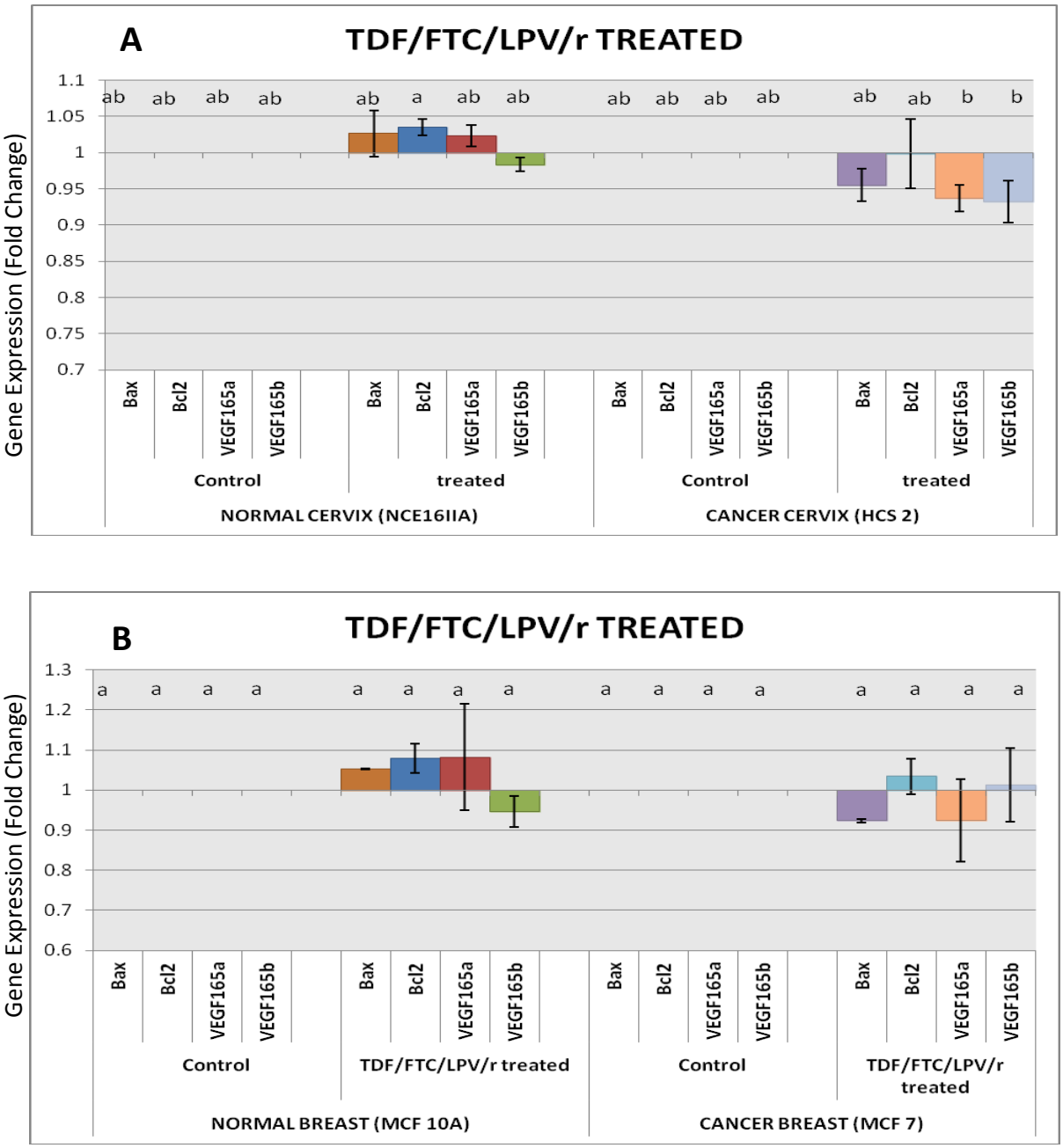

Figure 3.16: Effects of TDF/FTC/LPV/r on *BAX*, *BCL-2*, *VEGF*$_{165a}$ *and VEGF*$_{165b}$ mRNA expression in (**A**) NCE16IIA (normal cervical); HCS-2 (cervical cancer) and (**B**) MCF-10A (normal breast); MCF-7 (breast cancer) cells. Cells were incubated with 0.3µg/ml TDF; 1.8µg/ml FTC; 9.8µg/ml LPV; 0.6µg/ml RTV for 96 hours. Data (mean ± SEM), are represented as fold changes of gene expression relative to values from the vehicle-treated cells (defined as 1) and representative of 3 independent experiments for RNA extraction. Groups not connected by the same letter are significantly ($p<0.05$) different.

Table 3.2: Summary of the effects of ARVs on *BAX*, *BCL-2*, *VEGF165A* and *VEGF165B* mRNA expression in normal and cancer cervical and normal and cancer breast cell lines. +/++/+++ (up-regulation); 0 (no change); -/--/--- (down-regulation).

Treatment	Gene Expresion	Normal Cervical (NCE16IIA)	Cancer Cervical (HCS-2)	Normal Breast (MCF-10A)	Breast Cancer (MCF-7)
0.3 µg/ml TDF	***BAX***	+	+	--	--
	BCL-2	+	+	+	--
	VEGF165A	+	-	+	--
	VEGF165B	0	-	0	0
1.8µg/ml FTC	***BAX***	+	0	+	--
	BCL-2	+	+	+	-
	VEGF165A	+	0	-	--
	VEGF165B	-	0	0	-
4.07µg/ml EFV	***BAX***	+	-	0	-
	BCL-2	-	-	+	--
	VEGF165A	+	-	-	--
	VEGF165B	-	-	0	+
ATRIPLA TDF/FTC/ EFV	***BAX***	+	-	+	--
	BCL-2	++	0	-	+
	VEGF165A	+	-	-	--
	VEGF165B	0	-	+	-
9.8µg/ml LPV	***BAX***	+	-	-	--
	BCL-2	+	-	-	+
	VEGF165A	+	-	-	--
	VEGF165B	+	--	-	0
0.6 µg/ml RTV	***BAX***	+	-	+	--
	BCL-2	+	+	--	-
	VEGF165A	+	-	0	--
	VEGF165B	+	-	+	-
KALETRA (LPV/r)	***BAX***	+	-	-	-
	BCL-2	+	-	+	-
	VEGF165A	+	-	+	-
	VEGF165B	-	--	0	+
TDF/FTC/ LPVr	***BAX***	+	-	+	-
	BCL-2	+	0	+	+
	VEGF165A	+	-	+	-
	VEGF165B	-	-	-	0

3.3. Immunofluorescence of BAX, BCL-2 and VEGF165b proteins in cancer (HCS-2) and normal cervical (NCE16IIA) and cancer (MCF-7) and normal breast (MCF-10A) cells exposed to antiretroviral drugs

The effects of the antiretroviral drugs on BAX, BCL-2 protein expression (localisation and intensity) in all cell lines were investigated after a 96 hour exposure. The protein expression levels of the anti-angiogenic VEGFA splice variant ($VEGF_{165b}$) was also investigated. Negative control groups were set up to ensure that the secondary antibodies were specific for their primary antibodies. The primary antibodies were substituted with 0.1% BSA/PBS and the normal protocol was carried out. In a second negative control, the cells were treated in the same way as the experimental slides, but the secondary antibodies were substituted with PBS. There was lack of non-specific staining in the negative controls and representative fluorescence micrographs of untreated cells serving as no primary antibody control are shown in the last slides labelled 'K' for each antibody staining.

3.3.1 Immunofluorescence of BAX and BCL-2 proteins in cervical cancer (HCS-2) and normal cervical (NCE16IIA) cells exposed to antiretroviral drugs

In the untreated group of HCS-2 cells (Fig. 3.17 A), BAX and BCL-2 proteins are expressed and co-localised in the nuclei and cytoplasm. Mean fluorescent intensities of BAX and BCL-2 in the nuclei and cytoplasm were statistically analysed (ANOVA) between the untreated/vehicle control and the treated groups (Graphical representation presented in Figs. 3.25-3.32; Data summaries shown in Appendix E). There are no differences in protein staining, localisation and intensity of vehicle (0.01% methanol) treated group as compared to growth medium alone (Fig. 3.17B). Both BAX and BCL-2 localisation remained unaltered across treatment groups. Fig. 3.17 C-J illustrates the effect of the antiretroviral drugs on the localisation of BAX and BCL-2 in HCS-2 cell cultures.

Figs. 3.17 C-J are representative images illustrating the effects of the antiretroviral drugs on BAX and BCL-2 expression in the HCS-2 cell cultures. The untreated group of NCE16IIA cells (Fig 3.18A) shows the expression and localisation of BAX. BCL-2 oncoprotein was found to be unexpressed in this normal cervical cell line. There are no differences in protein staining, localisation and intensity of vehicle (0.01% methanol) treated group as compared to growth medium alone (Fig. 3.18B). Fig. 3.18 C-J illustrates the effect of the antiretroviral drugs on expression of BAX and BCL-2 in the NCE16IIA cell cultures. Figs. 3.18 C-J are representative images illustrating the effects of the antiretroviral drugs on expression of BAX and BCL-2 in NCE16IIA cell cultures. BAX and BCL-2 localisation remain unchanged across treatment groups. Mean fluorescent intensities of BAX and BCL-2 in the nuclei and cytoplasm were statistically analysed (ANOVA) between the untreated/vehicle control and the treated groups (Graphical representation presented in Figs. 3.25-3.32; Data summaries shown in Appendix E).

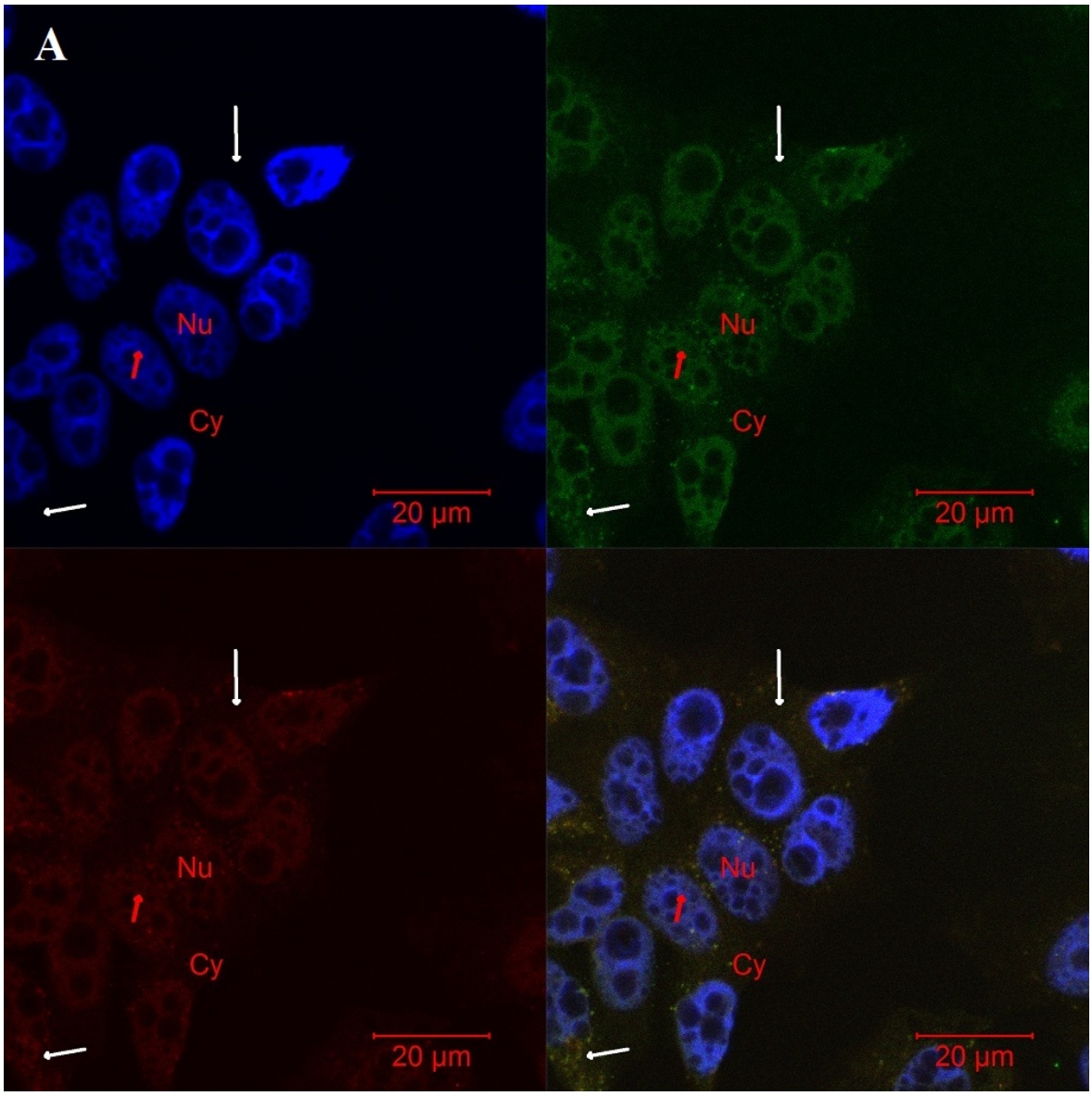

Figure 3.17 A: Fluorescence micrographs of HCS-2 cells exposed to Growth Medium for 96 hours. BCL-2 was stained with Monoclonal Anti-BCL-2 and Goat Anti-Mouse IgG, FITC conjugated (Green channel-Right Upper quadrant). BAX was stained with Polyclonal rabbit Anti-BAX and Goat Anti-Rabbit IgG, Rhodamine conjugated (Red channel-Left Lower quadrant). Nuclei were counterstained with DAPI (Blue channel-Left Upper quadrant). Combined Images are represented in the Right Lower quadrant. Nu=Nucleus, Cy=Cytoplasm. Red arrow points to nuclear staining and White arrow points to cytoplasmic staining. Representative Fluorescence micrographs of untreated cells serving as no primary antibody control are shown in Fig.3.17K.

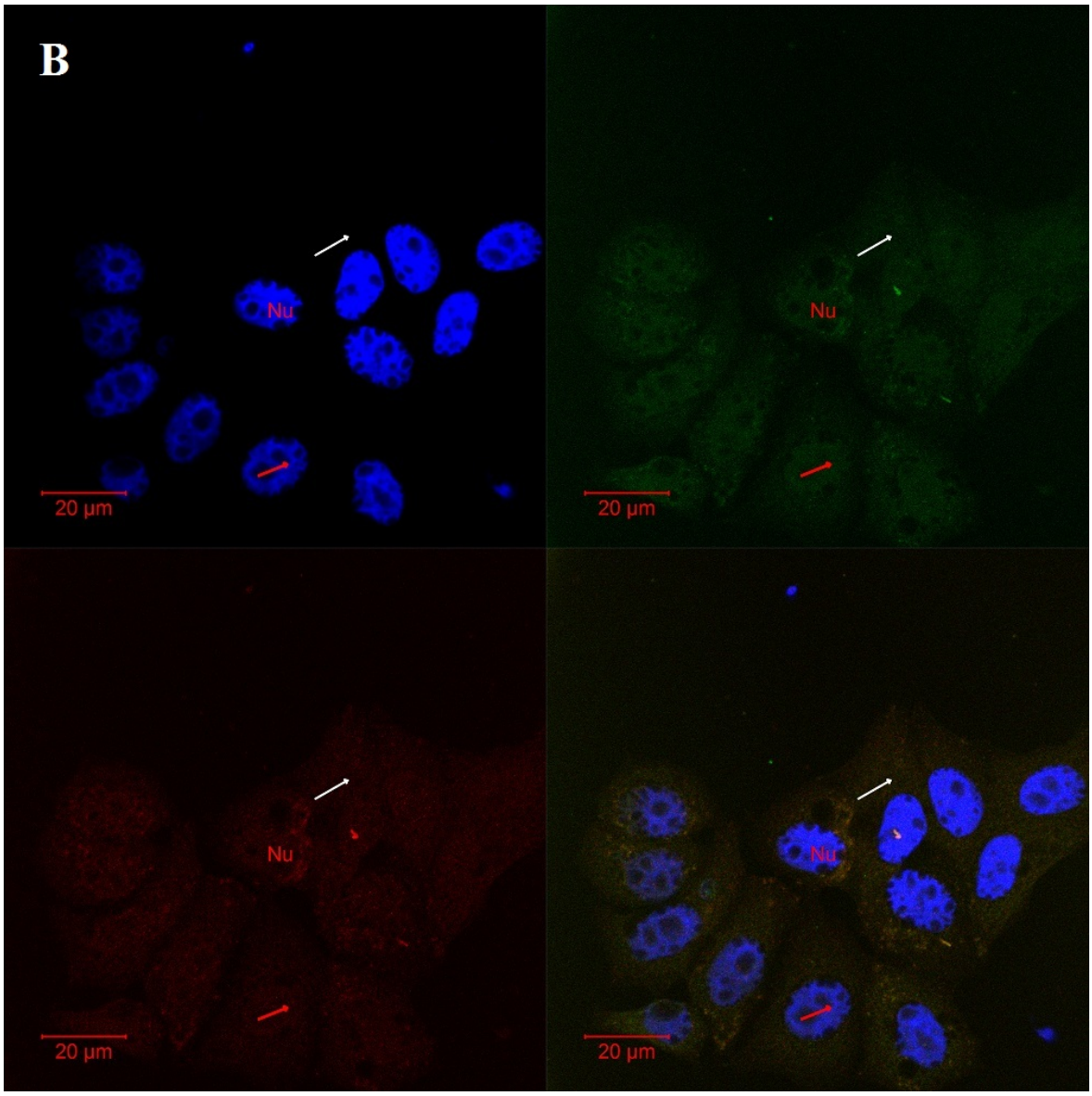

Figure 3.17 B: Fluorescence micrographs representing HCS-2 cells exposed to Vehicle-0.01% Methanol for 96 hours. BCL-2 was stained with Monoclonal Anti-BCL-2 and Goat Anti-Mouse IgG, FITC conjugated (Green channel-Right Upper quadrant). BAX was stained with Polyclonal rabbit Anti-BAX and Goat Anti-Rabbit IgG, Rhodamine conjugated (Red channel-Left Lower quadrant). Nuclei were counterstained with DAPI (Blue channel-Left Upper quadrant). Combined Images are represented in the Right Lower quadrant. Nu=Nucleus, Cy=Cytoplasm. Red arrow points to nuclear staining and White arrow points to cytoplasmic staining. There are no differences in protein staining, localisation and intensity as compared to growth medium alone. Representative Fluorescence micrographs of untreated cells serving as no primary antibody control are shown in Fig.3.17K.

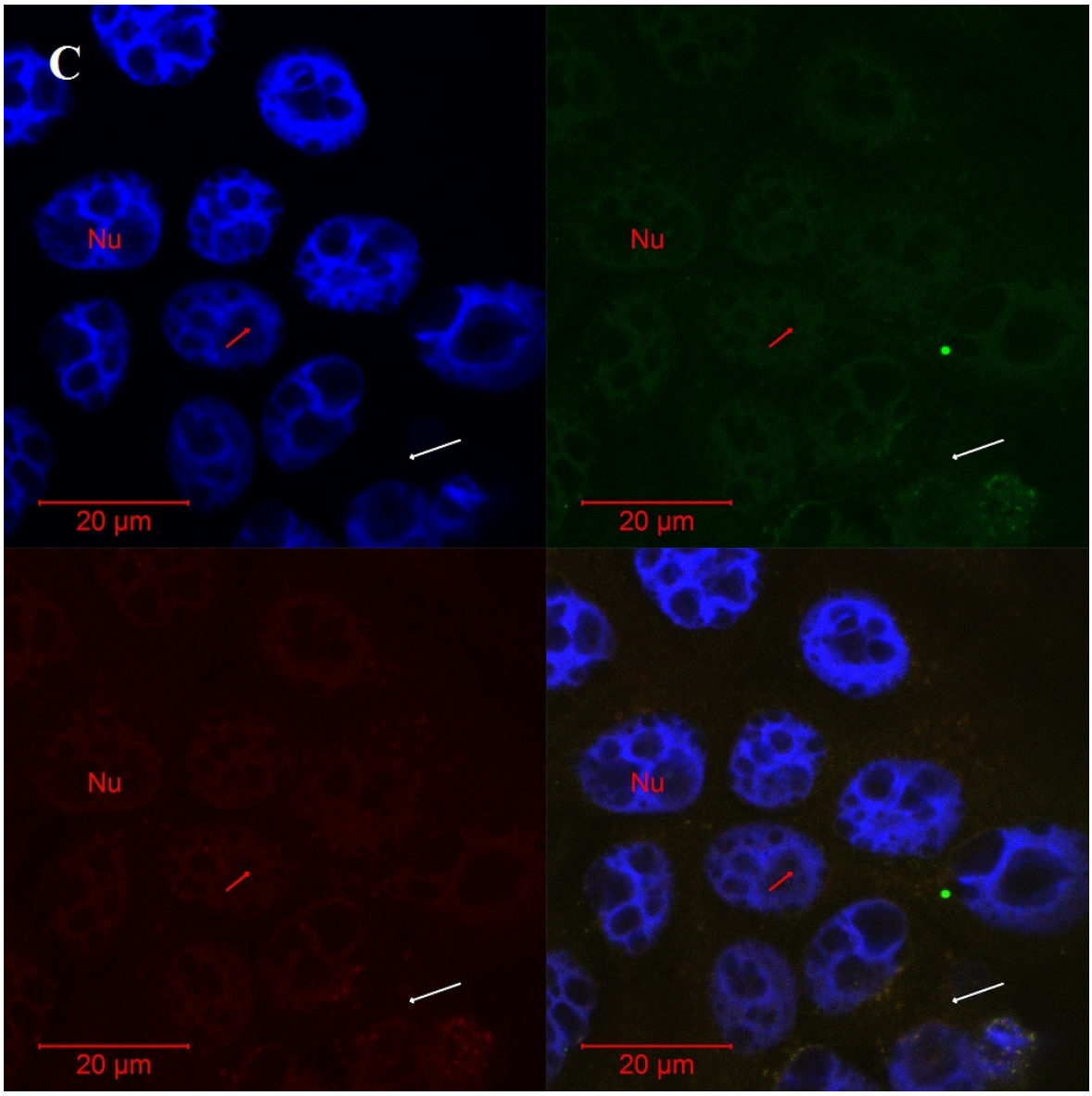

Figure 3.17C: Fluorescence micrographs representing HCS-2 cells exposed to 0.3µg/ml TDF for 96 hours. BCL-2 was stained with Monoclonal Anti-BCL-2 and Goat Anti-Mouse IgG, FITC conjugated (Green channel-Right Upper quadrant). BAX was stained with Polyclonal rabbit Anti-BAX and Goat Anti-Rabbit IgG, Rhodamine conjugated (Red channel-Left Lower quadrant). Nuclei were counterstained with DAPI (Blue channel-Left Upper quadrant). Combined Images are represented in the Right Lower quadrant. Nu=Nucleus, Cy=Cytoplasm. Red arrow points to nuclear staining and White arrow points to cytoplasmic staining. Representative Fluorescence micrographs of untreated cells serving as no primary antibody control are shown in Fig.3.17K.

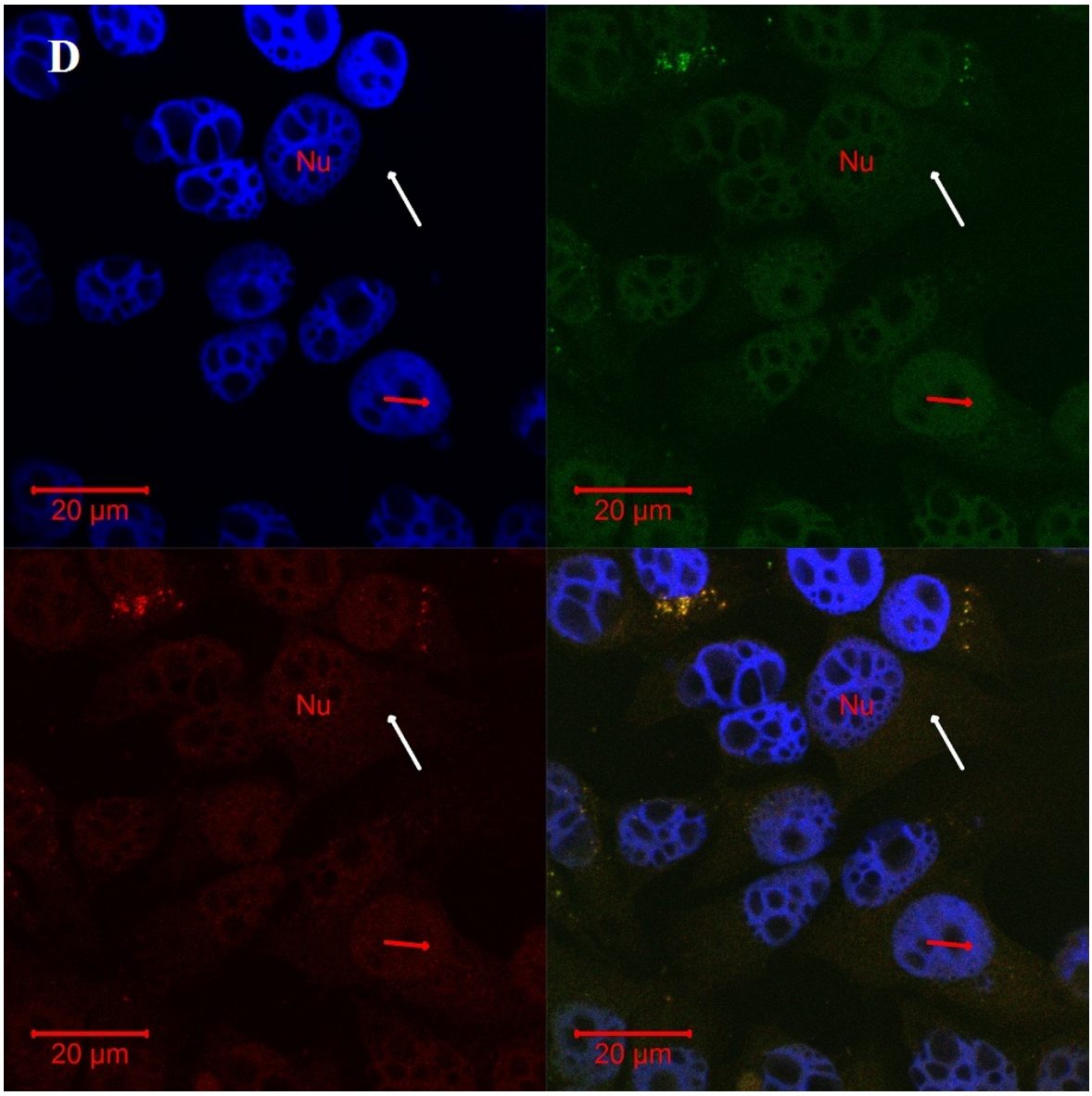

Figure 3.17D: Fluorescence micrographs representing HCS-2 cells exposed to 1.8µg/ml FTC for 96 hours. BCL-2 was stained with Monoclonal Anti-BCL-2 and Goat Anti-Mouse IgG, FITC conjugated (Green channel-Right Upper quadrant). BAX was stained with Polyclonal rabbit Anti-BAX and Goat Anti-Rabbit IgG, Rhodamine conjugated (Red channel-Left Lower quadrant). Nuclei were counterstained with DAPI (Blue channel-Left Upper quadrant). Combined Images are represented in the Right Lower quadrant. Nu=Nucleus, Cy=Cytoplasm. Red arrow points to nuclear staining and White arrow points to cytoplasmic staining. Representative Fluorescence micrographs of untreated cells serving as no primary antibody control are shown in Fig.3.17K.

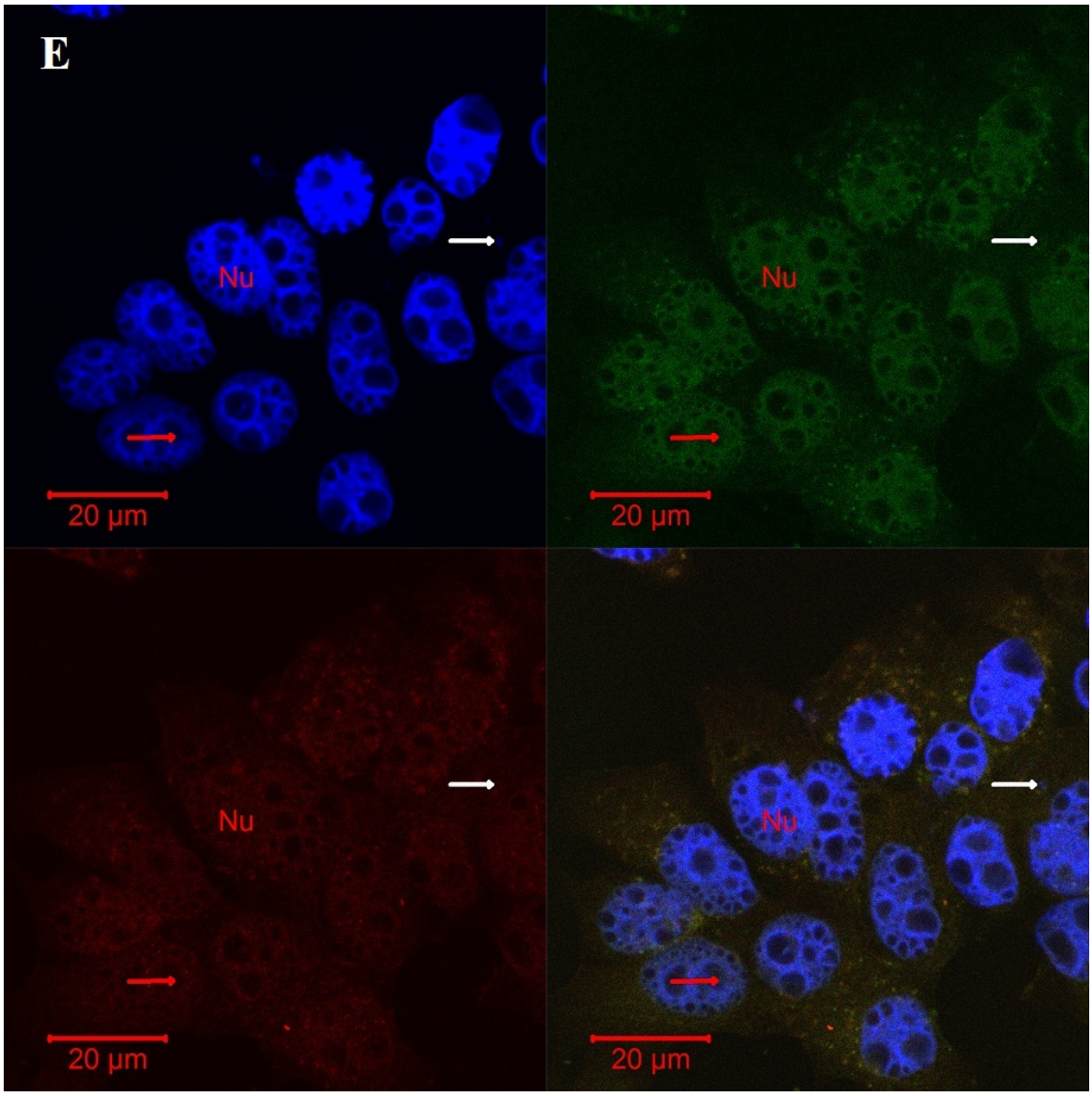

Figure 3.17E: Fluorescence micrographs representing HCS-2 cells exposed to 4.07µg/ml EFV for 96 hours. BCL-2 was stained with Monoclonal Anti-BCL-2 and Goat Anti-Mouse IgG, FITC conjugated (Green channel-Right Upper quadrant). BAX was stained with Polyclonal rabbit Anti-BAX and Goat Anti-Rabbit IgG, Rhodamine conjugated (Red channel-Left Lower quadrant). Nuclei were counterstained with DAPI (Blue channel-Left Upper quadrant). Combined Images are represented in the Right Lower quadrant. Nu=Nucleus. Red arrow points to nuclear staining and White arrow points to cytoplasmic staining. Representative Fluorescence micrographs of untreated cells serving as no primary antibody control are shown in Fig.3.17K.

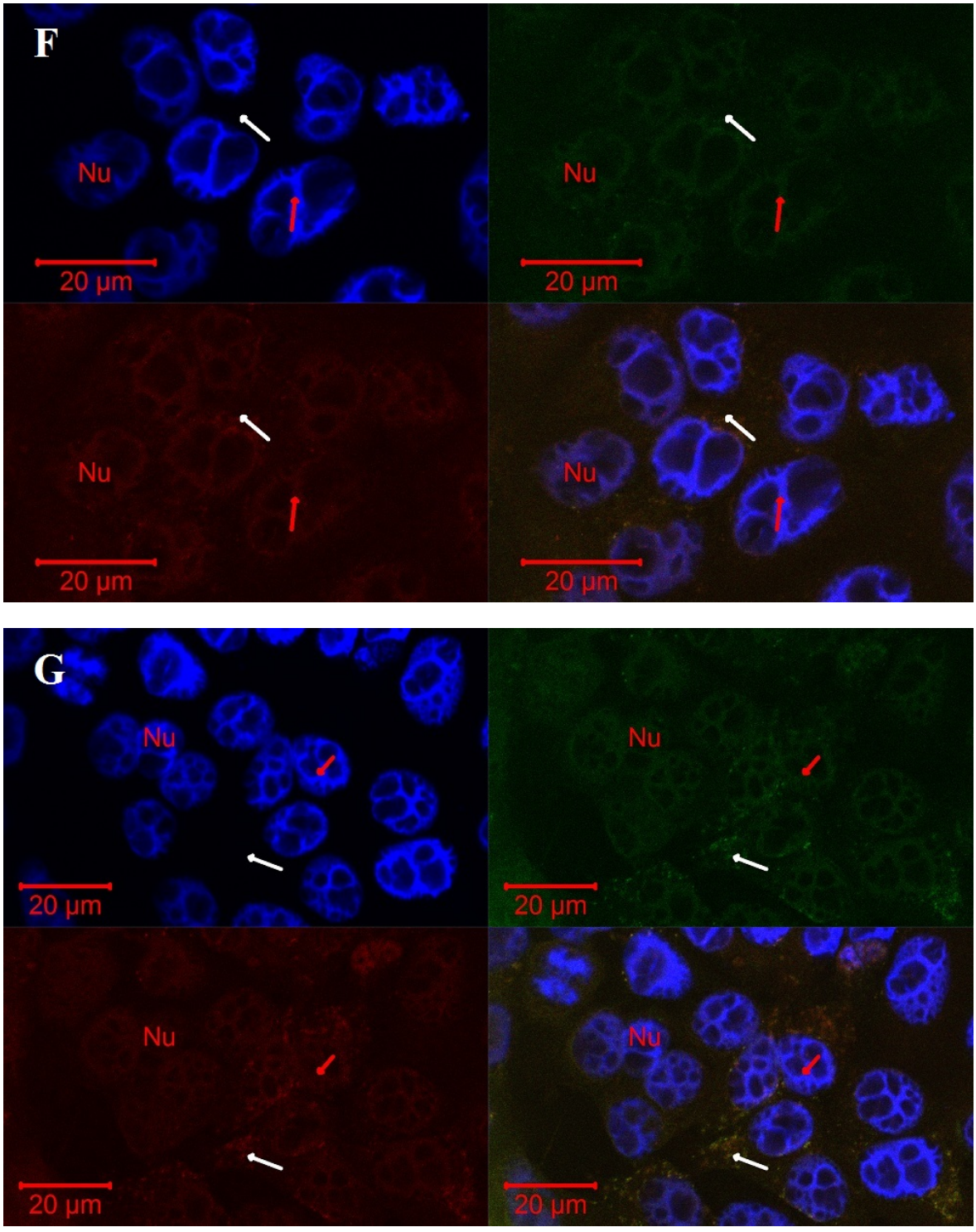

Figures 3.17F and G: Fluorescence micrographs representing HCS-2 cells exposed to **(F)** 0.3µg/ml TDF, 1.8µg/ml FTC, 4.07µg/ml EFV and 9.8µg/ml LPV for 96 hours. BCL-2 was stained with Monoclonal Anti-BCL-2 and Goat Anti-Mouse IgG, FITC conjugated (Green channel-Right Upper quadrant). BAX was stained with Polyclonal rabbit Anti-BAX and Goat Anti-Rabbit IgG, Rhodamine conjugated (Red channel-Left Lower quadrant). Nuclei were counterstained with DAPI (Blue channel-Left Upper quadrant). Combined Images are represented in the Right Lower quadrant. Nu=Nucleus. Red arrow points to nuclear staining and White arrow points to cytoplasmic staining.

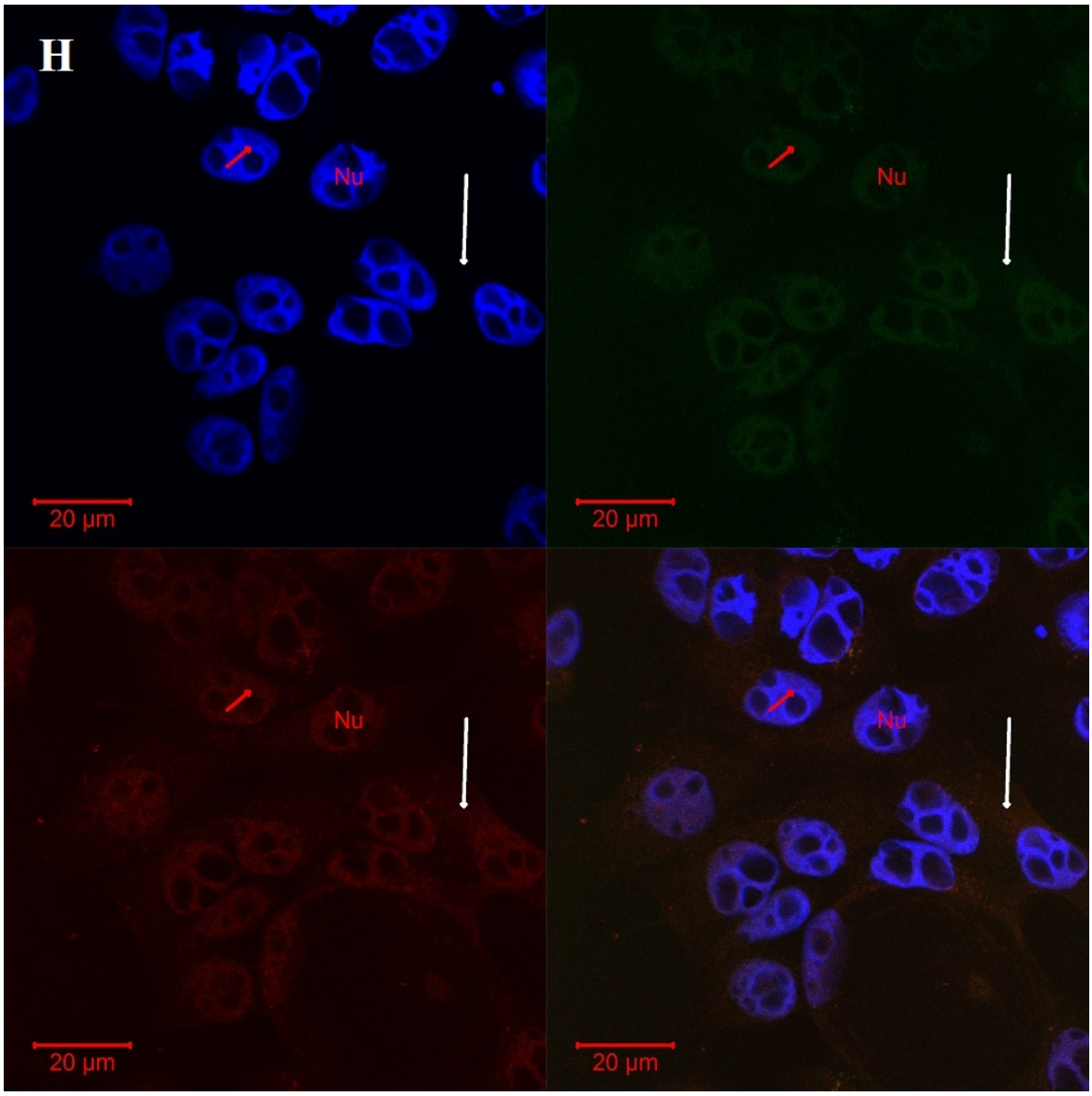

Figure 3.17H: Fluorescence micrographs representing HCS-2 cells exposed to 0.6µg/ml RTV for 96 hours. BCL-2 was stained with Monoclonal Anti-BCL-2 and Goat Anti-Mouse IgG, FITC conjugated (Green channel-Right Upper quadrant). BAX was stained with Polyclonal rabbit Anti-BAX and Goat Anti-Rabbit IgG, Rhodamine conjugated (Red channel-Left Lower quadrant). Nuclei were counterstained with DAPI (Blue channel-Left Upper quadrant). Combined Images are represented in the Right Lower quadrant. Nu=Nucleus. Red arrow points to nuclear staining and White arrow points to cytoplasmic staining. Representative Fluorescence micrographs of untreated cells serving as no primary antibody control are shown in Fig.3.17K.

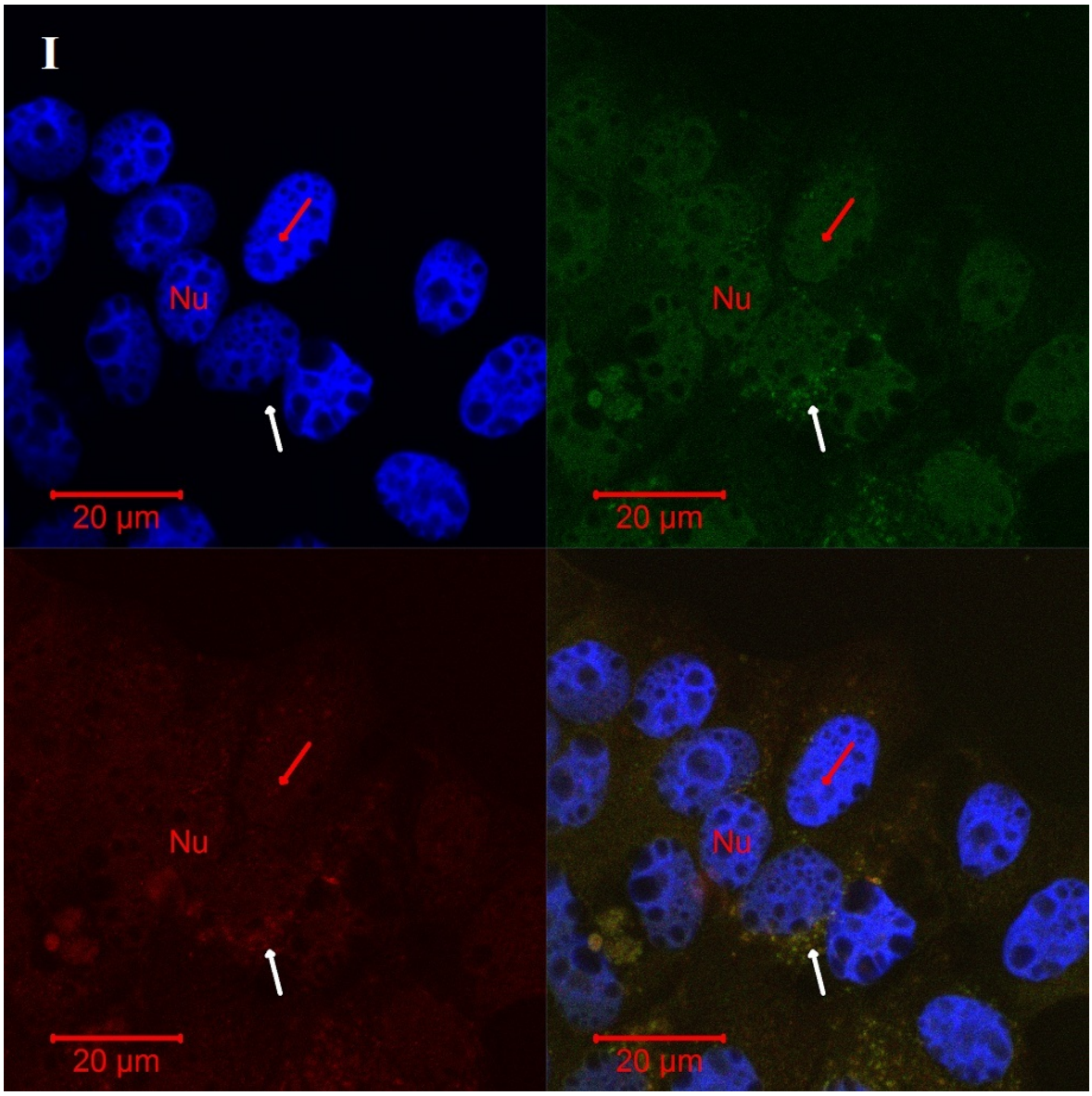

Figure 3.17I: Fluorescence micrographs representing HCS-2 cells exposed to 9.8µg/ml LPV; 0.6µg/ml RTV for 96 hours. BCL-2 was stained with Monoclonal Anti-BCL-2 and Goat Anti-Mouse IgG, FITC conjugated (Green channel-Right Upper quadrant). BAX was stained with Polyclonal rabbit Anti-BAX and Goat Anti-Rabbit IgG, Rhodamine conjugated (Red channel-Left Lower quadrant). Nuclei were counterstained with DAPI (Blue channel-Left Upper quadrant). Combined Images are represented in the Right Lower quadrant. Nu=Nucleus. Red arrow points to nuclear staining and White arrow points to cytoplasmic staining. Representative Fluorescence micrographs of untreated cells serving as no primary antibody control are shown in Fig.3.17K.

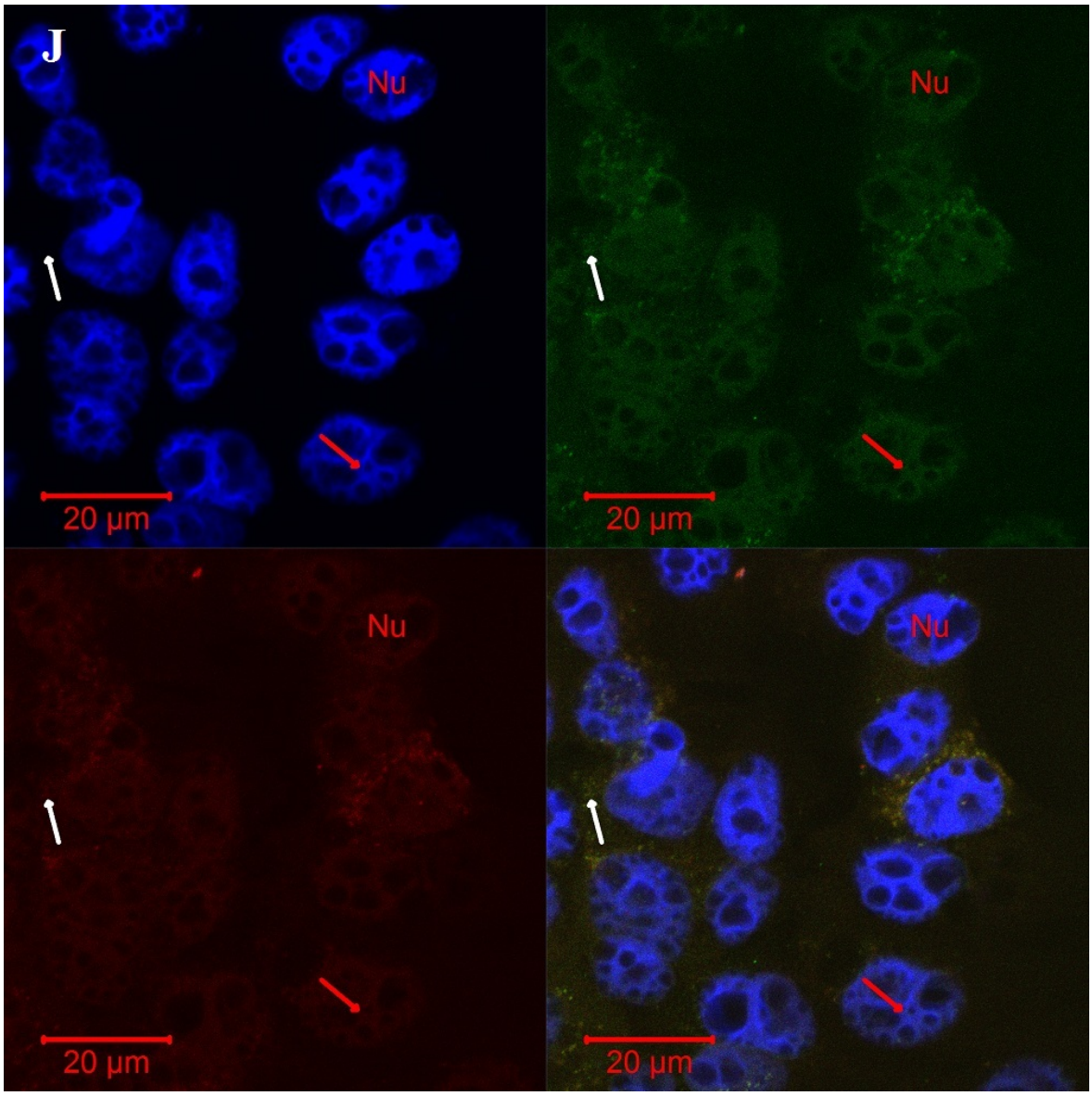

Figure 3.17J: Fluorescence micrographs representing HCS-2 cells exposed to 0.3µg/ml TDF; 1.8µg/ml FTC; 9.8µg/ml LPV; 0.6µg/ml RTV for 96 hours. BCL-2 was stained with Monoclonal Anti-BCL-2 and Goat Anti-Mouse IgG, FITC conjugated (Green channel-Right Upper quadrant). BAX was stained with Polyclonal rabbit Anti-BAX and Goat Anti-Rabbit IgG, Rhodamine conjugated (Red channel-Left Lower quadrant). Nuclei were counterstained with DAPI (Blue channel-Left Upper quadrant). Combined Images are represented in the Right Lower quadrant. Nu=Nucleus. Red arrow points to nuclear staining and White arrow points to cytoplasmic staining. Representative Fluorescence micrographs of untreated cells serving as no primary antibody control are shown in Fig.3.17K.

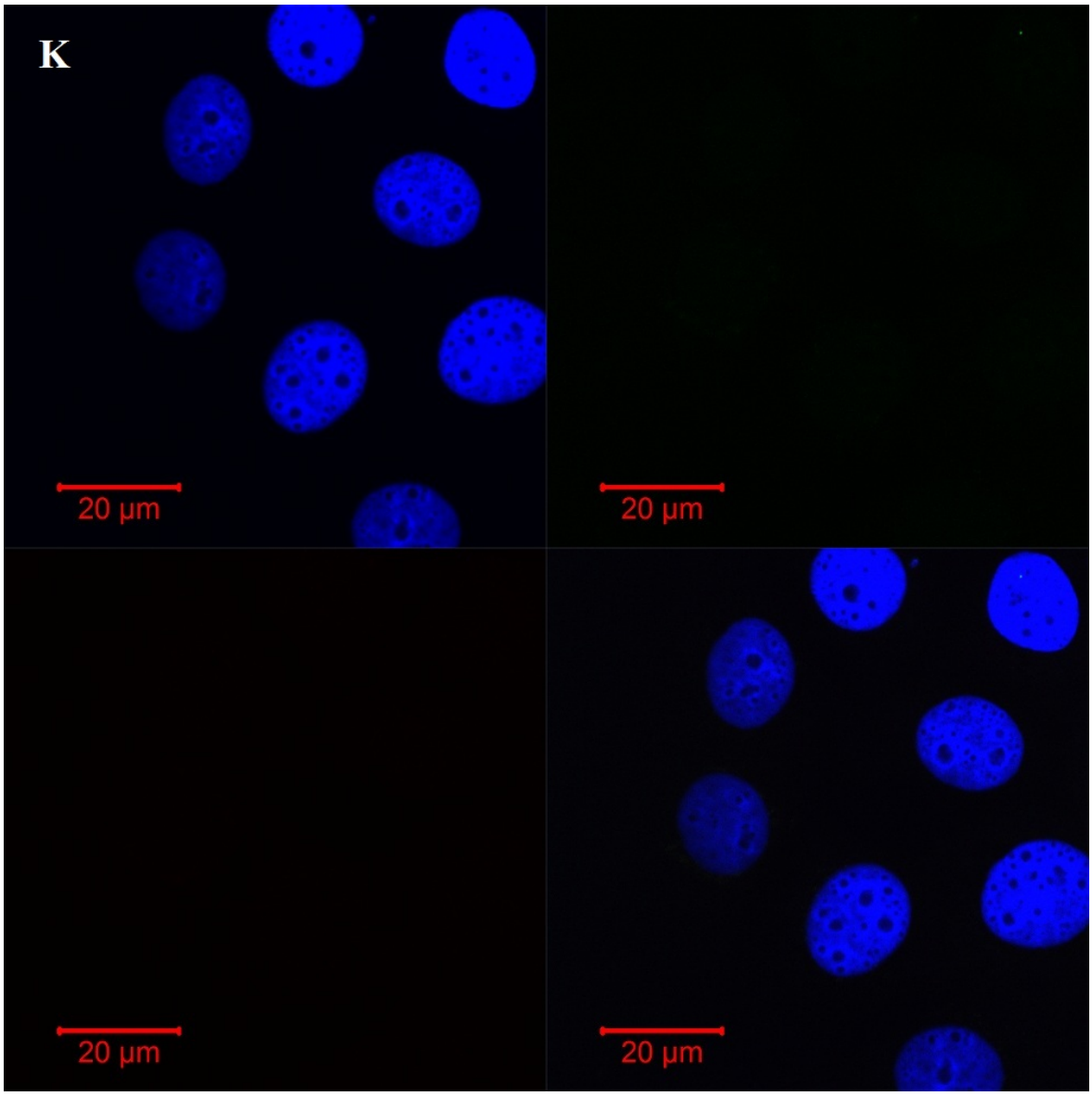

Figure3.17K: Fluorescence micrographs of untreated HCS-2 cells serving as no primary antibody control. Cells were incubated with goat serum in place of primary antibodies and incubated with Goat Anti-Mouse IgG, FITC conjugated (Green channel-Right Upper quadrant) and Goat Anti-Rabbit IgG, Rhodamine conjugated (Red channel-Left Lower quadrant). Nuclei were counterstained with DAPI (Blue channel-Left Upper quadrant). Combined Images are represented in the Right Lower quadrant.

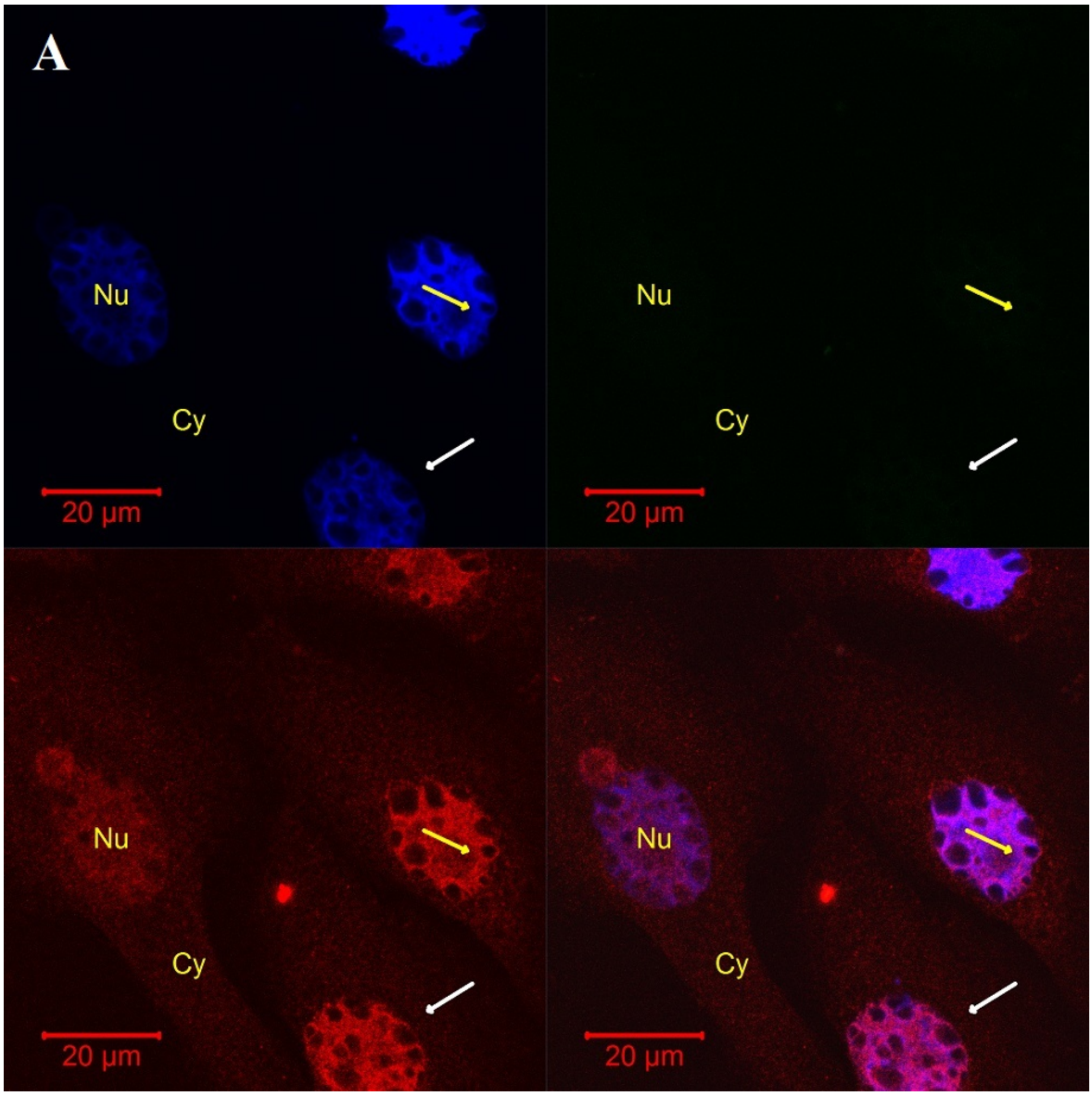

Figure 3.18A: Fluorescence micrographs of cervical NCE16IIA cells exposed to Growth Medium for 96 hours. BCL-2 was stained with Monoclonal Anti-BCL-2 and Goat Anti-Mouse IgG, FITC conjugated (Green channel-Right Upper quadrant). BAX was stained with Polyclonal rabbit Anti-BAX and Goat Anti-Rabbit IgG, Rhodamine conjugated (Red channel-Left Lower quadrant). Nuclei were counterstained with DAPI (Blue channel-Left Upper quadrant). Combined Images are represented in the Right Lower quadrant. Nu=Nucleus, Cy=Cytoplasm. Yellow arrow points to nuclear staining and White arrow points to cytoplasmic staining. Representative Fluorescence micrographs of untreated cells serving as no primary antibody control are shown in Fig.3.18K.

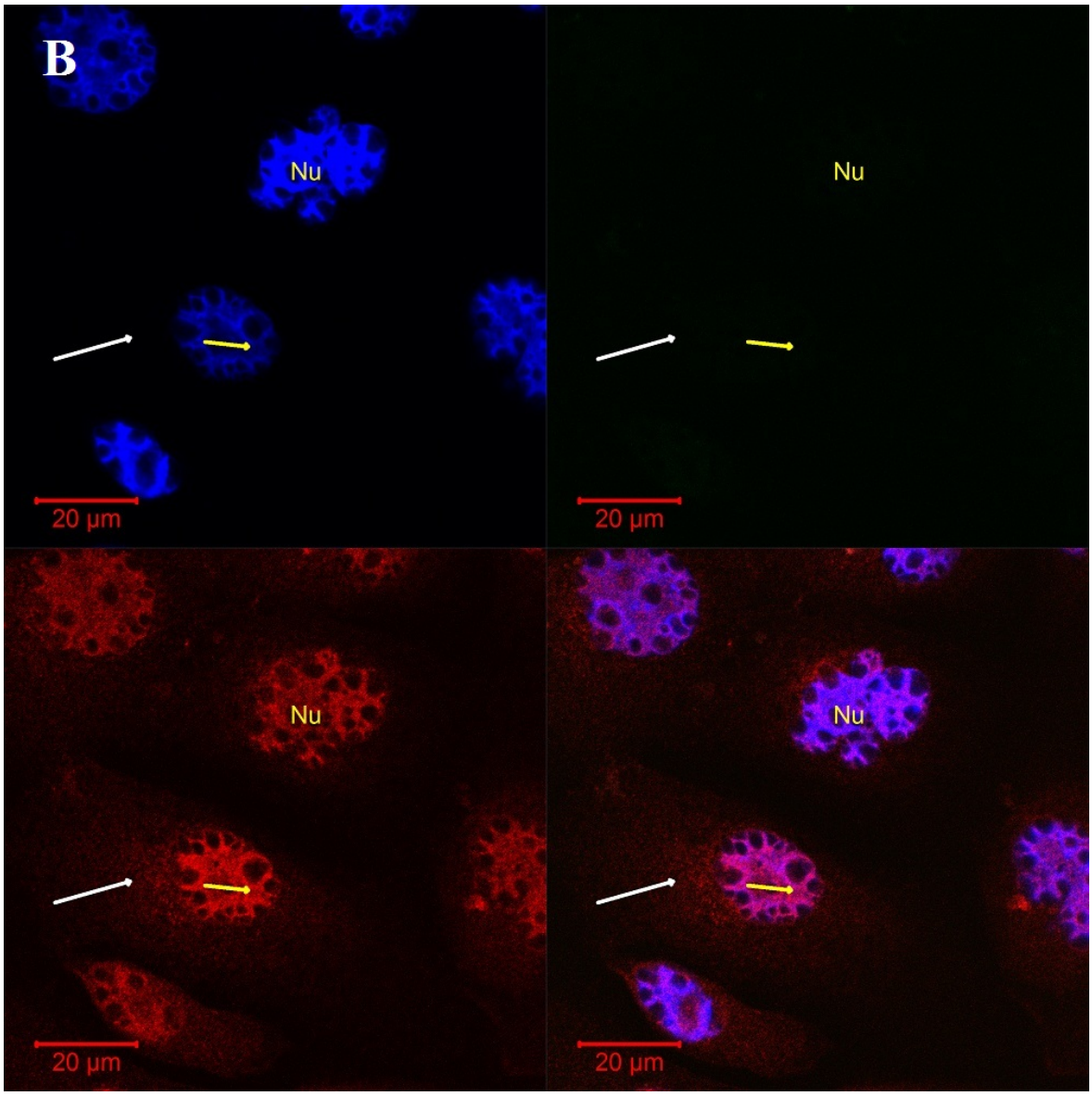

Figure 3.18 B: Fluorescence micrographs of cervical NCE16IIA cells exposed to Vehicle-0.01% Methanol for 96 hours. BCL-2 was stained with Monoclonal Anti-BCL-2 and Goat Anti-Mouse IgG, FITC conjugated (Green channel-Right Upper quadrant). BAX was stained with Polyclonal rabbit Anti-BAX and Goat Anti-Rabbit IgG, Rhodamine conjugated (Red channel-Left Lower quadrant). Nuclei were counterstained with DAPI (Blue channel-Left Upper quadrant). Combined Images are represented in the Right Lower quadrant. Nu=Nucleus. Yellow arrow points to nuclear staining and White arrow points to cytoplasmic staining. There are no differences in protein staining, localisation and intensity as compared to growth medium alone. Representative Fluorescence micrographs of untreated cells serving as no primary antibody control are shown in Fig.3.18K.

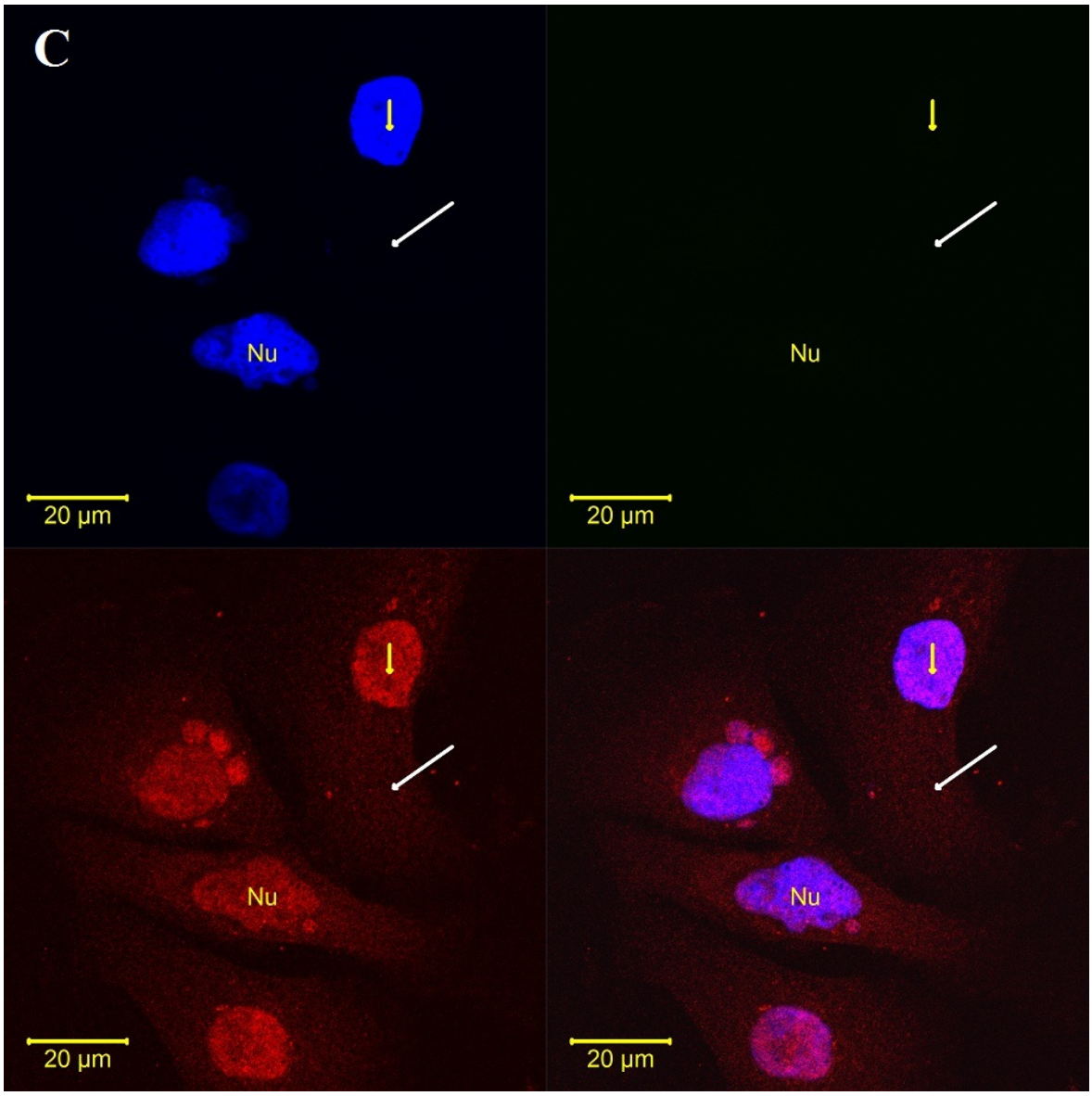

Figure 3.18C: Fluorescence micrographs of cervical NCE16IIA cells exposed to 0.3µg/ml TDF for 96 hours. BCL-2 was stained with Monoclonal Anti-BCL-2 and Goat Anti-Mouse IgG, FITC conjugated (Green channel-Right Upper quadrant). BAX was stained with Polyclonal rabbit Anti-BAX and Goat Anti-Rabbit IgG, Rhodamine conjugated (Red channel-Left Lower quadrant). Nuclei were counterstained with DAPI (Blue channel-Left Upper quadrant). Combined Images are represented in the Right Lower quadrant. Nu=Nucleus. Yellow arrow points to nuclear staining and White arrow points to cytoplasmic staining. Representative Fluorescence micrographs of untreated cells serving as no primary antibody control are shown in Fig.3.18K.

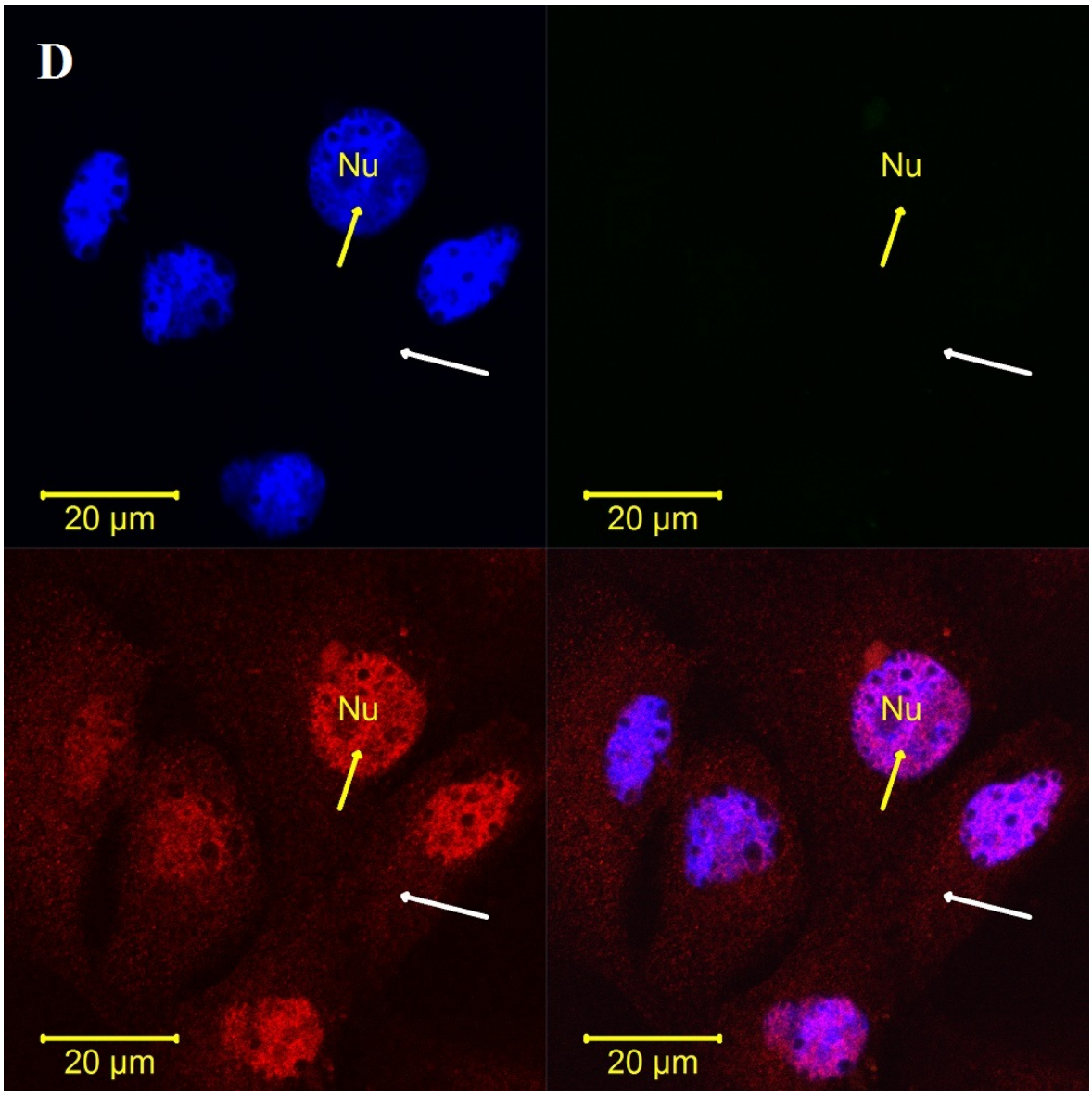

Figure 3.18D: Fluorescence micrographs of cervical NCE16IIA cells exposed to 1.8µg/ml FTC for 96 hours. BCL-2 was stained with Monoclonal Anti-BCL-2 and Goat Anti-Mouse IgG, FITC conjugated (Green channel-Right Upper quadrant). BAX was stained with Polyclonal rabbit Anti-BAX and Goat Anti-Rabbit IgG, Rhodamine conjugated (Red channel-Left Lower quadrant). Nuclei were counterstained with DAPI (Blue channel-Left Upper quadrant). Combined Images are represented in the Right Lower quadrant. Nu=Nucleus. Yellow arrow points to nuclear staining and White arrow points to cytoplasmic staining. Representative Fluorescence micrographs of untreated cells serving as no primary antibody control are shown in Fig.3.18K.

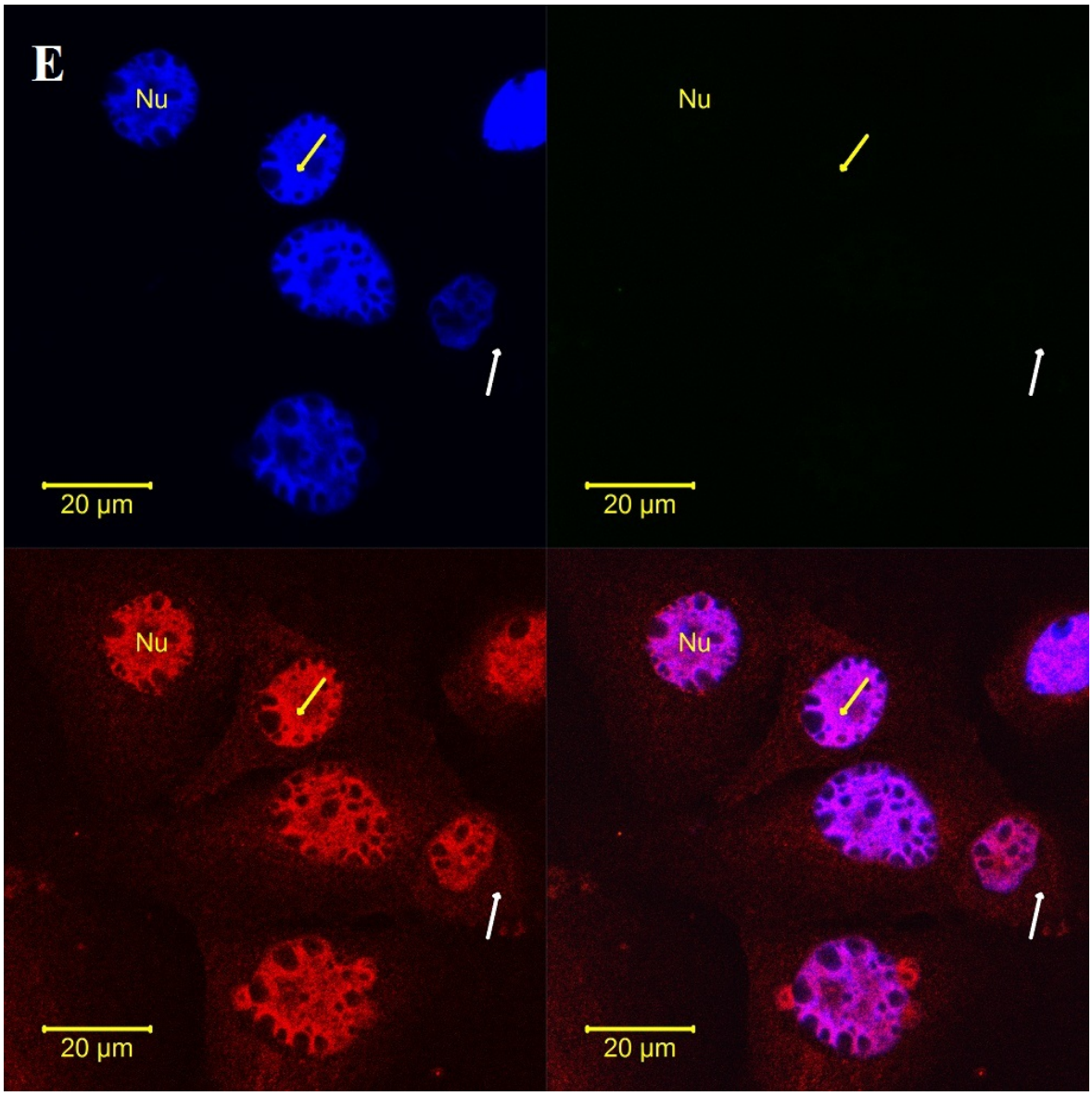

Figure 3.18E: Fluorescence micrographs of cervical NCE16IIA cells exposed to 4.07µg/ml EFV for 96 hours. BCL-2 was stained with Monoclonal Anti-BCL-2 and Goat Anti-Mouse IgG, FITC conjugated (Green channel-Right Upper quadrant). BAX was stained with Polyclonal rabbit Anti-BAX and Goat Anti-Rabbit IgG, Rhodamine conjugated (Red channel-Left Lower quadrant). Nuclei were counterstained with DAPI (Blue channel-Left Upper quadrant). Combined Images are represented in the Right Lower quadrant. Nu=Nucleus. Yellow arrow points to nuclear staining and White arrow points to cytoplasmic staining. Representative Fluorescence micrographs of untreated cells serving as no primary antibody control are shown in Fig.3.18K.

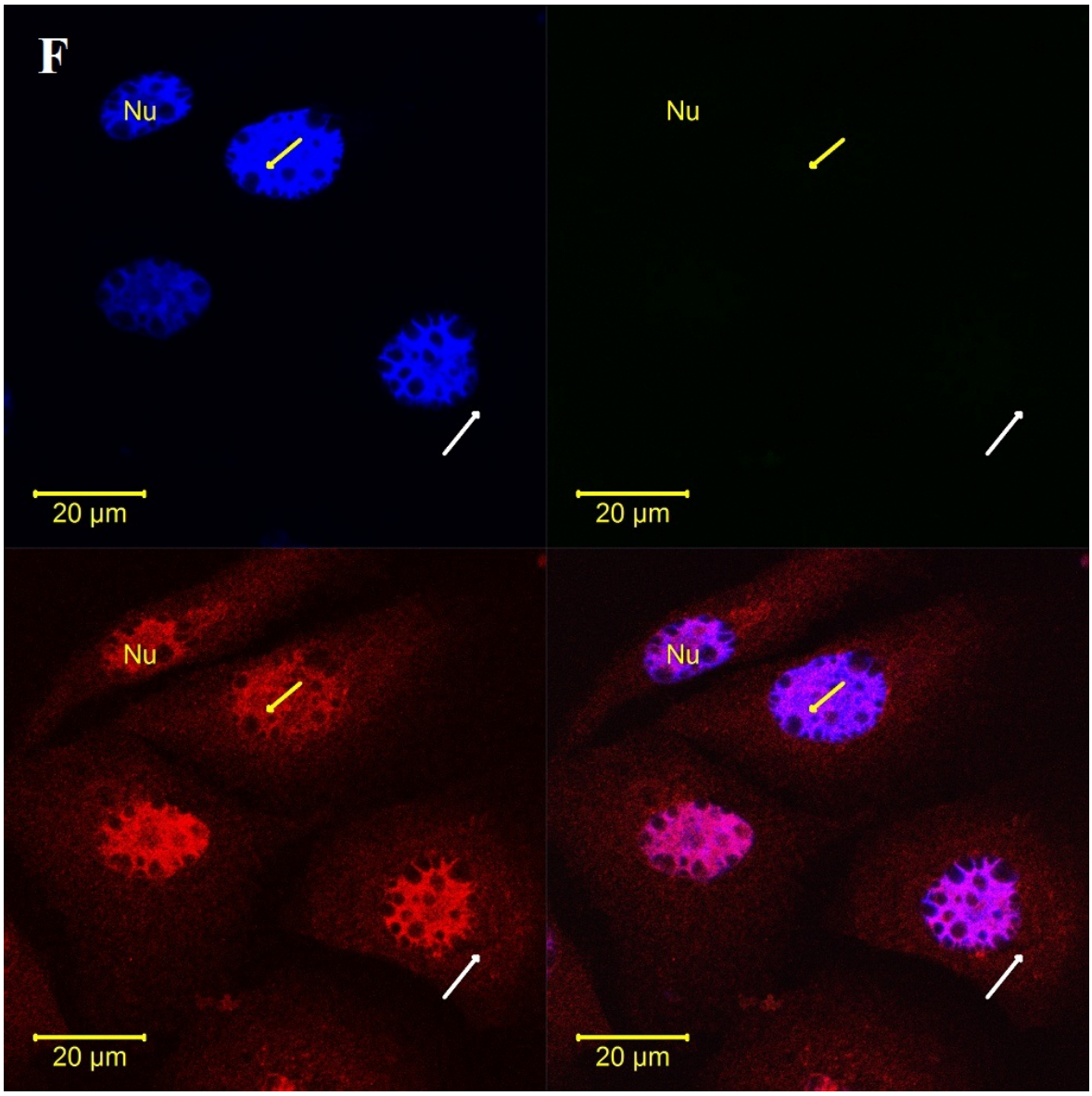

Figure 3.18F: Fluorescence micrographs of cervical NCE16IIA cells exposed to 0.3µg/ml TDF; 1.8µg/ml FTC; 4.07µg/ml EFV for 96 hours. BCL-2 was stained with Monoclonal Anti-BCL-2 and Goat Anti-Mouse IgG, FITC conjugated (Green channel-Right Upper quadrant). BAX was stained with Polyclonal rabbit Anti-BAX and Goat Anti-Rabbit IgG, Rhodamine conjugated (Red channel-Left Lower quadrant). Nuclei were counterstained with DAPI (Blue channel-Left Upper quadrant). Combined Images are represented in the Right Lower quadrant. Nu=Nucleus. Yellow arrow points to nuclear staining and White arrow points to cytoplasmic staining. Representative Fluorescence micrographs of untreated cells serving as no primary antibody control are shown in Fig.3.18K.

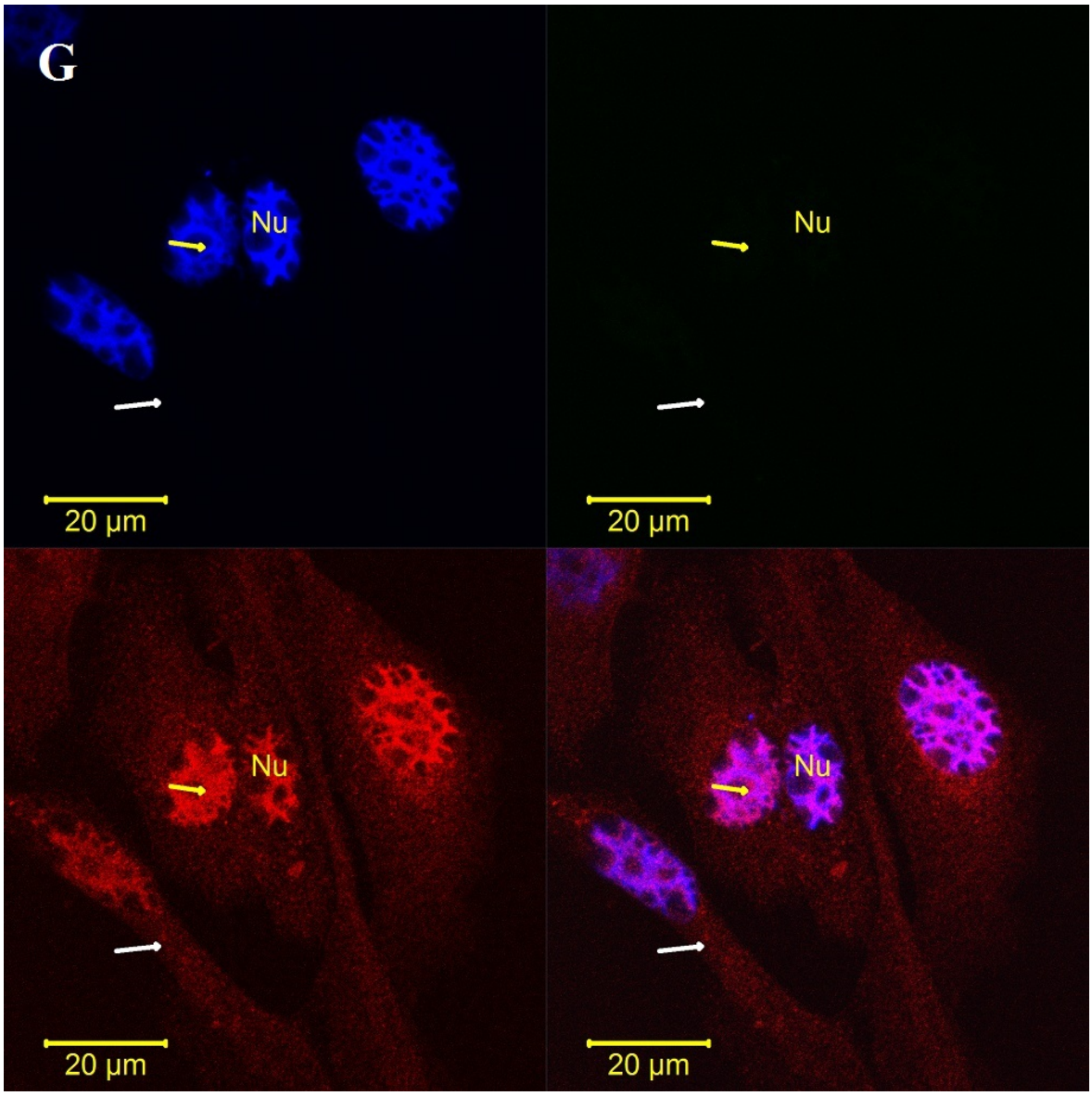

Figure 3.18G: Fluorescence micrographs of cervical NCE16IIA cells exposed to 9.8µg/ml LPV for 96 hours. BCL-2 was stained with Monoclonal Anti-BCL-2 and Goat Anti-Mouse IgG, FITC conjugated (Green channel-Right Upper quadrant). BAX was stained with Polyclonal rabbit Anti-BAX and Goat Anti-Rabbit IgG, Rhodamine conjugated (Red channel-Left Lower quadrant). Nuclei were counterstained with DAPI (Blue channel-Left Upper quadrant). Combined Images are represented in the Right Lower quadrant. Nu=Nucleus. Yellow arrow points to nuclear staining and White arrow points to cytoplasmic staining. Representative Fluorescence micrographs of untreated cells serving as no primary antibody control are shown in Fig.3.18K.

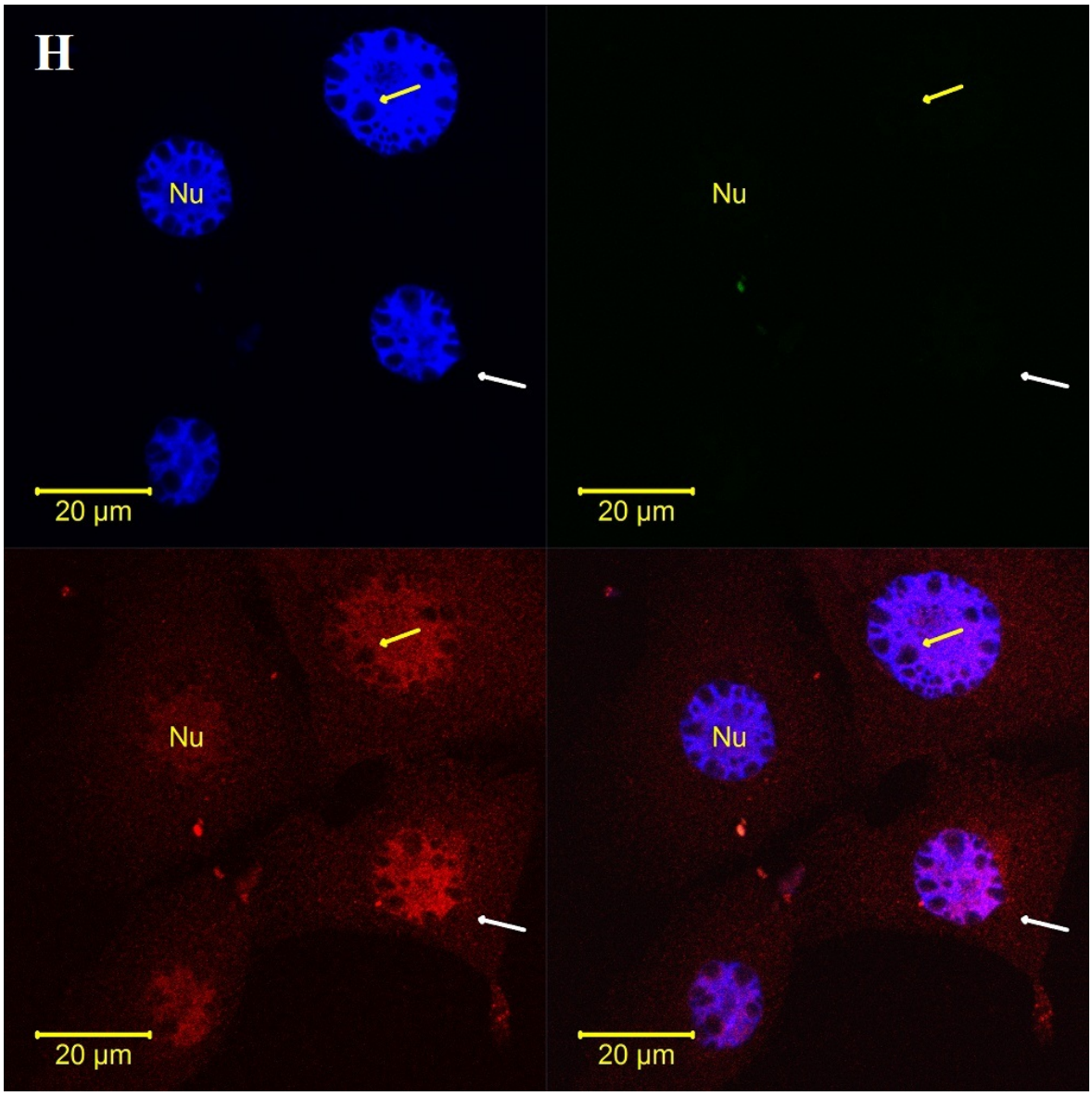

Figure 3.18H: Fluorescence micrographs of cervical NCE16IIA cells exposed to 0.6µg/ml RTV for 96 hours. BCL-2 was stained with Monoclonal Anti-BCL-2 and Goat Anti-Mouse IgG, FITC conjugated (Green channel-Right Upper quadrant). BAX was stained with Polyclonal rabbit Anti-BAX and Goat Anti-Rabbit IgG, Rhodamine conjugated (Red channel-Left Lower quadrant). Nuclei were counterstained with DAPI (Blue channel-Left Upper quadrant). Combined Images are represented in the Right Lower quadrant. Nu=Nucleus. Yellow arrow points to nuclear staining and White arrow points to cytoplasmic staining. Representative Fluorescence micrographs of untreated cells serving as no primary antibody control are shown in Fig.3.18K.

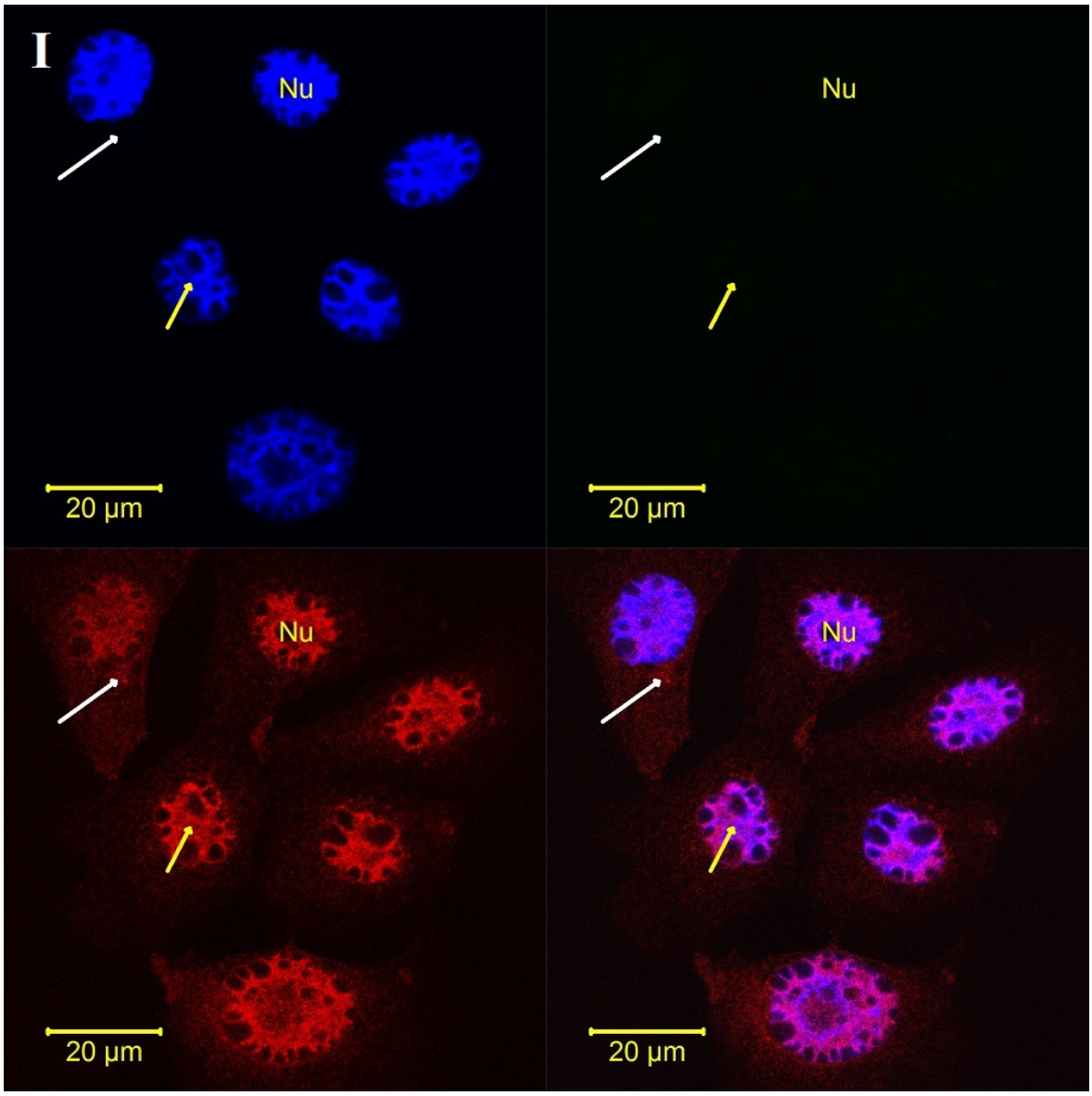

Figure 3.18I: Fluorescence micrographs of cervical NCE16IIA cells exposed to 9.8µg/ml LPV, 0.6µg/ml RTV for 96 hours. BCL-2 was stained with Monoclonal Anti-BCL-2 and Goat Anti-Mouse IgG, FITC conjugated (Green channel-Right Upper quadrant). BAX was stained with Polyclonal rabbit Anti-BAX and Goat Anti-Rabbit IgG, Rhodamine conjugated (Red channel-Left Lower quadrant). Nuclei were counterstained with DAPI (Blue channel-Left Upper quadrant). Combined Images are represented in the Right Lower quadrant. Nu=Nucleus. Yellow arrow points to nuclear staining and White arrow points to cytoplasmic staining. Representative Fluorescence micrographs of untreated cells serving as no primary antibody control are shown in Fig.3.18K.

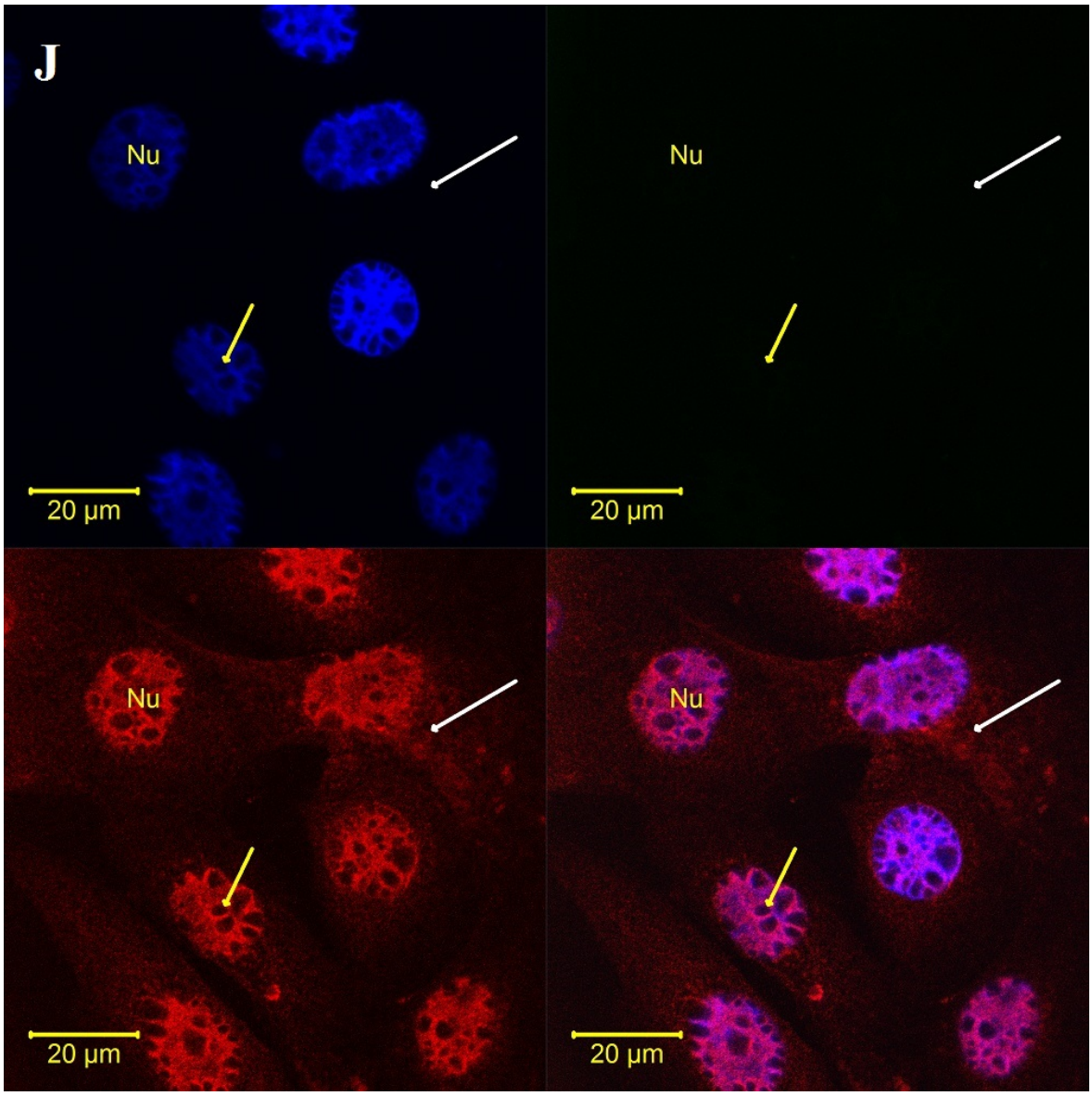

Figure 3.18J: Fluorescence micrographs of cervical NCE16IIA cells exposed to 0.3µg/ml TDF; 1.8µg/ml FTC, 9.8µg/ml LPV, 0.6µg/ml RTV for 96 hours. BCL-2 was stained with Monoclonal Anti-BCL-2 and Goat Anti-Mouse IgG, FITC conjugated (Green channel-Right Upper quadrant). BAX was stained with Polyclonal rabbit Anti-BAX and Goat Anti-Rabbit IgG, Rhodamine conjugated (Red channel-Left Lower quadrant). Nuclei were counterstained with DAPI (Blue channel-Left Upper quadrant). Combined Images are represented in the Right Lower quadrant. Nu=Nucleus. Yellow arrow points to nuclear staining and White arrow points to cytoplasmic staining. Representative Fluorescence micrographs of untreated cells serving as no primary antibody control are shown in Fig.3.18K.

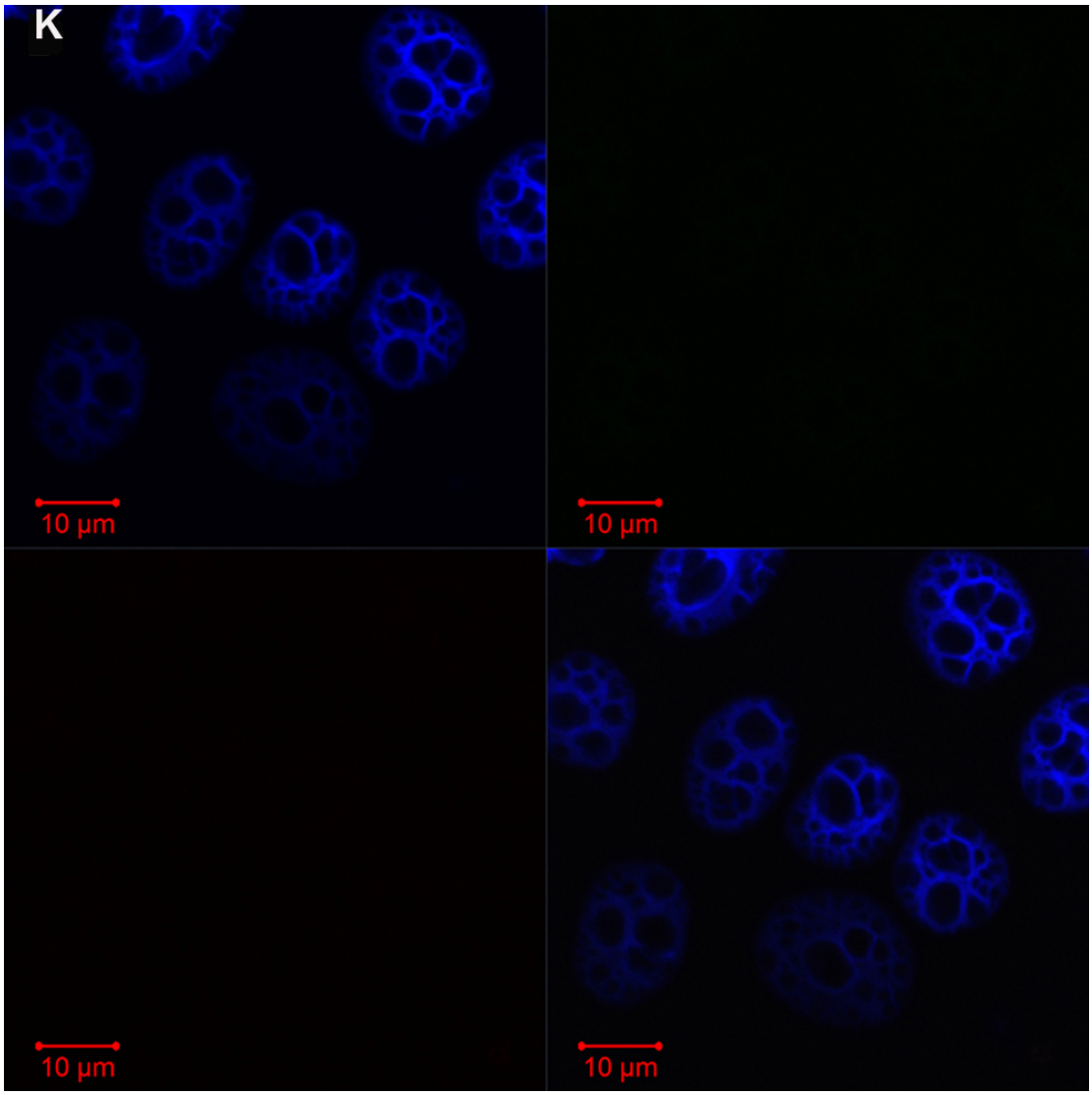

Figure 3.18K: Fluorescence micrographs of untreated cervical NCE16IIA cells serving as no primary antibody control. Cells were incubated with goat serum in place of primary antibodies and incubated with Goat Anti-Mouse IgG, FITC conjugated (Green channel-Right Upper quadrant) and Goat Anti-Rabbit IgG, Rhodamine conjugated (Red channel-Left Lower quadrant). Nuclei were counterstained with DAPI (Blue channel-Left Upper quadrant). Combined Images are represented in the Right Lower quadrant.

3.3.2 Immunofluorescence of BAX and BCL-2 proteins in breast cancer (MCF-7) and normal breast (MCF-10A) cells exposed to antiretroviral drugs

In the untreated group of MCF-7 cells (Fig 3.19 A), BAX and BCL-2 proteins are expressed and co-localised in the nuclei and cytoplasm. Mean Fluorescence intensities of BAX and BCL-2 in the nuclei and cytoplasm were statistically analysed (ANOVA) between the untreated/vehicle control and the treated groups. (Graphical representation presented in Figs. 3.25-3.32; Data summaries shown in Appendix E).There are no differences in protein staining, localisation and intensity of vehicle (0.01% methanol) treated group as compared to growth medium alone (Fig. 3.19B). Fig 3.19 C-J shows the effects of antiretroviral drugs on the localisation of BAX and BCL-2 in MCF-7 cell cultures. Fig. 3.19 C-J are representative images illustrating the effects of the antiretroviral drugs on expression of BAX and BCL-2 in MCF-7 cell cultures. BAX and BCL-2, localisation remains unaltered across treatment groups.

The untreated group of MCF-10A cells (Fig 3.20A) demonstrates the expression and localisation of BAX and BCL-2. Mean Fluorescence intensities of BAX and BCL-2 in the nuclei and cytoplasm were statistically analysed (ANOVA) between the untreated/vehicle control and the treated groups. (Graphical representation presented in Figs. 3.25-3.32; Data summaries shown in Appendix E). There are no differences in protein staining, localisation and intensity of vehicle (0.01% methanol) treated group as compared to growth medium alone (Fig. 3.20B). Fig 3.20 C-J illustrates the effect of the antiretroviral drugs on expression of BAX and BCL-2 in MCF-10A cell cultures. Fig. 3.20 C-J are representative images illustrating the effects of the antiretroviral drugs on expression of BAX and BCL-2 in MCF-10A cell cultures. BAX and BCL-2 localisation remain unchanged across treatment groups.

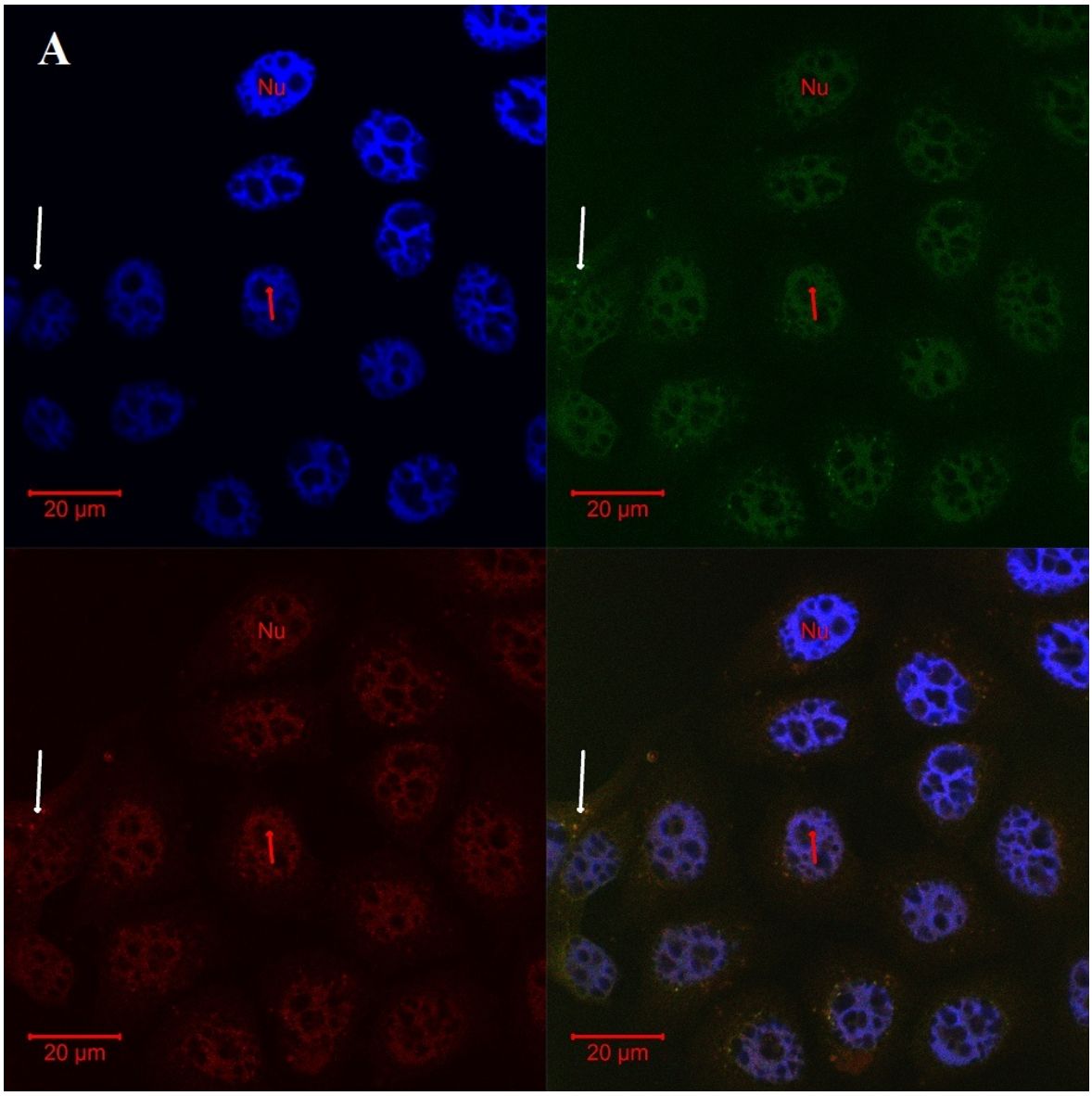

Figure 3.19A: Fluorescence micrographs of MCF-7 cells exposed to Growth Medium for 96 hours. BCL-2 was stained with Monoclonal Anti-BCL-2 and Goat Anti-Mouse IgG, FITC conjugated (Green channel-Right Upper quadrant). BAX was stained with Polyclonal rabbit Anti-BAX and Goat Anti-Rabbit IgG, Rhodamine conjugated (Red channel-Left Lower quadrant). Nuclei were counterstained with DAPI (Blue channel-Left Upper quadrant). Combined Images are represented in the Right Lower quadrant. Nu=Nucleus. Red arrow points to nuclear staining and White arrow points to cytoplasmic staining. Representative Fluorescence micrographs of untreated cells serving as no primary antibody control are shown in Fig.3.19K.

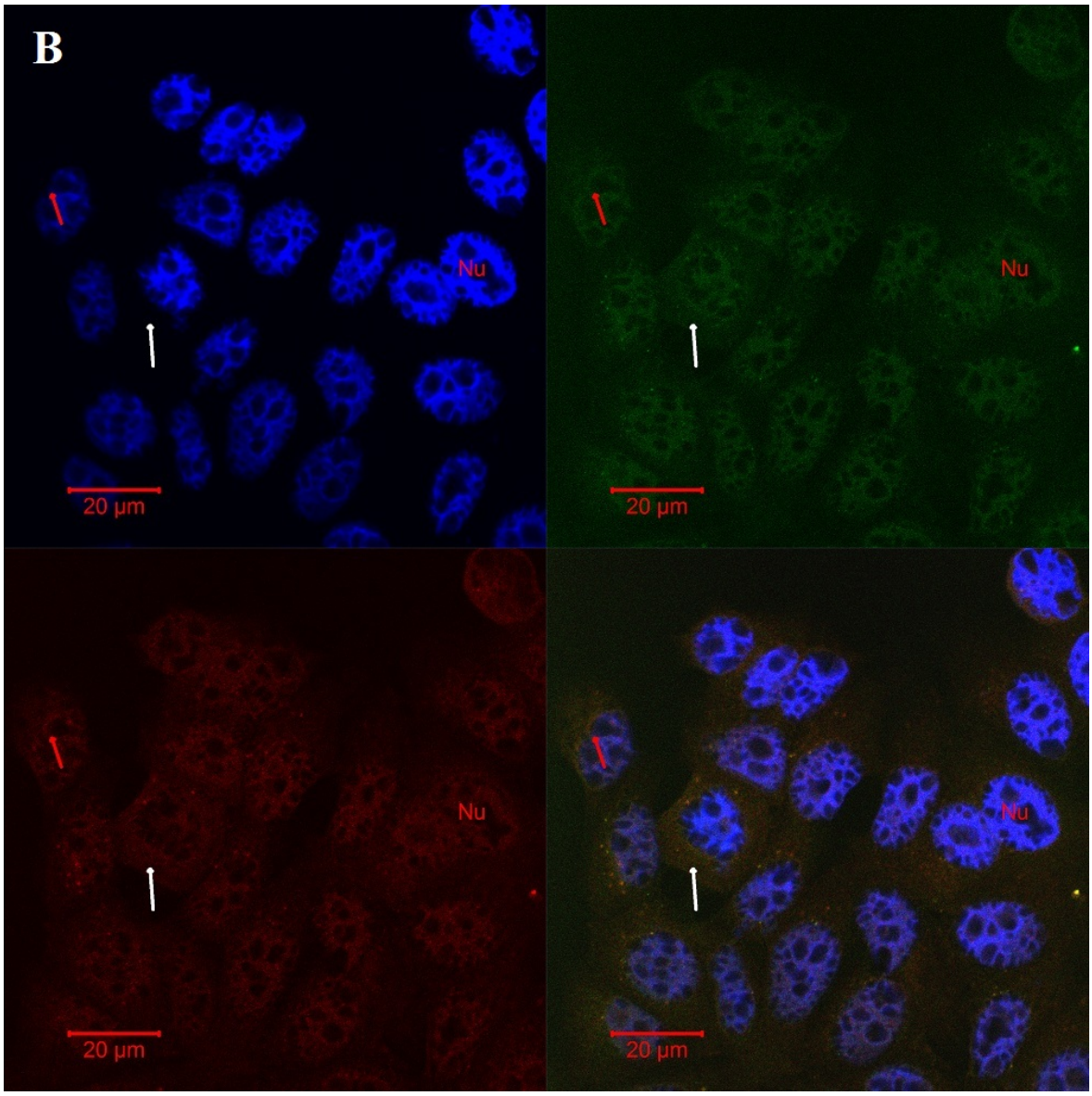

Figure 3.19B: Fluorescence micrographs of MCF-7 cells exposed to Vehicle-0.01% Methanol for 96 hours. BCL-2 was stained with Monoclonal Anti-BCL-2 and Goat Anti-Mouse IgG, FITC conjugated (Green channel-Right Upper quadrant). BAX was stained with Polyclonal rabbit Anti-BAX and Goat Anti-Rabbit IgG, Rhodamine conjugated (Red channel-Left Lower quadrant). Nuclei were counterstained with DAPI (Blue channel-Left Upper quadrant). Combined Images are represented in the Right Lower quadrant. Nu=Nucleus. Red arrow points to nuclear staining and White arrow points to cytoplasmic staining. There are no differences in protein staining, localisation and intensity as compared to growth medium alone. Representative Fluorescence micrographs of untreated cells serving as no primary antibody control are shown in Fig.3.19K.

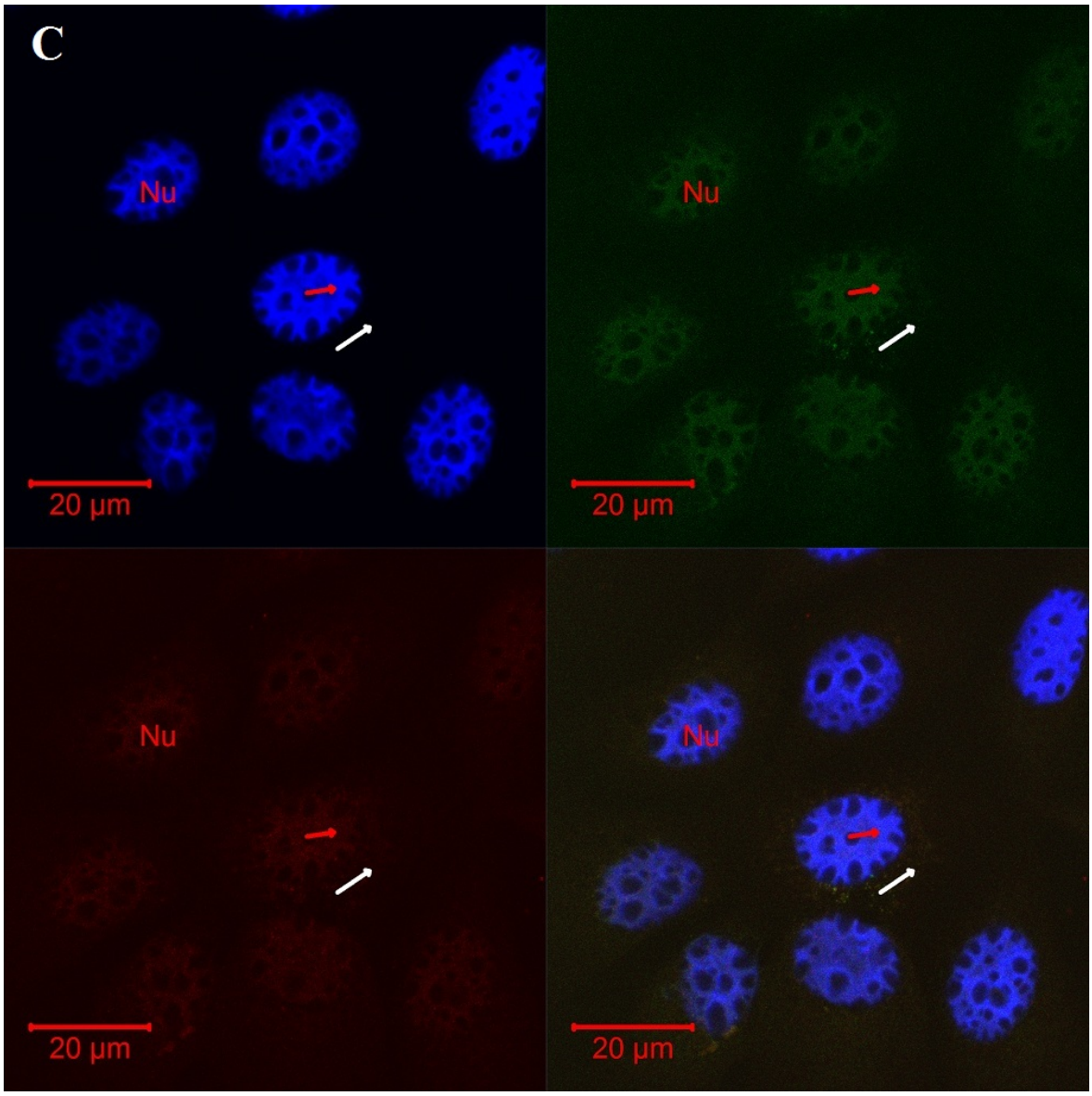

Figure 3.19C: Fluorescence micrographs of MCF-7 cells exposed to 0.3µg/ml TDF for 96 hours. BCL-2 was stained with Monoclonal Anti-BCL-2 and Goat Anti-Mouse IgG, FITC conjugated (Green channel-Right Upper quadrant). BAX was stained with Polyclonal rabbit Anti-BAX and Goat Anti-Rabbit IgG, Rhodamine conjugated (Red channel-Left Lower quadrant). Nuclei were counterstained with DAPI (Blue channel-Left Upper quadrant). Combined Images are represented in the Right Lower quadrant. Nu=Nucleus. Red arrow points to nuclear staining and White arrow points to cytoplasmic staining. Representative Fluorescence micrographs of untreated cells serving as no primary antibody control are shown in Fig.3.19K.

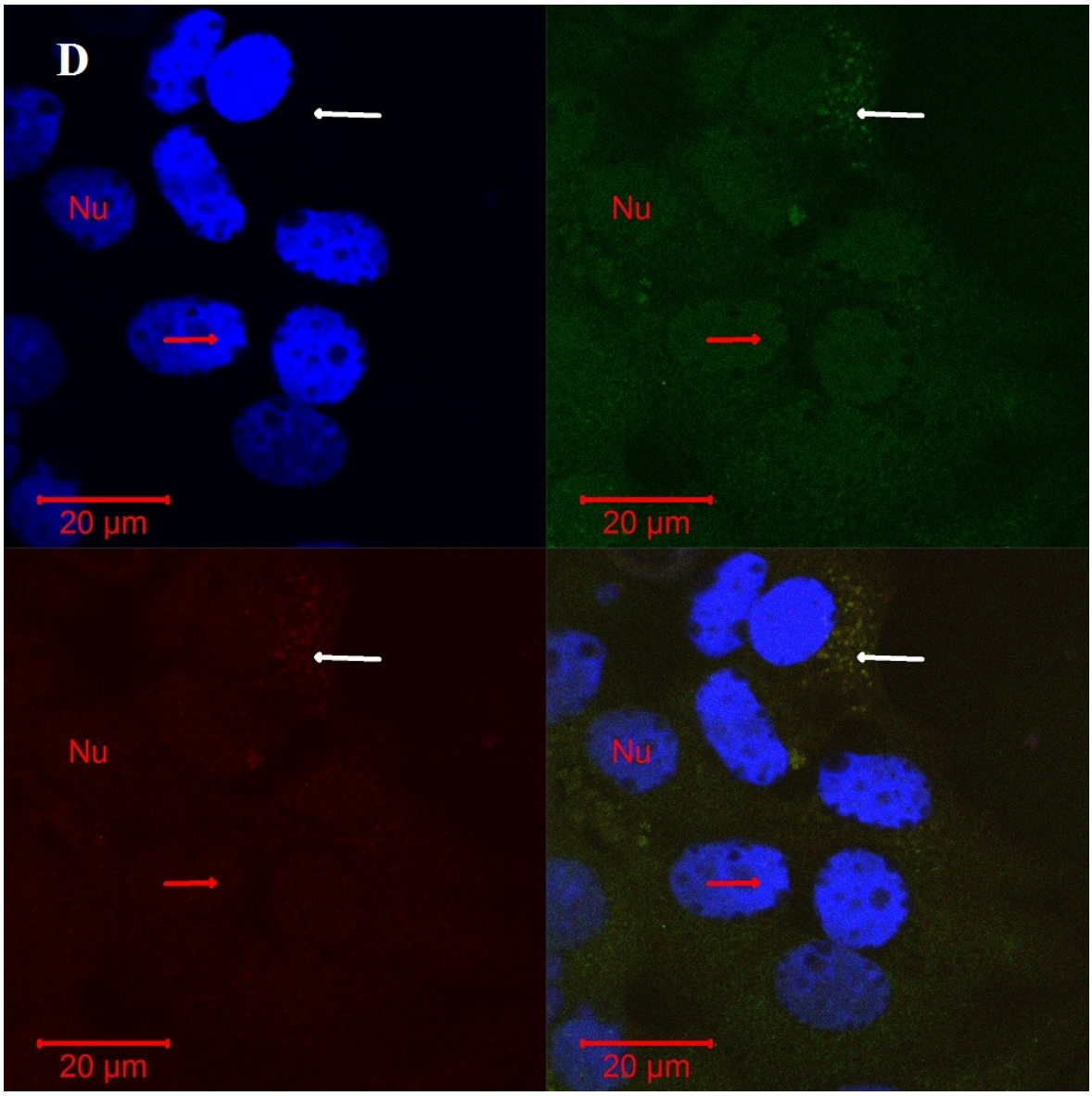

Figure 3.19D: Fluorescence micrographs of MCF-7 cells exposed to 1.8µg/ml FTC for 96 hours. BCL-2 was stained with Monoclonal Anti-BCL-2 and Goat Anti-Mouse IgG, FITC conjugated (Green channel-Right Upper quadrant). BAX was stained with Polyclonal rabbit Anti-BAX and Goat Anti-Rabbit IgG, Rhodamine conjugated (Red channel-Left Lower quadrant). Nuclei were counterstained with DAPI (Blue channel-Left Upper quadrant). Combined Images are represented in the Right Lower quadrant. Nu=Nucleus. Red arrow points to nuclear staining and White arrow points to cytoplasmic staining. Representative Fluorescence micrographs of untreated cells serving as no primary antibody control are shown in Fig.3.19K.

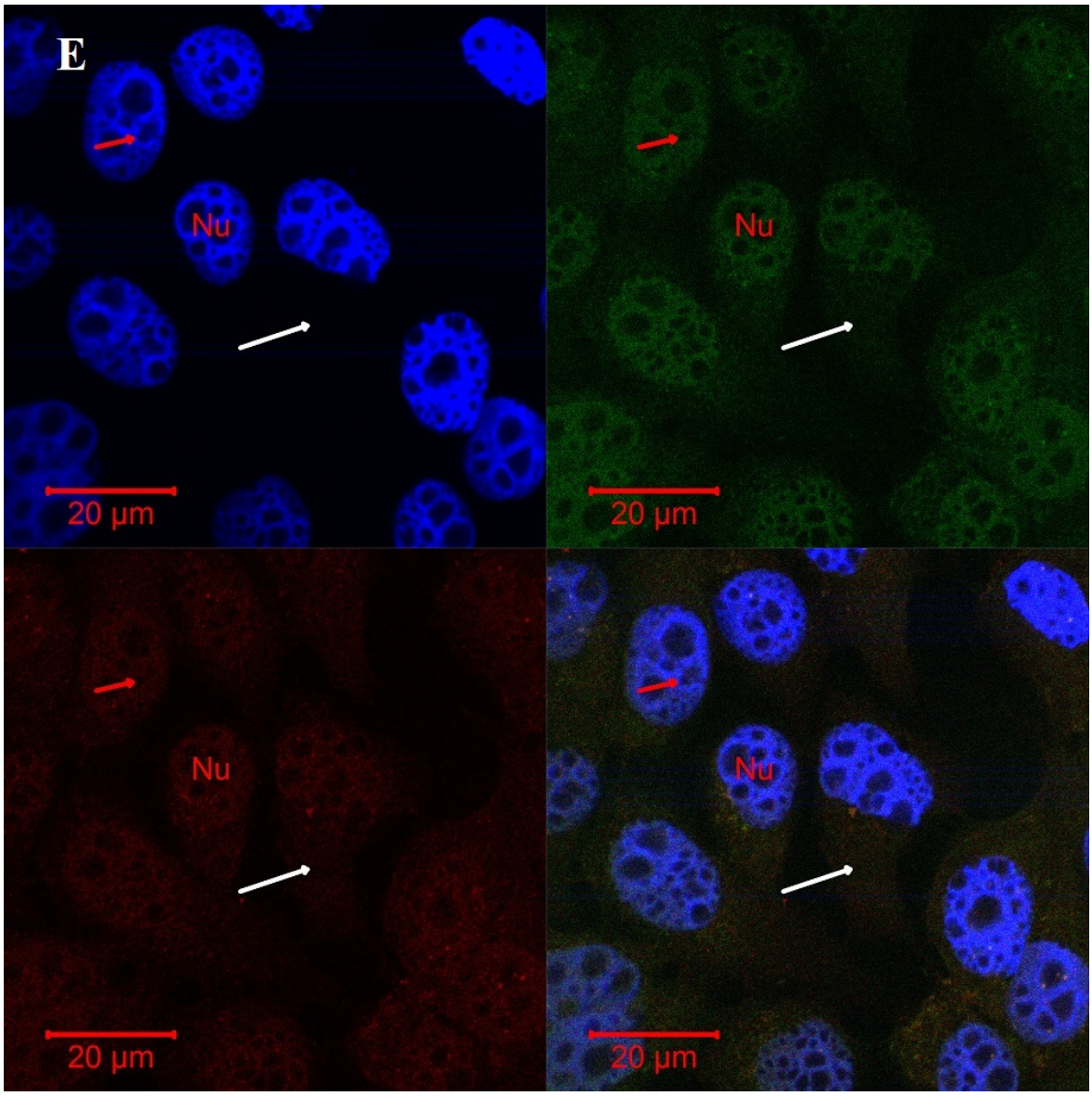

Figure 3.19E: Fluorescence micrographs of MCF-7 cells exposed to 4.07µg/ml EFV for 96 hours. BCL-2 was stained with Monoclonal Anti-BCL-2 and Goat Anti-Mouse IgG, FITC conjugated (Green channel-Right Upper quadrant). BAX was stained with Polyclonal rabbit Anti-BAX and Goat Anti-Rabbit IgG, Rhodamine conjugated (Red channel-Left Lower quadrant). Nuclei were counterstained with DAPI (Blue channel-Left Upper quadrant). Combined Images are represented in the Right Lower quadrant. Nu=Nucleus. Red arrow points to nuclear staining and White arrow points to cytoplasmic staining. Representative Fluorescence micrographs of untreated cells serving as no primary antibody control are shown in Fig.3.19K.

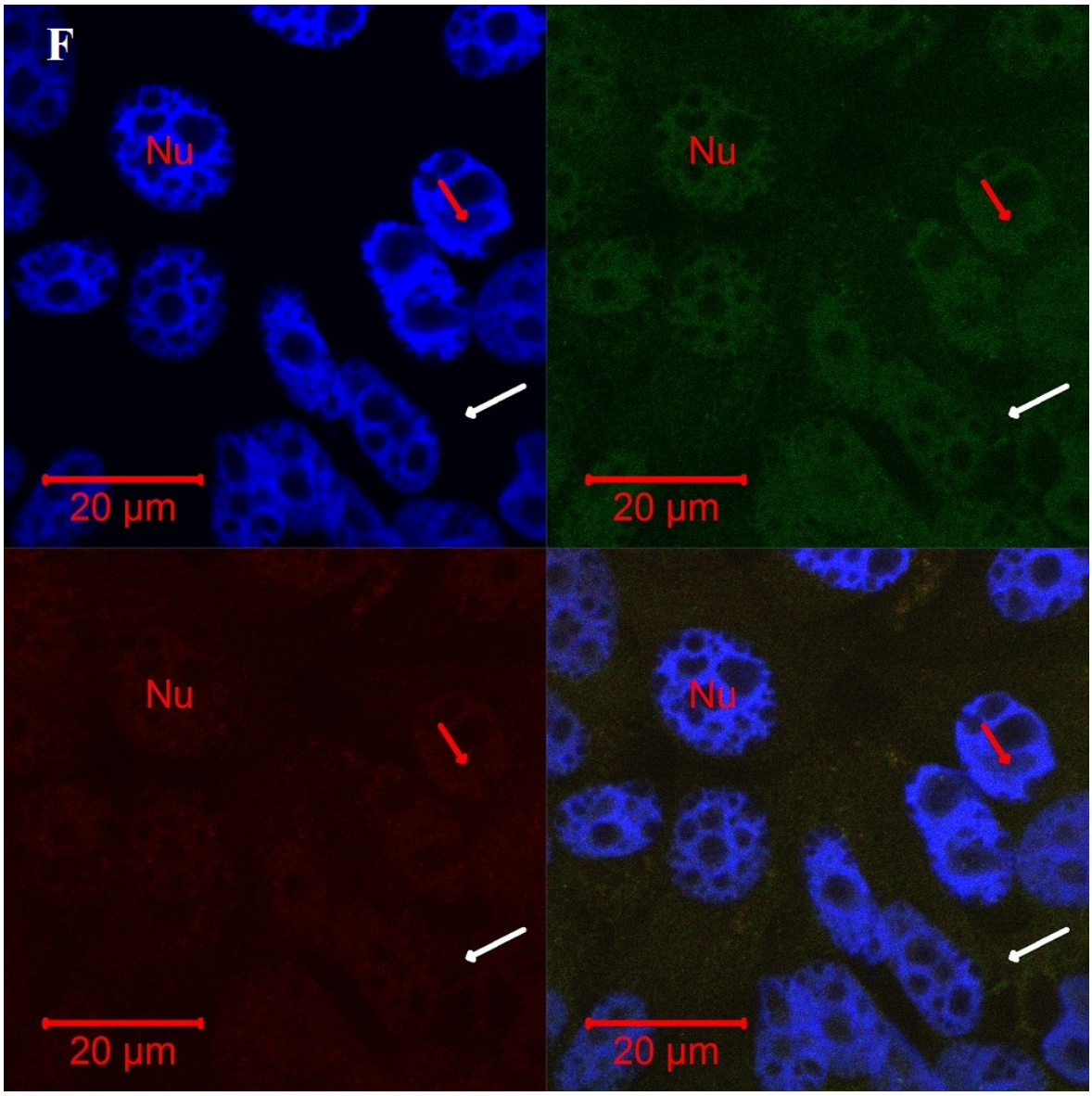

Figure 3.19F: Fluorescence micrographs of MCF-7 cells exposed to 0.3µg/ml TDF; 1.8µg/ml FTC; 4.07µg/ml EFV for 96 hours. BCL-2 was stained with Monoclonal Anti-BCL-2 and Goat Anti-Mouse IgG, FITC conjugated (Green channel-Right Upper quadrant). BAX was stained with Polyclonal rabbit Anti-BAX and Goat Anti-Rabbit IgG, Rhodamine conjugated (Red channel-Left Lower quadrant). Nuclei were counterstained with DAPI (Blue channel-Left Upper quadrant). Combined Images are represented in the Right Lower quadrant. Nu=Nucleus. Red arrow points to nuclear staining and White arrow points to cytoplasmic staining. Representative Fluorescence micrographs of untreated cells serving as no primary antibody control are shown in Fig.3.19K.

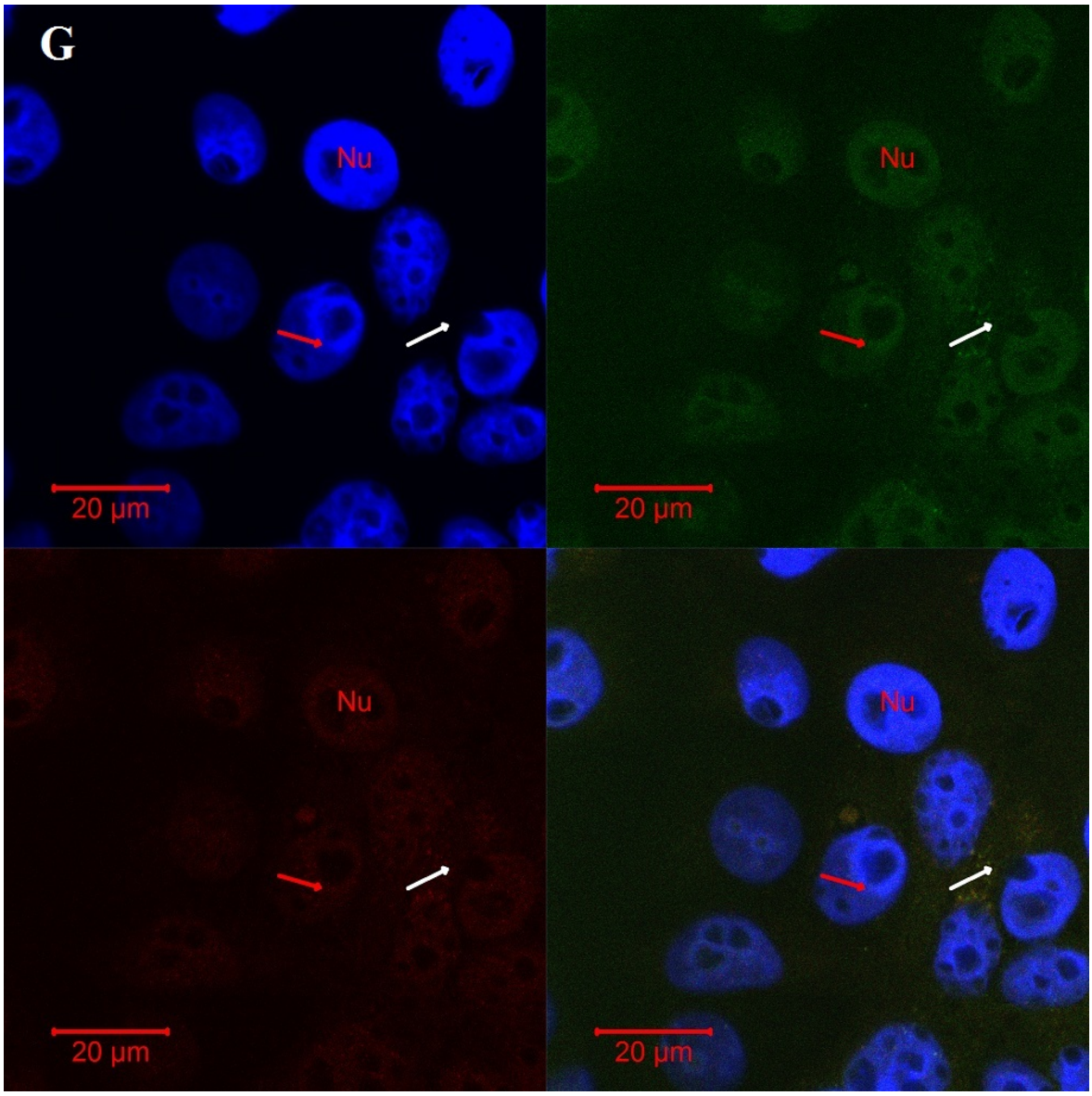

Figure 3.19G: Fluorescence micrographs of MCF-7 cells exposed to 9.8µg/ml LPV for 96 hours. BCL-2 was stained with Monoclonal Anti-BCL-2 and Goat Anti-Mouse IgG, FITC conjugated (Green channel-Right Upper quadrant). BAX was stained with Polyclonal rabbit Anti-BAX and Goat Anti-Rabbit IgG, Rhodamine conjugated (Red channel-Left Lower quadrant). Nuclei were counterstained with DAPI (Blue channel-Left Upper quadrant). Combined Images are represented in the Right Lower quadrant. Nu=Nucleus. Red arrow points to nuclear staining and White arrow points to cytoplasmic staining. Representative Fluorescence micrographs of untreated cells serving as no primary antibody control are shown in Fig.3.19K.

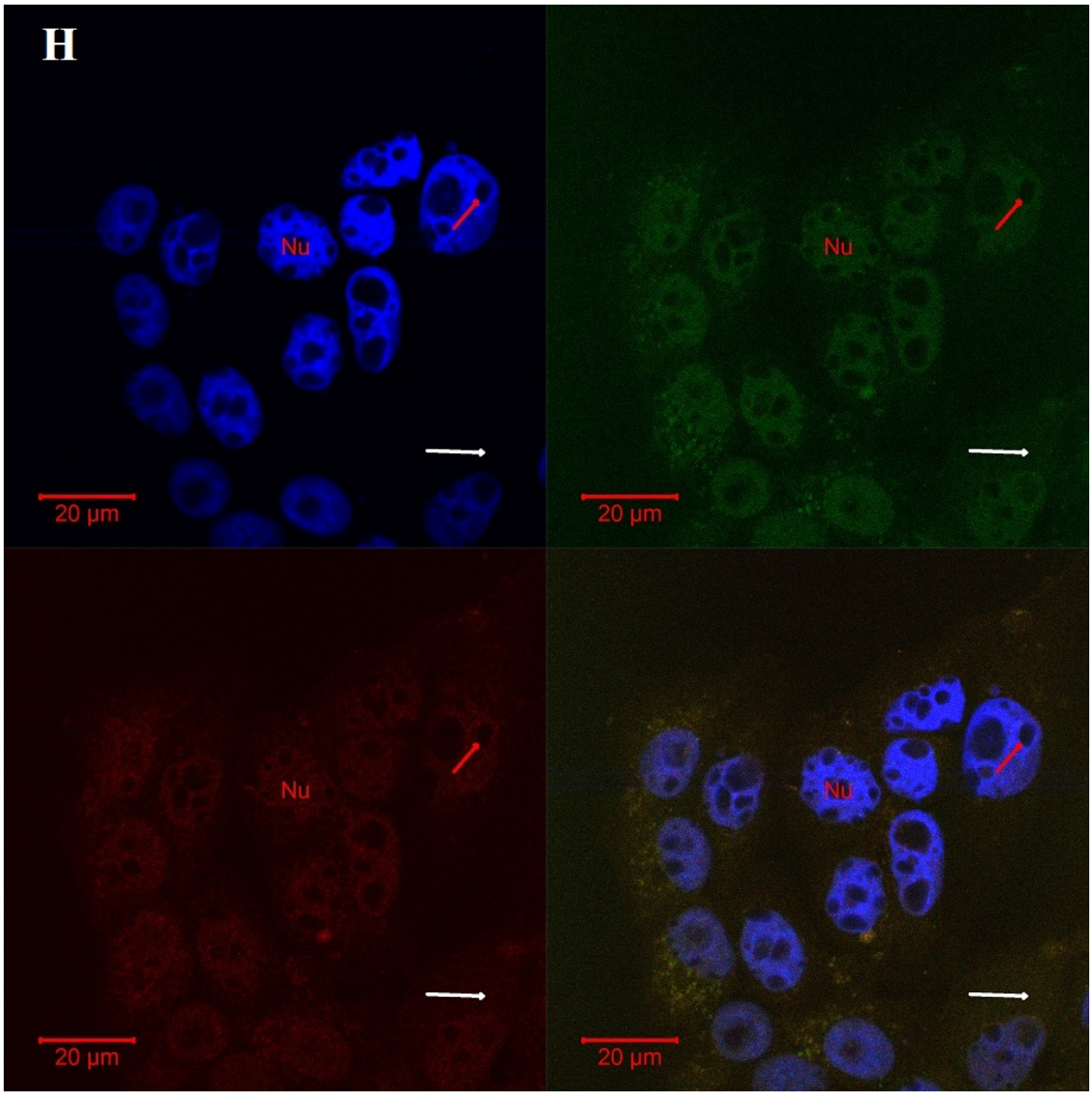

Figure 3.19H: Fluorescence micrographs of MCF-7 cells exposed to 0.6µg/ml RTV for 96 hours. BCL-2 was stained with Monoclonal Anti-BCL-2 and Goat Anti-Mouse IgG, FITC conjugated (Green channel-Right Upper quadrant). BAX was stained with Polyclonal rabbit Anti-BAX and Goat Anti-Rabbit IgG, Rhodamine conjugated (Red channel-Left Lower quadrant). Nuclei were counterstained with DAPI (Blue channel-Left Upper quadrant). Combined Images are represented in the Right Lower quadrant. Nu=Nucleus. Red arrow points to nuclear staining and White arrow points to cytoplasmic staining. Representative Fluorescence micrographs of untreated cells serving as no primary antibody control are shown in Fig.3.19K.

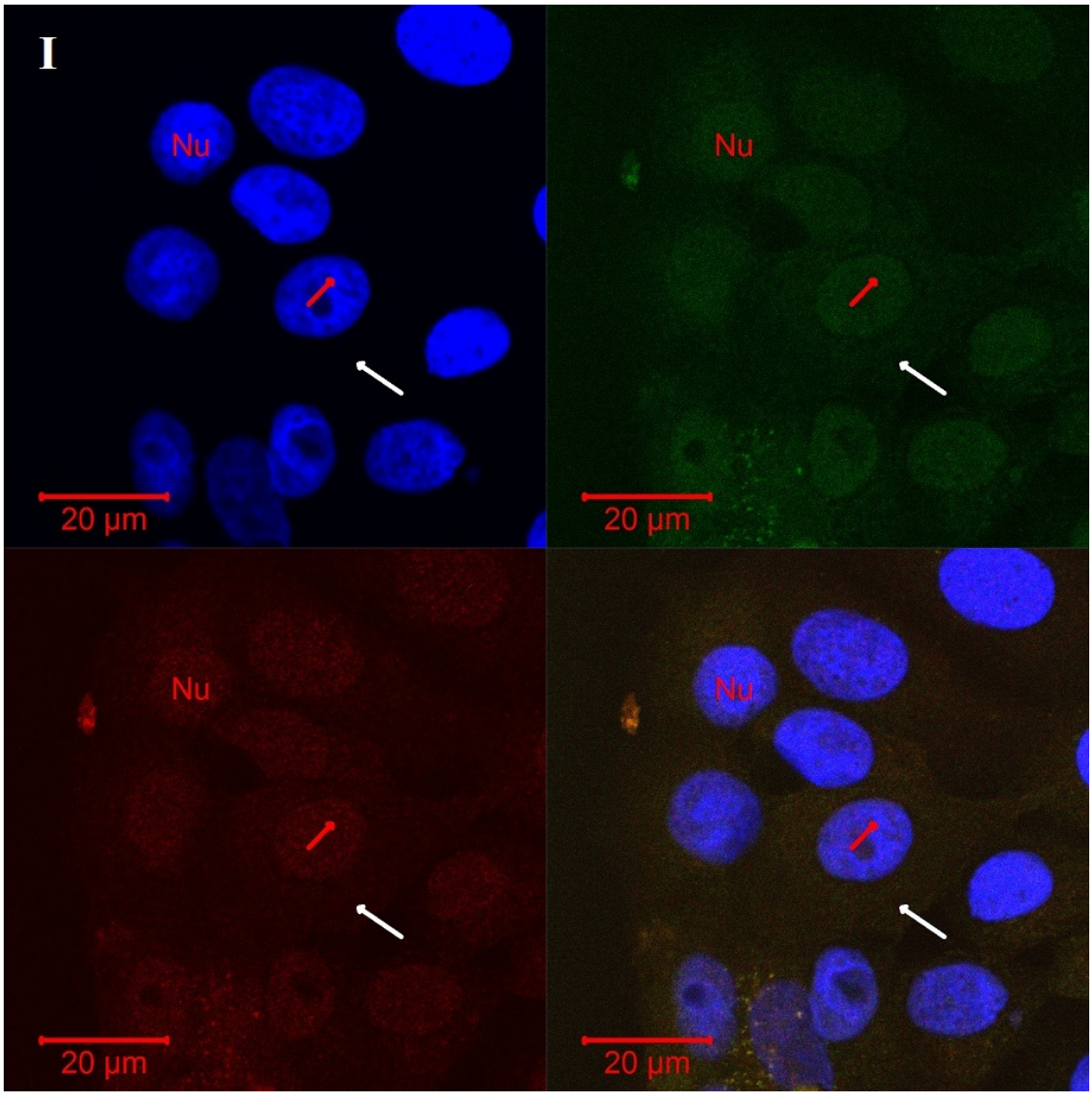

Figure 3.19I: Fluorescence micrographs of MCF-7 cells exposed to 9.8µg/ml LPV, 0.6µg/ml RTV for 96 hours. BCL-2 was stained with Monoclonal Anti-BCL-2 and Goat Anti-Mouse IgG, FITC conjugated (Green channel-Right Upper quadrant). BAX was stained with Polyclonal rabbit Anti-BAX and Goat Anti-Rabbit IgG, Rhodamine conjugated (Red channel-Left Lower quadrant). Nuclei were counterstained with DAPI (Blue channel-Left Upper quadrant). Combined Images are represented in the Right Lower quadrant. Nu=Nucleus. Red arrow points to nuclear staining and White arrow points to cytoplasmic staining. Representative Fluorescence micrographs of untreated cells serving as no primary antibody control are shown in Fig.3.19K.

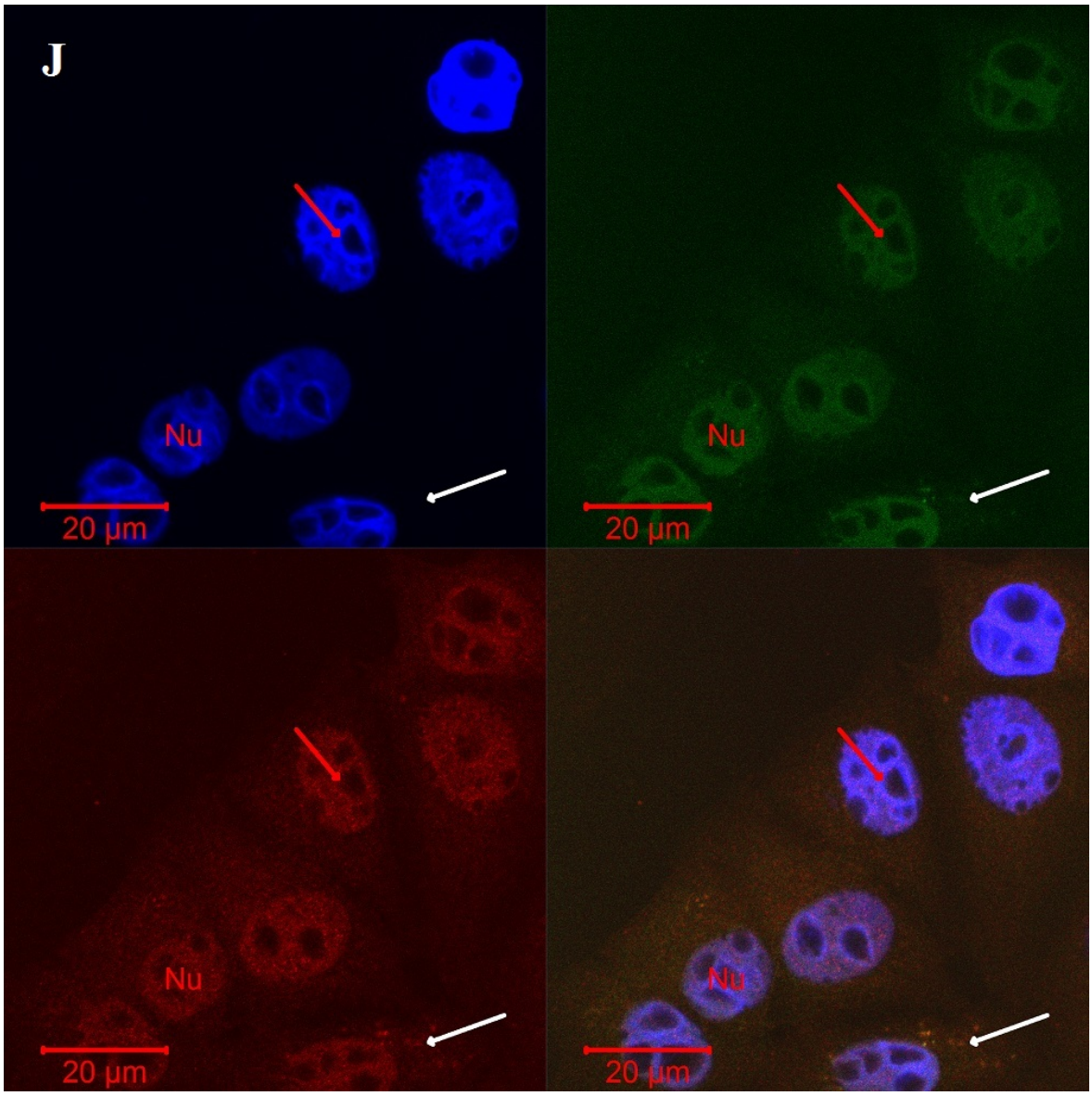

Figure 3.19J: Fluorescence micrographs of MCF-7 cells exposed to 0.3µg/ml TDF; 1.8µg/ml FTC; 9.8µg/ml LPV, 0.6µg/ml RTV for 96 hours. BCL-2 was stained with Monoclonal Anti-BCL-2 and Goat Anti-Mouse IgG, FITC conjugated (Green channel-Right Upper quadrant). BAX was stained with Polyclonal rabbit Anti-BAX and Goat Anti-Rabbit IgG, Rhodamine conjugated (Red channel-Left Lower quadrant). Nuclei were counterstained with DAPI (Blue channel-Left Upper quadrant). Combined Images are represented in the Right Lower quadrant. Nu=Nucleus. Red arrow points to nuclear staining and White arrow points to cytoplasmic staining. Representative Fluorescence micrographs of untreated cells serving as no primary antibody control are shown in Fig.3.19K.

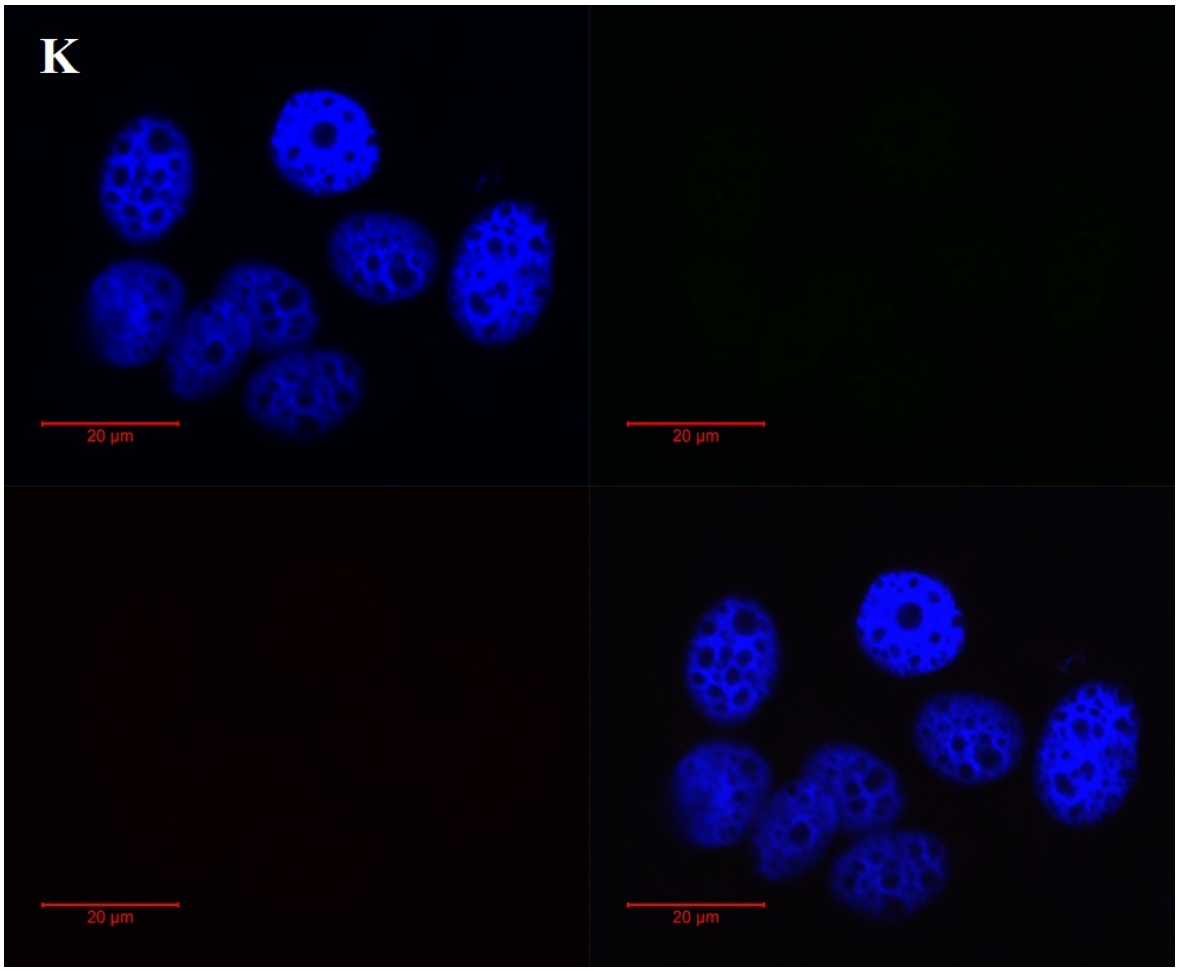

Figure 3.19K: Fluorescence micrographs of untreated breast MCF-7 cells serving as no primary antibody control. Cells were incubated with goat serum in place of primary antibodies and incubated with Goat Anti-Mouse IgG, FITC conjugated (Green channel-Right Upper quadrant) and Goat Anti-Rabbit IgG, Rhodamine conjugated (Red channel-Left Lower quadrant). Nuclei were counterstained with DAPI (Blue channel-Left Upper quadrant). Combined Images are represented in the Right Lower quadrant.

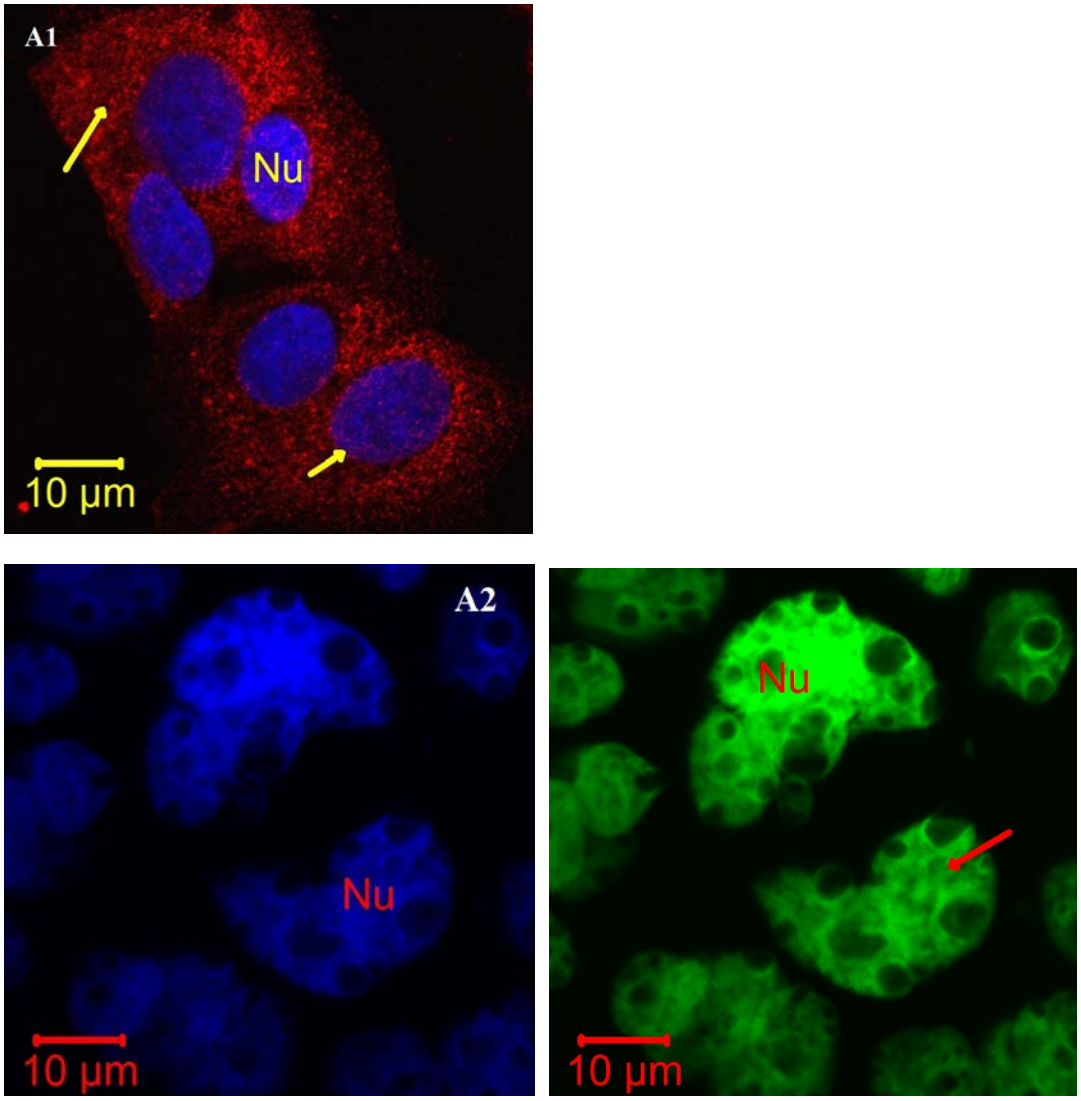

Figure 3.20 A: Fluorescence micrographs of breast MCF-10A cells exposed to Growth Medium for 96 hours. BAX (1) was stained with Polyclonal rabbit Anti-BAX and Goat Anti-Rabbit IgG, Rhodamine conjugated (Red channel). BCL-2 (2) was stained with Monoclonal Anti-BCL-2 and Goat Anti-Mouse IgG, FITC conjugated (Green channel). Nuclei were counterstained with DAPI (Blue channel). Nu=Nucleus. Red arrow point to nuclear staining and yellow arrow point to cytoplasmic staining. Representative Fluorescence micrographs of untreated cells serving as no primary antibody control are shown in Fig.3.20K.

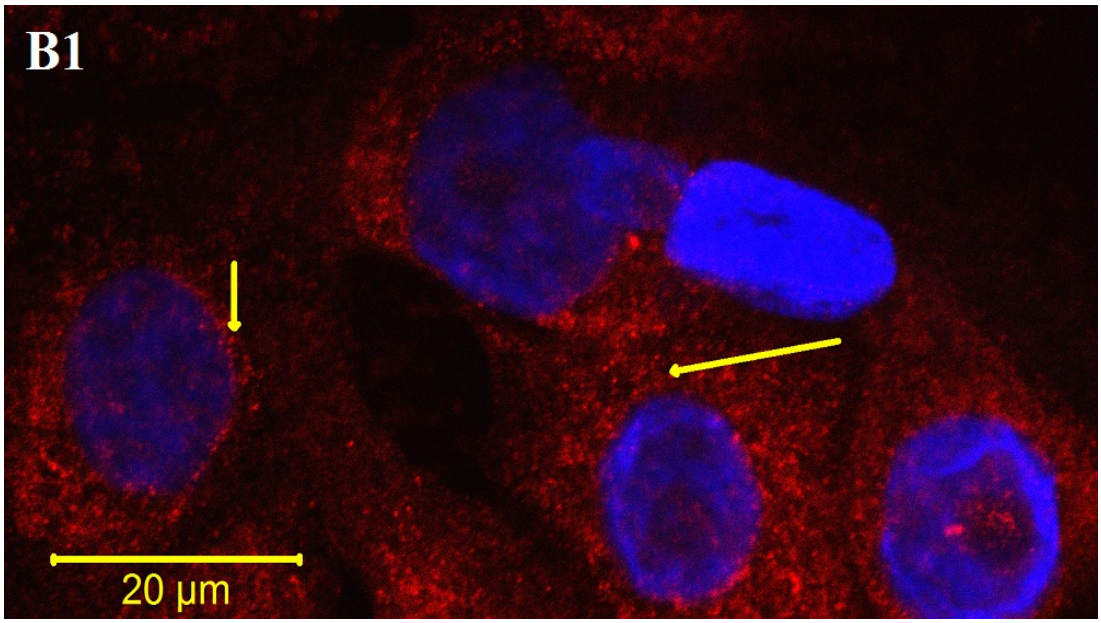

B2

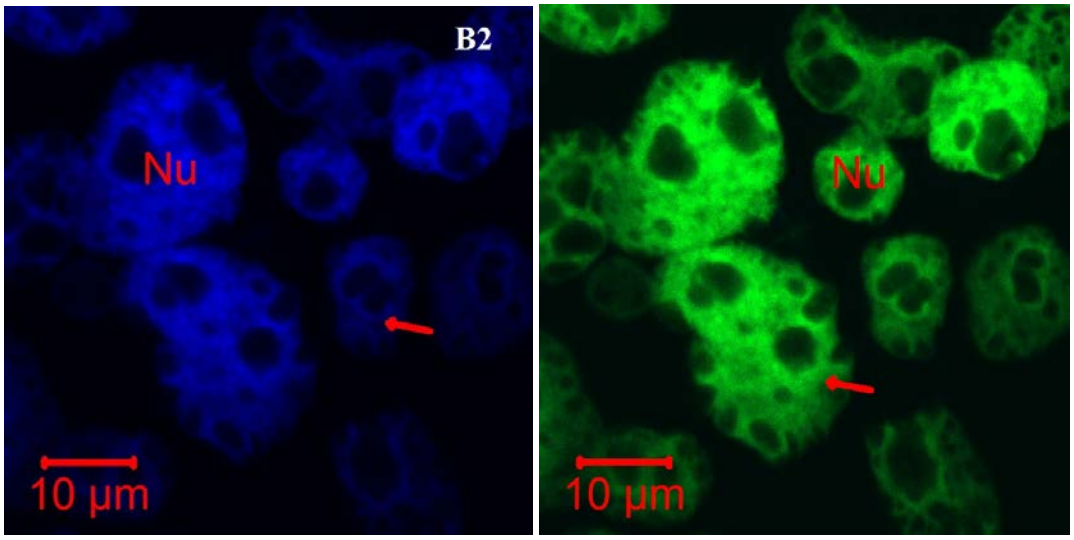

Figure 3.20B: Fluorescence micrographs of breast MCF-10A cells exposed to Vehicle-0.01% Methanol for 96 hours. BAX (1) was stained with Polyclonal rabbit Anti-BAX and Goat Anti-Rabbit IgG, Rhodamine conjugated (Red channel). BCL-2 (2) was stained with Monoclonal Anti-BCL-2 and Goat Anti-Mouse IgG, FITC conjugated (Green channel). Nuclei were counterstained with DAPI (Blue channel). Nu=Nucleus. Red arrow point to nuclear staining and yellow arrow point to cytoplasmic staining. There are no differences in protein staining, localisation and intensity as compared to growth medium alone. Representative Fluorescence micrographs of untreated cells serving as no primary antibody control are shown in Fig.3.20K.

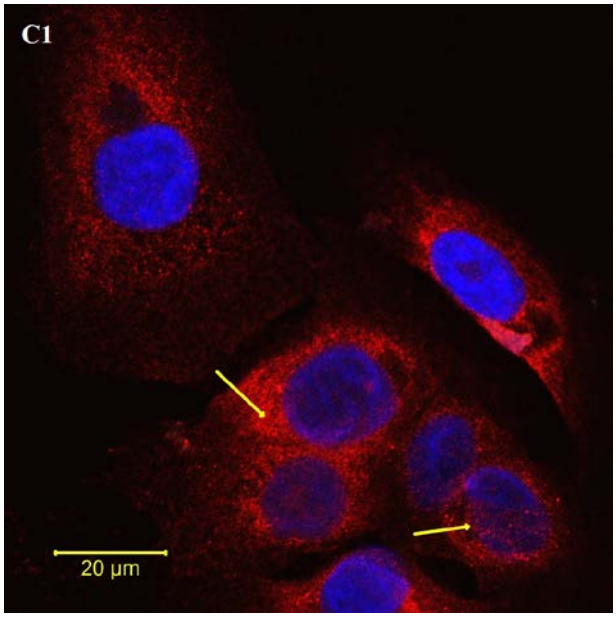

C2

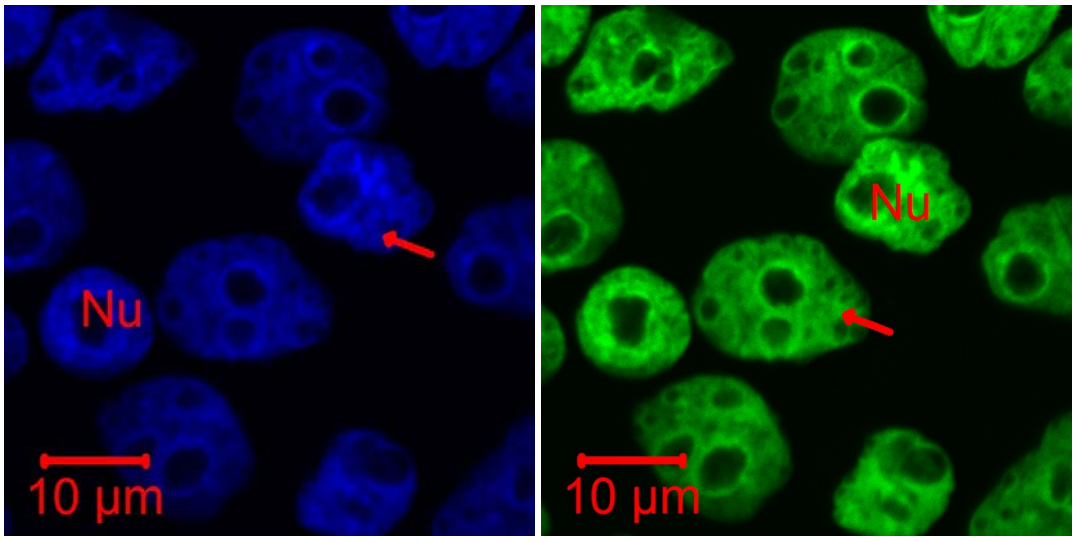

Figure 3.20C: Fluorescence micrographs of breast MCF-10A cells exposed to 0.3µg/ml TDF for 96 hours. BAX (1) was stained with Polyclonal rabbit Anti-BAX and Goat Anti-Rabbit IgG, Rhodamine conjugated (Red channel). BCL-2 (2) was stained with Monoclonal Anti-BCL-2 and Goat Anti-Mouse IgG, FITC conjugated (Green channel). Nuclei were counterstained with DAPI (Blue channel). Nu=Nucleus. Red arrow point to nuclear staining and yellow arrow point to cytoplasmic staining. Representative Fluorescence micrographs of untreated cells serving as no primary antibody control are shown in Fig.3.20K.

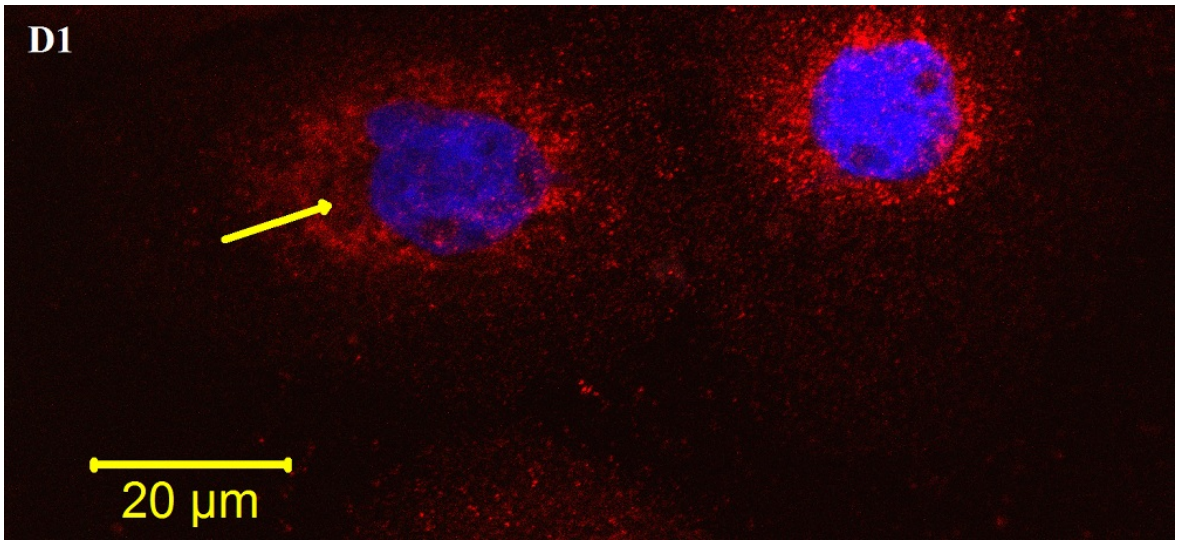

D2

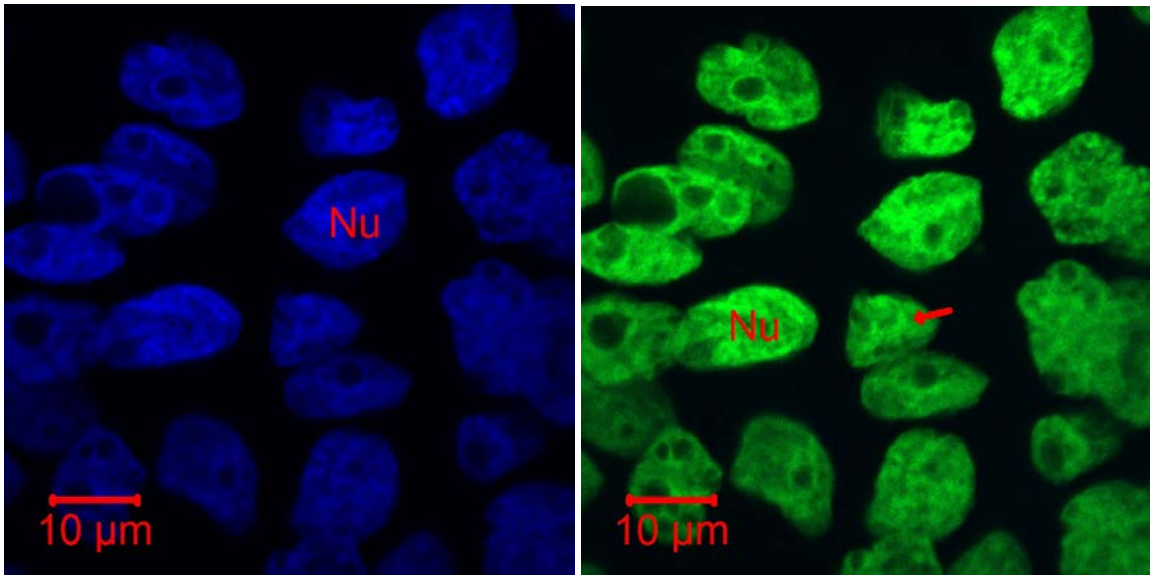

Figure 3.20D: Fluorescence micrographs of breast MCF-10A cells exposed to 1.8µg/ml FTC for 96 hours. BAX (1) was stained with Polyclonal rabbit Anti-BAX and Goat Anti-Rabbit IgG, Rhodamine conjugated (Red channel). BCL-2 (2) was stained with Monoclonal Anti-BCL-2 and Goat Anti-Mouse IgG, FITC conjugated (Green channel). Nuclei were counterstained with DAPI (Blue channel). Nu=Nucleus. Red arrow point to nuclear staining and yellow arrow point to cytoplasmic staining. Representative Fluorescence micrographs of untreated cells serving as no primary antibody control are shown in Fig.3.20K.

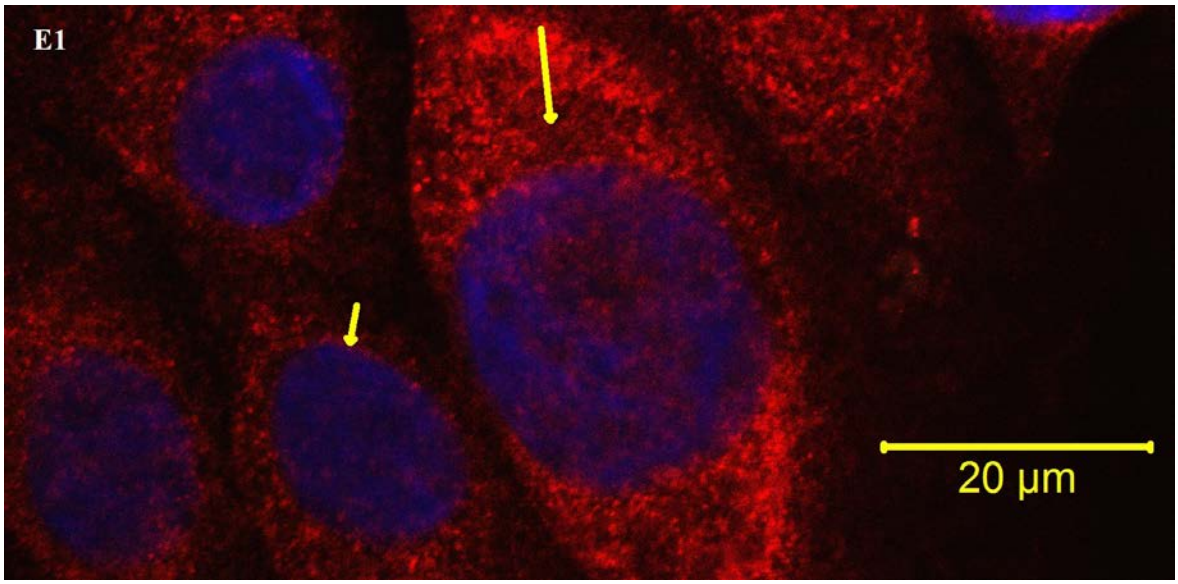

E2

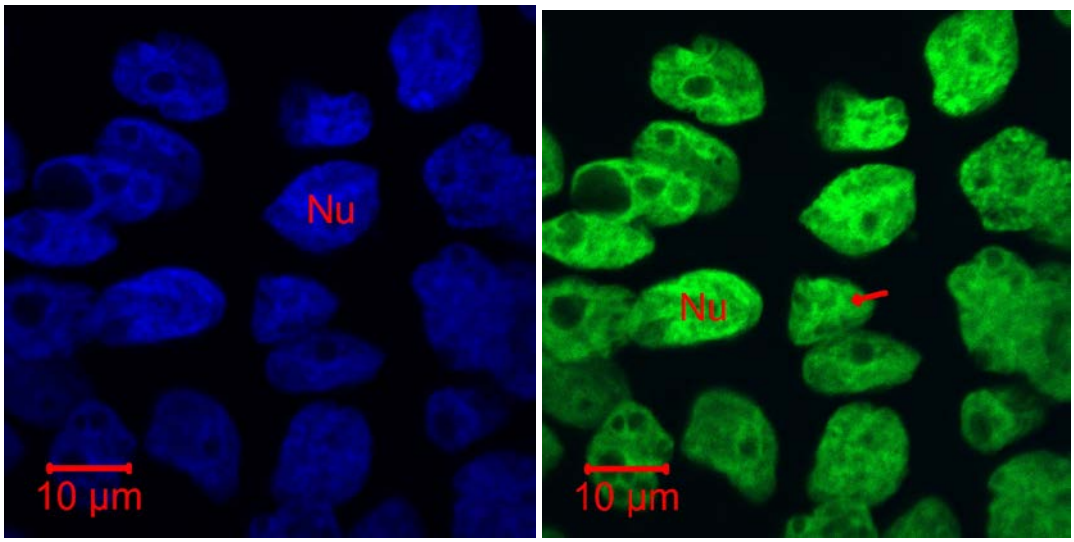

Figure 3.20E: Fluorescence micrographs of breast MCF-10A cells exposed to 4.07µg/ml EFV for 96 hours. BAX (1) was stained with Polyclonal rabbit Anti-BAX and Goat Anti-Rabbit IgG, Rhodamine conjugated (Red channel). BCL-2 (2) was stained with Monoclonal Anti-BCL-2 and Goat Anti-Mouse IgG, FITC conjugated (Green channel). Nuclei were counterstained with DAPI (Blue channel). Nu=Nucleus. Red arrow point to nuclear staining and yellow arrow point to cytoplasmic staining. Representative Fluorescence micrographs of untreated cells serving as no primary antibody control are shown in Fig.3.20K.

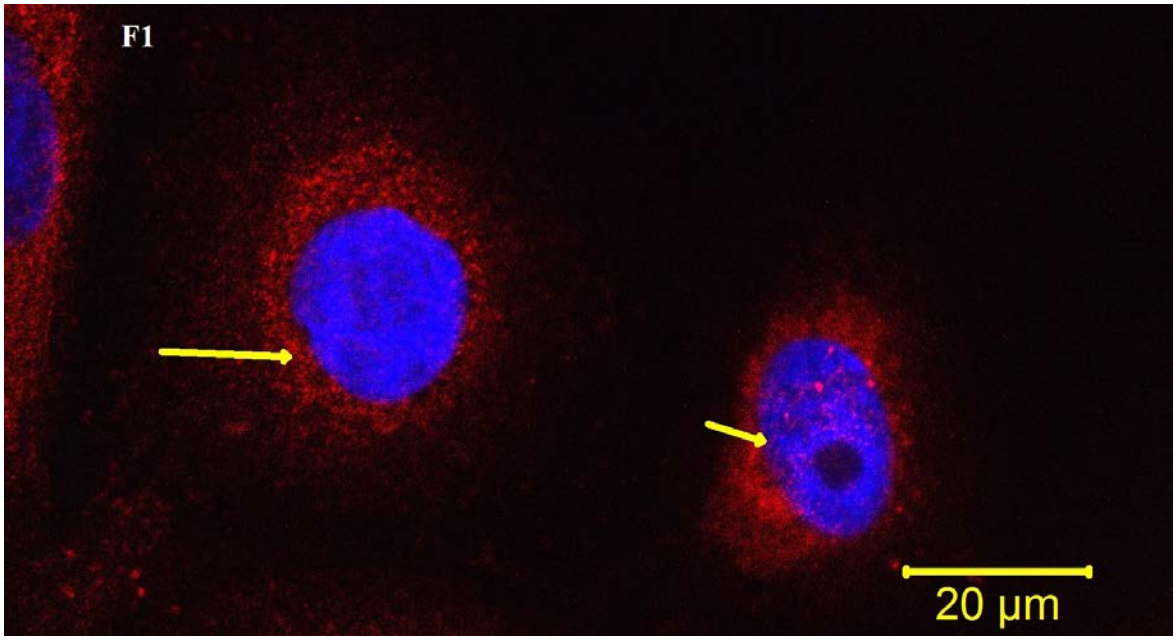

F2

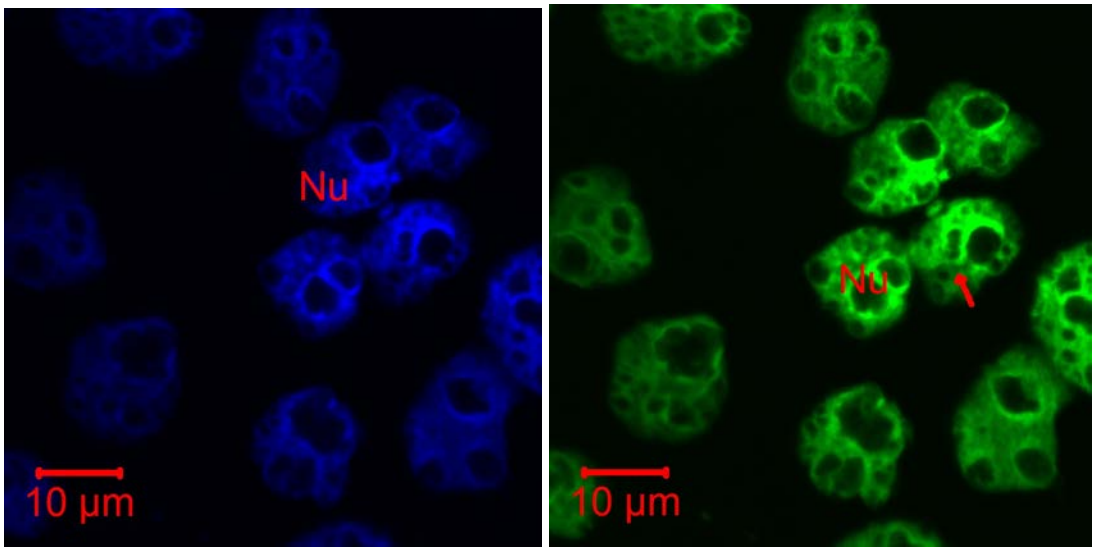

Figure 3.20F: Fluorescence micrographs of breast MCF-10A cells exposed to 0.3µg/ml TDF; 1.8µg/ml FTC; 4.07µg/ml EFV for 96 hours. BAX (1) was stained with Polyclonal rabbit Anti-BAX and Goat Anti-Rabbit IgG, Rhodamine conjugated (Red channel). BCL-2 (2) was stained with Monoclonal Anti-BCL-2 and Goat Anti-Mouse IgG, FITC conjugated (Green channel). Nuclei were counterstained with DAPI (Blue channel). Nu=Nucleus. Red arrow point to nuclear staining and yellow arrow point to cytoplasmic staining. Representative Fluorescence micrographs of untreated cells serving as no primary antibody control are shown in Fig.3.20K.

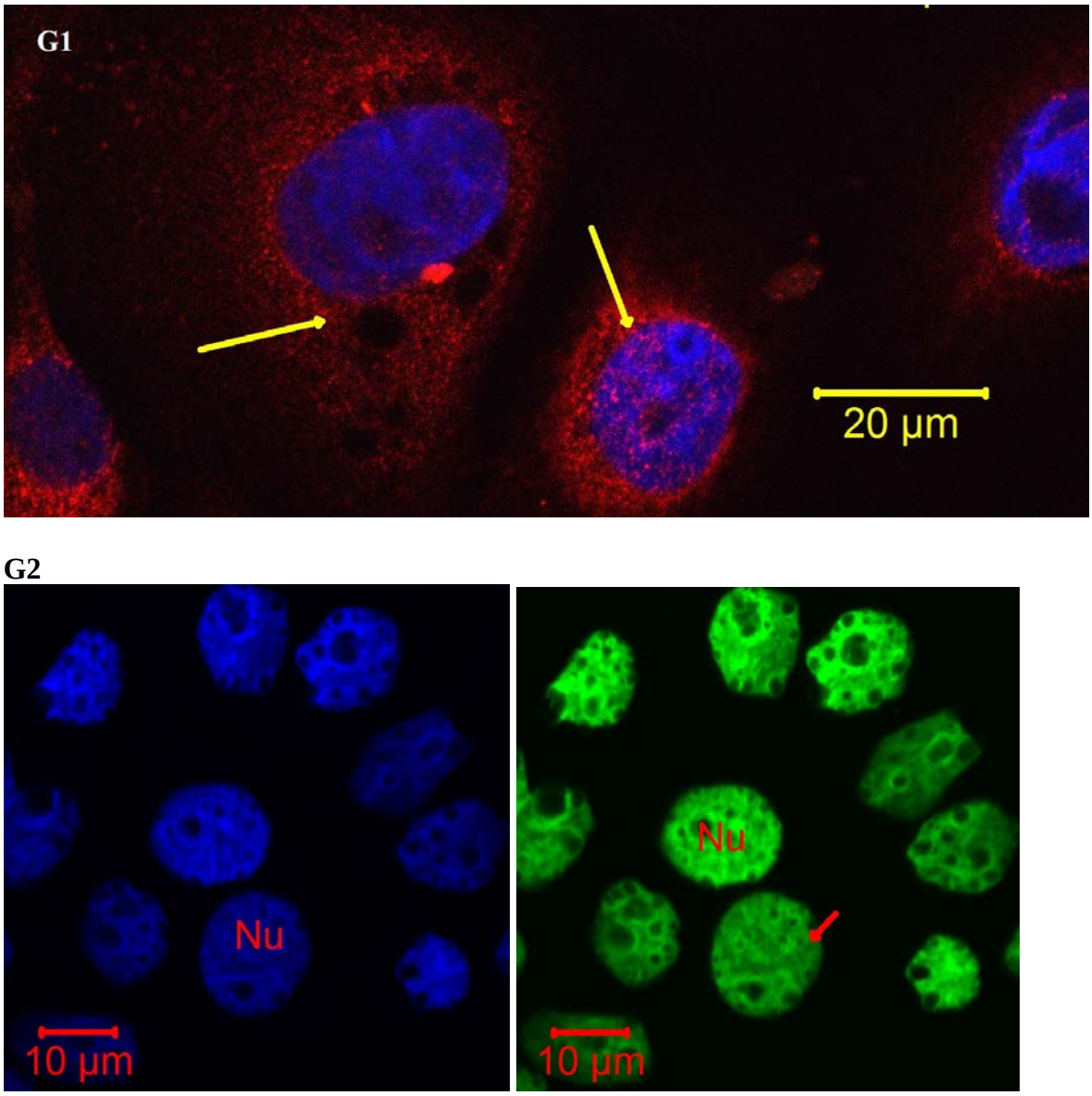

Figure 3.20G: Fluorescence micrographs of breast MCF-10A cells exposed to 9.8µg/ml LPV for 96 hours. BAX (1) was stained with Polyclonal rabbit Anti-BAX and Goat Anti-Rabbit IgG, Rhodamine conjugated (Red channel). BCL-2 (2) was stained with Monoclonal Anti-BCL-2 and Goat Anti-Mouse IgG, FITC conjugated (Green channel). Nuclei were counterstained with DAPI (Blue channel). Nu=Nucleus. Red arrow point to nuclear staining and yellow arrow point to cytoplasmic staining. Representative Fluorescence micrographs of untreated cells serving as no primary antibody control are shown in Fig.3.20K.

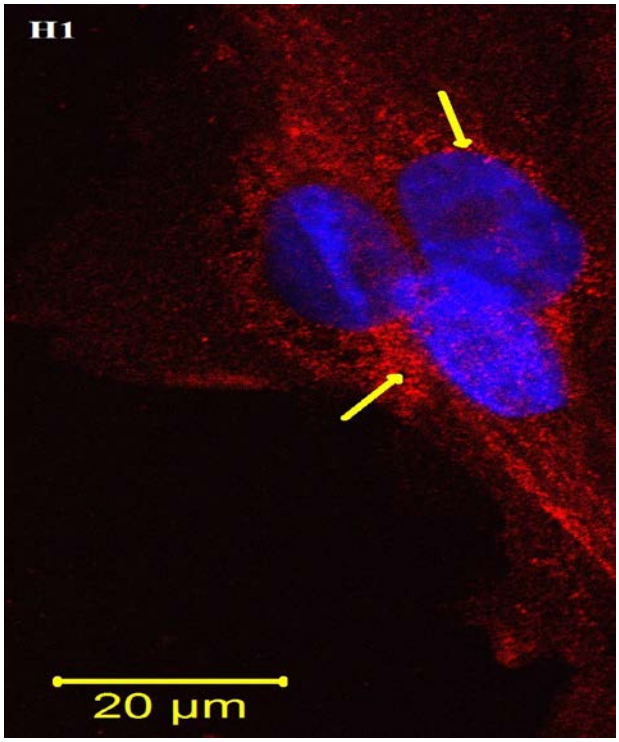

H2

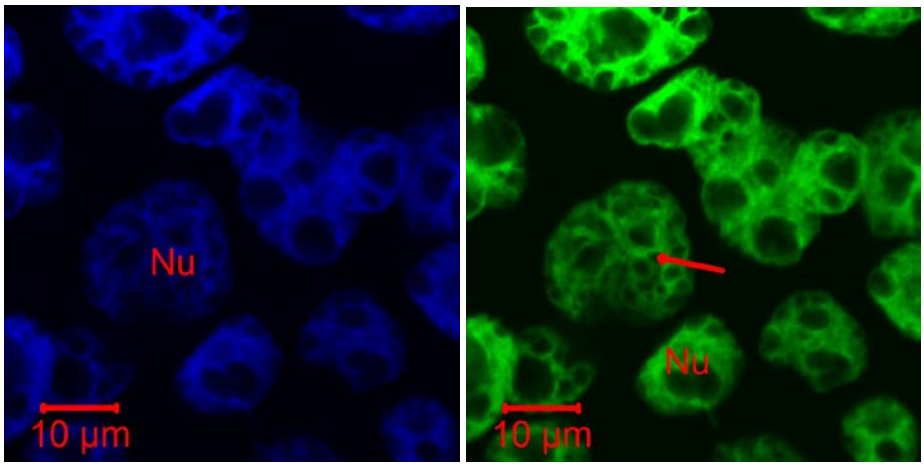

Figure 3.20H: Fluorescence micrographs of breast MCF-10A cells exposed to 0.6µg/ml RTV for 96 hours. BAX (1) was stained with Polyclonal rabbit Anti-BAX and Goat Anti-Rabbit IgG, Rhodamine conjugated (Red channel). BCL-2 (2) was stained with Monoclonal Anti-BCL-2 and Goat Anti-Mouse IgG, FITC conjugated (Green channel). Nuclei were counterstained with DAPI (Blue channel). Nu=Nucleus. Red arrow point to nuclear staining and yellow arrow point to cytoplasmic staining. Representative Fluorescence micrographs of untreated cells serving as no primary antibody control are shown in Fig.3.20K.

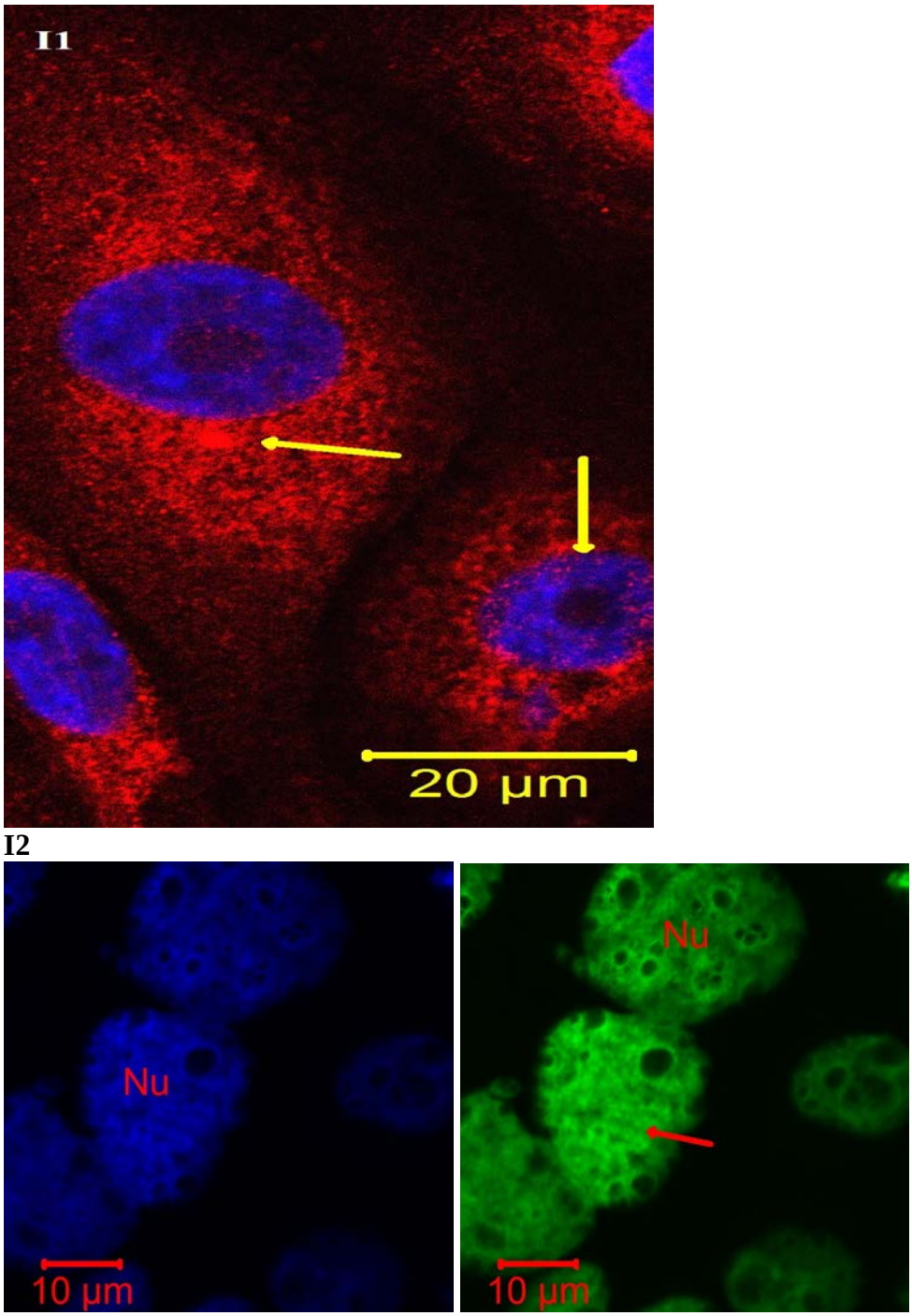

Figure 3.20I: Fluorescence micrographs of breast MCF-10A cells exposed to 9.8µg/ml LPV; 0.6µg/ml RTV for 96 hours. BAX (1) was stained with Polyclonal rabbit Anti-BAX and Goat Anti-Rabbit IgG, Rhodamine conjugated (Red channel). BCL-2 (2) was stained with Monoclonal Anti-BCL-2 and Goat Anti-Mouse IgG, FITC conjugated (Green channel). Nuclei were counterstained with DAPI (Blue channel). Nu=Nucleus. Red arrow point to nuclear staining and yellow arrow point to cytoplasmic staining. Representative Fluorescence micrographs of untreated cells serving as no primary antibody control are shown in Fig.3.20K.

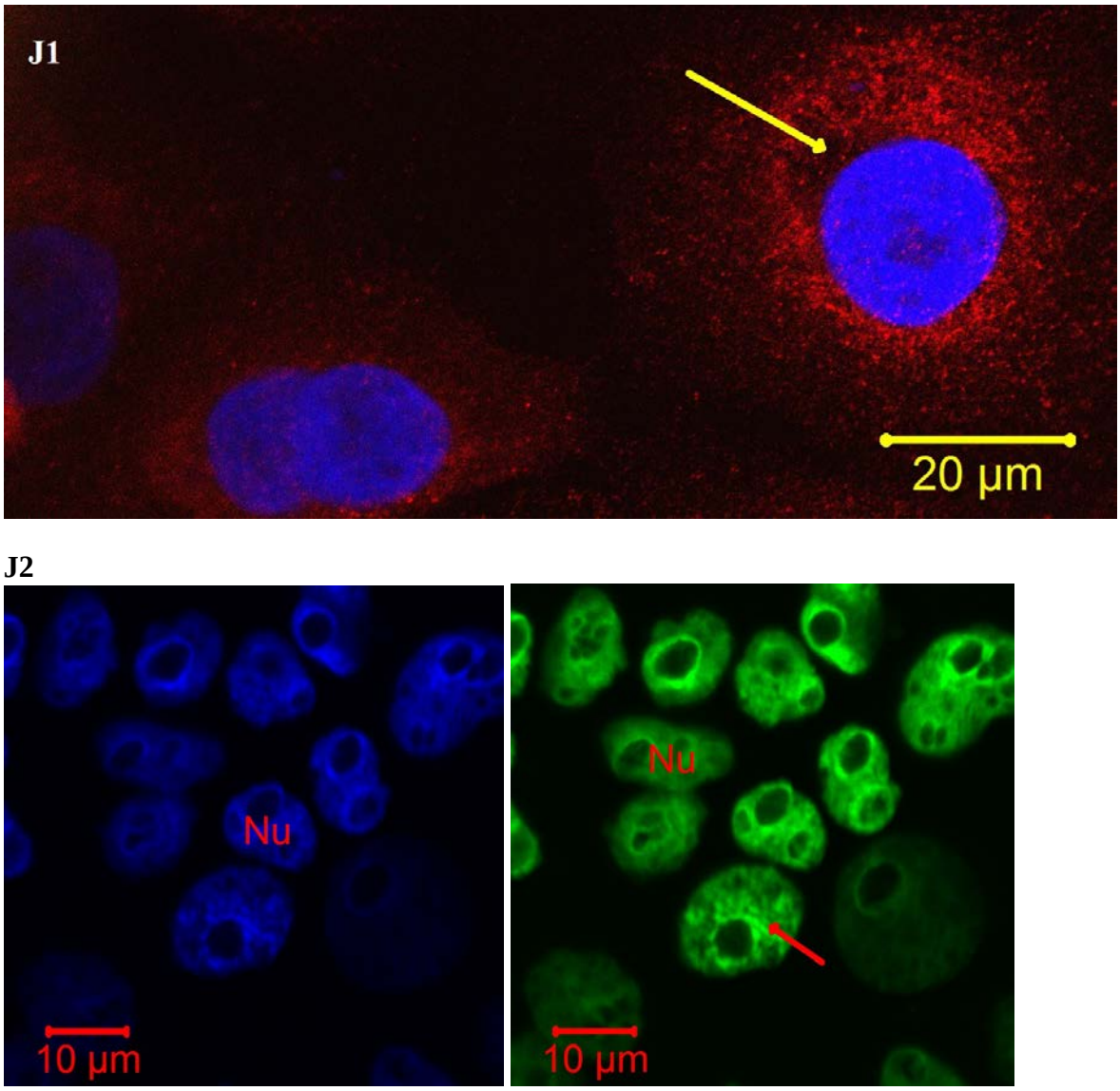

Figure 3.20J: Fluorescence micrographs of breast MCF-10A cells exposed to 0.3µg/ml TDF; 1.8µg/ml FTC; 9.8µg/ml LPV; 0.6µg/ml RTV for 96 hours. BAX (1) was stained with Polyclonal rabbit Anti-BAX and Goat Anti-Rabbit IgG, Rhodamine conjugated (Red channel). BCL-2 (2) was stained with Monoclonal Anti-BCL-2 and Goat Anti-Mouse IgG, FITC conjugated (Green channel). Nuclei were counterstained with DAPI (Blue channel). Nu=Nucleus. Red arrow point to nuclear staining and yellow arrow point to cytoplasmic staining. Representative Fluorescence micrographs of untreated cells serving as no primary antibody control are shown in Fig.3.20K.

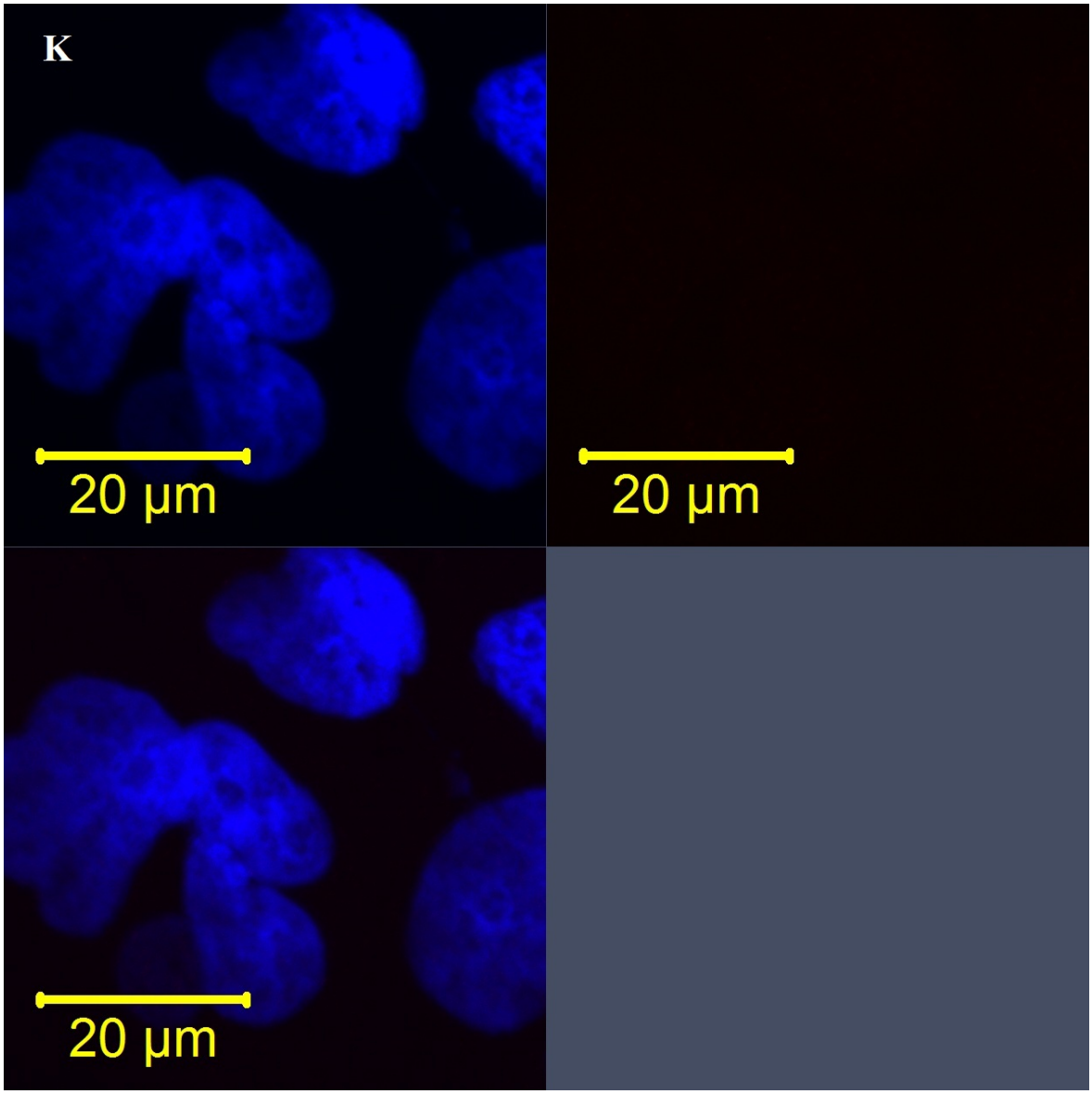

Figure 3.20K: Fluorescence micrographs of untreated breast MCF-10A cells serving as no primary antibody control. Cells were incubated with goat serum in place of primary antibodies and incubated with Goat Anti-Rabbit IgG, Rhodamine conjugated and Goat Anti-Mouse IgG, FITC conjugated (Right Upper quadrant). Nuclei were counterstained with DAPI (Blue channel-Left Upper quadrant). Combined Images are represented in the left Lower quadrant.

3.3.3 Immunofluorescence of anti-angiogenic VEGF $_{165b}$ protein in cervical cancer (HCS-2) and normal cervical (NCE16IIA) cells exposed to antiretroviral drugs

The anti-angiogenic $VEGF_{165b}$ protein, an inhibitor of the $VEGF_{165}$ mediated VEGF receptor 2 phosphorylation and signalling is expressed and localised in the nuclei and cytoplasm of HCS-2 (Fig 3.21 A) and NCE16IIA (Fig 3.22 A) cells. Mean fluorescence intensities of $VEGF_{165b}$ in the nuclei and cytoplasm were statistically analysed (ANOVA) between the untreated/vehicle control and the treated groups. (Graphical representation presented in Figs. 3.25-3.32; Data summaries shown in Appendix E). There are no differences in protein staining, localisation and intensity of vehicle (0.01% methanol) treated group as compared to growth medium alone (Fig. 3.21B and Fig. 3.22B). Exposing both cervical cells to the different antiretroviral drugs individually and in combination for 96 hours did not alter the localisation of $VEGF_{165b}$ (Figs. 3.21 C-J and Figs. 3.22 C-J) in both cell lines. Fig. 3.21 C-J are representative images illustrating the effects of the antiretroviral drugs on expression of $VEGF_{165b}$ in HCS-2 cell cultures. Figs. 3.22 C-J are representative images illustrating the effects of the antiretroviral drugs on expression of $VEGF_{165b}$ in NCE16IIA cell cultures.

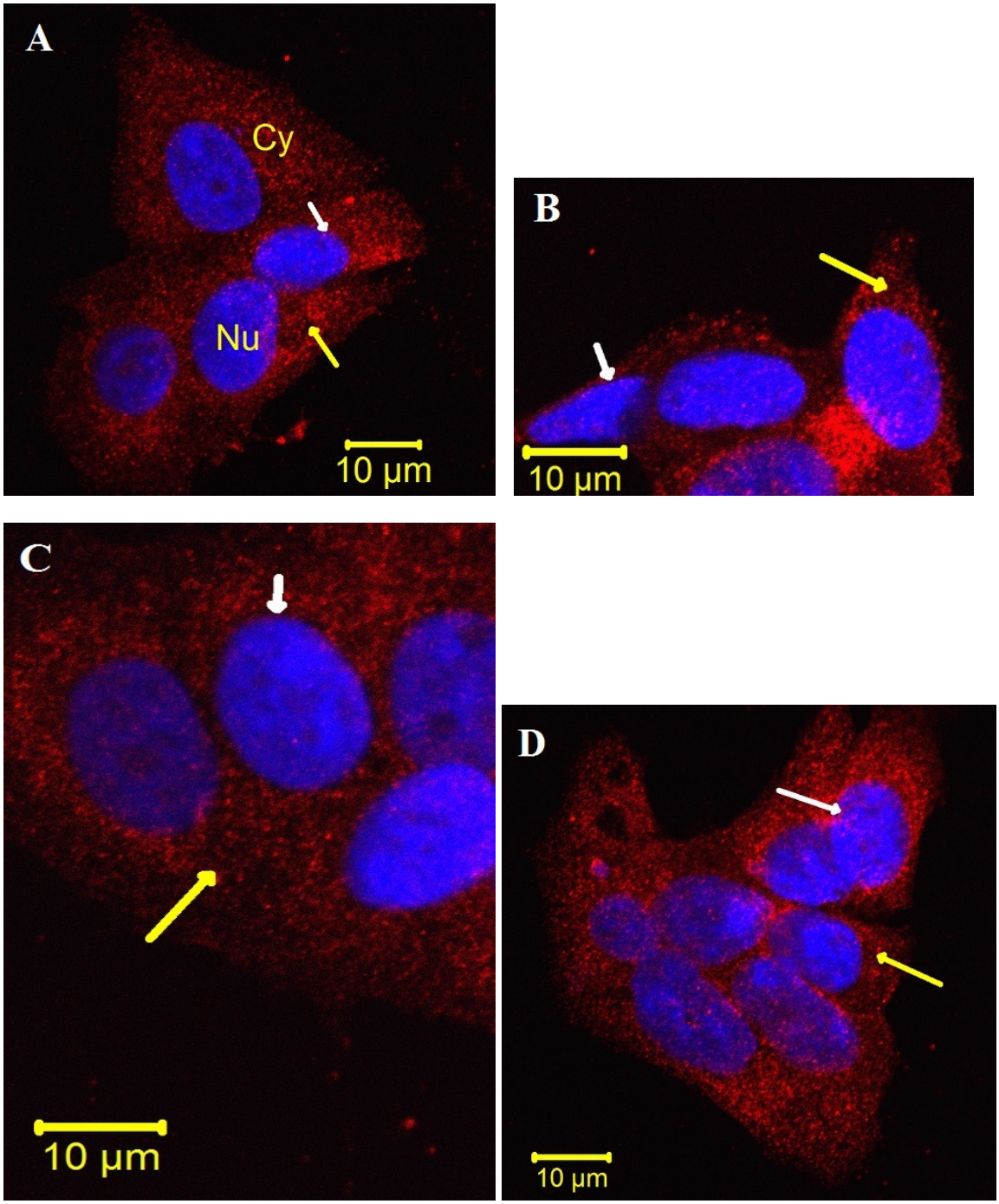

Figure 3.21 A-D: Fluorescence micrographs of HCS-2 cells exposed to Growth Medium **(A)**, Vehicle-0.01% Methanol **(B)**, 0.3µg/ml TDF **(C)**, 1.8µg/ml FTC **(D)** for 96 hours. $VEGF_{165b}$ was stained with polyclonal rabbit anti-human $VEGF_{165b}$ (5µg/ml) and Goat Anti-Rabbit IgG, Rhodamine conjugated (Red channel). Nuclei were counterstained with DAPI (Blue channel). Combined Images are shown. Nu=Nucleus. Cy=Cytoplasm. White arrow point to perinuclear staining and yellow arrow point to cytoplasmic staining. There are no differences in protein staining, localisation and intensity of vehicle treated **(B)** as compared to growth medium alone. Representative Fluorescence micrographs of untreated cells serving as no primary antibody control are shown in Fig.3.21K.

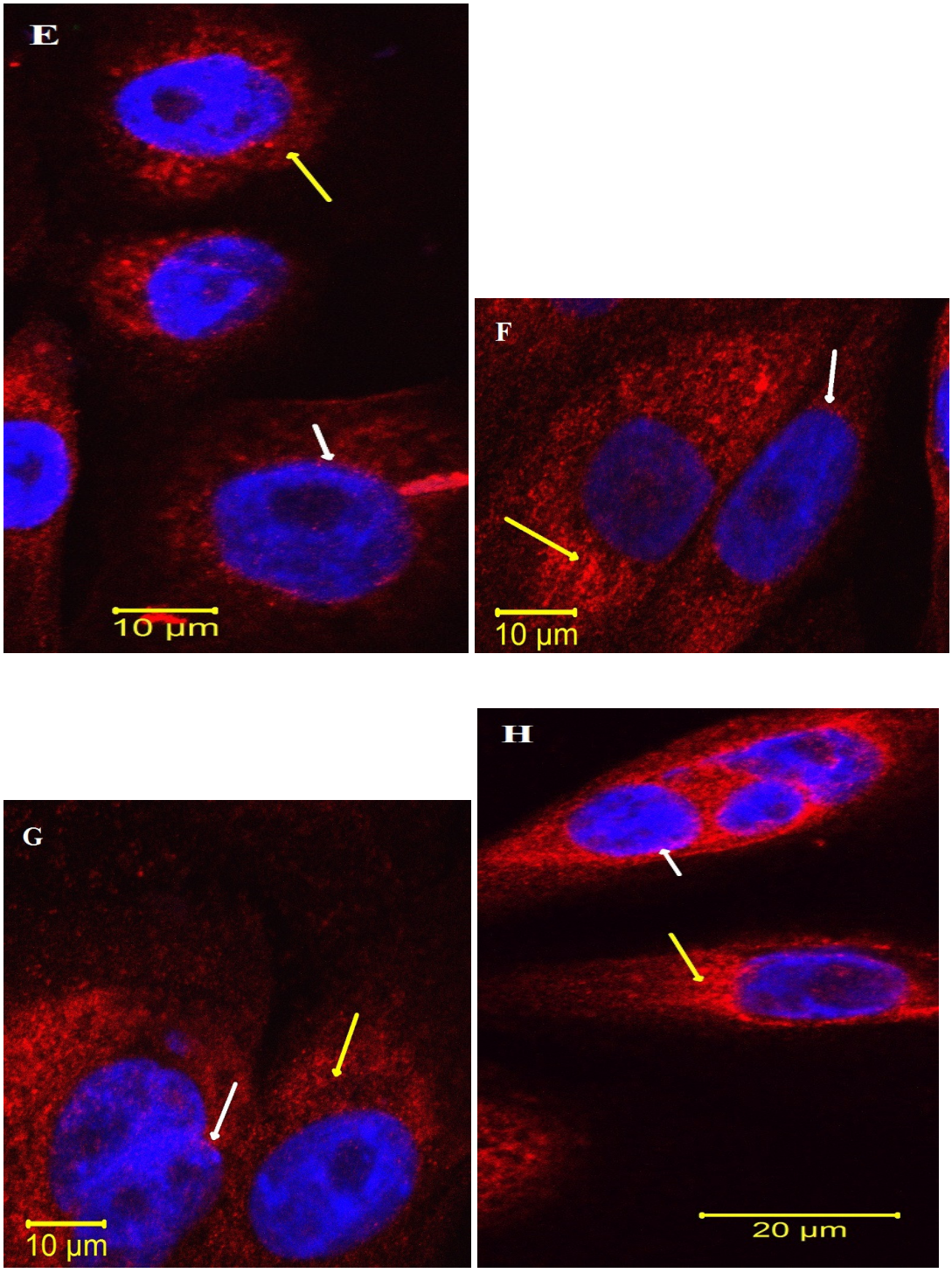

Figure 3.21 E-H: Fluorescence micrographs of HCS-2 cells exposed to 4.07µg/ml EFV **(E)**, 0.3µg/ml TDF, 1.8µg/ml FTC, 4.07µg/ml EFV **(F)**, 9.8µg/ml LPV **(G)**, 0.6µg/ml RTV **(H)** for 96 hours. $VEGF_{165b}$ was stained with polyclonal rabbit anti-human $VEGF_{165b}$ (5µg/ml) and Goat Anti-Rabbit IgG, Rhodamine conjugated (Red channel). Nuclei were counterstained with DAPI (Blue channel). Combined Images are shown. Nu=Nucleus. Cy=Cytoplasm. White arrow point to perinuclear staining and yellow arrow point to cytoplasmic staining. Representative Fluorescence micrographs of untreated cells serving as no primary antibody control are shown in Fig.3.21K.

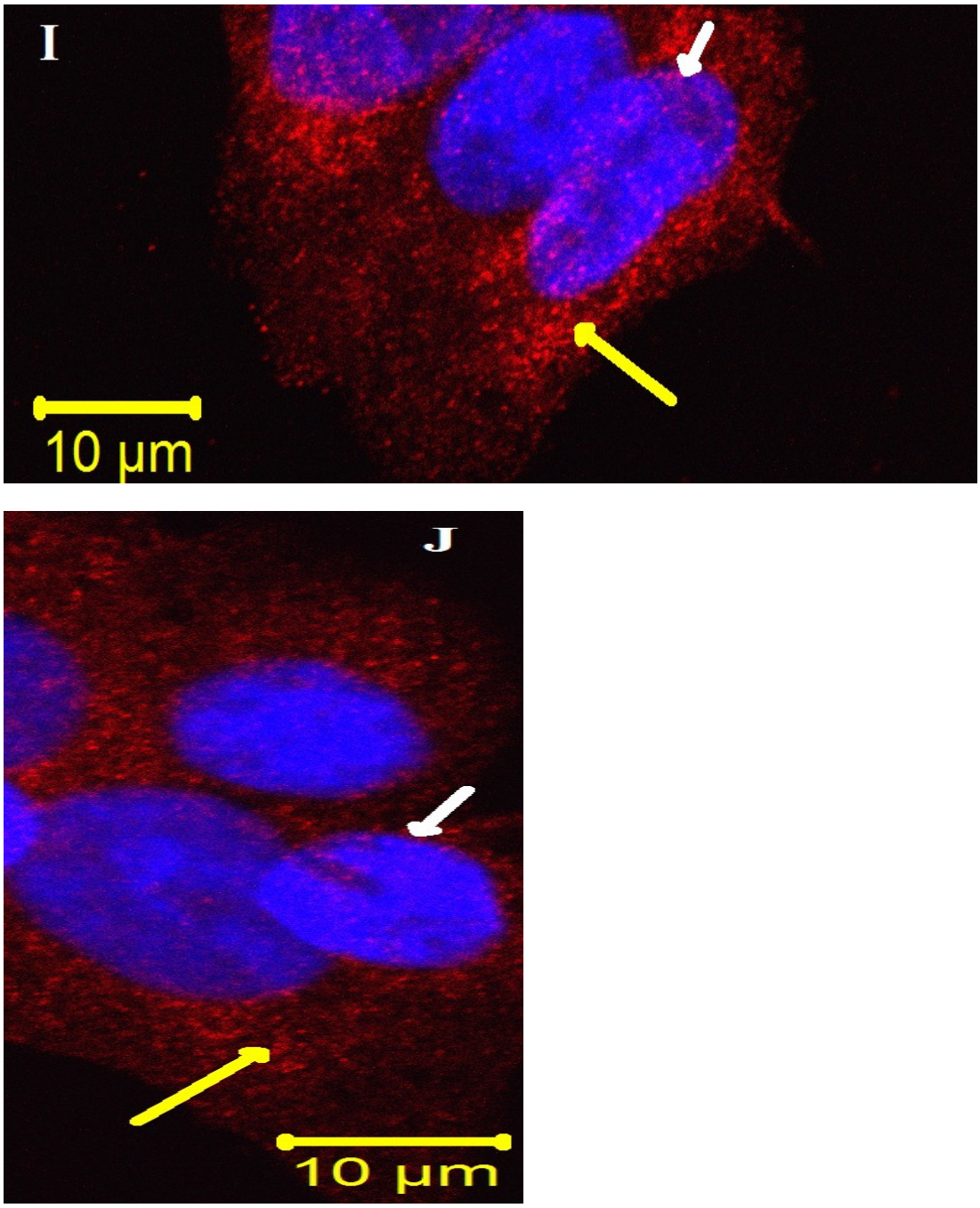

Figure 3.21 I-J: Fluorescence micrographs of HCS-2 cells exposed to 9.8µg/ml LPV; 0.6µg/ml RTV **(I)** and 0.3µg/ml TDF, 1.8µg/ml FTC, 9.8µg/ml LPV; 0.6µg/ml RTV **(J)** for 96 hours. $VEGF_{165b}$ was stained with polyclonal rabbit anti-human $VEGF_{165b}$ (5µg/ml) and Goat Anti-Rabbit IgG, Rhodamine conjugated (Red channel). Nuclei were counterstained with DAPI (Blue channel). Combined Images are shown. Nu=Nucleus. Cy=Cytoplasm. White arrow point to perinuclear staining and yellow arrow point to cytoplasmic staining. Representative Fluorescence micrographs of untreated cells serving as no primary antibody control are shown in Fig.3.21K.

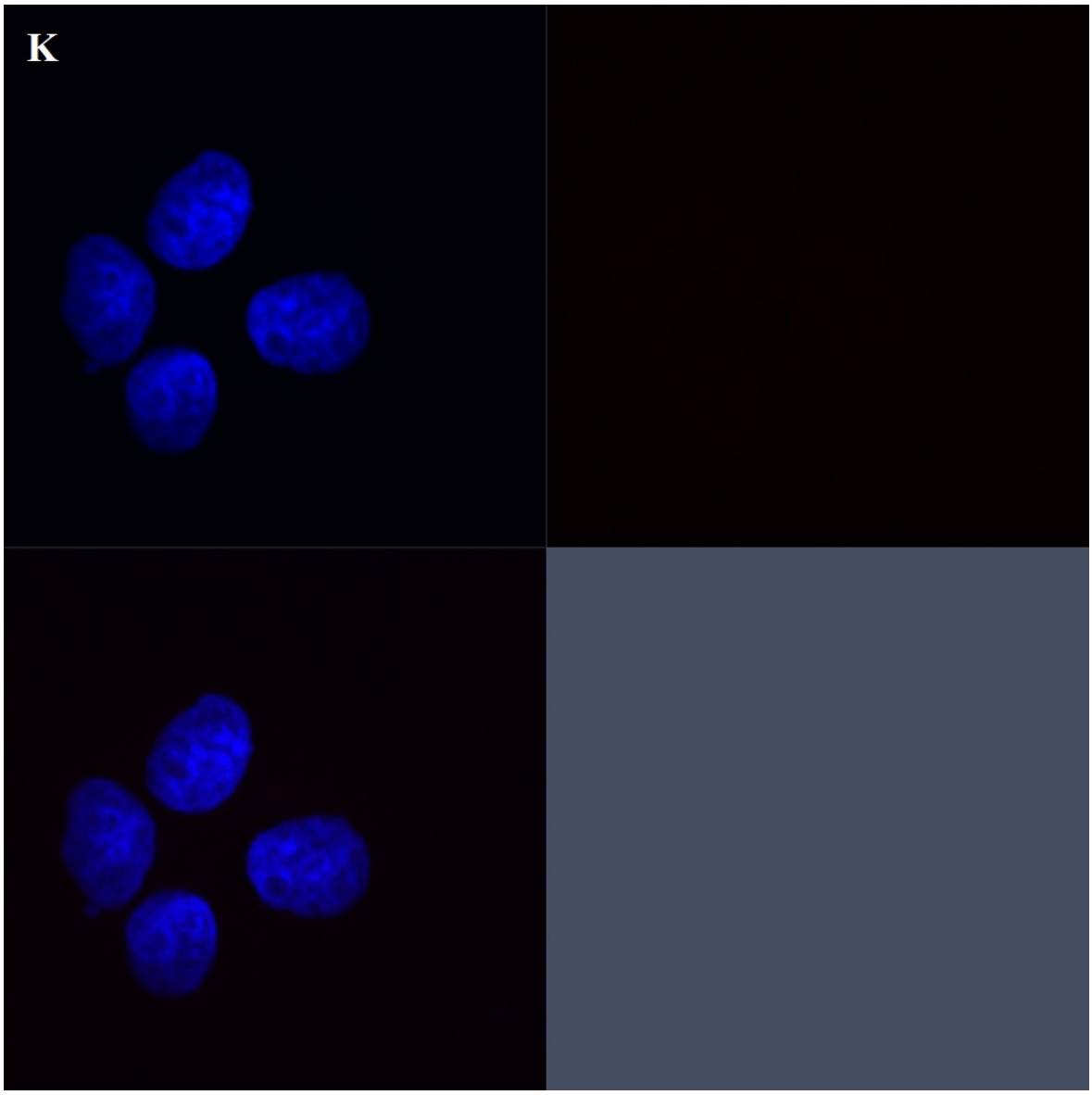

Figure 3.21K: Fluorescence micrographs of untreated cervical HCS-2 cells serving as no primary antibody control. Cells were incubated with goat serum in place of primary antibodies and incubated with Goat Anti-Rabbit IgG, Rhodamine conjugated (Red channel-Right Upper quadrant). Nuclei were counterstained with DAPI (Blue channel-Left upper quadrant). Combined images are shown-Left Lower quadrant.

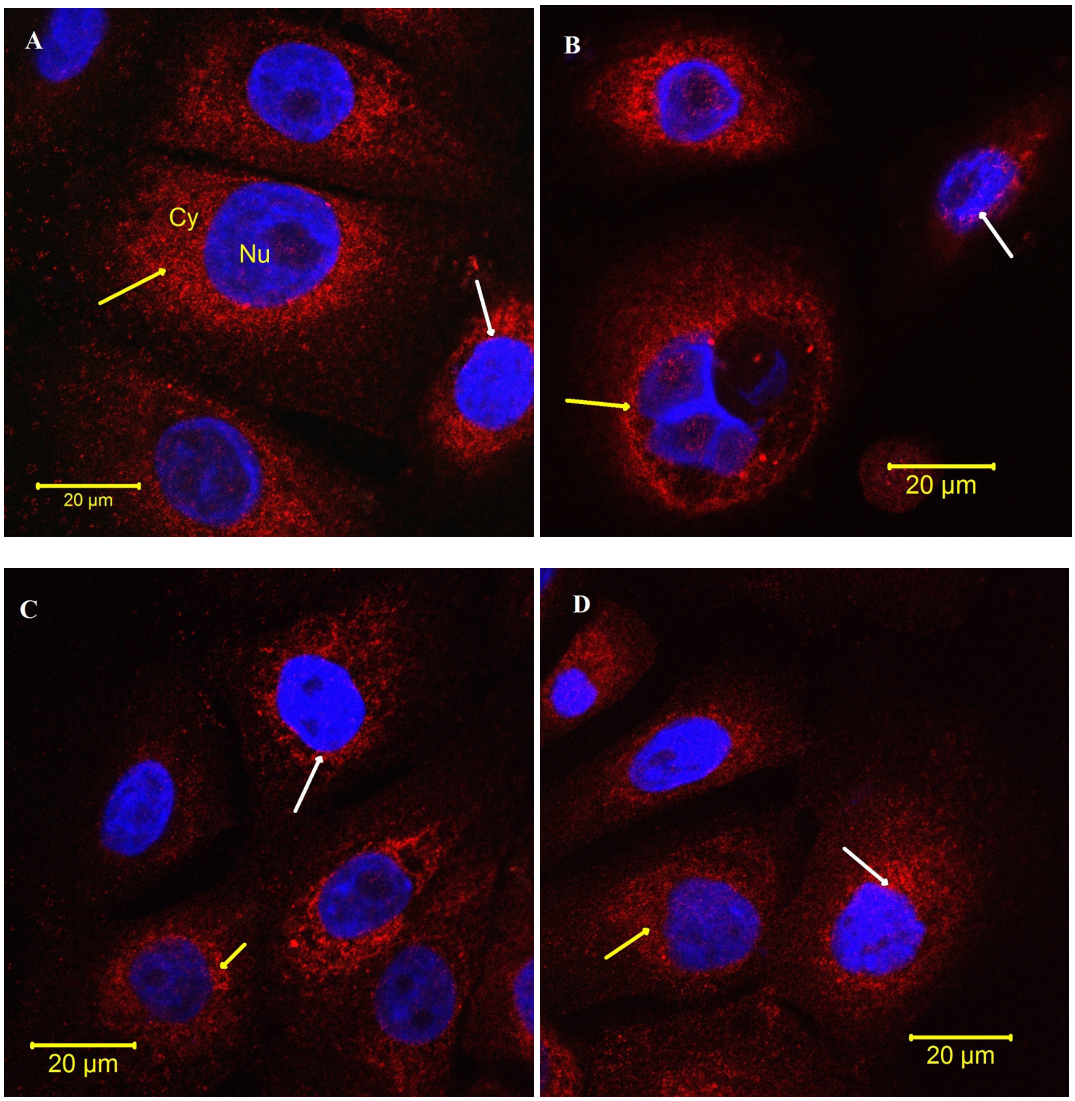

Figure 3.22 A-D: Fluorescence micrographs of Normal cervical NCE16IIA cells exposed to Growth Medium **(A)**, Vehicle-0.01% Methanol **(B)**, 0.3µg/ml TDF **(C)**, 1.8µg/ml FTC **(D)** for 96 hours. $VEGF_{165b}$ was stained with polyclonal rabbit anti-human $VEGF_{165b}$ (5µg/ml) and Goat Anti-Rabbit IgG, Rhodamine conjugated (Red channel). Nuclei were counterstained with DAPI (Blue channel). Combined Images are shown. Nu=Nucleus. Cy=Cytoplasm. White arrow point to perinuclear staining and yellow arrow point to cytoplasmic staining. There are no differences in protein staining, localisation and intensity of vehicle treated **(B)** as compared to growth medium alone. Representative Fluorescence micrographs of untreated cells serving as no primary antibody control are shown in Fig.3.22K.

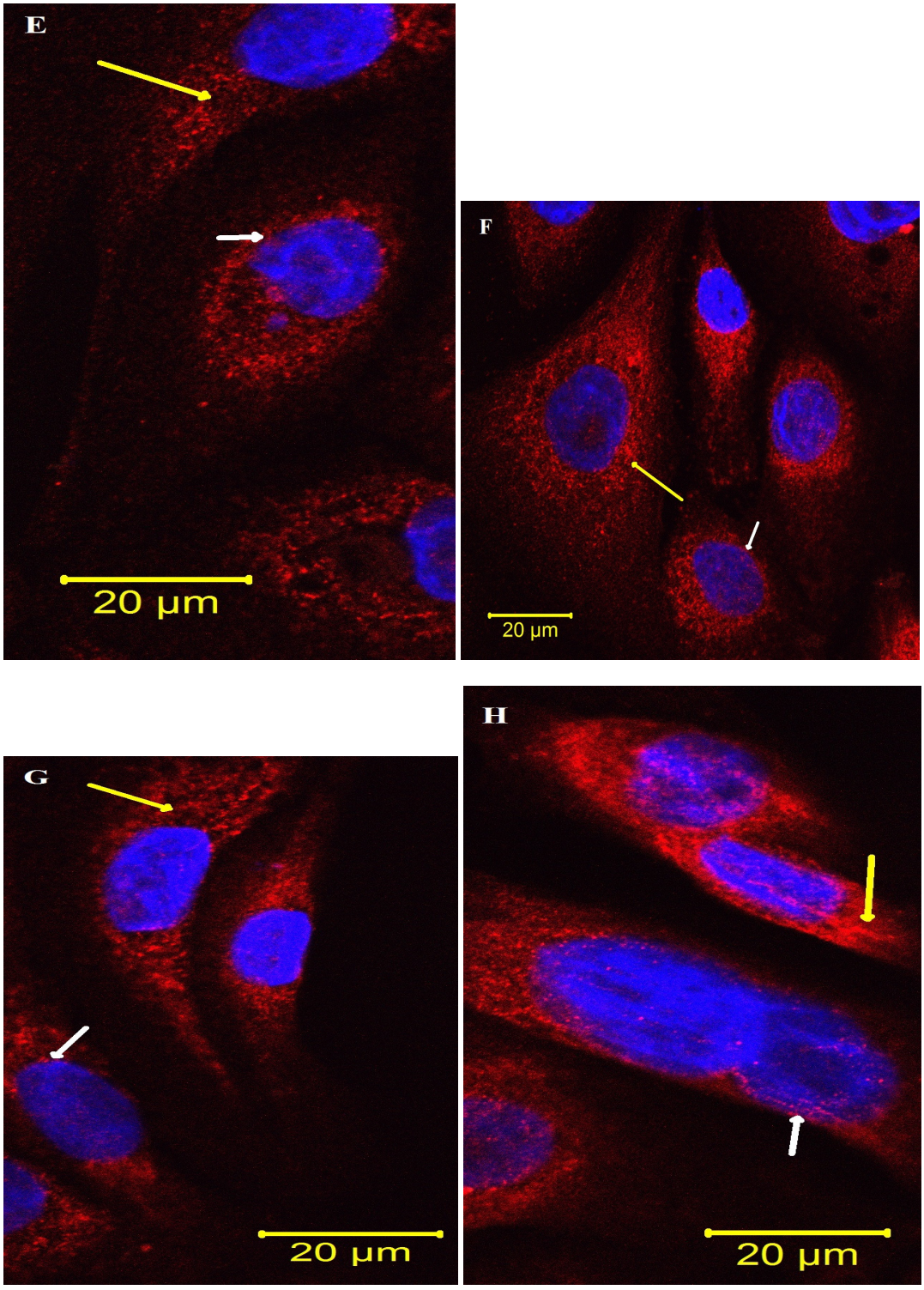

Figure 3.22 E-H: Fluorescence micrographs of Normal cervical (NCE16IIA) cells exposed to 4.07µg/ml EFV **(E)**, 0.3µg/ml TDF, 1.8µg/ml FTC, 4.07µg/ml EFV **(F)**, 9.8µg/ml LPV **(G)**, 0.6µg/ml RTV **(H)** for 96 hours. $VEGF_{165b}$ was stained with polyclonal rabbit anti-human $VEGF_{165b}$ (5µg/ml) and Goat Anti-Rabbit IgG, Rhodamine conjugated (Red channel). Nuclei were counterstained with DAPI (Blue channel). Combined Images are shown. Nu=Nucleus. Cy=Cytoplasm. White arrow point to perinuclear staining and yellow arrow point to cytoplasmic staining. Representative Fluorescence micrographs of untreated cells serving as no primary antibody control are shown in Fig.3.22K.

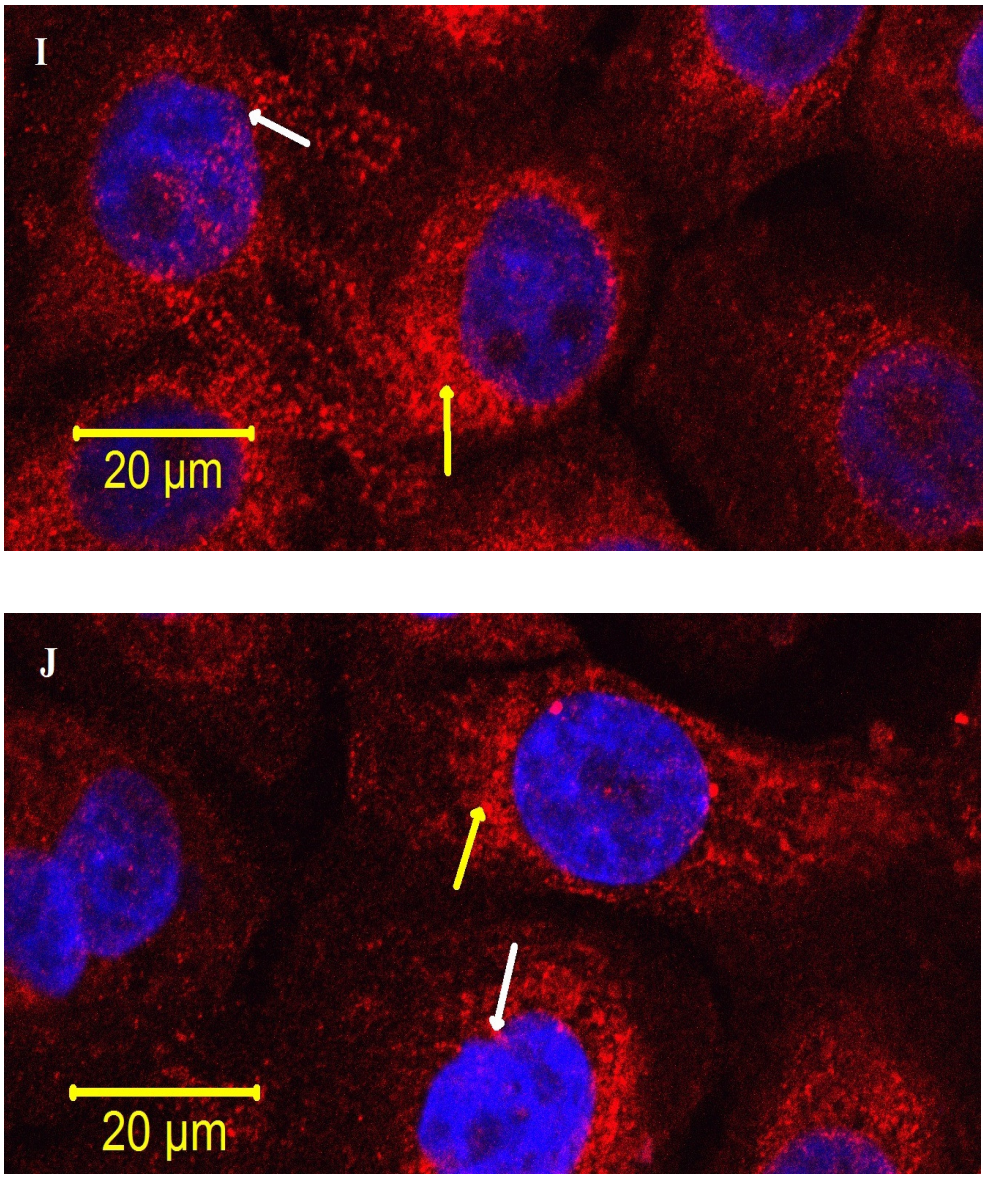

Figure 3.22 I-J: Fluorescence micrographs of Normal cervical (NCE16IIA) cells exposed to 9.8µg/ml LPV; 0.6µg/ml RTV **(I)** and 0.3µg/ml TDF, 1.8µg/ml FTC, 9.8µg/ml LPV; 0.6µg/ml RTV **(J)** for 96 hours. $VEGF_{165b}$ was stained with polyclonal rabbit anti-human $VEGF_{165b}$ (5µg/ml) and Goat Anti-Rabbit IgG, Rhodamine conjugated (Red channel). Nuclei were counterstained with DAPI (Blue channel). Combined Images are shown. Nu=Nucleus. Cy=Cytoplasm. White arrow point to perinuclear staining and yellow arrow point to cytoplasmic staining. Representative Fluorescence micrographs of untreated cells serving as no primary antibody control are shown in Fig.3.22K.

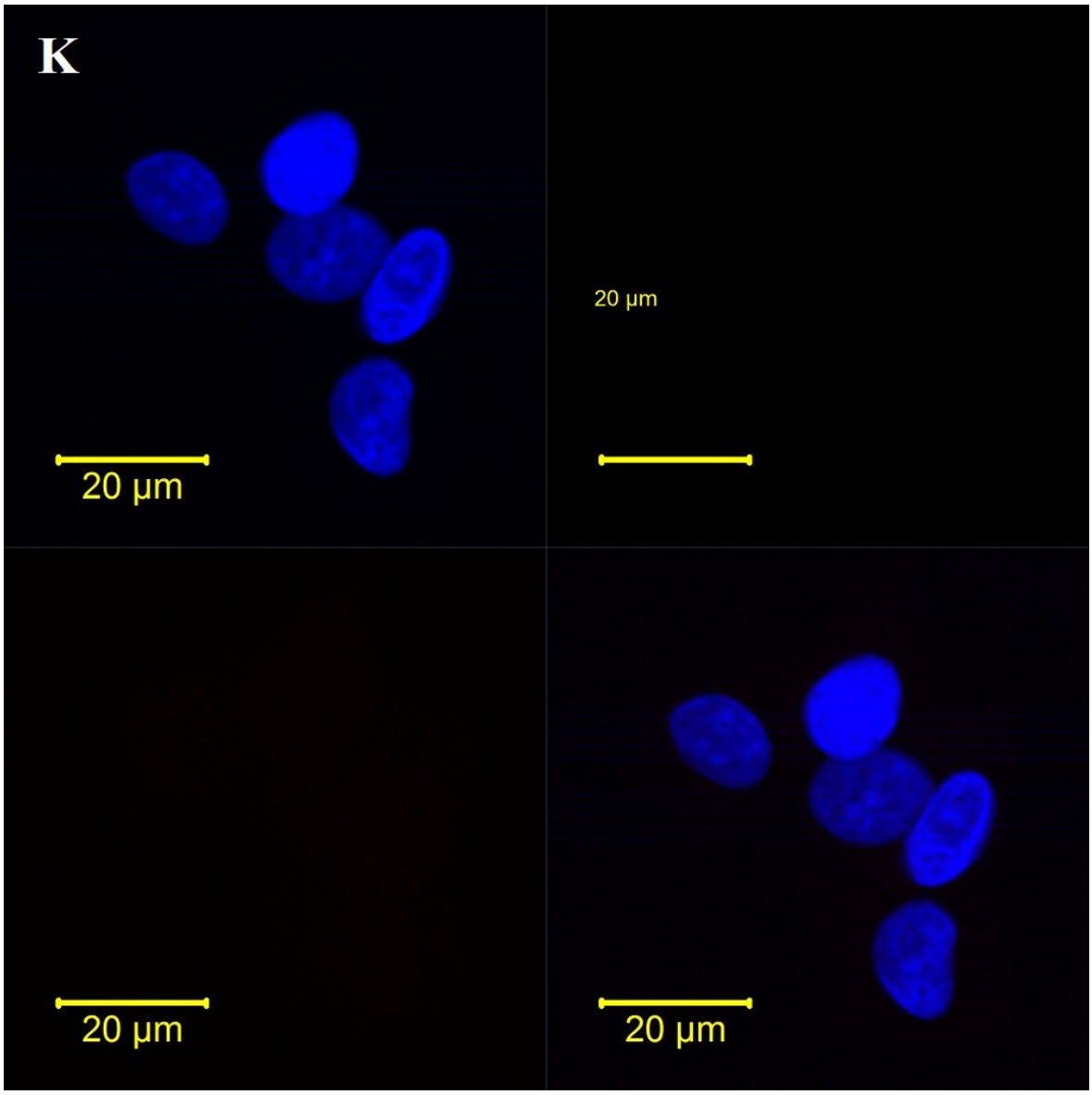

Figure 3.22K: Fluorescence micrographs of untreated cervical NCE16IIA cells serving as no primary antibody control. Cells were incubated with goat serum in place of primary antibodies and incubated with Goat Anti-Rabbit IgG, Rhodamine conjugated (Red channel-Left Lower quadrant). Nuclei were counterstained with DAPI (Blue channel-Left upper quadrant). Combined images are shown-Right lower quadrant.

3.3.4 Immunofluorescence of anti-angiogenic VEGF $_{165b}$ protein in breast cancer (MCF-7) and normal breast (MCF10-A) cells exposed to antiretroviral drugs

The anti-angiogenic $VEGF_{165b}$ protein is expressed and localised in the nuclei and cytoplasm of MCF-7 (Fig. 3.23 A) and MCF-10A (Fig. 3.24 A) cells. Mean fluorescence intensities of $VEGF_{165b}$ in the nuclei and cytoplasm were statistically analysed (ANOVA) between the untreated/vehicle control and the treated groups. (Graphical representation presented in Figs. 3.25-3.32; Data summaries shown in Appendix E). There are no differences in protein staining, localisation and intensity of vehicle (0.01% methanol) treated group as compared to growth medium alone (Fig. 3.23B and Fig. 3.24B). Exposing both breast cell lines to the different antiretroviral drugs individually and in combination for 96 hours showed no differences in the localisation of $VEGF_{165b}$ (Fig. 3.23 C-J and Fig. 3.24 C-J). Fig. 3.23 C-J are representative images illustrating the effects of the antiretroviral drugs on expression of $VEGF_{165b}$ in MCF-7 cell cultures. Fig. 3.24 C-J are representative images illustrating the effects of the antiretroviral drugs on expression of $VEGF_{165b}$ in MCF-10A cell cultures.

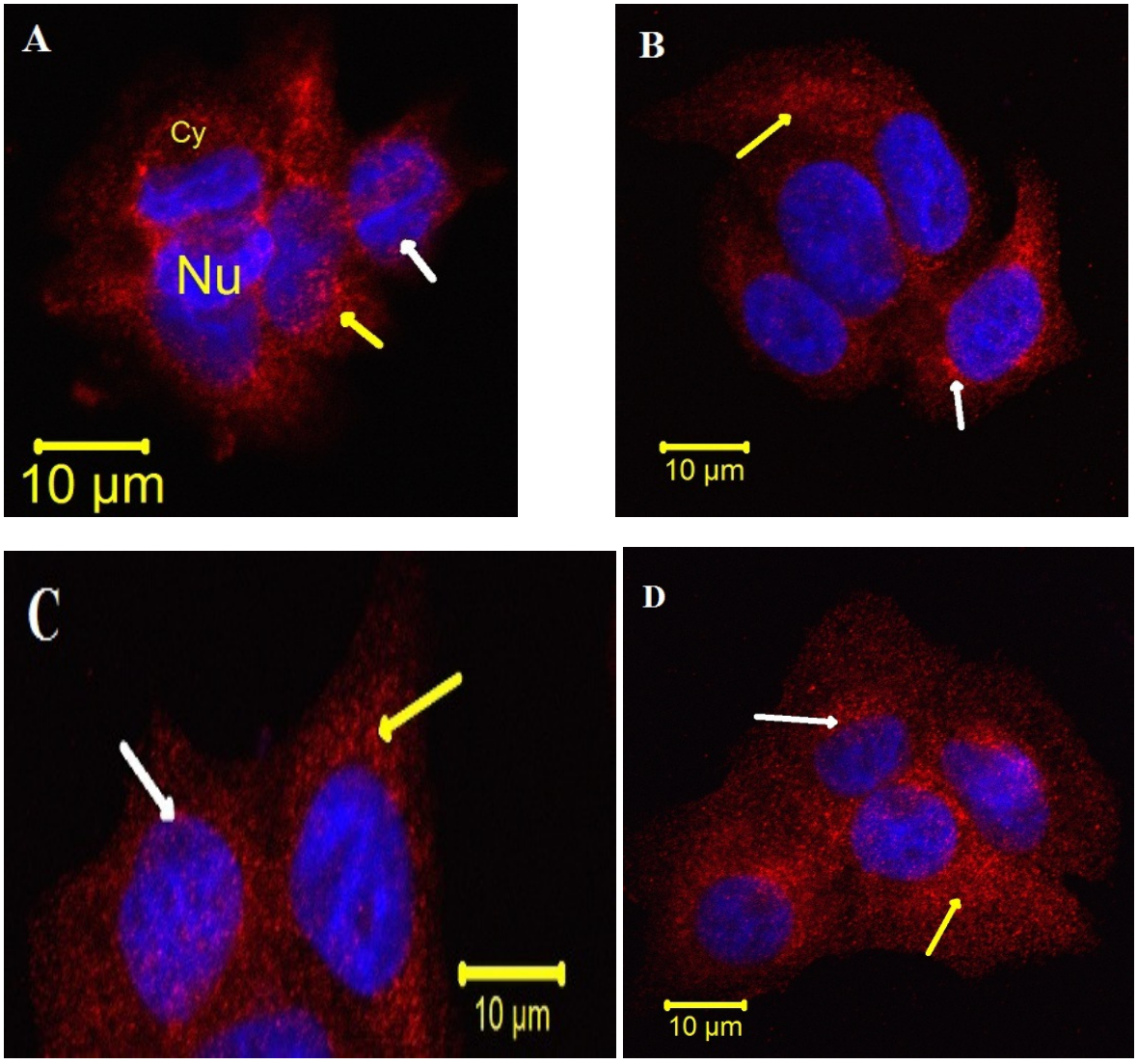

Figure 3.23 A-D: Fluorescence micrographs of Cancer breast MCF-7 cells exposed to Growth Medium **(A)**, Vehicle-0.01% Methanol **(B)**, 0.3µg/ml TDF **(C)**, 1.8µg/ml FTC **(D)** for 96 hours. $VEGF_{165b}$ was stained with polyclonal rabbit anti-human $VEGF_{165b}$ (5µg/ml) and Goat Anti-Rabbit IgG, Rhodamine conjugated (Red channel). Nuclei were counterstained with DAPI (Blue channel). Combined Images are shown. Nu=Nucleus. Cy=Cytoplasm. White arrow point to perinuclear staining and yellow arrow point to cytoplasmic staining. There are no differences in protein staining, localisation and intensity of vehicle treated **(B)** as compared to growth medium alone. Representative Fluorescence micrographs of untreated cells serving as no primary antibody control are shown in Fig.3.23K.

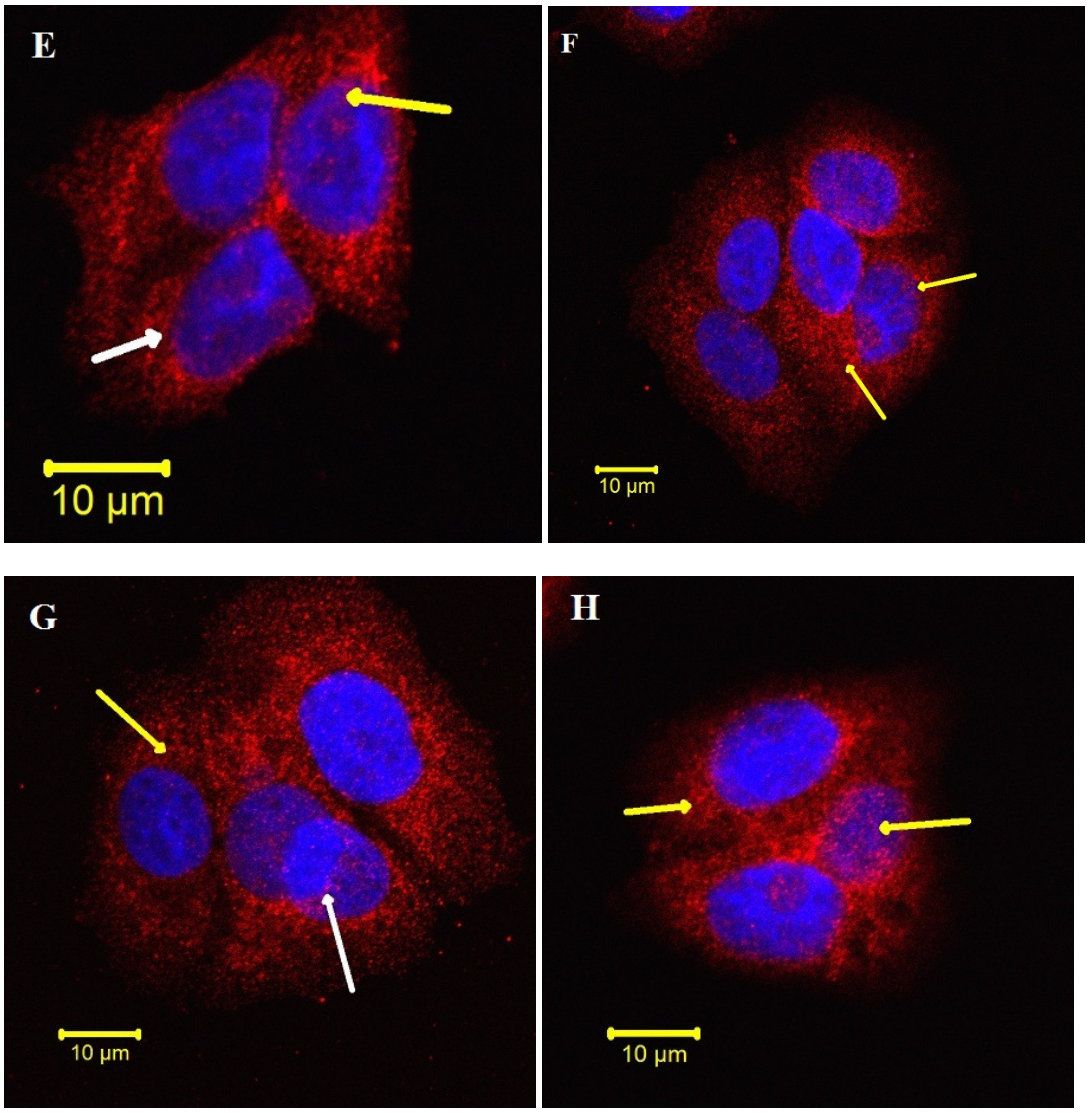

Figure 3.23 E-H: Fluorescence micrographs of Cancer breast MCF-7 cells exposed to 4.07µg/ml EFV **(E)**, 0.3µg/ml TDF, 1.8µg/ml FTC, 4.07µg/ml EFV **(F)**, 9.8µg/ml LPV **(G)**, 0.6µg/ml RTV **(H)** for 96 hours. $VEGF_{165b}$ was stained with polyclonal rabbit anti-human $VEGF_{165b}$ (5µg/ml) and Goat Anti-Rabbit IgG, Rhodamine conjugated (Red channel). Nuclei were counterstained with DAPI (Blue channel). Combined Images are shown. White arrow point to perinuclear staining and yellow arrow point to cytoplasmic staining. Representative Fluorescence micrographs of untreated cells serving as no primary antibody control are shown in Fig.3.23K.

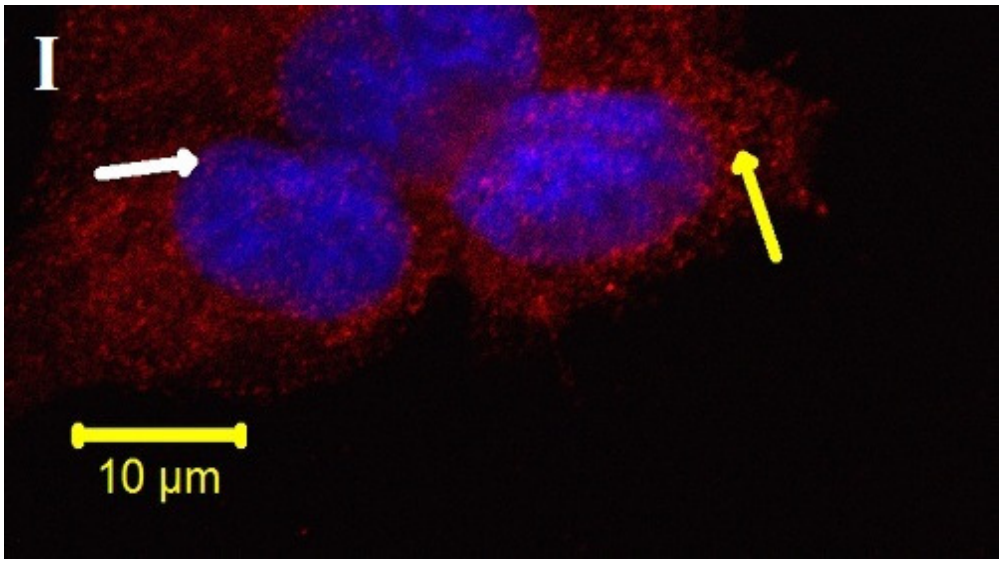

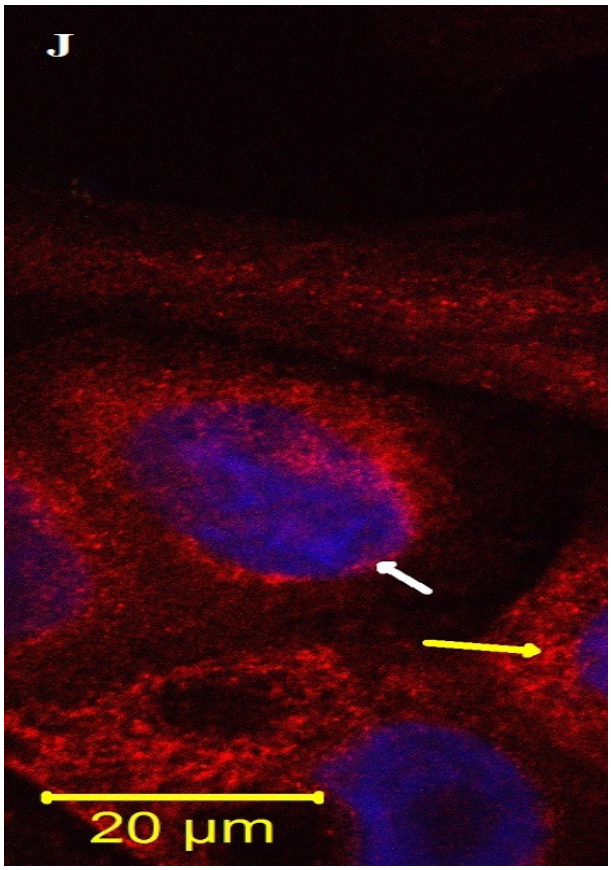

Figure 3.23 I-J: Fluorescence micrographs of Cancer breast MCF-7 cells exposed to 9.8µg/ml LPV; 0.6µg/ml RTV **(I)** and 0.3µg/ml TDF, 1.8µg/ml FTC, 9.8µg/ml LPV; 0.6µg/ml RTV **(J)** for 96 hours. $VEGF_{165b}$ was stained with polyclonal rabbit anti-human $VEGF_{165b}$ (5µg/ml) and Goat Anti-Rabbit IgG, Rhodamine conjugated (Red channel). Nuclei were counterstained with DAPI (Blue channel). Combined Images are shown. White arrow point to perinuclear staining and yellow arrow point to cytoplasmic staining. Representative Fluorescence micrographs of untreated cells serving as no primary antibody control are shown in Fig.3.23K.

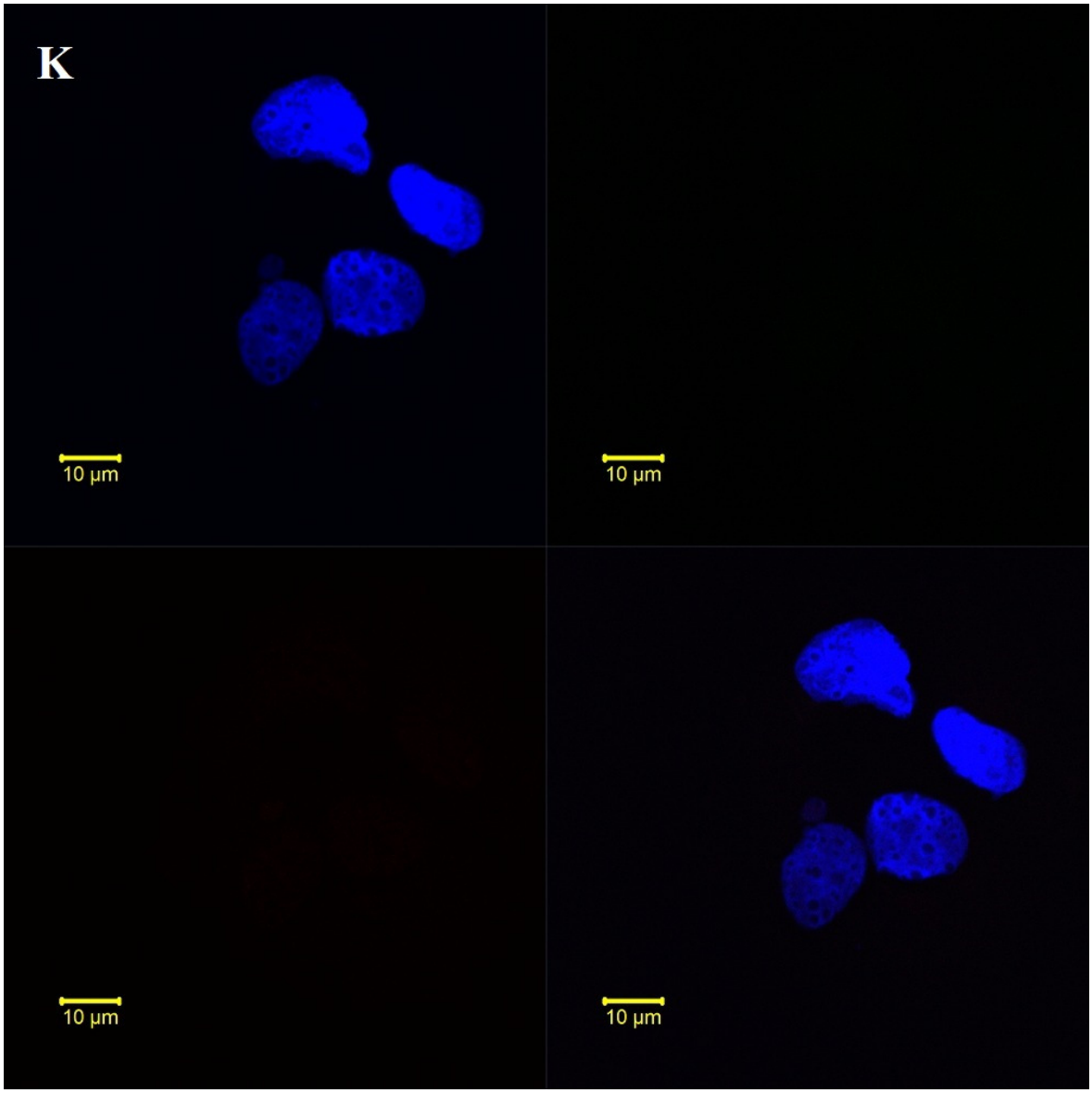

Figure 3.23K: Fluorescence micrographs of untreated breast MCF-7 cells serving as no primary antibody control. Cells were incubated with goat serum in place of primary antibodies and incubated with Goat Anti-Rabbit IgG, Rhodamine conjugated (Red channel-Left Lower quadrant). Nuclei were counterstained with DAPI (Blue channel-Left upper quadrant). Combined images are shown-Right lower quadrant.

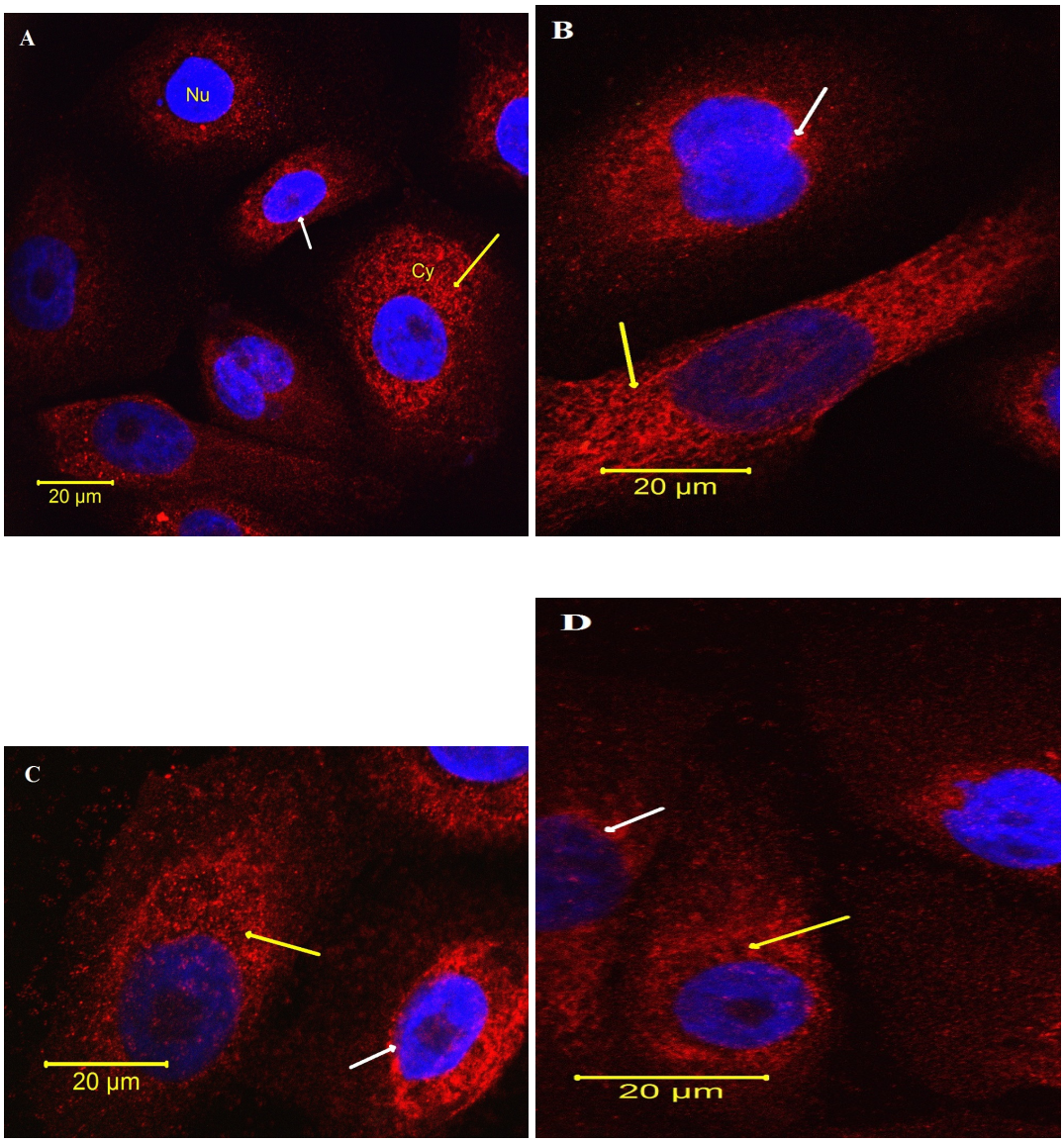

Figure 3.24 A-D: Fluorescence micrographs of normal breast MCF-10A cells exposed to Growth Medium **(A)**, Vehicle-0.01% Methanol **(B)**, 0.3µg/ml TDF **(C)**, 1.8µg/ml FTC **(D)** for 96 hours. $VEGF_{165b}$ was stained with polyclonal rabbit anti-human $VEGF_{165b}$ (5µg/ml) and Goat Anti-Rabbit IgG, Rhodamine conjugated (Red channel). Nuclei were counterstained with DAPI (Blue channel). Combined Images are shown. Nu=Nucleus. Cy=Cytoplasm. White arrow point to perinuclear staining and yellow arrow point to cytoplasmic staining. There are no differences in protein staining, localisation and intensity of vehicle treated **(B)** as compared to growth medium alone. Representative Fluorescence micrographs of untreated cells serving as no primary antibody control are shown in Fig.3.24K.

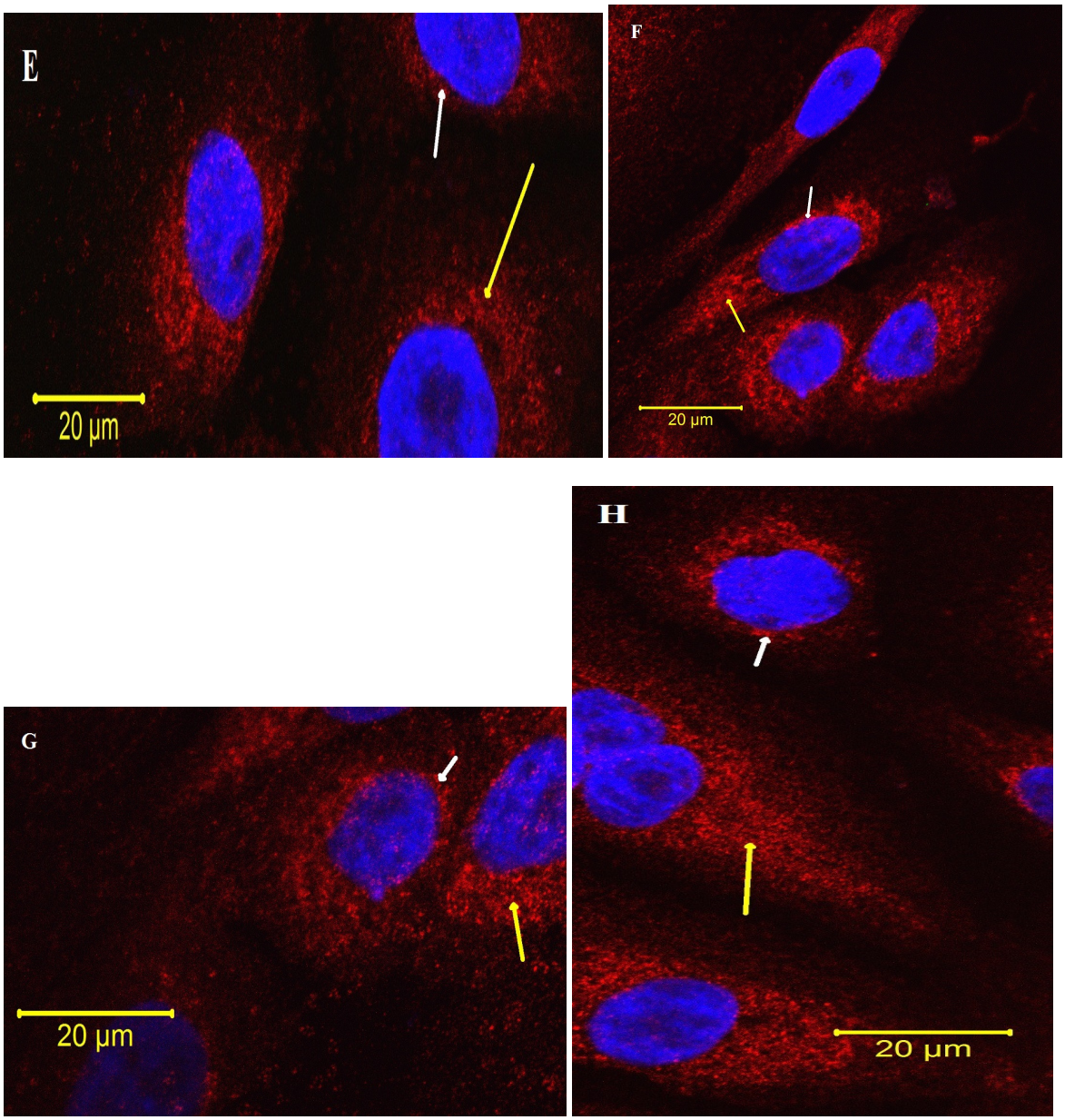

Figure 3.24 E-H: Fluorescence micrographs of normal breast MCF-10A cells exposed to 4.07µg/ml EFV **(E)**, 0.3µg/ml TDF, 1.8µg/ml FTC, 4.07µg/ml EFV **(F)**, 9.8µg/ml LPV **(G)**, 0.6µg/ml RTV **(H)** for 96 hours. $VEGF_{165b}$ was stained with polyclonal rabbit anti-human $VEGF_{165b}$ (5µg/ml) and Goat Anti-Rabbit IgG, Rhodamine conjugated (Red channel). Nuclei were counterstained with DAPI (Blue channel). Combined Images are shown. White arrow point to perinuclear staining and yellow arrow point to cytoplasmic staining. Representative Fluorescence micrographs of untreated cells serving as no primary antibody control are shown in Fig.3.24K.

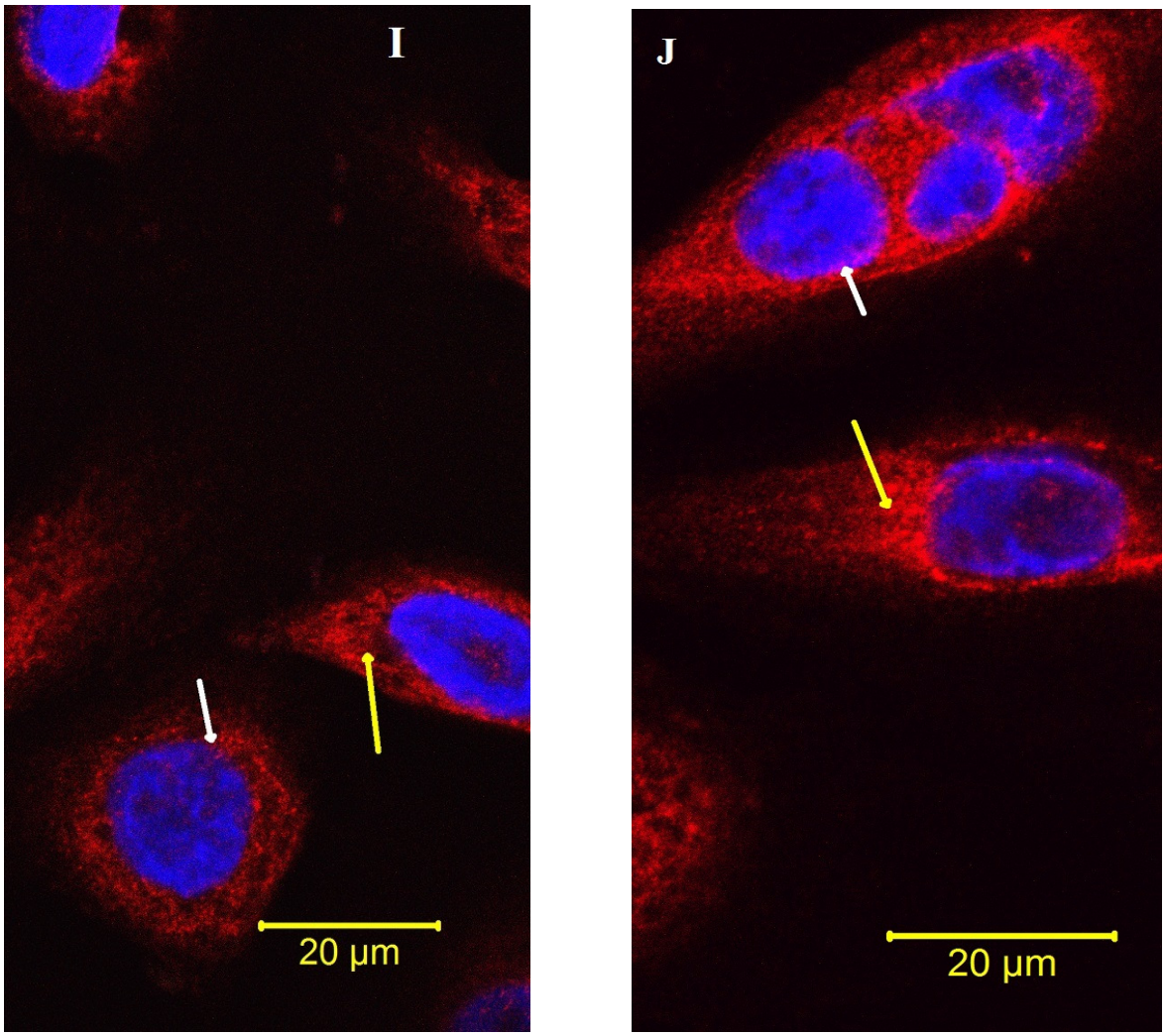

Figure 3.24 I-J: Fluorescence micrographs of normal breast MCF-10A cells exposed to 9.8µg/ml LPV; 0.6µg/ml RTV **(I)** and 0.3µg/ml TDF, 1.8µg/ml FTC, 9.8µg/ml LPV; 0.6µg/ml RTV **(J)** for 96 hours. $VEGF_{165b}$ was stained with polyclonal rabbit anti-human $VEGF_{165b}$ (5µg/ml) and Goat Anti-Rabbit IgG, Rhodamine conjugated (Red channel). Nuclei were counterstained with DAPI (Blue channel). Combined Images are shown. White arrow point to perinuclear staining and yellow arrow point to cytoplasmic staining. Representative Fluorescence micrographs of untreated cells serving as no primary antibody control are shown in Fig.3.24K.

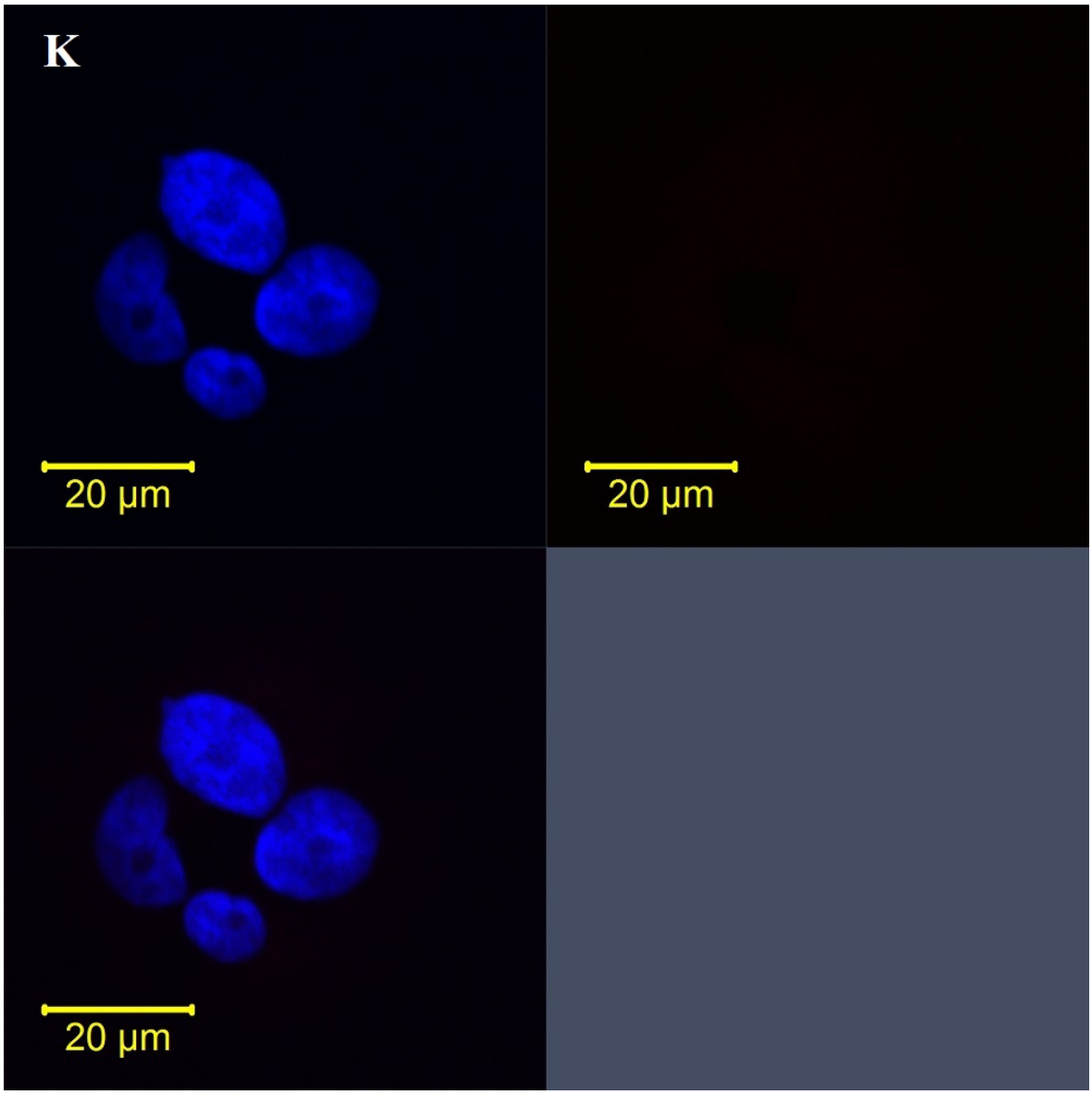

Figure 3.24K: Fluorescence micrographs of untreated breast MCF-10A cells serving as no primary antibody control. Cells were incubated with goat serum in place of primary antibodies and incubated with Goat Anti-Rabbit IgG, Rhodamine conjugated (Red channel- Right upper quadrant). Nuclei were counterstained with DAPI (Blue channel-Left upper quadrant). Combined images are shown- Left Lower quadrant.

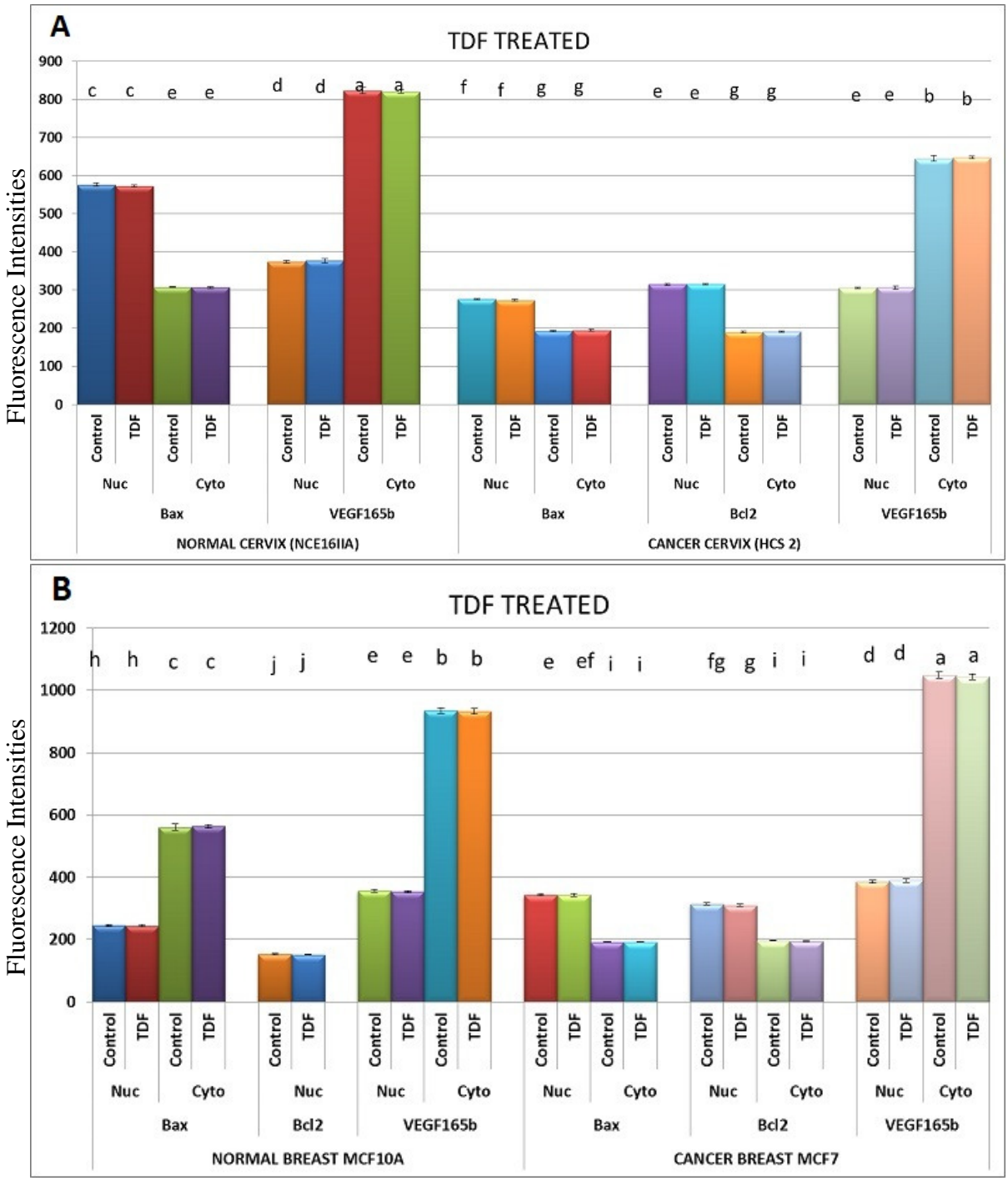

Figure 3.25: Effects of TDF on BAX, BCL-2 and $VEGF_{165b}$ protein expression in (**A**) NCE16IIA (normal cervical); HCS-2 (cervical cancer) and (**B**) MCF-10A (normal breast); MCF-7 (breast cancer) cells. Cells were incubated with 0.3µg/ml TDF for 96 hours. Data (mean ± SEM), are represented as fluorescence intensities of protein expression relative to values from the vehicle-treated cells and representative of 3 independent experiments for immunofluorescence staining. Groups not connected by the same letter are significantly ($p<0.05$) different.

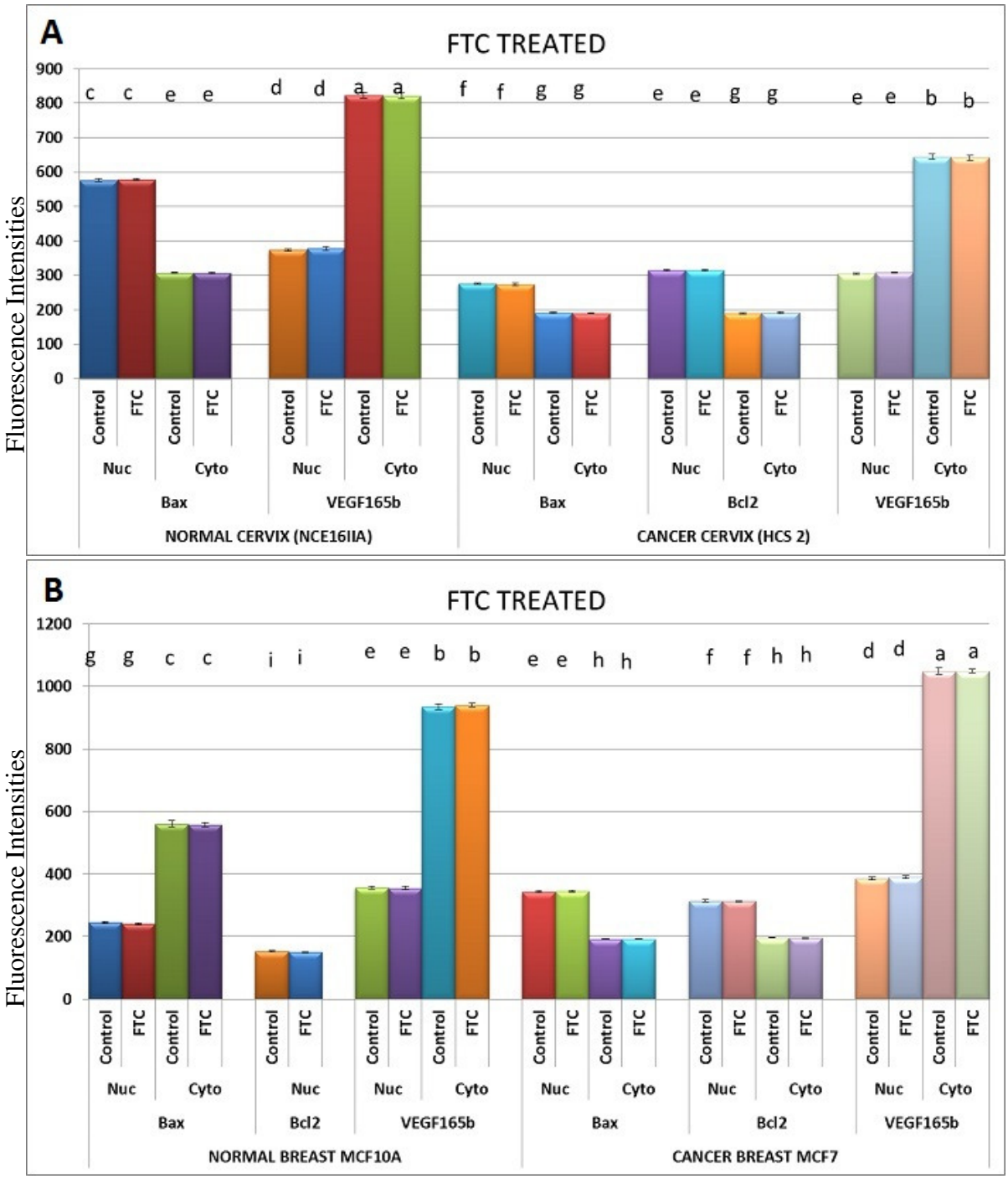

Figure 3.26: Effects of FTC on BAX, BCL-2 and $VEGF_{165b}$ protein expression in (**A**) NCE16IIA (normal cervical); HCS-2 (cervical cancer) and (**B**) MCF-10A (normal breast); MCF-7 (breast cancer) cells. Cells were incubated with 1.8µg/ml FTC for 96 hours. Data (mean ± SEM), are represented as fluorescence intensities of protein expression relative to values from the vehicle-treated cells and representative of 3 independent experiments for immunofluorescence staining. Groups not connected by the same letter are significantly ($p<0.05$) different.

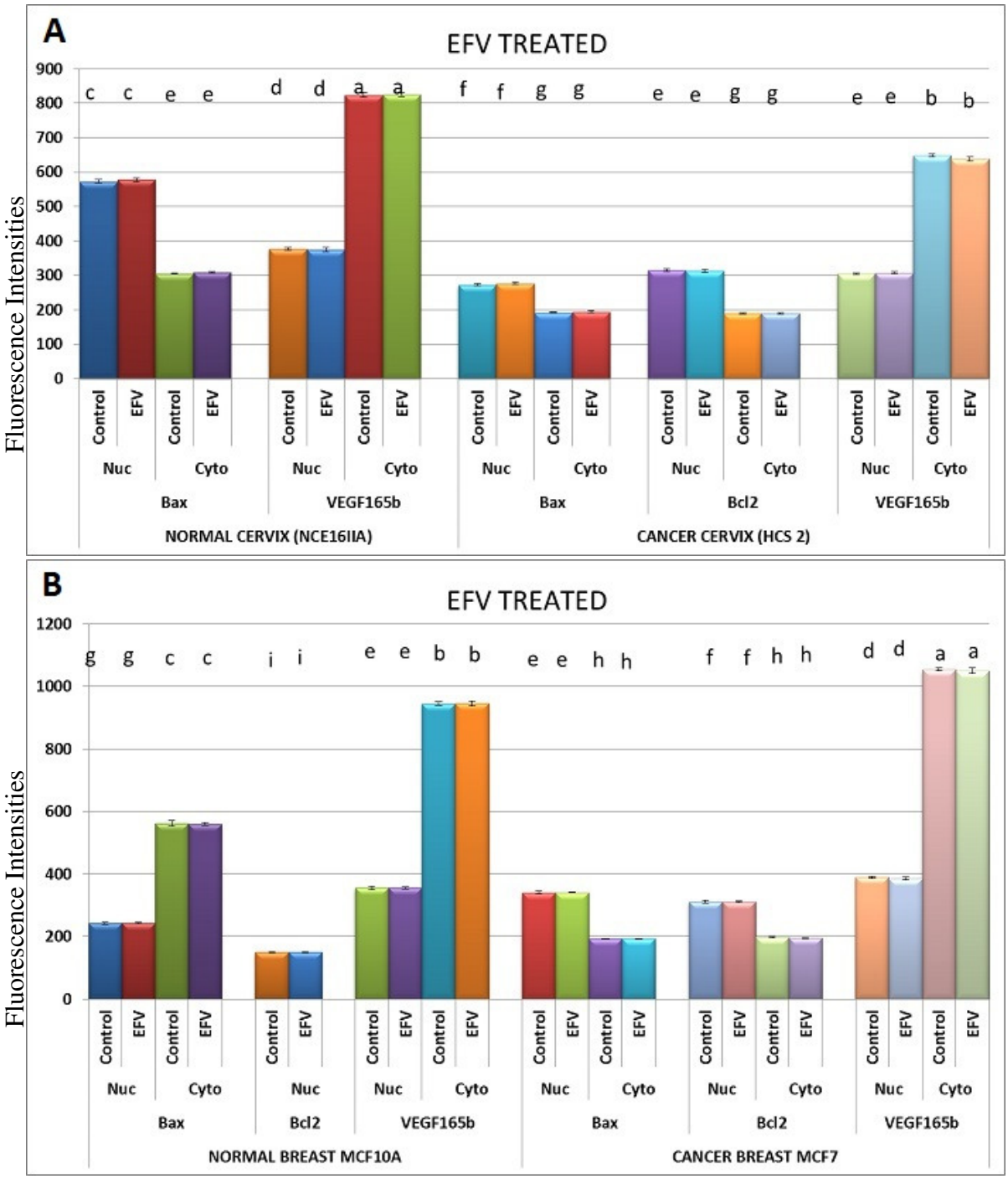

Figure 3.27: Effects of EFV on BAX, BCL-2 and $VEGF_{165b}$ protein expression in (**A**) NCE16IIA (normal cervical); HCS-2 (cervical cancer) and (**B**) MCF-10A (normal breast); MCF-7 (breast cancer) cells. Cells were incubated with 4.07µg/ml EFV for 96 hours. Data (mean ± SEM), are represented as fluorescence intensities of protein expression relative to values from the vehicle-treated cells and representative of 3 independent experiments for immunofluorescence staining. Groups not connected by the same letter are significantly ($p<0.05$) different.

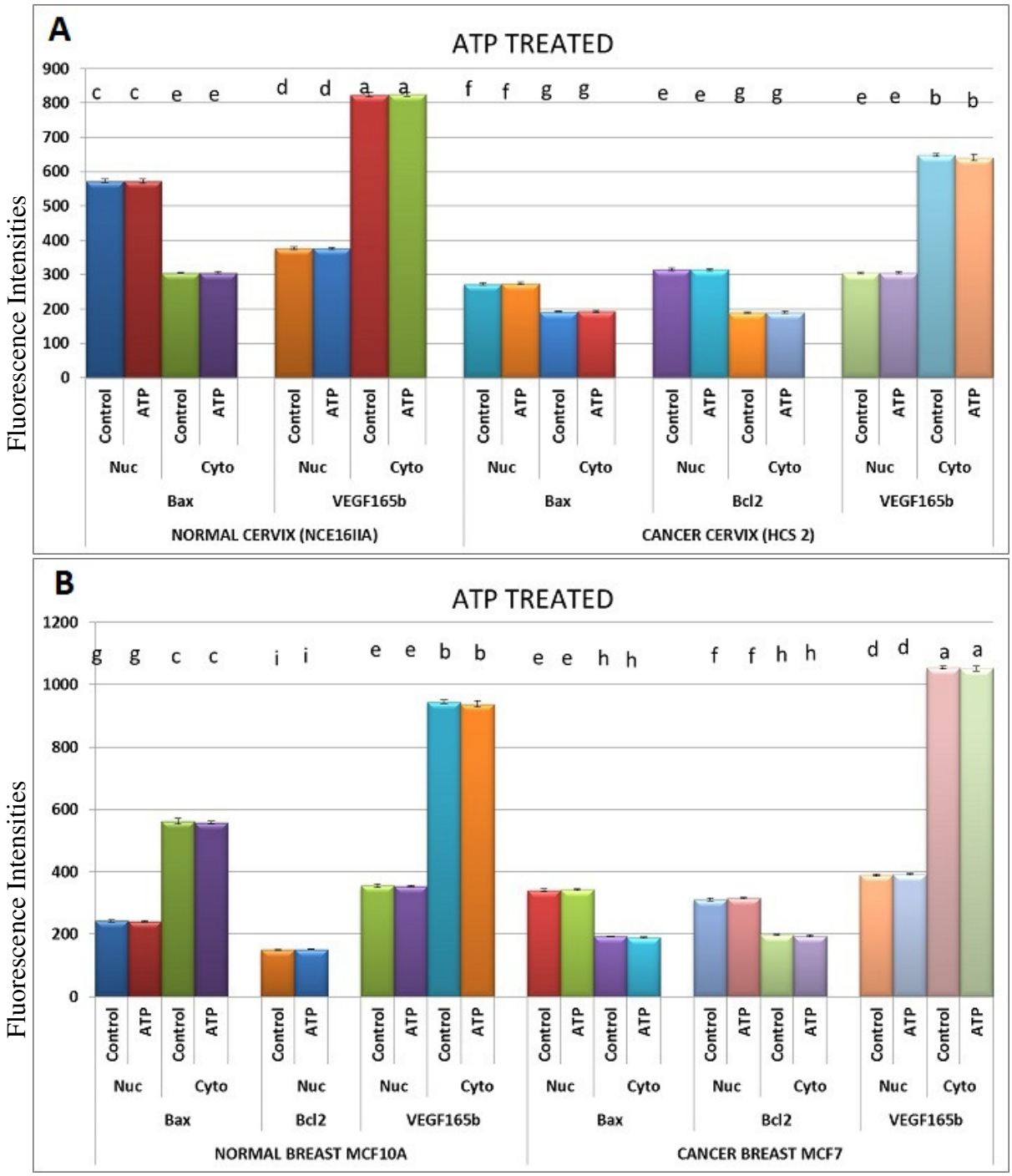

Figure 3.28: Effects of ATRIPLA on BAX, BCL-2 and $VEGF_{165b}$ protein expression in (**A**) NCE16IIA (normal cervical); HCS-2 (cervical cancer) and (**B**) MCF-10A (normal breast); MCF-7 (breast cancer) cells. Cells were incubated with 0.3µg/ml TDF; 1.8µg/ml FTC; 4.07µg/ml EFV for 96 hours. Data (mean ± SEM), are represented as fluorescence intensities of protein expression relative to values from the vehicle-treated cells and representative of 3 independent experiments for immunofluorescence staining. Groups not connected by the same letter are significantly ($p<0.05$) different.

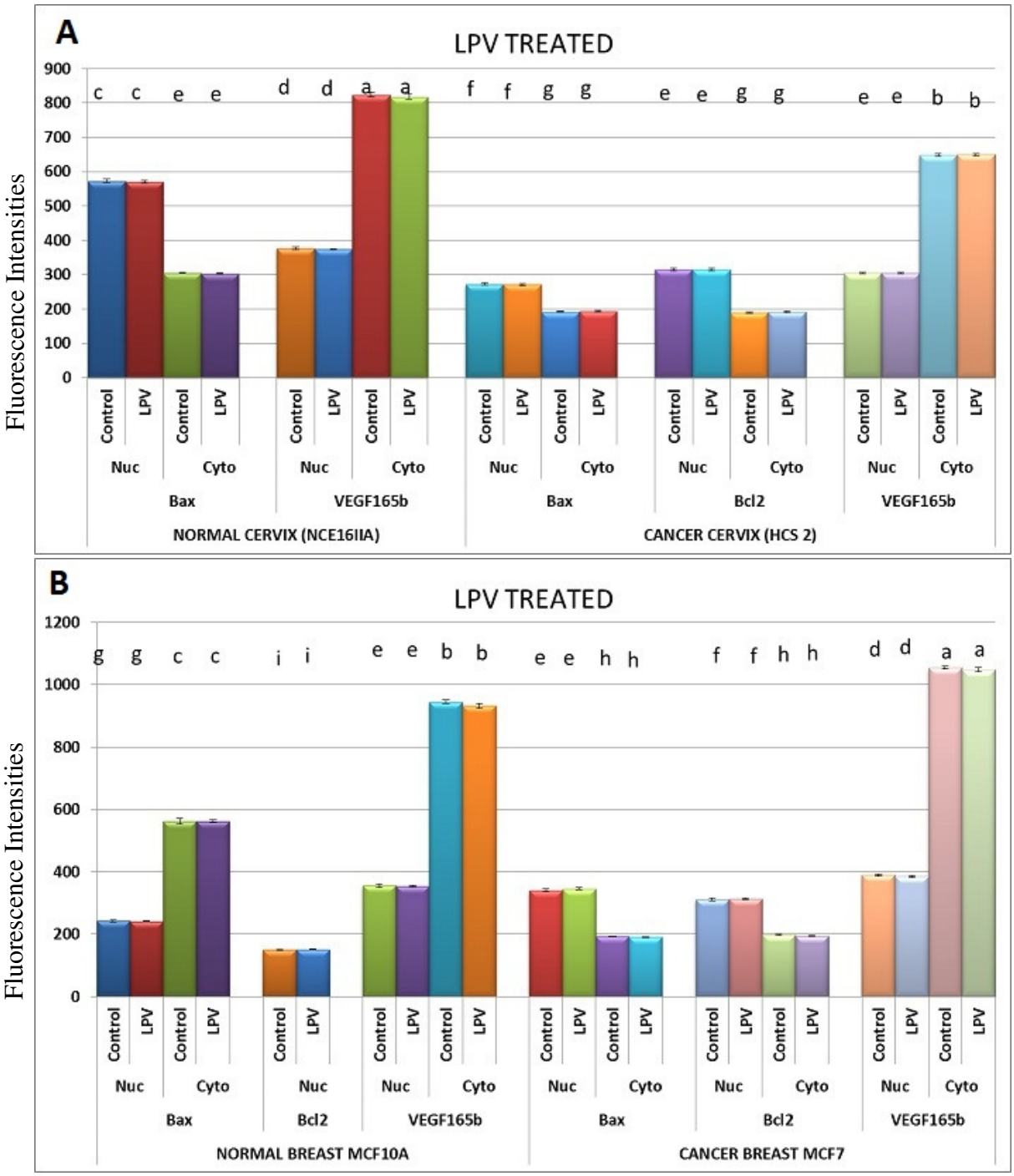

Figure 3.29: Effects of LPV on BAX, BCL-2 and $VEGF_{165b}$ protein expression in (**A**) NCE16IIA (normal cervical); HCS-2 (cervical cancer) and (**B**) MCF-10A (normal breast); MCF-7 (breast cancer) cells. Cells were incubated with 9.8µg/ml LPV for 96 hours. Data (mean ± SEM), are represented as fluorescence intensities of protein expression relative to values from the vehicle-treated cells and representative of 3 independent experiments for immunofluorescence staining. Groups not connected by the same letter are significantly ($p<0.05$) different.

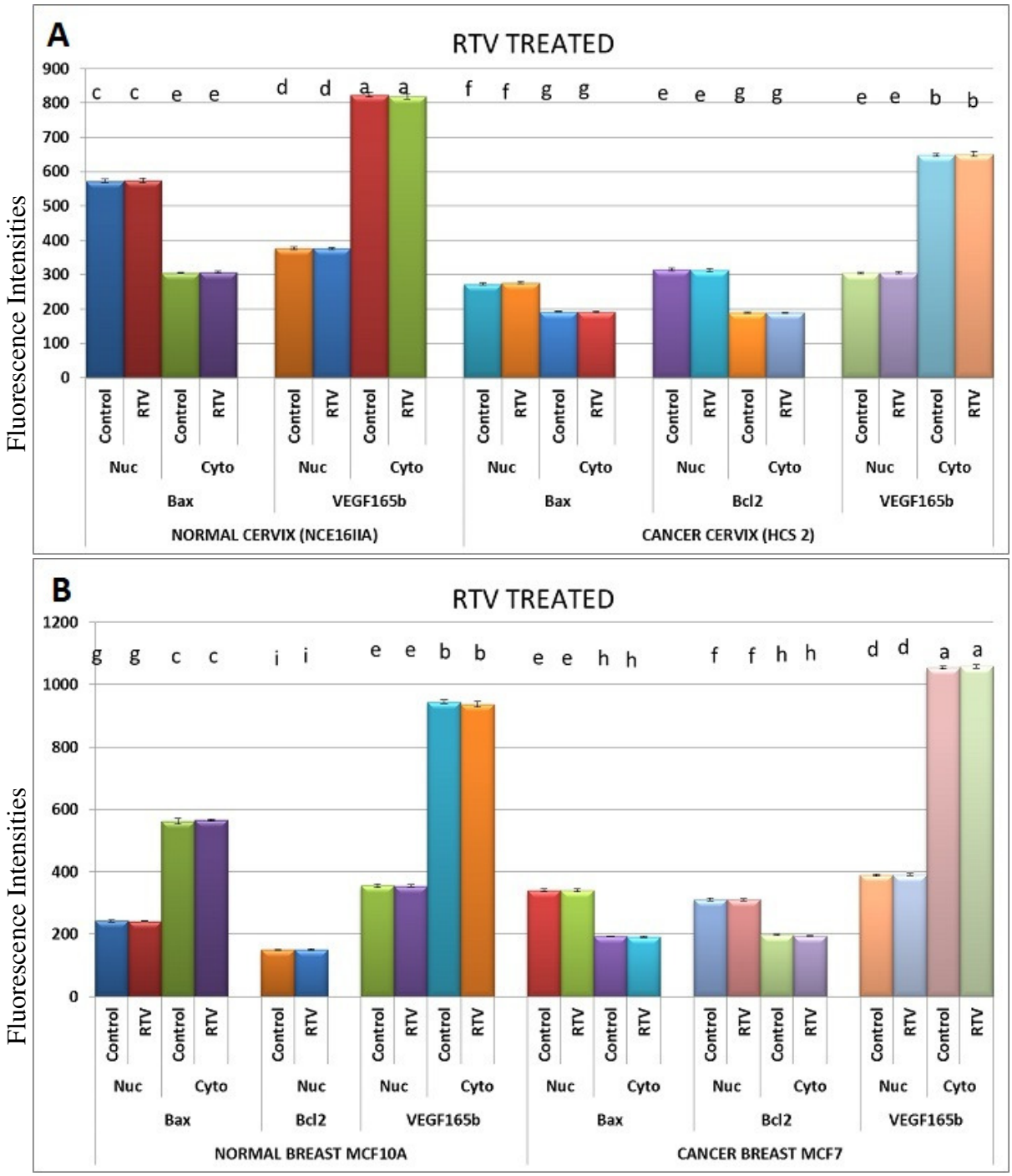

Figure 3.30: Effects of RTV on BAX, BCL-2 and $VEGF_{165b}$ protein expression in (**A**) NCE16IIA (normal cervical); HCS-2 (cervical cancer) and (**B**) MCF-10A (normal breast); MCF-7 (breast cancer) cells. Cells were incubated with 0.6µg/ml RTV for 96 hours. Data (mean ± SEM), are represented as fluorescence intensities of protein expression relative to values from the vehicle-treated cells and representative of 3 independent experiments for immunofluorescence staining. Groups not connected by the same letter are significantly ($p<0.05$) different.

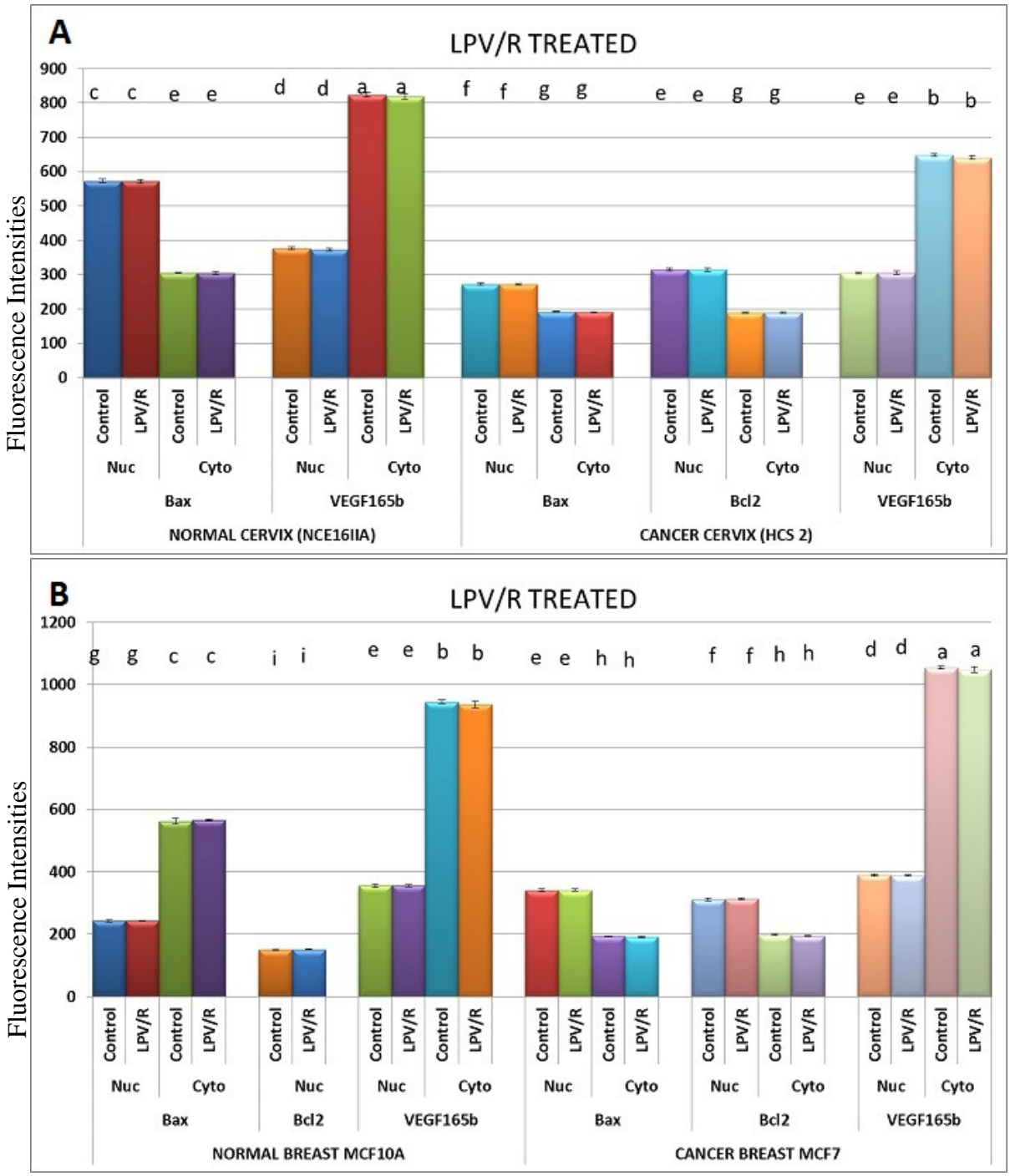

Figure 3.31: Effects of LPV/r on BAX, BCL-2 and $VEGF_{165b}$ protein expression in (**A**) NCE16IIA (normal cervical); HCS-2 (cervical cancer) and (**B**) MCF-10A (normal breast); MCF-7 (breast cancer) cells. Cells were incubated with 9.8µg/ml LPV; 0.6µg/ml RTV for 96 hours. Data (mean ± SEM), are represented as fluorescence intensities of protein expression relative to values from the vehicle-treated cells and representative of 3 independent experiments for immunofluorescence staining. Groups not connected by the same letter are significantly ($p<0.05$) different.

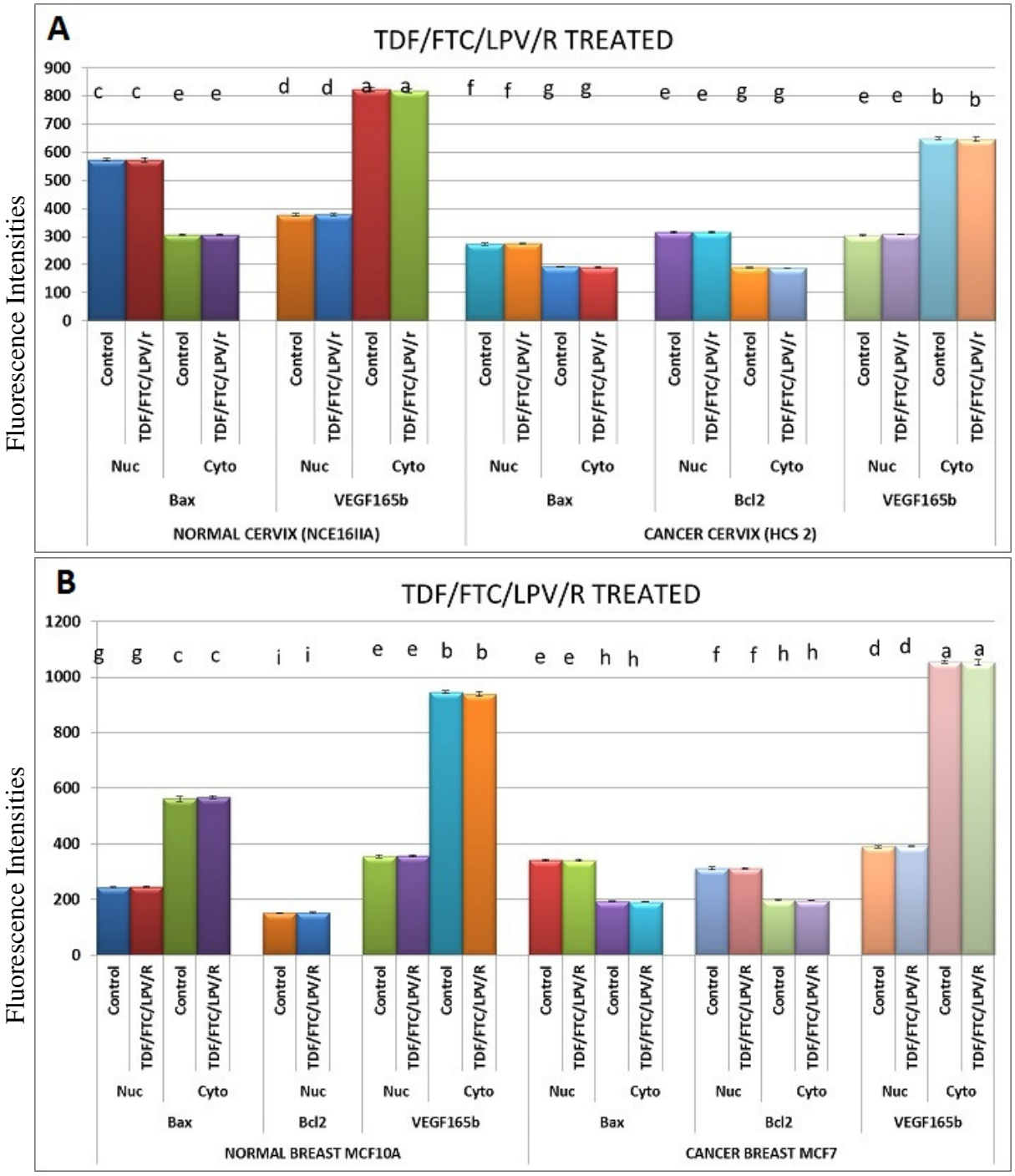

Figure 3.32: Effects of TDF/FTC/LPV/r on BAX, BCL-2 and $VEGF_{165b}$ protein expression in (**A**) NCE16IIA (normal cervical); HCS-2 (cervical cancer) and (**B**) MCF-10A (normal breast); MCF-7 (breast cancer) cells. Cells were incubated with 0.3µg/ml TDF; 1.8µg/ml FTC; 9.8µg/ml LPV; 0.6µg/ml RTV for 96 hours. Data (mean ± SEM), are represented as fluorescence intensities of protein expression relative to values from the vehicle-treated cells and representative of 3 independent experiments for immunofluorescence staining. Groups not connected by the same letter are significantly ($p<0.05$) different.

Table 3.3: Summary of the effects of ARVs on BAX, BCL-2 and VEGF165B protein expression (fluorescence intensity) and localisation in normal and cancer cervical and breast cell lines.

Treatment			Normal Cervical (NC)	Cancer Cervical (CC)	Normal Breast (NB)	Breast Cancer (BC)
Growth Medium	**BAX**	**Intensity**	Nuclear+++, Cyto++	Nuclear++, Cyto+	Nuclear+, Cyto+++	Nuclear++, Cyto+
		Localisation	Nuclear and Cytoplasm	Nuclear and Cytoplasm	Nuclear and Cytoplasm	Nuclear and Cytoplasm
	BCL2	**Intensity**	Nuclear 0, Cyto 0	Nuclear++, Cyto+	Nuclear++, Cyto 0	Nuclear++, Cyto+
		Localisation		Nuclear and Cytoplasm	Nuclear	Nuclear and Cytoplasm
	VEGF165b	**Intensity**	Nuclear+, Cyto+++	Nuclear+, Cyto+++	Nuclear+, Cyto+++	Nuclear+, Cyto+++
		Localisation	Nuclear and Cytoplasm	Nuclear and Cytoplasm	Nuclear and Cytoplasm	Nuclear and Cytoplasm
Vehicle Control 0.01% Methanol	**BAX**	**Intensity**	Nuclear+++, Cyto++	Nuclear++, Cyto+	Nuclear+, Cyto+++	Nuclear++, Cyto+
		Localisation	Nuclear and Cytoplasm	Nuclear and Cytoplasm	Nuclear and Cytoplasm	Nuclear and Cytoplasm
	BCL2	**Intensity**	Nuclear 0, Cyto 0	Nuclear++, Cyto+	Nuclear++, Cyto 0	Nuclear++, Cyto+
		Localisation		Nuclear and Cytoplasm	Nuclear	Nuclear and Cytoplasm
	VEGF165b	**Intensity**	Nuclear+, Cyto+++	Nuclear+, Cyto+++	Nuclear+, Cyto+++	Nuclear+, Cyto+++
		Localisation	Nuclear and Cytoplasm	Nuclear and Cytoplasm	Nuclear and Cytoplasm	Nuclear and Cytoplasm
0.3 µg/ml TDF	**BAX**	**Intensity**	Nuclear+++, Cyto++	Nuclear++, Cyto+	Nuclear+, Cyto+++	Nuclear++, Cyto+
		Localisation	Nuclear and Cytoplasm	Nuclear and Cytoplasm	Nuclear and Cytoplasm	Nuclear and Cytoplasm
	BCL2	**Intensity**	Nuclear 0, Cyto 0	Nuclear++, Cyto+	Nuclear++, Cyto 0	Nuclear++, Cyto+
		Localisation		Nuclear and Cytoplasm	Nuclear	Nuclear and Cytoplasm
	VEGF165b	**Intensity**	Nuclear+, Cyto+++	Nuclear+, Cyto+++	Nuclear+, Cyto+++	Nuclear+, Cyto+++
		Localisation	Nuclear and Cytoplasm	Nuclear and Cytoplasm	Nuclear and Cytoplasm	Nuclear and Cytoplasm
1.8µg/ml FTC	**BAX**	**Intensity**	Nuclear+++, Cyto++	Nuclear++, Cyto+	Nuclear+, Cyto+++	Nuclear+, Cyto+
		Localisation	Nuclear and Cytoplasm	Nuclear and Cytoplasm	Nuclear and Cytoplasm	Nuclear and Cytoplasm
	BCL2	**Intensity**	Nuclear 0, Cyto 0	Nuclear++, Cyto+	Nuclear++, Cyto 0	Nuclear++, Cyto+
		Localisation		Nuclear and Cytoplasm	Nuclear	Nuclear and Cytoplasm
	VEGF165b	**Intensity**	Nuclear+, Cyto+++	Nuclear+, Cyto+++	Nuclear+, Cyto+++	Nuclear+, Cyto+++
		Localisation	Nuclear and Cytoplasm	Nuclear and Cytoplasm	Nuclear and Cytoplasm	Nuclear and Cytoplasm
4.07µg/ml EFV	**BAX**	**Intensity**	Nuclear+++, Cyto++	Nuclear++, Cyto+	Nuclear+, Cyto+++	Nuclear++, Cyto+
		Localisation	Nuclear and Cytoplasm	Nuclear and Cytoplasm	Nuclear and Cytoplasm	Nuclear and Cytoplasm
	BCL2	**Intensity**	Nuclear 0, Cyto 0	Nuclear++, Cyto+	Nuclear++, Cyto 0	Nuclear++, Cyto+
		Localisation		Nuclear and Cytoplasm	Nuclear	Nuclear and Cytoplasm
	VEGF165b	**Intensity**	Nuclear+, Cyto+++	Nuclear+, Cyto+++	Nuclear+, Cyto+++	Nuclear+, Cyto+++
		Localisation	Nuclear and Cytoplasm	Nuclear and Cytoplasm	Nuclear and Cytoplasm	Nuclear and Cytoplasm
ATRIPLA TDF/FTC/ EFV	**BAX**	**Intensity**	Nuclear+++, Cyto++	Nuclear++, Cyto+	Nuclear+, Cyto+++	Nuclear++, Cyto+
		Localisation	Nuclear and Cytoplasm	Nuclear and Cytoplasm	Nuclear and Cytoplasm	Nuclear and Cytoplasm
	BCL2	**Intensity**	Nuclear 0, Cyto 0	Nuclear++, Cyto+	Nuclear++, Cyto 0	Nuclear++, Cyto+
		Localisation		Nuclear and Cytoplasm	Nuclear	Nuclear and Cytoplasm
	VEGF165b	**Intensity**	Nuclear+, Cyto+++	Nuclear+, Cyto+++	Nuclear+, Cyto+++	Nuclear+, Cyto+++
		Localisation	Nuclear and Cytoplasm	Nuclear and Cytoplasm	Nuclear and Cytoplasm	Nuclear and Cytoplasm
9.8µg/ml LPV	**BAX**	**Intensity**	Nuclear+++, Cyto++	Nuclear++, Cyto+	Nuclear+, Cyto+++	Nuclear++, Cyto+
		Localisation	Nuclear and Cytoplasm	Nuclear and Cytoplasm	Nuclear and Cytoplasm	Nuclear and Cytoplasm
	BCL2	**Intensity**	Nuclear 0, Cyto 0	Nuclear++, Cyto+	Nuclear++, Cyto 0	Nuclear++, Cyto+
		Localisation		Nuclear and Cytoplasm	Nuclear	Nuclear and Cytoplasm
	VEGF165b	**Intensity**	Nuclear+, Cyto+++	Nuclear+, Cyto+++	Nuclear+, Cyto+++	Nuclear+, Cyto+++
		Localisation	Nuclear and Cytoplasm	Nuclear and Cytoplasm	Nuclear and Cytoplasm	Nuclear and Cytoplasm
0.6 µg/ml RTV	**BAX**	**Intensity**	Nuclear+++, Cyto++	Nuclear++, Cyto+	Nuclear+, Cyto+++	Nuclear++, Cyto+
		Localisation	Nuclear and Cytoplasm	Nuclear and Cytoplasm	Nuclear and Cytoplasm	Nuclear and Cytoplasm
	BCL2	**Intensity**	Nuclear 0, Cyto 0	Nuclear++, Cyto+	Nuclear++, Cyto 0	Nuclear++, Cyto+
		Localisation		Nuclear and Cytoplasm	Nuclear	Nuclear and Cytoplasm
	VEGF165b	**Intensity**	Nuclear+, Cyto+++	Nuclear+, Cyto+++	Nuclear+, Cyto+++	Nuclear+, Cyto+++
		Localisation	Nuclear and Cytoplasm	Nuclear and Cytoplasm	Nuclear and Cytoplasm	Nuclear and Cytoplasm
KALETRA (LPV/r)	**BAX**	**Intensity**	Nuclear+++, Cyto++	Nuclear+, Cyto+	Nuclear+, Cyto+++	Nuclear++, Cyto+
		Localisation	Nuclear and Cytoplasm	Nuclear and Cytoplasm	Nuclear and Cytoplasm	Nuclear and Cytoplasm
	BCL2	**Intensity**	Nuclear 0, Cyto 0	Nuclear++, Cyto+	Nuclear++, Cyto 0	Nuclear++, Cyto+
		Localisation		Nuclear and Cytoplasm	Nuclear	Nuclear and Cytoplasm
	VEGF165b	**Intensity**	Nuclear+, Cyto+++	Nuclear+, Cyto+++	Nuclear+, Cyto+++	Nuclear+, Cyto+++
		Localisation	Nuclear and Cytoplasm	Nuclear and Cytoplasm	Nuclear and Cytoplasm	Nuclear and Cytoplasm
TDF/FTC/ LPVr	**BAX**	**Intensity**	Nuclear+++, Cyto++	Nuclear++, Cyto+	Nuclear+, Cyto+++	Nuclear++, Cyto+
		Localisation	Nuclear and Cytoplasm	Nuclear and Cytoplasm	Nuclear and Cytoplasm	Nuclear and Cytoplasm
	BCL2	**Intensity**	Nuclear 0, Cyto 0	Nuclear++, Cyto+	Nuclear++, Cyto 0	Nuclear++, Cyto+
		Localisation		Nuclear and Cytoplasm	Nuclear	Nuclear and Cytoplasm
	VEGF165b	**Intensity**	Nuclear+, Cyto+++	Nuclear+, Cyto+++	Nuclear+, Cyto+++	Nuclear+, Cyto+++
		Localisation	Nuclear and Cytoplasm	Nuclear and Cytoplasm	Nuclear and Cytoplasm	Nuclear and Cytoplasm

3.3.5 Effects of ARVs on the nuclear morphology of normal and cancer cervical and breast cell lines.

The major (long) and minor (short) axes of the nuclei were measured (in μm). This approach was found to be more reliable than the degree of nuclei compactness because the different cultures (passages) of the same untreated cell line exhibited different degrees of compactness and DAPI bright and DAPI dim areas. For example, while cell nuclei appeared compacted in NCE166IIA (normal cervical) cell culture preparation (passage) for VEGF165 staining (Fig. 3.22), they appeared less compacted in the same cell line (different passage) for BAX/BCL-2 staining (Fig. 3.18). Another example is Fig. 3.20A1-J1 (for BAX staining) compared to Fig.3.20A2-J2 (for BCL-2 staining). The morphological differences observed were not due to treatment with ARVs because there were notable differences between two groups of untreated cells (the same cell line but different cultures). These differences could be therefore be passage dependent.

Nuclear dimensions were therefore used as a more reliable measure of the effects of the ARVs on nuclear morphology and presented in the graphs below (Fig. 3.33). Mean values were statistically analysed (ANOVA) between the untreated, vehicle control and the treated groups. Fig. 3.33A illustrates the effects of the antiretroviral drugs on the major and minor axes of untreated, vehicle treated and ARV treated normal cervical NCE16IIA cells. Fig. 3.33B illustrates the effect of the antiretroviral drugs on the major and minor axes of untreated, vehicle treated and ARV treated cancer cervical HCS-2 cells. Fig. 3.33C illustrates the effect of the antiretroviral drugs on the major and minor axes of untreated, vehicle treated and ARV treated normal breast MCF-10A cells. Fig. 3.33D illustrates the effect of the antiretroviral drugs on the major and minor axes of untreated, vehicle treated and ARV treated cancer breast MCF-7 cells. Statistical analysis was performed using JMP® (Version 10.0 SAS Institute Inc., Cary, NC). Data are reported as mean $\pm$ standard

deviation. After verifying the normal distribution and the homogeneity of the variance using an F test ($p < 0.05$), a one way analysis of variance (where a significance level of $p < 0.05$ was set) was used to compare the results. All means were then compared using the Tukey-Kramer HSD. Data summaries are presented in Appendix F. There were no significant ($p<0.05$) differences observed between untreated, vehicle treated and ARV treated groups.

Table 3.4: Summary of the effects of ARVs on the nuclear morphology of normal and cancer cervical and breast cell lines

Treatment	**Normal Cervical (NCE16IIA)**	**Cancer Cervical (HCS-2)**	**Normal Breast (MCF-10A)**	**Breast Cancer (MCF-7)**
Growth Medium	Nuclei with round to oval shape. Major to minor axis ratio is approximately 1.5	Oval to round Nuclei with major and minor nuclei axis ratio approximately 1.6	Round to oval nuclei. Major and minor nuclei axis ratio approximately 1.5	Round Nuclei with major and minor nuclei axis ratio approximately 1.6
Vehicle Control (0.01% Methanol)	Nuclei with round to oval shape. Major to minor axis ratio similar to untreated control	Oval to round Nuclei with major to minor nuclei axis ratio similar to untreated control	Round to oval nuclei similar to untreated control. Major and minor nuclei axis ratio similar to untreated control	Round Nuclei with major to minor nuclei axis ratio similar to untreated control
TREATMENT: 0.3 µg/ml TDF, 1.8µg/ml FTC, 4.07µg/ml EFV, ATRIPLA, 9.8µg/ml LPV, 0.6 µg/ml RTV, KALETRA, TDF/FTC/LPVr	Nuclei with round to oval shape. Major to minor axis ratio not significantly $p<(0.05)$ different from controls	Oval to round Nuclei with major to minor nuclei axis ratio not significantly $p<(0.05)$ different from controls	Round to oval nuclei similar to untreated control. Major and minor nuclei axis ratio similar to and not significantly $p<(0.05)$ different from controls	Round Nuclei with major to minor nuclei axis ratio not significantly $p<(0.05)$ different from controls

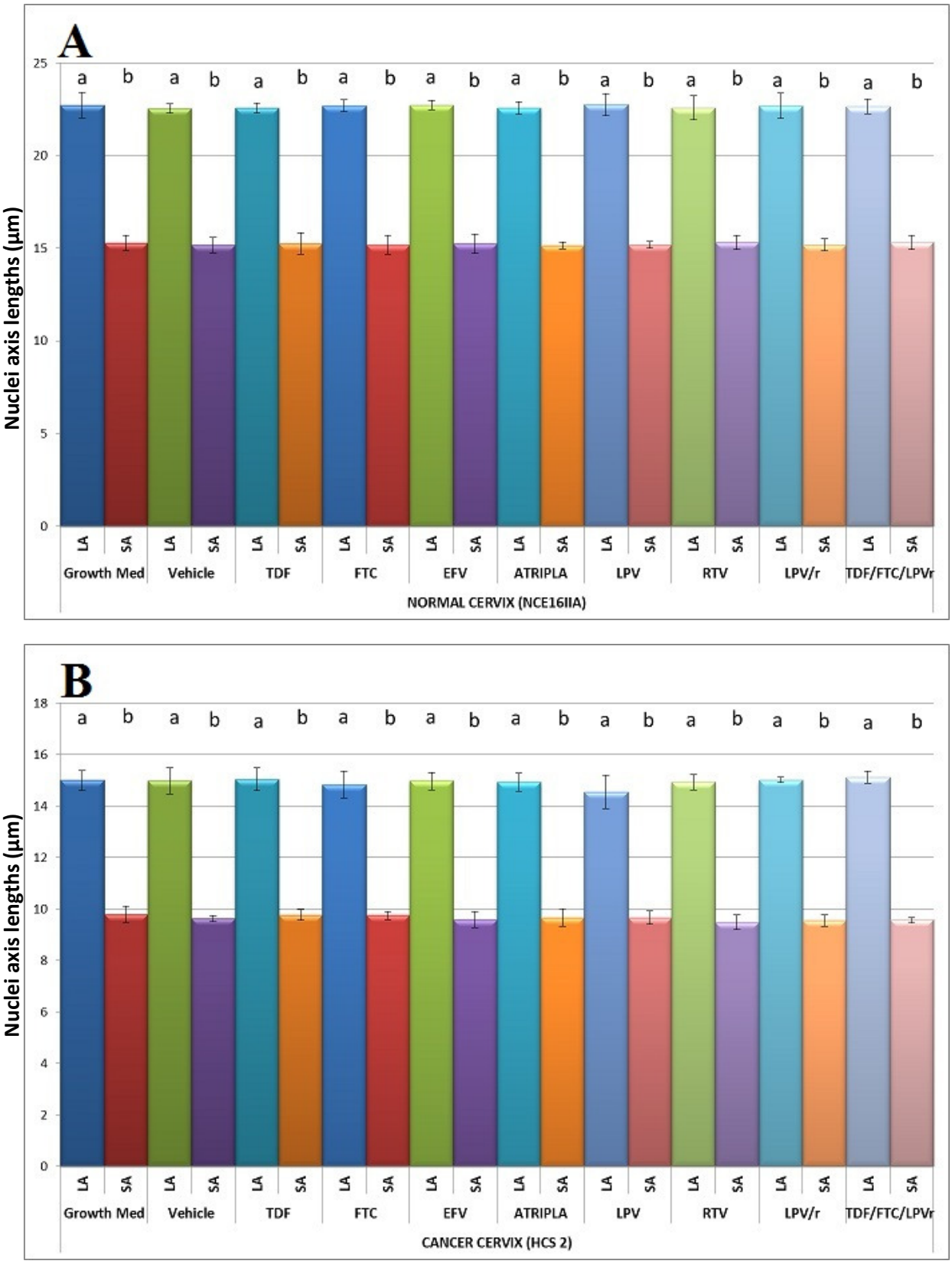

Figure 3.33A and B: Effects of ARVs on the long (LA) and short (SA) axes lengths (**µm**) of the nuclei of normal cervical NCE16IIA (A) and cancer cervical HCS-2 (B) cells. Data are represented as (mean ± SD). Groups not connected by the same letter are significantly ($p<0.05$) different.

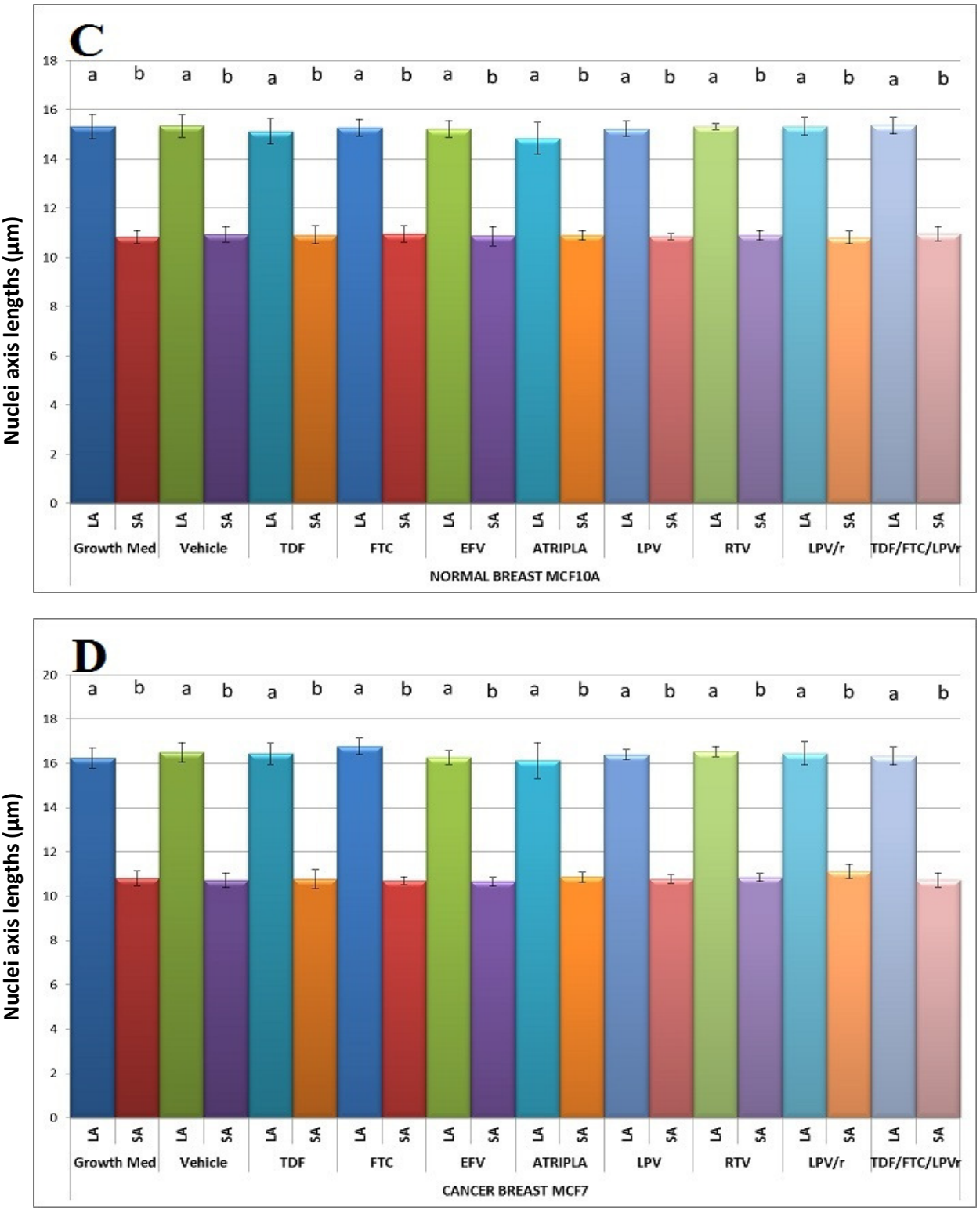

Figure 3.33C and D: Effects of ARVs on the long (LA) and short (SA) axes lengths (**µm**) of the nuclei of normal breast MCF-10A (C) and cancer breast MCF-7 (D) cells. Data are represented as (mean ± SD). Groups not connected by the same letter are significantly ($p<0.05$) different.

3.4 Protease Inhibitors and Apoptosis Inhibition

It has been previously shown (Phenix et al, 2001, Badley, 2005, Vlahakis *et al.,* 2007, Rizza and Badley, 2008) that protease inhibitors have potent anti-apoptotic effects in different cellular systems, the majority of which are immune cells. The anti-apoptotic effect of LPV/r was assessed to test whether these generalised effects are seen in the currently investigated cell lines and to test whether they alter apoptosis via a pathway other than the *BAX/BCL-2* pathway, since they had no significant effect on *BAX* and *BCL-2* mRNA expression (Figs. 3.9 – 3.16). From an evaluation of the many methods currently used to analyse apoptosis, chromatin condensation and nuclear fragmentation remain the hallmarks of apoptotic cells (Ribble *et al.,* 2005). Because it had been suggested that, as a rule, classification of cell death in a given model should always include morphological examination coupled with at least one other assay (Renvoize *et al.,* 1998), the Acridine Orange staining for morphological evaluation and an ELISA based method for the quantitative analysis of DNA fragmentation were thus chosen.

3.4.1 Protease Inhibitors and apoptosis inhibition in cervical cancer HCS-2 and normal cervical NCE16IIA cells

From previous optimisation experiments, it was determined that 25 μM and 5 μM Camptothecin (CPT) significantly induced apoptosis in the HCS-2 and NCE16IIA cells, respectively, after six hours. Figures 3.34 and 3.35 represent data (acquired and analysed as described in section 2.7.2) from AO staining showing that a 96 hour exposure to LPV/r significantly ($p<0.05$) inhibited apoptosis in the cervical cancer HCS-2 but not in the normal cervical NCE16IIA cells. A total of 600 cells per cell line per group were counted from 3 independent experiments to determine the percentage of apoptotic cells. Data analysis was performed using JMP® (Version 10.0 SAS Institute Inc., Cary, NC). Data are reported as mean $\pm$ standard deviation. After verifying the normal distribution and the homogeneity of the variance using an F test ($p < 0.05$), a one way analysis of variance (significance level $p < 0.05$) was used to compare the results. If there was a significant difference between the means ($p<0.05$) then a Tukey-Kramer *post hoc* analysis was performed to determine which treatment groups were significantly different from each other. Data summaries are shown in Appendix G.

Figure 3.36 represent data (acquired and analysed as described in section 2.8) quantifying DNA fragmentation between groups (Data summaries are shown in Appendix G). The ELISA results also confirm that LPV/r significantly inhibited drug induced apoptosis in the cancer HCS-2 but not in the NCE16IIA cells.

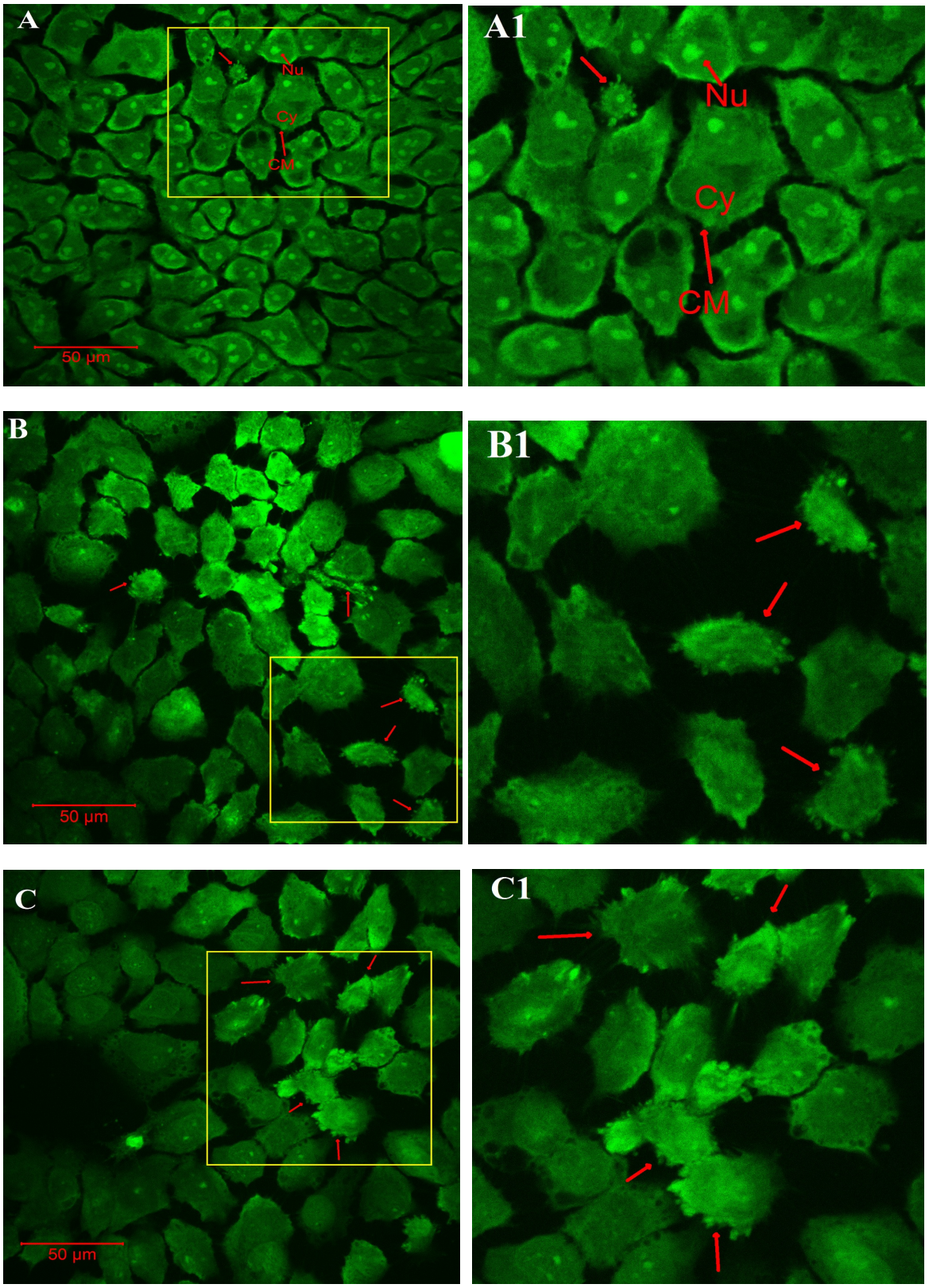

Figure legend and the graphical representation of percentage apoptosis on next page. Nu-Nucleus, Cy-Cytoplasm, CM-Cell membrane. Area within yellow box magnified to the right.

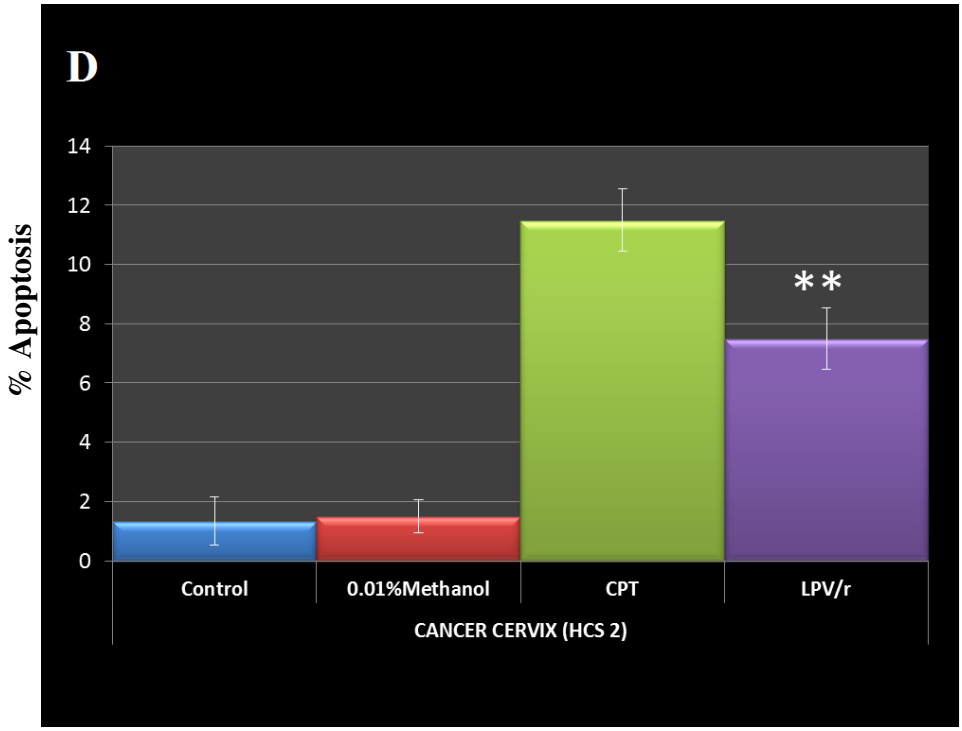

Figure 3.34A-D: Effects of LPV/r on CPT mediated apoptosis in HCS-2 cells. HCS-2 cells (untreated-A) were stimulated with 25μM CPT for 6 hours without prior exposure to LPV/r (B), while C shows cells incubated with LPV/r prior to apoptosis induction. Apoptosis was assessed using acridine orange staining. Arrows point to apoptotic bodies and cells undergoing apoptosis with the characteristic feature of membrane blebbing. Areas within the yellow box are magnified to the right (A1, B1 C1). A total of 600 cells per group were counted from 3 independent experiments to determine the percentage of apoptotic cells. LPV/r significantly ($p<0.05$) inhibited CPT induced apoptosis.

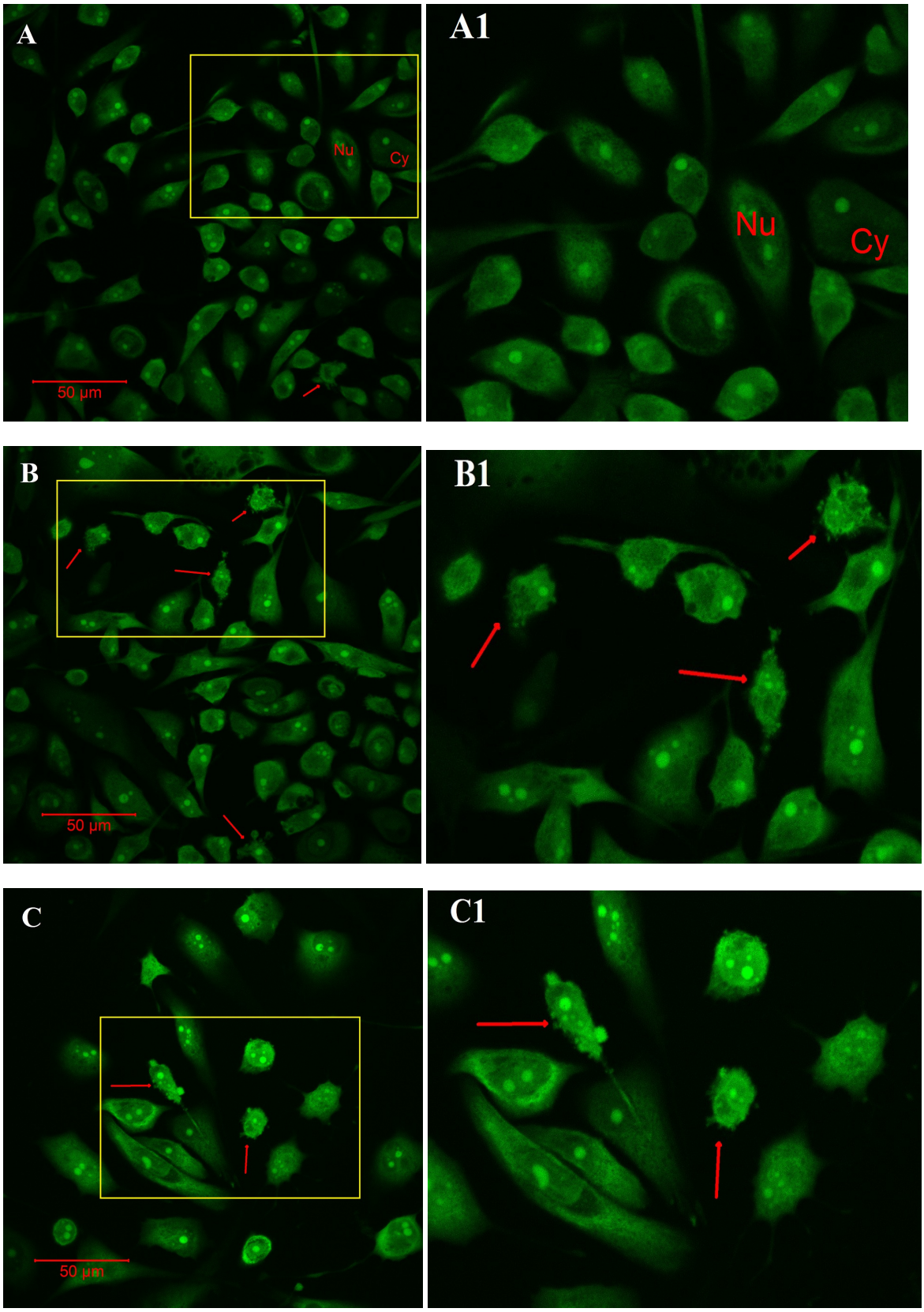

Figure legend and the graphical representation of percentage apoptosis on next page. Nu-Nucleus, Cy-Cytoplasm. Area within yellow box magnified to the right.

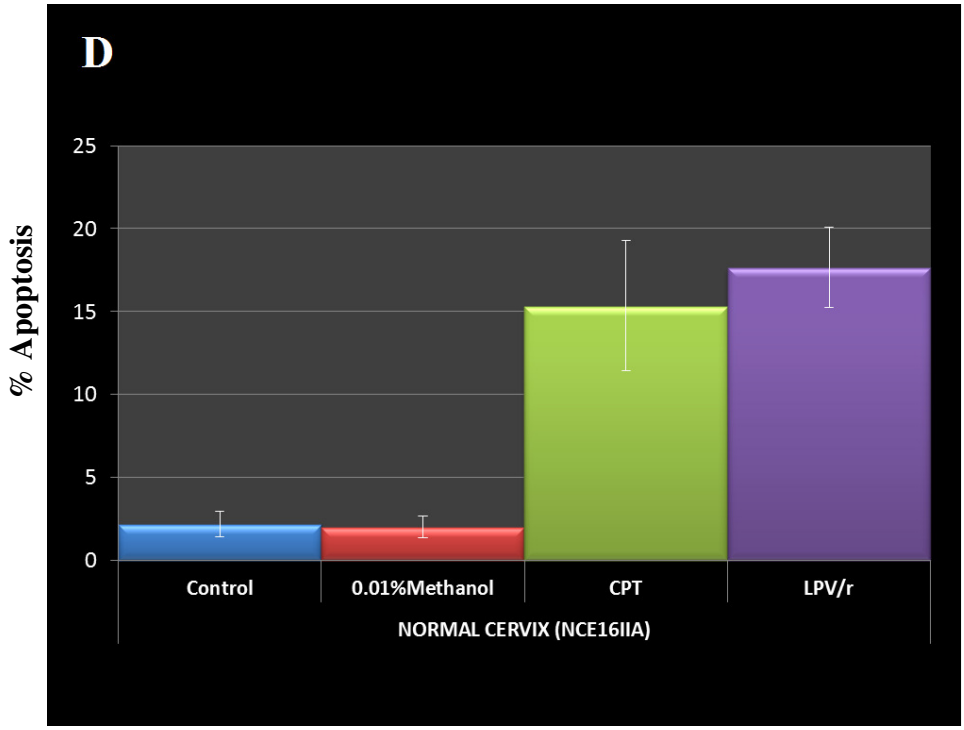

Figure 3.35A-D: Effects of LPV/r on CPT mediated apoptosis in NCE16IIA cells. NCE16IIA cells (untreated-A) were stimulated with 5μM CPT for 6 hours without prior exposure to LPV/r (B). C shows cells incubated with LPV/r prior to apoptosis induction. Apoptosis was assessed using acridine orange staining. Arrows point to apoptotic bodies and cells undergoing apoptosis with the characteristic feature of membrane blebbing. Areas within the yellow box are magnified to the right (A1, B1 C1). A total of 600 cells per group were counted from 3 independent experiments to determine the percentage of apoptotic cells. LPV/r has no significant effects on CPT induced apoptosis in NCE16IIA cells (D).

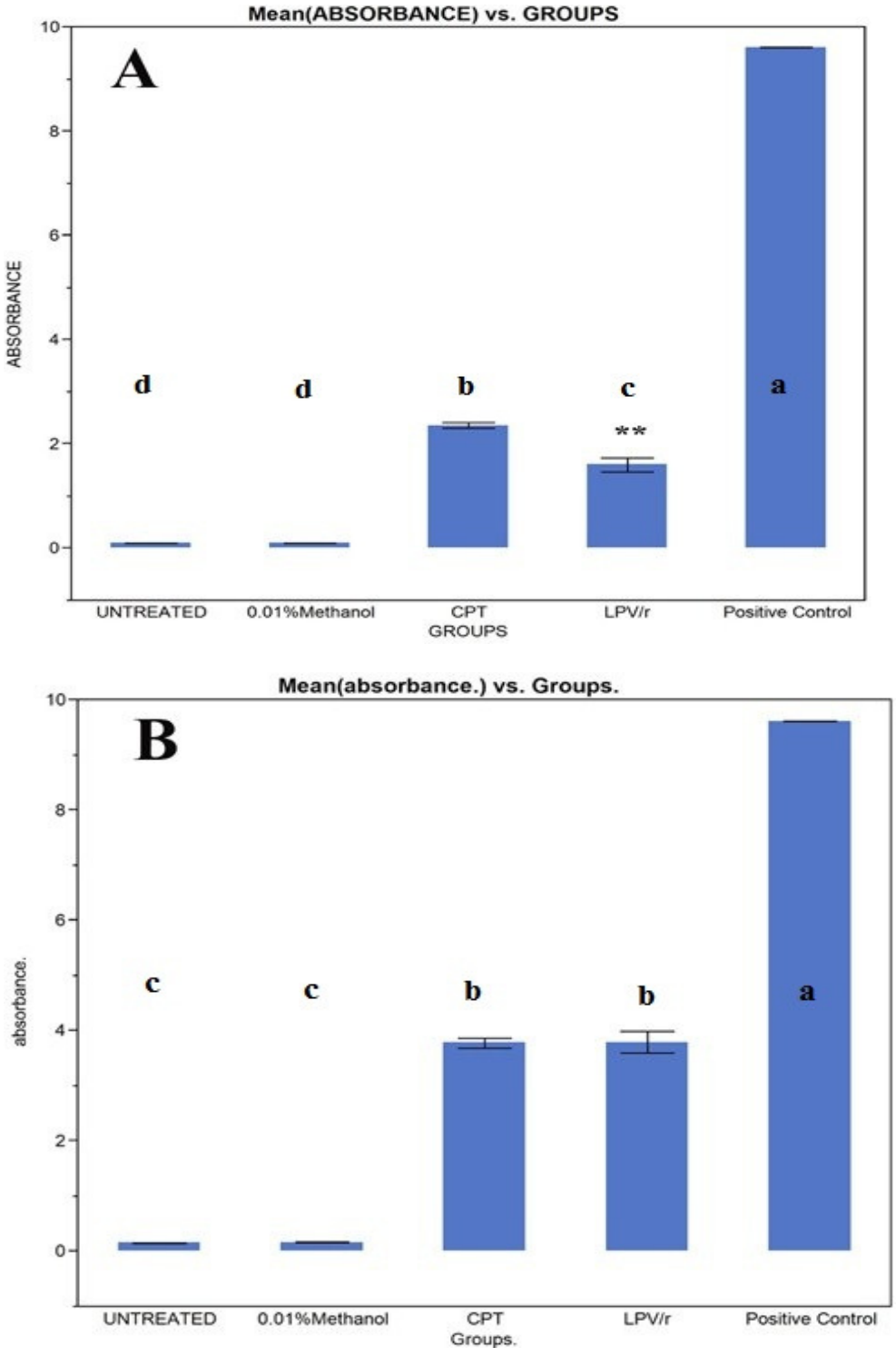

Figure 3.36A-B: Effects of LPV/r on CPT mediated apoptosis in HCS-2 and NCE16IIA cells evaluated by the Cell Death Detection ELISA. (**A**) HCS-2 cells were treated with methanol or LPV/r for 96 hours and stimulated with 25μM CPT. Apoptosis was assessed by quantifying internucleosomal DNA fragmentation. LPV/r treatment significantly ($p<0.05$) inhibited CPT induced apoptosis. (**B**) NCE16IIA cells were treated with methanol or LPV/r for 96 hours and stimulated with 5μM CPT. Apoptosis was assessed by quantifying internucleosomal DNA fragmentation. LPV/r treatment did not inhibit CPT induced apoptosis. Levels not connected by same letter are significantly different.

3.4.2 Protease Inhibitors and apoptosis inhibition in breast cancer (MCF-7) and normal breast (MCF10-A) cells

From previous optimisation experiments, it was determined that 1 μM and 30 μM CPT significantly induced apoptosis in the MCF-7 and MCF10-A cells respectively after six hours. Figures 3.37 and 3.38 represent data (acquired and analysed as described in section 2.7.2) from AO staining showing that a 96 hour exposure to LPV/r did not significantly ($p<0.05$) inhibit apoptosis in both breast cell lines. A total of 600 cells per cell line per group were counted from 3 independent experiments to determine the percentage of apoptotic cells. Data analysis was performed using JMP® (Version 10.0 SAS Institute Inc., Cary, NC). Data are reported as mean $\pm$ standard deviation. After verifying the normal distribution and the homogeneity of the variance using an F test ($p < 0.05$), a one way analysis of variance (significance level $p < 0.05$) was used to compare the results. If there was a significant difference between the means ($p<0.05$) then a Tukey-Kramer *post hoc* analysis was performed to determine which treatment groups were significantly different from each other. Data summaries are shown in Appendix G.

Figure 3.39 represents data (acquired and analysed as described in section 2.8) quantifying DNA fragmentation between groups (Data summaries are shown in Appendix G). These ELISA results also confirm that LPV/r did not significantly inhibit drug induced apoptosis in the breast MCF-7 and MCF-10A cells.

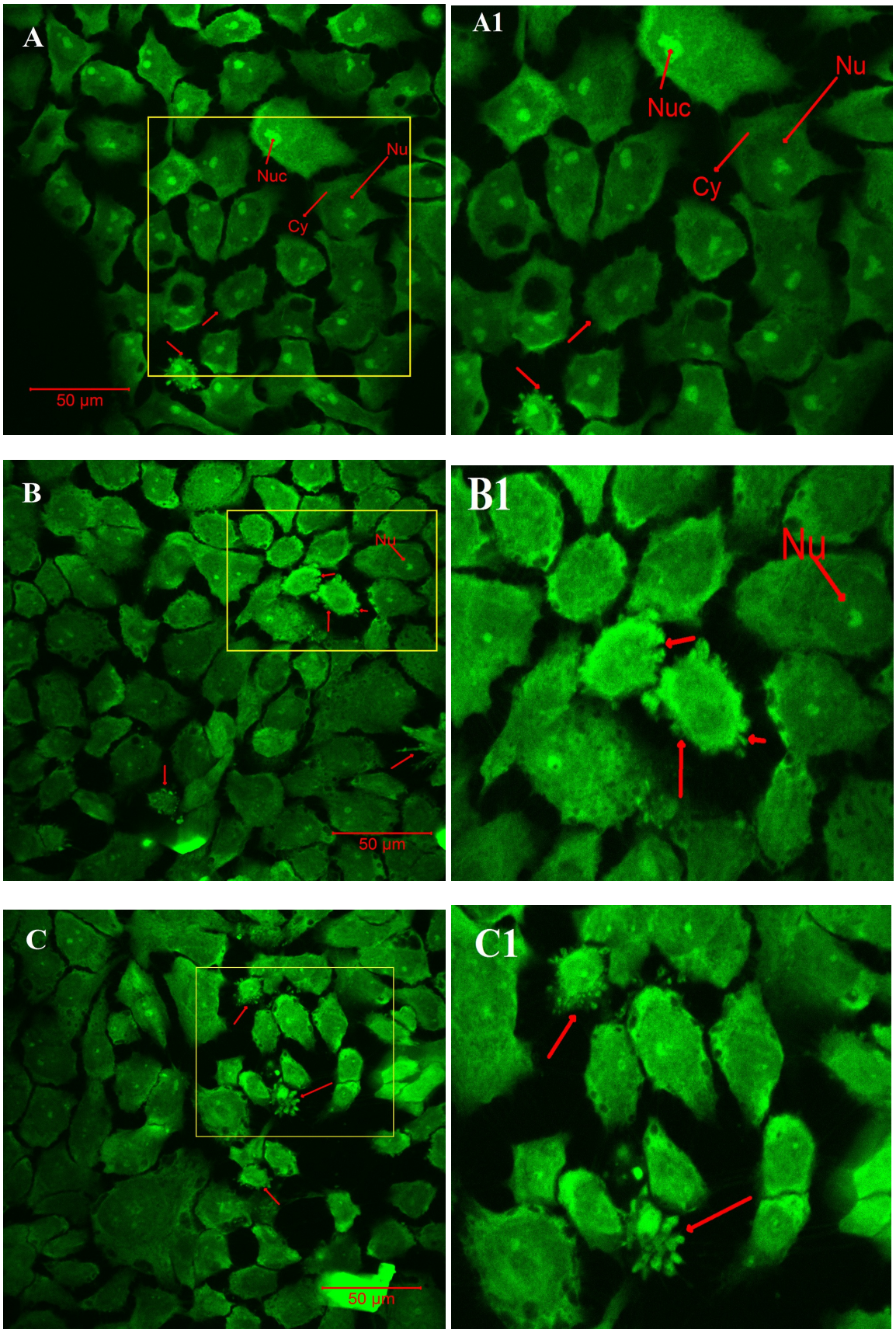

Figure legend and the graphical representation of percentage apoptosis on next page. Nu-Nucleus, Cy-Cytoplasm. Area within yellow box magnified to the right.

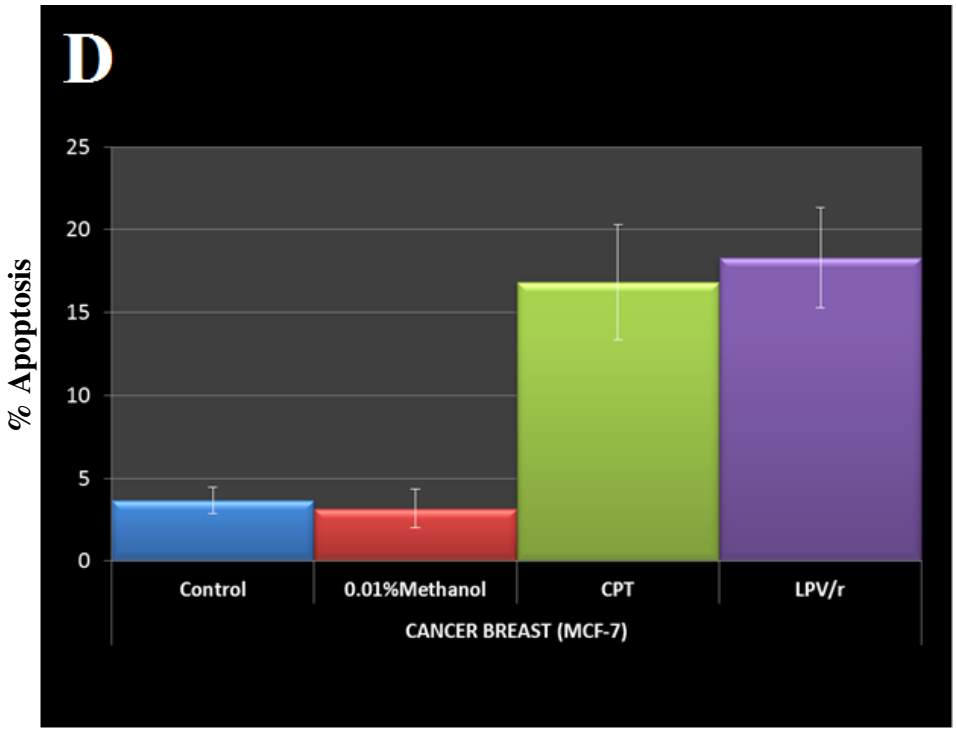

Figure 3.37A-D: Effects of LPV/r on CPT mediated apoptosis in MCF-7 cells. MCF-7 cells (untreated-A) were stimulated with 1μM CPT for 6 hours without prior exposure to LPV/r (B). C shows cells incubated with LPV/r prior to apoptosis induction. Apoptosis was assessed using acridine orange staining. Arrows point to apoptotic bodies and cells undergoing apoptosis with the characteristic feature of membrane blebbing. Areas within the yellow box are magnified to the right (A1, B1 C1). A total of 600 cells per group were counted from 3 independent experiments to determine the percentage of apoptotic cells. LPV/r has no significant inhibitory effects on CPT induced apoptosis in MCF-7 cells (D).

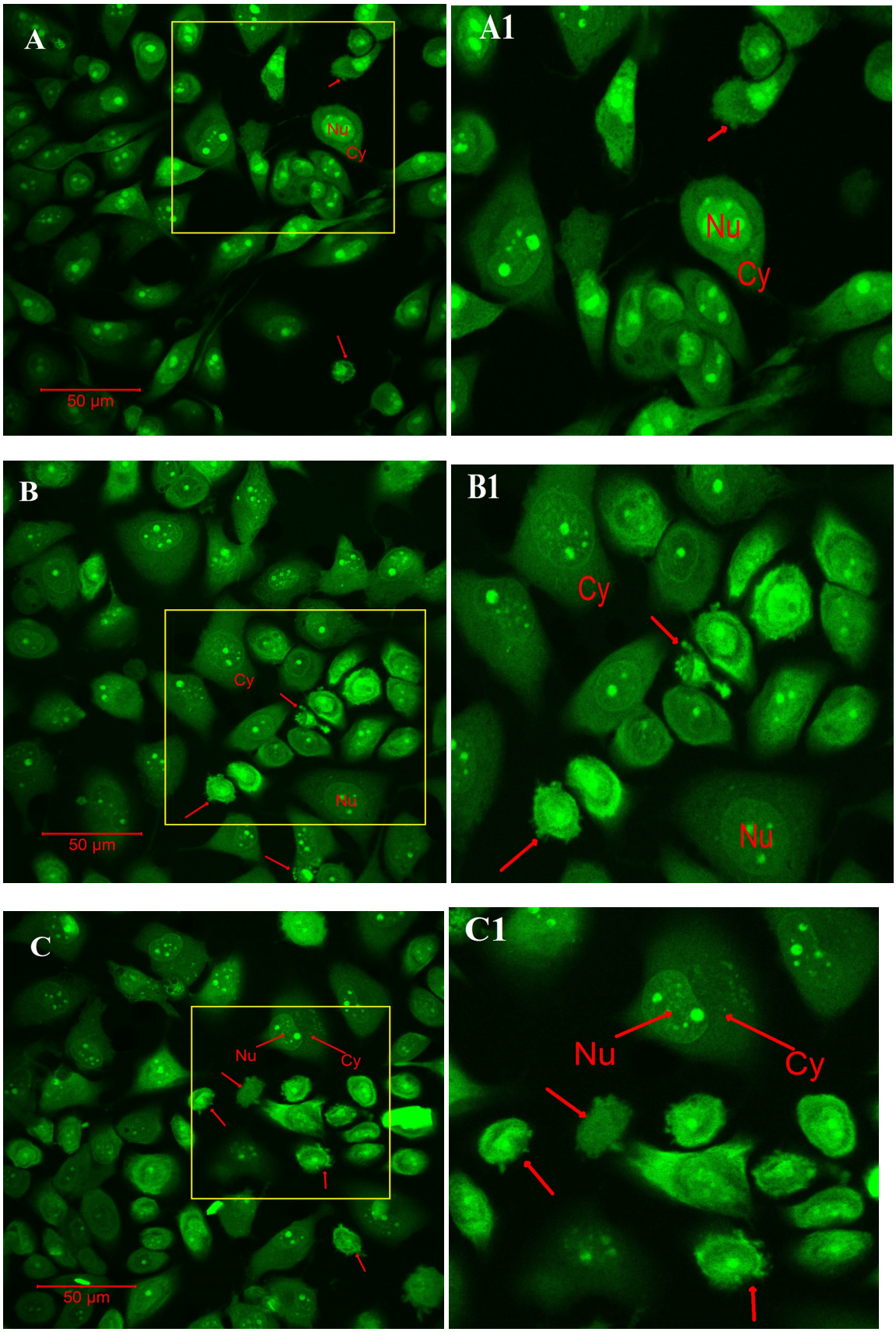

Figure legend and the graphical representation of percentage apoptosis on next page. Nu-Nucleus, Cy-Cytoplasm. Area within yellow box magnified to the right.

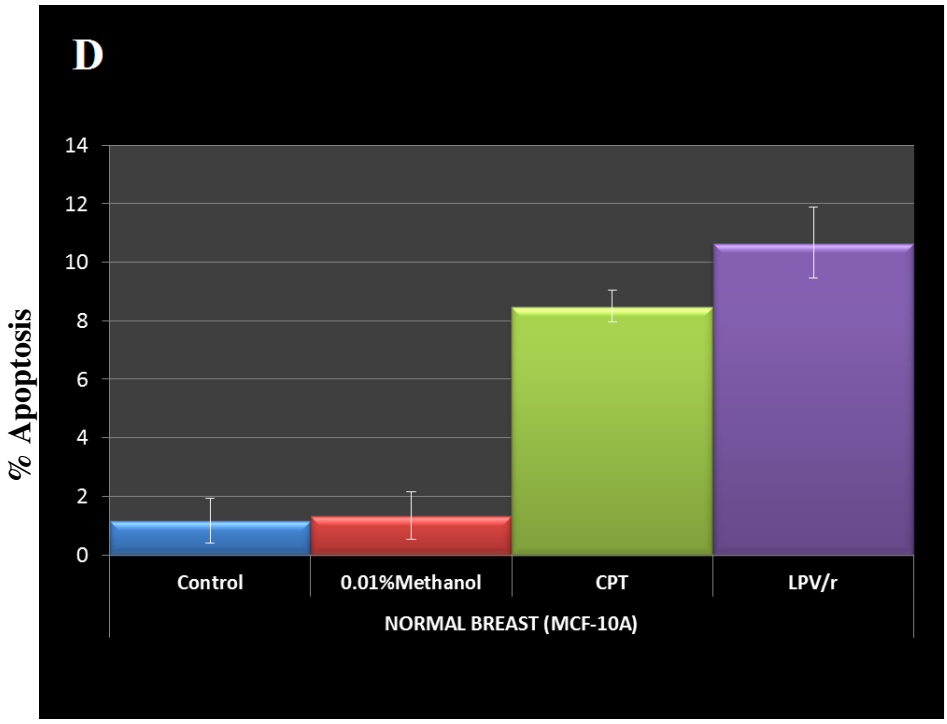

Figure 3.38A-D: Effects of LPV/r on CPT mediated apoptosis in MCF-10A cells. MCF-10A cells (untreated-**A**) were stimulated with 30µM CPT for 6 hours without prior exposure to LPV/r **(B)**. **C** shows cells incubated with LPV/r prior to apoptosis induction. Apoptosis was assessed using acridine orange staining. Arrows point to apoptotic bodies and cells undergoing apoptosis with the characteristic feature of membrane blebbing. Areas within the yellow box are magnified to the right (A1, B1 C1). A total of 600 cells per group were counted from 3 independent experiments to determine the percentage of apoptotic cells. LPV/r has no significant inhibitory effects on CPT induced apoptosis in MCF-10A cells **(D)**.

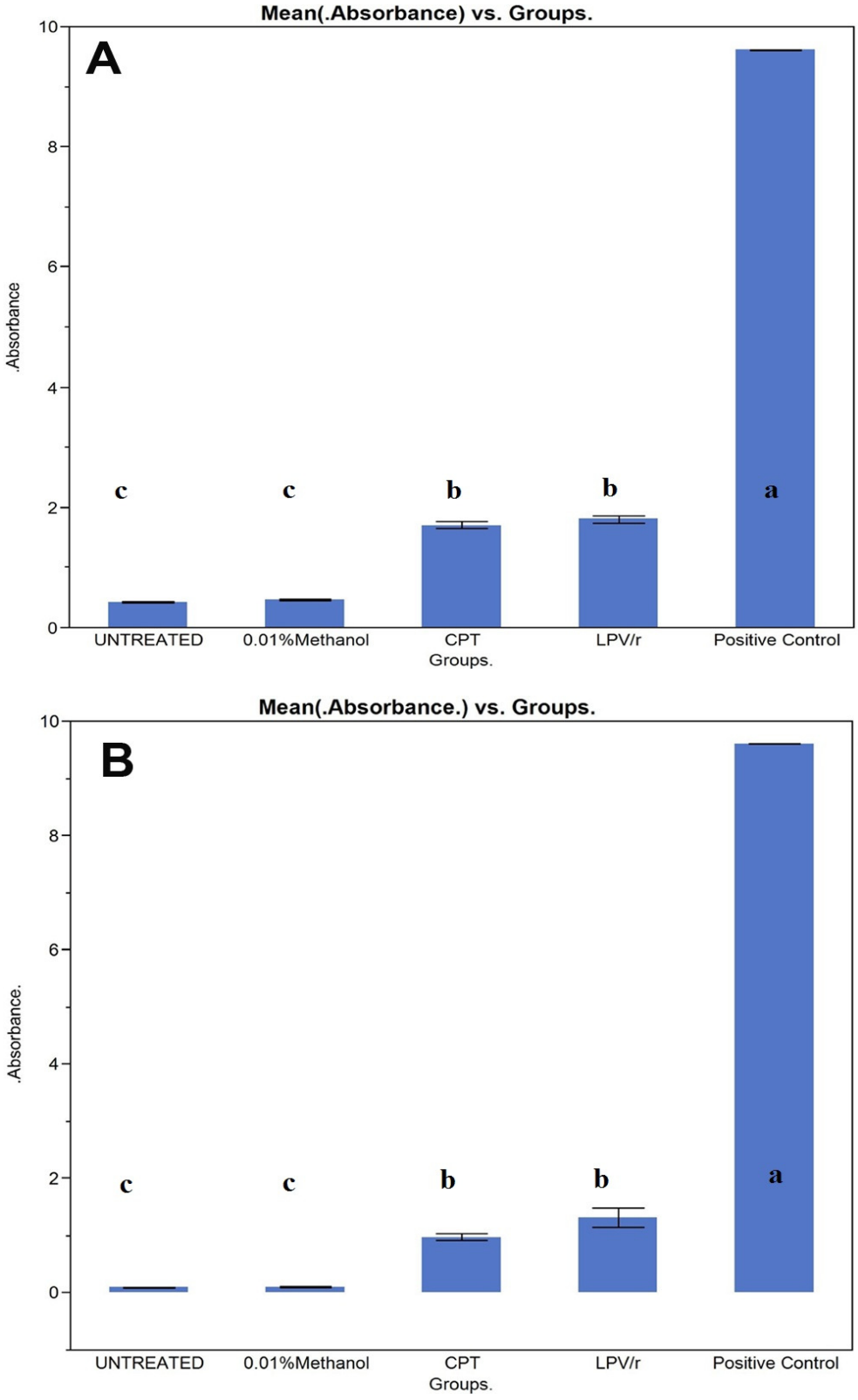

Figure 3.39A-B: Effects of LPV/r on CPT mediated apoptosis in MCF-7 and MCF-10A cells evaluated by the Cell Death Detection ELISA. MCF-7 **(A)** and MCF-10A **(B)** cells were treated with methanol or LPV/r for 96 hours and stimulated with CPT (1μM and 30μM respectively) and apoptosis was assessed by quantifying internucleosomal DNA fragmentation. LPV/r treatment did not significantly ($p<0.05$) inhibit CPT induced apoptosis in both cell lines. Levels not connected by same letter are significantly different.

CHAPTER 4: DISCUSSION

4.1 Introduction

To determine whether the use of antiretroviral drugs could be a risk factor for the initiation or development of cancer in patients receiving HAART, this study tested the effects of different classes of antiretroviral drugs (individually and in combination) on normal (NCE16IIA) and cancer (HCS-2) cervical and normal (MCF-10A) and cancer (MCF-7) breast cell lines. The cervix was chosen as a model of AIDS-defining malignancies while the breast was chosen as a model of non-AIDS-defining malignancies.

The findings reported here show that the antiretroviral drugs; tenofovir disoproxil fumarate, emtricitabine, efavirenz, lopinavir, ritonavir and the two triple combinations (all at clinically relevant concentrations which reflect their steady-state peak plasma concentrations in patients receiving these drugs (Apostolova *et al.*, 2010; Bumpus, 2011)) demonstrated some form of cytotoxicity in the breast and cervical cells, which may alter the activity of the nuclear and mitochondrial genome of cells and may cause genotoxic effects largely related to the tumor initiation processes (Bishop and Schiestl, 2001; Olivero, 2007; Wu *et al.*, 2012).

Negative effects of antiretroviral drugs have been widely reported. Olivero *et al.* (2005) and Gills *et al.* (2007) emphasised the need to determine the risks associated with individual classes of ARV drugs because the oncogenic potential of the different antiretroviral drug classes may be different. Powles *et al.* (2009) suggest that drugs within the cocktail may have effects on the host cell DNA leading to genomic instability and carcinogenesis. Individual NRTIs are implicated as possible chemical carcinogens and mutagens (Olivero *et al.*, 1997; Blanche *et al.*, 1999; IARC 2000; Torres *et al.*, 2007).

Studies by Torres *et al.* (2007) suggest that the continuous use of NRTI drug pairs may lead to additive or synergistic effects that compound the long-term risk for cancer gene mutations and potential carcinogenesis. HIV PIs at low (clinical, serum) concentrations inhibit apoptosis (Vlahakis *et al.*, 2007; Rizza and Badley, 2008), which may lead to the development of cancer.

In order to initiate and/or promote cancer, we formulated the hypothesis that the antiretroviral drugs at clinically relevant concentrations might alter the expression of *BAX* and *BCL-2* (which are key regulatory genes involved in carcinogenesis and apoptotic signalling) and $VEGF_{165a}$ and $VEGF_{165b}$ (pro- and anti-angiogenic related splice variants of the *VEGFA* gene, which are important factors regulating tumor angiogenesis).

4.2 Antiretroviral drugs and Cytotoxicity

The NRTI, TDF, has an initial cytotoxic effect on cell survival in the normal breast and a slow ongoing effect in both cervical cells. Generally, TDF seems to promote normal cell survival over cancer cells. TDF did not show any cytotoxic effects on the normal cervical cell line following a 96 hour exposure, but it did significantly increase the percentage viability of the normal cervical cells from 24 to 48 hours. On the other hand, after 72 hours of treatment, TDF became significantly cytotoxic to the cervical cancer cells. However, the possibility that TDF can increase the viability of normal cervical cells, when compared with the untreated control, may be an indication towards the initiation of cancer. However, the significant increase in percentage viability disappeared with continuous administration of TDF.

In the breast, TDF demonstrated significant cytotoxic effects in the normal breast MCF-10A cell lines after 24 hours of administration. This initial cytotoxic effect disappeared with continuous administration. The fact that TDF can produce an initial cytotoxic effect in

the normal breast cells supports the suggestion of Powles *et al.* (2009) that drugs within the HAART cocktail may have effects on the host cell DNA which may result in genomic instability and carcinogenesis. TDF-containing regimens have been linked to mutagenesis in the *in-vitro* mouse lymphoma assay (Drug information, VIREAD® Gilead Sciences, 2010) and nephrotoxicity (Gitman *et al.*, 2007).

The other NRTI used in this study, FTC, decreased the percentage viability of the normal cervical (NCE16IIA) cells with prolonged administration (96 hours). Even though the reduction was not statistically significant when compared to the vehicle control group, the reduction in percentage viability was significantly different from the effects of FTC on the cervical cancer HCS-2 cells at the same time point. Again this supports the claim that antiretroviral drugs may have effects on the host cell DNA which may cause genomic instability and carcinogenesis (Powles *et al.*, 2009).

FTC did not significantly alter the percentage viability of the normal breast MCF-10A cells from 24 to 96 hours, but it did significantly reduce the viability of the breast cancer MCF-7 cells after 48 hours of treatment. With continuous administration, the cytotoxic effects of FTC on the breast cancer cells disappeared. The potential genotoxicity of these drugs involves a network of complex events that may lead to genomic instability due to incorporation of the drug into the DNA, mutagenesis, and telomere deterioration (Olivero, 2007; Benhammou *et al.*, 2008). NRTIs have been shown to directly alter the activity of the nuclear and mitochondrial genome of cells and may cause genotoxic effects largely related to tumor initiation processes (Bishop and Schiestl, 2001; Olivero, 2007).

Studies by Brüning *et al.* (2012) showed that most of the NRTIs they tested did not alter the viability of selected cancer cells, while Tenofovir and FTC only reduced cancer cell viability at concentrations far beyond plasma levels of the drugs in HIV patients receiving

HAART. NRTI medications are phosphorylated by enzymes in host cells to their active triphosphate (TP) anabolites (Robbins *et al.,* 1998; Wang *et al.,* 2004). Intracellular NRTI triphosphates have been identified in clinical toxicities and many of them have been associated with inhibition of mitochondrial DNA polymerase gamma, just as they inhibit HIV DNA replication (Kakuda, 2000). This non-specificity leads to decreased mitochondrial DNA and reduced RNA and protein output, leading to mitochondrial dysfunction with resultant anaerobic respiration, lactic acid production, oxidative damage and a variety of other clinical presentations (Mallon *et al.,* 2005; Kohler and Lewis, 2007; Maagaard and Kvale, 2009) However, neither TDF nor FTC effectively inhibit DNA polymerase gamma when compared to other NRTIs as evaluated by *in-vitro* cellular and enzymatic assays (Johnson *et al.,* 2001; Birkus *et al.,* 2002; Feng *et al.,* 2004).

The NNRTI, EFV, reduced the percentage viability of the normal cervical cells after 48 hours and the cervical cancer cells after 72 to 96 hours of treatment but did not significantly change the percentage viability of the two cervical cell lines at the indicated concentration over 96 hours. This result corresponds with the findings of Apostolova *et al.* (2010) in which they reported that EFV, at similar concentrations reported here, failed to show significant cytotoxic effects in human Hep3B cells following a 3 day treatment period. However, the present study found that EFV (12.8 μM) showed significant cytotoxicity on the non-tumorigenic breast MCF-10A cells that was consistent throughout the period of exposure (24 to 96 hours). Again, the DNA damage associated with cytotoxicity is related to the processes of tumor initiation (Guimarães *et al.,* 2010). Bumpus (2011) reported similar EFV cytotoxic effects on primary human hepatocytes at similar concentrations (10μM). Bumpus (2011) further showed that the mechanism of cell death induced by EFV in primary human hepatocytes was apoptotic, evidenced by an

increase in caspase-3 activity and decreased mitochondrial membrane potential. This is also supported by the findings of Apostolova *et al.* (2010), Blas-Garcia *et al.* (2010) and Apostolova *et al.* (2011). This EFV cytotoxic effect was not observed in the breast cancer MCF-7 cell line at the tested concentration. Instead, EFV appeared to favour breast cancer cell growth, although the increase in cell viability did not reach statistical significance. A previous study (Thabethe *et al.,* 2013) reported that TDF, FTC and EFV significantly increased MCF-7 cell viability after 24 hours of exposure at the respective 1X Cmax concentrations of the drugs. However, this effect was no longer seen after 48 hours of exposure. The study (Thabethe *et al.,* 2013) used the maximum concentration (0.5% (v/v)) of diluent (either DMSO or methanol) in the final stock solution as recommended by the National Toxicology Programme (NTP) Interagency Centre for the Evaluation of Alternative Toxicological Methods (NICEATM, 2003). The NRTIs (TDF and FTC) were dissolved in DMSO to a final concentration of 0.5% and EFV dissolved in methanol to a final concentration of 0.5%. This present study, however, dissolved TDF and FTC in distilled water (thereby eliminating the effects of DMSO) and dissolved EFV in methanol to a final concentration of 0.01%. The differences in vehicle controls used in both studies could explain the differences observed in the effects of the antiretroviral drugs on MCF-7 cell viability.

A Study by Sikora *et al.* (2010) showed that EFV induced the growth of ER-positive breast cancer MCF-7 and T47D, but not ZR-75-1 cell lines after 6 days of treatment. They found that the MCF-7 growth induction was about 1.2-fold higher than that induced by vehicle treatment. The efavirenz concentrations that induced growth in their cell model ranged from 1 to 10μM which falls within the therapeutic plasma concentration range achieved after daily oral administration of 600 mg daily (mean steady-state minimum and maximum concentrations of 5.6 and 12.9 μM). They also showed that higher efavirenz concentrations

(50 or 100 μM) inhibited the growth of the MCF-7, T47D and ZR-75-1 cells. In the present study, however, the concentration of EFV (12.8 μM) utilised neither showed MCF-7 growth stimulation nor inhibition (Fig. 3.3). This might be because in MCF-7 cells, EFV stimulates growth at lower concentrations, inhibits growth at higher concentrations (Sikora *et al.,* 2010), and reaches an equilibrium of neither stimulatory nor inhibitory effects at the concentrations used in this study.

Evaluating the effects of the NNRTIs nevirapine and efavirenz on the viability of human adipocytes, Díaz-Delfín *et al.* (2011) found that nevirapine was not cytotoxic to human adipocytes at any of the concentrations tested and that efavirenz at lower concentrations (0.5 and 4 μM) was not significantly cytotoxic, but caused extensive cell death at 20 μM. Non-nucleoside reverse transcriptase inhibitor-based regimens, including those containing EFV, have been linked to negative effects such as oxidative stress, skin rash and toxicity (Kontorinis and Dieterich, 2003; Abrescia *et al.*, 2005; Vrouenraets *et al.,* 2007). Evidence exists for the likely role of efavirenz in causing gynaecomastia and an increased incidence of AIDS-defining and some non-AIDS-defining malignancies, including breast cancer, in HIV infected patients (Shiels *et al.,* 2009; Sikora *et al.,* 2010). The combined antiretroviral therapy has also been shown to be protective for AIDS-defining cancers, but whether this protection exists for non-AIDS-defining cancers has not been clearly elucidated (Sikora *et al.,* 2010).

From this study, the triple combination of TDF, FTC and EFV, as combined in the one pill a day drug 'ATRIPLA®', favours the survival of cancer cells compared to the normal cells. It decreased the viability of the NCE166IIA cells as determined by the Neutral Red Uptake assay. These cytotoxic effects were not statistically significant when compared to their vehicle controls but were significantly cytotoxic when compared to the cervical cancer

HCS-2 cells at 48 and 72 hours. ATRIPLA did not show cytotoxic effects on the cervical HCS-2 but did increase their percentage viability at all time points, even though it was not statistically significant.

ATP was significantly cytotoxic to the normal breast cells after 24 hours of administration. The cytotoxic effect disappeared with continuous administration; 48 to 96 hours (Fig. 3.4B). ATP did not significantly alter the percentage viability of the breast cancer cells from 24 to 96 hours. The initial cytotoxic effect on the normal breast cells can lead to DNA damage and mutations in the genes involved in genomic integrity – including the ones involved in chromosomal segregation and DNA repair, thereby increasing the probability of the occurrence of cancerous cells. The use of ATP has been linked to acute hepatic failure due to hepatotoxicity after 3 months of treatment in a patient without pre-existing liver disease or risk factors (Qayyum *et al.,* 2012).

The protease inhibitor LPV showed cytotoxic effects on the normal cervical NCE16IIA cells although these effects were not statistically significant (Fig. 3.5A) when compared with their vehicle controls at all the time points. However, when compared with the cervical cancer cells at 24 and 48 hours, LPV significantly reduced the viability of the normal cervical cells. LPV did not significantly alter the viability of the cervical HCS-2 cells at all time points when compared to their vehicle controls.

LPV showed an initial cytotoxic effect on the MCF-10A cells after 24hours of exposure. Even though this cytotoxic effect disappeared after 48, 72 and 96 hours of exposure, this initial cytotoxicity can produce genomic rearrangements that may act as the primary step toward carcinogenesis. LPV did not significantly alter the percentage viability of the cervical cancer HCS-2 cells from 24 to 96 hours.

The second protease inhibitor used in this study, RTV, did not significantly alter the viability of the normal and cervical cancer cells throughout all the time points measured. RTV, however, was significantly cytotoxic to the normal breast MCF-10A cells at 24 hours, when compared with the control group and the breast cancer MCF-7 cells. The cytotoxic effects of RTV on the normal breast disappeared with continuous administration but can lead to DNA damage and may trigger the processes of cancer initiation in normal breast cells.

The combination of lopinavir and ritonavir, as combined in KALETRA®, demonstrated cytotoxic effects on the normal cervical cells, but the effects did not reach statistical significance from 24 to 96 hours. LPV/r did not significantly alter the percentage viability of the cancer cervical HCS-2 or the two breast cell lines.

Evaluating the cytotoxicity of TDF/FTC/LPV/r, a protease inhibitor based second line regimen administered in South Africa, it is shown here that this combination was significantly cytotoxic to the normal cervical (NCE16IIA) cells after 24 hours of administration when compared to the control group and at 48 hours when compared to the cervical cancer treated group. The TDF/FTC/LPV/r combination demonstrated no significant alteration of the viability of the cervical cancer cells from 24 to 48 hours but increased the viability (albeit not significantly $p<0.05$) of the cervical cancer cells at 48 hours (Fig. 3.8). It can be inferred that this combination may support the viability of cervical cancer cells and at the same time be genotoxic to the normal cervical cells and favour the complex processes leading to cancer initiation.

4.3 Do antiretroviral drugs alter the expression of apoptotic regulatory genes?

Taking it further, this study evaluated the effects of the drugs on *BAX* and *BCL-2* mRNA expression and protein localisation. The landmark discovery of the genes responsible for cell death by Horvitz (1999) began a new direction of research into the mechanisms and genetics of apoptosis. The protein products of two *C. elegans* (the nematode, *Caenorhabditis elegans* - *C. elegans*) cell death genes (CED-3 and CED-4) were shown to be necessary for apoptosis in early development, with CED-9 being the functional homolog to the mammalian protein BCL-2 (Danial and Korsmeyer, 2004; Schaffitzel and Hertweck, 2006; Pecina-Slaus, 2009). The role of BCL-2, a foundation member of the BCL-2 family of apoptosis regulator proteins, has been clearly shown in tumorigenesis to dysregulate apoptotic pathways (Vaux *et al.,* 1988; Hanahan and Weinberg, 2000). In contrast to the nematode, the mammalian mitochondria exhibits a greater influence in controlling apoptosis by releasing numerous apoptogenic mediators from the mitochondrial intermembrane space, leading to a cascade of downstream reactions involving caspases (proteases that split key cellular proteins) (Susin *et al.,* 2000; Mohamad *et al.*,2005; Fan *et al.,* 2005; Li and Yuan, 2008). In mammals, the mitochondrion houses the intrinsic apoptotic pathway while the extrinsic apoptotic pathway involves death receptors. BCL-2 expression has been shown to block the morphologic characteristics of apoptosis, such as blebbing of the plasma membrane, condensation of the nucleus and DNA cleavage (Mohamad *et al.,* 2005). BCL-2 influences cell survival and inhibit cell death induced by a variety of stimuli; such as chemical agents, heat shock, and irradiation, implying that BCL-2 is an inhibitor of cell death. This anti-apoptotic role has also been demonstrated *in vivo*. *BCL-2* knockout mice showed a variety of abnormal manifestations such as excessive apoptosis (Ola *et al.,* 2011).

Members of the BCL-2 family of pro-apoptotic proteins are subdivided into two groups based on the number of BCL-2 homology (BH) domains (e.g., BCL-2 associated X protein - BAX, BCL-2 antagonistic killer - BAK, and BCL-2 related ovarian killer - BOX) or those with the BH3 domain alone (e.g., BCL-2 interacting domain death agonist - BID, BCL-2 interacting mediator of cell death - BIM, and BCL-2 antagonist of cell death - BAD) (Ola *et al.,* 2011). BID, BAD, and BIM are located in the cytosol with respect to the mitochondria. When the death signal is triggered, the BH3 domain-only proteins, also called minimal death domain, neutralises or inhibits anti-apoptotic BCL-2 proteins allowing pro-apoptotic proteins like BAX/BAK-like proteins to induce apoptosis (Wang *et al.,* 1996; Brunelle and Letai 2009). Generally, the relative ratio of pro-survival (BCL-2) and anti-survival (BAX and BH3-only) proteins is believed to determine cell sensitivity or resistance to the apoptotic stimuli (Ola *et al.,* 2011).

To promote cancer, the antiretroviral drugs, either individually or in combination at the clinically relevant concentrations tested, were expected to up-regulate the anti-apoptotic *BCL-2* mRNA and/or protein expression and down-regulate pro-apoptotic *BAX* mRNA and/or protein expression. The findings reported here show that the NRTIs and NNRTIs did not significantly alter *BAX* and *BCL-2* mRNA expression and protein localisation in the two cervical and breast cell lines after a 96 hour exposure. However, in response to TDF treatment, opposing trends of BAX mRNA expression were observed between the cervical and breast cell lines; while *BAX* was slightly up-regulated in the cervical cells, it was down-regulated in the breast cell lines. The expression of *BCL*-2 also followed opposite patterns in the two cancer cell lines; increased in the cervical cancer and decreased in the breast cancer cells. If the trends showed by TDF on *BAX* and *BCL*-2 expression in the normal breast MCF-10A cells were significant, that would have been an important

indication for the increased risk of cancer initiation because anti-apoptotic *BCL*-2 was up-regulated and pro-apoptotic *BAX* was down-regulated. FTC treatment produced opposing trends of *BAX* and *BCL*-2 mRNA expression in the two cancer cell lines; slight up-regulation in the cervical cancer and down-regulation in the breast cancer cell line. FTC also slightly decreased the *BAX* /*BCL*-2 ratio in the normal cervical NCE16IIA cells, which if it were significant, might have suggested the initiation of cancer. EFV treatment produced opposing trends of *BCL*-2 mRNA expression in the two normal cell lines; slight down-regulation in the normal cervical and up-regulation in the normal breast cell line. In response to ATP treatment, opposite trends of *BCL*-2 mRNA expression were observed in the two normal cell lines; slight up-regulation in the normal cervical and down-regulation in the normal breast cell line. ATP also slightly decreased the *BAX* /*BCL*-2 ratio in the normal cervical NCE16IIA cells, which, if significant, might have suggested the initiation of cancer.

The PIs also did not significantly alter the mRNA expression of *BAX* and *BCL-2*, neither did they alter the localisation of these proteins immunocytochemically in the cervical and breast cell lines. However, LPV treatment produced opposing trends of *BAX* and *BCL*-2 mRNA expression in the two normal cell lines; slight up-regulation in the normal cervical and down-regulation in the normal breast cell line. RTV also produced similar *BCL*-2 trends as LPV. LPV/r produced similar trends of *BAX* and *BCL*-2 mRNA expression in the two cancer cell lines. The PI containing combination of TDF/FTC/LPV/r also showed similar trends between the cervical and breast cell lines. The following correlations between gene expression and protein fluorescence staining intensity were also observed; LPV/r showed the same trends in the cancer cervical cells by decreasing *BAX* gene expression and slightly decreased nuclear BAX staining. In the cancer breast cells, FTC

demonstrated the same trends by decreasing *BAX* gene expression and slightly decreasing nuclear BAX staining intensity, even though these trends are not statistically significant.

These results are consistent with the findings of other researchers. Reports by Gomez-Sucerquia *et al.* (2012) showed that EFV at similar concentrations did not alter the mRNA expression of *BAX* and *BCL2 like 1* genes following a 24 hour treatment period in human Hep3B cells. Phenix *et al.* (2001), Badley (2005) and Rizza and Badley (2008) reported that protease inhibitors, including lopinavir, did not alter the mRNA expression and protein synthesis of BAX, BCL-2 and some other key apoptotic genes following a 3 day exposure in immune cells. Some other proteins and/or genes of this or another pathway, however, might be involved.

Antiretroviral drugs have been implicated in the production of reactive oxygen species (ROS) (from the mitochondrial electron transport chain enzymes), leading to mitochondrial dysfunction without a concomitant increase in apoptosis (Hebert *et al.,* 2004; Jiang *et al.,* 2007). Studies by Jiang *et al.* (2007) showed that azidothymidine (a representative NRTI) and indinavir (a representative PI), (individually and in combination at concentrations similar to therapeutic doses in humans) caused the generation of mitochondria derived ROS in *in vitro* cultures of human umbilical vein endothelial cells and compromised mitochondria function by a 40-50% reduction in cellular oxygen consumption/availability. The drugs also caused a decrease in mitochondrial transmembrane potential which further highlights mitochondrial dysfunction. However, the same treatment did not produce significant morphological or biochemical apoptotic characteristics in the endothelial cells (Jiang *et al.,* 2007).

4.4 Antiretroviral drugs and the expression of angiogenic related genes

Majority of the studies conducted before the discovery of anti-angiogenic VEGF variants utilised *in situ* hybridisation riboprobes, antibodies, and ELISAs that detect both $VEGF_{165a}$ and $VEGF_{165b}$ isoforms (Manetti *et al.*, 2011). Part of the specific aims of the current study therefore was to investigate whether the expression of pro- and anti-angiogenic VEGF splice variants ($VEGF_{165a}$ and $VEGF_{165b}$) would be altered in breast and cervical cell lines exposed to different classes of antiretroviral drugs.

The findings of the current study show that the NRTIs and NNRTIs do not alter $VEGF_{165a}$ and $VEGF_{165b}$ mRNA expression in the two cervical and breast cell lines after a 96 hour exposure. However, TDF treatment produced opposing trends of pro-angiogenic $VEGF_{165a}$ mRNA expression between the normal and cancer cell lines; slight up-regulation in the normal cell lines and down-regulation in the cancer cell lines. In the normal cervical cells, though not statistically significant, TDF administration seems to favour angiogenesis by increasing pro-angiogenic $VEGF_{165a}$ mRNA expression and slightly decreasing anti-angiogenic $VEGF_{165b}$ mRNA expression. On the other hand, FTC appeared to produce opposing trends of $VEGF_{165a}$ expression between the normal cell lines and between the cancer cell lines; slight up-regulation in the normal cervical and down-regulation in the normal breast and more down-regulation in the breast cancer than in the cervical cancer cells. FTC also appeared to produce opposing trends of $VEGF_{165b}$ expression between the cancer cell lines. In the normal cervical cells, though not statistically significant, FTC administration also seems to favour angiogenesis by increasing pro-angiogenic $VEGF_{165a}$ mRNA expression and slightly decreasing anti-angiogenic $VEGF_{165b}$ mRNA expression. In response to EFV, the cancer trends appear similar but the normal cells seem opposite. In the normal cervical cells, though not statistically significant, EFV administration also

seems to favour angiogenesis by increasing pro-angiogenic *VEGF$_{165a}$* mRNA expression and slightly decreasing anti-angiogenic *VEGF$_{165b}$* mRNA expression.

The PIs also did not alter the mRNA expression of *VEGF$_{165}$* and *VEGF$_{165b}$* in the cervical and breast cell lines. However, LPV treatment produced opposing trends of *VEGF$_{165a}$ and VEGF$_{165b}$* mRNA expression in the two normal cell lines; slight up-regulation in the normal cervical and down-regulation in the normal breast cell line. And while both angiogenic genes were slightly up-regulated in the normal cervical cells, they were slightly down-regulated in the cervical cancer cells. RTV and LPV/r produced similar trends as LPV on the expression of both angiogenic genes between the normal cervical and cervical cancer cells. LPV/r produced similar trends between the normal and cancer breast cell lines too. In the normal cervical and breast cells, though not statistically significant, the combination of TDF/FTC/LPV/r seems to favour angiogenesis by increasing pro-angiogenic *VEGF$_{165a}$* mRNA expression and slightly decreasing anti-angiogenic *VEGF$_{165b}$* mRNA expression. The NRTIs and NNRTIs did not alter VEGF$_{165b}$ protein localisation in the two cervical and breast cell lines after a 4 day exposure. The PIs also did not alter the localisation of the VEGF$_{165b}$ protein immunocytochemically in the cervical and breast cell lines (Fig. 3.21 - 3.24).

Studies investigating the effects of antiretroviral drugs on the mRNA expression of *VEGF* splice variants *VEGF$_{165a}$* and *VEGF$_{165b}$*, *in-vitro*, *in-vivo* or even in other cell lines were not found in the literature. In a glioblastoma cell line, HIV protease inhibitors, – nelfinavir and amprenavir reduced the expression of vascular endothelial growth factor (VEGF) and hypoxia inducible factor-alpha (Pore *et al.*, 2006). The same drugs, however, did not produce any decrease in VEGF expression in immortalized human astrocytes (Pore *et al.*, 2006).

Cancer development, invasion, and metastases require that cancer cells possess the ability to proliferate and invade tissues when the extracellular matrix is compromised. Inflammatory and stromal cells entering tumours take part in these processes by producing paracrine factors, matrix metalloproteinases and other proteases that increase cancer-cell growth and extracellular-matrix degradation (Carmeliet and Jain, 2000; Egeblad and Werb, 2002). As a result, the invasion, spread and proliferation of cancer cells, together with extracellular matrix and basement membrane degradation are needed for angiogenesis and progression of tumours (Carmeliet and Jain, 2000; Egeblad and Werb, 2002). Protease inhibitors are considered to be strongly anti-angiogenic compounds (Sgadari *et al.,* 2002; Sgadari *et al.,* 2003). Sgadari *et al.* (2002) demonstrated that PIs inhibited Kaposi's's sarcoma growth with the histological characteristics of treated mice showing that the regression of lesions was because the protease inhibitors restrict the formation of new blood vessels. Because Kaposi's's sarcoma is hastened by angiogenic factors secreted by Kaposi's sarcoma cells in human or mice lesions, they examined the effects of protease inhibitors, indinavir and saquinavir, on angiogenesis stimulated by subcutaneous injection of bFGF and VEGF in nude mice. Treatment with protease inhibitors was shown to block the formation of lesions and significantly reduce the amount of bFGF-induced angio-proliferative macroscopic lesions. Under microscopic examination, the sites of bFGF injection showed significantly reduced angiogenesis and spindle-cell growth in mice treated with protease inhibitors compared to control animals treated with saline. The protease inhibitors (at concentrations similar to those present in plasma from treated patients) were also found to block angiogenesis induced by both bFGF and VEGF individually in the chorioallantoic membrane—an established *in vivo* method for determining angiogenesis and evaluating the potency of anti-angiogenic agents (Sgadari *et al.,* 2002). The protease inhibitors indinavir and saquinavir, however, were not shown to

significantly affect bFGF-promoted multiplication, growth, and survival of endothelial cells derived from macrovasculature (Sgadari *et al.,* 2002). Their data suggests that protease inhibitors effectively blocked tumour growth and tumour associated angiogenesis in xenograft tumour models, without creating extreme toxic effects. Protease inhibitors, however, are also considered to be anti-apoptotic (Rizza and Badley, 2008), and are therefore implicated in the development of cancer. This study, however, did not show any association between PIs, NRTIs and NNRTIs and altered mRNA expression of proangiogenic $VEGF_{165a}$ and anti-angiogenic $VEGF_{165b}$ in the two cervical and breast cell lines.

4.5 Apoptosis Induction by Camptothecin

In the present study and as utilised in others (Nieves-Neira and Pommier, 1999; Rastogi *et al.,* 2006; Rudolf *et al.,* 2011), Camptothecin (CPT) was used to induce apoptosis in the different cell lines. CPT is a class I DNA topoisomerase inhibitor that reversibly induces single-strand breaks, and as a result altering the replication capacity of the cell. Camptothecin binds to and stabilises the topoisomerase 1/DNA complex (Legarza and Yang, 2006). These topoisomerase-linked DNA strand breaks are rescindable pre-lethal lesions that inhibit DNA metabolism (Bertrand *et al.,* 1991; Pommier, 1997). But, when a DNA replication fork comes into contact with the cleavable complex, single-strand breaks are transformed to irreversible double-strand breaks (Hsiang *et al.,* 1985; 1989). Then, apoptosis is facilitated by the activation of caspases (Sanchez-Alcazar *et al.,* 2000). The action of caspases result in the proteolysis of precise structural and homoeostatic proteins leading to an irrevocable commitment of cells to undergo the morphological changes typical of apoptosis, characterized by cytoplasmic shrinkage, membrane blebbing, chromatin condensation, and extensive DNA breakage (Alnemri, 1997); Sanchez-Alcazar

et al., 2000; Pizzolato and Saltz, 2003). This mechanism of CPT induced apoptosis requires active DNA replication and results in S-phase-specific cytotoxicity (Pizzolato and Saltz, 2003).

Apart from S-phase dependent pathways, S-phase independent pathways have also been described. Bendixen *et al.* (1990) reported an interference with transcription, describing that one of the initial reactions to CPT is quick cessation of RNA synthesis.

In Addition, Mosesso *et al.* (2000) reported the induction of chromosomal aberrations in the G2-phase connected to RNA polymerase while cell lines, in which RNA synthesis was inhibited, demonstrated a significant reduction in the chromosomal aberrations (Mosesso *et al.*, 2000). Additional S-phase independent pathways not related to the synthesis of RNA have also been described. In one investigation, neurones were treated with CPT with the proposition that CPT would not be cytotoxic to non-mitotic, differentiated cell lines. Contrary to the supposition, CPT induced apoptotic cell death in the neuronal cell lines. Apoptotic cell death also occurred in the nerve cells, when treated independently with substances inhibiting DNA polymerase, RNA transcription, and DNA synthesis, alluding to an apoptotic mechanism that is not dependent on S-phase and mitosis (Morris and Geller, 1996; Legarza and Yang, 2006).

4.6 Protease Inhibitors and Inhibition of Apoptosis

It has been shown previously that protease inhibitors have potent anti-apoptotic effects in different cellular systems, the majority of which are immune cells (Phenix et al, 2001; Badley, 2005; Vlahakis *et al.*, 2007; Rizza and Badley, 2008). These studies reported that the protease inhibitors investigated inhibited drug induced apoptosis. This anti-apoptotic property, (exhibited by protease inhibitors at concentrations similar to those levels

achieved in patients receiving the drugs) is a key step in the development of cancer. The anti-apoptotic effect of LPV/r was therefore assessed to test whether these generalised effects are seen in the currently investigated cell lines and to test whether they alter apoptosis via an alternate pathway other than the *BAX*/*BCL-2* pathway, since they had no significant effects on *BAX* and *BCL-2* mRNA expression.

Pre-incubation with LPV/r for 96 hours significantly inhibited the development of apoptosis in the cervical cancer HCS-2 but not the normal immortalised cervical NCE16IIA cell line. These findings were consistent between the AO morphological apoptotic evaluation and the Cell Death ELISA assessment of DNA fragmentation. In the breast cell lines, pre-incubation with LPV/r did not significantly inhibit CPT induced apoptosis in either breast cell lines. The Cell Death ELISA assessment of DNA fragmentation showed similar results (Fig. 3.39).

Phenix *et al.* (2001) demonstrated that the HIV protease inhibitor - nelfinavir inhibited Jurkat T-cell apoptosis induced by a variety of different stimuli, including CPT. They also reported that inhibition of apoptotic death was not associated with alterations of mRNA expression levels of a variety of pro- and anti-apoptotic factors, and did not depend on protein synthesis.

On the other hand, high-dose PIs have been shown to demonstrate paradoxical pro-apoptotic effects, as demonstrated in implanted mouse models and transformed cell lines (Badley, 2005; Gills *et al.,* 2007). They display pleiotropic anti-tumorigenic effects, inhibit the production of inflammatory cytokines, and induce apoptotic cell death (Chow *et al.,* 2009). HIV protease inhibitors and other antiretroviral drugs holding similar promise are a new class of FDA approved drugs that are being investigated for anti-tumour effects (Chow *et al.,* 2009). For instance, Dewan *et al.* (2006) reported that ritonavir, an HIV

protease inhibitor, induced apoptosis and inhibited transcriptional activation of NFκB in cultured Adult T-cell leukaemia cells. Ritonavir was shown to inhibit the expression of BIRC5. BIRC5 (survivin) is an important and widely studied member of the inhibitors of apoptosis (IAP) protein family which are involved in cell death, immunity, inflammation, cell cycle and migration (Almagro and Vucic, 2012). The members of this protein family are characterized by the presence of one to three baculoviral IAP repeats (BIR) domains and are overexpressed in cancer cells and malignancies making them highly resistant to therapy (Almagro and Vucic, 2012). In other studies, Nordgren *et al.* (2012) reported that ritonavir (HIV PI) alone or in combination with vincristine inhibited proliferation and induced apoptosis in Mantle Cell Lymphoma (MCL) cell lines. They also reported significant downregulation of some NFκB transcriptional targets including BIRC5 (surviving, an important IAP) following ritonavir exposure. However, they found that utilising ritonavir in treating MCL as a single agent has insignificant efficacy and suggested that while ritonavir did not exhibit any *in vivo* activity against MCL as a single agent, evidence from *in vitro* studies displayed possible therapeutic potential for its utilisation in a combinatorial regimen for the treatment of Mantle Cell Lymphoma (Nordgren *et al.*, 2012).

There are several theories explaining how HIV PIs hold cellular apoptosis in check. Because HIV PIs restrict the activity of HIV-1 viral protease, it was assumed that they might exercise similar effects on other cellular proteases (Rizza and Badley, 2008). It was also hypothesised that HIV PIs may inhibit the family members of the caspases and inhibits apoptosis because of the earlier observations that HIV PIs inhibits FAS-mediated apoptosis (Phenix *et al.*, 2001). While this model could be plausible, caspases are known to be cysteine proteases while HIV protease is an aspartyle protease (Chou *et al.*, 1997; Chou

et al., 2000). Studies investigating the effects of HIV protease inhibitors on the activity of caspases found that the HIV protease inhibitors restricted HIV protease cleavage of *gag/pol,* but did not inhibit the activity of any of the caspases (Phenix *et al.,* 2001). In other studies, the activity of caspases -3, -6, and -8 were not inhibited by indinavir in U937 cells at drug concentrations that effectively inhibited U937 apoptosis (Ghibelli *et al.,* 2003), while nelfinavir failed to inhibit the activation of caspases -1, -3, -4, -5, -9, and -8 in Jurkat T cells undergoing FAS-mediated apoptosis (Chavan *et al.,* 2001). Calpains, calcium dependent cysteine proteases, are other proteases that are associated with programmed cell death and have been considered as possible targets for HIV protease inhibitors to modulate apoptosis (Spinedi *et al.,* 1998). It has been postulated that HIV PIs alter apoptosis by blocking calpain activation and calpain function because the PIs inhibit the HIV-1 aspartyle protease (Rizza and Badley, 2008). It has been demonstrated that PIs - indinavir and ritonavir block m-calpain activation and directly inhibit apoptosis in cells where calpains are activated (Ghibelli *et al.,* 2003). In addition, another study found that ritonavir inhibited the activity of calpain isoforms -μ and m- competitively in PC12 cells (Wan and DePetrillo, 2002). Cuerrier *et al.* (2005), however, reported that HIV Protease Inhibitors did not inhibit μ- and m- calpain activation, postulating that previous studies suggesting otherwise used ritonavir concentrations near its maximum solubility and this could have affected the results.

Stabilisation of the mitochondria is the most alluded to mechanism through which HIV PIs might influence apoptosis (Rizza and Badley, 2008). The mitochrondrial permeability transition pore complex (PTPC) maintains the mitochondrial trans-membrane potential that is as a result of the unequal distribution of ions on the two sides of the inner mitochondrial membrane. It has been said that subsequent to an apoptotic trigger, the PTPC opens, alters

the membrane potential, and makes apoptogenic factors, such as pro-caspase-9 and cytochrome c, available. Hence, the mitochondria represent a regulatory checkpoint of apoptotic signaling, where many apoptotic regulatory proteins (including the BCL-2 family members) interact to influence apoptosis (Rizza and Badley, 2008). In CD4+T cells, over a narrow concentration range, it was shown that nelfinavir, but not other HIV PIs, inhibit cellular apoptosis (Garg and Blumenthal, 2006). Other studies have also shown that HIV PIs inhibit the loss of the mitochondrial trans-membrane potential in different models of apoptosis (Phenix *et al.*, 2001; Badley *et al.,* 2003; Matarrese *et al.,* 2003; Matarrese *et al.*, 2005; Miro *et al.*, 2005; Weaver *et al.*, 2005).

In vivo and *in vitro* studies by Hisatomi *et al.* (2008) showed that protease inhibitors demonstrated anti-apoptosis in a model in which the PIs (NFV and RTV) were administered after apoptosis induction. They demonstrated that HIV PIs suppresses the translocation of cytochrome *c* and prevents the release of AIF from the mitochondria, and provided experimental evidence indicating that HIV PIs disrupt both the caspase-dependent (cytochrome *c*/ Apaf-1/caspase-9–mediated) and the caspase-independent (AIFmediated) mitochondria apoptotic pathways. They reported that PIs significantly reduced the mitochondria-nuclear AIF translocation and the stimulation of caspase-3 and -9, leading to reduced apoptotic photoreceptor cell death (Hisatomi *et al.*, 2008). AIF, released from mitochondria, speeds up MOMP in a positive feed-forward loop (Susin *et al.*, 1999). AIF also stimulates refined mitochondria to release cytochrome *c* which binds Apaf-1 that in turn activates caspase-9, which also can directly affect mitochondrial function and/or disrupt the permeability of the mitochondrial membrane (Susin*et al.,* 1997; Hisatomi *et al.*, 2008). Both pathways appear to be activated after MOMP and simultaneously coordinate corresponding pathways climaxing in cellular death (Hisatomi

et al., 2008), but the PIs blocked cell death by stabilisation of MOMP (Hisatomi *et al.*, 2008).

Whether HIV protease inhibitors alter the expression of proteins regulating apoptosis provides another plausible explanation for the anti-apoptotic effects of PIs. Matarrese *et al.* (2003) investigated the effects of HIV PI treatment on intracellular levels of apoptotic regulatory proteins; BAX, BCL-2 and BCL-$_{XL}$ by flow cytometry and found that the protein levels were unchanged. Estaquier *et al.* (2002) reported an alteration in FAS expression after PI treatment. Other studies, however, did not show a relationship between altered FAS levels and HIV PI therapy (Sloand *et al.*, 1999; Lu and Andrieu, 2000; Isgro *et al.*, 2005). While HIV PIs have been reported to block FAS and TNF-induced apoptosis (Estaquier *et al.*, 2002; Matarrese *et al.*, 2003; Wolf *et al.*, 2003), this anti-apoptotic effect does not appear to be due to changes in intra- or extracellular apoptotic regulatory protein levels (Rizza and Badley, 2008). This view is corroborated by the findings of the present study because the combination of lopinavir and ritonavir as combined in KALETRA® significantly inhibited drug induced apoptosis in the cervical cancer HCS-2 cells without altering the expression of BAX and BCL-2.

4.7 HAART and Cervical Cancer

The introduction of the highly active antiretroviral therapy in 1996 (Dal Maso *et al.*, 2009) has led to significant improvement of clinical outcomes and life expectancies for people living with HIV/AIDS (PLWHA) (Heard, 2009). It also provided the hope that the resulting improved immunological status would translate into better removal of human papilloma virus (HPV) infection in HIV-infected women, in the same manner as other opportunistic and AIDS-related infections, and lead to a significant reduction in the incidence and progression of cervical neoplasia (Heard, 2009). However, a review (Bratcher and Sahasrabuddhe, 2010) of data from numerous studies did not point to a clear decrease in the burden and severity of cervical disease with introduction of the combined antiretroviral therapy, in marked difference to the other AIDS-associated malignancies, especially Kaposi's sarcoma and non-Hodgkin's lymphoma. Bratcher and Sahasrabuddhe (2010) reported that while the majority of published literature suggested that being on HAART does not reduce the incidence of cervical precancerous lesions and cervical intraepithelial neoplasia in HIV-infected women, some studies found a higher risk in the post-HAART era. Because of the unclear collaborations between HIV, HPV, HAART and the development of cervical neoplasia, this study investigated the probability that some of the commonly used ARVs might alter apoptotic gene expression which may lead to the initiation or development of cancer in the cervix.

The findings of this study, however, are not totally inconsistent with the notion of a possible role of antiretroviral drugs in the mechanisms involved in the initiation and/or development of cervical cancer because the protease inhibitors LPV/r inhibited drug induced apoptosis in cervical cancer cells.

To further tease out the effects of HAART on site specific malignancies, future studies should examine the effects of ARVs on cervical cells in the presence of HPV infection as it has been determined (Moubayed *et al.,* 2004) that HPV increases the sensitivity of conjunctival cells to ultraviolet induced mutagenesis.

4.8 HAART and Non-AIDS-Defining Malignancies

An analysis of the incidence of non-AIDS-defining cancers in HIV-infected patients suggests that the incidence of breast cancer in these patients has significantly increased since the introduction and implementation of the combined antiretroviral therapy (Shiels *et al.,* 2009), creating the need to effectively establish or rule out the possibility that candidate antiretroviral drugs may promote cancer.

In the HAART era, it is a paradox that people living with HIV and AIDS are now at an increased risk for developing several specific non-AIDS-defining malignancies (NADMs) (Engels *et al.,* 2008; Silverberg *et al.,* 2009; Spano *et al.,* 2012; Calabresi *et al.,* 2013; Franzetti *et al.,* 2013; Cutrell and Bedimo 2013), including breast cancer (Shiels *et al.,* 2009; Franzetti *et al.,* 2013). Such that, despite the immune reconstitution induced by HAART, excess NADMs deaths have been reported amongst HIV patients (Zucchetto *et al.,* 2010). It has also been reported that patients with NADMs often have more aggressive cancers and display more advanced stages of the disease (Grulich *et al.,* 2007; Deeken *et al.,* 2012), with breast cancer metastasising early and usually more poorly differentiated (Gewurz *et al.,* 2005).

The effects of HAART on the risk for NADMs have not been clearly established. Research evidence has been conflicting as to whether or which antiretroviral drugs or classes decrease, increase, or have no effect on the risk of developing NADMs (Burgi *et al.,* 2005;

Deeken *et al.*, 2012), with no definite pattern emerging from such studies. These inconsistencies partly arise from data obtained from disparate researchers. A lack of agreement for instance, arises from contradictions in population definition of AIDS or HIV/AIDS. A specific calendar period may also not be a correct representation of actual use of HAART. Hessol *et al.* (2007) reported differing NADM risks when comparing HAART era (pre-HAART versus HAART era) to HAART use. Even with this more specific classification, HAART use but not HAART era was linked to a lower risk for liver cancer, whereas HAART era but not HAART use was connected to a higher risk for anal cancer among patients with AIDS (Hessol *et al.*, 2007). Shiels *et al.* (2009), in a meta-analysis, reported that the standardised incidence ratio (SIR) of individual NADMs (specifically breast and kidney) but not all NADMs were significantly different in the pre-HAART and HAART era. They discovered a greater than three-fold reduction in AIDS-defining malignancy cases from 1991–2005 (34,587 to 10,325 cancers) in contrast to an approximately three-fold increment in NADM cases over the same period (3193 to 10,059 cancers). Clifford *et al.* (2005), in a large prospective cohort of people (called the Swiss HIV Cohort Study) surveyed for a median of 4.8 years after the introduction of HAART, reported no definite effects of HAART on SIRs of non–AIDS-defining malignancies. In an HIV/AIDS cohort in England, however, Powles *et al.* (2009) reported that HAART treatment was independently linked to a significant increase in the risk for NADMs. In addition, Crum-Cianflone *et al.* (2009) did not find any significant decrease in the incidence of malignancies in patients on HAART regimens containing protease inhibitors despite the chemo-preventive effects of this class of antiretroviral drugs on malignancy by inducing apoptosis of cancer cells. The exact mechanisms for the development of non-AIDs-defining malignancies remain to be fully elucidated (Cutrell and Bedimo 2013).

Use of the combined antiretroviral therapy has led to increased life expectancy among people living with HIV/AIDs and this has been predicted to lead to the increased incidence of NADMs (Nguyen *et al.,* 2010; Cutrell and Bedimo 2013). The effect of improved life expectancy as a risk for developing NADMs was underscored by the US military cohort by Burgi *et al.* (2005), which showed a very significant increase in any NADM among people 40 years and above. Interestingly, in spite of this effect, PLWHA are diagnosed with many different types of NADMs at younger ages when compared to the HIV negative controls (Brau *et al.,* 2007; Suneja *et al.,* 2013).

AIDS-defining malignancy rates have been shown to be strongly associated with the degree of immune suppression based on CD4 count (Nguyen *et al.,* 2010), but the association between CD4 count and the risk for NADMs has provided conflicting reports. Initial reports did not show any correlation between lower CD4 counts and higher NADM risk (Mbulaiteye *et al.,* 2003; Clifford *et al.,* 2005). However, more recently, studies have shown significant correlations between currently reduced CD4 counts or continuous exposure to reduced CD4 counts and NADM risk (Bedimo *et al.,* 2009; Powles *et al.,* 2009; Bruyand *et al.,* 2009; Guiguet *et al.,* 2009; Prosperi *et al.,* 2010; Reekie *et al.,* 2010; Kesselring *et al.,* 2011; Krishnan *et al.,* 2011). There was better correlation for some infection-related NADMs, while the association with the extent of immune-suppression for other non infection related cancer subtypes is described as more complicated or subtle (Dubrow *et al.,* 2012).

Whether the HIV virus itself exerts direct oncogenic threats on host cellular mechanisms provides one possible explanation for the pathogenesis of increased cancers in PLWHA. It has been reported that the HIV tat protein can inhibit the activity of tumor suppressor genes (Harrod *et al.,* 2003; De Falco *et al.,* 2003) and mobilise pro-oncogenes (Wright *et*

al., 1994). This HIV protein can also block cellular apoptosis (Campioni *et al.*, 1995), alter cell cycle dynamics (Colombrino *et al.*, 2004; Nyagol *et al.*, 2006), subject tissues to the effects of chemical carcinogens (Altavilla *et al.*, 2000) and also encourage angiogenic pathways necessary for cancer progression and metastasis (Corallini *et al.*, 1996).

The higher prevalence of oncogenic viral coinfection provides a plausible explanation for the higher occurrence of particular cancer subtypes, such as cervical cancer (HPV), liver (hepatitis B and C virus) and Hodgkin's lymphoma (Epstein-Barr virus) (Cutrell and Bedimo 2013). However, data from numerous studies has not pointed to a significant reduction in the burden and severity of cervical disease with the introduction of the combined antiretroviral treatment, while some studies have reported a higher risk in the post-HAART period (Bratcher and Sahasrabuddhe, 2010).

4.9 Conclusion

With universal adoption of highly active antiretroviral therapy and increased life expectancy among people living with HIV/AIDS, there have been chronic adverse effects leading to an increased burden of cancers contributing to an increasing percentage of deaths among the HIV population (Powles *et al.,* 2009; Nguyen *et al.,* 2010; Franzetti *et al.,* 2013). Reducing the mortality associated with increased cancer in the HAART era will require a better understanding of risk factors and their pathogenesis, which will then lead to the improvement of prevention and therapeutic interventions.

The speculation that some antiretroviral drugs or combinations may have an adverse effect on the risk of carcinogenesis among PLWHA under HAART led to this study. The results reported here show that tenofovir disoproxil fumarate, emtricitabine efavirenz, lopinavir, ritonavir and the two triple combinations demonstrated some form of cytotoxicity in the breast and cervical cells, which may alter the activity of the nuclear and mitochondrial genome of cells and may cause genotoxic effects largely related to tumor initiation processes (Bishop and Schiestl, 2001; Olivero, 2007; Wu *et al.,* 2012). The results of the qPCR data demonstrated differences in the response of the two tissue types (breast and cervical) used in this study, which, though, not statistically significant, showed trends and often opposite trends between the breast and cervical cell lines. The antiretroviral drugs; tenofovir disoproxil fumarate, emtricitabine, efavirenz, Atripla, lopinavir, ritonavir, Kaletra and a combination of TDF/FTC/LPV/r; all at clinically relevant concentrations (which reflect their steady-state peak plasma concentrations) do not alter the mRNA expression of apoptosis related *BAX* and *BCL-2* and angiogenic related $VEGF_{165a}$ and $VEGF_{165b}$ genes, neither do they alter the localisation of their proteins in the human cervical cancer cell line HCS-2, normal immortalised human cervical cell line NCE16IIA, human breast cancer cell

line MCF-7 and non tumorigenic immortalised breast cell line MCF-10A. If the ARVs initiate or promote cancer, these pathways are not likely to be involved, so the effects of these agents need to be investigated on other oncogenic pathways.

LPV/r, however, was found to significantly inhibit drug induced apoptosis in the cervical cancer cell line but not in the transformed normal cervical cell line nor in the two breast cell lines investigated. This inhibition of apoptosis, although so far not associated with RNA or protein synthesis is a key step in the development of cancer. This suggests that the PIs LPV/r at the clinically relevant concentrations tested might contribute to the progression of cancer of the cervix but are probably not involved in the development of breast cancer in patients under the combined antiretroviral regimen.

Recommendations and future directions

As better understanding of the effects of the class, combination and duration of ARV exposure on cancer risk is required, *in-vitro* and *in-vivo* studies of longer duration need to be conducted to determine whether the trends observed in the gene expression data of this study might eventually become significant. The effects of these agents also need to be investigated on other oncogenic pathways in order to characterise, more precisely, the genetic and molecular mechanisms underlying the interesting observations of this study.

With regards to patient management, a comprehensive family history of cancers should be obtained and optimal treatment protocols should be well-defined in HIV patients. Individual approach to patient management based on the measurement of the expression levels and activities of certain genes might provide useful predictive values when planning antiretroviral therapy. Hence, concerted efforts are required amongst medical oncologists, HIV specialists, and clinical pharmacists for optimising antiretroviral regimens.

REFERENCES

Abdool Karim, S. S., G. J. Churchyard, Q. A. Karim, and S. D. Lawn. 2009. HIV infection and tuberculosis in south africa: An urgent need to escalate the public health response. *Lancet* 374 (9693) (Sep 12): 921-33.

Abrescia, N., M. D'Abbraccio, M. Figoni, A. Busto, A. Maddaloni, and M. De Marco. 2005. Hepatotoxicity of antiretroviral drugs. *Current Pharmaceutical Design* 11 (28): 3697-710.

Achen, M. G., M. Jeltsch, E. Kukk, T. Makinen, A. Vitali, A. F. Wilks, K. Alitalo, and S. A. Stacker. 1998. Vascular endothelial growth factor D (VEGF-D) is a ligand for the tyrosine kinases VEGF receptor 2 (Flk1) and VEGF receptor 3 (Flt4). *Proceedings of the National Academy of Sciences of the United States of America* 95 (2) (Jan 20): 548-53.

Alnemri, E. S. 1997. Mammalian cell death proteases: A family of highly conserved aspartate specific cysteine proteases. *Journal of Cellular Biochemistry* 64 (1) (Jan): 33-42.

Altavilla, G., A. Caputo, M. Lanfredi, C. Piola, G. Barbanti-Brodano, and A. Corallini. 2000. Enhancement of chemical hepatocarcinogenesis by the HIV-1 tat gene. *The American Journal of Pathology* 157 (4) (Oct): 1081-9.

Andersen, M. H., S. Reker, P. Kvistborg, J. C. Becker, and P. thor Straten. 2005. Spontaneous immunity against bcl-xL in cancer patients. *Journal of Immunology (Baltimore, Md.: 1950)* 175 (4) (Aug 15): 2709-14.

Anderson, P. L., J. J. Kiser, E. M. Gardner, J. E. Rower, A. Meditz, and R. M. Grant. 2011. Pharmacological considerations for tenofovir and emtricitabine to prevent HIV infection. *The Journal of Antimicrobial Chemotherapy* 66 (2) (Feb): 240-50.

Andrade, A. C., P. M. Luz, V. G. Veloso, S. W. Cardoso, R. I. Moreira, B. Grinsztejn, and R. K. Friedman. 2011. Breast cancer in a cohort of human immunodeficiency virus (HIV)-infected women from rio de janeiro, brazil: A cases series report and an incidence rate estimate. *The Brazilian Journal of Infectious Diseases* 15 (4) (Jul-Aug): 387-93.

Apostolova, N., L. J. Gomez-Sucerquia, A. Gortat, A. Blas-Garcia, and J. V. Esplugues. 2011. Compromising mitochondrial function with the antiretroviral drug efavirenz induces cell survival-promoting autophagy. *Hepatology (Baltimore, Md.)* 54 (3) (Sep 2): 1009-19.

Apostolova, N., L. J. Gomez-Sucerquia, A. Moran, A. Alvarez, A. Blas-Garcia, and J. V. Esplugues. 2010. Enhanced oxidative stress and increased mitochondrial mass during efavirenz-induced apoptosis in human hepatic cells. *British Journal of Pharmacology* 160 (8) (Aug): 2069-84.

Arts, E. J., and D. J. Hazuda. 2012. HIV-1 antiretroviral drug therapy. *Cold Spring Harbor Perspectives in Medicine* 2 (4) (Apr): a007161.

Autran, B., G. Carcelain, T. S. Li, C. Blanc, D. Mathez, R. Tubiana, C. Katlama, P. Debre, and J. Leibowitch. 1997. Positive effects of combined antiretroviral therapy on CD4+ T cell homeostasis and function in advanced HIV disease. *Science (New York, N.Y.)* 277 (5322) (Jul 4): 112-6.

Badley, A. D. 2005. In vitro and in vivo effects of HIV protease inhibitors on apoptosis. *Cell Death and Differentiation* 12 Suppl 1 (Aug): 924-31.

Badley, A. D., T. Roumier, J. J. Lum, and G. Kroemer. 2003. Mitochondrion-mediated apoptosis in HIV-1 infection. *Trends in Pharmacological Sciences* 24 (6) (Jun): 298-305.

Barbaro, G., and G. Barbarini. 2007. HIV infection and cancer in the era of highly active antiretroviral therapy (review). *Oncology Reports* 17 (5) (May): 1121-6.

Basu, A., and S. Haldar. 1998. The relationship between BcI2, bax and p53: Consequences for cell cycle progression and cell death. *Molecular Human Reproduction* 4 (12) (Dec): 1099-109.

Bates, D. O., T. G. Cui, J. M. Doughty, M. Winkler, M. Sugiono, J. D. Shields, D. Peat, D. Gillatt, and S. J. Harper. 2002. VEGF165b, an inhibitory splice variant of vascular endothelial growth factor, is down-regulated in renal cell carcinoma. *Cancer Research* 62 (14) (Jul 15): 4123-31.

Bedimo, R. J., K. A. McGinnis, M. Dunlap, M. C. Rodriguez-Barradas, and A. C. Justice. 2009. Incidence of non-AIDS-defining malignancies in HIV-infected versus noninfected patients in the HAART era: Impact of immunosuppression. *Journal of Acquired Immune Deficiency Syndromes (1999)* 52 (2) (Oct 1): 203-8.

Benhammou, V., J. Warszawski, S. Bellec, F. Doz, N. Andre, B. Lacour, M. Levine, et al. 2008. Incidence of cancer in children perinatally exposed to nucleoside reverse transcriptase inhibitors. *AIDS (London, England)* 22 (16) (Oct 18): 2165-77.

Bertrand, R., M. Sarang, J. Jenkin, D. Kerrigan, and Y. Pommier. 1991. Differential induction of secondary DNA fragmentation by topoisomerase II inhibitors in human tumor cell lines with amplified c-myc expression. *Cancer Research* 51 (23 Pt 1) (Dec 1): 6280-5.

Birkus, G., M. J. Hitchcock, and T. Cihlar. 2002. Assessment of mitochondrial toxicity in human cells treated with tenofovir: Comparison with other nucleoside reverse transcriptase inhibitors. *Antimicrobial Agents and Chemotherapy* 46 (3) (Mar): 716-23.

Bishop, A. J., and R. H. Schiestl. 2001. Homologous recombination as a mechanism of carcinogenesis. *Biochimica Et Biophysica Acta* 1471 (3) (Mar 21): M109-21.

Blanche, S., M. Tardieu, P. Rustin, A. Slama, B. Barret, G. Firtion, N. Ciraru-Vigneron, et al. 1999. Persistent mitochondrial dysfunction and perinatal exposure to antiretroviral nucleoside analogues. *Lancet* 354 (9184) (Sep 25): 1084-9.

Blas-Garcia, A., N. Apostolova, D. Ballesteros, D. Monleon, J. M. Morales, M. Rocha, V. M. Victor, and J. V. Esplugues. 2010. Inhibition of mitochondrial function by efavirenz increases lipid content in hepatic cells. *Hepatology (Baltimore, Md.)* 52 (1) (Jul): 115-25.

Boom, R., C. J. Sol, M. M. Salimans, C. L. Jansen, P. M. Wertheim-van Dillen, and J. van der Noordaa. 1990. Rapid and simple method for purification of nucleic acids. *Journal of Clinical Microbiology* 28 (3) (Mar): 495-503.

Borenfreund, E., and J. A. Puerner. 1985. Toxicity determined in vitro by morphological alterations and neutral red absorption. *Toxicology Letters* 24 (2-3) (Feb-Mar): 119-24.

Bratcher, L. F., and V. V. Sahasrabuddhe. 2010. The impact of antiretroviral therapy on HPV and cervical intraepithelial neoplasia: Current evidence and directions for future research. *Infectious Agents and Cancer* 5 (May 12): 8,9378-5-8.

Brau, N., R. K. Fox, P. Xiao, K. Marks, Z. Naqvi, L. E. Taylor, A. Trikha, et al. 2007. Presentation and outcome of hepatocellular carcinoma in HIV-infected patients: A U.S.-canadian multicenter study. *Journal of Hepatology* 47 (4) (Oct): 527-37.

Brunelle, J. K., and A. Letai. 2009. Control of mitochondrial apoptosis by the bcl-2 family. *Journal of Cell Science* 122 (Pt 4) (Feb 15): 437-41.

Bruning, A., P. Burger, A. Gingelmaier, and I. Mylonas. 2012. The HIV reverse transcriptase inhibitor tenofovir induces cell cycle arrest in human cancer cells. *Investigational New Drugs* 30 (4) (Aug): 1389-95.

Bruyand, M., R. Thiebaut, S. Lawson-Ayayi, P. Joly, A. J. Sasco, P. Mercie, J. L. Pellegrin, et al. 2009. Role of uncontrolled HIV RNA level and immunodeficiency in the occurrence of malignancy in HIV-infected patients during the combination antiretroviral therapy era: Agence nationale de recherche sur le sida (ANRS) CO3 aquitaine cohort. *Clinical Infectious Diseases : An Official Publication of the Infectious Diseases Society of America* 49 (7) (Oct 1): 1109-16.

Bumpus, N. N. 2011. Efavirenz and 8-hydroxyefavirenz induce cell death via a JNK- and BimEL-dependent mechanism in primary human hepatocytes. *Toxicology and Applied Pharmacology* 257 (2) (Dec 1): 227-34.

Burgi, A., S. Brodine, S. Wegner, M. Milazzo, M. R. Wallace, K. Spooner, D. L. Blazes, et al. 2005. Incidence and risk factors for the occurrence of non-AIDS-defining cancers among human immunodeficiency virus-infected individuals. *Cancer* 104 (7) (Oct 1): 1505-11.

Bustin, S. A. 2002. Quantification of mRNA using real-time reverse transcription PCR (RT-PCR): Trends and problems. *Journal of Molecular Endocrinology* 29 (1) (Aug): 23-39.

Bustin, S. A., V. Benes, J. A. Garson, J. Hellemans, J. Huggett, M. Kubista, R. Mueller, et al. 2009. The MIQE guidelines: Minimum information for publication of quantitative real-time PCR experiments. *Clinical Chemistry* 55 (4) (Apr): 611-22.

Calabresi, A., A. Ferraresi, A. Festa, C. Scarcella, F. Donato, F. Vassallo, R. Limina, F. Castelli, E. Quiros-Roldan, and Brescia HIV Cancer Study Group. 2013. Incidence of AIDS-defining cancers and virus-related and non-virus-related non-AIDS-defining cancers among HIV-infected patients compared with the general population in a large health district of northern italy, 1999-2009. *HIV Medicine* 14 (8) (Sep): 481-90.

Campioni, D., A. Corallini, G. Zauli, L. Possati, G. Altavilla, and G. Barbanti-Brodano. 1995. HIV type 1 extracellular tat protein stimulates growth and protects cells of BK virus/tat transgenic mice from apoptosis. *AIDS Research and Human Retroviruses* 11 (9) (Sep): 1039-48.

Canete, M., A. Juarranz, P. Lopez-Nieva, C. Alonso-Torcal, A. Villanueva, and J. C. Stockert. 2001. Fixation and permanent mounting of fluorescent probes after vital labelling of cultured cells. *Acta Histochemica* 103 (2) (Apr): 117-26.

Carmeliet, P. 2000. VEGF gene therapy: Stimulating angiogenesis or angioma-genesis? *Nature Medicine* 6 (10) (Oct): 1102-3.

Carmeliet, P., and R. K. Jain. 2000. Angiogenesis in cancer and other diseases. *Nature* 407 (6801) (Sep 14): 249-57.

Chavan, S., S. Kodoth, R. Pahwa, and S. Pahwa. 2001. The HIV protease inhibitor indinavir inhibits cell-cycle progression in vitro in lymphocytes of HIV-infected and uninfected individuals. *Blood* 98 (2) (Jul 15): 383-9.

Chomczynski, P., and N. Sacchi. 1987. Single-step method of RNA isolation by acid guanidinium thiocyanate-phenol-chloroform extraction. *Analytical Biochemistry* 162 (1) (Apr): 156-9.

Chou, K. C., D. Jones, and R. L. Heinrikson. 1997. Prediction of the tertiary structure and substrate binding site of caspase-8. *FEBS Letters* 419 (1) (Dec 8): 49-54.

Chou, K. C., A. G. Tomasselli, and R. L. Heinrikson. 2000. Prediction of the tertiary structure of a caspase-9/inhibitor complex. *FEBS Letters* 470 (3) (Mar 31): 249-56.

Chow, W. A., C. Jiang, and M. Guan. 2009. Anti-HIV drugs for cancer therapeutics: Back to the future? *The Lancet Oncology* 10 (1) (Jan): 61-71.

Cihlar, T., and A. S. Ray. 2010. Nucleoside and nucleotide HIV reverse transcriptase inhibitors: 25 years after zidovudine. *Antiviral Research* 85 (1) (Jan): 39-58.

Clay, P. G., T. A. Taylor, A. G. Glaros, M. McRae, C. Williams, D. McCandless, and M. Oelklaus. 2008. "One pill, once daily": What clinicians need to know about atriplatrade mark. *Therapeutics and Clinical Risk Management* 4 (2) (Apr): 291-302.

Clifford, G. M., J. Polesel, M. Rickenbach, L. Dal Maso, O. Keiser, A. Kofler, E. Rapiti, et al. 2005. Cancer risk in the swiss HIV cohort study: Associations with immunodeficiency, smoking, and highly active antiretroviral therapy. *Journal of the National Cancer Institute* 97 (6) (Mar 16): 425-32.

Coligan, J.E., Kruisbeek, A.M., Margulies, D.H., Shevach, E.M., Strober, W. Current Protocols in Immunology. In *Related isolation procedures and functional assays Volume 1*. Edited by: Coico R. John Wiley & Sons, Inc: 1995:3.17.1

Colombrino, E., E. Rossi, G. Ballon, L. Terrin, S. Indraccolo, L. Chieco-Bianchi, and A. De Rossi. 2004. Human immunodeficiency virus type 1 tat protein modulates cell cycle and apoptosis in epstein-barr virus-immortalized B cells. *Experimental Cell Research* 295 (2) (May 1): 539-48.

Cooksley, C. D., L. Y. Hwang, D. K. Waller, and C. E. Ford. 1999. HIV-related malignancies: Community-based study using linkage of cancer registry and HIV registry data. *International Journal of STD & AIDS* 10 (12) (Dec): 795-802.

Corallini, A., D. Campioni, C. Rossi, A. Albini, L. Possati, M. Rusnati, G. Gazzanelli, et al. 1996. Promotion of tumour metastases and induction of angiogenesis by native HIV-1 tat protein from BK virus/tat transgenic mice. *AIDS (London, England)* 10 (7) (Jun): 701-10.

Crum-Cianflone, N. F., K. H. Hullsiek, V. Marconi, A. Weintrob, A. Ganesan, R. V. Barthel, S. Fraser, M. P. Roediger, B. Agan, and S. Wegner. 2009. The impact of nelfinavir exposure on cancer development among a large cohort of HIV-infected patients. *Journal of Acquired Immune Deficiency Syndromes (1999)* 51 (3) (Jul 1): 305-9.

Cuerrier, D., Z. Nie, A. D. Badley, and P. L. Davies. 2005. Ritonavir does not inhibit calpain in vitro. *Biochemical and Biophysical Research Communications* 327 (1) (Feb 4): 208-11.

Cutrell, J., and R. Bedimo. 2013. Non-AIDS-defining cancers among HIV-infected patients. *Current HIV/AIDS Reports* 10 (3) (Sep): 207-16.

Dal Maso, L., J. Polesel, D. Serraino, M. Lise, P. Piselli, F. Falcini, A. Russo, et al. 2009. Pattern of cancer risk in persons with AIDS in italy in the HAART era. *British Journal of Cancer* 100 (5) (Mar 10): 840-7.

Danial, N. N., and S. J. Korsmeyer. 2004. Cell death: Critical control points. *Cell* 116 (2) (Jan 23): 205-19.

de Almagro, M. C., and D. Vucic. 2012. The inhibitor of apoptosis (IAP) proteins are critical regulators of signaling pathways and targets for anti-cancer therapy. *Experimental Oncology* 34 (3) (Oct): 200-11.

De Clercq, E. 2005. Antiviral drug discovery and development: Where chemistry meets with biomedicine. *Antiviral Research* 67 (2) (Aug): 56-75.

De Falco, G., C. Bellan, S. Lazzi, P. Claudio, D. La Sala, C. Cinti, P. Tosi, A. Giordano, and L. Leoncini. 2003. Interaction between HIV-1 tat and pRb2/p130: A possible mechanism in the pathogenesis of AIDS-related neoplasms. *Oncogene* 22 (40) (Sep 18): 6214-9.

Deeken, J. F., A. Tjen-A-Looi, M. A. Rudek, C. Okuliar, M. Young, R. F. Little, and B. J. Dezube. 2012. The rising challenge of non-AIDS-defining cancers in HIV-infected patients. *Clinical Infectious Diseases : An Official Publication of the Infectious Diseases Society of America* 55 (9) (Nov): 1228-35.

Denny, L. 2006. Cervical cancer: The south african perspective. FIGO 26th annual report on the results of treatment in gynecological cancer. *International Journal of Gynaecology and Obstetrics: The Official Organ of the International Federation of Gynaecology and Obstetrics* 95 Suppl 1 (Nov): S211-4.

Department of Health. 2004, Monitoring and Evaluation Framework for the Comprehensive HIV and AIDS Care, Management and Treatment Plan for South Africa. Pretoria, South Africa.

Derks, N. M., M. Muller, B. Gaszner, D. T. Tilburg-Ouwens, E. W. Roubos, and L. T. Kozicz. 2008. Housekeeping genes revisited: Different expressions depending on gender, brain area and stressor. *Neuroscience* 156 (2) (Oct 2): 305-9.

Diaz-Delfin, J., M. del Mar Gutierrez, J. M. Gallego-Escuredo, J. C. Domingo, M. Gracia Mateo, F. Villarroya, P. Domingo, and M. Giralt. 2011. Effects of nevirapine and efavirenz on human adipocyte differentiation, gene expression, and release of adipokines and cytokines. *Antiviral Research* 91 (2) (Aug): 112-9.

Drug Information EMTRIVA™ GILEAD SCIENCES 2010

Drug Information KALETRA™ ABBOTT LABORATORIES 2011

Drug Information NORVIR™ ABBOTT LABORATORIES 2013

Drug Information SUSTIVA™ GILEAD SCIENCES 2010

Drug Information VIREAD™ GILEAD SCIENCES 2010

Product Information **(S)-(+)**-CAMPTOTHECIN, SIGMA 2012

Dubrow, R., M. J. Silverberg, L. S. Park, K. Crothers, and A. C. Justice. 2012. HIV infection, aging, and immune function: Implications for cancer risk and prevention. *Current Opinion in Oncology* 24 (5) (Sep): 506-16.

Egeblad, M., and Z. Werb. 2002. New functions for the matrix metalloproteinases in cancer progression. *Nature Reviews.Cancer* 2 (3) (Mar): 161-74.

Eggink, D., B. Berkhout, and R. W. Sanders. 2010. Inhibition of HIV-1 by fusion inhibitors. *Current Pharmaceutical Design* 16 (33): 3716-28.

Engels, E. A., R. J. Biggar, H. I. Hall, H. Cross, A. Crutchfield, J. L. Finch, R. Grigg, et al. 2008. Cancer risk in people infected with human immunodeficiency virus in the united states. *International Journal of Cancer.Journal International Du Cancer* 123 (1) (Jul 1): 187-94.

Ergorul, C., A. Ray, W. Huang, D. Darland, Z. K. Luo, and C. L. Grosskreutz. 2008. Levels of vascular endothelial growth factor-A165b (VEGF-A165b) are elevated in experimental glaucoma. *Molecular Vision* 14 (Aug 18): 1517-24.

Estaquier, J., J. D. Lelievre, F. Petit, T. Brunner, L. Moutouh-De Parseval, D. D. Richman, J. C. Ameisen, and J. Corbeil. 2002. Effects of antiretroviral drugs on human immunodeficiency virus type 1-induced CD4(+) T-cell death. *Journal of Virology* 76 (12) (Jun): 5966-73.

Eum, K. H., and M. Lee. 2011. Crosstalk between autophagy and apoptosis in the regulation of paclitaxel-induced cell death in v-ha-ras-transformed fibroblasts. *Molecular and Cellular Biochemistry* 348 (1-2) (Feb): 61-8.

Fan, T. J., L. H. Han, R. S. Cong, and J. Liang. 2005. Caspase family proteases and apoptosis. *Acta Biochimica Et Biophysica Sinica* 37 (11) (Nov): 719-27.

Feng, J. Y., E. Murakami, S. M. Zorca, A. A. Johnson, K. A. Johnson, R. F. Schinazi, P. A. Furman, and K. S. Anderson. 2004. Relationship between antiviral activity and host toxicity: Comparison of the incorporation efficiencies of 2',3'-dideoxy-5-fluoro-3'-thiacytidine-triphosphate analogs by human immunodeficiency virus type 1 reverse transcriptase and human mitochondrial DNA polymerase. *Antimicrobial Agents and Chemotherapy* 48 (4) (Apr): 1300-6.

Ferrara, N. 2004. Vascular endothelial growth factor: Basic science and clinical progress. *Endocrine Reviews* 25 (4) (Aug): 581-611.

Fiebig, A. A., W. Zhu, C. Hollerbach, B. Leber, and D. W. Andrews. 2006. Bcl-XL is qualitatively different from and ten times more effective than bcl-2 when expressed in a breast cancer cell line. *BMC Cancer* 6 (Aug 23): 213.

Finzi, D., J. Blankson, J. D. Siliciano, J. B. Margolick, K. Chadwick, T. Pierson, K. Smith, et al. 1999. Latent infection of CD4+ T cells provides a mechanism for lifelong persistence of HIV-1, even in patients on effective combination therapy. *Nature Medicine* 5 (5) (May): 512-7.

Finzi, D., M. Hermankova, T. Pierson, L. M. Carruth, C. Buck, R. E. Chaisson, T. C. Quinn, et al. 1997. Identification of a reservoir for HIV-1 in patients on highly active antiretroviral therapy. *Science (New York, N.Y.)* 278 (5341) (Nov 14): 1295-300.

Fleige, S., and M. W. Pfaffl. 2006. RNA integrity and the effect on the real-time qRT-PCR performance. *Molecular Aspects of Medicine* 27 (2-3) (Apr-Jun): 126-39.

Franzetti, M., F. Adorni, C. Parravicini, B. Vergani, S. Antinori, L. Milazzo, M. Galli, and A. L. Ridolfo. 2013. Trends and predictors of non-AIDS-defining cancers in men and women with HIV infection: A single-institution retrospective study before and after the introduction of HAART. *Journal of Acquired Immune Deficiency Syndromes (1999)* 62 (4) (Apr 1): 414-20.

Fvasconcellos, 2008, "Skeletal formula of efavirenz" http://en.wikipedia.org/wiki/File:Efavirenz_skeletal.svg

Gabriel, U., C. Bolenz, A. Becker, A. Schaaf, A. Steidler, L. Trojan, C. Weiss, and M. S. Michel. 2008. Evaluation of cytotoxic effects induced by bcl-2 and bcl-xL antisense-oligodeoxynucleotides in normal urothelium and transitional cell carcinoma. *Oncology Reports* 20 (6) (Dec): 1419-23.

Garg, H., and R. Blumenthal. 2006. HIV gp41-induced apoptosis is mediated by caspase-3-dependent mitochondrial depolarization, which is inhibited by HIV protease inhibitor nelfinavir. *Journal of Leukocyte Biology* 79 (2) (Feb): 351-62.

Gaym, A., Mashego, M., Harvey, A., Walldorf, J., Frohlich, J., Karim, Q. 2007, "High prevalence of abnormal Pap smears among young women co-infected with HIV in rural South Africa-implications for cervical cancer screening policies in high HIV prevalence populations". *South African Medical Journal*, 97**,** 130

Gee, J. M., J. F. Robertson, I. O. Ellis, P. Willsher, R. A. McClelland, H. B. Hoyle, S. R. Kyme, P. Finlay, R. W. Blamey, and R. I. Nicholson. 1994. Immunocytochemical localization of BCL-2 protein in human breast cancers and its relationship to a series of prognostic markers and response to endocrine therapy. *International Journal of Cancer.Journal International Du Cancer* 59 (5) (Dec 1): 619-28.

Gewurz, B. E., B. J. Dezube, and L. Pantanowitz. 2005. HIV and the breast. *The AIDS Reader* 15 (8) (Aug): 392,6, 399-402.

Ghibelli, L., F. Mengoni, M. Lichtner, S. Coppola, M. De Nicola, A. Bergamaschi, C. Mastroianni, and V. Vullo. 2003. Anti-apoptotic effect of HIV protease inhibitors via direct inhibition of calpain. *Biochemical Pharmacology* 66 (8) (Oct 15): 1505-12.

Gills, J. J., J. Lopiccolo, J. Tsurutani, R. H. Shoemaker, C. J. Best, M. S. Abu-Asab, J. Borojerdi, et al. 2007. Nelfinavir, A lead HIV protease inhibitor, is a broad-spectrum, anticancer agent that induces endoplasmic reticulum stress, autophagy, and apoptosis in vitro and in vivo. *Clinical Cancer Research : An Official Journal of the American Association for Cancer Research* 13 (17) (Sep 1): 5183-94.

Gitman, M. D., D. Hirschwerk, C. H. Baskin, and P. C. Singhal. 2007. Tenofovir-induced kidney injury. *Expert Opinion on Drug Safety* 6 (2) (Mar): 155-64.
Gomez-Sucerquia, L. J., A. Blas-Garcia, M. Marti-Cabrera, J. V. Esplugues, and N. Apostolova. 2012. Profile of stress and toxicity gene expression in human hepatic cells treated with efavirenz. *Antiviral Research* 94 (3) (Jun): 232-41.
Grizzi, F., and M. Chiriva-Internati. 2006. Cancer: Looking for simplicity and finding complexity. *Cancer Cell International* 6 (Feb 15): 4.
Grulich, A. E., M. T. van Leeuwen, M. O. Falster, and C. M. Vajdic. 2007. Incidence of cancers in people with HIV/AIDS compared with immunosuppressed transplant recipients: A meta-analysis. *Lancet* 370 (9581) (Jul 7): 59-67.
Guiguet, M., F. Boue, J. Cadranel, J. M. Lang, E. Rosenthal, D. Costagliola, and Clinical Epidemiology Group of the FHDH-ANRS CO4 cohort. 2009. Effect of immunodeficiency, HIV viral load, and antiretroviral therapy on the risk of individual malignancies (FHDH-ANRS CO4): A prospective cohort study. *The Lancet Oncology* 10 (12) (Dec): 1152-9.
Guimaraes, N. N., H. H. de Andrade, M. Lehmann, R. R. Dihl, and K. S. Cunha. 2010. The genetic toxicity effects of lamivudine and stavudine antiretroviral agents. *Expert Opinion on Drug Safety* 9 (5) (Sep): 771-81.
Hajjar, M., D. Lacoste, G. Brossard, P. Morlat, M. Dupon, L. R. Salmi, and F. Dabis. 1992. Non-acquired immune deficiency syndrome-defining malignancies in a hospital-based cohort of human immunodeficiency virus-infected patients: Bordeaux, france, 1985-1991. groupe d'epidemiologie clinique du SIDA en aquitaine. *Journal of the National Cancer Institute* 84 (20) (Oct 21): 1593-5.
Hameed, D. A., A. M. Abdel Raheem, E. Mosad, H. M. Hammouda, N. A. Kamel, and M. A. Abdel Aziz. 2008. Bcl-XL and bcl-2 expression in bilharzial squamous cell carcinoma of the urinary bladder: Which protein is prognostic? *Urology* 72 (2) (Aug): 374-8.
Hampson, L., H. C. Kitchener, and I. N. Hampson. 2006. Specific HIV protease inhibitors inhibit the ability of HPV16 E6 to degrade p53 and selectively kill E6-dependent cervical carcinoma cells in vitro. *Antiviral Therapy* 11 (6): 813-25.
Hanahan, D., and R. A. Weinberg. 2000. The hallmarks of cancer. *Cell* 100 (1) (Jan 7): 57-70.
Harrod, R., J. Nacsa, C. Van Lint, J. Hansen, T. Karpova, J. McNally, and G. Franchini. 2003. Human immunodeficiency virus type-1 Tat/co-activator acetyltransferase interactions inhibit p53Lys-320 acetylation and p53-responsive transcription. *The Journal of Biological Chemistry* 278 (14) (Apr 4): 12310-8.
Heard, I. 2009. Prevention of cervical cancer in women with HIV. *Current Opinion in HIV and AIDS* 4 (1) (Jan): 68-73.
Hellemans, J., G. Mortier, A. De Paepe, F. Speleman, and J. Vandesompele. 2007. qBase relative quantification framework and software for management and automated analysis of real-time quantitative PCR data. *Genome Biology* 8 (2): R19.
Hessol, N. A., S. Pipkin, S. Schwarcz, R. D. Cress, P. Bacchetti, and S. Scheer. 2007. The impact of highly active antiretroviral therapy on non-AIDS-defining cancers among adults with AIDS. *American Journal of Epidemiology* 165 (10) (May 15): 1143-53.
Hisatomi, T., T. Nakazawa, K. Noda, L. Almulki, S. Miyahara, S. Nakao, Y. Ito, et al. 2008. HIV protease inhibitors provide neuroprotection through inhibition of mitochondrial apoptosis in mice. *The Journal of Clinical Investigation* 118 (6) (Jun): 2025-38.
Hoeben, A., B. Landuyt, M. S. Highley, H. Wildiers, A. T. Van Oosterom, and E. A. De Bruijn. 2004. Vascular endothelial growth factor and angiogenesis. *Pharmacological Reviews* 56 (4) (Dec): 549-80.
Horvitz, H. R. 1999. Genetic control of programmed cell death in the nematode caenorhabditis elegans. *Cancer Research* 59 (7 Suppl) (Apr 1): 1701s-6s.
Houck, K. A., N. Ferrara, J. Winer, G. Cachianes, B. Li, and D. W. Leung. 1991. The vascular endothelial growth factor family: Identification of a fourth molecular species and characterization of alternative splicing of RNA. *Molecular Endocrinology (Baltimore, Md.)* 5 (12) (Dec): 1806-14.

Huber-Ruano, I., and M. Pastor-Anglada. 2009. Transport of nucleoside analogs across the plasma membrane: A clue to understanding drug-induced cytotoxicity. *Current Drug Metabolism* 10 (4) (May): 347-58.

Hsiang, Y. H., R. Hertzberg, S. Hecht, and L. F. Liu. 1985. Camptothecin induces protein-linked DNA breaks via mammalian DNA topoisomerase I. *The Journal of Biological Chemistry* 260 (27) (Nov 25): 14873-8.

Hsiang, Y. H., M. G. Lihou, and L. F. Liu. 1989. Arrest of replication forks by drug-stabilized topoisomerase I-DNA cleavable complexes as a mechanism of cell killing by camptothecin. *Cancer Research* 49 (18) (Sep 15): 5077-82.

IARC. 2000, "IARC Monographs on the Evaluation of Carcinogenic Risks to Humans". World Health Organization. IARC Scientific Publications No. 76, IARC, Lyon, France, pp. 1—521

Isgro, A., A. Aiuti, I. Mezzaroma, L. Ruco, M. Pinti, A. Cossarizza, and F. Aiuti. 2005. HIV type 1 protease inhibitors enhance bone marrow progenitor cell activity in normal subjects and in HIV type 1-infected patients. *AIDS Research and Human Retroviruses* 21 (1) (Jan): 51-7.

Jiang, B., V. Y. Hebert, Y. Li, J. M. Mathis, J. S. Alexander, and T. R. Dugas. 2007. HIV antiretroviral drug combination induces endothelial mitochondrial dysfunction and reactive oxygen species production, but not apoptosis. *Toxicology and Applied Pharmacology* 224 (1) (Oct 1): 60-71.

Jochmans, D. 2008. Novel HIV-1 reverse transcriptase inhibitors. *Virus Research* 134 (1-2) (Jun): 171-85.

Johnson, A. A., A. S. Ray, J. Hanes, Z. Suo, J. M. Colacino, K. S. Anderson, and K. A. Johnson. 2001. Toxicity of antiviral nucleoside analogs and the human mitochondrial DNA polymerase. *The Journal of Biological Chemistry* 276 (44) (Nov 2): 40847-57.

Joukov, V., K. Pajusola, A. Kaipainen, D. Chilov, I. Lahtinen, E. Kukk, O. Saksela, N. Kalkkinen, and K. Alitalo. 1996. A novel vascular endothelial growth factor, VEGF-C, is a ligand for the Flt4 (VEGFR-3) and KDR (VEGFR-2) receptor tyrosine kinases. *The EMBO Journal* 15 (2) (Jan 15): 290-8.

Jover, F., J. M. Cuadrado, P. Roig, M. Rodriguez, L. Andreu, and J. Merino. 2004. Efavirenz-associated gynecomastia: Report of five cases and review of the literature. *The Breast Journal* 10 (3) (May-Jun): 244-6.

Kakuda, T. N. 2000. Pharmacology of nucleoside and nucleotide reverse transcriptase inhibitor-induced mitochondrial toxicity. *Clinical Therapeutics* 22 (6) (Jun): 685-708.

Kearney, B. P., J. F. Flaherty, and J. Shah. 2004. Tenofovir disoproxil fumarate: Clinical pharmacology and pharmacokinetics. *Clinical Pharmacokinetics* 43 (9): 595-612.

Kesselring, A., L. Gras, C. Smit, G. van Twillert, A. Verbon, F. de Wolf, P. Reiss, and F. Wit. 2011. Immunodeficiency as a risk factor for non-AIDS-defining malignancies in HIV-1-infected patients receiving combination antiretroviral therapy. *Clinical Infectious Diseases : An Official Publication of the Infectious Diseases Society of America* 52 (12) (Jun 15): 1458-65.

Kienzle, N., D. Young, S. Zehntner, G. Bushell, and T. B. Sculley. 1996. DNaseI treatment is a prerequisite for the amplification of cDNA from episomal-based genes. *Biotechniques* 20 (4) (Apr): 612-6.

Klassen, M. K., M. Lewin-Smith, S. S. Frankel, and A. M. Nelson. 1997. Pathology of human immunodeficiency virus infection: Noninfectious conditions. *Annals of Diagnostic Pathology* 1 (1) (Oct): 57-64.

Kohler, J. J., and W. Lewis. 2007. A brief overview of mechanisms of mitochondrial toxicity from NRTIs. *Environmental and Molecular Mutagenesis* 48 (3-4) (Apr-May): 166-72.

Komanduri, K. V., M. N. Viswanathan, E. D. Wieder, D. K. Schmidt, B. M. Bredt, M. A. Jacobson, and J. M. McCune. 1998. Restoration of cytomegalovirus-specific CD4+ T-lymphocyte responses after ganciclovir and highly active antiretroviral therapy in individuals infected with HIV-1. *Nature Medicine* 4 (8) (Aug): 953-6.

Kontorinis, N., and D. T. Dieterich. 2003. Toxicity of non-nucleoside analogue reverse transcriptase inhibitors. *Seminars in Liver Disease* 23 (2) (May): 173-82.

Kranzer, K., J. Zeinecker, P. Ginsberg, C. Orrell, N. N. Kalawe, S. D. Lawn, L. G. Bekker, and R. Wood. 2010. Linkage to HIV care and antiretroviral therapy in cape town, south africa. *PloS One* 5 (11) (Nov 2): e13801.

Krishnan, S., J. T. Schouten, D. L. Jacobson, C. A. Benson, A. C. Collier, S. L. Koletar, J. Santana, F. R. Sattler, R. Mitsuyasu, and ACTG-ALLRT Protocol Team. 2011. Incidence of non-AIDS-defining cancer in antiretroviral treatment-naive subjects after antiretroviral treatment initiation: An ACTG longitudinal linked randomized trials analysis. *Oncology* 80 (1-2): 42-9.

Kwok, S., and R. Higuchi. 1989. Avoiding false positives with PCR. *Nature* 339 (6221) (May 18): 237-8.

Lederman, M. M., E. Connick, A. Landay, D. R. Kuritzkes, J. Spritzler, M. St Clair, B. L. Kotzin, et al. 1998. Immunologic responses associated with 12 weeks of combination antiretroviral therapy consisting of zidovudine, lamivudine, and ritonavir: Results of AIDS clinical trials group protocol 315. *The Journal of Infectious Diseases* 178 (1) (Jul): 70-9.

Legarza, K., and L. X. Yang. 2006. New molecular mechanisms of action of camptothecin-type drugs. *Anticancer Research* 26 (5A) (Sep-Oct): 3301-5.

Lewis, W., W. C. Copeland, and B. J. Day. 2001. Mitochondrial dna depletion, oxidative stress, and mutation: Mechanisms of dysfunction from nucleoside reverse transcriptase inhibitors. *Laboratory Investigation; a Journal of Technical Methods and Pathology* 81 (6) (Jun): 777-90.

Lewis, W., B. J. Day, and W. C. Copeland. 2003. Mitochondrial toxicity of NRTI antiviral drugs: An integrated cellular perspective. *Nature Reviews.Drug Discovery* 2 (10) (Oct): 812-22.

Li, J., and J. Yuan. 2008. Caspases in apoptosis and beyond. *Oncogene* 27 (48) (Oct 20): 6194-206.

Li, Q., T. Schacker, J. Carlis, G. Beilman, P. Nguyen, and A. T. Haase. 2004. Functional genomic analysis of the response of HIV-1-infected lymphatic tissue to antiretroviral therapy. *The Journal of Infectious Diseases* 189 (4) (Feb 15): 572-82.

Li, Y., X. Ye, C. Tan, J. A. Hongo, J. Zha, J. Liu, D. Kallop, M. J. Ludlam, and L. Pei. 2009. Axl as a potential therapeutic target in cancer: Role of axl in tumor growth, metastasis and angiogenesis. *Oncogene* 28 (39) (Oct 1): 3442-55.

Liu, C. Y., A. Takemasa, W. C. Liles, R. B. Goodman, M. Jonas, H. Rosen, E. Chi, R. K. Winn, J. M. Harlan, and P. I. Chuang. 2003. Broad-spectrum caspase inhibition paradoxically augments cell death in TNF-alpha -stimulated neutrophils. *Blood* 101 (1) (Jan 1): 295-304.

Livak, K. J., and T. D. Schmittgen. 2001. Analysis of relative gene expression data using real-time quantitative PCR and the 2(-delta delta C(T)) method. *Methods (San Diego, Calif.)* 25 (4) (Dec): 402-8.

Llambi, Fabien, and Douglas R. Green. 2011. Apoptosis and oncogenesis: Give and take in the BCL-2 family. *Current Opinion in Genetics & Development* 21 (1) (2): 12-20.

Lu, W., and J. M. Andrieu. 2000. HIV protease inhibitors restore impaired T-cell proliferative response in vivo and in vitro: A viral-suppression-independent mechanism. *Blood* 96 (1) (Jul 1): 250-8.

Maagaard, A., and D. Kvale. 2009. Mitochondrial toxicity in HIV-infected patients both off and on antiretroviral treatment: A continuum or distinct underlying mechanisms? *The Journal of Antimicrobial Chemotherapy* 64 (5) (Nov): 901-9.

Mallon, P. W., P. Unemori, R. Sedwell, A. Morey, M. Rafferty, K. Williams, D. Chisholm, et al. 2005. In vivo, nucleoside reverse-transcriptase inhibitors alter expression of both mitochondrial and lipid metabolism genes in the absence of depletion of mitochondrial DNA. *The Journal of Infectious Diseases* 191 (10) (May 15): 1686-96.

Manetti, M., S. Guiducci, E. Romano, C. Ceccarelli, S. Bellando-Randone, M. L. Conforti, L. Ibba-Manneschi, and M. Matucci-Cerinic. 2011. Overexpression of VEGF165b, an inhibitory splice variant of vascular endothelial growth factor, leads to insufficient angiogenesis in patients with systemic sclerosis. *Circulation Research* 109 (3) (Jul 22): e14-26.

Maqutu, D., T. Zewotir, D. North, K. Naidoo, and A. Grobler. 2011. Determinants of optimal adherence over time to antiretroviral therapy amongst HIV positive adults in south africa: A longitudinal study. *AIDS and Behavior* 15 (7) (Oct): 1465-74.

Matarrese, P., L. Gambardella, A. Cassone, S. Vella, R. Cauda, and W. Malorni. 2003. Mitochondrial membrane hyperpolarization hijacks activated T lymphocytes toward the apoptotic-prone phenotype: Homeostatic mechanisms of HIV protease inhibitors. *Journal of Immunology (Baltimore, Md.: 1950)* 170 (12) (Jun 15): 6006-15.

Matarrese, P., A. Tinari, L. Gambardella, E. Mormone, P. Narilli, M. Pierdominici, R. Cauda, and W. Malorni. 2005. HIV protease inhibitors prevent mitochondrial hyperpolarization and redox imbalance and decrease endogenous uncoupler protein-2 expression in gp 120-activated human T lymphocytes. *Antiviral Therapy* 10 Suppl 2 : M29-45.

Matthews, W., C. T. Jordan, M. Gavin, N. A. Jenkins, N. G. Copeland, and I. R. Lemischka. 1991. A receptor tyrosine kinase cDNA isolated from a population of enriched primitive hematopoietic cells and exhibiting close genetic linkage to c-kit. *Proceedings of the National Academy of Sciences of the United States of America* 88 (20) (Oct 15): 9026-30.

Mbulaiteye, S. M., R. J. Biggar, J. J. Goedert, and E. A. Engels. 2003. Immune deficiency and risk for malignancy among persons with AIDS. *Journal of Acquired Immune Deficiency Syndromes (1999)* 32 (5) (Apr 15): 527-33.

Messiaen, P., A. M. Wensing, A. Fun, M. Nijhuis, N. Brusselaers, and L. Vandekerckhove. 2013. Clinical use of HIV integrase inhibitors: A systematic review and meta-analysis. *PloS One* 8 (1): e52562.

Miro, O., J. Villarroya, G. Garrabou, S. Lopez, M. Rodriguez de la Concepcion, E. Pedrol, E. Martinez, et al. 2005. In vivo effects of highly active antiretroviral therapies containing the protease inhibitor nelfinavir on mitochondrially driven apoptosis. *Antiviral Therapy* 10 (8): 945-51.

Mironova, E. V., A. A. Evstratova, and S. M. Antonov. 2007. A fluorescence vital assay for the recognition and quantification of excitotoxic cell death by necrosis and apoptosis using confocal microscopy on neurons in culture. *Journal of Neuroscience Methods* 163 (1) (Jun 15): 1-8.

Mohamad, N., A. Gutierrez, M. Nunez, C. Cocca, G. Martin, G. Cricco, V. Medina, E. Rivera, and R. Bergoc. 2005. Mitochondrial apoptotic pathways. *Biocell : Official Journal of the Sociedades Latinoamericanas De Microscopia Electronica ...Et.Al* 29 (2) (Aug): 149-61.

Monini, P., C. Sgadari, G. Barillari, and B. Ensoli. 2003. HIV protease inhibitors: Antiretroviral agents with anti-inflammatory, anti-angiogenic and anti-tumour activity. *The Journal of Antimicrobial Chemotherapy* 51 (2) (Feb): 207-11.

Morris, E. J., and H. M. Geller. 1996. Induction of neuronal apoptosis by camptothecin, an inhibitor of DNA topoisomerase-I: Evidence for cell cycle-independent toxicity. *The Journal of Cell Biology* 134 (3) (Aug): 757-70.

Mosesso, P., P. Pichierri, A. Franchitto, and F. Palitti. 2000. Evidence that camptothecin-induced aberrations in the G(2) phase of cell cycle of chinese hamster ovary (CHO) cell lines is associated with transcription. *Mutation Research* 452 (2) (Sep 18): 189-95.

Moubayed, P., H. Mwakyoma, and D. T. Schneider. 2004. High frequency of human papillomavirus 6/11, 16, and 18 infections in precancerous lesions and squamous cell carcinoma of the conjunctiva in subtropical tanzania. *American Journal of Clinical Pathology* 122 (6) (Dec): 938-43.

Mudduluru, G., and H. Allgayer. 2008. The human receptor tyrosine kinase axl gene--promoter characterization and regulation of constitutive expression by Sp1, Sp3 and CpG methylation. *Bioscience Reports* 28 (3) (Jun): 161-76.

Mullis, K. B., and F. A. Faloona. 1987. Specific synthesis of DNA in vitro via a polymerase-catalyzed chain reaction. *Methods in Enzymology* 155 : 335-50.

Nachega, J. B., D. M. Stein, D. A. Lehman, D. Hlatshwayo, R. Mothopeng, R. E. Chaisson, and A. S. Karstaedt. 2004. Adherence to antiretroviral therapy in HIV-infected adults in soweto, south africa. *AIDS Research and Human Retroviruses* 20 (10) (Oct): 1053-6.

Naesens, L., N. Bischofberger, P. Augustijns, P. Annaert, G. Van den Mooter, M. N. Arimilli, C. U. Kim, and E. De Clercq. 1998. Antiretroviral efficacy and pharmacokinetics of oral bis(isopropyloxycarbonyloxymethyl)-9-(2-phosphonylmethoxypropyl)adenine in mice. *Antimicrobial Agents and Chemotherapy* 42 (7) (Jul): 1568-73.

Neufeld, G., T. Cohen, H. Gitay-Goren, Z. Poltorak, S. Tessler, R. Sharon, S. Gengrinovitch, and B. Z. Levi. 1996. Similarities and differences between the vascular endothelial growth factor (VEGF) splice variants. *Cancer Metastasis Reviews* 15 (2) (Jun): 153-8.

Nguyen, M. L., K. J. Farrell, and C. J. Gunthel. 2010. Non-AIDS-defining malignancies in patients with HIV in the HAART era. *Current Infectious Disease Reports* 12 (1) (Jan): 46-55.

Nieves-Neira, W., and Y. Pommier. 1999. Apoptotic response to camptothecin and 7-hydroxystaurosporine (UCN-01) in the 8 human breast cancer cell lines of the NCI anticancer drug screen: Multifactorial relationships with topoisomerase I, protein kinase C, bcl-2, p53, MDM-2 and caspase pathways. *International Journal of Cancer.Journal International Du Cancer* 82 (3) (Jul 30): 396-404.

Nordgren TM, Hegde GV, Joshi SS. 2012. Ritonavir Exhibits Limited Efficacy as a Single Agent in Treating Aggressive Mantle Cell Lymphoma. J Cancer Sci Ther 4: 061-068. doi:10.4172/1948-5956.1000112

Nowak, D. G., J. Woolard, E. M. Amin, O. Konopatskaya, M. A. Saleem, A. J. Churchill, M. R. Ladomery, S. J. Harper, and D. O. Bates. 2008. Expression of pro- and anti-angiogenic isoforms of VEGF is differentially regulated by splicing and growth factors. *Journal of Cell Science* 121 (Pt 20) (Oct 15): 3487-95.

NTP. 1999, "Technical report on the toxicology and carcinogenesis studies of AZT (CAS no. 30516-87-1) and AZT/α-interferon A/D in B6C3F_1 mice (gavage studies)". TR 469; NIH Publication No. 99-3959.http://ntp.niehs.nih.gov/ntp/htdocs/LT_rpts/tr469.pdf.

Nyagol, J., E. Leucci, A. Onnis, G. De Falco, C. Tigli, F. Sanseverino, M. Torriccelli, et al. 2006. The effects of HIV-1 tat protein on cell cycle during cervical carcinogenesis. *Cancer Biology & Therapy* 5 (6) (Jun): 684-90.

Ola, M. S., M. Nawaz, and H. Ahsan. 2011. Role of bcl-2 family proteins and caspases in the regulation of apoptosis. *Molecular and Cellular Biochemistry* 351 (1-2) (May): 41-58.

Olivero, O. A. 2007. Mechanisms of genotoxicity of nucleoside reverse transcriptase inhibitors. *Environmental and Molecular Mutagenesis* 48 (3-4) (Apr-May): 215-23.

Olivero, O. A., L. M. Anderson, B. A. Diwan, D. C. Haines, S. W. Harbaugh, T. J. Moskal, A. B. Jones, et al. 1997. Transplacental effects of 3'-azido-2',3'-dideoxythymidine (AZT): Tumorigenicity in mice and genotoxicity in mice and monkeys. *Journal of the National Cancer Institute* 89 (21) (Nov 5): 1602-8.

Olivero, O. A., A. M. Tejera, J. J. Fernandez, B. J. Taylor, S. Das, R. L. Divi, and M. C. Poirier. 2005. Zidovudine induces S-phase arrest and cell cycle gene expression changes in human cells. *Mutagenesis* 20 (2) (Mar): 139-46.

Olofsson, B., K. Pajusola, A. Kaipainen, G. von Euler, V. Joukov, O. Saksela, A. Orpana, R. F. Pettersson, K. Alitalo, and U. Eriksson. 1996. Vascular endothelial growth factor B, a novel growth factor for endothelial cells. *Proceedings of the National Academy of Sciences of the United States of America* 93 (6) (Mar 19): 2576-81.

Oluwole, Soji F., Ayoola O. Ali, Zahra Shafaee, and Hector A. Depaz. 2005. Breast cancer in women with HIV/AIDS: Report of five cases with a review of the literature. *Journal of Surgical Oncology* 89 (1): 23-7.

Ouyang, L., Z. Shi, S. Zhao, F. -T Wang, T. -T Zhou, B. Liu, and J. -K Bao. 2012. Programmed cell death pathways in cancer: A review of apoptosis, autophagy and programmed necrosis. *Cell Proliferation* 45 (6): 487-98.

Pace, C. S., A. M. Martin, E. L. Hammond, C. D. Mamotte, D. A. Nolan, and S. A. Mallal. 2003. Mitochondrial proliferation, DNA depletion and adipocyte differentiation in subcutaneous adipose tissue of HIV-positive HAART recipients. *Antiviral Therapy* 8 (4) (Aug): 323-31.

Pajusola, K., O. Aprelikova, J. Korhonen, A. Kaipainen, L. Pertovaara, R. Alitalo, and K. Alitalo. 1992. FLT4 receptor tyrosine kinase contains seven immunoglobulin-like loops and is expressed in multiple human tissues and cell lines. *Cancer Research* 52 (20) (Oct 15): 5738-43.

Palefsky, J. 2009. Human papillomavirus-related disease in people with HIV. *Current Opinion in HIV and AIDS* 4 (1) (Jan): 52-6.

Pan, Y., L. Wang, and J. L. Dai. 2006. Suppression of breast cancer cell growth by Na+/H+ exchanger regulatory factor 1 (NHERF1). *Breast Cancer Research : BCR* 8 (6): R63.

Pantanowitz, Liron, and James L. Connolly. 2002. Pathology of the breast associated with HIV/AIDS. *The Breast Journal* 8 (4): 234-43.

Patil, P., B. Elem, and A. Zumla. 1995. Pattern of adult malignancies in zambia (1980-1989) in light of the human immunodeficiency virus type 1 epidemic. *The Journal of Tropical Medicine and Hygiene* 98 (4) (Aug): 281-4.

Pecina-Slaus, N. 2009. Genetic and molecular insights into apoptosis. *Acta Medica Croatica : Casopis Hravatske Akademije Medicinskih Znanosti* 63 Suppl 2 (Oct): 13-9.

Perez-Molina, J. A., P. Domingo, E. Martinez, and S. Moreno. 2008. The role of efavirenz compared with protease inhibitors in the body fat changes associated with highly active antiretroviral therapy. *The Journal of Antimicrobial Chemotherapy* 62 (2) (Aug): 234-45.

Perrin, R. M., O. Konopatskaya, Y. Qiu, S. Harper, D. O. Bates, and A. J. Churchill. 2005. Diabetic retinopathy is associated with a switch in splicing from anti- to pro-angiogenic isoforms of vascular endothelial growth factor. *Diabetologia* 48 (11) (Nov): 2422-7.

Phenix, B. N., J. J. Lum, Z. Nie, J. Sanchez-Dardon, and A. D. Badley. 2001. Antiapoptotic mechanism of HIV protease inhibitors: Preventing mitochondrial transmembrane potential loss. *Blood* 98 (4) (Aug 15): 1078-85.

Phillips, A. A., and J. E. Justman. 2009. Screening HIV-infected patients for non-AIDS-defining malignancies. *Current HIV/AIDS Reports* 6 (2) (May): 83-92.

Pierone, G.,Jr, J. Mieras, D. Bulgin-Coleman, C. Kantor, J. Shearer, L. Fontaine, M. Fath, and M. Norton. 2006. A pilot study of switch to lopinavir/ritonavir (LPV/r) monotherapy from nonnucleoside reverse transcriptase inhibitor-based therapy. *HIV Clinical Trials* 7 (5) (Sep-Oct): 237-45.

Pizzolato, J. F., and L. B. Saltz. 2003. The camptothecins. *Lancet* 361 (9376) (Jun 28): 2235-42.

Plouet, J., and H. Moukadiri. 1990. Characterization of the receptor to vasculotropin on bovine adrenal cortex-derived capillary endothelial cells. *The Journal of Biological Chemistry* 265 (36) (Dec 25): 22071-4.

Pore, N., A. K. Gupta, G. J. Cerniglia, and A. Maity. 2006. HIV protease inhibitors decrease VEGF/HIF-1alpha expression and angiogenesis in glioblastoma cells. *Neoplasia (New York, N.Y.)* 8 (11) (Nov): 889-95.

Powles, T., D. Robinson, J. Stebbing, J. Shamash, M. Nelson, B. Gazzard, S. Mandelia, H. Moller, and M. Bower. 2009. Highly active antiretroviral therapy and the incidence of non-AIDS-defining cancers in people with HIV infection. *Journal of Clinical Oncology : Official Journal of the American Society of Clinical Oncology* 27 (6) (Feb 20): 884-90.

Product Information **(S)-(+)-**Camptothecin, Sigma, 2012.

Prosperi, M. C., A. Cozzi-Lepri, A. Castagna, C. Mussini, R. Murri, A. Giacometti, C. Torti, et al. 2010. Incidence of malignancies in HIV-infected patients and prognostic role of current CD4 cell count: Evidence from a large italian cohort study. *Clinical Infectious Diseases : An Official Publication of the Infectious Diseases Society of America* 50 (9) (May 1): 1316-21.

Pugh, D. J., E. Ab, A. Faro, P. T. Lutya, E. Hoffmann, and D. J. Rees. 2006. DWNN, a novel ubiquitin-like domain, implicates RBBP6 in mRNA processing and ubiquitin-like pathways. *BMC Structural Biology* 6 (Jan 5): 1.

Qayyum, S., H. Dong, D. Kovacic, S. Sohail, B. Waters, C. Thornton, and C. E. Corbett. 2012. Combination therapy efavirenz/emtricitabine/tenofovir disoproxil fumarate associated with hepatic failure. *Current Drug Safety* 7 (5) (Nov 1): 391-3.

Qiu, Y., C. Hoareau-Aveilla, S. Oltean, S. J. Harper, and D. O. Bates. 2009. The anti-angiogenic isoforms of VEGF in health and disease. *Biochemical Society Transactions* 37 (Pt 6) (Dec): 1207-13.

Rastogi, S., B. Joshi, G. Fusaro, and S. Chellappan. 2006. Camptothecin induces nuclear export of prohibitin preferentially in transformed cells through a CRM-1-dependent mechanism. *The Journal of Biological Chemistry* 281 (5) (Feb 3): 2951-9.

Razandi, M., G. Alton, A. Pedram, S. Ghonshani, P. Webb, and E. R. Levin. 2003. Identification of a structural determinant necessary for the localization and function of estrogen receptor alpha at the plasma membrane. *Molecular and Cellular Biology* 23 (5) (Mar): 1633-46.

Reekie, J., C. Kosa, F. Engsig, Ad Monforte, A. Wiercinska-Drapalo, P. Domingo, F. Antunes, et al. 2010. Relationship between current level of immunodeficiency and non-acquired immunodeficiency syndrome-defining malignancies. *Cancer* 116 (22) (Nov 15): 5306-15.

Rennel, E. S., S. J. Harper, and D. O. Bates. 2009. Therapeutic potential of manipulating VEGF splice isoforms in oncology. *Future Oncology (London, England)* 5 (5) (Jun): 703-12.

Renvoize, C., A. Biola, M. Pallardy, and J. Breard. 1998. Apoptosis: Identification of dying cells. *Cell Biology and Toxicology* 14 (2) (Mar): 111-20.
Ribble, D., N. B. Goldstein, D. A. Norris, and Y. G. Shellman. 2005. A simple technique for quantifying apoptosis in 96-well plates. *BMC Biotechnology* 5 (May 10): 12.
Richman, D. D. 2001. HIV chemotherapy. *Nature* 410 (6831) (Apr 19): 995-1001.
Rizza, S. A., and A. D. Badley. 2008. HIV protease inhibitors impact on apoptosis. *Medicinal Chemistry (Shariqah (United Arab Emirates))* 4 (1) (Jan): 75-9.
Robbins, B. L., R. V. Srinivas, C. Kim, N. Bischofberger, and A. Fridland. 1998. Anti-human immunodeficiency virus activity and cellular metabolism of a potential prodrug of the acyclic nucleoside phosphonate 9-R-(2-phosphonomethoxypropyl)adenine (PMPA), bis(isopropyloxymethylcarbonyl)PMPA. *Antimicrobial Agents and Chemotherapy* 42 (3) (Mar): 612-7.
Roskoski, R.,Jr. 2007. Vascular endothelial growth factor (VEGF) signaling in tumor progression. *Critical Reviews in oncology/hematology* 62 (3) (Jun): 179-213.
Rosse, T., R. Olivier, L. Monney, M. Rager, S. Conus, I. Fellay, B. Jansen, and C. Borner. 1998. Bcl-2 prolongs cell survival after bax-induced release of cytochrome c. *Nature* 391 (6666) (Jan 29): 496-9.
Roucou, X., P. N. Giannopoulos, Y. Zhang, J. Jodoin, C. G. Goodyer, and A. LeBlanc. 2005. Cellular prion protein inhibits proapoptotic bax conformational change in human neurons and in breast carcinoma MCF-7 cells. *Cell Death and Differentiation* 12 (7) (Jul): 783-95.
Rudolf, E., K. Rudolf, and M. Cervinka. 2011. Camptothecin induces p53-dependent and -independent apoptogenic signaling in melanoma cells. *Apoptosis : An International Journal on Programmed Cell Death* 16 (11) (Nov): 1165-76.
Saiki, R. K., D. H. Gelfand, S. Stoffel, S. J. Scharf, R. Higuchi, G. T. Horn, K. B. Mullis, and H. A. Erlich. 1988. Primer-directed enzymatic amplification of DNA with a thermostable DNA polymerase. *Science (New York, N.Y.)* 239 (4839) (Jan 29): 487-91.
Sambrook, J., Russell, D.W. 2001 Molecular Cloning: A Laboratory Manual, the third edition, Cold Spring Harbor Laboratory Press, Cold Spring Harbor, New York
Sanchez-Alcazar, J. A., J. G. Ault, A. Khodjakov, and E. Schneider. 2000. Increased mitochondrial cytochrome c levels and mitochondrial hyperpolarization precede camptothecin-induced apoptosis in jurkat cells. *Cell Death and Differentiation* 7 (11) (Nov): 1090-100.
Schaffitzel, E., and M. Hertweck. 2006. Recent aging research in caenorhabditis elegans. *Experimental Gerontology* 41 (6) (Jun): 557-63.
Sgadari, C., G. Barillari, E. Toschi, D. Carlei, I. Bacigalupo, S. Baccarini, C. Palladino, et al. 2002. HIV protease inhibitors are potent anti-angiogenic molecules and promote regression of kaposi sarcoma. *Nature Medicine* 8 (3) (Mar): 225-32.
Sgadari, C., P. Monini, G. Barillari, and B. Ensoli. 2003. Use of HIV protease inhibitors to block kaposi's sarcoma and tumour growth. *The Lancet Oncology* 4 (9) (Sep): 537-47.
Shibuya, M., S. Yamaguchi, A. Yamane, T. Ikeda, A. Tojo, H. Matsushime, and M. Sato. 1990. Nucleotide sequence and expression of a novel human receptor-type tyrosine kinase gene (flt) closely related to the fms family. *Oncogene* 5 (4) (Apr): 519-24.
Shiels, M. S., S. R. Cole, G. D. Kirk, and C. Poole. 2009. A meta-analysis of the incidence of non-AIDS cancers in HIV-infected individuals. *Journal of Acquired Immune Deficiency Syndromes (1999)* 52 (5) (Dec): 611-22.
Sikora, M. J., J. M. Rae, M. D. Johnson, and Z. Desta. 2010. Efavirenz directly modulates the oestrogen receptor and induces breast cancer cell growth. *HIV Medicine* 11 (9) (Oct 1): 603-7.
Silverberg, M. J., and D. I. Abrams. 2007. AIDS-defining and non-AIDS-defining malignancies: Cancer occurrence in the antiretroviral therapy era. *Current Opinion in Oncology* 19 (5) (Sep): 446-51.
Silverberg, M. J., C. Chao, W. A. Leyden, L. Xu, B. Tang, M. A. Horberg, D. Klein, C. P. Quesenberry Jr, W. J. Towner, and D. I. Abrams. 2009. HIV infection and the risk of cancers with and without a known infectious cause. *AIDS (London, England)* 23 (17) (Nov 13): 2337-45.
Sjostrom, J., and J. Bergh. 2001. How apoptosis is regulated, and what goes wrong in cancer. *BMJ (Clinical Research Ed.)* 322 (7301) (Jun 23): 1538-9.

Sloand, E. M., P. N. Kumar, S. Kim, A. Chaudhuri, F. F. Weichold, and N. S. Young. 1999. Human immunodeficiency virus type 1 protease inhibitor modulates activation of peripheral blood CD4(+) T cells and decreases their susceptibility to apoptosis in vitro and in vivo. *Blood* 94 (3) (Aug 1): 1021-7.

Spano, J. P., E. Lanoy, N. Mounier, C. Katlama, D. Costagliola, and I. Heard. 2012. Breast cancer among HIV infected individuals from the ONCOVIH study, in france: Therapeutic implications. *European Journal of Cancer (Oxford, England : 1990)* 48 (18) (Dec): 3335-41.

Spina, M., G. Nasti, C. Simonelli, G. Bertola, C. Rossi, and U. Tirelli. 1994. Breast cancer in a woman with HIV infection: A case report. *Annals of Oncology : Official Journal of the European Society for Medical Oncology / ESMO* 5 (7) (Sep): 661-2.

Spinedi, A., S. Oliverio, F. Di Sano, and M. Piacentini. 1998. Calpain involvement in calphostin C-induced apoptosis. *Biochemical Pharmacology* 56 (11) (Dec 1): 1489-92.

Splettstoesser, T. 2013, "Schematic description of the mechanism of the four classes of currently available antiviral drugs against HIV", http://commons.wikimedia.org/wiki/File:HIV-drug-classes.svg#

Stamataki, P., A. Papazafiropoulou, I. Elefsiniotis, M. Giannakopoulou, H. Brokalaki, E. Apostolopoulou, P. Sarafis, and G. Saroglou. 2010. Prevalence of HPV infection among greek women attending a gynecological outpatient clinic. *BMC Infectious Diseases* 10 (Feb 15): 27,2334-10-27.

Suneja, G., M. S. Shiels, S. K. Melville, M. A. Williams, R. Rengan, and E. A. Engels. 2013. Disparities in the treatment and outcomes of lung cancer among HIV-infected individuals. *AIDS (London, England)* 27 (3) (Jan 28): 459-68.

Susin, S. A., E. Daugas, L. Ravagnan, K. Samejima, N. Zamzami, M. Loeffler, P. Costantini, et al. 2000. Two distinct pathways leading to nuclear apoptosis. *The Journal of Experimental Medicine* 192 (4) (Aug 21): 571-80.

Szwagierczak, A., S. Bultmann, C. S. Schmidt, F. Spada, and H. Leonhardt. 2010. Sensitive enzymatic quantification of 5-hydroxymethylcytosine in genomic DNA. *Nucleic Acids Research* 38 (19) (Oct): e181.

Tan, C., L. Q. Cai, W. Wu, Y. Qiao, J. Imperato-McGinley, G. Q. Chen, and Y. S. Zhu. 2009. NSC606985, a novel camptothecin analog, induces apoptosis and growth arrest in prostate tumor cells. *Cancer Chemotherapy and Pharmacology* 63 (2) (Jan): 303-12.

Tan, J., B. Wang, and L. Zhu. 2009. Regulation of survivin and bcl-2 in HepG2 cell apoptosis induced by quercetin. *Chemistry & Biodiversity* 6 (7) (Jul): 1101-10.

Terman, B. I., M. E. Carrion, E. Kovacs, B. A. Rasmussen, R. L. Eddy, and T. B. Shows. 1991. Identification of a new endothelial cell growth factor receptor tyrosine kinase. *Oncogene* 6 (9) (Sep): 1677-83.

Terman, B. I., M. Dougher-Vermazen, M. E. Carrion, D. Dimitrov, D. C. Armellino, D. Gospodarowicz, and P. Bohlen. 1992. Identification of the KDR tyrosine kinase as a receptor for vascular endothelial cell growth factor. *Biochemical and Biophysical Research Communications* 187 (3) (Sep 30): 1579-86.

Torres, S. M., D. M. Walker, M. M. Carter, D. L. Cook Jr, C. L. McCash, E. M. Cordova, O. A. Olivero, M. C. Poirier, and V. E. Walker. 2007. Mutagenicity of zidovudine, lamivudine, and abacavir following in vitro exposure of human lymphoblastoid cells or in utero exposure of CD-1 mice to single agents or drug combinations. *Environmental and Molecular Mutagenesis* 48 (3-4) (Apr-May): 224-38.

Thabethe K. Adefolaju G. Hosie M. 2013. An *In Vitro* Study of the Effects of Emtricitabine, Tenofovir Disoproxil Fumarate and Efavirenz on a Breast Cancer Cell Line, MCF-7. *J. Basic. Appl. Sci. Res.*, 3(4)444-452

The National Toxicology Programme (NTP) Interagency Centre for the Evaluation of Alternative Toxicological Methods (NICEATM), 2003. Test method protocol for the NHK neutral red uptake cytotoxicity test. pp. 1-20.

The South African Antiretroviral Treatment Guidelines, 2010. Department of Health. Republic of South Africa

Tsuruta, F., N. Masuyama, and Y. Gotoh. 2002. The phosphatidylinositol 3-kinase (PI3K)-akt pathway suppresses bax translocation to mitochondria. *The Journal of Biological Chemistry* 277 (16) (Apr 19): 14040-7.

Tu, H. P., Y. T. Chen, H. C. Chiu, Y. T. Chin, S. M. Huang, L. C. Cheng, E. Fu, and C. Y. Chiang. 2009. Cyclosporine A enhances apoptosis in gingival keratinocytes of rats and in OECM1 cells via the mitochondrial pathway. *Journal of Periodontal Research* 44 (6) (Dec): 767-75.

UNAIDS 2013, Joint United Nations Programme on HIV/AIDS Update on the Global AIDS epidemic.

UNAIDS/WHO 2012. UNAIDS Report on the Global AIDS epidemic.

Vaisman, N., Gospodarowicz, D., Neufeld, G. 1990, "Characterization of the receptors for vascular endothelial growth factor". *The Journal of Biological Chemistry*, 265:19461–6.

van der Burg, S. H., and J. M. Palefsky. 2009. Human immunodeficiency virus and human papilloma virus - why HPV-induced lesions do not spontaneously resolve and why therapeutic vaccination can be successful. *Journal of Translational Medicine* 7 (Dec 18): 108,5876-7-108.

Van Phuc, P., P. L. Nhan, T. H. Nhung, N. T. Tam, N. M. Hoang, V. G. Tue, D. T. Thuy, and P. K. Ngoc. 2011. Downregulation of CD44 reduces doxorubicin resistance of CD44CD24 breast cancer cells. *OncoTargets and Therapy* 4 : 71-8.

Vaux, D. L., S. Cory, and J. M. Adams. 1988. Bcl-2 gene promotes haemopoietic cell survival and cooperates with c-myc to immortalize pre-B cells. *Nature* 335 (6189) (Sep 29): 440-2.

Venhoff, N., B. Setzer, K. Melkaoui, and U. A. Walker. 2007. Mitochondrial toxicity of tenofovir, emtricitabine and abacavir alone and in combination with additional nucleoside reverse transcriptase inhibitors. *Antiviral Therapy* 12 (7): 1075-85.

Vlahakis, S. R., S. A. Bennett, S. N. Whitehead, and A. D. Badley. 2007. HIV protease inhibitors modulate apoptosis signaling in vitro and in vivo. *Apoptosis : An International Journal on Programmed Cell Death* 12 (5) (May): 969-77.

Voutsadakis, I. A., and L. R. Silverman. 2002. Breast cancer in HIV-positive women: A report of four cases and review of the literature. *Cancer Investigation* 20 (4): 452-7.

Vrouenraets, S. M., F. W. Wit, J. van Tongeren, and J. M. Lange. 2007. Efavirenz: A review. *Expert Opinion on Pharmacotherapy* 8 (6) (Apr): 851-71.

Wall, Monroe E., M. C. Wani, C. E. Cook, Keith H. Palmer, A. T. McPhail, and G. A. Sim. 1966. Plant antitumor agents. I. the isolation and structure of camptothecin, a novel alkaloidal leukemia and tumor inhibitor from camptotheca acuminata1,2. *Journal of the American Chemical Society* 88 (16) (08/01; 2014/07): 3888-90

Wan, W., and P. B. DePetrillo. 2002. Ritonavir inhibition of calcium-activated neutral proteases. *Biochemical Pharmacology* 63 (8) (Apr 15): 1481-4.

Wang, K., X. M. Yin, D. T. Chao, C. L. Milliman, and S. J. Korsmeyer. 1996. BID: A novel BH3 domain-only death agonist. *Genes & Development* 10 (22) (Nov 15): 2859-69.

Wang, L. H., J. Begley, R. L. St Claire 3rd, J. Harris, C. Wakeford, and F. S. Rousseau. 2004. Pharmacokinetic and pharmacodynamic characteristics of emtricitabine support its once daily dosing for the treatment of HIV infection. *AIDS Research and Human Retroviruses* 20 (11) (Nov): 1173-82.

Weaver, J. G., A. Tarze, T. C. Moffat, M. Lebras, A. Deniaud, C. Brenner, G. D. Bren, et al. 2005. Inhibition of adenine nucleotide translocator pore function and protection against apoptosis in vivo by an HIV protease inhibitor. *The Journal of Clinical Investigation* 115 (7) (Jul): 1828-38.

Wickstrom, S. A., K. C. Masoumi, S. Khochbin, R. Fassler, and R. Massoumi. 2010. CYLD negatively regulates cell-cycle progression by inactivating HDAC6 and increasing the levels of acetylated tubulin. *The EMBO Journal* 29 (1) (Jan 6): 131-44.

Wolf, T., S. Findhammer, B. Nolte, E. B. Helm, and H. R. Brodt. 2003. Inhibition of TNF-alpha mediated cell death by HIV-1 specific protease inhibitors. *European Journal of Medical Research* 8 (1) (Jan 28): 17-24.

Woolard, J., W. Y. Wang, H. S. Bevan, Y. Qiu, L. Morbidelli, R. O. Pritchard-Jones, T. G. Cui, et al. 2004. VEGF165b, an inhibitory vascular endothelial growth factor splice variant: Mechanism of action, in vivo effect on angiogenesis and endogenous protein expression. *Cancer Research* 64 (21) (Nov 1): 7822-35.

Wright, S., X. Lu, and B. M. Peterlin. 1994. Human immunodeficiency virus type 1 tat directs transcription through attenuation sites within the mouse c-myc gene. *Journal of Molecular Biology* 243 (4) (Nov 4): 568-73.

Wu, K. M., M. W. Powley, and H. Ghantous. 2012. Timing of carcinogenicity studies and predictability of genotoxicity for tumorigenicity in anti-HIV drug development. *International Journal of Toxicology* 31 (3) (Jun): 211-21.

Yang, S., M. Liu, N. Liang, Q. Zhao, Y. Zhang, W. Xue, and S. Yang. 2013. Discovery and antitumor activities of constituents from cyrtomium fortumei (J.) smith rhizomes. *Chemistry Central Journal* 7 (1) (Feb 4): 24,153X-7-24.

Yikrazuul, 2008, "Structural formula of ritonavir" http://en.wikipedia.org/wiki/File:Ritonavir.svg

Zeng, C. W., X. J. Zhang, K. Y. Lin, H. Ye, S. Y. Feng, H. Zhang, and Y. Q. Chen. 2012. Camptothecin induces apoptosis in cancer cells via microRNA-125b-mediated mitochondrial pathways. *Molecular Pharmacology* 81 (4) (Apr): 578-86.

Zucchetto, A., B. Suligoi, A. De Paoli, S. Pennazza, J. Polesel, S. Bruzzone, G. Rezza, P. De Paoli, L. Dal Maso, and D. Serraino. 2010. Excess mortality for non-AIDS-defining cancers among people with AIDS. *Clinical Infectious Diseases : An Official Publication of the Infectious Diseases Society of America* 51 (9) (Nov 1): 1099-101.

APPENDIX A

A1

Solutions recipes

Phosphate Buffered Saline (PBS) pH 7.4; 8g NaC*l*, 1.15g Na_2HPO4, 0.2g KC*l*, 0.2g KH_2PO4.
Dissolve the salts in 800ml distilled water (dH_2O); adjust the pH of the solution to 7.4. Add 200ml dH_2O to make up 1*l*.

10% Phosphate buffered Formalin: Formaldehyde (37-40%) 100 ml, Distilled water 900 ml, NaH_2PO_4 4.0 g, Na_2HPO_4 (anhydrous) 6.5 g, pH 7.2 ± 0.5

4% Formaldehyde in PBS; 400µl formaldehyde, 9.6ml PBS
Mix the above solutions to make-up 10ml of 4% formaldehyde in PBS.

1% BSA in PBS; 10g bovine serum albumin (BSA), 1litre PBS
Dissolve 10g of BSA in 1*l* of PBS.

10X PBS; 80g NaC*l*, 11.5g Na_2HPO4, 2g KC*l*, 2g KH_2PO4
Dissolve the salts in 800ml dH2O adjust the pH of the solution to 7.4. Add 200ml dH_2O to make up 1*l*.

Blocking buffer (1XPBS/5% normal goat serum/ 0.3% Triton X-100); 2.5ml of 10X PBS, 1.25ml normal goat serum, 21.25ml dH_2O. Mix the solutions well and add 75µl of Triton X-100 while stirring to make-up 25ml of the blocking buffer.

Antibody dilution buffer (1X PBS/1%BSA/0.3% Triton X-100); 4ml of 10X PBS, 36ml dH_2O, 0.4g BSA. Mix the solutions with BSA and add 120µl of Triton X-100 while stirring, to make up 40ml of the antibody dilution buffer

10x TBE; 0.9 M Tris, 0.89 M boric acid and 25 mM EDTA, pH 8.3. This stock solution was diluted 1/10 for the electrophoresis of agarose gels.

10x TE; 1M Tris; Tris (hydroxymethyl) aminomethane - 60.57 g in 0.5L milliQ water (pH to 8.0 using HC*l*) 0.5M EDTA; Diaminoethane tetraacetic acid - 18.6 g in 100ml milliQ water (pH to 8.0 using NaOH - EDTA will not be soluble until pH reaches 8.0)
Component for 500ml TE buffer; 1M Tris pH 8* 5ml, 0.5M EDTA pH 8 1ml, dH_2O 496ml. TE buffer was used to solubilise DNA, while protecting it from degradation.

6 Glycerol BPB Gel-loading Buffer: 30 % glycerol, 0.3 % Bromophenol blue and 0.3 % Xylene cyanol.

10x MOPS: 200 mM 3-[N-mophonolino] propane sulphuric acid (MOPS), 50 mM sodium acetate, 10 mM EDTA.

A2

Table A1: List of reagents and suppliers

CHEMICAL	**SUPPLIER**
Absolute ethanol	Merck KGaA, Darmstadt, Germany
Bovine serum albumin V	Roche, Mannheim, Germany
DAPI (4', 6'-diamidino-2-phenylindole)	Sigma, Munich, Germany
Diethylpyrocarbonate	Sigma, Munich, Germany
EDTA (Ethylene diamine tetra acetic acid)	Sigma, Munich, Germany
Glacial acetic acid	Merck KGaA, Darmstadt, Germany
Hydrochloric acid	Merck KGaA, Darmstadt, Germany
Methanol	Sigma, Munich, Germany
MOPS (4-Morpholine propanesulphonic acid)	Sigma, Munich, Germany
Paraformaldehyde	Sigma, Munich, Germany
Sodium hydroxide	Merck KGaA, Darmstadt, Germany
Tris (Tris[hydroxymethyl] aminoethane)	Merck KGaA, Darmstadt, Germany
Triton X-100 (iso-octylphenoxypoly-ethoxyethanol)	Sigma, Munich, Germany
Trypsin	Invitrogen, Paisley, UK

A3

JCRB1090 [NCE 16IIA]

Profile: HPV16 transformed normal cells derived from human cervix.

Date accepted:	04/04/2001
Previous cell Number:	NIHS0265
Animal:	human
Sex and Age:	F :adult
Race:	Japanese
Scientific Name:	Homo sapiens
Classification:	transformed
Tissue prepared:	cervix
History of the cell:	Cells deposited from the original developper.
Medium:	MCDB153 medium with hormones, serum free medium. Less than 0.5% serum can be added in stead of hormones. See the Extra documents on details.
Passage method:	Cells are harvested with 0.1% trypsin and 0.1% EDTA. Medium change every 2 days and subculture every 10 days.
Cell no. at passage:	1.5 - 2.4 x 10^5 cells/sq.cm.
Genetics:	teromerase positive, HPV16, p75 NTR positive.
Life span:	infinite
Morphology:	epithelial-like
Characteristics:	HPV16 transformed noraml human cells from cervix
DNA Profile:	D5S818:12 D13S317:11,12 D7S820:8,11 D16S539:11,12 VWA:16,18 TH01:7 Amelogenin:X TPOX:9,12 CSF1PO:11,12
Established by	Yasumoto, S.
Deposited by	Yasumoto, S.
Special notice:	Not applied.
Cell bank:	NIHS(JCRB)

JCRB1203 [HCS-2]

Profile: Human squamous cell carcinoma from uterine cervix.

Date accepted: 04/15/2005	
Previous cell Number:	NIHS0405
Animal:	human
Sex and Age:	F :42
Race:	Japanese
Scientific Name:	Homo sapiens
Classification:	tumor
Tissue prepared:	uterine cervix
Origin of tumor:	squamous cell carcinoma
Date cell culture started:	11/08/1983
History of the cell:	Kitasato Univ. -> JCRB Cell Bank
Medium:	Eagle's minimal essential medium with 15% fetal calf serum.
Passage method:	Harvested with 0.1% trypsin and 0.02% EDTA
CO_2 Concentration:	5%
Cell no. at passage:	1 x 10^5 cells/ml
Genetics:	squamous cell carcinma
Life span:	Infinite
Morphology:	epithelial-like
Characteristics:	squamous cell carcinoma
Cell ID data:	**Available**
DNA Profile (STR):	D5S818:11,12 D13S317:11 D7S820:10,12 D16S539:9,10 VWA:18 TH01:6 Amelogenin:X TPOX:9,11 CSF1PO:10
Virus DNA detected:	CMV(-), EBV(-), HHV6(-), HHV7(-), BKJ(-), JCV(-), ADV1(-), parvoB19(-), HBV(-), HTL HTLV2(-), HIV1(-), HIV2(-), HPV18(+) [-/negative, +/positive, nt/not tested]
Established by	Morisawa,T. & Kuramoto, H.
Deposited by	Kuramoto, H. **Cell bank:** NIHS(JCRB)

Cell Line Designation: MCF 10A
ATCC® Catalog No. CRL-10317™

Table of Contents:

- Cell Line Description
- Biosafety Level
- Use Restrictions
- Handling Procedure for Frozen Cells
- Handling Procedure for Flask Cultures
- Medium Renewal
- Complete Growth Medium
- Cryoprotectant Medium
- References
- Warranty

Cell Line Description

Organism: *Homo sapiens* (human)

Tissue: mammary gland; breast; fibrocystic disease;
Age: 36 years

Gender: female **Morphology:**
epithelial **Growth properties:**
adherent

Tumorigenic: no; The cells were not tumorigenic in immunosuppressed mice, but did form colonies in semisolid medium.

DNA profile (STR analysis):

Amelogenin: X
CSF1PO: 10,12
D13S317: 8,9
D16S539: 11,12
D5S818: 10,13
D7S820: 10,11
TH01: 8,9.3
TPOX: 9,11
vWA: 15,17

Depositors: Michigan Cancer Foundation

Comments: The MCF 10A cell line is a non-tumorigenic epithelial cell line. The line was produced by long term culture in serum free medium with low Ca++ concentration.

MCF 10A was derived from adherent cells in the population. Cells derived from a floating population are available (see MCF 10F, ATCC CRL-10318). The cells are positive for epithelial sialomucins, cytokeratins and milk fat globule antigen.

They exhibit three dimensional growth in collagen, and form domes in confluent cultures. Thus far, the cells have shown no signs of terminal differentiation or senescence.

The line is responsive to insulin, glucocorticoids, cholera enterotoxin, and epidermal growth factor (EGF). By electron microscopy the cells display characteristics of luminal ductal cells but not of myoepithelial cells. They also express breast specific antigens as detected by positive reaction with MFA-Breast and MC-5 monoclonal antibodies. The calcium content of the medium exerts a strong effect on the morphology of the cells.

Karyotype: aneuploid human female; 48, XX, +8, +16, 3p-, 6p+, 9p+

Note: Cytogenetic information is based on initial seed stock at ATCC. Cytogenetic instability has been reported in the literature for some cell lines.

Biosafety Level: 1

Appropriate safety procedures should always be used with this material. Laboratory safety is discussed in the following publication: *Biosafety in Microbiological and Biomedical Laboratories,* 5th ed. HHS Publication No. (CDC) 93-8395. U.S. Department of Health and Human Services, Centers for Disease Control and Prevention. Washington DC: U.S. Government Printing Office; 2007. The entire text is available online at www.cdc.gov/od/ohs/biosfty/bmbl4/bmbl4toc.htm.

Use Restrictions

These cells are distributed for research purposes only.

Cell lines and hybridomas deposited for patent purposes are not always screened for contamination, antibody production or characterized by the ATCC. Release of a culture, the use of which may be claimed in a patent, from the ATCC during the effective term of any such patent is not meant to carry with it, and does not grant any license, express or implied, under any patent, or the right to use a culture in any process described in a patent.

The above culture was deposited in the ATCC in connection with a patent application. Copies of U.S. Patents may be obtained from the Commissioner of Patents, U.S. Patent and Trademark Office, Box 9, Washington, D.C. 20231.

This material is cited in a U.S and/or other Patent and may not be used to infringe the patent claims

ATCC

Product Sheet

MCF7 (ATCC® HTB-22™)

Please read this FIRST

Storage Temp.
liquid nitrogen vapor phase

Biosafety Level
1

Intended Use

This product is intended for research use only. It is not intended for any animal or human therapeutic or diagnostic use.

Complete Growth Medium

The base medium for this cell line is ATCC-formulated Eagle's Minimum Essential Medium, Catalog No. 30-2003. To make the complete growth medium, add the following components to the base medium: 0.01 mg/ml human recombinant insulin; fetal bovine serum to a final concentration of 10%.

Citation of Strain

If use of this culture results in a scientific publication, it should be cited in that manuscript in the following manner: MCF7 (ATCC® HTB-22™)

Description

Organism: *Homo sapiens*, human
Tissue:
mammary gland/breast; derived from metastatic site: pleural effusion **Disease:** adenocarcinoma
Cell Type: epithelial
Age: 69 years adult
Gender: female
Morphology: epithelial
Growth Properties: adherent
Isoenzymes:
AK-1, 1
ES-D, 1-2
G6PD, B
GLO-I, 1-2
PGM1, 1-2
PGM3, 1
DNA Profile:
Amelogenin: X
CSF1PO: 10
D13S317: 11
D16S539:
11,12 D5S818:
11,12 D7S820:
8,9 THO1: 6
TPOX: 9,12
vWA: 14,15
Cytogenetic Analysis: modal number = 82; range = 66 to 87.
The stemline chromosome numbers ranged from hypertriploidy to hypotetraploidy, with the 2S component occurring at 1%. There were 29 to 34 marker chromosomes per S metaphase; 24 to 28 markers occurred in at least 30% of cells, and generally one large submetacentric (M1) and 3 large subtelocentric (M2, M3, and M4) markers were recognizable in over 80% of metaphases. No DM were detected. Chromosome 20 was nullisomic and X was disomic.

Batch-Specific Information

Refer to the Certificate of Analysis for batch-specific test results.

SAFETY PRECAUTION

ATCC highly recommends that protective gloves and clothing always be used and a full face mask always be worn when handling frozen vials. It is important to note that some vials leak when submersed in liquid nitrogen and will slowly fill with liquid nitrogen. Upon thawing, the conversion of the liquid nitrogen back to its gas phase may result in the vessel exploding or blowing off its cap with dangerous force creating flying debris.

Unpacking & Storage Instructions

1. Check all containers for leakage or breakage.
2. Remove the frozen cells from the dry ice packaging and immediately place the cells at a temperature below -130°C, preferably in liquid nitrogen vapor, until ready for use.

American Type Culture Collection
PO Box 1549
Manassas, VA 20108
USA www.atcc.org

800.638.6597 or 703.365.2700 Fax: 703.365.2750
Email: Tech@atcc.org

Or contact your local distributor

APPENDIX B

B1 Procedure for total RNA extraction

The growth medium was removed from the cells ($5x10^6$ cells were used per extraction). Cells were rinsed once with PBS to remove residual medium. After discarding PBS, cells were detached from the culture dish by trypsinization. Cells were transfered into a microcentrifuge tube and pelleted by centrifugation for 5 min at 250 x g. The supernatant was discarded and the cells were resuspended in 600 µl of Lysis Buffer supplemented with β-mercaptoethanol. The mixture was vortexed for 10 sec to mix thoroughly. Due to the fact that incomplete homogenisation will result in a significant reduction of RNA yields, the mixture was homogenised with a disposable homogeniser-QIAshredder (QIAGEN®, USA) for 5 mins at 14000g (Hermle Z229, Zeiss, West Germany). After homogenisation, 360 µl of ethanol (96-100%) was added and the lysate mixed by pipetting. Up to 700 µl of lysate was added to the GeneJET RNA Purification Column inserted in a collection tube. The column was centrifuged (Hermle Z229, Zeiss, West Germany) for 1 min at 12000 x g. The flow-through was discarded and the purification column placed back into the collection tube. This step was repeated until all of the lysate has been transferred into the column and centrifuged. The collection tube containing the flow-through solution was then discarded. The GeneJET RNA Purification Column was then placed into a new 2 ml collection tube. 700 µl of Wash Buffer 1 (supplemented with ethanol) was added to the GeneJET RNA Purification Column and centrifuged (Hermle Z229, Zeiss, West Germany) for 1 min at 12000 x g. The flow-through was discarded and the purification column placed back into the collection tube. Wash Buffer 2 (600 µl) (supplemented with ethanol) was added to the GeneJET RNA Purification Column and centrifuged (Hermle Z229, Zeiss, West Germany) for 1 min at 12000 x g. The flow-through was discarded and the purification column placed back into the collection tube. Wash Buffer 2 (supplemented with ethanol) (250 µl) was added to the GeneJET RNA Purification Column and centrifuged (Hermle Z229, Zeiss, West Germany) for 2 min at 12000 x g. Residual solution was removed in the purification column by emptying the collection tube and re-spinning the column for 1 min at maximum speed. The collection tube containing the flow-through solution was discarded and the GeneJET RNA Purification Column was transferred to a sterile 1.5 ml RNase-free microcentrifuge tube. Nuclease-free water (100 µl), was added to the center of the

GeneJET RNA Purification Column membrane and centrifuged (Hermle Z229, Zeiss, West Germany) for 1 min at 12000 x g to elute RNA.

B2 Procedure for RNA Gel Electrophoresis

A 10X FA gel buffer to pour the gel and to make enough FA gel running buffer to fill the electrophoresis tank was prepared. An appropriate amount of agarose, 10X FA gel buffer, and RNase-free water was prepared in a flask in the ratio; 1 g agarose, 10 ml 10X FA gel buffer and RNase-free water to 100 ml. The mixture was heated in a microwave, swirled occasionally until the agarose was dissolved. Care was taken not to let the agarose solution boil over as it becomes super-heated. The agarose was cooled to 65-70°C in a water bath and swirled to prevent uneven cooling. After cooling, 1.8 ml of 37% [12.3 M] formaldehyde and 1 μl of a 10 mg/ml ethidium bromide stock solution were added. The agarose solution was then poured onto a gel tray in a fume hood to a thickness of 3-5 mm and the comb inserted immediately before pouring. The gel was allowed to set for 30 minutes. It was ensured that there was enough space between the bottom of the comb and the gel tray (0.5-1.0 mm) to allow proper well formation and avoid sample leakage. Leaving the comb in the gel, the gel was placed in the electrophoresis tank. The tank was filled with 1X FA gel running buffer up to 1mm of liquid above the surface of the gel. Prior to running the gel, the comb was carefully removed and the gel was allowed to equilibrate in the 1X FA gel running buffer for 30 minutes. 5X RNA loading buffer was prepared and mixed with RNA samples in a ratio of 1: 4, incubated for 3-5 minutes at 65°C to denature RNA and chilled on ice. Denatured samples were added to the wells already submerged in the electrophoresis buffer. The electrodes of the electrophoresis apparatus were connected so that the RNA migrated towards the anode (positive lead, red). The gel was run in a fume hood because of the formaldehyde fumes. The gel was run at 5-7V/cm until the bromophenol blue dye has migrated approximately 2/3 of the way through the gel. Ethidium bromide in the gel allows visualisation of the RNA with the UV light. Ethidium bromide-RNA complexes display increased fluorescence compared to the un-complexed dye in solution.

B3 Procedure for Genomic DNA (gDNA) Removal

Genomic DNA contamination was removed from total RNA according to the manufacturer's instructions, using the DNase I, RNase-free kit (Thermo Scientific, Pittsburgh PA. USA). 1 μg RNA was added to an RNase-free tube together with 10X reaction buffer containing $MgCl_2$ (1 μl), DNase I, RNase-free (1unit) and nuclease free water is added to 10 μl. The mixture was incubated at 37°C for 30 min. The DNAase I treated RNA was again cleaned with the GeneJET RNA Purification kit (Thermo Scientific, Pittsburgh PA. USA), re-quantified and stored at -80°C until used.

B4 Optimization for Immunofluorescence

A guide for cell staining was provided with the datasheet accompanying the primary and secondary antibodies used in this study, but to ensure specific antibody binding and optimal visualization of the target proteins, the following parameters required initial optimization; primary and secondary antibody dilutions, the blocking solution and duration and the duration of incubation with primary and secondary antibodies. The recommended dilution for polyclonal rabbit antihuman BAX (DAKO) was 1:1500 but a serial dilution of 1:500, 1:1000, 1:1500 and 1:2000 were tested and a final dilution of 1:1000 was considered optimal. The recommended dilution for monoclonal mouse antihuman Bcl2 (DAKO) was 1:50-1:100. Four serial dilutions at 1:50, 1:100, 1:200 and 1:500 were optimised and the 1:100 dilution considered optimal. The recommended dilution for polyclonal rabbit anti-human $VEGF_{165b}$ (ABCAM) was 5 μg/ml, but a concentration of 10 μg/ml was found to be optimal. Incubating cells with 10 % normal goat serum for 60 min was found to be more effective than 1% BSA in PBST for 30 min (according to the ABCAM double immunofluorescence – simultaneous protocol) at blocking unspecific binding of the antibodies. Incubating the cells with the primary antibodies overnight at 4°C gave better results compared to incubating the cells with the primary antibodies for 2 hours at room temperature.

B5

Double immunofluorescence – simultaneous protocol

abcam®
discover more

In order to be able to examine the co-distribution of two (or more) different antigens in the same sample, a double immunofluorescence procedure can be carried out. Primary antibodies raised in different species can be used either in parallel (in a mixture) or in a sequential way.

Preparation of slides and samples

1. Cell lines, cytology smears, cytospin preparations

1.1. Coat coverslips with polyethylineimine or poly-L-lysine for 1 hr at room temperature.

1.2. Rinse coverslips well with sterile H_2O (3 times 5 min each).

1.3. Allow coverslips to dry completely and sterilize them under UV light for at least 4 hrs.

1.4. Grow cells on glass coverslips or prepare cytospin or smear preparation.

1.5. Rinse briefly in phosphate-buffered saline (PBS).

2. Frozen (cryostat) sections

2.1. Snap frozen fresh tissue in liquid nitrogen or isopentane pre-cooled in liquid nitrogen. Store frozen blocks at -80°C.

2.2. Cut 4-8 µm thick cryostat sections and mount on superfrost or gelatin coated slides. You can store slides at -80°C until needed.

2.3. Before IF staining, warm up slides at room temperature for 30 minutes.

3. Paraffin-embedded sections

3.1. Deparaffinize sections in xylene 2x5 min.

3.2. Hydrate with 100% ethanol 2x3 min.

3.3. Hydrate with 95% ethanol 1 min.

3.4. Rinse in distilled water and then follow procedure for fixation and antigen retrieval as required (please see IHC protocol for formalin-fixed paraffin-embedded tissue sections for further details).

Fixation

1. Fix the samples either in ice-cold methanol, acetone (1-10 min) or in 3-4% paraformaldehyde in PBS pH 7.4 for 15 min at room temperature.
2. Wash the samples twice with ice cold PBS.

Permeabilization

If the target protein is expressed intracellularly, it is very important to permeabilize the cells. Note: acetone fixed samples do not require permeabilization.

3. Incubate the samples for 10 min with PBS containing 0.25% Triton X-100 (or 100 µM digitonin or 0.5% saponin). Triton X-100 is the most popular detergent for improving the penetration of the antibody. However, it is not appropriate for the use of membrane-associated antigens since it destroys membranes.

4. Wash cells in PBS three times for 5 mins.

Blocking and simultaneous incubation

5. Incubate cells with 1% BSA in PBST for 30 min to block unspecific binding of the antibodies (alternative blocking solutions are 1% gelatin or 10% serum from the species that the secondary antibody was raised in).

6. Incubate cells in **the mixture of two primary antibodies** (e.g. rabbit against human target-1 and mouse against human target-2, if the targets are human proteins) in 1% BSA in PBST in a humidified chamber for 1 hr at room temperature or overnight at 4°C.

7. Decant the mixture solution and wash the cells three times in PBS, 5 mins each wash.

8. Incubate cells with **the mixture of two secondary antibodies** which are raised in different species (with two different fluorochromes, i.e. Texas Red-conjugated against rabbit and FITC-conjugated against mouse) in 1% BSA for 1 hr at room temperature in dark.

9. Decant the mixture of the secondary antibody solution and wash three times with PBS for 5 min each in dark.

Counter staining

10. Incubate cells on 0.1-1 µg/ml Hoechst or DAPI (DNA stain) for 1 min.

11. Rinse with PBS.

Mounting

12. Mount coverslip with a drop of mounting medium.

13. Seal coverslip with nail polish to prevent drying and movement under microscope.

14. Store in dark at -20°C or 4°C.

APPENDIX C

Appendix C1: Primer properties and products on target templates for all genes

Table C1: *BAX* primer properties and products on target templates

	Forward primer	**Reverse primer**		
Sequence (5'->3')	CCTTTTCTACTTTGCCAGCAAAC	GAGGCCGTCCCAACCAC		
Length	23	17		
Tm	58.95	60.01		
GC%	43.48	70.59		
Self complementarity	8	4		
Self 3' complementarity	6	0		
Products on target templates			>NM_138763.3 Homo sapiens BCL2-associated X protein (*BAX*), transcript variant delta, mRNA	>NM_138761.3 Homo sapiens BCL2-associated X protein (*BAX*), transcript variant alpha, mRNA
Product Length			148	148
Forward primer Template			258 280	405 427
Reverse primer Template			405 389	552 536

Table C2: *BCL-2* primer properties and products on target templates

	Forward primer	**Reverse primer**		
Sequence (5'->3')	ATGTGTGTGGAGAGC GTCAACC	GCATCCCAGCCTC CGTTATC		
Length	22	20		
Tm	59.6	60.6		
GC%	50	60		
Self complementarity	2	3		
Self 3' complementarity	0	2		
Products on target templates			>NM_000633.2 Homo sapiens B-cell CLL/lymphoma 2 (BCL2), transcript variant alpha, mRNA	>NM_000657.2 Homo sapiens B-cell CLL/lymphoma 2 (BCL2), transcript variant beta, mRNA
Product Length			122	122
Forward primer Template			962……..981	962…....981
Reverse primer Template			1083…...1064	1083… 1064

Table C3: *VEGF165A* primer properties and products on target templates

	Forward primer	**Reverse primer**	
Sequence (5'->3')	CAAGATCCGCAG ACGTGTAA	GCTTGTCACATCT GCAAGTA	
Length	20	20	
Tm	58.01	56.07	
GC%	50	45	
Self complementarity	4	8	
Self 3' complementarity	1	4	
Products on target templates			>NM_001025368.2 Homo sapiens vascular endothelial growth factor A (VEGFA), transcript variant 4, mRNA

Product Length			100
Forward primer Template			1504.....1523
Reverse primer Template			1603…….....1584

Table C4: *VEGF165B* primer properties and products on target templates

	Forward primer	**Reverse primer**	
Sequence (5'->3')	CGCAGACGTGTAAATGTTCCTG	TTCCTGGTGAGAGATCTGCAAG	
Length	22	22	
Tm	60.16	59.76	
GC%	50	50	
Self complementarity	4	6	
Self 3' complementarity	2	2	
Products on target templates			>NM_001033756.2 Homo sapiens vascular endothelial growth factor A (VEGFA), transcript variant 7, mRNA
Product Length			97
Forward primer Template			1511…….. 1532
Reverse primer Template			1607…….....1586

Appendix C2: Amplification Plots of primer pairs for all genes

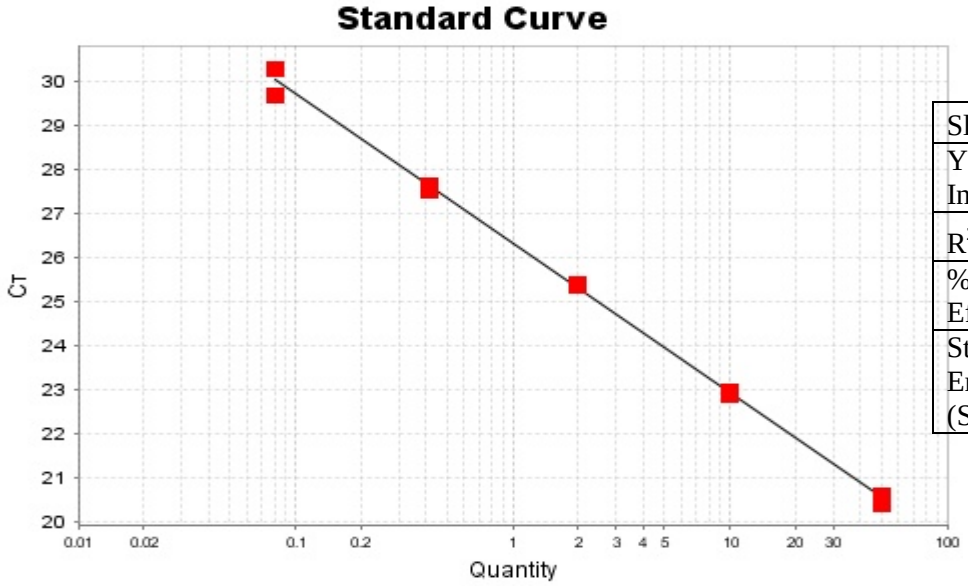

Slope	-3.38
Y-Intercept	26.29
R^2	0.99
% Efficiency	97.27
Standard Error (SE)	0.008

Figure C1: Amplification Plots of *BAX* primer pairs

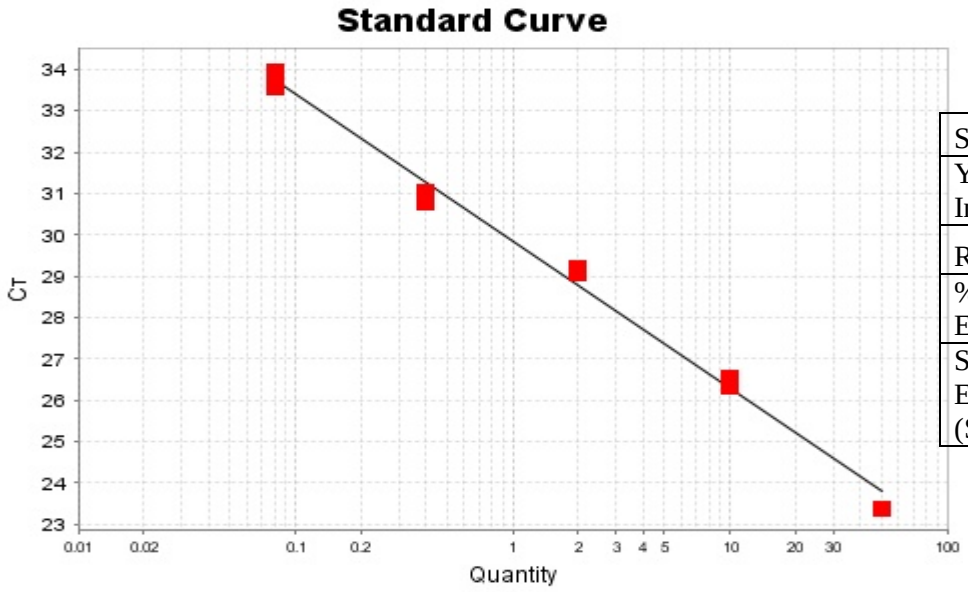

Slope	-3.55
Y-Intercept	29.8
R^2	0.99
% Efficiency	91.19
Standard Error (SE)	0.016

Figure C2: Amplification Plots of *BCL-2* primer pairs

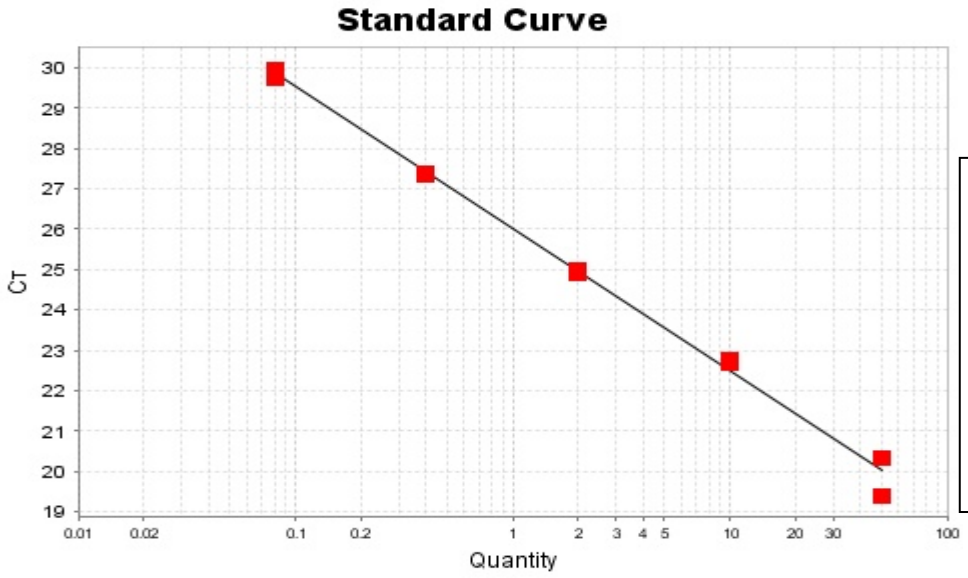

Slope	-3.53
Y-Intercept	26
R^2	0.99
% Efficiency	92.1
Standard Error (SE)	0.011

Figure C3: Amplification Plots of *VEGF165A* primer pairs

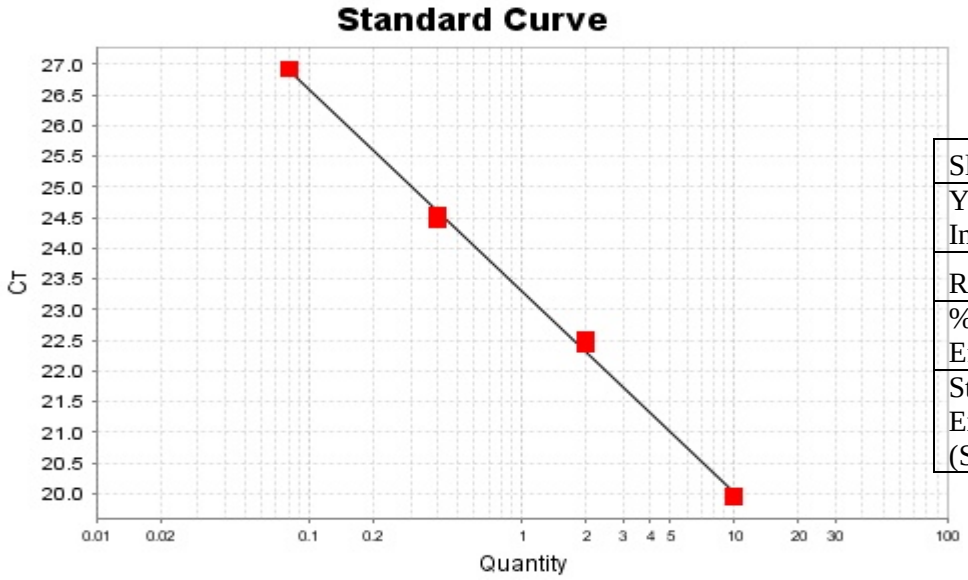

Slope	-3.28
Y-Intercept	23.29
R^2	0.99
% Efficiency	101.7
Standard Error (SE)	0.009

Figure C4: Amplification Plots of *VEGF165B* primer pairs

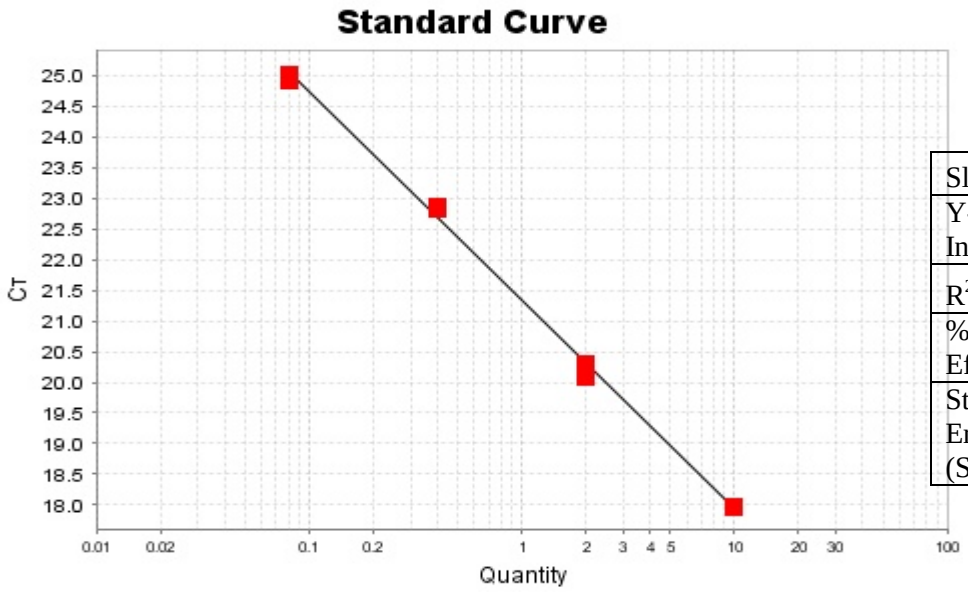

Slope	-3.39
Y-Intercept	21.33
R^2	0.99
% Efficiency	97.16
Standard Error (SE)	0.01

Figure C5: Amplification Plots of *TBP* primer pairs

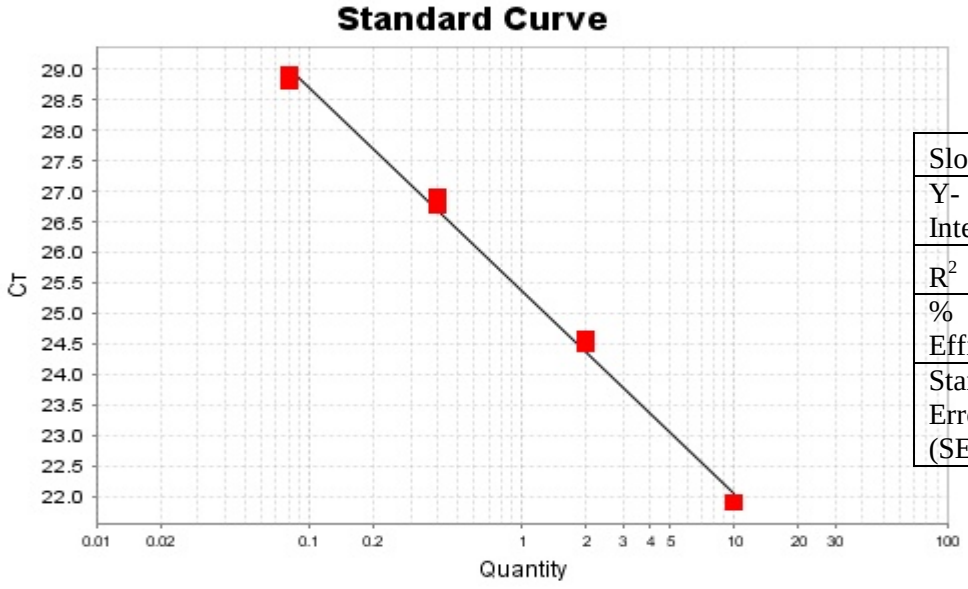

Slope	-3.31
Y-Intercept	25.37
R^2	0.99
% Efficiency	100.5
Standard Error (SE)	0.014

Figure C6: Amplification Plots of *TFRC* primer pairs

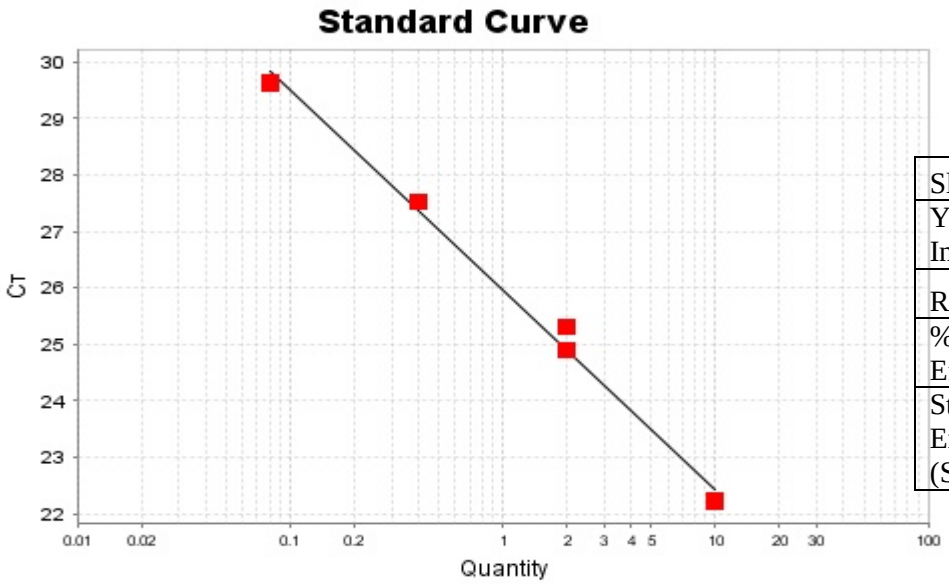

Slope	-3.53
Y-Intercept	25.95
R^2	0.99
% Efficiency	91.95
Standard Error (SE)	0.016

Figure C7: Amplification Plots of *RPLP0* primer pairs

Appendix C3: Melt curves generated for PCR products for all primer pairs to confirm the absence of primer dimers and nonspecific amplification.

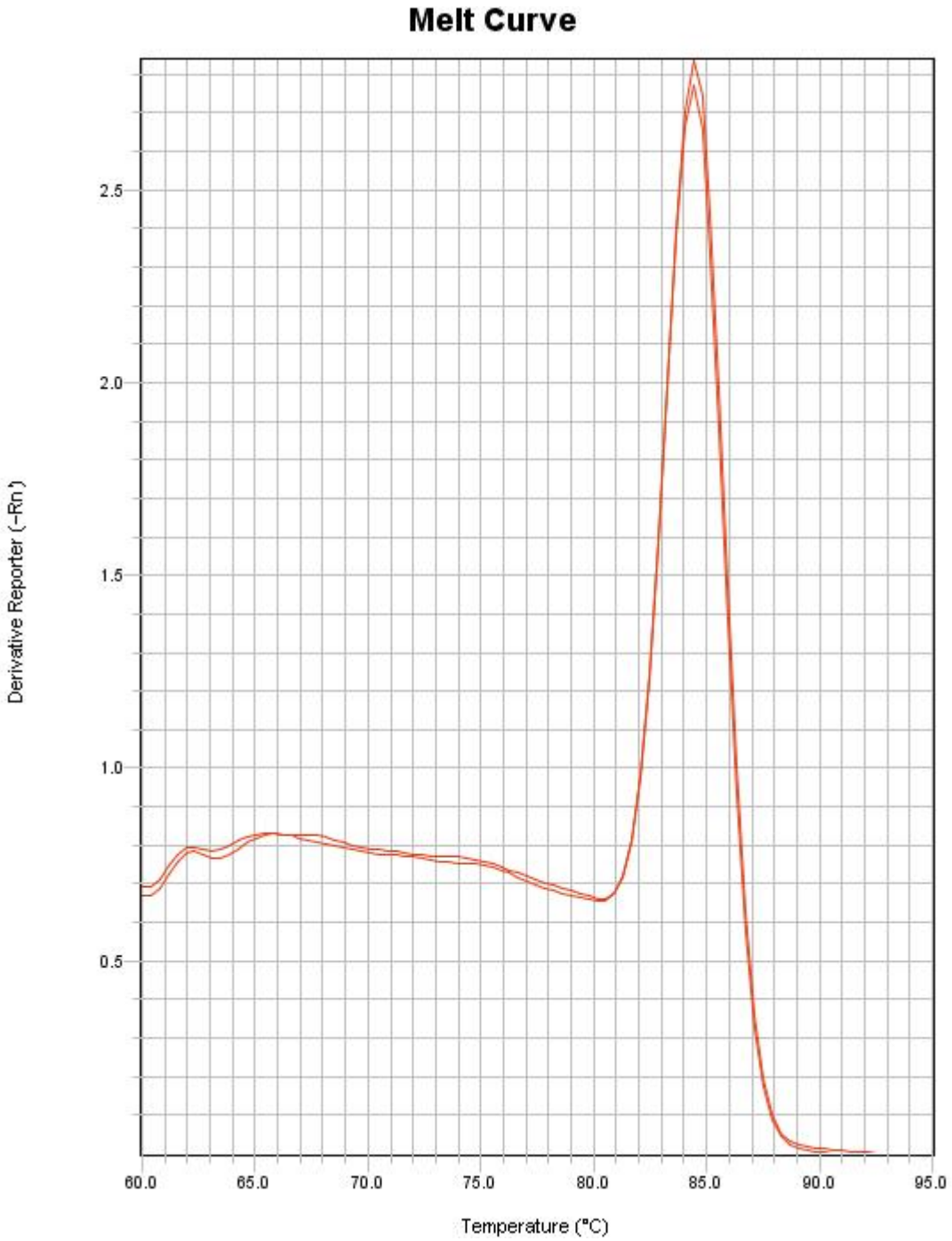

Figure C8: Melt curves generated for *BAX* PCR product to confirm the absence of primer dimers and nonspecific amplification. Melting Temperature of *BAX* PCR product=84.5^{0}C

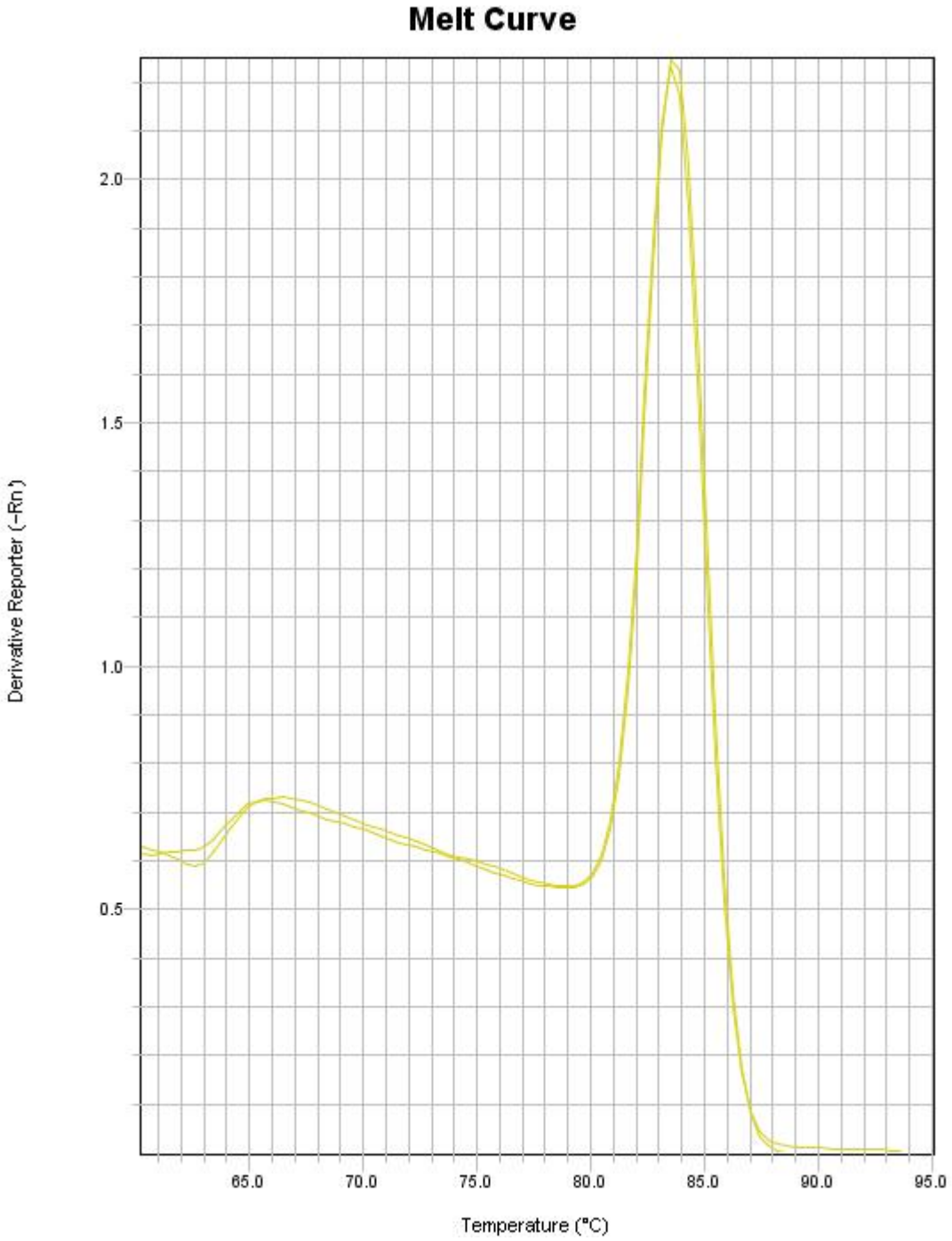

Figure C9: Melt curves generated for *BCL-2* PCR product to confirm the absence of primer dimers and nonspecific amplification. Melting Temperature of *BCL-2* PCR product=83.5^{0}C

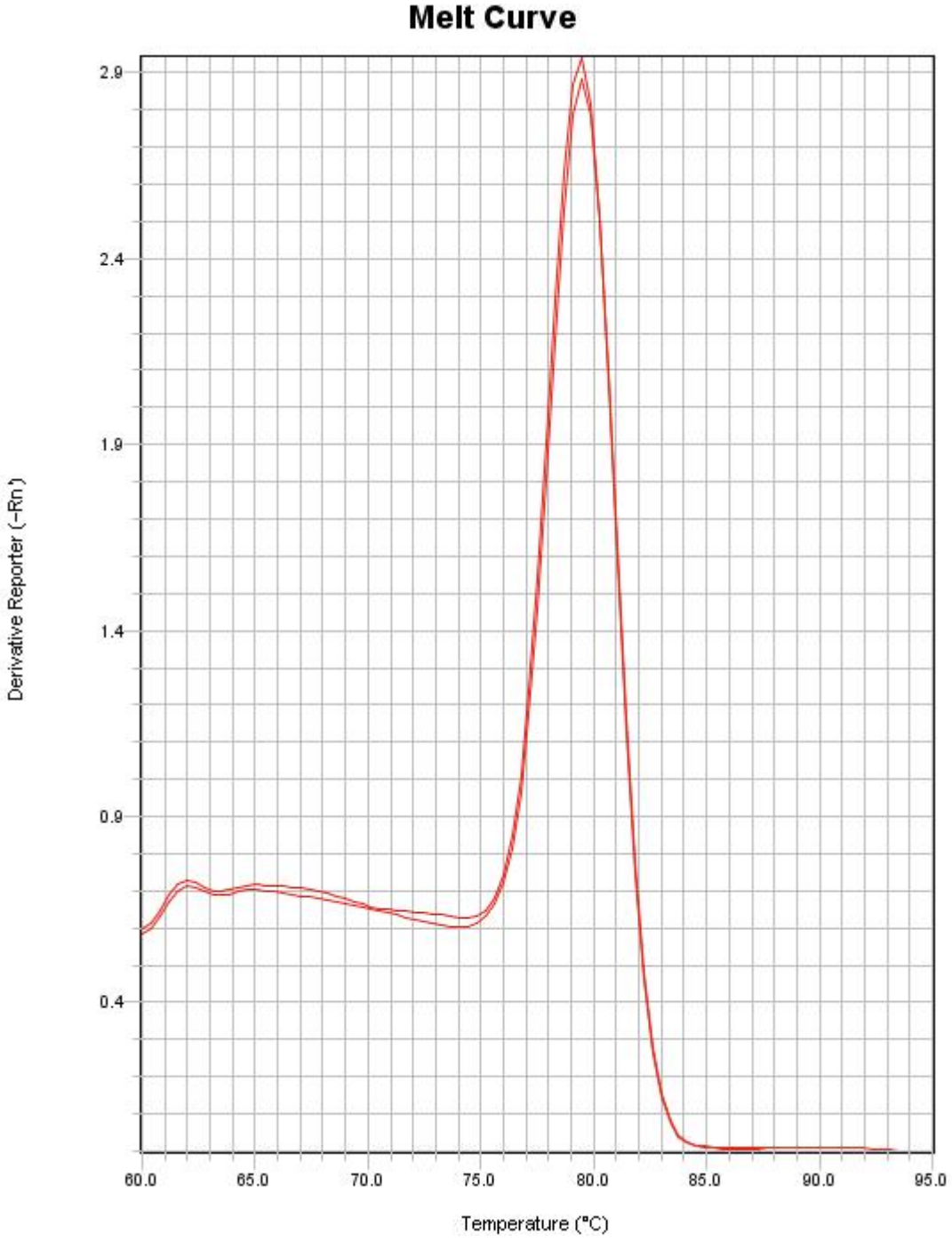

Figure C10: Melt curves generated for *VEGF165A* PCR product to confirm the absence of primer dimers and nonspecific amplification. Melting Temperature of *VEGF165A* PCR product=79.5^{0}C

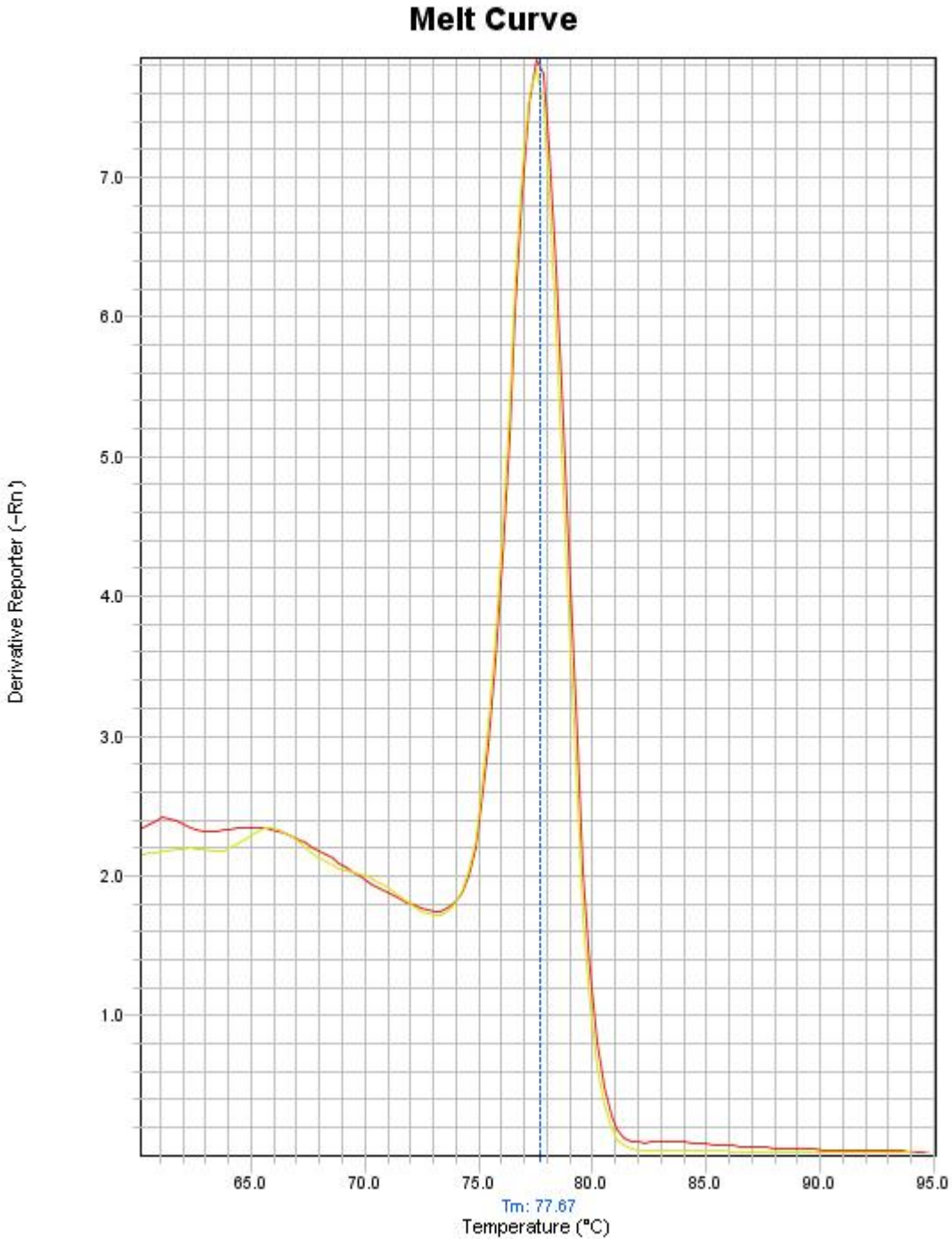

Figure C11: Melt curves generated for *VEGF165B* PCR product to confirm the absence of primer dimers and nonspecific amplification. Melting Temperature of *VEGF165B* PCR product=77.67^{0}C

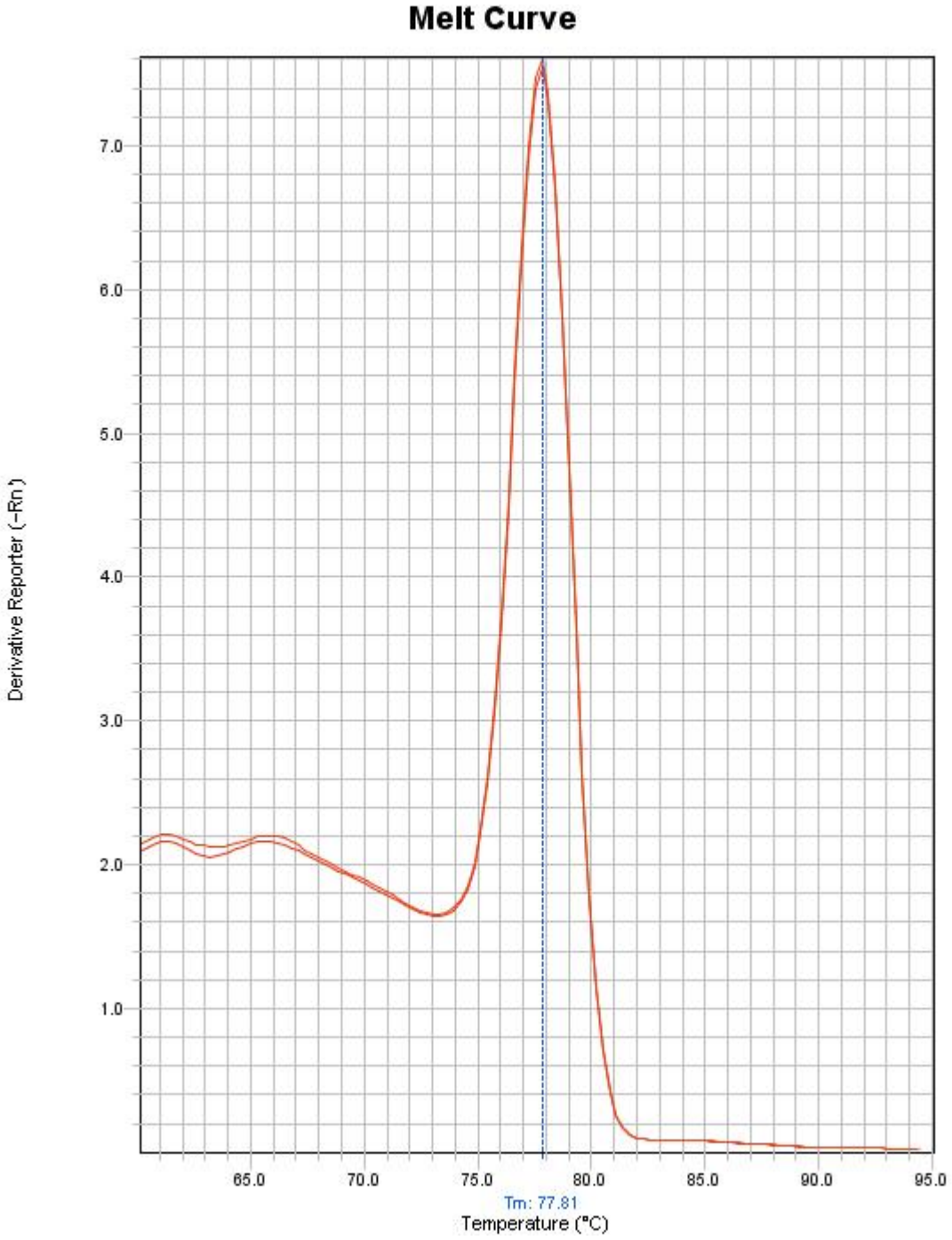

Figure C12: Melt curves generated for *TBP* PCR product to confirm the absence of primer dimers and nonspecific amplification. Melting Temperature of *TBP* PCR product=77.81^{0}C

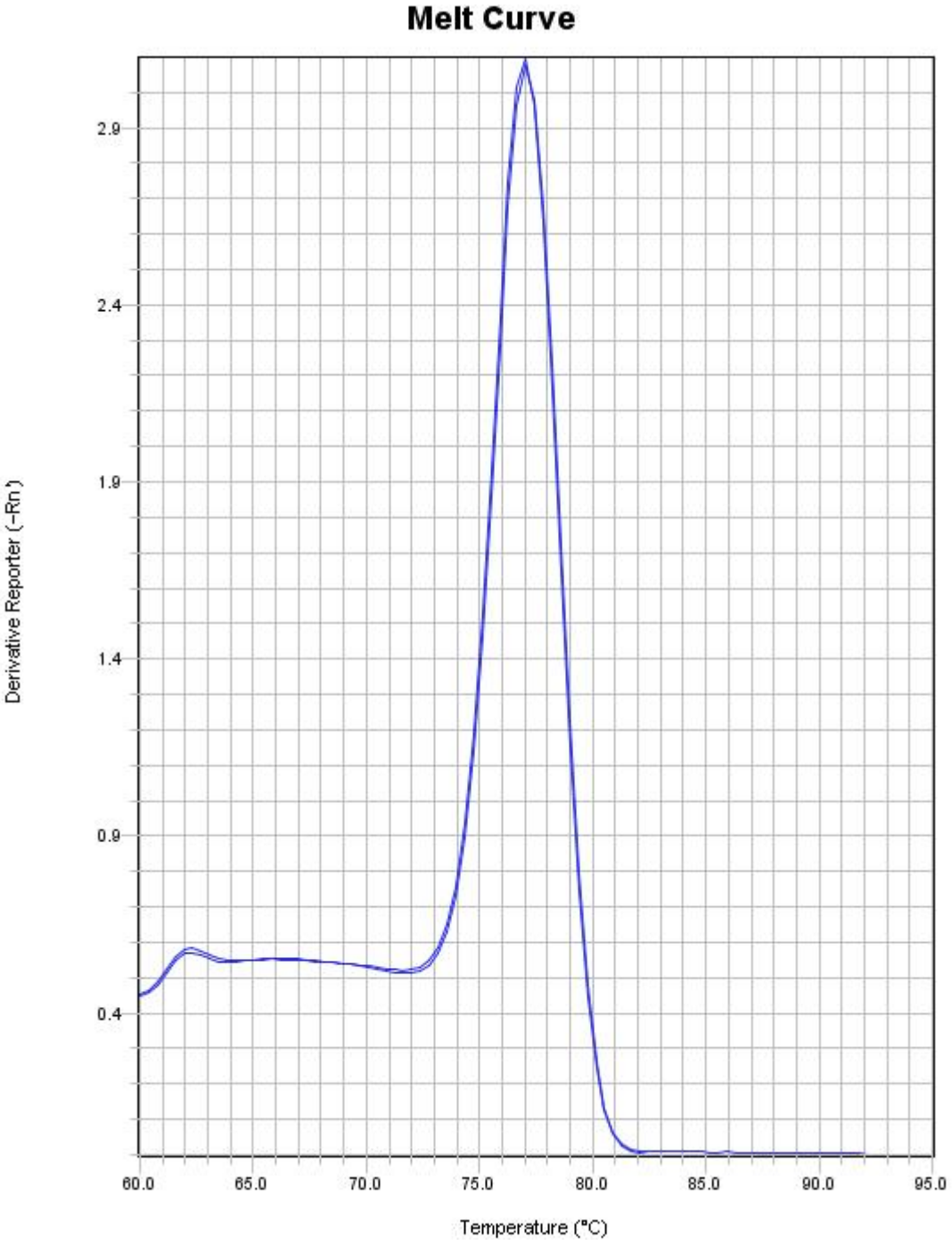

Figure C13: Melt curves generated for *TFRC* PCR product to confirm the absence of primer dimers and nonspecific amplification. Melting Temperature of *TFRC* PCR product=77.1^{0}C

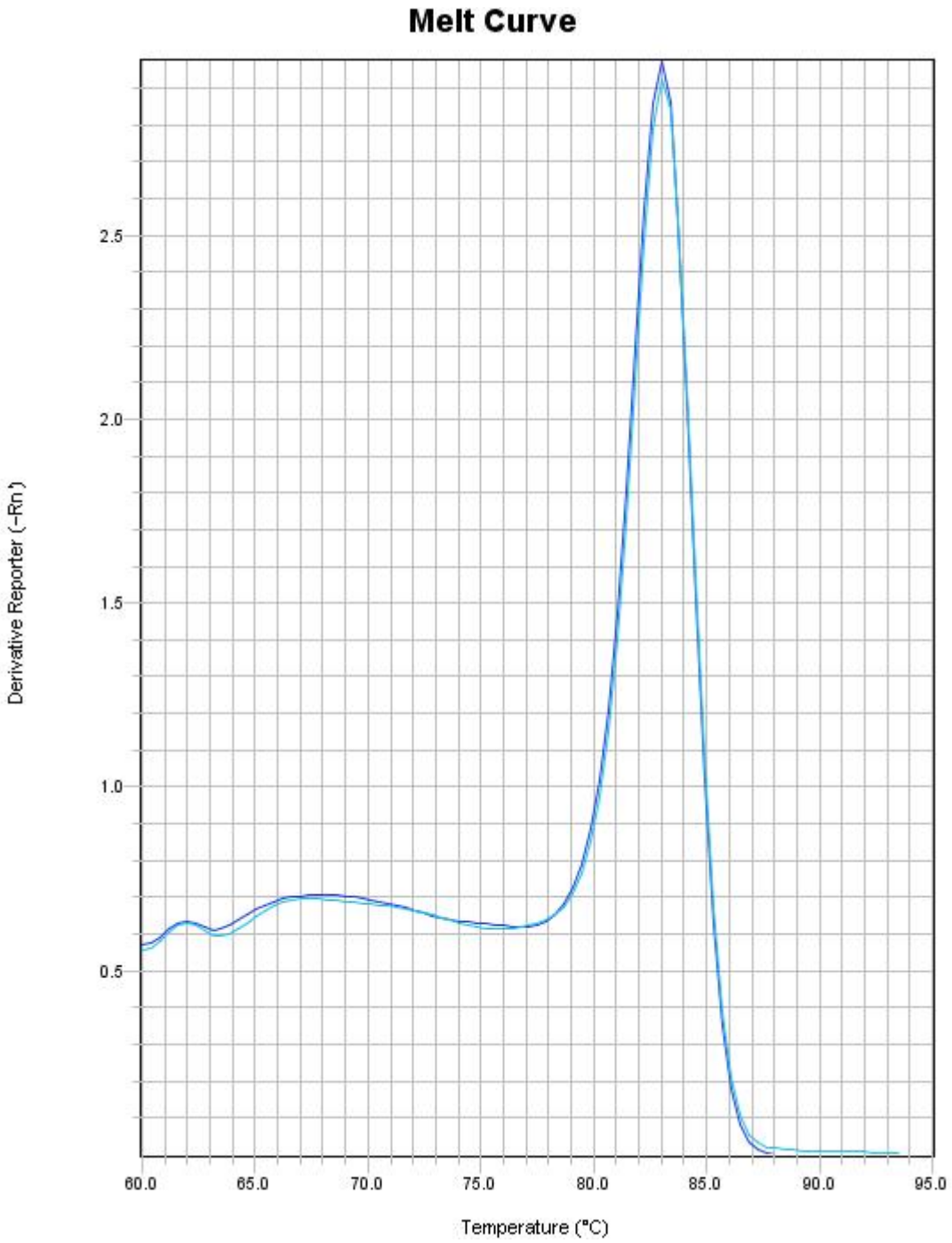

Figure C14: Melt curves generated for *RPLP0* PCR product to confirm the absence of primer dimers and nonspecific amplification. Melting Temperature of *RPLP0* PCR product=83.4^{0}C

Appendix C4

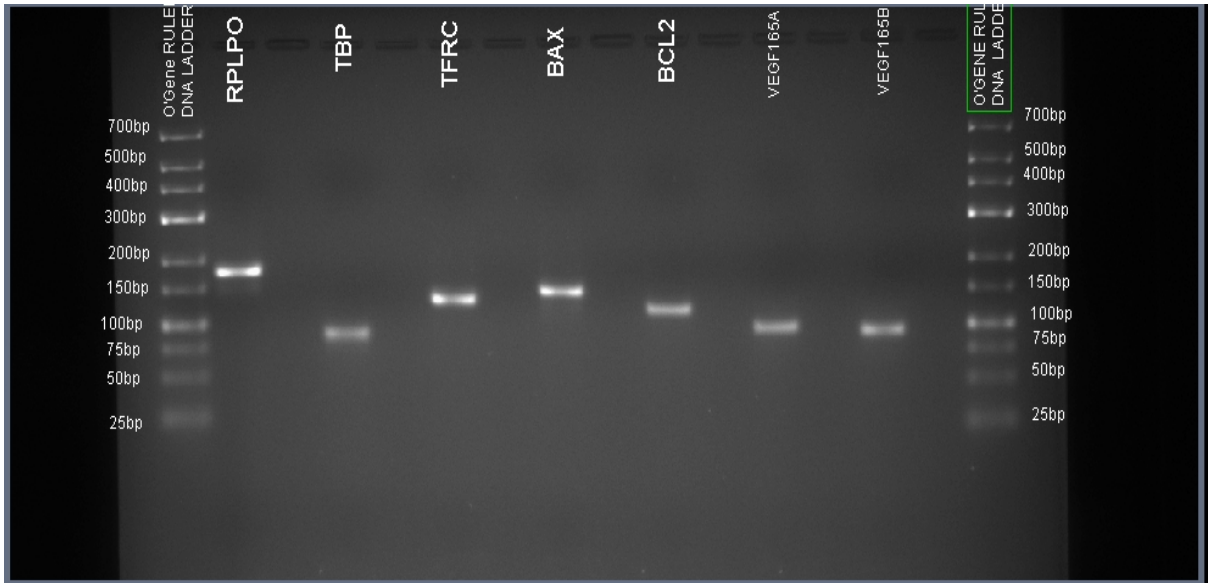

Figure C15: Agarose gel electrophoresis of PCR products confirming the absence of nonspecific amplification. The range of the DNA Ladder (O'GeneRuler Low Range - Thermo Scientific, Pittsburgh PA, USA) is 25bp to 700bp. *BAX* PCR product size (148bp), *BCL-2* PCR product size (122bp), *VEGF165A* PCR product size (100bp), *VEGF165B* PCR product size (97bp), *TBP* PCR product size (86bp), *TFRC* PCR product size (133bp), *RPLP0* PCR product size (178bp).

APPENDIX D1

Oneway Analysis of effects of TDF on % Viability of Cervical cells by Time

Summary of Fit

Rsquare	0.400157
Adj Rsquare	0.349034
Root Mean Square Error	10.27655
Mean of Response	101.2925
Observations (or Sum Wgts)	192

Analysis of Variance

Source	DF	Sum of Squares	Mean Square	F Ratio	Prob > F
Time	15	12399.399	826.627	7.8273	<.0001*
Error	176	18586.932	105.608		
C. Total	191	30986.332			

Means and Std Deviations

Level	Number	Mean	Std Dev	Std Err Mean	Lower 95%	Upper 95%
Normal control 24hrs	12	100.000	0.0000	0.0000	100.00	100.00
Normal control 48hrs	12	100.000	0.0000	0.0000	100.00	100.00
Normal control 72hrs	12	100.000	0.0000	0.0000	100.00	100.00
Normal control 96hrs	12	100.000	0.0000	0.0000	100.00	100.00
Normal treated 24hrs	12	117.818	12.0711	3.4846	110.15	125.49
Normal treated 48hrs	12	116.427	15.0109	4.3333	106.89	125.96
Normal treated 72hrs	12	110.505	10.5715	3.0517	103.79	117.22
Normal treated 96hrs	12	100.927	10.9538	3.1621	93.97	107.89
Cancer control 24hrs	12	100.000	0.0000	0.0000	100.00	100.00
Cancer control 48hrs	12	100.000	0.0000	0.0000	100.00	100.00
Cancer control 72hrs	12	100.000	0.0000	0.0000	100.00	100.00
Cancer control 96hrs	12	100.000	0.0000	0.0000	100.00	100.00
Cancer treated 24hrs	12	104.682	23.4962	6.7828	89.75	119.61
Cancer treated 48hrs	12	94.824	14.8406	4.2841	85.39	104.25
Cancer treated 72hrs	12	85.245	10.4093	3.0049	78.63	91.86
Cancer treated 96hrs	12	90.251	14.3622	4.1460	81.13	99.38

Comparisons for all pairs using Tukey-Kramer HSD

Confidence Quantile

q*	Alpha
3.47644	0.05

Connecting Letters Report

Level					Mean
Normal treated 24hrs	A				117.81796
Normal treated 48hrs	A				116.42730
Normal treated 72hrs	A	B			110.50502
Cancer treated 24hrs	A	B	C		104.68199
Normal treated 96hrs		B	C		100.92713
Normal control 24hrs		B	C		100.00000
Normal control 48hrs		B	C		100.00000
Normal control 72hrs		B	C		100.00000
Normal control 96hrs		B	C		100.00000
Cancer control 24hrs		B	C		100.00000
Cancer control 48hrs		B	C		100.00000
Cancer control 72hrs		B	C		100.00000
Cancer control 96hrs		B	C		100.00000
Cancer treated 48hrs			C	D	94.82405
Cancer treated 96hrs			C	D	90.25056
Cancer treated 72hrs				D	85.24546

Levels not connected by same letter are significantly different.

APPENDIX D2

Oneway Analysis of effects of TDF on % Viability of Breast cells by Time

Summary of Fit

Rsquare	0.386011
Adj Rsquare	0.333683
Root Mean Square Error	11.31143
Mean of Response	99.53261
Observations (or Sum Wgts)	192

Analysis of Variance

Source	DF	Sum of Squares	Mean Square	F Ratio	Prob > F
Time	15	14157.526	943.835	7.3767	<.0001*
Error	176	22518.928	127.948		
C. Total	191	36676.453			

Means and Std Deviations

Level	Number	Mean	Std Dev	Std Err Mean	Lower 95%	Upper 95%
Normal control 24hrs	12	100.000	0.0000	0.0000	100.00	100.00
Normal control 48hrs	12	100.000	0.0000	0.0000	100.00	100.00
Normal control 72hrs	12	100.000	0.0000	0.0000	100.00	100.00
Normal control 96hrs	12	100.000	0.0000	0.0000	100.00	100.00
Normal treated 24hrs	12	76.470	17.2227	4.9718	65.53	87.41
Normal treated 48hrs	12	113.955	12.6810	3.6607	105.90	122.01
Normal treated 72hrs	12	110.192	11.0624	3.1934	103.16	117.22
Normal treated 96hrs	12	111.891	10.1976	2.9438	105.41	118.37
Cancer control 24hrs	12	100.000	0.0000	0.0000	100.00	100.00
Cancer control 48hrs	12	100.000	0.0000	0.0000	100.00	100.00
Cancer control 72hrs	12	100.000	0.0000	0.0000	100.00	100.00
Cancer control 96hrs	12	100.000	0.0000	0.0000	100.00	100.00
Cancer treated 24hrs	12	98.432	23.5714	6.8045	83.46	113.41
Cancer treated 48hrs	12	87.056	18.0025	5.1969	75.62	98.49
Cancer treated 72hrs	12	95.741	19.8731	5.7369	83.11	108.37
Cancer treated 96hrs	12	98.784	9.4199	2.7193	92.80	104.77

Comparisons for all pairs using Tukey-Kramer HSD

Confidence Quantile

q*	Alpha
3.47644	0.05

Connecting Letters Report

Level					Mean
Normal treated 48hrs	A				113.95521
Normal treated 96hrs	A				111.89087
Normal treated 72hrs	A	B			110.19218
Normal control 24hrs	A	B	C		100.00000
Normal control 48hrs	A	B	C		100.00000
Normal control 72hrs	A	B	C		100.00000
Normal control 96hrs	A	B	C		100.00000
Cancer control 24hrs	A	B	C		100.00000
Cancer control 48hrs	A	B	C		100.00000
Cancer control 72hrs	A	B	C		100.00000
Cancer control 96hrs	A	B	C		100.00000
Cancer treated 96hrs	A	B	C		98.78367
Cancer treated 24hrs	A	B	C		98.43235
Cancer treated 72hrs		B	C		95.74097
Cancer treated 48hrs			C	D	87.05630
Normal treated 24hrs				D	76.47019

Levels not connected by same letter are significantly different.

APPENDIX D3

Oneway Analysis of effects of FTC on % Viability of Cervical cells by Time

Summary of Fit

Rsquare	0.229495
Adj Rsquare	0.163827
Root Mean Square Error	12.00947
Mean of Response	101.7945
Observations (or Sum Wgts)	192

Analysis of Variance

Source	DF	Sum of Squares	Mean Square	F Ratio	Prob > F
Time	15	7560.620	504.041	3.4948	<.0001*
Error	176	25384.013	144.227		
C. Total	191	32944.633			

Means and Std Deviations

Level	Number	Mean	Std Dev	Std Err Mean	Lower 95%	Upper 95%
Normal control 24hrs	12	100.000	0.0000	0.0000	100.00	100.00
Normal control 48hrs	12	100.000	0.0000	0.0000	100.00	100.00
Normal control 72hrs	12	100.000	0.0000	0.0000	100.00	100.00
Normal control 96hrs	12	100.000	0.0000	0.0000	100.00	100.00
Normal treated 24hrs	12	110.055	15.2043	4.3891	100.39	119.72
Normal treated 48hrs	12	108.949	15.9227	4.5965	98.83	119.07
Normal treated 72hrs	12	112.925	15.8747	4.5826	102.84	123.01
Normal treated 96hrs	12	85.292	14.5986	4.2142	76.02	94.57
Cancer control 24hrs	12	100.000	0.0000	0.0000	100.00	100.00
Cancer control 48hrs	12	100.000	0.0000	0.0000	100.00	100.00
Cancer control 72hrs	12	100.000	0.0000	0.0000	100.00	100.00
Cancer control 96hrs	12	100.000	0.0000	0.0000	100.00	100.00
Cancer treated 24hrs	12	103.477	18.3350	5.2929	91.83	115.13
Cancer treated 48hrs	12	95.236	22.1724	6.4006	81.15	109.32
Cancer treated 72hrs	12	105.845	9.4188	2.7190	99.86	111.83
Cancer treated 96hrs	12	106.932	21.0074	6.0643	93.58	120.28

Comparisons for all pairs using Tukey-Kramer HSD

Confidence Quantile

q*	Alpha
3.47644	0.05

Connecting Letters Report

Level				Mean
Normal treated 72hrs	A			112.92539
Normal treated 24hrs	A	B		110.05504
Normal treated 48hrs	A	B		108.94937
Cancer treated 96hrs	A	B		106.93161
Cancer treated 72hrs	A	B		105.84543
Cancer treated 24hrs	A	B		103.47662
Normal control 24hrs	A	B	C	100.00000
Normal control 48hrs	A	B	C	100.00000
Normal control 72hrs	A	B	C	100.00000
Normal control 96hrs	A	B	C	100.00000
Cancer control 24hrs	A	B	C	100.00000
Cancer control 48hrs	A	B	C	100.00000
Cancer control 72hrs	A	B	C	100.00000
Cancer control 96hrs	A	B	C	100.00000
Cancer treated 48hrs		B	C	95.23612
Normal treated 96hrs			C	85.29229

Levels not connected by same letter are significantly different.

APPENDIX D4

Oneway Analysis of effects of FTC on % Viability of Breast cells by Time

Summary of Fit

Rsquare	0.157168
Adj Rsquare	0.085335
Root Mean Square Error	12.05697
Mean of Response	98.62692
Observations (or Sum Wgts)	192

Analysis of Variance

Source	DF	Sum of Squares	Mean Square	F Ratio	Prob > F
Time	15	4771.018	318.068	2.1880	0.0083*
Error	176	25585.218	145.371		
C. Total	191	30356.236			

Means and Std Deviations

Level	Number	Mean	Std Dev	Std Err Mean	Lower 95%	Upper 95%
Normal control 24hrs	12	100.000	0.0000	0.0000	100.00	100.00
Normal control 48hrs	12	100.000	0.0000	0.0000	100.00	100.00
Normal control 72hrs	12	100.000	0.0000	0.0000	100.00	100.00
Normal control 96hrs	12	100.000	0.0000	0.0000	100.00	100.00
Normal treated 24hrs	12	109.333	12.8693	3.7150	101.16	117.51
Normal treated 48hrs	12	95.577	19.2952	5.5700	83.32	107.84
Normal treated 72hrs	12	93.355	15.1454	4.3721	83.73	102.98
Normal treated 96hrs	12	96.473	13.5340	3.9069	87.87	105.07
Cancer control 24hrs	12	100.000	0.0000	0.0000	100.00	100.00
Cancer control 48hrs	12	100.000	0.0000	0.0000	100.00	100.00
Cancer control 72hrs	12	100.000	0.0000	0.0000	100.00	100.00
Cancer control 96hrs	12	100.000	0.0000	0.0000	100.00	100.00
Cancer treated 24hrs	12	100.008	24.2170	6.9909	84.62	115.39
Cancer treated 48hrs	12	83.908	20.3348	5.8701	70.99	96.83
Cancer treated 72hrs	12	98.053	17.5382	5.0628	86.91	109.20
Cancer treated 96hrs	12	101.323	8.2402	2.3787	96.09	106.56

Comparisons for all pairs using Tukey-Kramer HSD

Confidence Quantile

q*	Alpha
3.47644	0.05

Connecting Letters Report

Level				Mean
Normal treated 24hrs	A			109.33316
Cancer treated 96hrs	A			101.32328
Cancer treated 24hrs	A	B		100.00809
Normal control 24hrs	A	B		100.00000
Normal control 48hrs	A	B		100.00000
Normal control 72hrs	A	B		100.00000
Normal control 96hrs	A	B		100.00000
Cancer control 24hrs	A	B		100.00000
Cancer control 48hrs	A	B		100.00000
Cancer control 72hrs	A	B		100.00000
Cancer control 96hrs	A	B		100.00000
Cancer treated 72hrs	A	B		98.05292
Normal treated 96hrs	A	B	C	96.47257
Normal treated 48hrs	A	B	C	95.57695
Normal treated 72hrs	A	B	C	93.35545
Cancer treated 48hrs			C	83.90825

Levels not connected by same letter are significantly different.

APPENDIX D5

Oneway Analysis of effects of EFV on % Viability of Cervical cells by Time

Summary of Fit

Rsquare	0.196665
Adj Rsquare	0.128199
Root Mean Square Error	15.3541
Mean of Response	100.0608
Observations (or Sum Wgts)	192

Analysis of Variance

Source	DF	Sum of Squares	Mean Square	F Ratio	Prob > F
Time	15	10157.614	677.174	2.8724	0.0005*
Error	176	41491.741	235.749		
C. Total	191	51649.355			

Means and Std Deviations

Level	Number	Mean	Std Dev	Std Err Mean	Lower 95%	Upper 95%
Normal control 24hrs	12	104.620	8.4035	2.4259	99.28	109.96
Normal control 48hrs	12	104.914	11.9183	3.4405	97.34	112.49
Normal control 72hrs	12	97.948	10.1678	2.9352	91.49	104.41
Normal control 96hrs	12	95.198	6.9494	2.0061	90.78	99.61
Normal treated 24hrs	12	105.911	20.4551	5.9049	92.91	118.91
Normal treated 48hrs	12	88.266	16.7104	4.8239	77.65	98.88
Normal treated 72hrs	12	99.019	12.2719	3.5426	91.22	106.82
Normal treated 96hrs	12	99.964	10.1948	2.9430	93.49	106.44
Cancer control 24hrs	12	102.842	13.2754	3.8323	94.41	111.28
Cancer control 48hrs	12	99.088	20.0293	5.7820	86.36	111.81
Cancer control 72hrs	12	101.878	24.8176	7.1642	86.11	117.65
Cancer control 96hrs	12	101.461	23.3571	6.7426	86.62	116.30
Cancer treated 24hrs	12	104.742	14.6382	4.2257	95.44	114.04
Cancer treated 48hrs	12	117.604	12.2421	3.5340	109.83	125.38
Cancer treated 72hrs	12	89.259	14.2236	4.1060	80.22	98.30
Cancer treated 96hrs	12	88.259	12.2522	3.5369	80.47	96.04

Comparisons for all pairs using Tukey-Kramer HSD

Confidence Quantile

q*	Alpha
3.47644	0.05

Connecting Letters Report

Level			Mean
Cancer treated 48hrs	A		117.60408
Normal treated 24hrs	A	B	105.91089
Normal control 48hrs	A	B	104.91403
Cancer treated 24hrs	A	B	104.74211
Normal control 24hrs	A	B	104.61958
Cancer control 24hrs	A	B	102.84158
Cancer control 72hrs	A	B	101.87779
Cancer control 96hrs	A	B	101.46113
Normal treated 96hrs	A	B	99.96434
Cancer control 48hrs	A	B	99.08842
Normal treated 72hrs	A	B	99.01855
Normal control 72hrs	A	B	97.94781
Normal control 96hrs	A	B	95.19797
Cancer treated 72hrs		B	89.25888
Normal treated 48hrs		B	88.26624
Cancer treated 96hrs		B	88.25888

Levels not connected by same letter are significantly different.

APPENDIX D6

Oneway Analysis of effects of EFV on % Viability of Breast cells by Time

Summary of Fit

Rsquare	0.75515
Adj Rsquare	0.734282
Root Mean Square Error	13.36748
Mean of Response	90.00757
Observations (or Sum Wgts)	192

Analysis of Variance

Source	DF	Sum of Squares	Mean Square	F Ratio	Prob > F
Time	15	96994.18	6466.28	36.1872	<.0001*
Error	176	31449.36	178.69		
C. Total	191	128443.54			

Means and Std Deviations

Level	Number	Mean	Std Dev	Std Err Mean	Lower 95%	Upper 95%
Normal control 24hrs	12	100.961	6.2315	1.7989	97.00	104.92
Normal control 48hrs	12	98.395	8.3918	2.4225	93.06	103.73
Normal control 72hrs	12	97.312	9.2757	2.6777	91.42	103.21
Normal control 96hrs	12	99.229	10.6578	3.0767	92.46	106.00
Normal treated 24hrs	12	24.714	8.9620	2.5871	19.02	30.41
Normal treated 48hrs	12	62.743	12.1717	3.5137	55.01	70.48
Normal treated 72hrs	12	65.743	18.9262	5.4635	53.72	77.77
Normal treated 96hrs	12	66.743	11.8115	3.4097	59.24	74.25
Cancer control 24hrs	12	103.253	13.7016	3.9553	94.55	111.96
Cancer control 48hrs	12	100.011	15.2025	4.3886	90.35	109.67
Cancer control 72hrs	12	97.947	16.0481	4.6327	87.75	108.14
Cancer control 96hrs	12	99.864	7.8385	2.2628	94.88	104.84
Cancer treated 24hrs	12	105.537	15.9173	4.5949	95.42	115.65
Cancer treated 48hrs	12	94.874	12.5722	3.6293	86.89	102.86
Cancer treated 72hrs	12	110.440	18.4099	5.3145	98.74	122.14
Cancer treated 96hrs	12	112.356	18.3246	5.2899	100.71	124.00

Comparisons for all pairs using Tukey-Kramer HSD

Confidence Quantile

q*	Alpha
3.47644	0.05

Connecting Letters Report

Level			Mean
Cancer treated 96hrs	A		112.35627
Cancer treated 72hrs	A		110.43960
Cancer treated 24hrs	A		105.53700
Cancer control 24hrs	A		103.25258
Normal control 24hrs	A		100.96127
Cancer control 48hrs	A		100.01121
Cancer control 96hrs	A		99.86396
Normal control 96hrs	A		99.22855
Normal control 48hrs	A		98.39523
Cancer control 72hrs	A		97.94729
Normal control 72hrs	A		97.31189
Cancer treated 48hrs	A		94.87380
Normal treated 96hrs		B	66.74290
Normal treated 72hrs		B	65.74289
Normal treated 48hrs		B	62.74289
Normal treated 24hrs			C 24.71374

Levels not connected by same letter are significantly different.

APPENDIX D7

Oneway Analysis of effects of ATP on % Viability of Cervical cells by Time

Summary of Fit

Rsquare	0.247947
Adj Rsquare	0.183852
Root Mean Square Error	16.28944
Mean of Response	102.4568
Observations (or Sum Wgts)	192

Analysis of Variance

Source	DF	Sum of Squares	Mean Square	F Ratio	Prob > F
Time	15	15396.981	1026.47	3.8684	<.0001*
Error	176	46700.870	265.35		
C. Total	191	62097.851			

Means and Std Deviations

Level	Number	Mean	Std Dev	Std Err Mean	Lower 95%	Upper 95%
Normal control 24hrs	12	104.620	8.4035	2.4259	99.28	109.96
Normal control 48hrs	12	104.914	11.9183	3.4405	97.34	112.49
Normal control 72hrs	12	97.948	10.1678	2.9352	91.49	104.41
Normal control 96hrs	12	95.198	6.9494	2.0061	90.78	99.61
Normal treated 24hrs	12	91.607	19.0147	5.4891	79.53	103.69
Normal treated 48hrs	12	90.582	17.3888	5.0197	79.53	101.63
Normal treated 72hrs	12	94.726	11.2261	3.2407	87.59	101.86
Normal treated 96hrs	12	91.815	8.6674	2.5021	86.31	97.32
Cancer control 24hrs	12	102.842	13.2754	3.8323	94.41	111.28
Cancer control 48hrs	12	99.088	20.0293	5.7820	86.36	111.81
Cancer control 72hrs	12	101.878	24.8176	7.1642	86.11	117.65
Cancer control 96hrs	12	101.461	23.3571	6.7426	86.62	116.30
Cancer treated 24hrs	12	110.655	13.9327	4.0220	101.80	119.51
Cancer treated 48hrs	12	118.129	14.6240	4.2216	108.84	127.42
Cancer treated 72hrs	12	120.341	22.0432	6.3633	106.34	134.35
Cancer treated 96hrs	12	113.507	19.5793	5.6521	101.07	125.95

Comparisons for all pairs using Tukey-Kramer HSD

Confidence Quantile

q*	Alpha
3.47644	0.05

Connecting Letters Report

Level				Mean
Cancer treated 72hrs	A			120.34065
Cancer treated 48hrs	A	B		118.12880
Cancer treated 96hrs	A	B	C	113.50732
Cancer treated 24hrs	A	B	C	110.65505
Normal control 48hrs	A	B	C	104.91403
Normal control 24hrs	A	B	C	104.61958
Cancer control 24hrs	A	B	C	102.84158
Cancer control 72hrs	A	B	C	101.87779
Cancer control 96hrs	A	B	C	101.46113
Cancer control 48hrs	A	B	C	99.08842
Normal control 72hrs	A	B	C	97.94781
Normal control 96hrs		B	C	95.19797
Normal treated 72hrs			C	94.72556
Normal treated 96hrs			C	91.81477
Normal treated 24hrs			C	91.60749
Normal treated 48hrs			C	90.58152

Levels not connected by same letter are significantly different.

APPENDIX D8

Oneway Analysis of effects of ATP on % Viability of Breast cells by Time

Summary of Fit

Rsquare	0.200193
Adj Rsquare	0.132027
Root Mean Square Error	14.32635
Mean of Response	99.60847
Observations (or Sum Wgts)	192

Analysis of Variance

Source	DF	Sum of Squares	Mean Square	F Ratio	Prob > F
Time	15	9041.622	602.775	2.9369	0.0004*
Error	176	36122.987	205.244		
C. Total	191	45164.609			

Means and Std Deviations

Level	Number	Mean	Std Dev	Std Err Mean	Lower 95%	Upper 95%
Normal control 24hrs	12	100.961	6.2315	1.7989	97.00	104.92
Normal control 48hrs	12	98.395	8.3918	2.4225	93.06	103.73
Normal control 72hrs	12	97.312	9.2757	2.6777	91.42	103.21
Normal control 96hrs	12	99.229	10.6578	3.0767	92.46	106.00
Normal treated 24hrs	12	80.202	21.4543	6.1933	66.57	93.83
Normal treated 48hrs	12	99.450	17.6067	5.0826	88.26	110.64
Normal treated 72hrs	12	98.616	13.7489	3.9690	89.88	107.35
Normal treated 96hrs	12	99.700	21.5245	6.2136	86.02	113.38
Cancer control 24hrs	12	103.253	13.7016	3.9553	94.55	111.96
Cancer control 48hrs	12	100.011	15.2025	4.3886	90.35	109.67
Cancer control 72hrs	12	97.947	16.0481	4.6327	87.75	108.14
Cancer control 96hrs	12	99.864	7.8385	2.2628	94.88	104.84
Cancer treated 24hrs	12	109.558	15.2805	4.4111	99.85	119.27
Cancer treated 48hrs	12	101.093	17.5171	5.0568	89.96	112.22
Cancer treated 72hrs	12	114.314	14.9684	4.3210	104.80	123.82
Cancer treated 96hrs	12	93.830	7.0836	2.0449	89.33	98.33

Comparisons for all pairs using Tukey-Kramer HSD

Confidence Quantile

q*	Alpha
3.47644	0.05

Connecting Letters Report

Level				Mean
Cancer treated 72hrs	A			114.31409
Cancer treated 24hrs	A	B		109.55800
Cancer control 24hrs	A	B		103.25258
Cancer treated 48hrs	A	B		101.09348
Normal control 24hrs	A	B		100.96127
Cancer control 48hrs	A	B	C	100.01121
Cancer control 96hrs	A	B	C	99.86396
Normal treated 96hrs	A	B	C	99.69982
Normal treated 48hrs	A	B	C	99.44982
Normal control 96hrs	A	B	C	99.22855
Normal treated 72hrs	A	B	C	98.61649
Normal control 48hrs	A	B	C	98.39523
Cancer control 72hrs	A	B	C	97.94729
Normal control 72hrs	A	B	C	97.31189
Cancer treated 96hrs		B	C	93.83001
Normal treated 24hrs			C	80.20178

Levels not connected by same letter are significantly different.

APPENDIX D9

Oneway Analysis of effects of LPV on % Viability of Cervical cells by Time

Summary of Fit

Rsquare	0.246833
Adj Rsquare	0.182643
Root Mean Square Error	15.80714
Mean of Response	98.97962
Observations (or Sum Wgts)	192

Analysis of Variance

Source	DF	Sum of Squares	Mean Square	F Ratio	Prob > F
Time	15	14412.244	960.816	3.8453	<.0001*
Error	176	43976.369	249.866		
C. Total	191	58388.613			

Means and Std Deviations

Level	Number	Mean	Std Dev	Std Err Mean	Lower 95%	Upper 95%
Normal control 24hrs	12	104.620	8.4035	2.4259	99.28	109.96
Normal control 48hrs	12	104.914	11.9183	3.4405	97.34	112.49
Normal control 72hrs	12	97.948	10.1678	2.9352	91.49	104.41
Normal control 96hrs	12	95.198	6.9494	2.0061	90.78	99.61
Normal treated 24hrs	12	83.305	16.5049	4.7646	72.82	93.79
Normal treated 48hrs	12	86.671	15.5202	4.4803	76.81	96.53
Normal treated 72hrs	12	94.027	13.1159	3.7862	85.69	102.36
Normal treated 96hrs	12	96.724	19.5782	5.6517	84.28	109.16
Cancer control 24hrs	12	102.842	13.2754	3.8323	94.41	111.28
Cancer control 48hrs	12	99.088	20.0293	5.7820	86.36	111.81
Cancer control 72hrs	12	101.878	24.8176	7.1642	86.11	117.65
Cancer control 96hrs	12	101.461	23.3571	6.7426	86.62	116.30
Cancer treated 24hrs	12	115.366	15.2685	4.4076	105.66	125.07
Cancer treated 48hrs	12	116.027	17.5876	5.0771	104.85	127.20
Cancer treated 72hrs	12	92.136	13.2591	3.8276	83.71	100.56
Cancer treated 96hrs	12	91.470	10.3803	2.9965	84.87	98.07

Comparisons for all pairs using Tukey-Kramer HSD

Confidence Quantile

q*	Alpha
3.47644	0.05

Connecting Letters Report

Level			Mean
Cancer treated 48hrs	A		116.02716
Cancer treated 24hrs	A		115.36553
Normal control 48hrs	A	B	104.91403
Normal control 24hrs	A	B	104.61958
Cancer control 24hrs	A	B	102.84158
Cancer control 72hrs	A	B	101.87779
Cancer control 96hrs	A	B	101.46113
Cancer control 48hrs	A	B	99.08842
Normal control 72hrs	A	B	97.94781
Normal treated 96hrs	A	B	96.72358
Normal control 96hrs	A	B	95.19797
Normal treated 72hrs	A	B	94.02653
Cancer treated 72hrs		B	92.13641
Cancer treated 96hrs		B	91.46974
Normal treated 48hrs		B	86.67140
Normal treated 24hrs		B	83.30528

Levels not connected by same letter are significantly different.

APPENDIX D10

Oneway Analysis of effects of LPV on % Viability of Breast cells by Time

Summary of Fit

Rsquare	0.463325
Adj Rsquare	0.417585
Root Mean Square Error	13.27362
Mean of Response	101.7714
Observations (or Sum Wgts)	192

Analysis of Variance

Source	DF	Sum of Squares	Mean Square	F Ratio	Prob > F
Time	15	26771.029	1784.74	10.1297	<.0001*
Error	176	31009.243	176.19		
C. Total	191	57780.272			

Means and Std Deviations

Level	Number	Mean	Std Dev	Std Err Mean	Lower 95%	Upper 95%
Normal control 24hrs	12	100.961	6.2315	1.7989	97.00	104.92
Normal control 48hrs	12	98.395	8.3918	2.4225	93.06	103.73
Normal control 72hrs	12	97.312	9.2757	2.6777	91.42	103.21
Normal control 96hrs	12	99.229	10.6578	3.0767	92.46	106.00
Normal treated 24hrs	12	63.991	10.1815	2.9391	57.52	70.46
Normal treated 48hrs	12	111.708	11.9766	3.4574	104.10	119.32
Normal treated 72hrs	12	114.542	17.5199	5.0576	103.41	125.67
Normal treated 96hrs	12	113.208	15.0140	4.3342	103.67	122.75
Cancer control 24hrs	12	103.253	13.7016	3.9553	94.55	111.96
Cancer control 48hrs	12	100.011	15.2025	4.3886	90.35	109.67
Cancer control 72hrs	12	97.947	16.0481	4.6327	87.75	108.14
Cancer control 96hrs	12	99.864	7.8385	2.2628	94.88	104.84
Cancer treated 24hrs	12	106.649	13.7934	3.9818	97.88	115.41
Cancer treated 48hrs	12	94.477	18.0611	5.2138	83.00	105.95
Cancer treated 72hrs	12	112.481	15.8847	4.5855	102.39	122.57
Cancer treated 96hrs	12	114.314	14.9684	4.3210	104.80	123.82

Comparisons for all pairs using Tukey-Kramer HSD

Confidence Quantile

q*	Alpha
3.47644	0.05

Connecting Letters Report

Level				Mean
Normal treated 72hrs	A			114.54158
Cancer treated 96hrs	A			114.31409
Normal treated 96hrs	A	B		113.20826
Cancer treated 72hrs	A	B		112.48076
Normal treated 48hrs	A	B		111.70824
Cancer treated 24hrs	A	B		106.64879
Cancer control 24hrs	A	B		103.25258
Normal control 24hrs	A	B		100.96127
Cancer control 48hrs	A	B		100.01121
Cancer control 96hrs	A	B		99.86396
Normal control 96hrs	A	B		99.22855
Normal control 48hrs	A	B		98.39523
Cancer control 72hrs	A	B		97.94729
Normal control 72hrs	A	B		97.31189
Cancer treated 48hrs		B		94.47673
Normal treated 24hrs			C	63.99143

Levels not connected by same letter are significantly different.

APPENDIX D11

Oneway Analysis of effects of RTV on % Viability of Cervical cells by Time

Summary of Fit

Rsquare	0.085086
Adj Rsquare	0.00711
Root Mean Square Error	15.71516
Mean of Response	99.74839
Observations (or Sum Wgts)	192

Analysis of Variance

Source	DF	Sum of Squares	Mean Square	F Ratio	Prob > F
Time	15	4042.297	269.486	1.0912	0.3676
Error	176	43466.066	246.966		
C. Total	191	47508.363			

Means and Std Deviations

Level	Number	Mean	Std Dev	Std Err Mean	Lower 95%	Upper 95%
Normal control 24hrs	12	104.620	8.4035	2.4259	99.280	109.96
Normal control 48hrs	12	104.914	11.9183	3.4405	97.341	112.49
Normal control 72hrs	12	97.948	10.1678	2.9352	91.487	104.41
Normal control 96hrs	12	95.198	6.9494	2.0061	90.783	99.61
Normal treated 24hrs	12	92.413	11.9950	3.4627	84.792	100.03
Normal treated 48hrs	12	95.155	19.8640	5.7343	82.534	107.78
Normal treated 72hrs	12	98.074	13.0692	3.7728	89.770	106.38
Normal treated 96hrs	12	89.363	7.8654	2.2705	84.365	94.36
Cancer control 24hrs	12	102.842	13.2754	3.8323	94.407	111.28
Cancer control 48hrs	12	99.088	20.0293	5.7820	86.362	111.81
Cancer control 72hrs	12	101.878	24.8176	7.1642	86.109	117.65
Cancer control 96hrs	12	101.461	23.3571	6.7426	86.621	116.30
Cancer treated 24hrs	12	101.336	15.2671	4.4072	91.636	111.04
Cancer treated 48hrs	12	105.268	14.6369	4.2253	95.968	114.57
Cancer treated 72hrs	12	104.333	22.3094	6.4402	90.158	118.51
Cancer treated 96hrs	12	102.083	11.4924	3.3176	94.781	109.38

Comparisons for all pairs using Tukey-Kramer HSD

Confidence Quantile

q*	Alpha
3.47644	0.05

Connecting Letters Report

Level		Mean
Cancer treated 48hrs	A	105.26825
Normal control 48hrs	A	104.91403
Normal control 24hrs	A	104.61958
Cancer treated 72hrs	A	104.33294
Cancer control 24hrs	A	102.84158
Cancer treated 96hrs	A	102.08294
Cancer control 72hrs	A	101.87779
Cancer control 96hrs	A	101.46113
Cancer treated 24hrs	A	101.33642
Cancer control 48hrs	A	99.08842
Normal treated 72hrs	A	98.07411
Normal control 72hrs	A	97.94781
Normal control 96hrs	A	95.19797
Normal treated 48hrs	A	95.15534
Normal treated 24hrs	A	92.41339
Normal treated 96hrs	A	89.36255

Levels not connected by same letter are significantly different.

APPENDIX D12

Oneway Analysis of effects of RTV on % Viability of Breast cells by Time

Summary of Fit

Rsquare	0.31555
Adj Rsquare	0.257216
Root Mean Square Error	13.32825
Mean of Response	102.4972
Observations (or Sum Wgts)	192

Analysis of Variance

Source	DF	Sum of Squares	Mean Square	F Ratio	Prob > F
Time	15	14414.019	960.935	5.4094	<.0001*
Error	176	31265.041	177.642		
C. Total	191	45679.060			

Means and Std Deviations

Level	Number	Mean	Std Dev	Std Err Mean	Lower 95%	Upper 95%
Normal control 24hrs	12	100.961	6.2315	1.7989	97.00	104.92
Normal control 48hrs	12	98.395	8.3918	2.4225	93.06	103.73
Normal control 72hrs	12	97.312	9.2757	2.6777	91.42	103.21
Normal control 96hrs	12	99.229	10.6578	3.0767	92.46	106.00
Normal treated 24hrs	12	79.907	12.3541	3.5663	72.06	87.76
Normal treated 48hrs	12	113.163	12.4211	3.5857	105.27	121.06
Normal treated 72hrs	12	117.163	15.3658	4.4357	107.40	126.93
Normal treated 96hrs	12	115.663	17.3576	5.0107	104.63	126.69
Cancer control 24hrs	12	103.253	13.7016	3.9553	94.55	111.96
Cancer control 48hrs	12	100.011	15.2025	4.3886	90.35	109.67
Cancer control 72hrs	12	97.947	16.0481	4.6327	87.75	108.14
Cancer control 96hrs	12	99.864	7.8385	2.2628	94.88	104.84
Cancer treated 24hrs	12	112.159	17.7029	5.1104	100.91	123.41
Cancer treated 48hrs	12	101.031	20.6438	5.9593	87.91	114.15
Cancer treated 72hrs	12	101.115	13.3510	3.8541	92.63	109.60
Cancer treated 96hrs	12	102.782	5.7841	1.6697	99.11	106.46

Comparisons for all pairs using Tukey-Kramer HSD

Confidence Quantile

q*	Alpha
3.47644	0.05

Connecting Letters Report

Level				Mean
Normal treated 72hrs	A			117.16314
Normal treated 96hrs	A	B		115.66314
Normal treated 48hrs	A	B		113.16314
Cancer treated 24hrs	A	B		112.15945
Cancer control 24hrs	A	B		103.25258
Cancer treated 96hrs	A	B		102.78180
Cancer treated 72hrs	A	B		101.11513
Cancer treated 48hrs	A	B		101.03066
Normal control 24hrs	A	B		100.96127
Cancer control 48hrs	A	B		100.01121
Cancer control 96hrs	A	B		99.86396
Normal control 96hrs	A	B		99.22855
Normal control 48hrs	A	B	C	98.39523
Cancer control 72hrs		B	C	97.94729
Normal control 72hrs		B	C	97.31189
Normal treated 24hrs			C	79.90671

Levels not connected by same letter are significantly different.

APPENDIX D13

Oneway Analysis of effects of LPV/r on % Viability of Cervical cells by Time

Summary of Fit

Rsquare	0.118332
Adj Rsquare	0.04319
Root Mean Square Error	18.20467
Mean of Response	100.0854
Observations (or Sum Wgts)	192

Analysis of Variance

Source	DF	Sum of Squares	Mean Square	F Ratio	Prob > F
Time	15	7828.479	521.899	1.5748	0.0848
Error	176	58328.165	331.410		
C. Total	191	66156.643			

Means and Std Deviations

Level	Number	Mean	Std Dev	Std Err Mean	Lower 95%	Upper 95%
Normal control 24hrs	12	104.620	8.4035	2.4259	99.280	109.96
Normal control 48hrs	12	104.914	11.9183	3.4405	97.341	112.49
Normal control 72hrs	12	97.948	10.1678	2.9352	91.487	104.41
Normal control 96hrs	12	95.198	6.9494	2.0061	90.783	99.61
Normal treated 24hrs	12	89.863	13.1722	3.8025	81.494	98.23
Normal treated 48hrs	12	90.555	17.0542	4.9231	79.719	101.39
Normal treated 72hrs	12	98.096	22.0108	6.3540	84.111	112.08
Normal treated 96hrs	12	89.020	13.1967	3.8096	80.635	97.40
Cancer control 24hrs	12	102.842	13.2754	3.8323	94.407	111.28
Cancer control 48hrs	12	99.088	20.0293	5.7820	86.362	111.81
Cancer control 72hrs	12	101.878	24.8176	7.1642	86.109	117.65
Cancer control 96hrs	12	101.461	23.3571	6.7426	86.621	116.30
Cancer treated 24hrs	12	112.535	20.8060	6.0062	99.316	125.75
Cancer treated 48hrs	12	109.047	18.8896	5.4529	97.045	121.05
Cancer treated 72hrs	12	102.776	25.1405	7.2574	86.803	118.75
Cancer treated 96hrs	12	101.526	25.5853	7.3858	85.270	117.78

Comparisons for all pairs using Tukey-Kramer HSD

Confidence Quantile

q*	Alpha
3.47644	0.05

Connecting Letters Report

Level		Mean
Cancer treated 24hrs	A	112.53509
Cancer treated 48hrs	A	109.04665
Normal control 48hrs	A	104.91403
Normal control 24hrs	A	104.61958
Cancer control 24hrs	A	102.84158
Cancer treated 72hrs	A	102.77611
Cancer control 72hrs	A	101.87779
Cancer treated 96hrs	A	101.52611
Cancer control 96hrs	A	101.46113
Cancer control 48hrs	A	99.08842
Normal treated 72hrs	A	98.09628
Normal control 72hrs	A	97.94781
Normal control 96hrs	A	95.19797
Normal treated 48hrs	A	90.55475
Normal treated 24hrs	A	89.86316
Normal treated 96hrs	A	89.01976

Levels not connected by same letter are significantly different.

APPENDIX D14

Oneway Analysis of effects of LPV/r on % Viability of Breast cells by Time

Summary of Fit

Rsquare	0.048589
Adj Rsquare	-0.0325
Root Mean Square Error	14.97004
Mean of Response	99.13889
Observations (or Sum Wgts)	192

Analysis of Variance

Source	DF	Sum of Squares	Mean Square	F Ratio	Prob > F
Time	15	2014.308	134.287	0.5992	0.8730
Error	176	39441.993	224.102		
C. Total	191	41456.301			

Means and Std Deviations

Level	Number	Mean	Std Dev	Std Err Mean	Lower 95%	Upper 95%
Normal control 24hrs	12	100.961	6.2315	1.7989	97.002	104.92
Normal control 48hrs	12	98.395	8.3918	2.4225	93.063	103.73
Normal control 72hrs	12	97.312	9.2757	2.6777	91.418	103.21
Normal control 96hrs	12	99.229	10.6578	3.0767	92.457	106.00
Normal treated 24hrs	12	92.949	27.3322	7.8901	75.583	110.32
Normal treated 48hrs	12	99.228	13.0793	3.7757	90.917	107.54
Normal treated 72hrs	12	98.311	14.0731	4.0625	89.369	107.25
Normal treated 96hrs	12	98.965	15.8492	4.5753	88.895	109.03
Cancer control 24hrs	12	103.253	13.7016	3.9553	94.547	111.96
Cancer control 48hrs	12	100.011	15.2025	4.3886	90.352	109.67
Cancer control 72hrs	12	97.947	16.0481	4.6327	87.751	108.14
Cancer control 96hrs	12	99.864	7.8385	2.2628	94.884	104.84
Cancer treated 24hrs	12	103.564	16.4679	4.7539	93.101	114.03
Cancer treated 48hrs	12	91.417	16.4340	4.7441	80.976	101.86
Cancer treated 72hrs	12	101.575	17.0906	4.9336	90.716	112.43
Cancer treated 96hrs	12	103.242	18.3903	5.3088	91.557	114.93

Comparisons for all pairs using Tukey-Kramer HSD

Confidence Quantile

q*	Alpha
3.47644	0.05

Connecting Letters Report

Level		Mean
Cancer treated 24hrs	A	103.56390
Cancer control 24hrs	A	103.25258
Cancer treated 96hrs	A	103.24172
Cancer treated 72hrs	A	101.57506
Normal control 24hrs	A	100.96127
Cancer control 48hrs	A	100.01121
Cancer control 96hrs	A	99.86396
Normal control 96hrs	A	99.22855
Normal treated 48hrs	A	99.22756
Normal treated 96hrs	A	98.96482
Normal control 48hrs	A	98.39523
Normal treated 72hrs	A	98.31089
Cancer control 72hrs	A	97.94729
Normal control 72hrs	A	97.31189
Normal treated 24hrs	A	92.94904
Cancer treated 48hrs	A	91.41729

Levels not connected by same letter are significantly different.

APPENDIX D15

Oneway Analysis of effects of TDF/FTC/LPV/r on % Viability of Cervical cells by Time

Summary of Fit

Rsquare	0.19781
Adj Rsquare	0.129442
Root Mean Square Error	15.32801
Mean of Response	99.20963
Observations (or Sum Wgts)	192

Analysis of Variance

Source	DF	Sum of Squares	Mean Square	F Ratio	Prob > F
Time	15	10196.613	679.774	2.8933	0.0004*
Error	176	41350.823	234.948		
C. Total	191	51547.436			

Means and Std Deviations

Level	Number	Mean	Std Dev	Std Err Mean	Lower 95%	Upper 95%
Normal control 24hrs	12	104.620	8.4035	2.4259	99.28	109.96
Normal control 48hrs	12	104.914	11.9183	3.4405	97.34	112.49
Normal control 72hrs	12	97.948	10.1678	2.9352	91.49	104.41
Normal control 96hrs	12	95.198	6.9494	2.0061	90.78	99.61
Normal treated 24hrs	12	83.183	12.2129	3.5255	75.42	90.94
Normal treated 48hrs	12	86.893	18.3546	5.2985	75.23	98.56
Normal treated 72hrs	12	92.028	9.4739	2.7349	86.01	98.05
Normal treated 96hrs	12	96.122	14.5087	4.1883	86.90	105.34
Cancer control 24hrs	12	102.842	13.2754	3.8323	94.41	111.28
Cancer control 48hrs	12	99.088	20.0293	5.7820	86.36	111.81
Cancer control 72hrs	12	101.878	24.8176	7.1642	86.11	117.65
Cancer control 96hrs	12	101.461	23.3571	6.7426	86.62	116.30
Cancer treated 24hrs	12	105.201	10.6723	3.0808	98.42	111.98
Cancer treated 48hrs	12	114.515	13.5614	3.9148	105.90	123.13
Cancer treated 72hrs	12	101.190	17.7801	5.1327	89.89	112.49
Cancer treated 96hrs	12	100.273	15.9906	4.6161	90.11	110.43

Comparisons for all pairs using Tukey-Kramer HSD

Confidence Quantile

q*	Alpha
3.47644	0.05

Connecting Letters Report

Level				Mean
Cancer treated 48hrs	A			114.51456
Cancer treated 24hrs	A	B		105.20077
Normal control 48hrs	A	B		104.91403
Normal control 24hrs	A	B		104.61958
Cancer control 24hrs	A	B		102.84158
Cancer control 72hrs	A	B	C	101.87779
Cancer control 96hrs	A	B	C	101.46113
Cancer treated 72hrs	A	B	C	101.19009
Cancer treated 96hrs	A	B	C	100.27342
Cancer control 48hrs	A	B	C	99.08842
Normal control 72hrs	A	B	C	97.94781
Normal treated 96hrs	A	B	C	96.12198
Normal control 96hrs	A	B	C	95.19797
Normal treated 72hrs		B	C	92.02849
Normal treated 48hrs		B	C	86.89318
Normal treated 24hrs			C	83.18326

Levels not connected by same letter are significantly different.

APPENDIX D16

Oneway Analysis of effects of TDF/FTC/LPV/r on % Viability of Breast cells by Time

Summary of Fit

Rsquare	0.273928
Adj Rsquare	0.212047
Root Mean Square Error	12.70453
Mean of Response	102.8484
Observations (or Sum Wgts)	192

Analysis of Variance

Source	DF	Sum of Squares	Mean Square	F Ratio	Prob > F
Time	15	10717.335	714.489	4.4267	<.0001*
Error	176	28407.312	161.405		
C. Total	191	39124.648			

Means and Std Deviations

Level	Number	Mean	Std Dev	Std Err Mean	Lower 95%	Upper 95%
Normal control 24hrs	12	100.961	6.2315	1.7989	97.00	104.92
Normal control 48hrs	12	98.395	8.3918	2.4225	93.06	103.73
Normal control 72hrs	12	97.312	9.2757	2.6777	91.42	103.21
Normal control 96hrs	12	99.229	10.6578	3.0767	92.46	106.00
Normal treated 24hrs	12	90.612	16.7531	4.8362	79.97	101.26
Normal treated 48hrs	12	113.225	11.6850	3.3732	105.80	120.65
Normal treated 72hrs	12	116.225	14.9957	4.3289	106.70	125.75
Normal treated 96hrs	12	114.808	11.0426	3.1877	107.79	121.82
Cancer control 24hrs	12	103.253	13.7016	3.9553	94.55	111.96
Cancer control 48hrs	12	100.011	15.2025	4.3886	90.35	109.67
Cancer control 72hrs	12	97.947	16.0481	4.6327	87.75	108.14
Cancer control 96hrs	12	99.864	7.8385	2.2628	94.88	104.84
Cancer treated 24hrs	12	99.797	13.5684	3.9169	91.18	108.42
Cancer treated 48hrs	12	93.647	12.5528	3.6237	85.67	101.62
Cancer treated 72hrs	12	108.562	16.0556	4.6349	98.36	118.76
Cancer treated 96hrs	12	111.728	13.1261	3.7892	103.39	120.07

Comparisons for all pairs using Tukey-Kramer HSD

Confidence Quantile

q*	Alpha
3.47644	0.05

Connecting Letters Report

Level				Mean
Normal treated 72hrs	A			116.22456
Normal treated 96hrs	A	B		114.80768
Normal treated 48hrs	A	B		113.22456
Cancer treated 96hrs	A	B		111.72844
Cancer treated 72hrs	A	B	C	108.56177
Cancer control 24hrs	A	B	C	103.25258
Normal control 24hrs	A	B	C	100.96127
Cancer control 48hrs	A	B	C	100.01121
Cancer control 96hrs	A	B	C	99.86396
Cancer treated 24hrs	A	B	C	99.79685
Normal control 96hrs	A	B	C	99.22855
Normal control 48hrs	A	B	C	98.39523
Cancer control 72hrs		B	C	97.94729
Normal control 72hrs		B	C	97.31189
Cancer treated 48hrs			C	93.64720
Normal treated 24hrs			C	90.61158

Levels not connected by same letter are significantly different.

APPENDIX E1

Oneway Analysis of Fluorescence Intensity of effects of ARVs on Cervical cells

Oneway Analysis of Fluorescence Intensity of TDF on Cervical cells

Summary of Fit

Rsquare	0.998224
Adj Rsquare	0.997887
Root Mean Square Error	9.196458
Mean of Response	400.421
Observations (or Sum Wgts)	120

Analysis of Variance

Source	DF	Sum of Squares	Mean Square	F Ratio	Prob > F
Gene	19	4753633.2	250191	2958.223	<.0001*
Error	100	8457.5	85		
C. Total	119	4762090.7			

Means for Oneway Anova

Means and Std Deviations

Level	Number	Mean	Std Dev	Std Err Mean	Lower 95%	Upper 95%
Normal control Bax Nucleus	6	576.077	9.9957	4.0807	565.59	586.57
Normal treated Bax Nucleus	6	572.468	6.5711	2.6826	565.57	579.36
Normal control Bax Cytoplasm	6	307.727	3.4534	1.4098	304.10	311.35
Normal treated Bax Cytoplasm	6	306.628	6.0649	2.4760	300.26	312.99
Normal Control VEGF165b Nucleus	6	373.772	8.9153	3.6397	364.42	383.13
Normal treated VEGF 165b Nucleus	6	376.739	12.5491	5.1232	363.57	389.91
Normal Control VEGF 165b Cytoplasm	6	822.998	20.2078	8.2498	801.79	844.20
Normal treated VEGF 165b Cytoplasm	6	819.989	9.5117	3.8831	810.01	829.97
Cancer Control Bax Nucleus	6	276.353	4.7441	1.9368	271.37	281.33
Cancer treated Bax Nucleus	6	273.537	6.8808	2.8091	266.32	280.76
Cancer Control Bax Cytoplasm	6	192.531	5.1956	2.1211	187.08	197.98
Cancer treated Bax Cytoplasm	6	194.570	5.4018	2.2053	188.90	200.24
Cancer control Bcl2 Nucleus	6	314.768	6.6436	2.7122	307.80	321.74
Cancer Treated Bcl2 Nucleus	6	315.693	4.9127	2.0056	310.54	320.85
Cancer control Bcl2 Cytoplasm	6	189.813	5.0311	2.0539	184.53	195.09
Cancer Treated Bcl2 Cytoplasm	6	190.597	4.8863	1.9948	185.47	195.72
Cancer Control VEGF 165b Nucleus	6	305.645	4.9207	2.0089	300.48	310.81
Cancer treated VEGF 165b Nucleus	6	306.305	9.5898	3.9150	296.24	316.37
Cancer Control VEGF 165b Cytoplasm	6	644.643	18.1028	7.3905	625.65	663.64
Cancer treated VEGF 165b Cytoplasm	6	647.568	8.7479	3.5713	638.39	656.75

Means Comparisons

Comparisons for all pairs using Tukey-Kramer HSD

Confidence Quantile

q*	Alpha
3.64086	0.05

Connecting Letters Report

Level					Mean
Normal Control VEGF 165b Cytoplasm	A				822.99761
Normal treated VEGF 165b Cytoplasm	A				819.98866
Cancer treated VEGF 165b Cytoplasm		B			647.56755
Cancer Control VEGF 165b Cytoplasm		B			644.64310
Normal control Bax Nucleus			C		576.07677
Normal treated Bax Nucleus			C		572.46816
Normal treated VEGF 165b Nucleus				D	376.73941

Level				Mean
Normal Control VEGF165b Nucleus	D			373.77185
Cancer Treated Bcl2 Nucleus		E		315.69289
Cancer control Bcl2 Nucleus		E		314.76758
Normal control Bax Cytoplasm		E		307.72696
Normal treated Bax Cytoplasm		E		306.62818
Cancer treated VEGF 165b Nucleus		E		306.30500
Cancer Control VEGF 165b Nucleus		E		305.64500
Cancer Control Bax Nucleus			F	276.35280
Cancer treated Bax Nucleus			F	273.53700
Cancer treated Bax Cytoplasm				G 194.57001
Cancer Control Bax Cytoplasm				G 192.53124
Cancer Treated Bcl2 Cytoplasm				G 190.59672
Cancer control Bcl2 Cytoplasm				G 189.81300

Levels not connected by same letter are significantly different.

Oneway Analysis of Fluorescence Intensity of FTC on Cervical cells
Summary of Fit

Rsquare	0.997771
Adj Rsquare	0.997348
Root Mean Square Error	10.31391
Mean of Response	400.5181
Observations (or Sum Wgts)	120

Analysis of Variance

Source	DF	Sum of Squares	Mean Square	F Ratio	Prob > F
Gene	19	4762765.7	250672	2356.452	<.0001*
Error	100	10637.7	106		
C. Total	119	4773403.3			

Means and Std Deviations

Level	Number	Mean	Std Dev	Std Err Mean	Lower 95%	Upper 95%
Normal control Bax Nucleus	6	576.077	9.9957	4.0807	565.59	586.57
Normal treated Bax Nucleus	6	578.506	6.3650	2.5985	571.83	585.19
Normal control Bax Cytoplasm	6	307.727	3.4534	1.4098	304.10	311.35
Normal treated Bax Cytoplasm	6	306.852	5.3769	2.1951	301.21	312.50
Normal Control VEGF165b Nucleus	6	373.772	8.9153	3.6397	364.42	383.13
Normal treated VEGF 165b Nucleus	6	378.112	11.1957	4.5706	366.36	389.86
Normal Control VEGF 165b Cytoplasm	6	822.998	20.2078	8.2498	801.79	844.20
Normal treated VEGF 165b Cytoplasm	6	821.337	18.9896	7.7525	801.41	841.27
Cancer Control Bax Nucleus	6	276.353	4.7441	1.9368	271.37	281.33
Cancer treated Bax Nucleus	6	274.176	11.3968	4.6527	262.22	286.14
Cancer Control Bax Cytoplasm	6	192.531	5.1956	2.1211	187.08	197.98
Cancer treated Bax Cytoplasm	6	190.582	1.8121	0.7398	188.68	192.48
Cancer control Bcl2 Nucleus	6	314.768	6.6436	2.7122	307.80	321.74
Cancer Treated Bcl2 Nucleus	6	315.711	5.4703	2.2333	309.97	321.45
Cancer control Bcl2 Cytoplasm	6	189.813	5.0311	2.0539	184.53	195.09
Cancer Treated Bcl2 Cytoplasm	6	190.824	5.4796	2.2370	185.07	196.57
Cancer Control VEGF 165b Nucleus	6	305.645	4.9207	2.0089	300.48	310.81
Cancer treated VEGF 165b Nucleus	6	307.923	3.3419	1.3643	304.42	311.43
Cancer Control VEGF 165b Cytoplasm	6	644.643	18.1028	7.3905	625.65	663.64
Cancer treated VEGF 165b Cytoplasm	6	642.011	17.2429	7.0394	623.92	660.11

Means Comparisons
Comparisons for all pairs using Tukey-Kramer HSD
Confidence Quantile

q*	Alpha
3.64086	0.05

Connecting Letters Report

Level							Mean
Normal Control VEGF 165b Cytoplasm	A						822.99761
Normal treated VEGF 165b Cytoplasm	A						821.33750
Cancer Control VEGF 165b Cytoplasm		B					644.64310
Cancer treated VEGF 165b Cytoplasm		B					642.01050
Normal treated Bax Nucleus			C				578.50632
Normal control Bax Nucleus			C				576.07677
Normal treated VEGF 165b Nucleus				D			378.11178
Normal Control VEGF165b Nucleus				D			373.77185
Cancer Treated Bcl2 Nucleus					E		315.71124
Cancer control Bcl2 Nucleus					E		314.76758
Cancer treated VEGF 165b Nucleus					E		307.92333
Normal control Bax Cytoplasm					E		307.72696
Normal treated Bax Cytoplasm					E		306.85245
Cancer Control VEGF 165b Nucleus					E		305.64500
Cancer Control Bax Nucleus						F	276.35280
Cancer treated Bax Nucleus						F	274.17620
Cancer Control Bax Cytoplasm							G 192.53124
Cancer Treated Bcl2 Cytoplasm							G 190.82426
Cancer treated Bax Cytoplasm							G 190.58184
Cancer control Bcl2 Cytoplasm							G 189.81300

Levels not connected by same letter are significantly different.

Oneway Analysis of Fluorescence Intensity of EFV on Cervical cells
Summary of Fit

Rsquare	0.997764
Adj Rsquare	0.99734
Root Mean Square Error	10.34972
Mean of Response	400.5535
Observations (or Sum Wgts)	120

Analysis of Variance

Source	DF	Sum of Squares	Mean Square	F Ratio	Prob > F
Gene	19	4780635.4	251612	2348.955	<.0001*
Error	100	10711.7	107		
C. Total	119	4791347.1			

Means and Std Deviations

Level	Number	Mean	Std Dev	Std Err Mean	Lower 95%	Upper 95%
Normal control Bax Nucleus	6	573.104	13.0980	5.3472	559.36	586.85
Normal treated Bax Nucleus	6	577.811	14.0923	5.7532	563.02	592.60
Normal control Bax Cytoplasm	6	305.715	4.5406	1.8537	300.95	310.48
Normal treated Bax Cytoplasm	6	309.040	5.4424	2.2219	303.33	314.75
Normal Control VEGF165b Nucleus	6	377.585	10.5504	4.3072	366.51	388.66
Normal treated VEGF 165b Nucleus	6	375.038	13.4286	5.4822	360.95	389.13
Normal Control VEGF 165b Cytoplasm	6	824.282	19.7112	8.0471	803.60	844.97
Normal treated VEGF 165b Cytoplasm	6	825.421	14.4638	5.9048	810.24	840.60

Level	Number	Mean	Std Dev	Std Err Mean	Lower 95%	Upper 95%
Cancer Control Bax Nucleus	6	272.730	7.8329	3.1978	264.51	280.95
Cancer treated Bax Nucleus	6	276.970	5.6517	2.3073	271.04	282.90
Cancer Control Bax Cytoplasm	6	192.489	3.0724	1.2543	189.26	195.71
Cancer treated Bax Cytoplasm	6	194.673	5.9368	2.4237	188.44	200.90
Cancer control Bcl2 Nucleus	6	315.272	8.7886	3.5879	306.05	324.50
Cancer Treated Bcl2 Nucleus	6	312.976	9.1597	3.7394	303.36	322.59
Cancer control Bcl2 Cytoplasm	6	189.515	5.5464	2.2643	183.69	195.34
Cancer Treated Bcl2 Cytoplasm	6	189.700	5.0531	2.0629	184.40	195.00
Cancer Control VEGF 165b Nucleus	6	304.397	5.2417	2.1399	298.90	309.90
Cancer treated VEGF 165b Nucleus	6	307.788	6.5457	2.6723	300.92	314.66
Cancer Control VEGF 165b Cytoplasm	6	648.631	10.6315	4.3403	637.47	659.79
Cancer treated VEGF 165b Cytoplasm	6	637.934	17.1409	6.9977	619.95	655.92

Means Comparisons
Comparisons for all pairs using Tukey-Kramer HSD
Confidence Quantile

q*	Alpha
3.64086	0.05

Connecting Letters Report

Level								Mean
Normal treated VEGF 165b Cytoplasm	A							825.42136
Normal Control VEGF 165b Cytoplasm	A							824.28228
Cancer Control VEGF 165b Cytoplasm		B						648.63135
Cancer treated VEGF 165b Cytoplasm		B						637.93385
Normal treated Bax Nucleus			C					577.81098
Normal control Bax Nucleus			C					573.10382
Normal Control VEGF165b Nucleus				D				377.58481
Normal treated VEGF 165b Nucleus				D				375.03771
Cancer control Bcl2 Nucleus					E			315.27240
Cancer Treated Bcl2 Nucleus					E			312.97569
Normal treated Bax Cytoplasm					E			309.03955
Cancer treated VEGF 165b Nucleus					E			307.78833
Normal control Bax Cytoplasm					E			305.71493
Cancer Control VEGF 165b Nucleus					E			304.39667
Cancer treated Bax Nucleus						F		276.97040
Cancer Control Bax Nucleus						F		272.73013
Cancer treated Bax Cytoplasm							G	194.67279
Cancer Control Bax Cytoplasm							G	192.48892
Cancer Treated Bcl2 Cytoplasm							G	189.70005
Cancer control Bcl2 Cytoplasm							G	189.51469

Levels not connected by same letter are significantly different.

Oneway Analysis of Fluorescence Intensity of ATP on Cervical cells
Summary of Fit

Rsquare	0.997624
Adj Rsquare	0.997172
Root Mean Square Error	10.67895
Mean of Response	400.0672
Observations (or Sum Wgts)	120

Analysis of Variance

Source	DF	Sum of Squares	Mean Square	F Ratio	Prob > F

Source	DF	Sum of Squares	Mean Square	F Ratio	Prob > F
Gene	19	4787710.0	251985	2209.616	<.0001*
Error	100	11404.0	114		
C. Total	119	4799114.0			

Means and Std Deviations

Level	Number	Mean	Std Dev	Std Err Mean	Lower 95%	Upper 95%
Normal control Bax Nucleus	6	573.104	13.0980	5.3472	559.36	586.85
Normal treated Bax Nucleus	6	571.923	14.7126	6.0064	556.48	587.36
Normal control Bax Cytoplasm	6	305.715	4.5406	1.8537	300.95	310.48
Normal treated Bax Cytoplasm	6	305.231	7.1985	2.9388	297.68	312.78
Normal Control VEGF165b Nucleus	6	377.585	10.5504	4.3072	366.51	388.66
Normal treated VEGF 165b Nucleus	6	376.044	6.5215	2.6624	369.20	382.89
Normal Control VEGF 165b Cytoplasm	6	824.282	19.7112	8.0471	803.60	844.97
Normal treated VEGF 165b Cytoplasm	6	825.194	15.0897	6.1604	809.36	841.03
Cancer Control Bax Nucleus	6	272.730	7.8329	3.1978	264.51	280.95
Cancer treated Bax Nucleus	6	274.538	7.8387	3.2001	266.31	282.76
Cancer Control Bax Cytoplasm	6	192.489	3.0724	1.2543	189.26	195.71
Cancer treated Bax Cytoplasm	6	192.700	7.1707	2.9274	185.17	200.22
Cancer control Bcl2 Nucleus	6	315.272	8.7886	3.5879	306.05	324.50
Cancer Treated Bcl2 Nucleus	6	314.763	8.0695	3.2944	306.29	323.23
Cancer control Bcl2 Cytoplasm	6	189.515	5.5464	2.2643	183.69	195.34
Cancer Treated Bcl2 Cytoplasm	6	190.269	6.9923	2.8546	182.93	197.61
Cancer Control VEGF 165b Nucleus	6	304.397	5.2417	2.1399	298.90	309.90
Cancer treated VEGF 165b Nucleus	6	305.833	6.8830	2.8100	298.61	313.06
Cancer Control VEGF 165b Cytoplasm	6	648.631	10.6315	4.3403	637.47	659.79
Cancer treated VEGF 165b Cytoplasm	6	641.130	21.3712	8.7248	618.70	663.56

Means Comparisons

Comparisons for all pairs using Tukey-Kramer HSD

Confidence Quantile

q*	Alpha
3.64086	0.05

Connecting Letters Report

Level							Mean
Normal treated VEGF 165b Cytoplasm	A						825.19418
Normal Control VEGF 165b Cytoplasm	A						824.28228
Cancer Control VEGF 165b Cytoplasm		B					648.63135
Cancer treated VEGF 165b Cytoplasm		B					641.12980
Normal control Bax Nucleus			C				573.10382
Normal treated Bax Nucleus			C				571.92322
Normal Control VEGF165b Nucleus				D			377.58481
Normal treated VEGF 165b Nucleus				D			376.04370
Cancer control Bcl2 Nucleus					E		315.27240
Cancer Treated Bcl2 Nucleus					E		314.76261
Cancer treated VEGF 165b Nucleus					E		305.83333
Normal control Bax Cytoplasm					E		305.71493
Normal treated Bax Cytoplasm					E		305.23051
Cancer Control VEGF 165b Nucleus					E		304.39667
Cancer treated Bax Nucleus						F	274.53840
Cancer Control Bax Nucleus						F	272.73013
Cancer treated Bax Cytoplasm						G	192.69959
Cancer Control Bax Cytoplasm						G	192.48892
Cancer Treated Bcl2 Cytoplasm						G	190.26891
Cancer control Bcl2 Cytoplasm						G	189.51469

Levels not connected by same letter are significantly different.

Oneway Analysis of Fluorescence Intensity of LPV on Cervical cells
Summary of Fit

Rsquare	0.998161
Adj Rsquare	0.997811
Root Mean Square Error	9.381051
Mean of Response	399.7788
Observations (or Sum Wgts)	120

Analysis of Variance

Source	DF	Sum of Squares	Mean Square	F Ratio	Prob > F
Gene	19	4776215.7	251380	2856.455	<.0001*
Error	100	8800.4	88		
C. Total	119	4785016.2			

Means and Std Deviations

Level	Number	Mean	Std Dev	Std Err Mean	Lower 95%	Upper 95%
Normal control Bax Nucleus	6	573.104	13.0980	5.3472	559.36	586.85
Normal treated Bax Nucleus	6	570.441	8.9215	3.6422	561.08	579.80
Normal control Bax Cytoplasm	6	305.715	4.5406	1.8537	300.95	310.48
Normal treated Bax Cytoplasm	6	303.657	4.5796	1.8696	298.85	308.46
Normal Control VEGF165b Nucleus	6	377.585	10.5504	4.3072	366.51	388.66
Normal treated VEGF 165b Nucleus	6	374.171	3.8839	1.5856	370.09	378.25
Normal Control VEGF 165b Cytoplasm	6	824.282	19.7112	8.0471	803.60	844.97
Normal treated VEGF 165b Cytoplasm	6	817.907	19.4362	7.9348	797.51	838.30
Cancer Control Bax Nucleus	6	272.730	7.8329	3.1978	264.51	280.95
Cancer treated Bax Nucleus	6	271.164	6.7775	2.7669	264.05	278.28
Cancer Control Bax Cytoplasm	6	192.489	3.0724	1.2543	189.26	195.71
Cancer treated Bax Cytoplasm	6	194.087	3.9941	1.6306	189.90	198.28
Cancer control Bcl2 Nucleus	6	315.272	8.7886	3.5879	306.05	324.50
Cancer Treated Bcl2 Nucleus	6	315.138	9.0493	3.6944	305.64	324.64
Cancer control Bcl2 Cytoplasm	6	189.515	5.5464	2.2643	183.69	195.34
Cancer Treated Bcl2 Cytoplasm	6	191.215	5.6173	2.2932	185.32	197.11
Cancer Control VEGF 165b Nucleus	6	304.397	5.2417	2.1399	298.90	309.90
Cancer treated VEGF 165b Nucleus	6	304.325	6.0617	2.4747	297.96	310.69
Cancer Control VEGF 165b Cytoplasm	6	648.631	10.6315	4.3403	637.47	659.79
Cancer treated VEGF 165b Cytoplasm	6	649.749	6.5782	2.6855	642.85	656.65

Means Comparisons
Comparisons for all pairs using Tukey-Kramer HSD
Confidence Quantile

q*	Alpha
3.64086	0.05

Connecting Letters Report

Level						Mean
Normal Control VEGF 165b Cytoplasm	A					824.28228
Normal treated VEGF 165b Cytoplasm	A					817.90736
Cancer treated VEGF 165b Cytoplasm		B				649.74922
Cancer Control VEGF 165b Cytoplasm		B				648.63135
Normal control Bax Nucleus			C			573.10382
Normal treated Bax Nucleus			C			570.44136
Normal Control VEGF165b Nucleus				D		377.58481
Normal treated VEGF 165b Nucleus				D		374.17077
Cancer control Bcl2 Nucleus					E	315.27240
Cancer Treated Bcl2 Nucleus					E	315.13838
Normal control Bax Cytoplasm					E	305.71493

Level				Mean
Cancer Control VEGF 165b Nucleus	E			304.39667
Cancer treated VEGF 165b Nucleus	E			304.32500
Normal treated Bax Cytoplasm	E			303.65701
Cancer Control Bax Nucleus		F		272.73013
Cancer treated Bax Nucleus		F		271.16447
Cancer treated Bax Cytoplasm			G	194.08721
Cancer Control Bax Cytoplasm			G	192.48892
Cancer Treated Bcl2 Cytoplasm			G	191.21516
Cancer control Bcl2 Cytoplasm			G	189.51469

Levels not connected by same letter are significantly different.

Oneway Analysis of Fluorescence Intensity of RTV on Cervical cells
Summary of Fit

Rsquare	0.997696
Adj Rsquare	0.997259
Root Mean Square Error	10.51859
Mean of Response	400.4318
Observations (or Sum Wgts)	120

Analysis of Variance

Source	DF	Sum of Squares	Mean Square	F Ratio	Prob > F
Gene	19	4792022.0	252212	2279.554	<.0001*
Error	100	11064.1	111		
C. Total	119	4803086.1			

Means and Std Deviations

Level	Number	Mean	Std Dev	Std Err Mean	Lower 95%	Upper 95%
Normal control Bax Nucleus	6	573.104	13.0980	5.3472	559.36	586.85
Normal treated Bax Nucleus	6	574.577	14.2574	5.8206	559.61	589.54
Normal control Bax Cytoplasm	6	305.715	4.5406	1.8537	300.95	310.48
Normal treated Bax Cytoplasm	6	307.887	5.2155	2.1292	302.41	313.36
Normal Control VEGF165b Nucleus	6	377.585	10.5504	4.3072	366.51	388.66
Normal treated VEGF 165b Nucleus	6	376.292	6.6290	2.7063	369.34	383.25
Normal Control VEGF 165b Cytoplasm	6	824.282	19.7112	8.0471	803.60	844.97
Normal treated VEGF 165b Cytoplasm	6	818.542	19.0366	7.7717	798.56	838.52
Cancer Control Bax Nucleus	6	272.730	7.8329	3.1978	264.51	280.95
Cancer treated Bax Nucleus	6	276.841	7.5305	3.0743	268.94	284.74
Cancer Control Bax Cytoplasm	6	192.489	3.0724	1.2543	189.26	195.71
Cancer treated Bax Cytoplasm	6	191.437	6.0060	2.4519	185.13	197.74
Cancer control Bcl2 Nucleus	6	315.272	8.7886	3.5879	306.05	324.50
Cancer Treated Bcl2 Nucleus	6	313.282	8.3450	3.4068	304.52	322.04
Cancer control Bcl2 Cytoplasm	6	189.515	5.5464	2.2643	183.69	195.34
Cancer Treated Bcl2 Cytoplasm	6	188.846	2.7162	1.1089	186.00	191.70
Cancer Control VEGF 165b Nucleus	6	304.397	5.2417	2.1399	298.90	309.90
Cancer treated VEGF 165b Nucleus	6	305.732	6.7635	2.7612	298.63	312.83
Cancer Control VEGF 165b Cytoplasm	6	648.631	10.6315	4.3403	637.47	659.79
Cancer treated VEGF 165b Cytoplasm	6	651.480	18.6855	7.6283	631.87	671.09

Means Comparisons
Comparisons for all pairs using Tukey-Kramer HSD
Confidence Quantile

q*	Alpha
3.64086	0.05

Connecting Letters Report

Level	Mean

Level								Mean
Normal Control VEGF 165b Cytoplasm	A							824.28228
Normal treated VEGF 165b Cytoplasm	A							818.54182
Cancer treated VEGF 165b Cytoplasm		B						651.48025
Cancer Control VEGF 165b Cytoplasm		B						648.63135
Normal treated Bax Nucleus			C					574.57690
Normal control Bax Nucleus			C					573.10382
Normal Control VEGF165b Nucleus				D				377.58481
Normal treated VEGF 165b Nucleus				D				376.29183
Cancer control Bcl2 Nucleus					E			315.27240
Cancer Treated Bcl2 Nucleus					E			313.28180
Normal treated Bax Cytoplasm					E			307.88696
Cancer treated VEGF 165b Nucleus					E			305.73167
Normal control Bax Cytoplasm					E			305.71493
Cancer Control VEGF 165b Nucleus					E			304.39667
Cancer treated Bax Nucleus						F		276.84120
Cancer Control Bax Nucleus						F		272.73013
Cancer Control Bax Cytoplasm							G	192.48892
Cancer treated Bax Cytoplasm							G	191.43692
Cancer control Bcl2 Cytoplasm							G	189.51469
Cancer Treated Bcl2 Cytoplasm							G	188.84616

Levels not connected by same letter are significantly different.

Oneway Analysis of Fluorescence Intensity of LPV/R on Cervical cells
Summary of Fit

Rsquare	0.997672
Adj Rsquare	0.99723
Root Mean Square Error	10.55208
Mean of Response	399.321
Observations (or Sum Wgts)	120

Analysis of Variance

Source	DF	Sum of Squares	Mean Square	F Ratio	Prob > F
Gene	19	4772426.9	251180	2255.848	<.0001*
Error	100	11134.6	111		
C. Total	119	4783561.5			

Means and Std Deviations

Level	Number	Mean	Std Dev	Std Err Mean	Lower 95%	Upper 95%
Normal control Bax Nucleus	6	573.104	13.0980	5.3472	559.36	586.85
Normal treated Bax Nucleus	6	571.528	13.8961	5.6731	556.94	586.11
Normal control Bax Cytoplasm	6	305.715	4.5406	1.8537	300.95	310.48
Normal treated Bax Cytoplasm	6	304.245	8.9752	3.6641	294.83	313.66
Normal Control VEGF165b Nucleus	6	377.585	10.5504	4.3072	366.51	388.66
Normal treated VEGF 165b Nucleus	6	372.959	9.2655	3.7826	363.24	382.68
Normal Control VEGF 165b Cytoplasm	6	824.282	19.7112	8.0471	803.60	844.97
Normal treated VEGF 165b Cytoplasm	6	820.022	19.9263	8.1349	799.11	840.93
Cancer Control Bax Nucleus	6	272.730	7.8329	3.1978	264.51	280.95
Cancer treated Bax Nucleus	6	272.496	4.9677	2.0280	267.28	277.71
Cancer Control Bax Cytoplasm	6	192.489	3.0724	1.2543	189.26	195.71
Cancer treated Bax Cytoplasm	6	191.500	2.5169	1.0275	188.86	194.14
Cancer control Bcl2 Nucleus	6	315.272	8.7886	3.5879	306.05	324.50
Cancer Treated Bcl2 Nucleus	6	314.221	11.5475	4.7142	302.10	326.34
Cancer control Bcl2 Cytoplasm	6	189.515	5.5464	2.2643	183.69	195.34
Cancer Treated Bcl2 Cytoplasm	6	189.224	3.4496	1.4083	185.60	192.84

Level	Number	Mean	Std Dev	Std Err Mean	Lower 95%	Upper 95%
Cancer Control VEGF 165b Nucleus	6	304.397	5.2417	2.1399	298.90	309.90
Cancer treated VEGF 165b Nucleus	6	305.390	11.2981	4.6124	293.53	317.25
Cancer Control VEGF 165b Cytoplasm	6	648.631	10.6315	4.3403	637.47	659.79
Cancer treated VEGF 165b Cytoplasm	6	641.116	12.4557	5.0850	628.04	654.19

Means Comparisons
Comparisons for all pairs using Tukey-Kramer HSD
Confidence Quantile

q*	Alpha
3.64086	0.05

Connecting Letters Report

Level							Mean
Normal Control VEGF 165b Cytoplasm	A						824.28228
Normal treated VEGF 165b Cytoplasm	A						820.02183
Cancer Control VEGF 165b Cytoplasm		B					648.63135
Cancer treated VEGF 165b Cytoplasm		B					641.11615
Normal control Bax Nucleus			C				573.10382
Normal treated Bax Nucleus			C				571.52750
Normal Control VEGF165b Nucleus				D			377.58481
Normal treated VEGF 165b Nucleus				D			372.95937
Cancer control Bcl2 Nucleus					E		315.27240
Cancer Treated Bcl2 Nucleus					E		314.22125
Normal control Bax Cytoplasm					E		305.71493
Cancer treated VEGF 165b Nucleus					E		305.39000
Cancer Control VEGF 165b Nucleus					E		304.39667
Normal treated Bax Cytoplasm					E		304.24452
Cancer Control Bax Nucleus						F	272.73013
Cancer treated Bax Nucleus						F	272.49607
Cancer Control Bax Cytoplasm							G 192.48892
Cancer treated Bax Cytoplasm							G 191.50019
Cancer control Bcl2 Cytoplasm							G 189.51469
Cancer Treated Bcl2 Cytoplasm							G 189.22392

Levels not connected by same letter are significantly different.

Oneway Analysis of Fluorescence Intensity of TDF/FTC/LPV/R on Cervical cells
Summary of Fit

Rsquare	0.99754
Adj Rsquare	0.997072
Root Mean Square Error	10.85025
Mean of Response	400.124
Observations (or Sum Wgts)	120

Analysis of Variance

Source	DF	Sum of Squares	Mean Square	F Ratio	Prob > F
Gene	19	4773452.6	251234	2134.025	<.0001*
Error	100	11772.8	118		
C. Total	119	4785225.4			

Means and Std Deviations

Level	Number	Mean	Std Dev	Std Err Mean	Lower 95%	Upper 95%
Normal control Bax Nucleus	6	573.104	13.0980	5.3472	559.36	586.85
Normal treated Bax Nucleus	6	572.333	17.6780	7.2170	553.78	590.89
Normal control Bax Cytoplasm	6	305.715	4.5406	1.8537	300.95	310.48
Normal treated Bax Cytoplasm	6	306.051	7.5508	3.0826	298.13	313.97
Normal Control VEGF165b Nucleus	6	377.585	10.5504	4.3072	366.51	388.66
Normal treated VEGF 165b Nucleus	6	378.353	9.7607	3.9848	368.11	388.60
Normal Control VEGF 165b Cytoplasm	6	824.282	19.7112	8.0471	803.60	844.97
Normal treated VEGF 165b Cytoplasm	6	818.950	21.3011	8.6961	796.60	841.30
Cancer Control Bax Nucleus	6	272.730	7.8329	3.1978	264.51	280.95
Cancer treated Bax Nucleus	6	275.329	4.2477	1.7341	270.87	279.79
Cancer Control Bax Cytoplasm	6	192.489	3.0724	1.2543	189.26	195.71
Cancer treated Bax Cytoplasm	6	190.330	5.1141	2.0878	184.96	195.70
Cancer control Bcl2 Nucleus	6	315.272	8.7886	3.5879	306.05	324.50
Cancer Treated Bcl2 Nucleus	6	315.121	9.6775	3.9508	304.96	325.28
Cancer control Bcl2 Cytoplasm	6	189.515	5.5464	2.2643	183.69	195.34
Cancer Treated Bcl2 Cytoplasm	6	188.514	2.2562	0.9211	186.15	190.88
Cancer Control VEGF 165b Nucleus	6	304.397	5.2417	2.1399	298.90	309.90
Cancer treated VEGF 165b Nucleus	6	308.467	2.8416	1.1601	305.48	311.45
Cancer Control VEGF 165b Cytoplasm	6	648.631	10.6315	4.3403	637.47	659.79
Cancer treated VEGF 165b Cytoplasm	6	645.313	16.5438	6.7540	627.95	662.67

Means Comparisons

Comparisons for all pairs using Tukey-Kramer HSD

Confidence Quantile

q*	Alpha
3.64086	0.05

Connecting Letters Report

Level								Mean
Normal Control VEGF 165b Cytoplasm	A							824.28228
Normal treated VEGF 165b Cytoplasm	A							818.94977
Cancer Control VEGF 165b Cytoplasm		B						648.63135
Cancer treated VEGF 165b Cytoplasm		B						645.31270
Normal control Bax Nucleus			C					573.10382
Normal treated Bax Nucleus			C					572.33310
Normal treated VEGF 165b Nucleus				D				378.35287
Normal Control VEGF165b Nucleus				D				377.58481
Cancer control Bcl2 Nucleus					E			315.27240
Cancer Treated Bcl2 Nucleus					E			315.12072
Cancer treated VEGF 165b Nucleus					E			308.46667
Normal treated Bax Cytoplasm					E			306.05051
Normal control Bax Cytoplasm					E			305.71493
Cancer Control VEGF 165b Nucleus					E			304.39667
Cancer treated Bax Nucleus						F		275.32900
Cancer Control Bax Nucleus						F		272.73013
Cancer Control Bax Cytoplasm							G	192.48892
Cancer treated Bax Cytoplasm							G	190.33006
Cancer control Bcl2 Cytoplasm							G	189.51469
Cancer Treated Bcl2 Cytoplasm							G	188.51435

Levels not connected by same letter are significantly different.

APPENDIX E2

Oneway Analysis of Fluorescence Intensity of effects of ARVs on Breast cells

Oneway Analysis of Fluorescence Intensity of TDF on Breast cells

Summary of Fit

Rsquare	0.998159
Adj Rsquare	0.997808
Root Mean Square Error	13.47935
Mean of Response	429.829
Observations (or Sum Wgts)	132

Analysis of Variance

Source	DF	Sum of Squares	Mean Square	F Ratio	Prob > F
Gene	21	10838584	516123	2840.633	<.0001*
Error	110	19986	182		
C. Total	131	10858570			

Means and Std Deviations

Level	Number	Mean	Std Dev	Std Err Mean	Lower 95%	Upper 95%
Normal control Bax Nucleus	6	245.46	9.0193	3.6821	236.0	254.9
Normal treated Bax Nucleus	6	244.36	7.2360	2.9541	236.8	252.0
Normal control Bax Cytoplasm	6	560.54	24.0055	9.8002	535.3	585.7
Normal treated Bax Cytoplasm	6	563.56	15.4398	6.3033	547.4	579.8
Normal control Bcl2 Nucleus	6	152.66	4.8650	1.9861	147.6	157.8
Normal treated Bcl2 Nucleus	6	151.52	2.6058	1.0638	148.8	154.3
Normal Control VEGF165b Nucleus	6	356.76	10.1859	4.1584	346.1	367.5
Normal treated VEGF 165b Nucleus	6	353.39	10.7901	4.4050	342.1	364.7
Normal Control VEGF 165b Cytoplasm	6	935.70	22.5602	9.2102	912.0	959.4
Normal treated VEGF 165b Cytoplasm	6	933.66	21.8533	8.9216	910.7	956.6
Cancer Control Bax Nucleus	6	344.20	6.5877	2.6894	337.3	351.1
Cancer treated Bax Nucleus	6	343.30	9.0488	3.6941	333.8	352.8
Cancer Control Bax Cytoplasm	6	192.04	2.8324	1.1563	189.1	195.0
Cancer treated Bax Cytoplasm	6	192.82	3.8414	1.5682	188.8	196.8
Cancer control Bcl2 Nucleus	6	314.65	7.8314	3.1972	306.4	322.9
Cancer Treated Bcl2 Nucleus	6	310.37	10.8950	4.4479	298.9	321.8
Cancer control Bcl2 Cytoplasm	6	197.05	2.4784	1.0118	194.4	199.6
Cancer Treated Bcl2 Cytoplasm	6	194.99	4.6866	1.9133	190.1	199.9
Cancer Control VEGF 165b Nucleus	6	387.06	10.9729	4.4797	375.5	398.6
Cancer treated VEGF 165b Nucleus	6	389.63	14.8254	6.0525	374.1	405.2
Cancer Control VEGF 165b Cytoplasm	6	1048.77	24.1119	9.8436	1023.5	1074.1
Cancer treated VEGF 165b Cytoplasm	6	1043.76	23.1072	9.4335	1019.5	1068.0

Means Comparisons

Comparisons for all pairs using Tukey-Kramer HSD

Confidence Quantile

q*	Alpha
3.68436	0.05

Connecting Letters Report

Level				Mean
Cancer Control VEGF 165b Cytoplasm	A			1048.7683
Cancer treated VEGF 165b Cytoplasm	A			1043.7617
Normal Control VEGF 165b Cytoplasm		B		935.7000
Normal treated VEGF 165b Cytoplasm		B		933.6600
Normal treated Bax Cytoplasm			C	563.5617
Normal control Bax Cytoplasm			C	560.5400

Level									Mean
Cancer treated VEGF 165b Nucleus	D								389.6300
Cancer Control VEGF 165b Nucleus	D								387.0617
Normal Control VEGF165b Nucleus		E							356.7617
Normal treated VEGF 165b Nucleus		E							353.3883
Cancer Control Bax Nucleus		E							344.1988
Cancer treated Bax Nucleus		E	F						343.2955
Cancer control Bcl2 Nucleus			F	G					314.6500
Cancer Treated Bcl2 Nucleus				G					310.3700
Normal control Bax Nucleus					H				245.4617
Normal treated Bax Nucleus					H				244.3617
Cancer control Bcl2 Cytoplasm						I			197.0467
Cancer Treated Bcl2 Cytoplasm						I			194.9850
Cancer treated Bax Cytoplasm						I			192.8150
Cancer Control Bax Cytoplasm						I			192.0367
Normal control Bcl2 Nucleus							J		152.6600
Normal treated Bcl2 Nucleus							J		151.5233

Levels not connected by same letter are significantly different.

Oneway Analysis of Fluorescence Intensity of FTC on Breast cells
Summary of Fit

Rsquare	0.998535
Adj Rsquare	0.998255
Root Mean Square Error	12.05997
Mean of Response	430.2606
Observations (or Sum Wgts)	132

Analysis of Variance

Source	DF	Sum of Squares	Mean Square	F Ratio	Prob > F
Gene	21	10903653	519222	3569.936	<.0001*
Error	110	15999	145		
C. Total	131	10919652			

Means and Std Deviations

Level	Number	Mean	Std Dev	Std Err Mean	Lower 95%	Upper 95%
Normal control Bax Nucleus	6	245.46	9.0193	3.6821	236.0	254.9
Normal treated Bax Nucleus	6	240.92	8.4179	3.4366	232.1	249.8
Normal control Bax Cytoplasm	6	560.54	24.0055	9.8002	535.3	585.7
Normal treated Bax Cytoplasm	6	557.13	16.8189	6.8663	539.5	574.8
Normal control Bcl2 Nucleus	6	152.66	4.8650	1.9861	147.6	157.8
Normal treated Bcl2 Nucleus	6	150.56	1.6449	0.6715	148.8	152.3
Normal Control VEGF165b Nucleus	6	356.76	10.1859	4.1584	346.1	367.5
Normal treated VEGF 165b Nucleus	6	355.33	13.4362	5.4853	341.2	369.4
Normal Control VEGF 165b Cytoplasm	6	935.70	22.5602	9.2102	912.0	959.4
Normal treated VEGF 165b Cytoplasm	6	940.31	13.4421	5.4877	926.2	954.4
Cancer Control Bax Nucleus	6	344.20	6.5877	2.6894	337.3	351.1
Cancer treated Bax Nucleus	6	346.00	4.9552	2.0230	340.8	351.2
Cancer Control Bax Cytoplasm	6	192.04	2.8324	1.1563	189.1	195.0
Cancer treated Bax Cytoplasm	6	192.58	3.5000	1.4289	188.9	196.3
Cancer control Bcl2 Nucleus	6	314.65	7.8314	3.1972	306.4	322.9
Cancer Treated Bcl2 Nucleus	6	312.89	3.2828	1.3402	309.4	316.3
Cancer control Bcl2 Cytoplasm	6	197.05	2.4784	1.0118	194.4	199.6
Cancer Treated Bcl2 Cytoplasm	6	196.04	2.7705	1.1310	193.1	198.9
Cancer Control VEGF 165b Nucleus	6	387.06	10.9729	4.4797	375.5	398.6
Cancer treated VEGF 165b Nucleus	6	390.65	10.7043	4.3700	379.4	401.9

Level	Number	Mean	Std Dev	Std Err Mean	Lower 95%	Upper 95%
Cancer Control VEGF 165b Cytoplasm	6	1048.77	24.1119	9.8436	1023.5	1074.1
Cancer treated VEGF 165b Cytoplasm	6	1048.44	14.0559	5.7383	1033.7	1063.2

Means Comparisons

Comparisons for all pairs using Tukey-Kramer HSD

Confidence Quantile

q*	Alpha
3.68436	0.05

Connecting Letters Report

Level									Mean
Cancer Control VEGF 165b Cytoplasm	A								1048.7683
Cancer treated VEGF 165b Cytoplasm	A								1048.4433
Normal treated VEGF 165b Cytoplasm		B							940.3100
Normal Control VEGF 165b Cytoplasm		B							935.7000
Normal control Bax Cytoplasm			C						560.5400
Normal treated Bax Cytoplasm			C						557.1267
Cancer treated VEGF 165b Nucleus				D					390.6517
Cancer Control VEGF 165b Nucleus				D					387.0617
Normal Control VEGF165b Nucleus					E				356.7617
Normal treated VEGF 165b Nucleus					E				355.3267
Cancer treated Bax Nucleus					E				346.0035
Cancer Control Bax Nucleus					E				344.1988
Cancer control Bcl2 Nucleus						F			314.6500
Cancer Treated Bcl2 Nucleus						F			312.8850
Normal control Bax Nucleus							G		245.4617
Normal treated Bax Nucleus							G		240.9217
Cancer control Bcl2 Cytoplasm								H	197.0467
Cancer Treated Bcl2 Cytoplasm								H	196.0383
Cancer treated Bax Cytoplasm								H	192.5783
Cancer Control Bax Cytoplasm								H	192.0367
Normal control Bcl2 Nucleus									I 152.6600
Normal treated Bcl2 Nucleus									I 150.5617

Levels not connected by same letter are significantly different.

Oneway Analysis of Fluorescence Intensity of EFV on Breast cells

Summary of Fit

Rsquare	0.998818
Adj Rsquare	0.998593
Root Mean Square Error	10.9133
Mean of Response	430.8519
Observations (or Sum Wgts)	132

Analysis of Variance

Source	DF	Sum of Squares	Mean Square	F Ratio	Prob > F
Gene	21	11073126	527292	4427.297	<.0001*
Error	110	13101	119		
C. Total	131	11086228			

Means and Std Deviations

Level	Number	Mean	Std Dev	Std Err Mean	Lower 95%	Upper 95%
Normal control Bax Nucleus	6	243.48	8.1109	3.3113	235.0	252.0
Normal treated Bax Nucleus	6	243.34	5.4806	2.2374	237.6	249.1

Level	Number	Mean	Std Dev	Std Err Mean	Lower 95%	Upper 95%
Normal control Bax Cytoplasm	6	562.09	21.3875	8.7314	539.6	584.5
Normal treated Bax Cytoplasm	6	559.69	11.8261	4.8280	547.3	572.1
Normal control Bcl2 Nucleus	6	150.57	3.9908	1.6293	146.4	154.8
Normal treated Bcl2 Nucleus	6	150.72	1.7893	0.7305	148.8	152.6
Normal Control VEGF165b Nucleus	6	355.63	12.4854	5.0972	342.5	368.7
Normal treated VEGF 165b Nucleus	6	355.81	6.5286	2.6653	349.0	362.7
Normal Control VEGF 165b Cytoplasm	6	945.16	12.4112	5.0669	932.1	958.2
Normal treated VEGF 165b Cytoplasm	6	945.61	18.8638	7.7011	925.8	965.4
Cancer Control Bax Nucleus	6	340.73	10.8621	4.4344	329.3	352.1
Cancer treated Bax Nucleus	6	341.96	1.1745	0.4795	340.7	343.2
Cancer Control Bax Cytoplasm	6	193.11	2.3805	0.9718	190.6	195.6
Cancer treated Bax Cytoplasm	6	193.32	4.4619	1.8216	188.6	198.0
Cancer control Bcl2 Nucleus	6	311.60	10.0953	4.1214	301.0	322.2
Cancer Treated Bcl2 Nucleus	6	311.52	3.5745	1.4593	307.8	315.3
Cancer control Bcl2 Cytoplasm	6	197.98	6.6480	2.7140	191.0	205.0
Cancer Treated Bcl2 Cytoplasm	6	195.56	1.5925	0.6501	193.9	197.2
Cancer Control VEGF 165b Nucleus	6	389.71	10.4542	4.2679	378.7	400.7
Cancer treated VEGF 165b Nucleus	6	386.19	11.6610	4.7606	374.0	398.4
Cancer Control VEGF 165b Cytoplasm	6	1054.57	11.5117	4.6996	1042.5	1066.7
Cancer treated VEGF 165b Cytoplasm	6	1050.43	22.7030	9.2685	1026.6	1074.3

Means Comparisons

Comparisons for all pairs using Tukey-Kramer HSD

Confidence Quantile

q*	Alpha
3.68436	0.05

Connecting Letters Report

Level									Mean
Cancer Control VEGF 165b Cytoplasm	A								1054.5700
Cancer treated VEGF 165b Cytoplasm	A								1050.4283
Normal treated VEGF 165b Cytoplasm		B							945.6133
Normal Control VEGF 165b Cytoplasm		B							945.1600
Normal control Bax Cytoplasm			C						562.0883
Normal treated Bax Cytoplasm			C						559.6867
Cancer Control VEGF 165b Nucleus				D					389.7133
Cancer treated VEGF 165b Nucleus				D					386.1883
Normal treated VEGF 165b Nucleus					E				355.8117
Normal Control VEGF165b Nucleus					E				355.6250
Cancer treated Bax Nucleus					E				341.9588
Cancer Control Bax Nucleus					E				340.7252
Cancer control Bcl2 Nucleus						F			311.5967
Cancer Treated Bcl2 Nucleus						F			311.5150
Normal control Bax Nucleus							G		243.4750
Normal treated Bax Nucleus							G		243.3350
Cancer control Bcl2 Cytoplasm								H	197.9750
Cancer Treated Bcl2 Cytoplasm								H	195.5567
Cancer treated Bax Cytoplasm								H	193.3233
Cancer Control Bax Cytoplasm								H	193.1117
Normal treated Bcl2 Nucleus									I 150.7200
Normal control Bcl2 Nucleus									I 150.5650

Levels not connected by same letter are significantly different.

Oneway Analysis of Fluorescence Intensity of ATP on Breast cells
Summary of Fit

Rsquare	0.998786
Adj Rsquare	0.998554
Root Mean Square Error	11.04102
Mean of Response	430.9074
Observations (or Sum Wgts)	132

Analysis of Variance

Source	DF	Sum of Squares	Mean Square	F Ratio	Prob > F
Gene	21	11033511	525405	4309.987	<.0001*
Error	110	13409	122		
C. Total	131	11046921			

Means and Std Deviations

Level	Number	Mean	Std Dev	Std Err Mean	Lower 95%	Upper 95%
Normal control Bax Nucleus	6	243.48	8.1109	3.3113	235.0	252.0
Normal treated Bax Nucleus	6	242.60	5.5505	2.2660	236.8	248.4
Normal control Bax Cytoplasm	6	562.09	21.3875	8.7314	539.6	584.5
Normal treated Bax Cytoplasm	6	558.33	10.0050	4.0845	547.8	568.8
Normal control Bcl2 Nucleus	6	150.57	3.9908	1.6293	146.4	154.8
Normal treated Bcl2 Nucleus	6	151.60	2.1091	0.8610	149.4	153.8
Normal Control VEGF165b Nucleus	6	355.63	12.4854	5.0972	342.5	368.7
Normal treated VEGF 165b Nucleus	6	354.31	4.3220	1.7644	349.8	358.8
Normal Control VEGF 165b Cytoplasm	6	945.16	12.4112	5.0669	932.1	958.2
Normal treated VEGF 165b Cytoplasm	6	938.37	23.1829	9.4644	914.0	962.7
Cancer Control Bax Nucleus	6	340.73	10.8621	4.4344	329.3	352.1
Cancer treated Bax Nucleus	6	342.98	6.2511	2.5520	336.4	349.5
Cancer Control Bax Cytoplasm	6	193.11	2.3805	0.9718	190.6	195.6
Cancer treated Bax Cytoplasm	6	190.60	5.4838	2.2387	184.8	196.4
Cancer control Bcl2 Nucleus	6	311.60	10.0953	4.1214	301.0	322.2
Cancer Treated Bcl2 Nucleus	6	316.43	5.5660	2.2723	310.6	322.3
Cancer control Bcl2 Cytoplasm	6	197.98	6.6480	2.7140	191.0	205.0
Cancer Treated Bcl2 Cytoplasm	6	195.16	6.7883	2.7713	188.0	202.3
Cancer Control VEGF 165b Nucleus	6	389.71	10.4542	4.2679	378.7	400.7
Cancer treated VEGF 165b Nucleus	6	393.30	7.1313	2.9113	385.8	400.8
Cancer Control VEGF 165b Cytoplasm	6	1054.57	11.5117	4.6996	1042.5	1066.7
Cancer treated VEGF 165b Cytoplasm	6	1051.69	20.8017	8.4923	1029.9	1073.5

Means Comparisons
Comparisons for all pairs using Tukey-Kramer HSD
Confidence Quantile

q*	Alpha
3.68436	0.05

Connecting Letters Report

Level						Mean
Cancer Control VEGF 165b Cytoplasm	A					1054.5700
Cancer treated VEGF 165b Cytoplasm	A					1051.6867
Normal Control VEGF 165b Cytoplasm		B				945.1600
Normal treated VEGF 165b Cytoplasm		B				938.3717
Normal control Bax Cytoplasm			C			562.0883
Normal treated Bax Cytoplasm			C			558.3300
Cancer treated VEGF 165b Nucleus				D		393.2950
Cancer Control VEGF 165b Nucleus				D		389.7133
Normal Control VEGF165b Nucleus					E	355.6250
Normal treated VEGF 165b Nucleus					E	354.3083

Level							Mean
Cancer treated Bax Nucleus	E						342.9817
Cancer Control Bax Nucleus	E						340.7252
Cancer Treated Bcl2 Nucleus		F					316.4250
Cancer control Bcl2 Nucleus		F					311.5967
Normal control Bax Nucleus			G				243.4750
Normal treated Bax Nucleus			G				242.6033
Cancer control Bcl2 Cytoplasm				H			197.9750
Cancer Treated Bcl2 Cytoplasm				H			195.1617
Cancer Control Bax Cytoplasm				H			193.1117
Cancer treated Bax Cytoplasm				H			190.5967
Normal treated Bcl2 Nucleus					I		151.5983
Normal control Bcl2 Nucleus					I		150.5650

Levels not connected by same letter are significantly different.

Oneway Analysis Fluorescence Intensity of LPV on Breast cells
Summary of Fit

Rsquare	0.998896
Adj Rsquare	0.998685
Root Mean Square Error	10.50484
Mean of Response	430.2275
Observations (or Sum Wgts)	132

Analysis of Variance

Source	DF	Sum of Squares	Mean Square	F Ratio	Prob > F
Gene	21	10983781	523037	4739.733	<.0001*
Error	110	12139	110		
C. Total	131	10995919			

Means and Std Deviations

Level	Number	Mean	Std Dev	Std Err Mean	Lower 95%	Upper 95%
Normal control Bax Nucleus	6	243.48	8.1109	3.3113	235.0	252.0
Normal treated Bax Nucleus	6	242.33	4.0191	1.6408	238.1	246.5
Normal control Bax Cytoplasm	6	562.09	21.3875	8.7314	539.6	584.5
Normal treated Bax Cytoplasm	6	563.02	10.2409	4.1808	552.3	573.8
Normal control Bcl2 Nucleus	6	150.57	3.9908	1.6293	146.4	154.8
Normal treated Bcl2 Nucleus	6	151.46	2.7117	1.1070	148.6	154.3
Normal Control VEGF165b Nucleus	6	355.63	12.4854	5.0972	342.5	368.7
Normal treated VEGF 165b Nucleus	6	354.18	4.7369	1.9338	349.2	359.1
Normal Control VEGF 165b Cytoplasm	6	945.16	12.4112	5.0669	932.1	958.2
Normal treated VEGF 165b Cytoplasm	6	932.08	20.7826	8.4845	910.3	953.9
Cancer Control Bax Nucleus	6	340.73	10.8621	4.4344	329.3	352.1
Cancer treated Bax Nucleus	6	345.78	7.9642	3.2514	337.4	354.1
Cancer Control Bax Cytoplasm	6	193.11	2.3805	0.9718	190.6	195.6
Cancer treated Bax Cytoplasm	6	190.68	3.9724	1.6217	186.5	194.8
Cancer control Bcl2 Nucleus	6	311.60	10.0953	4.1214	301.0	322.2
Cancer Treated Bcl2 Nucleus	6	313.10	5.7813	2.3602	307.0	319.2
Cancer control Bcl2 Cytoplasm	6	197.98	6.6480	2.7140	191.0	205.0
Cancer Treated Bcl2 Cytoplasm	6	194.74	3.9739	1.6223	190.6	198.9
Cancer Control VEGF 165b Nucleus	6	389.71	10.4542	4.2679	378.7	400.7
Cancer treated VEGF 165b Nucleus	6	384.99	7.2961	2.9786	377.3	392.6
Cancer Control VEGF 165b Cytoplasm	6	1054.57	11.5117	4.6996	1042.5	1066.7
Cancer treated VEGF 165b Cytoplasm	6	1048.06	17.3985	7.1029	1029.8	1066.3

Means Comparisons
Comparisons for all pairs using Tukey-Kramer HSD
Confidence Quantile

q*	Alpha
3.68436	0.05

Connecting Letters Report

Level									Mean
Cancer Control VEGF 165b Cytoplasm	A								1054.5700
Cancer treated VEGF 165b Cytoplasm	A								1048.0550
Normal Control VEGF 165b Cytoplasm		B							945.1600
Normal treated VEGF 165b Cytoplasm		B							932.0817
Normal treated Bax Cytoplasm			C						563.0167
Normal control Bax Cytoplasm			C						562.0883
Cancer Control VEGF 165b Nucleus				D					389.7133
Cancer treated VEGF 165b Nucleus				D					384.9900
Normal Control VEGF165b Nucleus					E				355.6250
Normal treated VEGF 165b Nucleus					E				354.1750
Cancer treated Bax Nucleus					E				345.7832
Cancer Control Bax Nucleus					E				340.7252
Cancer Treated Bcl2 Nucleus						F			313.0983
Cancer control Bcl2 Nucleus						F			311.5967
Normal control Bax Nucleus							G		243.4750
Normal treated Bax Nucleus							G		242.3250
Cancer control Bcl2 Cytoplasm								H	197.9750
Cancer Treated Bcl2 Cytoplasm								H	194.7350
Cancer Control Bax Cytoplasm								H	193.1117
Cancer treated Bax Cytoplasm								H	190.6783
Normal treated Bcl2 Nucleus									I 151.4617
Normal control Bcl2 Nucleus									I 150.5650

Levels not connected by same letter are significantly different.

Oneway Analysis of Fluorescence Intensity of RTV on Breast cells
Summary of Fit

Rsquare	0.998902
Adj Rsquare	0.998693
Root Mean Square Error	10.5307
Mean of Response	431.1424
Observations (or Sum Wgts)	132

Analysis of Variance

Source	DF	Sum of Squares	Mean Square	F Ratio	Prob > F
Gene	21	11099147	528531	4766.023	<.0001*
Error	110	12199	111		
C. Total	131	11111346			

Means and Std Deviations

Level	Number	Mean	Std Dev	Std Err Mean	Lower 95%	Upper 95%
Normal control Bax Nucleus	6	243.48	8.1109	3.3113	235.0	252.0
Normal treated Bax Nucleus	6	242.56	4.9044	2.0022	237.4	247.7
Normal control Bax Cytoplasm	6	562.09	21.3875	8.7314	539.6	584.5
Normal treated Bax Cytoplasm	6	566.13	6.8715	2.8053	558.9	573.3
Normal control Bcl2 Nucleus	6	150.57	3.9908	1.6293	146.4	154.8
Normal treated Bcl2 Nucleus	6	150.74	4.2281	1.7261	146.3	155.2
Normal Control VEGF165b Nucleus	6	355.63	12.4854	5.0972	342.5	368.7

Level	Number	Mean	Std Dev	Std Err Mean	Lower 95%	Upper 95%
Normal treated VEGF 165b Nucleus	6	355.25	9.4655	3.8643	345.3	365.2
Normal Control VEGF 165b Cytoplasm	6	945.16	12.4112	5.0669	932.1	958.2
Normal treated VEGF 165b Cytoplasm	6	937.22	20.6352	8.4243	915.6	958.9
Cancer Control Bax Nucleus	6	340.73	10.8621	4.4344	329.3	352.1
Cancer treated Bax Nucleus	6	341.18	9.8620	4.0261	330.8	351.5
Cancer Control Bax Cytoplasm	6	193.11	2.3805	0.9718	190.6	195.6
Cancer treated Bax Cytoplasm	6	191.99	5.0352	2.0556	186.7	197.3
Cancer control Bcl2 Nucleus	6	311.60	10.0953	4.1214	301.0	322.2
Cancer Treated Bcl2 Nucleus	6	310.64	6.2444	2.5493	304.1	317.2
Cancer control Bcl2 Cytoplasm	6	197.98	6.6480	2.7140	191.0	205.0
Cancer Treated Bcl2 Cytoplasm	6	194.94	3.8133	1.5568	190.9	198.9
Cancer Control VEGF 165b Nucleus	6	389.71	10.4542	4.2679	378.7	400.7
Cancer treated VEGF 165b Nucleus	6	391.45	7.2022	2.9403	383.9	399.0
Cancer Control VEGF 165b Cytoplasm	6	1054.57	11.5117	4.6996	1042.5	1066.7
Cancer treated VEGF 165b Cytoplasm	6	1058.45	15.7002	6.4096	1042.0	1074.9

Means Comparisons

Comparisons for all pairs using Tukey-Kramer HSD

Confidence Quantile

q*	Alpha
3.68436	0.05

Connecting Letters Report

Level									Mean
Cancer treated VEGF 165b Cytoplasm	A								1058.4533
Cancer Control VEGF 165b Cytoplasm	A								1054.5700
Normal Control VEGF 165b Cytoplasm		B							945.1600
Normal treated VEGF 165b Cytoplasm		B							937.2150
Normal treated Bax Cytoplasm			C						566.1300
Normal control Bax Cytoplasm			C						562.0883
Cancer treated VEGF 165b Nucleus				D					391.4450
Cancer Control VEGF 165b Nucleus				D					389.7133
Normal Control VEGF165b Nucleus					E				355.6250
Normal treated VEGF 165b Nucleus					E				355.2483
Cancer treated Bax Nucleus					E				341.1767
Cancer Control Bax Nucleus					E				340.7252
Cancer control Bcl2 Nucleus						F			311.5967
Cancer Treated Bcl2 Nucleus						F			310.6400
Normal control Bax Nucleus							G		243.4750
Normal treated Bax Nucleus							G		242.5617
Cancer control Bcl2 Cytoplasm								H	197.9750
Cancer Treated Bcl2 Cytoplasm								H	194.9350
Cancer Control Bax Cytoplasm								H	193.1117
Cancer treated Bax Cytoplasm								H	191.9850
Normal treated Bcl2 Nucleus									I 150.7367
Normal control Bcl2 Nucleus									I 150.5650

Levels not connected by same letter are significantly different.

Oneway Analysis of Fluorescence Intensity of LPVr on Breast cells
Summary of Fit

Rsquare	0.998719
Adj Rsquare	0.998475
Root Mean Square Error	11.32883
Mean of Response	430.792
Observations (or Sum Wgts)	132

Analysis of Variance

Source	DF	Sum of Squares	Mean Square	F Ratio	Prob > F
Gene	21	11009422	524258	4084.841	<.0001*
Error	110	14118	128		
C. Total	131	11023540			

Means and Std Deviations

Level	Number	Mean	Std Dev	Std Err Mean	Lower 95%	Upper 95%
Normal control Bax Nucleus	6	243.48	8.1109	3.311	235.0	252.0
Normal treated Bax Nucleus	6	244.02	1.8067	0.738	242.1	245.9
Normal control Bax Cytoplasm	6	562.09	21.3875	8.731	539.6	584.5
Normal treated Bax Cytoplasm	6	566.04	7.8452	3.203	557.8	574.3
Normal control Bcl2 Nucleus	6	150.57	3.9908	1.629	146.4	154.8
Normal treated Bcl2 Nucleus	6	151.36	2.3337	0.953	148.9	153.8
Normal Control VEGF165b Nucleus	6	355.63	12.4854	5.097	342.5	368.7
Normal treated VEGF 165b Nucleus	6	356.24	7.8274	3.196	348.0	364.5
Normal Control VEGF 165b Cytoplasm	6	945.16	12.4112	5.067	932.1	958.2
Normal treated VEGF 165b Cytoplasm	6	936.90	25.3196	10.337	910.3	963.5
Cancer Control Bax Nucleus	6	340.73	10.8621	4.434	329.3	352.1
Cancer treated Bax Nucleus	6	341.73	6.3479	2.592	335.1	348.4
Cancer Control Bax Cytoplasm	6	193.11	2.3805	0.972	190.6	195.6
Cancer treated Bax Cytoplasm	6	191.80	6.1463	2.509	185.3	198.3
Cancer control Bcl2 Nucleus	6	311.60	10.0953	4.121	301.0	322.2
Cancer Treated Bcl2 Nucleus	6	313.67	7.4277	3.032	305.9	321.5
Cancer control Bcl2 Cytoplasm	6	197.98	6.6480	2.714	191.0	205.0
Cancer Treated Bcl2 Cytoplasm	6	195.10	4.6020	1.879	190.3	199.9
Cancer Control VEGF 165b Nucleus	6	389.71	10.4542	4.268	378.7	400.7
Cancer treated VEGF 165b Nucleus	6	388.00	5.4058	2.207	382.3	393.7
Cancer Control VEGF 165b Cytoplasm	6	1054.57	11.5117	4.700	1042.5	1066.7
Cancer treated VEGF 165b Cytoplasm	6	1047.97	22.5088	9.189	1024.3	1071.6

Means Comparisons
Comparisons for all pairs using Tukey-Kramer HSD
Confidence Quantile

q*	Alpha
3.68436	0.05

Connecting Letters Report

Level				Mean
Cancer Control VEGF 165b Cytoplasm	A			1054.5700
Cancer treated VEGF 165b Cytoplasm	A			1047.9700
Normal Control VEGF 165b Cytoplasm		B		945.1600
Normal treated VEGF 165b Cytoplasm		B		936.9017
Normal treated Bax Cytoplasm			C	566.0383

Connecting Letters Report **Mean**

Level								
Normal control Bax Cytoplasm	C							562.0883
Cancer Control VEGF 165b Nucleus		D						389.7133
Cancer treated VEGF 165b Nucleus		D						387.9967
Normal treated VEGF 165b Nucleus			E					356.2433
Normal Control VEGF165b Nucleus			E					355.6250
Cancer treated Bax Nucleus			E					341.7302
Cancer Control Bax Nucleus			E					340.7252
Cancer Treated Bcl2 Nucleus				F				313.6650
Cancer control Bcl2 Nucleus				F				311.5967
Normal treated Bax Nucleus					G			244.0150
Normal control Bax Nucleus					G			243.4750
Cancer control Bcl2 Cytoplasm						H		197.9750
Cancer Treated Bcl2 Cytoplasm						H		195.1033
Cancer Control Bax Cytoplasm						H		193.1117
Cancer treated Bax Cytoplasm						H		191.8000
Normal treated Bcl2 Nucleus							I	151.3550
Normal control Bcl2 Nucleus							I	150.5650

Levels not connected by same letter are significantly different.

Oneway Analysis of Fluorescence Intensity of TDF/FTC/LPV/r on Breast cells
Summary of Fit

Rsquare	0.998687
Adj Rsquare	0.998436
Root Mean Square Error	11.49501
Mean of Response	431.1353
Observations (or Sum Wgts)	132

Analysis of Variance

Source	DF	Sum of Squares	Mean Square	F Ratio	Prob > F
Gene	21	11053622	526363	3983.513	<.0001*
Error	110	14535	132		
C. Total	131	11068157			

Means and Std Deviations

Level	Number	Mean	Std Dev	Std Err Mean	Lower 95%	Upper 95%
Normal control Bax Nucleus	6	243.48	8.1109	3.311	235.0	252.0
Normal treated Bax Nucleus	6	245.75	3.9169	1.599	241.6	249.9
Normal control Bax Cytoplasm	6	562.09	21.3875	8.731	539.6	584.5
Normal treated Bax Cytoplasm	6	567.27	14.2712	5.826	552.3	582.2
Normal control Bcl2 Nucleus	6	150.57	3.9908	1.629	146.4	154.8
Normal treated Bcl2 Nucleus	6	151.87	3.5829	1.463	148.1	155.6
Normal Control VEGF165b Nucleus	6	355.63	12.4854	5.097	342.5	368.7
Normal treated VEGF 165b Nucleus	6	355.94	8.2213	3.356	347.3	364.6
Normal Control VEGF 165b Cytoplasm	6	945.16	12.4112	5.067	932.1	958.2
Normal treated VEGF 165b Cytoplasm	6	938.57	21.5284	8.789	916.0	961.2
Cancer Control Bax Nucleus	6	340.73	10.8621	4.434	329.3	352.1
Cancer treated Bax Nucleus	6	340.18	8.9627	3.659	330.8	349.6
Cancer Control Bax Cytoplasm	6	193.11	2.3805	0.972	190.6	195.6
Cancer treated Bax Cytoplasm	6	190.17	3.9897	1.629	186.0	194.4
Cancer control Bcl2 Nucleus	6	311.60	10.0953	4.121	301.0	322.2
Cancer Treated Bcl2 Nucleus	6	310.95	4.7263	1.930	306.0	315.9
Cancer control Bcl2 Cytoplasm	6	197.98	6.6480	2.714	191.0	205.0

Level	Number	Mean	Std Dev	Std Err Mean	Lower 95%	Upper 95%
Cancer Treated Bcl2 Cytoplasm	6	195.95	3.8492	1.571	191.9	200.0
Cancer Control VEGF 165b Nucleus	6	389.71	10.4542	4.268	378.7	400.7
Cancer treated VEGF 165b Nucleus	6	391.54	5.6698	2.315	385.6	397.5
Cancer Control VEGF 165b Cytoplasm	6	1054.57	11.5117	4.700	1042.5	1066.7
Cancer treated VEGF 165b Cytoplasm	6	1052.19	24.8573	10.148	1026.1	1078.3

Means Comparisons

Comparisons for all pairs using Tukey-Kramer HSD

Confidence Quantile

q*	Alpha
3.68436	0.05

Connecting Letters Report

Level									Mean
Cancer Control VEGF 165b Cytoplasm	A								1054.5700
Cancer treated VEGF 165b Cytoplasm	A								1052.1850
Normal Control VEGF 165b Cytoplasm		B							945.1600
Normal treated VEGF 165b Cytoplasm		B							938.5667
Normal treated Bax Cytoplasm			C						567.2717
Normal control Bax Cytoplasm			C						562.0883
Cancer treated VEGF 165b Nucleus				D					391.5433
Cancer Control VEGF 165b Nucleus				D					389.7133
Normal treated VEGF 165b Nucleus					E				355.9350
Normal Control VEGF165b Nucleus					E				355.6250
Cancer Control Bax Nucleus					E				340.7252
Cancer treated Bax Nucleus					E				340.1757
Cancer control Bcl2 Nucleus						F			311.5967
Cancer Treated Bcl2 Nucleus						F			310.9500
Normal treated Bax Nucleus							G		245.7450
Normal control Bax Nucleus							G		243.4750
Cancer control Bcl2 Cytoplasm								H	197.9750
Cancer Treated Bcl2 Cytoplasm								H	195.9533
Cancer Control Bax Cytoplasm								H	193.1117
Cancer treated Bax Cytoplasm								H	190.1733
Normal treated Bcl2 Nucleus									I 151.8733
Normal control Bcl2 Nucleus									I 150.5650

Levels not connected by same letter are significantly different.

APPENDIX F

Oneway Analysis of Nuclear Axis lengths (µm) By Treatment Groups

Oneway Analysis of Normal Cervix Nuc. Long Axis µm By GROUPS

Summary of Fit

Rsquare	0.029034
Adj Rsquare	-0.14574
Root Mean Square Error	0.479142
Mean of Response	22.64983
Observations (or Sum Wgts)	60

Analysis of Variance

Source	DF	Sum of Squares	Mean Square	F Ratio	Prob > F
GROUPS	9	0.343248	0.038139	0.1661	0.9966
Error	50	11.478850	0.229577		

Source	DF	Sum of Squares	Mean Square	F Ratio	Prob > F
C. Total	59	11.822098			

Means and Std Deviations

Level	Number	Mean	Std Dev	Std Err Mean	Lower 95%	Upper 95%
Untreated Control	6	22.7367	0.682574	0.27866	22.020	23.453
0.01%Methanol	6	22.5417	0.246367	0.10058	22.283	22.800
0.3 µg/ml TDF	6	22.5617	0.267014	0.10901	22.281	22.842
1.8µg/ml FTC	6	22.6917	0.316128	0.12906	22.360	23.023
4.07µg/ml EFV	6	22.7317	0.259647	0.10600	22.459	23.004
ATRIPLA	6	22.5633	0.337441	0.13776	22.209	22.917
9.8µg/ml LPV	6	22.7467	0.607607	0.24805	22.109	23.384
0.6 µg/ml RTV	6	22.5917	0.644590	0.26315	21.915	23.268
KALETRA(LPV/r)	6	22.6883	0.688169	0.28094	21.966	23.411
TDF/FTC/LPVr	6	22.6450	0.397982	0.16248	22.227	23.063

Means Comparisons

Comparisons for all pairs using Tukey-Kramer HSD

Confidence Quantile

q*	Alpha
3.31028	0.05

Connecting Letters Report

Level	
9.8µg/ml LPV	A
Untreated Control	A
4.07µg/ml EFV	A
1.8µg/ml FTC	A
KALETRA(LPV/r)	A
TDF/FTC/LPVr	A
0.6 µg/ml RTV	A
ATRIPLA	A
0.3 µg/ml TDF	A
0.01%Methanol	A

Levels not connected by same letter are significantly different.

Oneway Analysis of Normal Cervix Nuc. Short Axis µm By GROUPS

Summary of Fit

Rsquare	0.022329
Adj Rsquare	-0.15365
Root Mean Square Error	0.408818
Mean of Response	15.237
Observations (or Sum Wgts)	60

Analysis of Variance

Source	DF	Sum of Squares	Mean Square	F Ratio	Prob > F
GROUPS	9	0.1908600	0.021207	0.1269	0.9988
Error	50	8.3566000	0.167132		
C. Total	59	8.5474600			

Means and Std Deviations

Level	Number	Mean	Std Dev	Std Err Mean	Lower 95%	Upper 95%
Untreated Control	6	15.2800	0.423367	0.17284	14.836	15.724
0.01%Methanol	6	15.1833	0.413747	0.16891	14.749	15.618
0.3 µg/ml TDF	6	15.2667	0.579126	0.23643	14.659	15.874
1.8µg/ml FTC	6	15.1900	0.505767	0.20648	14.659	15.721
4.07µg/ml EFV	6	15.2483	0.511094	0.20865	14.712	15.785
ATRIPLA	6	15.1617	0.194362	0.07935	14.958	15.366
9.8µg/ml LPV	6	15.1933	0.191172	0.07805	14.993	15.394
0.6 µg/ml RTV	6	15.3217	0.387320	0.15812	14.915	15.728
KALETRA(LPV/r)	6	15.2000	0.318559	0.13005	14.866	15.534
TDF/FTC/LPVr	6	15.3250	0.377717	0.15420	14.929	15.721

Means Comparisons

Comparisons for all pairs using Tukey-Kramer HSD

Confidence Quantile

q*	Alpha
3.31028	0.05

Connecting Letters Report

Level	
TDF/FTC/LPVr	A
0.6 µg/ml RTV	A
Untreated Control	A
0.3 µg/ml TDF	A
4.07µg/ml EFV	A
KALETRA(LPV/r)	A
9.8µg/ml LPV	A
1.8µg/ml FTC	A
0.01%Methanol	A
ATRIPLA	A

Levels not connected by same letter are significantly different.

Oneway Analysis of Cancer Cervix Nuc. Long Axis µm By GROUPS

Summary of Fit

Rsquare	0.138576
Adj Rsquare	-0.01648
Root Mean Square Error	0.409774
Mean of Response	14.9365
Observations (or Sum Wgts)	60

Analysis of Variance

Source	DF	Sum of Squares	Mean Square	F Ratio	Prob > F
GROUPS	9	1.3506150	0.150068	0.8937	0.5377
Error	50	8.3957500	0.167915		
C. Total	59	9.7463650			

Means and Std Deviations

Level	Number	Mean	Std Dev	Std Err Mean	Lower 95%	Upper 95%

Level	Number	Mean	Std Dev	Std Err Mean	Lower 95%	Upper 95%
Untreated Control	6	15.0017	0.389996	0.15922	14.592	15.411
0.01%Methanol	6	14.9833	0.500466	0.20431	14.458	15.509
0.3 µg/ml TDF	6	15.0367	0.446169	0.18215	14.568	15.505
1.8µg/ml FTC	6	14.8250	0.518295	0.21159	14.281	15.369
4.07µg/ml EFV	6	14.9750	0.337268	0.13769	14.621	15.329
ATRIPLA	6	14.9300	0.342053	0.13964	14.571	15.289
9.8µg/ml LPV	6	14.5450	0.645376	0.26347	13.868	15.222
0.6 µg/ml RTV	6	14.9283	0.300361	0.12262	14.613	15.244
KALETRA(LPV/r)	6	15.0167	0.111654	0.04558	14.899	15.134
TDF/FTC/LPVr	6	15.1233	0.242789	0.09912	14.869	15.378

Means Comparisons

Comparisons for all pairs using Tukey-Kramer HSD

Confidence Quantile

q*	Alpha
3.31028	0.05

Connecting Letters Report

Level	
TDF/FTC/LPVr	A
0.3 µg/ml TDF	A
KALETRA(LPV/r)	A
Untreated Control	A
0.01%Methanol	A
4.07µg/ml EFV	A
ATRIPLA	A
0.6 µg/ml RTV	A
1.8µg/ml FTC	A
9.8µg/ml LPV	A

Levels not connected by same letter are significantly different.

Oneway Analysis of Cancer Cervix Nuc. Short Axis µm By GROUPS

Summary of Fit

Rsquare	0.153208
Adj Rsquare	0.000786
Root Mean Square Error	0.245944
Mean of Response	9.646167
Observations (or Sum Wgts)	60

Analysis of Variance

Source	DF	Sum of Squares	Mean Square	F Ratio	Prob > F
GROUPS	9	0.5472017	0.060800	1.0052	0.4485
Error	50	3.0244167	0.060488		
C. Total	59	3.5716183			

Means and Std Deviations

Level	Number	Mean	Std Dev	Std Err Mean	Lower 95%	Upper 95%

Level	Number	Mean	Std Dev	Std Err Mean	Lower 95%	Upper 95%
Untreated Control	6	9.78167	0.320775	0.13096	9.4450	10.118
0.01%Methanol	6	9.63000	0.117983	0.04817	9.5062	9.754
0.3 µg/ml TDF	6	9.76833	0.199641	0.08150	9.5588	9.978
1.8µg/ml FTC	6	9.75500	0.158461	0.06469	9.5887	9.921
4.07µg/ml EFV	6	9.58833	0.313332	0.12792	9.2595	9.917
ATRIPLA	6	9.66667	0.341389	0.13937	9.3084	10.025
9.8µg/ml LPV	6	9.66333	0.261891	0.10692	9.3885	9.938
0.6 µg/ml RTV	6	9.47667	0.286333	0.11690	9.1762	9.777
KALETRA(LPV/r)	6	9.55833	0.217937	0.08897	9.3296	9.787
TDF/FTC/LPVr	6	9.57333	0.101522	0.04145	9.4668	9.680

Means Comparisons

Comparisons for all pairs using Tukey-Kramer HSD

Confidence Quantile

q*	Alpha
3.31028	0.05

Connecting Letters Report

Level	
Untreated Control	A
0.3 µg/ml TDF	A
1.8µg/ml FTC	A
ATRIPLA	A
9.8µg/ml LPV	A
0.01%Methanol	A
4.07µg/ml EFV	A
TDF/FTC/LPVr	A
KALETRA(LPV/r)	A
0.6 µg/ml RTV	A

Levels not connected by same letter are significantly different.

Oneway Analysis of Normal Breast Nuc. Long Axis µm By GROUPS

Summary of Fit

Rsquare	0.13224
Adj Rsquare	-0.02396
Root Mean Square Error	0.418844
Mean of Response	15.23528
Observations (or Sum Wgts)	60

Analysis of Variance

Source	DF	Sum of Squares	Mean Square	F Ratio	Prob > F
GROUPS	9	1.336713	0.148524	0.8466	0.5776
Error	50	8.771515	0.175430		
C. Total	59	10.108228			

Means and Std Deviations

Level	Number	Mean	Std Dev	Std Err Mean	Lower 95%	Upper 95%

Level	Number	Mean	Std Dev	Std Err Mean	Lower 95%	Upper 95%
Untreated Control	6	15.3189	0.498624	0.20356	14.796	15.842
0.01%Methanol	6	15.3385	0.454163	0.18541	14.862	15.815
0.3 µg/ml TDF	6	15.1226	0.528383	0.21571	14.568	15.677
1.8µg/ml FTC	6	15.2740	0.344052	0.14046	14.913	15.635
4.07µg/ml EFV	6	15.2280	0.348213	0.14216	14.863	15.593
ATRIPLA	6	14.8366	0.656238	0.26791	14.148	15.525
9.8µg/ml LPV	6	15.2254	0.307662	0.12560	14.902	15.548
0.6 µg/ml RTV	6	15.3166	0.113286	0.04625	15.198	15.435
KALETRA(LPV/r)	6	15.3284	0.356844	0.14568	14.954	15.703
TDF/FTC/LPVr	6	15.3639	0.339301	0.13852	15.008	15.720

Means Comparisons

Comparisons for all pairs using Tukey-Kramer HSD

Confidence Quantile

q*	Alpha
3.31028	0.05

Connecting Letters Report

Level	
TDF/FTC/LPVr	A
0.01%Methanol	A
KALETRA(LPV/r)	A
Untreated Control	A
0.6 µg/ml RTV	A
1.8µg/ml FTC	A
4.07µg/ml EFV	A
9.8µg/ml LPV	A
0.3 µg/ml TDF	A
ATRIPLA	A

Levels not connected by same letter are significantly different.

Oneway Analysis of Normal Breast Nuc. Short Axis µm By GROUPS

Summary of Fit

Rsquare	0.038834
Adj Rsquare	-0.13418
Root Mean Square Error	0.28052
Mean of Response	10.89584
Observations (or Sum Wgts)	60

Analysis of Variance

Source	DF	Sum of Squares	Mean Square	F Ratio	Prob > F
GROUPS	9	0.1589695	0.017663	0.2245	0.9895
Error	50	3.9345653	0.078691		
C. Total	59	4.0935349			

Means and Std Deviations

Level	Number	Mean	Std Dev	Std Err Mean	Lower 95%	Upper 95%
Untreated Control	6	10.8340	0.258414	0.10550	10.563	11.105
0.01%Methanol	6	10.9445	0.305808	0.12485	10.624	11.265
0.3 µg/ml TDF	6	10.9200	0.363743	0.14850	10.538	11.302
1.8µg/ml FTC	6	10.9598	0.324512	0.13248	10.619	11.300
4.07µg/ml EFV	6	10.8707	0.389236	0.15890	10.462	11.279
ATRIPLA	6	10.8998	0.189029	0.07717	10.701	11.098
9.8µg/ml LPV	6	10.8455	0.112577	0.04596	10.727	10.964
0.6 µg/ml RTV	6	10.9070	0.192144	0.07844	10.705	11.109
KALETRA(LPV/r)	6	10.8104	0.268565	0.10964	10.529	11.092
TDF/FTC/LPVr	6	10.9667	0.282918	0.11550	10.670	11.264

Means Comparisons

Comparisons for all pairs using Tukey-Kramer HSD

Confidence Quantile

q*	Alpha
3.31028	0.05

Connecting Letters Report

Level	
TDF/FTC/LPVr	A
1.8µg/ml FTC	A
0.01%Methanol	A
0.3 µg/ml TDF	A
0.6 µg/ml RTV	A
ATRIPLA	A
4.07µg/ml EFV	A
9.8µg/ml LPV	A
Untreated Control	A
KALETRA(LPV/r)	A

Levels not connected by same letter are significantly different.

Oneway Analysis of Cancer Breast Nuc. Long Axis µm 2 By GROUPS

Summary of Fit

Rsquare	0.143803
Adj Rsquare	-0.01031
Root Mean Square Error	0.454352
Mean of Response	16.41
Observations (or Sum Wgts)	60

Analysis of Variance

Source	DF	Sum of Squares	Mean Square	F Ratio	Prob > F
GROUPS	9	1.733600	0.192622	0.9331	0.5052
Error	50	10.321800	0.206436		
C. Total	59	12.055400			

Means and Std Deviations

Level	Number	Mean	Std Dev	Std Err Mean	Lower 95%	Upper 95%

Level	Number	Mean	Std Dev	Std Err Mean	Lower 95%	Upper 95%
Untreated Control	6	16.2567	0.466762	0.19055	15.767	16.747
0.01%Methanol	6	16.5100	0.446497	0.18228	16.041	16.979
0.3 µg/ml TDF	6	16.4367	0.469283	0.19158	15.944	16.929
1.8µg/ml FTC	6	16.7750	0.371308	0.15159	16.385	17.165
4.07µg/ml EFV	6	16.2633	0.308199	0.12582	15.940	16.587
ATRIPLA	6	16.1350	0.806666	0.32932	15.288	16.982
9.8µg/ml LPV	6	16.3933	0.226774	0.09258	16.155	16.631
0.6 µg/ml RTV	6	16.5417	0.241447	0.09857	16.288	16.795
KALETRA(LPV/r)	6	16.4500	0.515946	0.21063	15.909	16.991
TDF/FTC/LPVr	6	16.3383	0.409166	0.16704	15.909	16.768

Means Comparisons

Comparisons for all pairs using Tukey-Kramer HSD

Confidence Quantile

q*	Alpha
3.31028	0.05

Connecting Letters Report

Level	
1.8µg/ml FTC	A
0.6 µg/ml RTV	A
0.01%Methanol	A
KALETRA(LPV/r)	A
0.3 µg/ml TDF	A
9.8µg/ml LPV	A
TDF/FTC/LPVr	A
4.07µg/ml EFV	A
Untreated Control	A
ATRIPLA	A

Levels not connected by same letter are significantly different.

Oneway Analysis of Cancer Breast Nuc. Short Axis µm By GROUPS

Summary of Fit

Rsquare	0.184926
Adj Rsquare	0.038213
Root Mean Square Error	0.282699
Mean of Response	10.809
Observations (or Sum Wgts)	60

Analysis of Variance

Source	DF	Sum of Squares	Mean Square	F Ratio	Prob > F
GROUPS	9	0.9066067	0.100734	1.2605	0.2816
Error	50	3.9959333	0.079919		
C. Total	59	4.9025400			

Means and Std Deviations

Level	Number	Mean	Std Dev	Std Err Mean	Lower 95%	Upper 95%

Level	Number	Mean	Std Dev	Std Err Mean	Lower 95%	Upper 95%
Untreated Control	6	10.8200	0.339588	0.13864	10.464	11.176
0.01%Methanol	6	10.7233	0.325924	0.13306	10.381	11.065
0.3 µg/ml TDF	6	10.7833	0.408542	0.16679	10.355	11.212
1.8µg/ml FTC	6	10.7183	0.183893	0.07507	10.525	10.911
4.07µg/ml EFV	6	10.6650	0.201569	0.08229	10.453	10.877
ATRIPLA	6	10.8650	0.237550	0.09698	10.616	11.114
9.8µg/ml LPV	6	10.7867	0.194285	0.07932	10.583	10.991
0.6 µg/ml RTV	6	10.8533	0.172704	0.07051	10.672	11.035
KALETRA(LPV/r)	6	11.1317	0.340495	0.13901	10.774	11.489
TDF/FTC/LPVr	6	10.7433	0.310398	0.12672	10.418	11.069

Means Comparisons

Comparisons for all pairs using Tukey-Kramer HSD

Confidence Quantile

q*	Alpha
3.31028	0.05

Connecting Letters Report

Level	
KALETRA(LPV/r)	A
ATRIPLA	A
0.6 µg/ml RTV	A
Untreated Control	A
9.8µg/ml LPV	A
0.3 µg/ml TDF	A
TDF/FTC/LPVr	A
0.01%Methanol	A
1.8µg/ml FTC	A
4.07µg/ml EFV	A

Levels not connected by same letter are significantly different.

APPENDIX G1
Oneway Analysis of % Apoptotic cells (Acridine Orange) By Groups

Oneway Analysis of % Apoptotic HCS-2 cells By Groups

Summary of Fit

Rsquare	0.965275
Adj Rsquare	0.960066
Root Mean Square Error	0.889757
Mean of Response	5.458333
Observations (or Sum Wgts)	24

Analysis of Variance

Source	DF	Sum of Squares	Mean Square	F Ratio	Prob > F
Groups	3	440.12500	146.708	185.3158	<.0001*
Error	20	15.83333	0.792		
C. Total	23	455.95833			

Means and Std Deviations

Level	Number	Mean	Std Dev	Std Err Mean	Lower 95%	Upper 95%

Level	Number	Mean	Std Dev	Std Err Mean	Lower 95%	Upper 95%
Control	6	1.3333	0.81650	0.33333	0.476	2.190
0.01%Methanol	6	1.5000	0.54772	0.22361	0.925	2.075
CPT	6	11.5000	1.04881	0.42817	10.399	12.601
LPV/r	6	7.5000	1.04881	0.42817	6.399	8.601

Means Comparisons
Comparisons for all pairs using Tukey-Kramer HSD
Confidence Quantile

q*	Alpha
2.79894	0.05

Connecting Letters Report

Level				Mean
CPT	A			11.500000
LPV/r		B		7.500000
0.01%Methanol			C	1.500000
Control			C	1.333333

Levels not connected by same letter are significantly different.

Oneway Analysis of %Apoptotic NCE16IIA cells By Groups
Summary of Fit

Rsquare	0.918907
Adj Rsquare	0.906743
Root Mean Square Error	2.361144
Mean of Response	9.291667
Observations (or Sum Wgts)	24

Analysis of Variance

Source	DF	Sum of Squares	Mean Square	F Ratio	Prob > F
Groups	3	1263.4583	421.153	75.5431	<.0001*
Error	20	111.5000	5.575		
C. Total	23	1374.9583			

Means and Std Deviations

Level	Number	Mean	Std Dev	Std Err Mean	Lower 95%	Upper 95%
Control	6	2.1667	0.75277	0.3073	1.377	2.957
0.01%Methanol	6	2.0000	0.63246	0.2582	1.336	2.664
CPT	6	15.3333	3.93277	1.6055	11.206	19.461
LPV/r	6	17.6667	2.42212	0.9888	15.125	20.209

Means Comparisons
Comparisons for all pairs using Tukey-Kramer HSD
Confidence Quantile

q*	Alpha
2.79894	0.05

Connecting Letters Report

Level		
LPV/r	A	
CPT	A	
Control		B
0.01%Methanol		B

Levels not connected by same letter are significantly different.

Oneway Analysis of %apoptotic MCF-7 cells By Groups
Summary of Fit

Rsquare	0.9124
Adj Rsquare	0.89926
Root Mean Square Error	2.411777
Mean of Response	10.5
Observations (or Sum Wgts)	24

Analysis of Variance

Source	DF	Sum of Squares	Mean Square	F Ratio	Prob > F
Groups	3	1211.6667	403.889	69.4365	<.0001*
Error	20	116.3333	5.817		
C. Total	23	1328.0000			

Means and Std Deviations

Level	Number	Mean	Std Dev	Std Err Mean	Lower 95%	Upper 95%
Control	6	3.6667	0.81650	0.3333	2.810	4.524
0.01%Methanol	6	3.1667	1.16905	0.4773	1.940	4.394
CPT	6	16.8333	3.48807	1.4240	13.173	20.494
LPV/r	6	18.3333	3.01109	1.2293	15.173	21.493

Means Comparisons
Comparisons for all pairs using Tukey-Kramer HSD
Confidence Quantile

q*	Alpha
2.79894	0.05

Connecting Letters Report

Level		
LPV/r	A	
CPT	A	
Control		B
0.01%Methanol		B

Levels not connected by same letter are significantly different.

Oneway Analysis of %Apoptotic MCF-10A cells By Groups
Summary of Fit

Rsquare	0.966355
Adj Rsquare	0.961308
Root Mean Square Error	0.866025
Mean of Response	5.416667
Observations (or Sum Wgts)	24

Analysis of Variance

Source	DF	Sum of Squares	Mean Square	F Ratio	Prob > F
Groups	3	430.83333	143.611	191.4815	<.0001*
Error	20	15.00000	0.750		
C. Total	23	445.83333			

Means and Std Deviations

Level	Number	Mean	Std Dev	Std Err Mean	Lower 95%	Upper 95%
Control	6	1.1667	0.75277	0.30732	0.3767	1.957
0.01%Methanol	6	1.3333	0.81650	0.33333	0.4765	2.190
CPT	6	8.5000	0.54772	0.22361	7.9252	9.075
LPV/r	6	10.6667	1.21106	0.49441	9.3957	11.938

Means Comparisons
Comparisons for all pairs using Tukey-Kramer HSD
Confidence Quantile

q*	Alpha
2.79894	0.05

Connecting Letters Report

Level			
LPV/r	A		
CPT		B	
0.01%Methanol			C
Control			C

Levels not connected by same letter are significantly different.

APPENDIX G2

Oneway Analysis of ELISA ABSORBANCE By GROUPS

Oneway Analysis of HCS-2 ABSORBANCE By GROUPS
Summary of Fit

Rsquare	0.998659
Adj Rsquare	0.998391
Root Mean Square Error	0.144882
Mean of Response	2.756757
Observations (or Sum Wgts)	25

Analysis of Variance

Source	DF	Sum of Squares	Mean Square	F Ratio	Prob > F
GROUPS	4	312.71758	78.1794	3724.449	<.0001*
Error	20	0.41982	0.0210		
C. Total	24	313.13739			

Means and Std Deviations

Level	Number	Mean	Std Dev	Std Err Mean	Lower 95%	Upper 95%
UNTREATED	5	0.10084	0.006382	0.00285	0.0929	0.1088
0.01%Methanol	5	0.10611	0.010164	0.00455	0.0935	0.1187
CPT	5	2.36066	0.125129	0.05596	2.2053	2.5160
LPV/r	5	1.60518	0.298238	0.13338	1.2349	1.9755
Positive Control	5	9.61100	0.014387	0.00643	9.5931	9.6289

Means Comparisons
Comparisons for all pairs using Tukey-Kramer HSD
Confidence Quantile

q*	Alpha
2.99238	0.05

Connecting Letters Report

Level				
Positive Control	A			
CPT		B		
LPV/r			C	
0.01%Methanol				D
UNTREATED				D

Levels not connected by same letter are significantly different.

Oneway Analysis of NCE16IIA Absorbance By GROUPS
Summary of Fit

Rsquare	0.996879

Adj Rsquare	0.996255
Root Mean Square Error	0.216366
Mean of Response	3.500777
Observations (or Sum Wgts)	25

Analysis of Variance

Source	DF	Sum of Squares	Mean Square	F Ratio	Prob > F
GROUPS	4	299.06240	74.7656	1597.073	<.0001*
Error	20	0.93628	0.0468		
C. Total	24	299.99868			

Means and Std Deviations

Level	Number	Mean	Std Dev	Std Err Mean	Lower 95%	Upper 95%
UNTREATED	5	0.15126	0.009573	0.00428	0.1394	0.1631
0.01%Methanol	5	0.16977	0.016262	0.00727	0.1496	0.1900
CPT	5	3.77706	0.200206	0.08953	3.5285	4.0256
LPV/r	5	3.79480	0.439801	0.19669	3.2487	4.3409
Positive Control	5	9.61100	0.014387	0.00643	9.5931	9.6289

Means Comparisons

Comparisons for all pairs using Tukey-Kramer HSD

Confidence Quantile

q*	Alpha
2.99238	0.05

Connecting Letters Report

Level		
Positive Control	A	
LPV/r		B
CPT		B
0.01%Methanol		C
UNTREATED		C

Levels not connected by same letter are significantly different.

Oneway Analysis of MCF-7 Absorbance By GROUPS

Summary of Fit

Rsquare	0.999511
Adj Rsquare	0.999413
Root Mean Square Error	0.085364
Mean of Response	2.806257
Observations (or Sum Wgts)	25

Analysis of Variance

Source	DF	Sum of Squares	Mean Square	F Ratio	Prob > F
GROUPS	4	298.01156	74.5029	10224.16	<.0001*
Error	20	0.14574	0.0073		
C. Total	24	298.15730			

Means and Std Deviations

Level	Number	Mean	Std Dev	Std Err Mean	Lower 95%	Upper 95%
UNTREATED	5	0.43109	0.027282	0.01220	0.3972	0.4650
0.01%Methanol	5	0.46880	0.026930	0.01204	0.4354	0.5022
CPT	5	1.71456	0.128368	0.05741	1.5552	1.8739
LPV/r	5	1.80584	0.135203	0.06046	1.6380	1.9737
Positive Control	5	9.61100	0.014387	0.00643	9.5931	9.6289

Means Comparisons
Comparisons for all pairs using Tukey-Kramer HSD
Confidence Quantile

q*	Alpha
2.99238	0.05

Connecting Letters Report

Level			
Positive Control	A		
LPV/r		B	
CPT		B	
0.01%Methanol			C
UNTREATED			C

Levels not connected by same letter are significantly different.

Oneway Analysis of MCF-10A Absorbance By GROUPS
Summary of Fit

Rsquare	0.998013
Adj Rsquare	0.997615
Root Mean Square Error	0.180819
Mean of Response	2.42632
Observations (or Sum Wgts)	25

Analysis of Variance

Source	DF	Sum of Squares	Mean Square	F Ratio	Prob > F
GROUPS	4	328.40751	82.1019	2511.102	<.0001*
Error	20	0.65391	0.0327		
C. Total	24	329.06142			

Means and Std Deviations

Level	Number	Mean	Std Dev	Std Err Mean	Lower 95%	Upper 95%
UNTREATED	5	0.10200	0.016432	0.00735	0.0816	0.1224
0.01%Methanol	5	0.11000	0.021213	0.00949	0.0837	0.1363
CPT	5	0.98400	0.131643	0.05887	0.8205	1.1475
LPV/r	5	1.32460	0.381078	0.17042	0.8514	1.7978
Positive Control	5	9.61100	0.014387	0.00643	9.5931	9.6289

Means Comparisons
Comparisons for all pairs using Tukey-Kramer HSD
Confidence Quantile

q*	Alpha
2.99238	0.05

Connecting Letters Report

Level			
Positive Control	A		
LPV/r		B	
CPT		B	
0.01%Methanol			C
UNTREATED			C

Levels not connected by same letter are significantly different.

APPENDIX H
Ethics Clearance Certificate

M10

UNIVERSITY OF THE WITWATERSRAND, JOHANNESBURG
Division of the Deputy Registrar (Research)

HUMAN RESEARCH ETHICS COMMITTEE (MEDICAL)
R14/49 Prof Margot Hosie

CLEARANCE CERTIFICATE	**M10905**
PROJECT	Determiining the link between HAART treatment and urine, cervical and breast carcinomas
INVESTIGATORS	Prof Margot Hosie.
DEPARTMENT	School of Anatomical Sciences
DATE CONSIDERED	01/10/2010
DECISION OF THE COMMITTEE*	Approved unconditionally

Unless otherwise specified this ethical clearance is valid for 5 years and may be renewed upon application.

DATE 18/02/2011 **CHAIRPERSON** .....
(Professor PE Cleaton-Jones)

*Guidelines for written 'informed consent' attached where applicable
cc: Supervisor : Pr M Hosie

DECLARATION OF INVESTIGATOR(S)

To be completed in duplicate and **ONE COPY** returned to the Secretary at Room 10004, 10th Floor, Senate House, University.
I/We fully understand the conditions under which I am/we are authorized to carry out the abovementioned research and I/we guarantee to ensure compliance with these conditions. Should any departure to be contemplated from the research procedure as approved I/we undertake to resubmit the protocol to the Committee. **I agree to a completion of a yearly progress report.**

PLEASE QUOTE THE PROTOCOL NUMBER IN ALL ENQUIRIES...